รายงานวิจัยฉบับสมบูรณ์

ทุนส่งเสริมกลุ่มวิจัย
โครงการฤทธิ์ทางชีวภาพขององค์ประกอบทางเคมีจากพืชในภาคอีสาน
ราในประเทศไทยและการพัฒนาผลิตภัณฑ์นาโนสำหรับภูมิคุ้มกันในพืช

**Bioactive Constituents from Isan Plants and Thai Fungi, and
Development of Nanoproduct for Plant Immunity**

โดย ศ.ดร.สมเดช กนกเมธากุล และคณะ

มกราคม 2562

รายงานวิจัยฉบับสมบูรณ์

ทุนส่งเสริมกลุ่มวิจัย
โครงการฤทธิ์ทางชีวภาพขององค์ประกอบทางเคมีจากพืชในภาคอีสาน
ราในประเทศไทยและการพัฒนาผลิตภัณฑ์นาโนสำหรับภูมิคุ้มกันในพืช

Bioactive Constituents from Isan Plants and Thai Fungi,

and Development of Nanoproduct for Plant Immunity

คณะผู้วิจัย   สังกัด

1. ศ.ดร.สมเดช กนกเมธากุล (Somdej Kanokmedhakul)   มหาวิทยาลัยขอนแก่น

2. ศ.ดร.ขวัญใจ กนกเมธากุล (Kwanjai Kanokmedhakul)   มหาวิทยาลัยขอนแก่น

3. รศ.ดร.เกษม สร้อยทอง (Kasem Soytong) สถาบันเทคโนโลยีพระจอมเกล้าเจ้าคุณทหารลาดกระบัง

4. ผศ.ดร.พนาวัลย์ หมู่โสภณ (Panawan Moosophon)   มหาวิทยาลัยขอนแก่น

5. ผศ.ดร.นุชนาฏ ผลเกิด (Nutchanat Phonkerd)   มหาวิทยาลัยขอนแก่น วิทยาเขตหนองคาย

6. ดร.นิคม วงศา (Nikhom Wongsa)   มหาวิทยาลัยราชภัฏอุดรธานี

7. ผศ.ดร.มงคล นนทกิตติเจริญ (Mongkol Nontakitticharoen)   มหาวิทยาลัยขอนแก่น

8. ผศ.ดร.ณัชชา พันธมา (Natcha Panthama)   มหาวิทยาลัยเทคโนโลยีราชมงคลอีสานนครราชสีมา

9. ผศ.ดร.รัศมี เหล็กพรม (Ratsami Lekphrom)   มหาวิทยาลัยขอนแก่น

10. ผศ.ดร.ชุลิดา เหมตะศิลป์ (Chulida Hemtasin)   มหาวิทยาลัยกาฬสินธุ์

11. ดร.เอื้ออาทร ราชจันทร์ (Oue-artorn Rajachan)   มหาวิทยาลัยมหาสารคาม

สารบัญ

PART I: Investigation on Bioactive Compounds from Isan Plants and Thai Fungi

Project 1: Investigate on Six Fungi : *Myrothecium roridum, Neosatorya hiralsukae,*
Neosatorya pseudofisheri, Chaetomium globosum 7s-1, and *Talaromyces*
macrosporus KKU-1NK8**,** and *Talaromyces trachyspermus EU23* and Four
Plants: *Rhodamnia duetorum, Uvaria cherrevensis, Asparagus racemosus*
and *Croton poomae*

Project 2: Investigate on two Fungi : *Apiospora montagnei* and *Botryotrichum*
piluliferum and Two Plants: *Miliusa velutina* and *Cissus rheifolia*

สารบัญ (ต่อ)

บทคัดย่อ

โครงการวิจัยเรื่องฤทธิ์ทางชีวภาพขององค์ประกอบทางเคมีจากพืชในภาคอีสาน ราใน ประเทศไทยและการพัฒนาผลิตภัณฑ์นาโนสำหรับภูมิคุ้มกันในพืช ได้รับการสนับสนุนจากทุนส่งเสริม กลุ่มวิจัย (เมธีวิจัยอาวุโส สกว.) ในระยะเวลา 3 ปี มีนักวิจัยในโครงการทั้งหมด 11 คน จาก มหาวิทยาลัย 6 แห่ง คือ มหาวิทยาลัยขอนแก่น มหาวิทยาลัยกาฬสินธุ์ มหาวิทยาลัยมหาสารคาม มหาวิทยาลัยราชภัฏอุดรธานี มหาวิทยาลัยราชมงคลอีสานนครราชสีมา และ สถาบันเทคโนโลยีพระ จอมเกล้าเจ้าคุณทหารลาดกระบัง โดยแบ่งงานวิจัยเป็น 2 ส่วน คือส่วนที่ 1 การศึกษาสารออกฤทธิ์ ทางชีวภาพจากพืชในภาคอีสานและราในประเทศไทย มี 10 โครงการประกอบด้วย 24 โครงการย่อย ซึ่งศึกษาตัวอย่างจากผลิตภัณฑ์ธรรมชาติ 2 แหล่ง คือ พืช และรา โดยศึกษาพืชในภาคอีสานจำนวน 14 ชนิด ได้แก่ พลองแก้มอ้น นมแมวป่า รากสามสิบ เปล้าภูวัว ขางหัวหมู หุนหูช้าง กระดูกค่าง มะม่วงหัวแมงวัน เครือตับปลา เปล้าตองแตก ลำไยป่า เครือตากวาง กาฝากก่อ และ ฝ้ายน้ำ จาก การแยกสารโดยวิธีทางโครมาโทกราฟี และวิเคราะห์โครงสร้างของสารด้วยสเปกโทรสโกปีได้สาร องค์ประกอบจำนวน 152 สาร ในจำนวนนี้เป็นสารใหม่จำนวน 38 สาร และจากราตัวอย่างจำนวน 9 ชนิด ได้แก่ *Myrothecium roridum, Neosatorya hiralsukae, Neosatorya pseudofisheri, Chaetomium globosum* 7s-1, *Talaromyces macrosporus* KKU-1NK8, *Talaromyces trachyspermus* EU23, *Apiospora montagnei, Botryotrichum piluliferum* และเห็ดเรืองแสงสิรินรัศมี (*Neonothopanus nambi* PW2) แยกได้สารเคมีองค์ประกอบจำนวน 122 สาร พบว่าเป็นสารใหม่ จำนวน 26 สาร โครงสร้างของสารเคมีที่แยกได้มีหลายกลุ่ม เช่น แอลคาลอยด์ เทอร์ปีนอยด์ สเตอ รอยด์ ฟลาวานอยด์ ไตรโคทีซีน แซนโทน ออกซาฟีนาลีโนน กลัยโคไซด์ และอื่นๆ พบว่ามีสาร จำนวนหนึ่งแสดงฤทธิ์ทางชีวภาพที่ดีต่อการทดสอบในห้องปฏิบัติการ เช่น ยับยั้งเชื้อมาลาเรีย *Plasmodium falciparum* ยับยั้งเชื้อวัณโรค *Mycobacterium tuberculosis* ยับยั้งเชื้อแบคทีเรียก่อโรค ในมนุษย์ ยับยั้งแอลฟากลูโคซิเดสที่เกี่ยวกับโรคเบาหวาน ยับยั้งเอนไซม์แอซีทิลโคลีนเอสเทอเรส ที่เกี่ยวกับโรคอัลไซเมอร์ และฤทธิ์ต้านอนุมูลอิสระ รวมถึงทดสอบความเป็นพิษต่อเซลล์มะเร็งชนิด ต่างๆ เป็นต้น ในส่วนที่ 2 เป็นการวิจัยและพัฒนาโดยเลือกราสกุลคีโตเมียมที่มีสารองค์ประกอบออก ฤทธิ์ยับยั้งโรคพืชเช่น โรครากเน่าในทุเรียน ส้มโอ โรคใบไหม้ในข้าว รวมทั้งผัก เช่น มะเขือเทศ และ พริก มาพัฒนาเป็นผลิตภัณฑ์นาโนเพื่อเพิ่มประสิทธิภาพและง่ายต่อการใช้งาน ซึ่งผลิตภัณฑ์นาโน จากราคีโตเมียม อยู่ระหว่างการเตรียมข้อมูลสำหรับจดอนุสิทธิบัตร

โครงการนี้สามารถสร้างนักวิจัยรุ่นใหม่ที่มีศักยภาพให้มหาวิทยาลัยในโครงการและสังคมวิจัย จำนวน 8 คน นักศึกษาระดับปริญญาเอก 10 คน ปริญญาโท 4 คน และปริญญาตรี 15 คน โดย ผลการวิจัยได้ตีพิมพ์ในวารสาร 22 เรื่อง อยู่ระหว่าง review 1 เรื่อง และอยู่ระหว่างเตรียมบทความ ต้นฉบับ 2 เรื่อง พบว่างานวิจัยจะดำเนินการได้ดีจะขึ้นกับนโยบายของแต่ละสถาบันที่จะสนับสนุนให้มี บรรยากาศที่เอื้อต่อการทำวิจัย

คำสำคัญ องค์ประกอบทางเคมี สารออกฤทธิ์ทางชีวภาพ คีโตเมียม ผลิตภัณฑ์นาโน

Abstract

This research project on Bioactive Constituents from Isan Plants and Thai Fungi, and Development of Nanoproducts for Plant Immunity, was funded by a TRF Research Team Promotion Grant, RTA for 3 years. There were 11 researchers from 6 universities, Khon Kaen University, Mahasarakham University, Kalasin University, Udon Thani Rajabhat University, Rajamangala University of Technology Isan Nakhon Ratchasima and King Mongkut's Institute of Technology Ladkrabang. The research was divided into 2 parts. The first part was Investigation of Bioactive Compounds from Isan Plants and Thai Fungi. There were 10 projects consisting of 24 sub-projects, for which research samples were taken from 2 natural sources, plants and fungi. Fourteen species of Isan plants, including *Rhodamnia duetorum*, *Uvaria cherrevensis*, *Asparagus racemosus*, *Croton poomae* Esser, *Miliusa velutina*, Cissus *rheifolia*, *Diospyros undulata*, *Buchanania lanzan*, *Solori thorelii*, *Baliospermum calycinum*, *Walsura trichostemon*, *Salacia chinensis* Linn., *Helixanthera parasitica* Lour and *Croton krabas* were investigated. Chromatographic separation and structural identification by spectroscopy of these samples resulted in 152 isolated compounds, 38 of which were new compounds. The isolation of 8 species of fungi, namely *Myrothecium roridum, Neosatorya hiralsukae, Neosatorya pseudofisheri, Chaetomium globosum* 7s-1, *Talaromyces. Macrosporus* KKU-1NK8, Talaromyces *trachyspermus* EU23, *Apiospora montagnei, Botryotrichum piluliferum* and a luminescent mushroom *Neonothopanus nambi* PW2 gave 122 isolated compounds, of which 26 were new compounds. The structures of these isolated compounds can be classified into many groups, such as alkaloids, terpenoids, steroids, flavonoids, trichothecenes, xanthone, oxaphenalenones, glycosides etc. Some of these compounds exhibited potent biological activities *in vitro*, such as anti-malarial (*Plasmodium falciparum*), anti-TB (*Mycobacterium tuberculosis*), antibacterial, inhibiting alpha-glucosidase related to diabetes, inhibiting acetylcholine esterase associated with Alzheimer's disease and antioxidant activities, as well as cytotoxicity toward various types of cancer cell lines. The second part was the research and development of selected fungi in the genus *Chaetomium*, which contained active compounds inhibiting plant photogenic fungi, causing root rot in durian, grapefruit, rice blast vegetables such as tomatoes and peppers. Nano products were developed to increase efficiency and ease of use. The petty patent for the *Chaetomium* nanoproduct is under preparation for submission.

Finally, this project created a network including researchers with good potential to serve the universities under the project and research society, consisting of 8 young researchers, 10 PhD, 4 MSc and 15 BSc students. The research results have been published as 22 articles, 1 article under review and 2 manuscripts in preparation. It was found that the research can be performed better with a policy in each university to support the research environment in their institutions.

Keywords: Chemical constituents, Bioactive compounds, *Chaetomium,* Nanoproducts

Executive Summary

ทุนส่งเสริมการวิจัย (RTA5980002)

โครงการ ฤทธิ์ทางชีวภาพขององค์ประกอบทางเคมีจากพืชในภาคอีสาน ราในประเทศไทย

และการพัฒนาผลิตภัณฑ์นาโนสำหรับภูมิคุ้มกันในพืช

รายงานสรุปผลงานฉบับสมบูรณ์

(1 สิงหาคม 2559 – 31 มกราคม 2562)

โครงการวิจัยเรื่องฤทธิ์ทางชีวภาพขององค์ประกอบทางเคมีจากพืชในภาคอีสาน ราใน
ประเทศไทยและการพัฒนาผลิตภัณฑ์นาโนสำหรับภูมิคุ้มกันในพืช ภายใต้การสนับสนุนจากทุน
ส่งเสริมการวิจัย สกว. ในระยะเวลา 3 ปี มีนักวิจัยในโครงการทั้งหมด 11 คน จากมหาวิทยาลัย 6 แห่ง
คือ มหาวิทยาลัยขอนแก่น มหาวิทยาลัยกาฬสินธุ์ มหาวิทยาลัยมหาสารคาม มหาวิทยาลัยราชภัฏ
อุดรธานี มหาวิทยาลัยราชมงคลอีสานนครราชสีมา และ สถาบันเทคโนโลยีพระจอมเกล้าเจ้าคุณทหาร
ลาดกระบัง โดยแบ่งงานวิจัยเป็น 2 ส่วน คือส่วนแรกเป็นการศึกษาสารออกฤทธิ์ทางชีวภาพจากพืชใน
ภาคอีสานและราในประเทศไทย มี 10 โครงการประกอบด้วย 24 โครงการย่อย ซึ่งศึกษาตัวอย่างจาก
ผลิตภัณฑ์ธรรมชาติ 2 แหล่ง คือ พืช และรา โดยศึกษาพืชในภาคอีสานจำนวน 14 ชนิด ได้แก่ พลอง
แก้มอ้น (*Rhodamnia duetorum*) นมแมวป่า (*Uvaria cherrevensis*) รากสามสิบ (*Asparagus
racemosus*) เปล้าภูวัว (*Croton poomae* Esser) ขางหัวหมู (*Miliusa velutina*) หุนหูช้าง (*Cissus
rheifolia*) กระดูกค่าง (*Diospyros undulata*) มะม่วงหัวแมงวัน (*Buchanania lanzan*) เครือตับปลา
(*Solori thorelii*) เปล้าตองแตก (*Baliospermum calycinum*) ลำไยป่า (*Walsura trichostemon*)
เครือตากวาง (*Salacia chinensis* Linn.) กาฝากก่อ (*Helixanthera parasitica* Lour) และ ฝ้ายน้ำ
(*Croton krabas*) รวมทั้งราจำนวน 9 ชนิด ได้แก่ *Myrothecium roridum, Neosatorya hiralsukae,
Neosatorya pseudofisheri, Chaetomium globosum* 7s-1, *Talaromyces macrosporus* KKU-1NK8,
Talaromyces trachyspermus EU23, *Apiospora montagnei, Botryotrichum piluliferum* และ เห็ด
เรืองแสงสิรินรัศมี (*Neonothopanus nambi* PW2) จากการแยกสารโดยวิธีทางโครมาโทกราฟี และ
วิเคราะห์โครงสร้างของสารด้วยสเปกโทร สโกปีได้สารเคมีองค์ประกอบทั้งหมด 274 สาร ในจำนวนนี้
พบว่าเป็นสารใหม่ 64 สาร โดยแบ่งสารที่แยกได้จากพืช 14 ชนิด แยกได้ 152 สาร เป็นสารใหม่ 38
สาร และจากรา 9 ชนิด แยกได้ 122 สาร เป็นสารใหม่ 26 สาร โครงสร้างของสารเคมีที่แยกได้มีหลาย
กลุ่ม เช่น แอลคาลอยด์ เทอร์ปีนอยด์ สเตอรอยด์ ฟลาวานอยด์ ไตรโคทีซีน แซนโทน ออกซาฟีนาลี
โนน กลัยโคไซด์ เป็นต้น พบว่ามีสารจำนวนหนึ่งแสดงฤทธิ์ทางชีวภาพที่ดีต่อการทดสอบใน

ห้องปฏิบัติการ เช่น ยับยั้งเชื้อมาลาเรีย (*Plasmodium falciparum*) ยับยั้งเชื้อวัณโรค (*Mycobacterium tuberculosis*) ยับยั้งเชื้อแบคทีเรียก่อโรคในมนุษย์ ยับยั้งแอลฟากลูโคซิเดสที่เกี่ยวกับโรคเบาหวาน ยับยั้งเอนไซม์แอซีทิลโคลีนเอสเทอเรสที่เกี่ยวกับโรคอัลไซเมอร์ และยับยั้งอนุมูลอิสระ รวมถึงทดสอบความเป็นพิษต่อเซลล์มะเร็งชนิดต่างๆ เป็นต้น องค์ความรู้ที่ได้จากงานวิจัยนี้นอกจากจะได้ทราบถึงสารองค์ประกอบทั้งที่เป็นสารใหม่และสารที่เคยมีรายงานโครงสร้างแล้ว จะเป็นการเพิ่มข้อมูลสำหรับฐานข้อมูลของสารผลิตภัณฑ์ธรรมชาติในระดับสากล รวมทั้งฤทธิ์ทางชีวภาพของสารนั้นๆ สามารถสนับสนุนการใช้พืชเหล่านี้เป็นยาสมุนไพรได้ ความรู้ใหม่เหล่านี้จะเผยแพร่เป็นบทความตีพิมพ์ในระดับนานาชาติเพื่อรอการวิจัยพัฒนาต่อยอดการใช้ประโยชน์ต่อไป นอกจากประโยชน์ทางด้านการแพทย์แล้ว ในส่วนที่สองเป็นการวิจัยและพัฒนาโดยเลือกราสกุลคีโตเมียมที่มีสารองค์ประกอบออกฤทธิ์ยับยั้งราก่อโรคพืช เช่น โรครากเน่าในทุเรียน ส้มโอ และโรคใบไหม้ในข้าว รวมทั้งผัก เช่น มะเขือเทศ และพริก มาพัฒนาเป็นผลิตภัณฑ์นาโนเพื่อเพิ่มประสิทธิภาพและง่ายต่อการใช้งาน ซึ่งผลิตภัณฑ์นาโนจากราคีโตเมียม กำลังอยู่ระหว่างการเตรียมข้อมูลสำหรับจดอนุสิทธิบัตร

โครงการได้บริหารการทำวิจัยผ่านโครงการย่อย โดยสนับสนุนสารเคมี อุปกรณ์ การทดสอบฤทธิ์ทางชีวภาพ ค่าใช้เครื่องมือต่างๆ มีการให้คำปรึกษา ประชุมกลุ่ม และประชุมประจำปี ทำให้โครงการสามารถสร้างนักวิจัยรุ่นใหม่ที่มีศักยภาพที่ดีให้มหาวิทยาลัยในโครงการได้ และมี Output ดังแสดงในข้อ ต่อไปนี้

2. ผลงานตีพิมพ์ในวารสารวิชาการระดับนานาชาติ (ดูภาคผนวก)

    2.1 ผลงานที่ได้รับตีพิมพ์จำนวน 21 เรื่อง

    2.2 ผลงานที่อยู่ระหว่างการตีพิมพ์ จำนวน 1 เรื่อง

    2.3 ผลงานที่อยู่ระหว่างการ review จำนวน 1 เรื่อง

    2.4 ผลงานที่อยู่ระหว่างเตรียม manuscript จำนวน 2 เรื่อง

3. การนำเสนอผลงานวิจัย

    ผู้วิจัยมีการนำเสนอผลงานระดับชาติ และนานาชาติจำนวนกว่า 17 ครั้ง

4. การสร้างนักวิจัย

    นักวิจัยหลัก 11 คน หลังจากโครงการเสร็จสิ้น มีนักวิจัยได้ตำแหน่งทางวิชาการสูงขึ้น 5 คน คือ ตำแหน่งศาสตราจารย์ 1 คน และผู้ช่วยศาสตราจารย์ 4 คน ทั้งนี้สามารถสร้างนักวิจัยระดับต่างๆดังนี้

    4.1 นักวิจัยรุ่นใหม่ 8 คน โดยมีนักวิจัย 3 คน ได้รับทุนส่งเสริมนักวิจัยรุ่นใหม่ สกว.

    และอีก 5 คน ได้รับทุนวิจัยจากแหล่งอื่น

4.2 ผู้ช่วยวิจัย 2 คน

 4.3   นักศึกษา ระดับปริญญาเอก 10 คน และ ปริญญาโท 4 คน ปริญญาตรี 15 คน

5. การเชื่อมโยงทางวิชาการกับนักวิชาการอื่น ๆ ทั้งในและต่างประเทศ

นักวิจัยในโครงการมีงานวิจัยและมีการติดต่อเชื่อมโยงกับนักวิจัยทั้งในและต่างประเทศ ได้แก่ ประเทศเยอรมันนี แคนาดา สาธารณรัฐเช็ก ออสเตรเลีย ญี่ปุ่นและสาธารณรัฐประชาชนจีน รวมทั้ง นักวิจัยไทยในมหาวิทยาลัยต่าง ๆ ผ่านรูปแบบกิจกรรมต่าง ๆ เช่น การบรรยายในการประชุมสัมมนา การแลกเปลี่ยนประสบการณ์การวิจัย การให้คำปรึกษา และการให้ความร่วมมือในการแลกเปลี่ยน ข้อมูล ซึ่งเป็นการเพิ่มพูนและเรียนรู้ความรู้ใหม่ ๆ ทางวิชาการอย่างต่อเนื่อง

6.การจัดการอบรม/ประชุมวิชาการ

นักวิจัยในโครงการมีการจัดอบรมและประชุมวิชาการทั้งระดับชาติและนานาชาติ จำนวน 3 ครั้ง

โครงการ ฤทธิ์ทางชีวภาพขององค์ประกอบทางเคมีจากพืชในภาคอีสาน ราในประเทศไทย
และการพัฒนาผลิตภัณฑ์นาโนสำหรับภูมิคุ้มกันในพืช
รายงานฉบับสมบูรณ์

ชื่อหัวหน้าโครงการวิจัยผู้รับทุน ศาสตราจารย์ สมเดช กนกเมธากุล

โครงการวิจัยนี้ประกอบด้วยงานวิจัย 2 ส่วน คือ Part I: Investigation on Bioactive Compounds from Isan Plants and Thai Fungi และ Part II: Development of Chaetoglobosin C as a Microbial Elicitor to be Nanoproduct for Plant Immunity โดยมีนักวิจัยในโครงการทั้งหมด 11 คน และมีกิจกรรมที่ได้ดำเนินการดังต่อไปนี้

PART I: Investigation on Bioactive Compounds from Isan Plants and Thai Fungi

There are 10 researchers under 10 projects of over all 24 subprojects.

Project 1: Investigate on Six Fungi : *Myrothecium roridum*, *Neosatorya hiralsukae*, *Neosatorya pseudofisheri*, *Chaetomium globosum 7s-1*, *Talaromyces macrosporus* KKU-1NK8 and *Talaromyces trachyspermus* EU23 and Four Plants: *Rhodamnia duetorum*, *Uvaria cherrevensis*, *Asparagus racemosus* and *Croton poomae* Esser

Researcher: Somdej Kanokmedhakul (Project Leader)

Project 1A: Investigate on the Fungus *Myrothecium roridum*

1) Keywords

Myrothecium roridum, macrocyclic trichothecenes, cytotoxicity

2) Objective

To investigate the chemical constituents and their bioactivity of the fungus *Myrothecium roridum*

3) Introduction

Myrothecium roridum is a plant pathogenic fungus causing various plant diseases such as leaf spot, stem canker, and fruit rot with a wide host range. It was worldwide distribution including, agronomic crop, fruit plants and ornamental plants such as tomato, potato, cucurbits, watermelon, cherry, corn, dumb cane, and aglaonema.[1–7] Previous investigations of secondary metabolites from *M. roridum* have presented in the isolation of compounds, most of which are macrocyclic trichothecene mycotoxins, for example roridin A,

verrucarin A, myrothecine A, 2',3'-epoxymyrothecine A, and myrotoxin A.[8-12] The trichothecene mycotoxins have also been isolated from various fungi, including species of *Fusarium*, *Cylindrocarpon*, *Phomopsis*, *Stachybotrys*, *Trichothecium*, and *Verticimonosporium*[13] as well as endophytic fungi including, *Baccharis coridifolia* and *Baccharis artemisioides*.[14] Trichothecenes are classifiled as a sesquiterpenoid derivartive, containing trichothecene ring system characterized by a common tetracyclic 12,13-epoxy-trichothec-9-ene skeleton (EPT), which distributed into four types (A-D). Type A trichothecenes consist of a hydroxyl group or an ester function or even no oxygen substitution at C-8. Type B trichothecenes have a keto functional group at C-8. Type C trichothecenes have an epoxide at C-7/C-8, whereas trichothecenes D have a cyclic diester or triester ring linking at C-4 and C-15 which considered to be some of the most toxic trichothecenes. Type A trichothecenes commonly more toxic than Type B trichothecenes. Their toxicity increases when an increasing oxygenation of EPT.[15-17] Trichothecene mycotoxins displayed a wide range of bioactivities such as antifungal, antimalarial, cytotoxic and tyrosinase inhibitory. However, these compounds are highly toxic to human and animals, which show an extremely potent inhibitors of protein translation in eukaryotic cell.[18] Contact to these toxins can cause immunological problems, feed refusal, vomiting, hemorrhagic lesions, skin dermatitis and high dose of the mycotoxin can cause shock-like death.[19] Our continuing search for bioactive constituents from fungi, the EtOAc and MeOH extracts of the culture biomass of *M. roridum* displayed antimalarial activity toward *Plasmodium falciparum* with IC_{50} values of 0.025 and 0.0034 µg/mL, respectively, and presented strong cytotoxicity against KB cell line with 89.4% and 91.1% inhibition, respectively, at a concentration of 50 µg/mL. Moreover, the MeOH extract showed cytotoxicity toward NCI-H187 cell line with 99.3% inhibition. The EtOAc extract also showed cytotoxicity toward *Vero* cell line with IC_{50} value of 0.045 µg/mL. We present herein the isolation, structural elucidation, and bioactivity of eight trichothecenes from the biomass of *M. roridum*.

4) Result and Discussion

The crude extract of dried fungal biomass of *M. roridum* was fractionated by flash column chromatography on silica gel and preparative TLC to give two new macrocyclic trichothecene, 6′,12′-epoxymyrotoxin A (**1A.1**), 7′-hydroxymytoxin B (**1A.2**), six known macrocyclic trichothecene (**1A.3-1A.8**) and ergosterol. The structures of these known compounds were identified by physical and spectroscopic data measurements (IR, 1D and 2D NMR) and MS and by comparing the data obtained with published values, as myrotoxin B (**1A.3**), myrotoxin D hydrate (**1A.4**), 2′,3′-epoxymyrothecine A (**1A.5**), miotoxin A (**1A.6**), roridin L-2 (**1A.7**), and trichoverritone (**1A.8**) as shown in Figure 1A.1.

Compound **1A.1** was obtained as colorless solid and its molecular formula, $C_{27}H_{32}O_9$, was determined from the HRESITOFMS (observed *m/z* 523.1960 [M + Na]$^+$), indicating 12 degrees of unsaturation. The IR spectrum of **1A.1** showed characteristics of carbonyl lactone (1754 cm^{-1}) and conjugated carbonyl lactone (1718 cm^{-1}) groups. The UV spectrum showed absorption maxima at 242 nm indicative of a conjugated carbonyl group. The ^1H and ^{13}C‑NMR spectroscopic data of **1A.1** were similar to those of myrotoxin A hydrate, except for the appearance of an epoxide at C-6′/C-12′ [$\delta_{H/C}$ 3.05/75.6 (H-12′) and δ_C 97.5 (C-6′)] in **1A.1**. The COSY and HMBC data supported the NMR assignments. The HMBC correlations of H-15 to C-1′; H-2′ to C-1′, C-3′, and C-12′; H-4′ to C-2′, C-3′, and C-12′; H-12′ to C-2′, C-3′, C-4′, and C-6′; H-5′ to C-3′, C-4′, and C-6′; H-8′ to C-6′, C-7′, and C-9′; H-10′ to C-11′; and H-4 to C-11′ confirmed the linkage between C-4 and C-15 of the macrocyclic ring. A first set of NOESY correlations between H-2 and H-3b, H-2, and H-13a and between H-13b and H-14 indicated that these protons are *β*-orientated, whereas correlations between H-3a and H-4, H-4 and H-15b, and H-11 and H-15a confirmed their *α*-orientation. This suggested the relative configuration of the EPT moiety to be 2*R*,4*R*,5*S*,6*R*,11*R*,12*S*, the same as that reported in literature. Moreover, a second set of NOESY correlations within the macrocyclic ring between H-2′ and H-12′, H-12′ and H-7′b indicated that these protons were located on the same side.   The configuration of **1A.1** was further confirmed by the comparison of its experimental and calculated ECD spectra. The calculation for two possible configurations at C-6′ and C-12′ of **1A.1**, **1Aa.1** (2*R*,4*R*,5*S*,6*R*,11*R*,12*S*,2'*S*,3'*R*,6'*R*,12'*R*) and **1Ab.1** (2*R*,4*R*,5*S*,6*R*,11*R*,12*S*,2'*S*,3'*R*,6'*S*,12'*S*) were performed using Gaussian 09 with TD-CAM-B3LYP/6-311++G**//B3LYP/6-31G*. The solvent effect was included using the Polarizable Continuum Model (PCM) for calculations in methanol. The calculated ECD spectrum of **1Aa.1** exhibited a Cotton effect at λ_{max} 225 nm ($\Delta\varepsilon$ +36.8), which agreed well with the experimental ECD spectrum of **1A.1**. Thus, the absolute configuration of **1A.1** was elucidated to be 2*R*,4*R*,5*S*,6*R*,11*R*,12*S*,2'*S*,3'*R*,6'*R*,12'*R*. Compound **1A.1** is a new macrocyclic tricothecene, and was named 6′,12′-epoxymyrotoxin A.

Compound **1A.2** was obtained as a white solid and its molecular formula, $C_{29}H_{36}O_{10}$, was determined from the HRESITOFMS (observed m/z 567.2208 [M + Na]$^+$), indicating 12 degrees of unsaturation. The IR spectrum of **1A.2** showed characteristics of hydroxyl (3432 cm^{-1}) and carbonyl (1710 cm^{-1}) groups. The UV spectrum showed absorption maxima at 243 nm indicative of a conjugated carbonyl group. The ^{13}C NMR and DEPT spectra of **1A.2** were similar to those of mytoxin B except for the appearance of a hydroxyl group at C-7′ by showing ^1H NMR signals at δ_H 4.18 (dd, *J* = 11.9 Hz, H-7′) ascribable to a hydroxymethine

group. This was confirmed by correlations of an oxymethine proton H-7′ to C-13′; H-8′ to C-7′, C-9′ and C-10′; H-9 to C-7′; H-12′ to C-2′, C-3′, C-5′, and C-7′ and H-14′ to C-6′ and C-12′ in the HMBC spectrum. The relative stereochemistry was determined by a combination of coupling constants and analysis of the NOESY spectrum, which was comparable to those of mytoxin B. Thus, the structure of compound **1A.2** was determined as 7′-hydroxymytoxin B.

Trichothecene mycotoxins are secondary metabolites produced by various fungi that colonize crop. Accordingly, the mycotoxins are highly toxic to humans and animals. However, these compounds also show a broad spectrum of bioactivities including, cytotoxic, antifungal, antimalarial, and tyrosinase inhibitory. The isolated compounds were tasted for antimalarial against (*Plasmodium falciparum*), antituberculosis (*Mycobacterium tuberculosis*), vero cell (African green monkey kidney cell line), and cytotoxicity toward NCI-H187, KB, and MCF-7 cancer cell lines. The results of bioactivity assays of the isolated compounds are shown in Table 1A.1. Compounds **1A.1**-**1A.8** exhibited strong antimalarial activity against *Plasmodium falciparum* with an IC_{50} values ranging from 0.57 nM to 3.07 μM and showed high cytotoxicity against two cancer cell lines (KB and NCI-H187) with IC_{50} values ranging from 0.59 nM to 12.64 μM. Compounds **1A.1**-**1A.3** and **1A.6** showed strong antimalarial activity *Plasmodium falciparum* with an IC_{50} values of 0.58, 0.70, 0.57, and 0.68 nM, respectively, which are lower than the control drug. Moreover, compounds **1A.1**-**1A.4** and **1A.6**-**1A.8** showed strong cytotoxic against KB cells with IC_{50} value of 0.60-497.88 nM. Compounds **1A.1-1A.4** and **1A.6** also exhibited strong cytotoxicity against the NCI-H187 cell line, with IC_{50} values in the range of 0.79–112.28 nM. However, all compounds also displayed strong cytotoxicity against *Vero* cells with IC_{50} values ranging from 1.50-30,990 nM (Table 1A.1). Comparison of the structures among trichothecene mycotoxins **1A.1**-**1A.8** suggests that the existence of an epoxide at C-12/C-13 and a macrocyclic ring in the skeleton played important roles in their biological activities. Moreover, the new trichothecene **1A.1** which contained one more epoxide ring at C-6′/C-12′ showed the strongest cytotoxicity towards both cancer NCI-H187 and normal *Vero* cell lines. On the other hand, the absence of an epoxide ring at C-12/C-13 and a double bond at C-9 in trichothecene **1A.5** led to a decrease in all activities tested. When comparing the macrocyclic derivative **1A.6** with the two non-cyclic congeners **1A.7** and **1A.8**, compound **1A.6** was found to be more toxic than **1A.7** and **1A.8** with an opened ring. It should be noted that most of the isolated trichothecenes, except **1A.5**, were more toxic than the standard drugs. Our data confirm by the way that contamination of agricultural and food products by the fungus *M. roridum* must be strictly controlled.
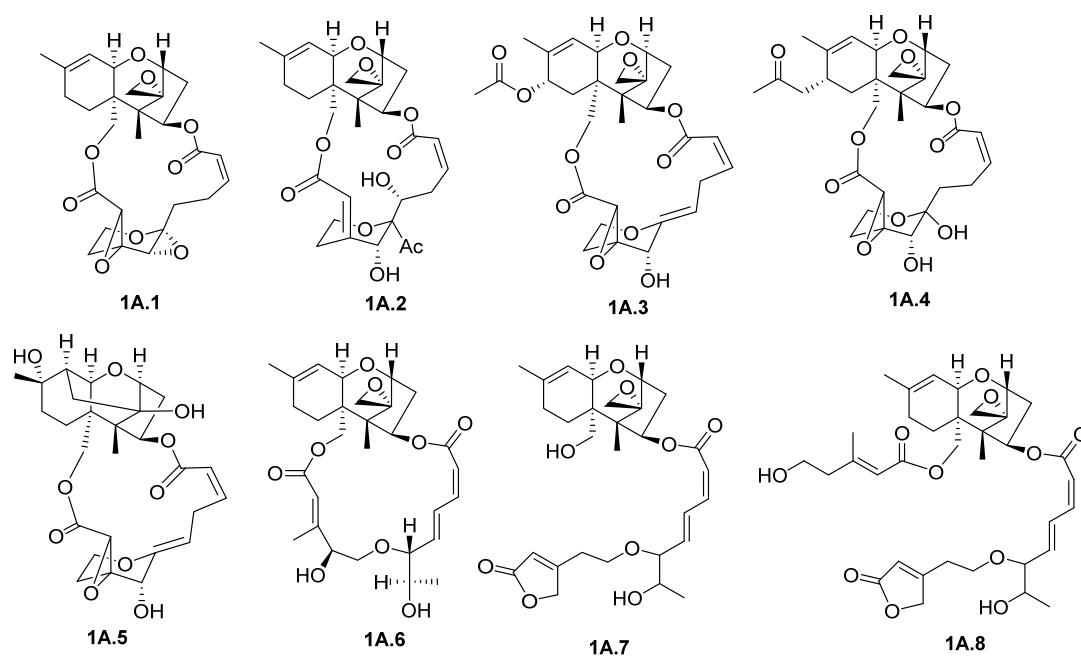
Figure 1A.1. Isolated compounds from the fungus *Myrothecium roridum*

Table 1A.1. Biological activity of compounds **1A.1**-**1A.8**.

Compound	anti-malarial IC$_{50}$ (nM)	Cytotoxicity IC$_{50}$ (nM)		
		KB[a]	NCI-H187[b]	*Vero* cell[c]
1A.1	0.58 nM	0.63 nM	0.79 nM	1.50 nM
1A.2	0.70 nM	2.81 nM	5.99 nM	5.75 nM
1A.3	0.57 nM	0.60 nM	20.60 nM	2.87 nM
1A.4	7.29 nM	48.77 nM	112.28 nM	46.51 nM
1A.5	3.07 μM	12.64 μM	12.10 μM	30.99 μM
1A.6	0.68 nM	6.24 nM	3.94 nM	11.49 nM
1A.7	265.91 nM	497.88 nM	731.73 nM	1.68 μM
1A.8	54.80 nM	77.84 nM	4.23 μM	2.12 μM
Dihydroartemisinin	2.09 nM			
Doxorubicin		0.68 μM	0.20 μM	
Ellipticine		4.87 μM	12.50 μM	3.40 μM

[a]Human epidermoid carcinoma in the mouth. [b]Human small cell lung cancer.
[c]African green monkey kidney.

References

1) Domsch, K. H.; Gams, W.; Anderson, T.-H. Compendium of soil fungi; Academic Press, London, 1980; Vol. 1, pp 483–484.

2) Fish WW, Bruton BD, Popham TW. Cucurbit host range of *Myrothecium roridum* isolated from watermelon. Am J Plant Sci 2012; 3: 353–359.

3) Chase, A. R. Influence of Host Plant and Isolate Source on *Myrothecium* Leaf Spot of Foliage Plants. *Plant Dis.* 1983, *67* (6), 668.

4) Ponnappa, K. M. On the pathogenicity of *Myrothecium roridum* Eichhornia crassipes isolate. Hyacinth Control Jnl 1970, *8*, 18–20.

5) Cabral, C. S.; Henz, G. P.; Moreira, A. J. A.; Reis, A. New cucurbitaceous hosts of *Myrothecium roridum* in Amazonas state, Brazil. *Trop. Plant Pathol.* 2009, *34* (6), 402–405.

6) Quezado Duval, A. M.; Henz, G. P.; Paz-Lima, M. L.; Medeiros, A. R.; Miranda, B. E. C.; Pfenning, L. H.; Reis, A. New hosts of *Myrothecium* spp. In brazil and a preliminary in vitro assay of fungicides. *Braz. J.* Microbiol. Publ. Braz. Soc. Microbiol. 2010, *41* (1), 246–252.

7) Hong, C. F.; Tsai, S. F.; Yeh, H. C.; Fan, M. C. First Report of Myrothecium roridum Causing Myrothecium Leaf Spot on Dieffenbachia picta "Camilla" in Taiwan. *Plant Dis.* 2013, *97* (9), 1253–1253.

8) Bloem RJ, Smitka TA, Bunge RH, French JC, Mazzola EP. Roridin-L-2, a new trichothecene. Tetrahedron Lett 1983; 24:249–252.

9) Jarvis BB, Vrudhula VM, Pavanasasivam G, Trichoverritone and 16-hydroxyroridin L-2, new trichothecenes from *Myrothecium roridum.* Tetrahedron Lett 1983; 24: 3539-3542

10) Lin T, Wang G, Zhou Y, Zeng D, Liu X, Ding R, Jiang X, Zhu D, Shan W, Chen H. Structure elucidation and biological activity of two new trichothecenes from an endophyte, *Myrothecium roridum*. J Agric Food Chem 2014; 62:5993–6000.

11) Wang T, Zhang Y, Pei Y. Two novel trichothecenes from *Myrothecium roridum*. Med Chem Res 2007; 16:155–161.

12) De Carvalho MP, Weich H, Abrahum WR. *Macrocyclic trichothecenes* as antifungal and anticancer compounds. Curr Med Chem 2016; 23:23–35.

13) He J, Zhou T, Young JC, Boland GJ, Scott PM. Chemical and biological transformations for detoxification of trichothecene mycotoxins in human and animal food chains: a review. Trends Food Sci Technol 2010; 21:67–76.

14) Rizzo I, Varsavky E, Haidukowski M, Frade H. Macrocyclic trichothecenes in *Baccharis coridifolia* plants and endophytes and Baccharis artemisioides plants. Toxicon 1997; 35:753–757.

15) McCormick SP, Stanley AM, Stover NA, Alexander NJ. Trichothecenes: from simple to complex mycotoxins. Toxins 2011; 3:802–814.

16) Islam Z, Shinozuka J, Harkema JR, Pestka JJ. Purification and comparative neurotoxicity of the trichothecenes satratoxin G and roridin L2 from *Stachybotrys chartarum*. J Toxicol Environ. Health A 2009; 72:1242–1251.

17) Zhang HJ, Tamez PA, Aydogmus Z, Tan GT, Saikawa Y, Hashimoto K, Nakata M, Hung NV, Xuan le T, Cuong NM, Soejarto DD, Pezzuto JM, Fong HH. Antimalarial agents from plants. III. Trichothecenes from Ficus fistulosa and R*haphidophora decursiva.* Planta Med 2002; 68:1088–1091.

18) Rocha O, Ansari K, Doohan FM. Effects of trichothecene mycotoxins on eukaryotic cells: a review. Food Addit Contam 2005; 22:369–378

19) Pestka JJ, Smolinski AT. Deoxynivalenol: toxicology and potential effects on humans. J Toxicol Environ Health B Crit Rev 2005; 8:39–69.

20) Jarvis BB, Lee YW, Cömezoḡlu FT, Cömezoḡlu SN, Bean GA. Myrotoxins: a new class of macrocyclic trichothecenes. Tetrahedron Lett 1985; 26:4859–4862.

5) Research Outcome

Publication

Lakornwong, W.; Kanokmedhakul, K.; Soytong, K.; Unartngam, A.; Tontapha, S.; Amornkitbamrung, V.; Kanokmedhakul, S. "Types A and D trichothecene mycotoxins from the fungus *Myrothecium roridum*" Planta Med. 2019, 85, 774-780.

Oral presentation

5.1) Lakornwong W, Kanokmedhakul S, Kanokmedhakul K, Soytong K. "Chemical constituents from *Myrothecium roridum* and their bioactivities", at 116th RGJ Seminar Series, at College of Local Administration, Khon Kaen University, Khonkaen, Thailand, 9-10 August 2016.

5.2) Lakornwong W, Kanokmedhakul S, Kanokmedhakul K, Soytong K. "Phytochemistry from the fungus *Myrothecium roridum*" at 5th International Conference on Integrating Science and Technology for Sustainable Development, at Cherry Queen Hotel, Southern Shan State, Myanmar, 26-27 November 2016.

Project 1B Investigate on Fungus *Neosatorya hiratsukae*

1) Keywords

Neosatorya, Neosatorya hiratsukae, cytotoxicity

2) Objective

To investigate secondary metabolizes and their cytotoxicity from the fungus *Neosatorya hiratsukae*

3) Introduction

The fungus *Neosartorya* species are sexual states of the *Aspergillus* species, family Trichocomaceae. They are distributed in soil worldwide [1]. This genus has been reported to produce many types of bioactive compounds such as sartorymensin [2], eurochevalierine [3] and fischerindoline [4], which display *in vitro* cytostatic effects in human U373 glioblastoma, MCF-7 breast cancer and A549 non-small-cell-lung cancer cell lines. Glabramycin [5], aszonapyrone [6], and sartorypyrone analogs [7] have been reported for their antibacterial properties. Previously, we reported the isolation and biological activity of tatenoic acid from *Neosartorya tatenoi* [8], meroterpenoid, spinosate analogs from *N. spinosa* [9], and tryptoquivaline V and brasiliamide G from *N. pseudofischeri* [10]. In our continuing search for bioactive compounds from fungi in the Neosartorya species, isolated from soil in Thailand [11], the EtOAc extract from biomass of the fungus *Neosartorya hiratsukae* showed antibacterial activity against *Bacillus cereus* ATCC 11778 with MIC 40 µg/mL.

4) Result and discussion

Chromatographic separation of n-hexane, EtOAc and MeOH extracts from biomass of *N. hiratsukae* gave twenty compounds (**1B.1**- **1B.20**), and four of them (**1B.1**-**1B.4**) were new compounds. The structures of known compounds were identified by their physical properties and spectroscopic analysis (^{1}H and ^{13}C NMR, and IR) as well as by comparison with the data obtained from published values as being chevalones A-C (**1B.5**-**1B.7**) [12], chevalone E (**1B.8**) [13], 11-hydroxychevalone C (**1B.9**) [9], sartorypyrone A (**1B.10**) [14], sartorypyrone D (**1B.11**) [7], α-pyrone meroterpenoid pyripyropene A (**1B.12**) [15], isochaetominine C (**1B.13**) [16], pyrrolobenzoxazine terpenoids, CJ-12662 (**1B.14**) and CJ-12663 (**1B.15**) [17], eurochevalierine (**1B.16**) [12], 1,4-diacetyl-2,5-dibenzylpiperazine derivative (**1B.17**), 2,4-dihydroxy-6-methylbenzoic acid (**1B.18**) [3], 1-methyl-4-quinolone (**1B.19**) [18] and diorcinol (**1B.20**) [19] as shown in Figure 1B.1.

Compound **1B.1** had a molecular formula $C_{26}H_{36}O_4$, deduced from the ^{13}C NMR and HRESITOFMS (m/z 435.2516 [M+Na]$^+$) data, revealing nine degrees of unsaturation. The UV spectrum showed absorption maxima at 207, 230 and 286 nm. The IR spectrum showed the

presence of α,β-unsaturated ester (1727 cm^{-1}) and alkene (1664 cm^{-1}) groups. The ^{1}H and ^{13}C NMR spectroscopic data of **1B.1** were similar to an isolated meroterpenoid, chevalone A (**1B.5**) [12], except for the absence of a hydroxyl group at C-3 in the A ring, which was replaced by a carbonyl group (δ_C 217.3). The HMBC spectrum presented correlations of methylene proton H-1 to C-2, C-3, C-5, C-10 and C-18; H-5 to C-7, C-10 and C-20; H-9 to C-5, C-10, C-18, C-8 and C-17, and H-17 to C-14, which confirmed the connectivity of A, B and C rings. The cross-peaks of correlations of H-15 to C-13, C-14 and C-3′ extended the connectivity between the two fragments, C and E, through the D ring junction. From the above evidence, compound **1B.1**, chevalone G was determined as a new meroterpenoid.

Compound **1B.2** had the molecular formula $C_{28}H_{40}O_5$, deduced from the ^{13}C NMR and HRESITOFMS (m/z 479.2780 [M+Na]$^+$) data, demonstrating nine degrees of unsaturation. The UV spectrum showed absorption maxima at 207, 236 and 288 nm. The IR spectrum showed the presence of hydroxyl (3380 cm^{-1}) and carbonyl (1702 and 1687 cm^{-1}) groups. The ^{1}H and ^{13}C NMR spectroscopic data of **1B.2** are close to the meroterpenoid, aszonapyrone A [20], except for the disconnection at C-8 and C-14 on the C ring in 2, which was arranged to form double bonds at C-7/C-8 and C-13/C-14. The NMR spectrum of **1B.2** showed two alkene groups at $\delta_{H/C}$ 5.33/121.2 (H-7/C-7) and δ_C 135.8 (C-8), and $\delta_{H/C}$ 5.17 (dd, J = 8.8, 4.3 Hz)/123.5 (H-14/C-14), and δ_C 135.6 (C-13). The COSY spectrum exhibited a cross coupling network between H-1/H-2/H-3, H-5/H-6/H-7, H-9/H-11/H-12, H-14/H-15 and H-5′/H-7′ (allylic coupling). The HMBC spectrum of **1B.2** displayed the correlations of the α-pyrone ring H-7′ to C-5′ and C-6′, H-5′ to C-3′, C-4′, C-6′ and C-7′, and bicyclic rings A and B of H-1 to C-10; H-3 to C-4, C-19, C-20 and the carbonyl carbon (C-1″); H-5 to C-1, C-6, C-9 and C-18; H-6 to C-8. While HMBC correlations of H-9 to C-7, C-8 and C-10, H-17 to C-7, C-8 and C-9, and H-11 to C-8, C-10 and C-13, H-12 to C-9, C-14 and C-16; H-16 to C-12 and C-14; H-14 to C-16; and H-15 to C-2′, C-4′ and C-13 extended the connectivity between bicyclic A, B rings and the α-pyrone ring. The relative configuration of **1B.2** was determined by coupling constant and NOESY spectral data. The coupling constant of H-3 (9.6 Hz) and the correlations of 1,3-diaxial between H-3 and H-5, and H-5 and H-9 in NOESY spectra indicated that these protons were placed in the axial orientation. Furthermore, the configurations of two double bonds at C7/C-8 and C-13/C14 were assigned to be Z and E by the NOESY correlations between H-7 and H3-17, and H3-16 and H-15, respectively. From the above evidence, compound **1B.2** was determined as a new meroterpenoid, and has been named aszonapyrone C. This is the first isolation of a new type of meroterpenoid pyrone and its structure could support it as an intermediate in the previously proposed biosynthetic pathway for meroterpenoid pyrones [12,14].
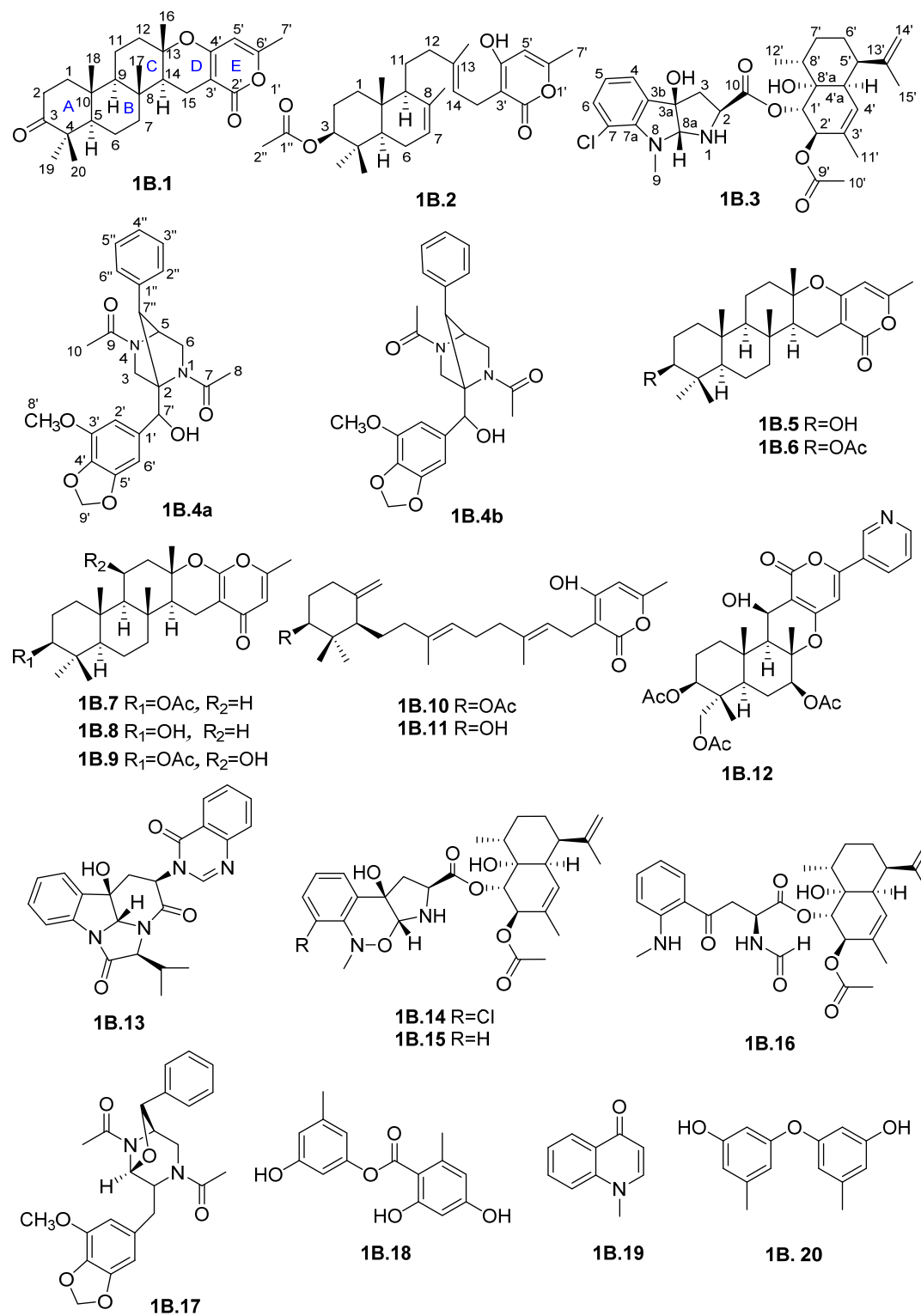
Figure 1B.1. Isolated compounds from the fungus *Neosatorya hiratsukae*.

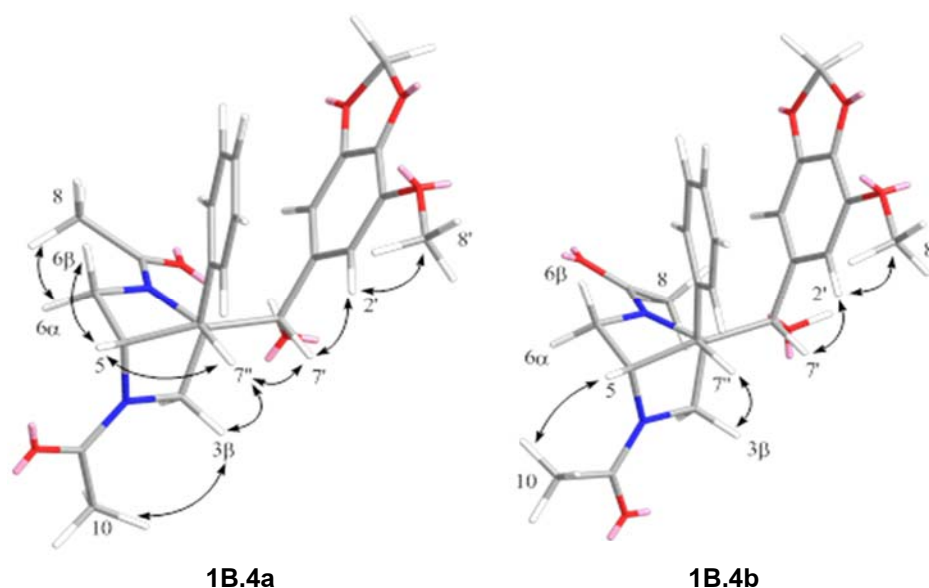1B.4a   1B.4b

Figure 1B.2. The key NOESY correlations of major (**1B.4a**), minor (**1B.4b**) and their energy-
minimized rotamer structures using MM2

Compound **1B.3** had the molecular formula $C_{29}H_{37}ClN_2O_6$, deduced from the[13]C NMR, and HRESITOFMS (m/z 567.2235 [M+Na]+ and m/z 569.2210 [M+2+Na]+) data, indicating twelve degrees of unsaturation. The UV spectrum showed absorption maxima at 212, 256 and 307 nm. The IR spectrum showed the presence of hydroxyl (3403 cm^{-1}), ester carbonyl (1743 cm^{-1}), and aromatic (1643 cm^{-1}) groups. The ^1H and ^{13}C NMR spectral data of 3 were similar to a known pyrroloindole terpenoid, fischerindoline [4], except that an aromatic proton at C-7 was replaced by a chloride atom (δ_C 133.2). The ^1H NMR spectrum showed resonances of aromatic protons at δ 7.03 (1H, d, J = 7.2 Hz, H-4), 6.65 (1H, dd, J = 7.2, 8.0 Hz, H-5), and 7.10 (1H, d, J = 8.0 Hz, H-6), indicating the presence of a 1,2,3-trisubstituted aromatic ring, as found in the isolated pyrrolobenzoxazine CJ-12662 (**1B.14**). The HMBC spectrum presented correlations of H-4 to C-6 and C-3a; H-5 to C-7 and C-3b; H-6 to C-4 and C-7a; H-9 to C-7a and C-8a; H-8a to C-3a, C-2, and C-9; H-2 to C-3, C-3a, and C-8a; and H-3 to C-3a, C-2, and C-10 to complete the assignment of the alkaloid moiety and its substituents. Thus, compound **1B.3** was determined as a new pyrroloindole terpenoid, and has been named 7-chlorofischerindoline.

The molecular formula of compound **1B.4**, $C_{24}H_{26}N_2O_6$, was derived from the ^{13}C NMR and HRESITOFMS (m/z 461.1683 [M+Na]$^+$) data, demonstrating thirteen indices of

hydrogen deficiency. The UV spectrum showed absorption maxima at 208, 249 and 257 nm. The IR spectrum showed the presence of hydroxyl (3266 cm^{-1}) and amide carbonyl (1638 cm^{-1}) groups. The ^{1}H and ^{13}C NMR spectra of **1B.4** showed two sets of resonances signals for two conformers, **1B.4a** and **1B.4b**, with the protons integration ratio of 4:1. Analysis of the ^{1}H and ^{13}C NMR spectral data of the major conformer, **1B.4a**, indicated a structure related to brasiliamide B [21] and brasiliamide G [10], which contain three parts including a benzyl, a 3-methoxy-4,5-methylenedioxyphenyl and a piperazine moiety. However, the structure of **1B.4** was different from those brasiliamide analogs by having a diazabicyclo[2.2.1]heptane unit with C-2 and C-5 of the piperazine ring linked at a benzylic carbon C-7″. The resonance signals of two benzylic protons in the structure appeared at $\delta_{H/C}$ 5.54 (s, H-7′)/70.3 and 2.66 (s, H-7″)/55.0. The HMBC exhibited correlations of a methine proton H-5 to C-2 and C-7″, and methylene protons H-3 to C-7″ and H-7″ to C-2″, C-6 confirmed the connectivity of a bicyclic structure. The conformational change of acetamides at N-1 and N-4 generated two conformers **1B.4a** and **1B.4b**, as reported in the literature [10], which were observed. The difference of NMR signals between **1B.4a** and **1B.4b** conformers caused by the rotation of the acetyl group of the N-4 amide, which affected the chemical shift values of H-3, H-5 and H-7″. The major conformer **1B.4a** was observed from NOESY correlations between H-10 and H-3α, H-8 and H-6α, H-5 and H-6α, and H-7′ and H-7″, H-2′ (Figure 1B.2), together with the chemical shifts of protons and carbons at positions H/C-5 ($\delta_{H/C}$ 4.60/58.8) and H/C-7″ ($\delta_{H/C}$ 2.66/55.0) [21,22]. The NOESY correlations between H-10 and H-5 supported the minor conformer **1B.4b**. In addition, the resonance signals of protons and carbons of H/C-3 ($\delta_{H/C}$ 3.97/53.5), H/C-5 ($\delta_{H/C}$ 4.08/61.8) and H/C-7″ ($\delta_{H/C}$ 2.73/56.2) were shielded compared to the corresponding protons of the major conformer **1B.4a** [3,10,21,22]. From the above evidence, compound **1B.4** was determined as a new brasiliamide with a bicyclic structure and has been named brasiliamide H.

The results of biological activity evaluation of the new compounds **1B.1**-**1B.4** found that they showed weak antibacterial activity against *Bacillus cereus*, *Staphylococcus aureus*, *Escherichia coli, Pseudomonas aeruginsa* and *Salmonella enterica* serovar typhimurium (Table 1B.1). Compound **1B.3** exhibited weak cytotoxicity towards HeLa, KB, MCF-7, HepG2, HT-29 and *Vero* cell lines, with IC$_{50}$ values ranging from 45.0 - 63.26 µg/mL (Table 1B.2).

Chevalone G (**1B.1**). white solid; R$_f$ = 0.74 (MeOH-CH$_2$Cl$_2$;1:19); mp 145-147 ^{o}C; $[\alpha]_D^{30}$ -50.9 (c 0.05, CHCl$_3$); CD (c 0.24 mM, MeOH) nm 203 (+17.4), 211 (-90.7), 277 (-3.9) UV (MeOH) λ_{max} (log ε) 207 (4.12), 230 (3.13), 286 (3.64) nm; IR (ATR) V_{max} 1727, 1664, 1584, 1244 cm^{-1}; HRESITOFMS m/z 435.2516 [M + Na]$^+$ (calcd for C$_{26}$H$_{36}$O$_4$ + Na, 435.2511).

Aszonapyrone C (**1B.2**). yellow solid; R_f = 0.50 (MeOH-CH$_2$Cl$_2$; 1:19); mp 118-120 ^{o}C; $[\alpha]_D^{30}$ -6.6 (c 0.1, CHCl$_3$); CD (c 0.22 mM, MeOH) nm 206 (-17.2), 215 (-7.8), 293 (-1.1); UV (MeOH) λ_{max} (log ε) 207 (4.10), 236 (3.59), 288 (3.64) nm; IR (ATR) v_{max} 3380, 2934, 1702, 1687, 1581, 1447, 1378, 1232, 1020 cm^{-1}; HRESITOFMS m/z 479.2780 [M+Na]$^+$ (calcd for C$_{28}$H$_{40}$O$_5$ + Na, 479.2773).

7-Chlorofischerindoline (**1B.3**). white solid; R_f = 0.65 (MeOH-CH$_2$Cl$_2$; 1:19); mp 124-126 ^{o}C; $[\alpha]_D^{30}$ -69.5 (c 0.1, CHCl$_3$); CD (c 57.05 μM, MeOH) nm 221 (-1.9), 252 (+3.2), 307 (-1.5); UV (MeOH) λ_{max} (log ε) 212 (4.4), 256 (3.9), 307 (3.4) nm; IR (ATR) v_{max} 3403, 3082, 2966, 2932, 2862, 1743, 1643, 1570, 1439, 1373, 1233, 1179, 1019, 754 cm^{-1}; ^{1}H NMR (CDCl$_3$, 400 MHz) δ 7.10 (1H, d, J = 8.0 Hz, H-6), 7.03 (1H, d, J = 7.2 Hz, H-4), 6.65 (1H, dd, J = 7.2, 8.0 Hz, H-5), 5.41 (1H, brs, H-4″), 5.29 (1H, brs, H-1′), 5.08 (1H, brs, H-2′), 4.98 (1H, brs, H-14′), 4.78 (1H, brs, H-8a), 4.73 (1H, brs, H-14′), 4.00 (1H, dd, J = 7.8, 2.0 Hz, H-2), 3.20 (1H, s, H-9), 2.72 (1H, brs, H-4′a), 2.63 (1H, d, J = 13.5 Hz, H-3α), 2.47 (1H, brd, J = 12.4 Hz, H-5′), 2.26 (1H, dd, J = 13.5, 7.8 Hz, H-3β), 2.09 (3H, s, H-10′), 1.95 (1H, m, H-8′),1.83 (3H, brs, H-15′), 1.64 (3H, s, H-11′), 1.53 (1H, brd, J = 12.0 Hz, H-6′), 1.50 (1H, m, H-7′), 1.44 (1H, m, H-7′), 1.31 (1H, m, H-6′), 0.74 (3H, d, J = 6.7 Hz, H-12′); ^{13}C NMR (100 MHz) δ 173.6 (C-10), 170.0 (C-9′), 146.7 (C-13′), 145.0 (C-7a), 133.2 (C-7), 131.9 (C-6), 129.5 (C-3′), 127.4 (C-4′), 121.4 (C-4), 119.5 (C-5), 115.2 (C-3b), 111.2 (C-14′), 93.8 (C-8a), 86.0 (C-3a), 74.3 (C-1′), 73.5 (C-8′a), 72.7 (C-2′), 60.3 (C-2), 42.3 (C-3α), 40.8 (C-5′), 39.0 (C-4′a), 35.9 (C-9), 30.5 (C-8′), 30.2 (C-7′), 25.7 (C-6′), 22.3 (C-15′), 20.8 (C-10′), 19.7 (C-11′), 14.6 (C-12′); HRESITOFMS m/z 567.2235 [M + Na]$^+$ and 569.2210 [M+2+Na]$^+$ (calcd for C$_{29}$H$_{37}$^{35}ClN$_2$O$_6$ + Na, 567.2238 and C$_{29}$H$_{37}$^{37}ClN$_2$O$_6$ + Na, 569.2209).

Brasiliamide H (**1B.4**). Yellow solid; R_f = 0.48 (MeOH-CH$_2$Cl$_2$; 1:19); mp 128-130 ^{o}C; $[\alpha]_D^{30}$ -45.4 (c 0.1, CHCl$_3$); CD (c 36.75 μM, MeOH) nm 228 (+4.4), 255 (+0.5), 277 (+0.8); UV (MeOH) λ_{max} (log ε) 208 (4.71), 249 (3.94), 275 (3.97) nm; IR (ATR) v_{max} 3266, 2928, 1638, 1541, 1428, 1369, 1321, 1239, 1188, 1091, 1038, 699 cm^{-1}; HRESITOFMS m/z 461.1683 [M+Na]+ (calcd for C$_{24}$H$_{26}$N$_2$O$_6$ + Na, 461.1689).

Table 1B.1 Antibacterial activity of compounds **1B.1**-**1B.4.**

Compound	Antibacterial activity (MIC, μg/mL)				
	Gram-positive		Gram-negative		
	B. cereus[a]	*S. aureus*[b]	*E. coli*[c]	*P. aeruginosa*[d]	*S. typhimurium*[e]
1B.1	128	128	>128	128	>128
1B.2	>128	>128	>128	128	>128
1B.3	>128	>128	>128	128	>128
1B.4	64	128	128	128	>128
Vancomyci	1.0	1.0	-	-	-
Gentamyci	-	-	2.0	0.5	0.5

[a]*Bacillus cereus* ATCC 11778

[b]*Staphylococcus aureus* ATCC 25923

[c]*Escherichia coli* ATCC 25922

[d]*Pseudomonas aeruginosa* ATCC 27853

[e]*Salmonella enterica* serovar Typhimurium ATCC 13311

Table 1B.2 Cytotoxicity of new compounds **1B.1-1B.4**.

Compound	Cytotoxicity IC$_{50}$ (μM)					
	HeLa[a]	KB[b]	MCF-7[c]	HepG2[d]	HT-29[e]	*Vero* cells[f]
1B.2	94.44±5.52	>100	>100	>100	>100	>100
1B.3	48.33±2.02	50.54±5.87	56.42±2.13	45.0±4.82	57.5±5.74	63.26±6.57
1B.4	>100	>100	>100	>100	>100	>100
Adriamycin	0.02±0.005	2.44±0.35	1.11±0.28	0.37±0.17	0.35±0.06	1.51±0.18
Etoposide	0.47±0.10	-	-	-	-	44.79±1.95

[a]Human cervical carcinoma

[b]Human epidermoid carcinoma in the mouth

[c]Human breast adenocarcinoma

[d]HepG2 Human hepatocellular carcinoma

[e]HT-29 colectal adenocarcinoma

[f]African green monkey kidney

References

1) R.A. Samson, S. Hong, S.W. Peterson, J.C. Frisvad, J. Varga, Polyphasic taxonomy of *Aspergillus section* Fumigati and its teleomorph *Neosartorya*, Stud. Mycol. 59 (2007) 147–203.

2) S. Buttachon, A. Chandrapatya, L. Manoch, A. Silva, L. Gales, C. Bruyère, R. Kiss, A. Kijjoa, Sartorymensin, a new indole alkaloid, and new analogues of tryptoquivaline and fiscalins produced by *Neosartorya siamensis* (KUFC 6349), Tetrahedron. 68 (2012) 3253-3262.

3) A. Eamvijarn, A. Kijjoa, C. Brúyere, V. Mathieu, L. Manoch, F. Lefranc, A. Silva, R. Kiss, W. Herz, Secondary metabolites from a culture of the fungus *Neosartorya pseusofischeri* and their in vitro cytostatic activity in human cancer cells, Planta Med. 78 (2012) 1767-1776.

4) M. Masi, A. Andolfi, V. Mathieu, A. Boari, A. Cimmino, L. Moreno Y Banuls, M. Vurro, A. Kornienko, R. Kiss, A. Evidente, Fischerindoline, a pyrroloindole sesquiterpenoid isolated from *Neosartorya pseudofischeri*, with in vitro growth inhibitory activity in human cancer cell lines, Tetrahedron. 69 (2013) 7466–7470.

5) H. Jayasuriya, D. Zink, A. Basilio, F. Vicente, J. Collado, G. Bills, M.L. Goldman, M. Motyl, J. Huber, G. Dezeny, K. Byrne, S.B. Singh, Discovery and antibacterial activity of glabramycin A-C from *Neosartorya glabra* by an antisense strategy, J. Antibiot. (Tokyo). 62 (2009) 265–269.

6) N.M. Gomes, L.J. Bessa, S. Buttachon, P.M. Costa, J. Buaruang, T. Dethoup, A.M.S. Silva, A. Kijjoa, Antibacterial and antibiofilm activities of tryptoquivalines and meroditerpenes isolated from the marine-derived fungi *Neosartorya paulistensis*, *N. laciniosa, N. tsunodae*, and the soil fungi *N. fischeri* and *N. siamensis*, Mar. Drugs. 12 (2014) 822–839.

7) S. Kaifuchi, M. Mori, K. Nonaka, R. Masuma, S. Ōmura, K. Shiomi, Sartorypyrone D : a new NADH-fumarate reductase inhibitor produced by *Neosartorya fischeri* FO-5897, J. Antibiot. (Tokyo). 68 (2015) 403–405.

8) T. Yim, K. Kanokmedhakul, Natural Product Research : Formerly Natural Product Letters, A new meroterpenoid tatenoic acid from the fungus *Neosartorya tatenoi* KKU-2NK23, Nat. Prod. Res. 28 (2014) 37–41.

9) O. Rajachan, K. Kanokmedhakul, W. Sanmanoch, S. Boonlue, S. Hannongbua, P. Saparpakorn, S. Kanokmedhakul, Chevalone C analogues and globoscinic acid derivatives from the fungus *Neosartorya spinosa* KKU-1NK1, Phytochemistry. 132 (2016) 68–75.

10) J. Paluka, K. Kanokmedhakul, M. Soytong, K. Soytong, S. Kanokmedhakul, Meroditerpene pyrone, tryptoquivaline and brasiliamide derivatives from the *fungus Neosartorya pseudofischeri,* Fitoterapia. 137 (2019) doi.org/10.1016/j.fitote.2019.104257.

11) M. Soytong, S. Poeaim, Isolation and identification of Trichocomaceae from soil by morphology and three regions DNA sequencing, J. Agric. Technol. 11 (2015) 315–326.

12) K. Kanokmedhakul, S. Kanokmedhakul, R. Suwannatrai, K. Soytong, S. Prabpai, P. Kongsaeree, Bioactive meroterpenoids and alkaloids from the fungus *Eurotium chevalieri*, Tetrahedron. 67 (2011) 5461–5468.

13) C. Prompanya, T. Dethoup, L.J. Bessa, M.M.M. Pinto, L. Gales, P.M. Costa, A.M.S. Silva, A. Kijjoa, New isocoumarin derivatives and meroterpenoids from the marine sponge-associated fungus *Aspergillus similanensis* sp. nov. KUFA 0013, Mar. Drugs. 12 (2014) 5160–5173.

14) A. Eamvijarn, N.M. Gomes, T. Dethoup, J. Buaruang, L. Manoch, A. Silva, M. Pedro, I. Marini, V. Roussis, A. Kijjoa, Bioactive meroditerpenes and indole alkaloids from the soil fungus *Neosartorya fischeri* (KUFC 6344), and the marine-derived fungi *Neosartorya laciniosa* (KUFC 7896) and *Neosartorya tsunodae* (KUFC 9213), Tetrahedron. 69 (2013) 8583–8591.

15) W.L. Liang, X. Le, H.J. Li, X.L. Yang, J.X. Chen, J. Xu, H.L. Liu, L.Y. Wang, K.T. Wang, K.C. Hu, D.P. Yang, W.J. Lan, Exploring the chemodiversity and biological activities of the secondary metabolites from the marine fungus *Neosartorya pseudofischeri*, Mar. Drugs. 12 (2014) 5657–5676.

16) W.J. Lan, S.J. Fu, M.Y. Xu, W.L. Liang, C.K. Lam, G.H. Zhong, J. Xu, D.P. Yang, H.J. Li, Five new cytotoxic metabolites from the marine fungus *Neosartorya pseudofischeri*, Mar. Drugs. 14 (2016) 1–13.

17) Y. Kojima, Y. Yamauchi, N. Kojima, B.F. Bishop, Antiparasitic pyrrolobenzoxazine compounds, Pfizer Pharm. Inc. Pat. Coop. (1995) Treaty WO 95/19363.

18) L. Zalibera, V. Milata, D. Ilavsky, ^{1}H and ^{13}C NMR spectra of 3-substituted 4-quinolones, Magn. Reson. Chem. 36 (1998) 681–684.

19) L.J. Fremlin, A.M. Piggott, E. Lacey, R.J. Capon, Cottoquinazoline A and Cotteslosins A and B, metabolites from an Australian marine-derived strain of *Aspergillus versicolor*, J. Nat. Prod. 72 (2009) 666–670.

20) Y. Kimura, T. Hamasaki, A. Isogai, H. Nakajima, Structure of aszonapyrone A, a new metabolite produced by *Aspergillus zonatus*, Agric. Biol. Chem. 46 (1982) 1963–1965.

21) T. Fujita, D. Makishima, K. Akiyama, H. Hayashi, New convulsive compounds, brasiliamides A and B, from *Penicillium brasilianum* Batista JV-379., Biosci. Biotechnol. Biochem. 66 (2002) 1697–1705.

22) T. Fujita, H. Hayashi, New brasiliamide congeners, brasiliamides C, D and E, from *Penicillium brasilianum* Batista JV-379., Biosci. Biotechnol. Biochem. 68 (2004) 820-826.

5) Research Outcome

 Publication

   J. Paluka, K. Kanokmedhakul, M. Soytong, K. Soytong, J. Yahuafaid, P. Siripongd, S. Kanokmedhakul, Meroterpenoid pyrones, alkaloid and brasiliamide derivative from the fungus *Neosartorya hiratsukae* Fitoterapia (2019 Under review).

Project 1C: Investigate on the Fungus *Neosatorya pseudofischeri*

1) Keyword:

   Neosatorya, *Neosatorya pseudofischeri*, cytotoxicity

2) Objective:

   To investigate secondary metabolizes and their cytotoxicity from the fungus *Neosatorya pseudofischeri*

3) Introduction

   The genus Neosartorya (Trichomaceae) is a source of bioactive secondary metabolites such as sesquiterpene alkaloids, sartorymensin analogs and meroterpenoids. These compounds show cytotoxicity against human U373 glioblastoma, MCF-7 breast cancer, and A549 non-small-cell-lung cancer cell lines [1-3]. The fungus *Neosartorya pseudofischeri* has been found in both marine and terrestrial sources, for example sea star (*Acanthaster planci*) [4-5] and soil [1, 6]. Various bioactive compounds have been reported from *N. pseudofischeri* such as pyripyropenes A, 1,4-diacetyl-2,5-dibenzylpiperazine-3,7″-oxide, pseudofischerine [1] neosartin analogs, bis-N-norgliovictin [4], trichodermamide A and indolyl-3-acetic acid methyl ester [5]. In our search for bioactive compounds from soil fungi isolated in Thailand, we have found that the n-hexane extract from biomass of the fungus *N. pseudofischeri* shows anti-mycobacterial activity against *Mycobacterium tuberculosis*, with 50% inhibition at a concentration of 50 µg/mL.

4) Result and discussion

Chromatographic separation of n-hexane, EtOAc and MeOH extracts from the fungal biomass of *N. pseudofischeri* gave seventeen compounds. Their structures were identified by spectroscopic data (UV, IR, ^{1}H and ^{13}C NMR), as well as by comparison to published data, as two new meroditerpene pyrones (**1C.1** and **1C.2**), a new tryptoquivaline analog (**1C.3**) and a new brasiliamide analog (**1C.4**)), as well as thirteen known compounds, chevalones A-C (**1C.5**-**1C.7**) [13], chevalone E (**1C.8**) [14], 11-hydroxychevalone C (**1C.9**) [15], pyripyropene A (**1C.10**) [4], isochaetominine C (**1C.11**) [16], pyrrolobenzoxazine terpenoids CJ-12662 (**1C.12**) and CJ-12663 (**1C.13**) [17], fischerindoline (**1C.14**) [18], eurochevalierine (**1C.15**) [13], 1,4-diacetyl-2,5-dibenzylpiperazine-3,7″-oxide (**1C.1 6**), and lecanorin (**1C.17**) [1] as shown in Figure 1C.1.

Compound **1C.1** had the molecular formula $C_{26}H_{36}O4$, deduced from the HRESITOFMS (m/z 435.2557 [M+Na]+), indicating nine degrees of unsaturation. The UV spectrum showed absorption maxima at 226, 245, and 259 nm. The IR spectrum showed the presence of ketone (1697 cm^{-1}), α,β-unsaturated ketone (1665 cm^{-1}), and alkene (1613 and 1585 cm^{-1}) functionalities. Analysis of ^{1}H and ^{13}C NMR as well as 2D-NMR (COSY, HMBC and NOESY) spectroscopic data indicated that the main skeleton of **1C.1** was the same as the isolated meroditerpene pyrone, chevalone C (**1C.8**), which was reported from *Eurotium chevalieri* [13]. However, the hydroxyl group at C-3 of 8 was replaced by a carbonyl group (δ_C-3 217.3) in **1C.1**. The HMBC spectrum showed the correlations of methylene protons, H-1 to C-3 and C-5; and H-5 to C-3 confirmed the position of a carbonyl group at C-3 in **1C.1**. Based on the above analysis, compound **1C.1** was determined as a new meroditerpene pyrone and has been named chevalone F.

Compound **1C.2** had the molecular formula $C_{26}H_{38}O_5$, deduced from the HRESITOFMS (m/z 453.2622 [M+Na]$^+$), indicating eight degrees of unsaturation. The UV spectrum showed absorption maxima at 203, 232, and 260 nm. The IR spectrum showed the presence of hydroxyl (3408 cm^{-1}), α,β-unsaturated ketone (1665 cm^{-1}), and alkene (1577 cm^{-1}) groups. The ^{1}H and ^{13}C NMR spectroscopic data are similar to those of a known isolate 11-hydroxychevalone C (**1C.9**), which was been reported from *Neosartorya spinosa* [15], except for an acetyl group at C-3 in **1C.9** which was replaced by a hydroxyl group ($\delta_{H/C}$ 3.06, dd/ 78.5) in **1C.2**. The COSY spectrum exhibited a cross coupling network between H-1/H-2/H-3 and H-9/H-11/H-12, as well as the HMBC spectrum displaying correlations of H-19, H-20 to C-3 and H-12 to C-11, supporting the positions of these two hydroxy groups at C-3 and C-11. Base on NOESY correlations and the coupling constants of these protons, the relative

configuration of **1C.2** was defined to be the same as that of **1C.9**. Thus, **1C.2** was assigned as a new meroditerpene pyrone and it has been named 11-hydroxychevalone E.

Compound **1C.3** had the molecular formula $C_{24}H_{22}N_4O_4$, deduced from the HRESITOFMS (m/z 453.1572 [M+Na]$^+$), indicating sixteen degrees of unsaturation. The UV spectrum showed absorption maxima at 209, 225, 255, and 301 nm. The IR spectrum showed the absorption bands of ester (1725 cm^{-1}), amide (1671 cm^{-1}), and alkene (1606 cm^{-1}) groups. The ^{13}C NMR and DEPT spectra showed 24 carbon signals, attributable to two methyl, one methylene, thirteen methine (including eight aromatic carbons), four aliphatic and one olefinic, together with eight quaternary (four aromatic, three carbonyl and one aliphatic) carbons. The ^{1}H NMR spectrum showed resonances of two doublets of methyl groups at δ 1.12 (d, J = 7.4 Hz, H3-28) and 1.10 (d, J = 7.4 Hz, H3-29), methylene protons at δ 2.68 (dd, J = 10.8, 11.4 Hz, H-13b) and 3.21, (dd, J = 9.8, 10.8 Hz, H-13a), four methine protons at δ 5.76 (s, H-2), 5.04 (dd, J = 9.8, 11.4 Hz, H-12), 3.85 (d, J = 3.9 Hz, H-15), and 2.23 (m, H-27), eight aromatic protons at δ 7.78 (d, J = 7.8 Hz, H-5), 7.28 (t, J = 7.8 Hz, H-6), 7.41 (t, J = 7.8 Hz, H-7), 7.52 (d, J = 7.8 Hz, H-8), 8.31 (d, J = 8.0 Hz, H-20), 7.55 (t, J = 8.0 Hz, H-21), 7.81 (t, J = 8.0 Hz, H-22), and 7.75 (d, J = 8.0 Hz, H-23) and an olefinic proton at δ 8.11 (s, H-26). Analysis of COSY and HMBC spectroscopic data suggested that **1C.3** has the same core structure as the tryptoquivaline U, which has previously been isolated from *Neosartorya takakii* [19]. However, there was a difference at the C-15 position, where a gem dimethyl group of tryptoquivaline U is replaced by an isopropyl group in **1C.3**. The COSY correlations between H-2/H-15/H-27/H-28/H-29, and the HMBC correlations of H-15 to C-14, C-28, and C-29; and H-28 and H-29 to C-15 confirmed the substituent of an isopropyl unit in the molecule. The relative configuration of **1C.3** was determined by NOESY correlations between H-28 and H-2, H-27 and H-15, H-13b and H-5, H-13a and H-12, and H-12 and H-26, suggesting each proton pairs were on the same phase (Figure 1C.2). The NOE-difference data also supported the same direction of H-12 and H-13a. Moreover, there was no correlation between H-2 and H-13 in NOESY, which was different from the corresponding position in tryptoquivaline U. In addition, the optical rotation of **1C.3** ([α]$_D^{28}$ +184.6 (c 0.1, CHCl$_3$)) showed significant difference from tryptoquivaline U ([α]$_D^{28}$ -196 (c 0.1, CHCl$_3$)) [19], indicating a different configuration between them. Since the absolute configuration at C-3 of tryptoquivaline U was assigned as 3S, the configuration at C-3 in **1C.3** should be 3R. Therefore, the relative configuration of **1C.3** was assigned as 2R, 3R, 12R and 15S. Based on above evidence, **1C.3** is a new tryptoquivaline analog, and it has been named tryptoquivaline V.

Compound **1C.4** had the molecular formula $C_{24}H_{26}N_2O_5$, deduced from the HRESITOFMS (m/z 445.1749 [M+Na]$^+$), indicating thirteen degrees of unsaturation. The UV spectrum showed absorption maxima at 205, 230, and 285 nm. The IR spectrum indicated the presence of amide (1627 cm^{-1}), and ether (1136 and 1037 cm^{-1}) functionalities. The ^{1}H NMR, ^{13}C NMR, COSY and HMBC spectroscopic data indicated the presence of three partial structures, including a benzyl moiety, a 3-methoxy-4,5-methylenedioxyphenyl unit, and a piperazine ring. The COSY and HMBC spectroscopic data indicated that a benzyl unit and a 3-methoxy-4,5-methylenedioxyphenyl unit were linked through the piperazine ring at C-5 and C-2, respectively. As a result, the core structure of **1C.4** was the same as a brasiliamide B, which has previously been isolated from *Penicillium brasilianum* [20]. However, the double bond in the piperazine ring C-2/C-3 (δ_C 121.4, $\delta_{H/C}$ 6.16/112.8) of brasiliamide B was isomerized to C-2/C-7' (δ_C 128.2, $\delta_{H/C}$ 6.35/126.5) in 4. Moreover, the HMBC spectrum confirmed the structure of 4 by showing the correlations of olefinic proton H-7' to C-1' of the methylenedioxyphenyl unit, aromatic protons H-2' and H-6' to C-7', and methylene proton H-3 to carbonyl carbon C-9. According to the literature, the NMR spectra of brasiliamide analogs show a mixture of resonances of their conformers for the piperazine unit and the protons nearby due to the rotational arrangement of carbonyl groups of both acetamides [1, 20, 21]. A similar observation was found for the brasiliamide derivative **1C.4**, by showing a mixture of resonances for a major 4a and a minor **1C.4b** conformers (Figure 1C.3) in the ratio of 3:1. The different NMR signals between **1C.4a** and **1C.4b** conformers was caused by the rotation of the acetyl group of the N-4 amide, which affects H-3, H-5, H-10 and H-7″. In addition, the NOESY spectrum showed correlations between H-5 and H-10, H-3α, H-6α; H-3α,β and H-2'; and H-8 and H-7', which supports that the carbonyl acetamides at N-1 and N-4 of **1C.4a** are arranged to C-6 and C-3 directions, respectively (Figure 1C.3). From the above evidence, the structure of **1C.4** was determined to be a new (2E)-1,4-diacetyl-5-benzyl-2-(3-methoxy-4,5-methylenedioxybenzylidene) piperazine and has been named brasiliamide G.

The new compounds **1C.1**-**1C.4** did not display anti-malarial and anti-TB activities, and were non-cytotoxic toward KB, MCF-7, and Vero cell lines. Since compounds **1C.7**, **1C.12**, and **1C.15** have previously been reported to have anti-mycobacterial activity against *M. tuberculosis* [13], these compounds should be responsible for the anti-TB activity of the *n*-hexane extract in our screening test. Compound **1C.13** showed weak cytotoxicity against KB and MCF-7 cell lines with IC_{50} values of 36.11 and 28.31 µg/mL, respectively, while compound **1C.14** exhibited weak cytotoxicity against the KB cell line, with an IC_{50} value of 35.23 µg/mL. Moreover, compounds **1C.13** and **1C.14** displayed weak cytotoxicity towards *Vero* cells, with IC_{50} values of 30.89 and 21.24 µg/mL, respectively. Compound **1C.2** showed

weak antibacterial activity against *E. coli* and *S.* typhimurium, both with MIC 128 µg/mL. Compounds **1C.7**, **1C.12**, **1C.13** and **1C.15** showed anti-bacterial activity against *B. cereus* with MIC values of 8, 64, 16, and 16 µg/mL, respectively, and they also exhibited activity against *S. aureus* with MIC values of 16, 128, 64, and 64 µg/mL, respectively (Table 1C.1).
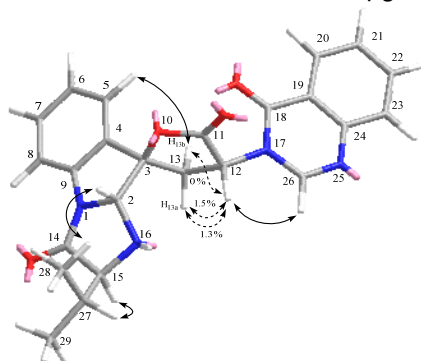

Figure 1C.2. The key NOESY correlations (⟷) and NOE-difference (⟵⟶) data of **1C.3**.

Table 1C.1 Antibacterial activity of compounds **1C.1-1C.17**.

Compound	Antibacterial activity (MIC, *µg/mL*)				
	Gram-positive		Gram-negative		
	B. cereus[a]	*S. aureus*[b]	*E. coli*[c]	*P. aeruginosa*[d]	*S. typhimurium*[e]
1C.1	>128	>128	>128	>128	>128
1C.2	>128	>128	128	>128	128
1C.3	>128	>128	>128	>128	>128
1C.4	>128	>128	>128	>128	>128
1C.5	>128	>128	>128	>128	>128
1C.6	128	>128	>128	>128	>128
1C.7	8	16	>128	>128	>128
1C.8	>128	>128	>128	>128	>128
1C.9	>128	>128	>128	>128	>128
1C.10	>128	>128	128	>128	>128
1C.11	>128	>128	128	>128	>128
1C.12	64	128	>128	>128	>128
1C.13	16	64	>128	>128	>128
1C.14	128	>128	>128	>128	>128
1C.15	16	64	>128	>128	>128
1C.16	>128	>128	128	>128	>128
1C.17	128	>128	128	>128	>128
Vancomycin	1.0	1.0	-	-	-
Gentamycin	-	-	2.0	0.5	0.5

[a]*Bacillus cereus* ATCC 11778   [b]*Staphylococcus aureus* ATCC 25923 [c]*Escherichia coli* ATCC 25922
[d]*Pseudomonas aeruginosa* ATCC 27853   [e]*Salmonella enterica* serovar Typhimurium ATCC 13311
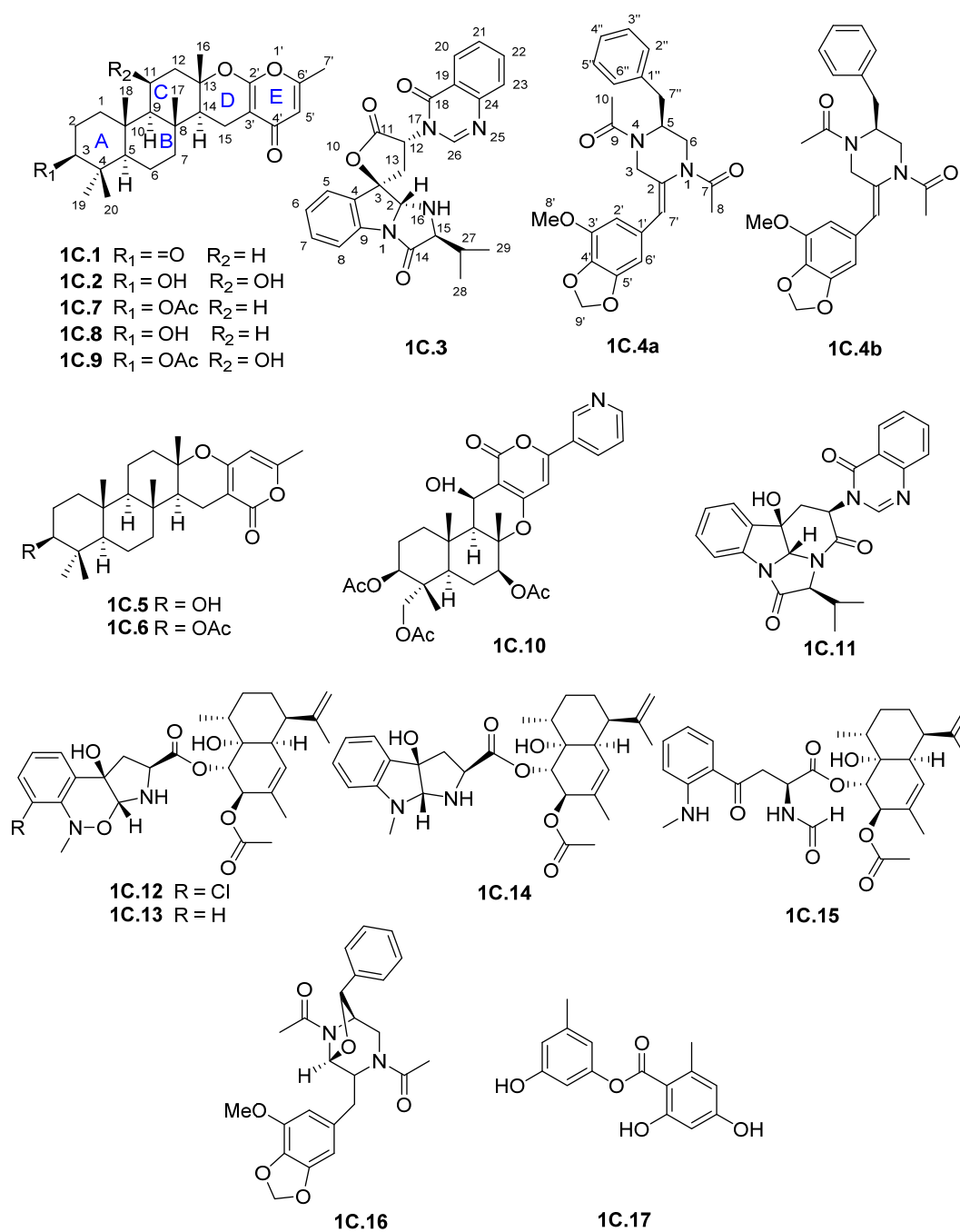
22

Figure 1C.1. Isolated compounds from the fungus *Neosatorya pseudofischeri*.
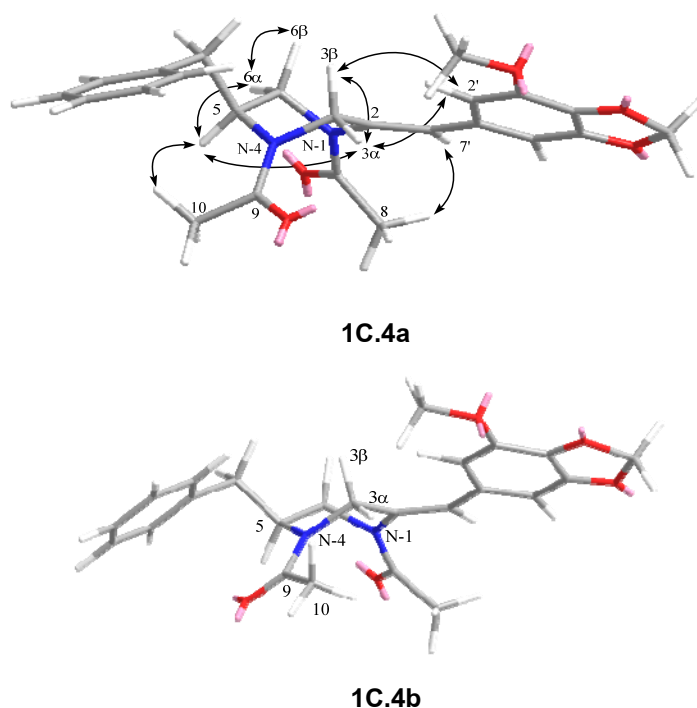
1C.4a

1C.4b

Figure 1C.3. The major (**1C.4a**), minor (**1C.4b**) rotamers and the key NOESY correlations.

References

1) A. Eamvijarn, A. Kijjoa, C. Bruyère, V. Mathieu, L. Manoch, F. Lefranc, A. Silva, R. Kiss, W. Herz, Secondary metabolites from a culture of the fungus *Neosartorya pseusofischeri* and their *in vitro* cytostatic activity in human cancer cells, Planta Med. 78 (2012) 1767–1776.

2) S. Buttachon, A. Chandrapatya, L. Manoch, A. Silva, L. Gales, C. Bruyère, R. Kiss, A. Kijjoa, Sartorymensin, a new indole alkaloid, and new analogues of tryptoquivaline and fiscalins produced by *Neosartorya siamensis* (KUFC 6349), Tetrahedron. 68 (2012) 3253–3262.

3) A. Eamvijarn, N.M. Gomes, T. Dethoup, J. Buaruang, L. Manoch, A. Silva, M. Pedro, I. Marini, V. Roussis, A. Kijjoa, Bioactive meroditerpenes and indole alkaloids from the soil fungus *Neosartorya fischeri* (KUFC 6344), and the marine-derived fungi *Neosartorya laciniosa* (KUFC 7896) and *Neosartorya tsunodae* (KUFC 9213), Tetrahedron. 69 (2013) 8583–8591.

4) W.L. Liang, X. Le, H.J. Li, X.L. Yang, J.X. Chen, J. Xu, H.L. Liu, L.Y. Wang, K.T. Wang, K.C. Hu, D.P. Yang, W.J. Lan, Exploring the chemodiversity and biological activities of the secondary metabolites from the marine fungus *Neosartorya pseudofischeri*, Mar. Drugs. 12 (2014) 5657–5676.

5) W.J. Lan, S.J. Fu, M.Y. Xu, W.L. Liang, C.K. Lam, G.H. Zhong, J. Xu, D.P. Yang, H.J. Li, Five new cytotoxic metabolites from the marine fungus *Neosartorya pseudofischeri*, Mar. Drugs. 14 (2016) 1–13.

6) M. Soytong, S. Poeaim, Isolation and identification of Trichocomaceae from soil by morphology and three regions DNA sequencing, J. Agric. Technol. 11 (2015) 315–326.

7) W. Trager, J.B. Jensen, Human malaria parasites in continuous culture, J. Parasitol. 91 (2005) 484–486.

8) R.E. Desjardins, C.J. Canfield, J.D. Haynes, J.D. Chulay, Quantitative assessment of antimalarial activity *in vitro* by a semiautomated microdilution technique., Antimicrob. Agents Chemother. 16 (1979) 710–718.

9) L. Collins, S.G. Franzblau, Microplate alamar blue assay versus BACTEC 460 system for high-throughput screening of compounds against *Mycobacterium tuberculosis* and *Mycobacterium avium*., Antimicrob. Agents Chemother. 41 (1997) 1004–1009.

10) J. O'Brien, I. Wilson, T. Orton, F. Pognan, Investigation of the alamar blue (resazurin) fluorescent dye for the assessment of mammalian cell cytotoxicity: Resazurin as a cytotoxicity assay, Eur. J. Biochem. 267 (2000) 5421–5426.

11) L. Hunt, M. Jordan, M. De Jesus, F.M. Wurm, GFP-expressing mammalian cells for fast, sensitive, noninvasive cell growth assessment in a kinetic mode, Biotechnol. Bioeng. 65 (1999) 201–205.

12) F.R. Cockerill, M.A. Wikler, J. Alder, M.N. Dudley, G.M. Eliopoulos, M.J. Ferraro, D.J. Hardy, D.W. Hecht, J.A. Hindler, J.B. Patel, M. Powell, J.M. Swenson, R.B. Thomson, M.M. Traczewski, J.D. Turnidge, M.P. Weinstein, B.L. Zimmer, Methods for dilution antimicrobial susceptibility tests for bacteria that grow aerobically ; approved standard - Ninth Edition, 2012.

13) K. Kanokmedhakul, S. Kanokmedhakul, R. Suwannatrai, K. Soytong, S. Prabpai, P. Kongsaeree, Bioactive meroterpenoids and alkaloids from the fungus *Eurotium chevalieri*, Tetrahedron. 67 (2011) 5461–5468.

14) C. Prompanya, T. Dethoup, L.J. Bessa, M.M.M. Pinto, L. Gales, P.M. Costa, A.M.S. Silva, A. Kijjoa, New isocoumarin derivatives and meroterpenoids from the marine sponge-associated fungus *Aspergillus similanensis* sp. nov. KUFA 0013, Mar. Drugs. 12 (2014) 5160–5173.

15) O. Rajachan, K. Kanokmedhakul, W. Sanmanoch, S. Boonlue, S. Hannongbua, P. Saparpakorn, S. Kanokmedhakul, Chevalone C analogues and globoscinic acid derivatives from the fungus *Neosartorya spinosa* KKU-1NK1, Phytochemistry. 132 (2016) 68–75.

16) L. Liao, M. You, B.K. Chung, D.C. Oh, K.B. Oh, J. Shin, Alkaloidal metabolites from a marine-derived *Aspergillus* sp. fungus, J. Nat. Prod. 78 (2015) 349–354.

17) Y. Kojima, Y. Yamauchi, N. Kojima, B.F. Bishop, Antiparasitic pyrrolobenzoxazine compounds, Pfizer Pharm. Inc. Pat. Coop. (1995) Treaty WO 95/19363.

18) M. Masi, A. Andolfi, V. Mathieu, A. Boari, A. Cimmino, L. Moreno Y Banuls, M. Vurro, A. Kornienko, R. Kiss, A. Evidente, Fischerindoline, a pyrroloindole sesquiterpenoid isolated from *Neosartorya pseudofischeri*, with in vitro growth inhibitory activity in human cancer cell lines, Tetrahedron. 69 (2013) 7466–7470.

19) W.W.M. Zin, S. Buttachon, J. Buaruang, L. Gales, J.A. Pereira, M.M.M. Pinto, A.M.S. Silva, A. Kijjoa, A new meroditerpene and a new tryptoquivaline analog from the algicolous fungus *Neosartorya takakii* KUFC 7898, Mar. Drugs. 13 (2015) 3776–3790.

20) T. Fujita, D. Makishima, K. Akiyama, H. Hayashi, New convulsive compounds, brasiliamides A and B, from *Penicillium brasilianum* Batista JV-379., Biosci. Biotechnol. Biochem. 66 (2002) 1697–1705.

21) T. Fujita, H. Hayashi, New brasiliamide congeners, brasiliamides C, D and E, from *Penicillium brasilianum* Batista JV-379., Biosci. Biotechnol. Biochem. 68 (2004) 820–826.

5) Research Outcome

Publication

J. Paluka, K. Kanokmedhakul, M. Soytong, K. Soytong, S. Kanokmedhakul, Meroditerpene pyrone, tryptoquivaline and brasiliamide derivatives from the fungus *Neosartorya pseudofischeri* Fitoterapia 137 (2019) 104257 (Online 03 July 2019).

Oral presentation

Jakkapat Paluka, Somdej Kanokmedhakul, Kwanjai Kanokmedhakul, Kasem Soytong. "Bioactive meroterpenoids and alkaloids from the fungus *Neosartorya pseudofischeri*" at 5th International Conference on Integrating Science and Technology for Sustainable Development, at Cherry Queen Hotel, Southern Shan State, Myanmar, 26-27 November 2016.

Project 1D: Investigate on the Fungus *Chaetomium globosum* 7s-1

1) Keywords

Chaetomium globosum, endophytic fungus, antimalarial, antibacterial, cytotoxicity, mytotoxin

2) Objective

To investigate the chemical constituents and their bioactivity from endophytic fungus *Chaetomium globosum* 7s-1

3) Introduction

Chaetomium globosum belongs to the Chaetomiaceae family.[1] It was isolated from water-damaged building materials,[2] animals,[3] soil,[4] and plants.[5,6] *C. globosum* is well-known to produce a variety of structural secondary metabolites, including of anthraquinones,[7,8] azaphilones,[3,9] azaphilone alkaloids,[3,10] cytochalasan alkaloids,[11-13] depsidones,[14] epipolythiodioxopiperazines,[15,16] indole alkaloids,[15] steroids,[17] xanthones,[8] and xanthoquinodins.[7] Most of them exhibited a wide range of biological activities such as antibacterial,[3,12] antifungal,[15] anti-HIV,[18] and cytotoxic[11,14] activities. It was also reported its ability to degrade cell walls of fungal pathogens, an oomycete (*Pythium ultimum*),[19] and inhibit the growth and reproduction of *Myzus persicae*.[20] Interestingly, derivatives of epipolythiodioxopiperazine toxins have therapeutic potential and roles in disease.[21,22] As part of our search for bioactive compounds from endophytic fungi, an EtOAc and MeOH extracts of *C. globosum* exhibited antibacterial activity against Gram positive and Gram negative bacteria at concentration 1 mg/mL. Moreover, they also showed cytotoxicity toward the KB cell line with IC_{50} values of 0.69 and 10.75 μg/mL, respectively.

4) Result and Discussion

Chromatographic separation of EtOAc and MeOH extracts of *C. globosum* gave one new xanthoquinodin B6 (**1D.1**), along with nine known compounds, xanthoquinodin A1 (**1D.2**),[23] xanthoquinodin A3 (**1D.3**),[23] chetomin (**1D.4**),[23] chaetocochin C (**1D.5**),[24] dethio-tetra(methylthio)chetomin (**1D.6**),[25] chrysophanol (**1D.7**),[26] emodin (**1D.8**),[27] alatinone (**1D.9**),[28] and ergosterol (**1D.10**)[26] (Figure 1D.1).

Compound **1D.1** had the molecular formula $C_{31}H_{24}O_{11}$, deduced from the ^{13}C NMR and HRESITOFMS (*m/z* 573.1390 [M + H]$^+$) data, implying 20 indices of hydrogen deficiency. The UV spectrum exhibited absorption maximum at 236, 273, and 360 nm, which were similar to that of xanthoquinodin type B.[29] The IR absorption indicated the presences of hydroxyl (3366), carbonyl (1718), and aromatic (1594) groups. The ^{13}C NMR and DEPT spectra of **1D.1** showed 31 carbon signals which attributed to a methoxyl (δ_C 52.9) and a methyl (δ_C

21.7) carbons, three sp^3 methylenes (δ_C 41.8, 36.0, and 26.0), two sp^3 methines (δ_C 74.3 and 46.0), two sp^3 quaternary carbons (δ_C 87.6 and 53.3), five sp^2 methines (δ_C 133.4, 133.1, 124.6, 119.9, and 113.5), and 15 sp^2 quaternary carbons [including three α,β-conjugated keto carbonyls (δ_C 200.2, 199.2, and 191.4) and an ester carbonyl (δ_C 174.9)]. The ^{1}H and ^{13}C NMR spectral data of **1D.1** agreed well with those of xanthoquinodin B1.[29] This data revealed signals of *cis* vinyl protons at δ_H 6.55 (1H, d, *J* = 8.3 Hz, H-13') and 6.34 (1H, dd, *J* = 8.3, 7.0 Hz, H-12') which coupled to H-11' at δ_H 4.63 (1H, d, *J* = 7.0 Hz). The three signals of aromatic protons appeared at δ_H 5.57 (1H, s), corresponded to a pentasubstituted aromatic H-11, while δ_H 7.39 (1H, s) and 6.98 (1H, s) corresponded to *meta*-coupling with H-3' and H-5', respectively. An oxymethine group at C-3 appeared at δ_H 4.22 (1H, dd, *J* = 12.5, 4.5 Hz). The ^{1}H NMR spectrum also displayed the signals of three methylene groups at δ_H 2.99 (1H, d, *J* = 17.0 Hz, H$_a$-15') and 2.70 (1H, d, *J* = 17.0 Hz, H$_b$-15'), 2.69 (1H, m, H-5), 2.49 (1H, dd, *J* = 18.0, 7.0 Hz, H-5), 2.20 (1H, m, H-4), and 1.98 (1H, m, H-4). Two singlet signals at δ_H 3.59 (3H, s) and 2.38 (3H, s) were resonances due to a methoxy carbonyl group of H-16 and a methyl group of H-16', respectively. The significant difference between compound **1D.1** and xanthoquinodin B1 was an arrangement of the keto-enolic system at C-6 (δ_C 191.4) and C-8 (δ_C 178.8). This was indicated by the different of chemical shift of protons and carbons at positions 2-5. The HMBC spectrum of **1D.1** clearly showed correlations of H-4 to C-6 (δ_C 191.4), H-5 to C-7 (δ_C 100.2), and ^4J correlation of the aromatic proton H-11 to C-8 (δ_C 178.8) confirming the location of the keto-enolic system at C-6 and C-8. In the NOESY experiment (measured in DMSO-d_6, supplementary data), the NOESY correlations of 3-OH with H-16 indicated that 3-hydroxyl should have the same orientation. The cross peak between H-11' and H-12' also implied that they are in the same orientation. The absolute configurations of **1D.1** were assigned by the predicted ECD curves of **1D.1** and its relevant enantiomer, which were optimized by the B3LYP/6-31G(d,p) method. The predicted ECD curve of **1D.1** was similar to the experimental one, therefore, the absolute configuration of **1D.1** was assigned as 2*S*, 3*S*, 11'*S*, and 14'*R*. Thus, compound **1D.1** was defined as a new xanthoquinodin type B and was named xanthoquinodin B6.

Compounds **1D.1**-**1D.6** were evaluated for their antibacterial activity gainst three Gram positive bacteria and three Gram negative bacteria. Xanthoquinodins **1D.1**-**1D.3** showed significant activity against *B. cereus* with MIC values of 0.87, 0.44, and 0.22 μM, respectively, which were lower than standard drugs, vancomycin (1.35 μM) and kanamycin (3.43 μM). They also exhibited activity against *S. aureus* and MRSA with MIC values ranging from 0.87 to 1.75 μM whereas vancomycin showed activity against *S. aureus* and MRSA with MIC value
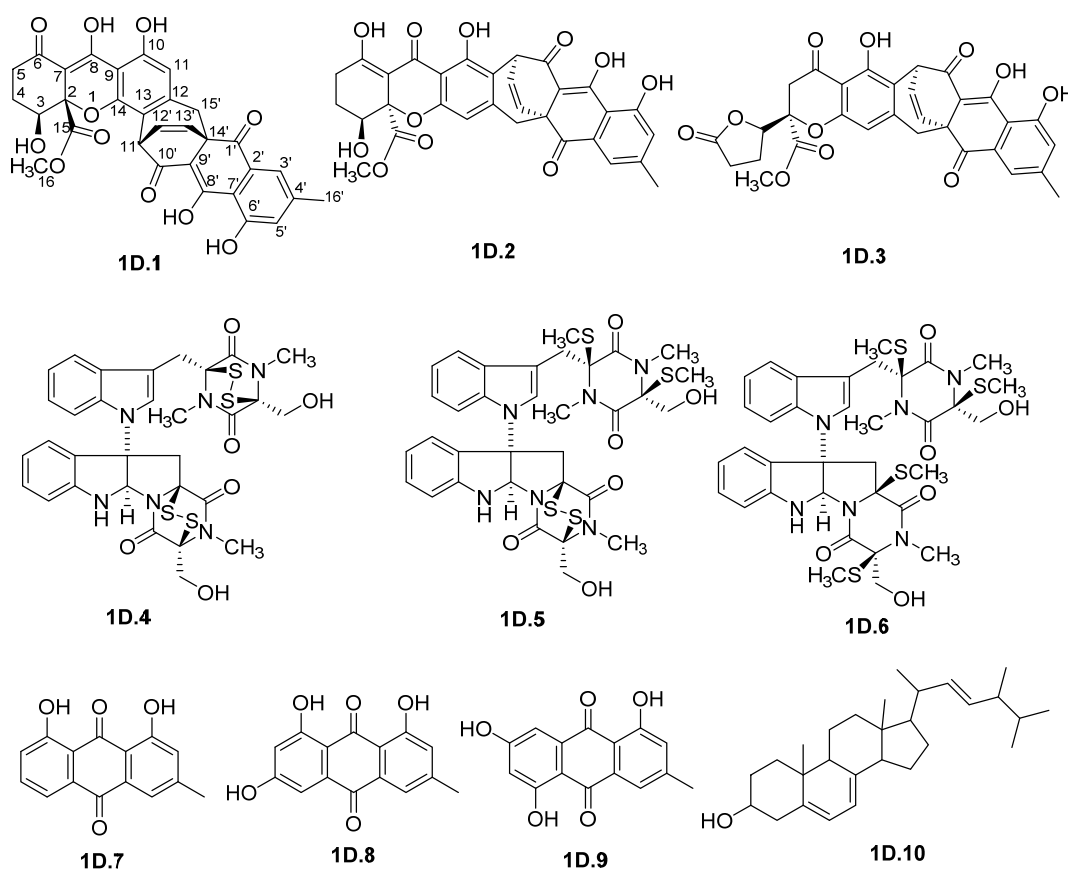
Figure 1D.1. Chemical constituents isolated from *C. globosum*.

of 0.67 μM, and kanamycin showed activity against *S .aureus* with MIC value of 1.72 μM .The antibacterial activity against *S .aureus* of **1D.2** and **1D.3** confirmed the previous study by Tabata using paper disc method.[30] Epipolythiodioxopiperazines **1D.4**-**1D.6** exhibited a potent activity against Gram positive bacteria with the MIC values ranging from 0.02 pM to 10.81 μM. Compound **1D.4** showed the highest activity toward *B. cereus*, *S. aureus*, and MRSA with MIC values of 0.35 μM, 10.74 pM, and 0.02 pM, respectively, which are remarkably lower than vancomycin (1.35, 0.67, and 0.67 μM). Among them (**1D.4**-**1D.6**), it should be noted that the activities against all Gram positive were decrease when the sulfide bridges were opened as in compounds **1D.5** and **1D.6**. However, in case of **1D.6** both sulfide bridges opened demonstrated activity against MRSA close to vancomycin. These results supported that two sulfide bridges have played an important role on activity against Gram positive bacteria as previously reports.[21,22,31] In contrast, all compounds showed weak activity against Gram negative bacteria tested (MICs of 45.06 to >223.72 μM). In addition, compounds **1D.1**-**1D.6** were also tested for their antimalarial, anti-TB, and cytotoxic activities. They showed

antimalarial activity against *P. falciparum* with IC$_{50}$ values in the range of 0.40-6.29 *µ*M. Epipolythiodioxopiperazines **1D.4**-**1D.6** were also active against *M. tuberculosis* with MICs of 0.55, 4.06, and 8.11 *µ*M, respectively, while xanthoquinodins **1D.1**-**1D.3** showed weak activity and inactive. Furthermore, they showed strong cytotoxicity against three human cancer cell lines, KB, MCF-7, and NCI-H187, with IC$_{50}$ ranging from 0.04 to 18.40 *µ*M. Compounds **1D.2**-**1D.6** showed cytotoxicity against MCF-7 cell line (IC$_{50}$ values of 1.09 to 13.12 *µ*M) which were lower than standard drug doxoburicin (17.24 *µ*M). Among them, **1D.4** exhibited cytotoxicity against NCI-H187 with IC$_{50}$ value of 0.04 *µ*M, which was lower than standard drugs doxoburicin (0.40 *µ*M) and ellipticine (9.54 *µ*M). It should be noted that compounds **1D.4** and **1D.5** contained sulfide bridged in the structures are more cytotoxicity against cancer cell line tested than a non-sulfide bridged structure, **1D.6**. However, all compounds **1D.1**−**1D.6** exhibited very strong cytotoxicity toward normal cell line (*Vero* cell) with IC$_{50}$ values ranging from 0.04 to 3.86 *µ*M, respectively, comparing to a control drug, ellipticine (4.22 *µ*M).

References

1) Youn, U. J.; Sripisut, T.; Park, E. J.; Kondratyuk, T. P.; Fatima, N.; Simmons, C. J.; Wall, M. M.; Sun, D.; Pezzuto, J. M.; Chang, L. C. *Bioorg. Med. Chem. Lett.* 2015, *25,* 4719.

2) Green, B. J.; Nayak, A. P.; Lemons, A. R.; Rittenour, W. R.; Hettick, J. M.; Beezhold, D. H. *Monoclon. Antib. Immunodiagn. Immunother.* 2014, *33*, 428.

3) Chen, C.; Wang, J.; Zhu, H.; Wang, J.; Xue, Y.; Wei, G.; Guo, Y.; Tan, D.; Zhang, J.; Yin, C.; Zhang, Y. *Chem. Biodivers.* 2016, *13*, 422.

4) Kanokmedhakul, S.; Kanokmedhakul, K.; Phonkerd, N.; Soytong, K.; Kongsaeree, P.; Suksamrarn, A. *Planta Med.* 2002, *68*, 834.

5) Hu, Y.; Zhang, W.; Zhang, P.; Ruan, W.; Zhu, X. *J. Agric. Food. Chem.* 2013, *61*, 41.

6) Christensen, C. M.; Nelson, G. H.; Mirocha, C. J.; Bates, F.; Dorworth, C. E. *Appl. Microbiol.* 1966, *14*, 774.

7) Xu, G. B.; He, G.; Bai, H. H.; Yang, T.; Zhang, G. L.; Wu, L. W.; Li, G. Y. *J. Nat. Prod.* 2015, *78*, 1479.

8) Wijeratne, E. M. K.; Turbyville, T. J.; Fritz, A.; Whitesell, L.; Gunatilaka, A. A. L. *Bioorg. Med. Chem.* 2006, *14*, 7917.

9) McMullin, D. R.; Sumarah, M. W.; Blackwell, B. A.; Miller, J. D. *Tetrahedron Lett.* 2013, *54*, 568.

10) Li, X.; Tian, Y.; Yang, S. X.; Zhang, Y. M.; Qin, J. C. *Bioorg. Med. Chem. Lett.* 2013, *23*, 2945.

11) Chen, C.; Wang, J.; Liu, J.; Zhu, H.; Sun, B.; Wang, J.; Zhang, J.; Luo, Z.; Yao, G.; Xue, Y.; Zhang, Y. *J. Nat. Prod.* 2015, *78*, 1193.

12) Guo, Z. L.; Zheng, J. J.; Cao, F.; Wang, C.; Wang, C.Y. *Chem. Nat. Compd.* 2017, *53*, 199.

13) Jiang, T.; Wang, M.; Li, L.; Si, J.; Song, B.; Zhou, C.; Yu, M.; Wang, X.; Zhang, Y.; Ding, G.; Zou, Z. *J. Nat. Prod.* 2016, *79*, 2487.

14) Li, G. Y.; Li, B. G.; Yang, T.; Liu, G. Y.; Guo, L. Z. *Helv. Chim. Acta.* 2008, *91*, 124.

15) Li, H. Q.; Li, X. J.; Wang, Y. L.; Zhang, Q.; Zhang, A. L.; Gao, J. M.; Zhang, X. C. *Biochem. Syst. Ecol.* 2011, *39*, 876.

16) Xu, G. B.; He, G.; Bai, H. H.; Yang, T.; Zhang, G. L.; Wu, L. W.; Li, G. Y. *J. Nat. Prod.* 2015, *78*, 1479.

17) Yu, F. X.; Li, Z.; Chen, Y.; Yang, Y. H.; Li, G.H.; Zhao, P.J. *Fitoterapia* 2017, *117*, 41.

18) Chen, C.; Zhu, H.; Wang, J.; Yang, J.; Li, X. N.; Wang, J.; Chen, K.; Wang, Y.; Luo, Z.; Yao, G.; Xue, Y.; Zhang, Y. *Eur. J. Org. Chem.* 2015, *2015*, 3086.

19) Inglis, G. D.; Kawchuk, L. M. *Can. J. Microbiol.* 2002, *48*, 60.

20) Qi, G.; Lan, N.; Ma, X.; Yu, Z.; Zhao, X. *J. Appl. Microbiol.* 2011, *110*, 1314.

21) Jordan, T. W.; Cordiner, S. J. *Trends Pharmacol. Sci.* 1987, *8*, 144.

22) Brewer, D.; Duncan, J. M.; Jerram, W. A.; Leach, C. K.; Safe, S.; Taylor, A.; Vining, L. C.; Archibald, R. McG.; Stevenson, R. G.; Mirocha, C. J.; Christensen, C. M. *Can. J. Microbiol.* 1972, *18*, 1129.

23) Fujimoto, H.; Sumino, M.; Okuyama, E.; Ishibashi, M. *J. Nat. Prod.* 2004, *67*, 98.

24) Li, G. Y.; Li, B. G.; Yang, T.; Yan, J. F.; Liu, G. Y.; Zhang, L. G. *J. Nat. Prod.* 2006, *69*, 1374.

25) Kikuchi, T.; Kadota, S.; Nakamura, K.; Nishi, A.; Taga, T.; Kaji, T.; Osaki, K.; Tubaki, K. *Chem. Pharm. Bull.* 1982, *30*, 3846.

26) Ghisalberti, E. L.; Narbey, M. J.; Dewan, M. M.; Sivasithamparam, K. *Plant Soil.* 1990, *121*, 287.

27) Zhou, X.; Song, B.; Jin, L.; Hu, D.; Diao, C.; Xu, G.; Zou, Z.; Yang, S. *Bioorg. Med. Chem. Lett.* 2006, *16*, 563.

28) Hemlata; Kalidhar, S. B. Phytochemistry. 1993, *32*, 1616.

29) Tabata, N.; Tomoda, H.; Matsuzaki, K.; Omura, S. *J. Am. Chem. Soc.* 1993, *115*, 8558.

30) Tabata, N.; Suzumura, Y.; Tomoda, H.; Masuma, R.; Haneda, K.; Kisni, M.; Iwai, Y.; Omura, S. *J. Antibiot.* 1993, *46*, 749.

31) Waksman, S. A.; Bugie, E. *J. Bateriol.* 1944, *48*, 527.

5) Research Outcome

Tantapakul, C., Promgool, T., Kanokmedhakul, K., Soytong, K., Song, J., Hadsadee, S.,
Jungsuttiwong, S., Kanokmedhakul, S., Bioactive xanthoquinodins and
epipolythiodioxopiperazines from *Chaetomium globosum* 7s-1, an endophytic fungus
isolated from *Rhapis cochinchinensis* (Lour.) Mart. Natural Product Research, Published
online: 2018 doi.org/10.1080/14786419.2018.1489392

Project 1E: Investigate on fungus *Talaromyces macrosporus* KKU-1NK8

1) **Keyword**

>*Talaromyces macrosporus,* oxaphenalenone, antibacterial, antimalarial, cytotoxicity

2) **Objective**

>To investigate the chemical constituents and their bioactivity from fungus
Talaromyces macrosporus KKU-1NK8

1) **Introduction**

>The genus Talaromyces, a sexual state of the Penicillium species, was
introduced by Benjamin in 1995. It belongs to the family Trichocomaceae [1]. Some
species were isolated from soil, plants, sponges, and foods. Many species are used in
food and agricultural production [2]. Previous reports on secondary metabolites from
Talaromyces species have resulted in the isolation of many different types of
compounds such as alkaloids [3], indole alkaloids [4], adenine [5], tetramic acid
derivatives [6], polyesters [7], diphenyl ether lactone derivatives [8], meroterpenoids
[9], oxaphenalenone dimers [8,10–13], quinones [14–16], steroids and terpenoids [17].
One interesting type is the oxaphenalenone dimer which is a polyketide-derived. Until
now, only 20 natural isolated members in this type have been reported [8,10–13,18].
They showed various bioactive activities such as cytotoxicity against cancer cell lines
[11] and antibacterial activity against Gram positive bacteria [8,12,13], as well as
acetylcholinesterase inhibition [11]. Therefore, searching for bioactive compounds
from the fungus Talaromyces is still of interest. Since no phytochemical investigation
of *T. macrosporus* has been reported, our investigation found that the crude EtOAc
extracts of *T. macrosporus* KKU-1NK8 exhibited cytotoxicity towards the KB cell line
with 40% inhibition at 50 μg/mL.

4) Result and Discussion

Chromatographic separation of extracts from the dried mycelium of the fungus *T. macrosporus* KKU-1NK8 obtained six new oxaphenalenone dimers (**1E.1-1E.6**) and eight known compounds (**1E.7-1E.14**). Their structures were elucidated by spectroscopic methods. Structures of known compounds were also compared with those reported in the literature. They were talaromycesone B (**1E.7**) [8], bacillisporin G (**1E.8**) [12], xenoclauxin (**1E.9**) [10], bacillisporin F (**1E.10**) and 1-epi-bacillisporin F (**1E.10b**) [12], bacillisporins A and B (**1E.11** and **1E.12**) [10,11] and bacillisporins D and E (**1E.13** and **1E.14**) [11] as shown in Figure 1E.1.
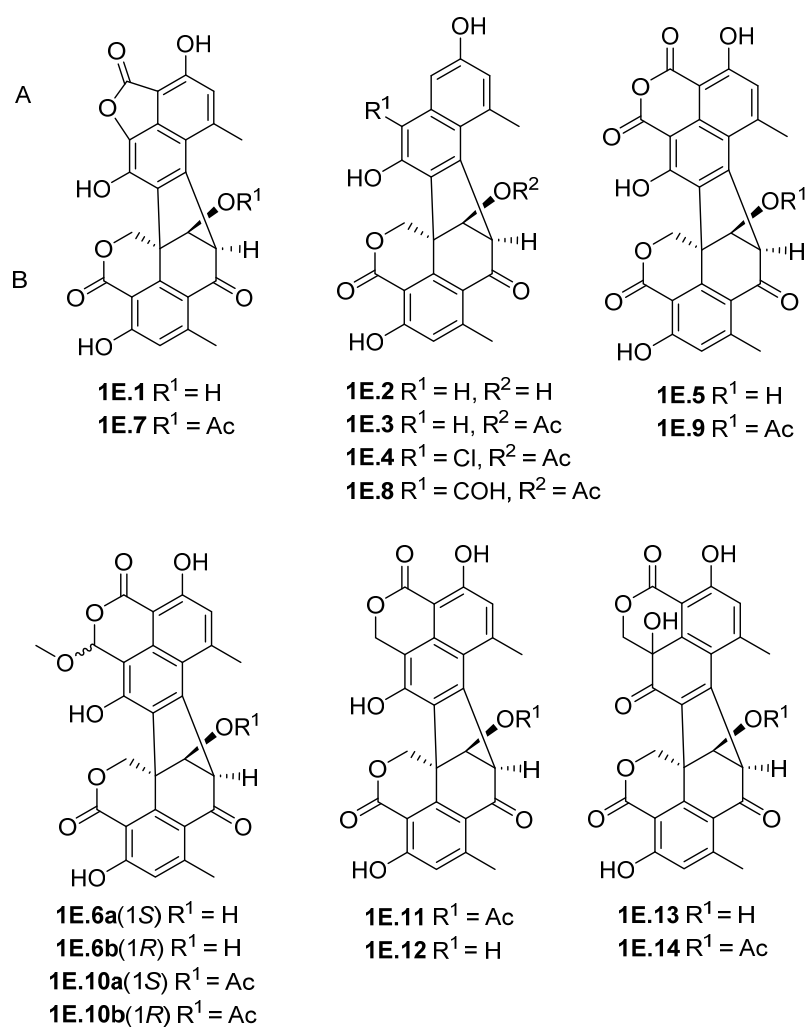

1E.1 R¹ = H
1E.7 R¹ = Ac

1E.2 R¹ = H, R² = H
1E.3 R¹ = H, R² = Ac
1E.4 R¹ = Cl, R² = Ac
1E.8 R¹ = COH, R² = Ac

1E.5 R¹ = H
1E.9 R¹ = Ac

1E.6a(1*S*) R¹ = H
1E.6b(1*R*) R¹ = H
1E.10a(1*S*) R¹ = Ac
1E.10b(1*R*) R¹ = Ac

1E.11 R¹ = Ac
1E.12 R¹ = H

1E.13 R¹ = H
1E.14 R¹ = Ac

Figure 1E.1. Isolated compounds from *Talaromyces macrosporus* KKU-1NK8

Compound **1E.1** possessed the molecular formula $C_{25}H_{16}O_9$, based on the ^{13}C NMR and HRESITOFMS (*m/z* 483.0684) [M+Na]+ data, implying 18 degrees of unsaturation. Analysis of the ^1H and ^{13}C NMR spectroscopic data of **1E.1** with the assistance of 2D NMR techniques (COSY, HMQC, HMBC, and NOESY) concluded that the structure of **1E.1** was similar to that of talaromycesone B (**1E.7**) [8], except for an acetyl group at C-9′ being replaced by a hydroxyl group in **1E.1**. The structure of **1** was confirmed by HMBC correlations of H-9′ to C-7, C-8, C-3'b, and C-7′. The absolute configuration of **1E.1** was determined by comparing its experimental and calculated ECD spectra. The ECD calculations were generated for three chiral centers of two selected possible stereoisomers, 8′*R*, 9′*S*, 9'a*S* and 8′*S*, 9′*R*, 9'a*R* using Gaussian 09 with DFT B3LYP/6-311++G (d,p). The ECD calculated spectrum of **1E.1** generated for the 8′*R*, 9′*S*, 9'a*S* isomer shows a Cotton effect at 215 nm ($\Delta\varepsilon$ −56.5), 239 ($\Delta\varepsilon$ 65.1), 258 ($\Delta\varepsilon$ 38.2) and 335 ($\Delta\varepsilon$ -9.1), which agrees well with its experimental ECD spectrum. From the above evidence, compound **1E.1** was named talaromycesone C and was determined to be a new oxaphenalenone dimer.

Compound **1E.2** had the molecular formula $C_{24}H_{18}O_7$, based on the ^{13}C NMR and HRESITOFMS (*m/z* 441.0940) [M+Na]+ data, indicating 16 degrees of unsaturation. The NMR spectroscopic data of **1E.2** were similar to those of bacillisporin G (**1E.8**) [12], expect for the absence of an aldehyde group at C-9a and that an acetyl group at C-9′ was replaced by a hydroxyl group. The ^1H NMR spectral data of unit A showed resonances of three aromatic protons at δ 6.62 (s, H-5), 6.65 (s,H-9a), and 6.57 (s, H-3a). The COSY data showed meta-coupling correlations between H-5/H-3a and H-3a/H-9a. The ^{13}C NMR spectral data of unit A showed three methine aromatic carbons at δ106.8 (C-3a), 119.2 (C-5) and 110.6 (C-9a), five quaternary aromatic carbons at δ 138.4 (C-3b), 136.4 (C-6), 121.0 (C-6a), 136.5 (C-7) and 130.9 (C-8), two oxy-aromatic carbons at δ 154.1 (C-4) and 152.0 (C-9), and a methyl at δ 24.3 (Me-6). The HMBC correlations of H-3a to C-4, C-5, C-6a and C-9a; H-5 to C-3a, C-4 and C-6a; H-9a to C-3a, C-6a, C-8 and C-9; and Me-6 to C-5, C-6 and C-6a confirmed the structure of unit A. The NMR spectroscopic data of unit B was similar to that of **1E.1**. The absolute configuration of **1E.2** was concluded to be 8′*R*, 9′S, 9'aS, the same as that of **1E.1**, by comparing their ECD spectra. Thus, compound **1E.2** was determined as a new oxaphenalenone dimer and was named macrosporusone A.

Compound **1E.3** had the molecular formula $C_{26}H_{20}O_8$, based on the ^{13}C NMR and HRESITOFMS (m/z 459.1088) [M-H]⁻ data, implying 17 degrees of unsaturation. The ^1H and ^{13}C NMR spectroscopic data of **1E.3** were similar to those of **1E.2**, except that the hydroxyl group at C-9′ was replaced by an acetoxyl group (δ_C carbonyl ester group 170.6 and methyl group $\delta_{H/C}$ 1.99 (s)/20.8). The complete interpretation of the NMR data of **1E.3** was

established as a result of conclusive DEPT, COSY, HMQC, HMBC, and NOESY experiments. The ECD spectrum of **1E.3** showed the same Cotton effect as that of **1E.1**. Therefor, the new compound **1E.3** was named macrosporusone B. Compound **1E.4** had the molecular formula $C_{26}H_{19}ClO_8$, based on the ^{13}C NMR and HRESITOFMS (m/z 495.0850) [M+H]$^+$, (m/z 497.0812) [M+H+2]$^+$ data, indicating 17 degrees of unsaturation. The ^1H and ^{13}C NMR spectroscopic data of **1E.4** were similar to those of **1E.3**. The major distinction was the presence of a chloride atom at C-9a in **1E.4** (δ_C 113.8) which was confirmed by the HMBC correlation of H-3a to C-9a. The absolute configuration of **1E.4** was determined by comparing its ECD spectrum with that of **1E.1**. Thus, compound **1E.4**, macrosporusone C, was assigned as a new oxaphenalenone dimer. It should be noted that this is the first oxaphenalenone dimer reported with a chlorine atom in the molecule.

Compound **1E.5** possesses the molecular formula $C_{26}H_{16}O_{10}$, based on the ^{13}C NMR and HRESITOFMS (m/z 487.0669) [M-H]$^-$ data, implying 19 indices of deficiency. The NMR spectroscopic data of **1E.5** were similar to those of the isolated xenoclauxin (**1E.9**) [10], except that an acetoxyl group at C-9′ was replaced by a hydroxyl group. The ^1H NMR spectroscopic data of unit A showed resonances of aromatic protons at δ 6.92 (s, H-5), and methyl protons at δ 3.06 (s, Me-6). The NMR spectral data of unit B were similar to those of **1E.1**. The absolute configuration of **1E.5** was assigned to be the same as that of **1E.1** by comparison of its ECD spectrum with that of **1E.1**. The complete structure of **1E.5** was confirmed by 2D NMR techniques, COSY, HMBC and NOESY. From the above evidence, compound **1E.5**, named macrosporusone D, was determined as a new oxaphenalenone dimer.

Compound **1E.6** had the molecular formula $C_{27}H_{20}O_{10}$, based on the ^{13}C NMR and HRESITOFMS (m/z 503.0975) [M-H]$^-$ data, implying 18 degrees of unsaturation. The NMR spectroscopic data of **1E.6** showed a mixture of epimers in the ratio of 1:1. Their resonance signals were similar to those of the mixture of bacillisporin F (**1E.10a**) and 1-epi-bacillisporin F (**1E.10b**) [12], except that an acetoxyl group at C-9′ was replaced by a hydroxyl group. The ^1H NMR spectral data of unit A showed a mixture of two sets of aromatic proton signals at δ 6.84/6.77 (s, H-5), methine protons at δ 6.44/6.37 (s, H-1), methoxy protons at δ 3.68/3.56 (s, MeO-1) and methyl protons at δ 2.99/2.97 (s, Me-6). The COSY spectrum showed an allylic coupling between H-5 and Me-6. The C-3, C-3b and C-9; H-5 to C-3, C-3a, C-4 and C-6a; and Me-6 to C-5, C-6 and C-6a. The NMR spectroscopic data of unit B was similar to that of **1E.1**. The configurations of 6a and 6b were determined as 1R, 8'R, 9'S, 9'aS and 1S, 8'R, 9'S, 9'aS by comparing their experimental ECD spectra with those of bacillisporin F (**1E.10a**)

and 1-epi-bacillisporin F (**1E.10b**) [12]. Therefore, the compound **1E.6** was deduced to be a mixture of two new oxaphenalenone dimers and they were named macrosporusone E (**1E.6a**) and 1-epi-macrosporusone E (**1E.6b**). The biological activities of the isolated compounds were evaluated. Compounds **1E.3** and **1E.8** exhibited antimalarial activity against *P. falciparum* with IC_{50} values of 10.28 and 8.07 μM, respectively. Compound **1E.3** also showed cytotoxicity against NCI-H187 cells with an IC_{50} value of 16.73 μM, while compound **1E.8** showed cytotoxicity against KB, MCF-7 and NCI-H187 cell lines with IC_{50} values of 5.86, 9.16 and 7.29 μM, respectively. Moreover, compounds **1E.2**, **1E.3**, **1E.5**, **1E.8** and **1E.10**–**1E.12** exhibited cytotoxicity against Vero cells with IC_{50} values in the range of 7.50–93.27 μM. In addition, compounds **1E.1**–**1E.3**, **1E.5**, **1E.7**–**1E.12** and **1E.14** were evaluated for their antibacterial activity against Gram positive and Gram negative bacteria. Among them, compounds **1E.11** and **1E.14** showed the most potent antibacterial activity against *B. cereus*, *S. aureus* and MRSA with MICs in the range of 1.94–15.03 μM.

References

1) N. Yilmaz, C.M. Visagie, J. Houbraken, J.C. Frisvad, R.A. Samson, Polyphasic taxonomy of the genus *Talaromyces*, Stud. Mycol. 78 (2014) 175–341.

2) M.M. Zhai, J. Li, C.X. Jiang, Y.P. Shi, D.L. Di, P. Crews, Q.X. Wu, The bioactive secondary metabolites from *Talaromyces* species, Nat. Products Bioprospect. 6 (2016) 1-24.

3) H. Yang, F. Li, N. Ji, Alkaloids from an algicolous strain of Talaromyces sp, Chin. J. Oceanol. Limnol. 34 (2016) 367–371.

4) J.P. Guo, J.L. Tan, Y.L. Wang, H.Y. Wu, C.P. Zhang, X.M. Niu, W.Z. Pan, X.W. Huang, K.Q. Zhang, Isolation of talathermophilins from the thermophilic fungus *Talaromyces thermophilus* YM3-4, J. Nat. Prod. 74 (2011) 2278–2281.

5) T. Morino, M. Nishimoto, A. Masuda, T. Nishikiori, S. Saito, NK374200, a novel insecticidal agent from *Talaromyces*, found by physicochemical screening, J. Antibiot. 48 (1995) 1509–1510.

6) S. Suzuki, T. Hosoe, K. Nozawa, K.I. Kawai, T. Yaguchi, S.I. Udagawa, Antifungal substances against pathogenic fungi, talaroconvolutins, from *Talaromyces convolutus*, J. Nat. Prod. 63 (2000) 768–772.

7) J.W. He, Z.Q. Mu, H. Gao, G.D. Chen, Q. Zhao, D. Hu, J.Z. Sun, X.X. Li, Y. Li, X.Z. Liu, X.S. Yao, New polyesters from *Talaromyces flavus*, Tetrahedron. 70 (2014) 4425–4430.

8) B. Wu, B. Ohlendorf, V. Oesker, J. Wiese, S. Malien, R. Schmaljohann, J.F. Imhoff, Acetylcholinesterase inhibitors from a marine fungus *Talaromyces* sp. strain LF458, Mar. Biotechnol. 17 (2015) 110–119.

9) H. Hayashi, Y. Oka, K. Kai, K. Akiyama, A new meroterpenoid, chrodrimanin C, from YO-2 of *Talaromyces* sp, Biosci. Biotechnol. Biochem. 76 (2012) 745–748.

10) M. Yamazaki, E. Okuyama, Isolation and structures of oxaphenalenone dimers from *Talaromyces bacillsporus*, Chem. Pharm. Bull. 28 (1980) 3649–3655.

11) T. Dethoup, L. Manoch, A. Kijjoa, M.S.J. Nascimento, P. Puaparoj, A.M.S. Silva, G. Eaton, W. Herz, Bacillisporins D and E, new oxyphenalenone dimers *from Talaromyces bacillisporus*, Planta Med. 72 (2006) 957–960.

12) Y. Zang, G. Genta-Jouve, A.E. Escargueil, A.K. Larsen, L. Guedon, B. Nay, S. Prado, Antimicrobial oligophenalenone dimers from the soil fungus *Talaromyces stipitatus,* J. Nat. Prod. 79 (2016) 2991–2996.

13) Y. Zang, G. Genta-jouve, P. Retailleau, A. Escargueil, S. Mann, B. Nay, S. Prado, Talaroketals A and B, unusual bis(oxaphenalenone) spiro and fused ketals from the soil fungus *Talaromyces stipitatus* ATCC 10500, Org. Biomol. Chem. 14 (2016) 2691–2697.

14) S. Natori, F. Sato, S. Udagawa, Anthraquinone metabolites of *Talaromyces avellaneus*, Chem. Pharm. Bull. 13 (1965) 385–386.

15) R. Bara, A.H. Aly, A. Pretsch, V. Wray, B. Wang, P. Proksch, A. Debbab, Antibiotically active metabolites from *Talaromyces wortmannii*, an endophyte of *Aloe vera*, J. Antibiot. (Tokyo) 66 (2013) 491–493.

16) R. Bara, I. Zerfass, A.H. Aly, H. Goldbach-Gecke, V. Raghavan, P. Sass, A. Mándi, V. Wray, P.L. Polavarapu, A. Pretsch, W. Lin, T. Kurtán, A. Debbab, H. Brötz-Oesterhelt, P. Proksch, Atropisomeric dihydroanthracenones as inhibitors of multiresista *Staphylococcus aureus,* J. Med. Chem. 56 (2013) 3257–3272.

17) H. Li, H. Huang, C. Shao, H. Huang, J. Jiang, X. Zhu, Y. Liu, L. Liu, Y. Lu, M. Li, Y. Lin, Z. She, Cytotoxic norsesquiterpene peroxides from the endophytic fungus *Talaromyces flavus* isolated from the mangrove plant *Sonneratia apetala*, J. Nat. Prod. 74 (2011) 1230–1235.

18) K.K. Chexa, C. Tamm, 186. Gilmaniellin and dechlorogilmaniellin, two novel dimeric oxaphenalenones, Helv. Chim. Acta. 62 (1979) 1785–1803.

5) Research Outcome

Publication

Chaiyosaeng, B.; Kanokmedhakul, K.; Sanmanoch, W.; Boonlue, S.; Hadsadee, S.; Jungsuttiwong, S.; Kanokmedhakul, S. "Bioactive oxaphenalenone dimers from the fungus *Talaromyces macrosporus* KKU-1NK8". Fitoterapia 2019, 134, 429-434.

Project 1F Investigate on the Fungus *Talaromyces trachyspermus EU23*

1) Keywords

Talaromyces, pyrrolobenzoxazine terpenoid, cytotoxicity, antibacterial activity

2) Objective

To investigate the chemical constituents and their cytotoxicity and antibacterial activity from *Talaromyces trachyspermus*

3) Introduction

Talaromyces trachyspermus, a perfect state of the *Penicillium* species belongs to the family Trichocomaceae (Yilmaz et al., 2014). Its colonies reach 19.52─25.35 mm on potato dextrose agar at 7 days. Colony is pale yellow and ascospores are broadly allipsoidal, 2.09 – 3.92 × 2.40–4.37 μm, spiny wall, no ridge (Soytong et al., 2015). These characteristics are similar to those reported by Domsch and Gams, 1993. Until now, only three secondary metabolites, a trachyspic acid (Sfflozawa et al., 1994), a γ-butenolide derivative, spiculisporic acid E (Kumla et al., 2014) and an 3-acetyl ergosterol 5, 8-endoperoxide (Kumla et al., 2014) have been reported from the fungus *T. trachyspermus*. However, several types of compounds such as meroterpenoids (Hayashi et al., 2012), alkaloids (Yang et al., 2016), oxaphenalenone dimers (Dethoup et al., 2006; Wu et al., 2015; Zang et al., 2016; Chaiyosang et. al., 2019), steroids and terpenoids (Li et al., 2011) have been reported from the genus *Talaromyces*. On our continue searching for bioactive compounds from fungi, the crude EtOAc extract from biomass of *T. trachyspermus* EU23 showed antibacterial activity against *Pseudomonas aeruginosa* with MIC value of 128 µg/mL. Therefore, the investigation on the fungus *T. trachyspermus* EU23 was our focus.

4) Result and Discussion

The chromatographic separation on the extracts from air-dried fungal biomass of *T. trachyspermus* EU23 gave three new pyrrolobenzoxazine terpenoids, pyrrolobenzoxazines A─C (**1F.1**─**1F.3**), together with fourteen known compounds, pyrrolobenzoxazines terpenoids CJ-12662 (**1F.4**) and CJ-12663 (**1F.5**) (Kojima et al., 1995), eurochevalierine (**1F.6**) (Kanokmedhakul et al., 2011), chevalones A─C (**1F.7**─**1F.9**) (Kanokmedhakul et al., 2011), chevalone E (**1F.10**) (Prompanya et al., 2014), α-pyrone meroterpenoid pyripyropene A (**1F.11**) (Masi et al., 2013), isochaetominine C (**1F.12**) (Lan et al., 2016), brasiliamide B (**1F.13**) (Eamvijarn et al., 2012), reessiate (**1F.14**) (Kitchawalit et al., 2014), diorcinol (**1F.15**) (Fremlin et al., 2009), ergosterol (**1F.16**) (Kwon et al., 2002), and 24(*R*)-5α,8α-

epidioxyergosta-6-22-diene-3*β*-ol (**1F.17**) (Jinming et al., 2001). Structures of known compounds were identified by spectroscopic data (^{1}H and ^{13}C NMR) and compared with data obtained in literature as shown in Figure 1F.1.
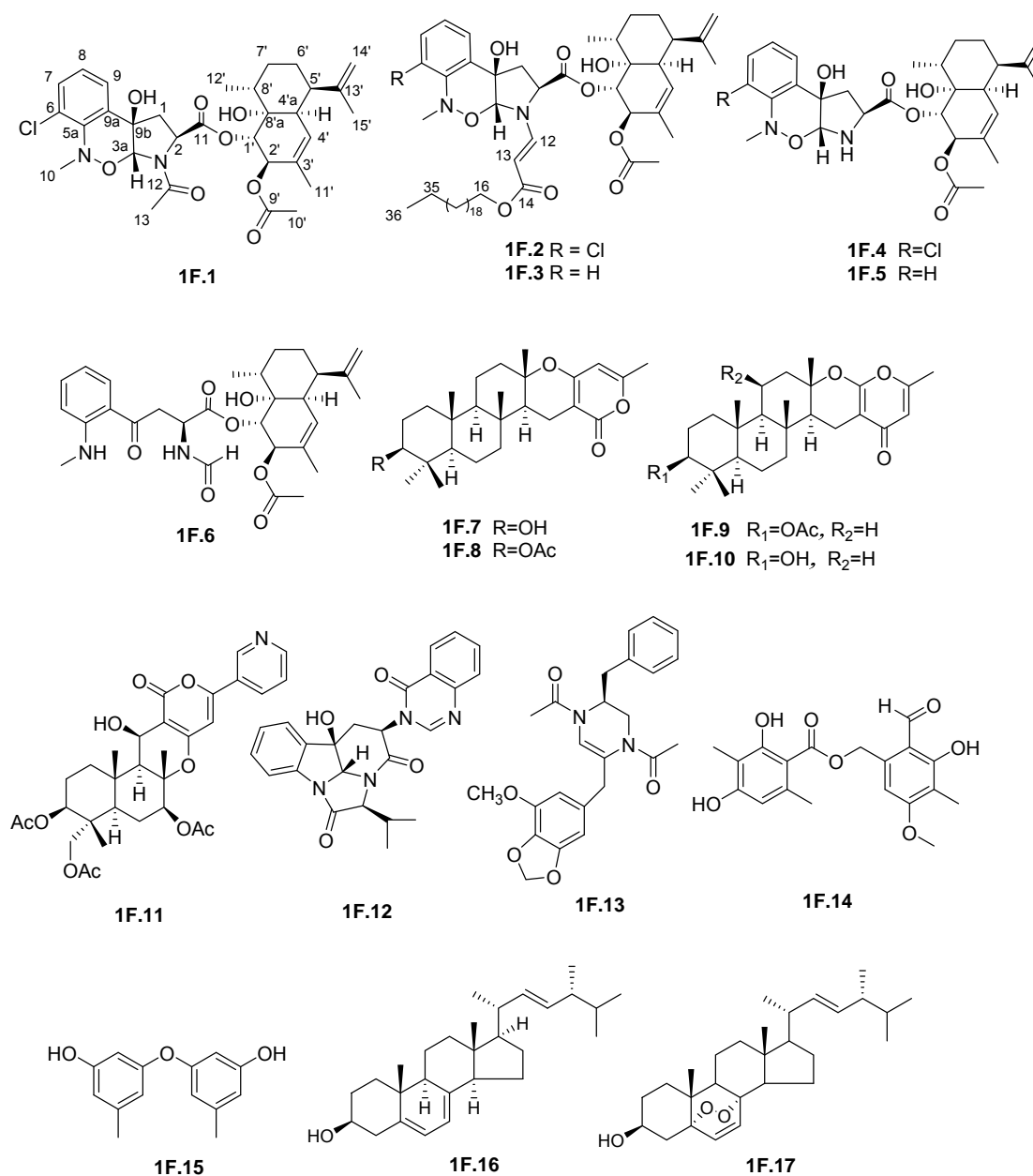
Figure 1F.1. Isolated compounds from *Talaromyces trachyspermus EU23*

Compound **1F.1** had the molecular formula $C_{31}H_{39}ClN_2O_8$, deduced from the HRESITOFMS (m/z 625.2297 [M + Na]$^+$ and 627.2268 [M + Na + 2]$^+$), indicating thirteen degrees of unsaturation. The UV spectrum showed absorption maxima at 204, 212, 246 and 248 nm. The IR spectrum showed absorption bands of hydroxyl (3455 cm^{-1}), ester carbonyl (1742 cm^{-1}) and amide (1657 cm^{-1}) functionalities. Analysis of the ^{1}H and ^{13}C NMR spectroscopic data as well as 2D NMR (HMQC, HMBC and NOESY) found that structure of **1F.1** was similar to a pyrrolobenzoxazine terpenoid, CJ-12662 (**1F.5**) (Kojma et al., 2009). The different between these two compounds was, a proton at N-3 of pyrrolidine ring in **1F.5** was replaced by an acetyl group (δ_C carbonyl amide 171.2 and methyl group $\delta_{H/C}$ 2.37 (s)/22.0). The COSY spectrum showed correlations of aromatic protons, H-7/H-8/H-9. The HMBC spectrum confirmed the position of an acetyl group in **1F.1** by showing the correlations of H-3a and H-2 to C-12. The absolute configuration of **1F.1** was characterized through the comparison of an experimental and calculated ECD spectra. The ECD calculations were generated for 6 chiral centers of two selected possible stereoisomers 1S, 2R, 4aR, 5R, 8R, 8aR and 1R, 2S, 4aS, 5S, 8S, 8aS using Gaussian09 with DFT B3LYP/6-31G (d,p). The ECD calculated spectrum of **1F.1** generated for the 1S, 2R, 4aR, 5R, 8R, 8aR isomer showed a Cotton effect at 182 nm ($\Delta\varepsilon$ −132.8), 197 ($\Delta\varepsilon$ +72.4), 222 ($\Delta\varepsilon$ −9.8) and 243 ($\Delta\varepsilon$ +4.0), which correspond to its experimental ECD spectrum. Thus, the compound **1F.1** was a new pyrrolobenzoxazine terpenoid and was named pyrrolobenzoxazine A (Figure 1F.1).

Compound **1F.2** had the molecular formula $C_{53}H_{81}ClN_2O_9$, deduced from the HRESITOFMS (m/z 925.5701 [M + H]$^+$ and 927.5695 [M + H + 2]$^+$), indicating fourteen degrees of unsaturation. The UV spectrum showed absorption maxima at 205, 211 and 272 nm. The IR spectrum showed the presence of hydroxyl (3472 cm^{-1}), alkyl (2922 and 2853 cm^{-1}) ester carbonyl (1744 cm^{-1}) and alkene (1621 cm^{-1}) functionalities. The ^{13}C NMR and DEPT spectrum showed 53 signals attributable to six methyl (including acetoxy group), twenty-four methylene (including vinylic), thirteen methine (including olefinic and aromatic), and ten quaternary (including three carbonyl groups) carbons. The ^{1}H and ^{13}C NMR spectroscopic data are similar to those of **1F.1**, except for an acetyl group at N-3 of pyrrolidine ring, which was replaced by a henicosyl acrylate unit. The ^{1}H NMR spectral data of **1F.2** exhibited resonance at δ 7.73 (d, J = 13.6 Hz, H-12), 4.96 (d, J = 13.6 Hz, H-13), 4.09 (td, J = 6.8 Hz, H-16), 1.62 (m, H-17), 0.87 (t, J = 1.7 Hz, H-36), and 1.32-1.25 (m, overlap, H-18—H-35). The COSY spectrum of **1F.2** showed correlations of H-12/H-13, H-16/H-17/H-18 and H-35/H-36, and aromatic protons, H-7/H-8/H-9. The key HMBC correlations of H-2 to C-3a and C-12; H-3a to C-12; H-12 to C-2, C-3a, and C-14; H-16 to C-14, C-17, and C-18; H-17 to C-18; H-36

to C-34 and C-35 confirmed the henicosyl acrylate moiety at N-3 of pyrrolidine ring. The *trans* geometric isomer of C-12/C-13 was determined from the coupling constant value (*J* = 13.6 Hz). Finally, the EIMS fragmentations ion peak at *m/z* 649.3938 [(M + H) - sesquiterpene]$^+$, 651.3963 [(M + 2 + H) - sesquiterpene]$^+$, 613.2304 [(M + H) - henicosanoxy]$^+$, 615.2281 [(M + 2 + H) - henicosanoxy]$^+$, 337.0577 [(M + H) - sesquiterpene - henicosanoxy]$^+$, 339.0479 [(M + 2 + H) - sesquiterpene - henicosanoxy]$^+$, and 217.1583 [(M + H) – acetate - henicosanoxy]$^+$ confirmed the structure of **1F.2**.. The ECD calculated spectrum of **1F.2** generated for the 1*S*, 2*R*, 4a*R*, 5*R*, 8*R*, 8a*R* showing a Cotton effect at 183 (*Δε* – 28.4), 197 (*Δε* + 47.8), 225 (*Δε* – 11.5), and 244 (*Δε* – 23.5), which agreed well with its experimental ECD spectrum. Thus, the compound **1F.2** was a new pyrrolobenzoxazine terpenoid, named pyrrolobenzoxazine B.

Compound **1F.3** had the molecular formula $C_{53}H_{82}N_2O_9$, deduced from the HRESITOFMS (*m/z* 891.6088 [M + H]$^+$) data, indicating fourteen degrees of unsaturation. The UV spectrum showed absorption maxima at 205, 231 and 270 nm. The IR spectrum showed the presence of hydroxyl (3463 cm^{-1}), alkyl (2921 and 2852 cm^{-1}), ester carbonyl (1744 cm^{-1}) and alkene (1620 cm^{-1}) groups. The ^{1}H and ^{13}C NMR spectroscopic data were similar to those of **2**, except for the absence of a chlorine atom at C-6 of an aromatic ring which was presented as a proton (δ_H 6.76, d, *J* = 8.0 Hz, δ_C 112.3). The complete interpretation of NMR spectroscopic data of **1F.3** was established as a result of conclusive DEPT, COSY, and HMBC techniques. The COSY spectrum showed correlations of aromatic protons, H-6/H-7/H-8/H-9. The HMBC spectrum of **1F.3** showed correlations of the side chain, henicosanoxyl moiety as in **1F.2**. Finally, the EIMS fragmentation ion peak at *m/z* 615.4361 [(M + H) - sesquiterpene]$^+$, 579.2700 [(M + H) - henicosanoxy]$^+$, 303.0985 [(M + H) - sesquiterpene - henicosanoxy]$^+$, and 217.1580 [(M + H) - acetate - henicosanoxy]$^+$ supported the structure of **1F.3**. The ECD calculated spectrum of **1F.3** generated for the 1*S*, 2*R*, 4a*R*, 5*R*, 8*R*, 8a*R* showing a Cotton effect at 184 (*Δε* – 117.7), 197 (*Δε* + 52.8), 204 (*Δε* + 43.0), 222 (*Δε* -5.3) and 243 (*Δε* –18.2), which agreed with its experimental ECD spectrum. Thus, the compound **1F.3** was a new pyrrolobenzoxazine terpenoid and was named pyrrolobenzoxazine C.

Compounds **1F.1** - **1F.3** were evaluated for cytotoxic activities. Compound **1F.1** showed moderate cytotoxicity against Hela, KB, HT-29, MCF-7 and HepG2 cell lines with IC$_{50}$ values of 6.89 ± 0.70, 10.64 ± 0.12, 8.74 ± 0.28, 12.20 ± 1.19 and 8.39 ± 0.86 *μ*M, respectively. However, compound **1F.1** also exhibited cytotoxicity against *Vero* cells with IC$_{50}$ value of 8.20 ± 1.90 μM. Whereas compounds **1F.2** and **1F.3** were not cytotoxic comparing to **1F.1** suggesting the steric effect from their side chain at N-3. Compounds **1F.1** – **1F.3** and **11F.14** were further evaluated for antibacterial activity against Gram-positive (*B. cereus*, *S. aureus* and *B. subtilis*) and Gram-negative bacteria (*E. coli*, *P. aeruginosa* and *S. sonnei*).

Compound **1F.1** showed weak antibacterial activity against *B. cereus*, *B. subtilis, E. coli* and *P. aeruginosa* with MICs 106.27, 212.54, 212.54 and 212.54 µM, respectively. While **1F.2** and **1F.3** showed weak antibacterial activity against *P. aeruginosa* with MICs 143.72 and 138.44 µM, respectively. In addition, the known compound **1F.14** was tested for antibacterial activity for the first time and its showed weak antibacterial against *B. cereus*, *B. subtilis* and *P. aeruginosa* with MICs 355.44 μM. Two standard drugs, kanamycin showed antibacterial activity against *B. cereus* and *B. subtilis* with MICs 2.06 μM and gentamicin showed antibacterial activity against *E. coli* and *P. aeruginosa* with MICs 2.09 and 1.05 μM, respectively.

References

Chaiyosang, B., Kanokmedhakul, K., Sanmanoch, W., Boonlue, S., Hadsadee, S., Jungsuttiwong, S., Kanokmedhakul, S. 2019. Bioactive oxaphenalenone dimers from the fungus *Talaromyces macrosporus* KKU-1NK8. Fitoterapia. 134, 429−433.

Dethoup, T., Manoch, L., Kijjoa, A., Nascimento, M.S.J., Puaparoj, P., Silva, A.M.S., Eaton, G., Herz, W., 2006. Bacillisporins D and E, new oxyphenalenone dimers from *Talaromyces bacillisporus*. Planta Med. 72, 957–960.

Domsch, K. and Gams, W., 1993. Compendium of soil fungi. IHW-Verlag, Ger. Vol.1., 859 p.

Fremlin, L.J., Piggott, A.M., Lacey, E., Capon, R.J., 2009. Cottoquinazoline A and cotteslosins A and B, Metabolites from an australian marine-derived strain of *Aspergillus Wersicolor*. J. Nat. Prod 72, 666–670.

Hayashi, H., Oka, Y., Kai, K., Akiyama, K., 2012. A New meroterpenoid, chrodrimanin C, from YO-2 of *Talaromyces* sp. Biosci. Biotechnol. Biochem. 76, 745–748.

Jinming, G., Lin, H., Jikai, L., 2001. A novel sterol from chinese truffles *Tuber indicum*. Steroids 66, 771–775.

Kanokmedhakul, K., Kanokmedhakul, S., Suwannatrai, R., Soytong, K., Prabpai, S., Kongsaeree, P., 2011. Bioactive meroterpenoids and alkaloids from the fungus *Eurotium chevalieri*. Tetrahedron 67, 5461–5468.

Kitchawalit, S., Kanokmedhakul, K., Kanokmedhakul, S., Soytong, K., 2014. A new benzyl ester and ergosterol derivatives from the fungus *Gymnoascus reessii*. Nat. Prod. Res. 28, 1045–1051.

Kojima, Y., Yamauchi, Y., Kojima, N., Bishop, B.F., 1995. Antiparasitic pyrrolobenzoxazine compounds, Pfzer Pharm. Inc. Pat. Coop. (Treaty WO 95/19363).

Kumla, D., Dethoup, T., Buttachon, S., Singburaudom, N., Silva, A.M.S., Kijjoa, A., 2014. Spiculisporic acid E, a new spiculisporic acid derivative and ergosterol derivatives from the marine-sponge associated fungus *Talaromyces trachyspermus* (KUFA 0021). Nat.

Prod. Commun. 9, 1147–1150.

Kwon, H.C., Zee, S.D., Cho, S.Y., Choi, S.U., Lee, K.R., 2002. Cytotoxic ergosterols from *paecilomyces* sp. J300. Arch. Pharm. Res. 25, 851–855.

Li, H., Huang, Hongbo, Shao, C., Huang, Huarong, Jiang, J., Zhu, X., Liu, Y., Liu, L., Lu, Y., Li, M., Lin, Y., She, Z., 2011. Cytotoxic norsesquiterpene peroxides from the endophytic fungus *Talaromyces flavus* isolated from the mangrove plant *Sonneratia apetala*. J. Nat. Prod. 74, 1230–1235.

Masi, M., Andolfi, A., Mathieu, V., Boari, A., Cimmino, A., Moreno Y Banuls, L., Vurro, M., Kornienko, A., Kiss, R., Evidente, A., 2013. Fischerindoline, a pyrroloindole sesquiterpenoid isolated from *Neosartorya pseudofischeri*, with in vitro growth inhibitory activity in human cancer cell lines. Tetrahedron 69, 7466–7470.

Prompanya, C., Dethoup, T., Bessa, L.J., Pinto, M.M.M., Gales, L., Costa, P.M., Silva, A.M.S., Kijjoa, A., 2014. New isocoumarin derivatives and meroterpenoids from the marine sponge-associated fungus *Aspergillus similanensis* sp. Nov. KUFA 0013. Mar. Drugs 12, 5160–5173.

Chaiyosang, B., Kanokmedhakul, K., Sanmanoch, W., Boonlue, S., Hadsadee, S., Jungsuttiwong, S., Kanokmedhakul, S. 2019. Bioactive oxaphenalenone dimers from the fungus *Talaromyces macrosporus* KKU-1NK8. Fitoterapia. 134, 429—433.

Dethoup, T., Manoch, L., Kijjoa, A., Nascimento, M.S.J., Puaparoj, P., Silva, A.M.S., Eaton, G., Herz, W., 2006. Bacillisporins D and E, new oxyphenalenone dimers from *Talaromyces bacillisporus*. Planta Med. 72, 957–960.

Domsch, K. and Gams, W., 1993. Compendium of soil fungi. IHW-Verlag, Ger. Vol.1., 859 p.

Fremlin, L.J., Piggott, A.M., Lacey, E., Capon, R.J., 2009. Cottoquinazoline A and cotteslosins A and B, Metabolites from an australian marine-derived strain of *Aspergillus Wersicolor*. J. Nat. Prod 72, 666–670.

Hayashi, H., Oka, Y., Kai, K., Akiyama, K., 2012. A New meroterpenoid, chrodrimanin C, from YO-2 of *Talaromyces* sp. Biosci. Biotechnol. Biochem. 76, 745–748.

Jinming, G., Lin, H., Jikai, L., 2001. A novel sterol from chinese truffles *Tuber indicum*. Steroids 66, 771–775.

Kanokmedhakul, K., Kanokmedhakul, S., Suwannatrai, R., Soytong, K., Prabpai, S., Kongsaeree, P., 2011. Bioactive meroterpenoids and alkaloids from the fungus *Eurotium chevalieri*. Tetrahedron 67, 5461–5468.

Kitchawalit, S., Kanokmedhakul, K., Kanokmedhakul, S., Soytong, K., 2014. A new benzyl ester and ergosterol derivatives from the fungus *Gymnoascus reessii*. Nat. Prod. Res. 28, 1045–1051.

Kojima, Y., Yamauchi, Y., Kojima, N., Bishop, B.F., 1995. Antiparasitic pyrrolobenzoxazine compounds, Pfzer Pharm. Inc. Pat. Coop. (Treaty WO 95/19363).

Kumla, D., Dethoup, T., Buttachon, S., Singburaudom, N., Silva, A.M.S., Kijjoa, A., 2014. Spiculisporic acid E, a new spiculisporic acid derivative and ergosterol derivatives from

the marine-sponge associated fungus *Talaromyces trachyspermus* (KUFA 0021). Nat. Prod. Commun. 9, 1147–1150.

Kwon, H.C., Zee, S.D., Cho, S.Y., Choi, S.U., Lee, K.R., 2002. Cytotoxic ergosterols *frompaecilomyces* sp. J300. Arch. Pharm. Res. 25, 851–855.

Li, H., Huang, Hongbo, Shao, C., Huang, Huarong, Jiang, J., Zhu, X., Liu, Y., Liu, L., Lu, Y., Li, M., Lin, Y., She, Z., 2011. Cytotoxic norsesquiterpene peroxides from the endophytic fungus *Talaromyces flavus* isolated from the mangrove plant *Sonneratia apetala*. J. Nat. Prod. 74, 1230–1235.

Masi, M., Andolfi, A., Mathieu, V., Boari, A., Cimmino, A., Moreno Y Banuls, L., Vurro, M., Kornienko, A., Kiss, R., Evidente, A., 2013. Fischerindoline, a pyrroloindole sesquiterpenoid isolated from *Neosartorya pseudofischeri*, with in vitro growth inhibitory activity in human cancer cell lines. Tetrahedron 69, 7466–7470.

Prompanya, C., Dethoup, T., Bessa, L.J., Pinto, M.M.M., Gales, L., Costa, P.M., Silva, A.M.S., Kijjoa, A., 2014. New isocoumarin derivatives and meroterpenoids from the marine sponge-associated fungus *Aspergillus similanensis* sp. Nov. KUFA 0013. Mar. Drugs 12, 5160–5173.

Soytong, Mayamor, Poeaim, S., 2015. Isolation and identification of Trichocomaceae from soil by morphology and three regions DNA sequencing. J. Agric. Technol. 11, 315–326.

Wu, B., Ohlendorf, B., Oesker, V., Wiese, J., Malien, S., Schmaljohann, R., Imhoff, J.F., 2015. Acetylcholinesterase inhibitors from a marine fungus *Talaromyces* sp. Strain LF458. Mar. Biotechnol. 17, 110–119.

Yang, H., Li, F., Ji, N., 2016. Alkaloids from an algicolous strain of *Talaromyces* sp. Chinese J. Oceanol. Limnol. 34, 367–371.

Yilmaz, N., Visagie, C.M., Houbraken, J., Frisvad, J.C., Samson, R.A., 2014. Polyphasic taxonomy of the genus *Talaromyces*. Stud. Mycol. 78, 175–341.

Zang, Y., Genta-Jouve, G., Escargueil, A.E., Larsen, A.K., Guedon, L., Nay, B., Prado, S., 2016. Antimicrobial Oligophenalenone dimers from the soil fungus *Talaromyces stipitatus*. J. Nat. Prod. 79, 2991–2996.

5) Research Outcome

Manuscript Preparation

Chaiyosang, B., Kanokmedhakul, K., Soytong, K., Soytong, M., Hadsadee, S., Jungsuttiwon, S., Yahuafai, J., Siripong, S., Kanokmedhakul, S. New pyrrolobenzoxazines terpenoid analogues from the fungus *Talaromyces trachyspermus* EU23.

The manuscript will be submitted to Phytochemistry.

Project 1G Investigate on Stems of *Rhodamnia dumetorum*

1) Keywords

   Rhodamnia dumetorum, Rhodamnia, bioactivity

2) Objective

   To investigate the chemical constituents and their bioactivity from *Rhodamnia dumetorum*

3) Introduction

   Rhodamnia dumetorum (DC.) Merr. & L.M. Perry (Myrtaceae) is a shrub or tree up to 15 m in height, growing in Cambodia, Laos, Malaysia, Thailand and Vietnam. It is known as 'Plong Kam Aon' in Thai (Smitinand 2001). The bark and leaves of *R. dumetorum* have been used as an astringent (Chansuwanit and Chanprasert 2011) and the roots has been used as an anti-pyretic in Thai traditional medicine (Ratanadomrongpinyo 2008). Moreover, the ethanol extract of the twigs of *R. dumetorum* from Vietnam has been reported to have inhibitory activity on AGEs formation (Choi et al. 2015). In a previous investigation of secondary metabolites from Rhodamnia species, only essential oil has been reported (Brophy et al. 1997).

4) Result and Discussion

   Hexane and EtOAc extracts from the stems of *R. dumetorum* were separated by chromatographic methods to give a new coruleoellagic acid derivative, 3,3′,4,4′,5′-pentamethylcoruleoellagic acid (**1G.1**) and nine known compounds, including hexamethylcoruleoellagic acid (**1G.2**) (Geevananda et al. 1979), 3,4,3′-tri-*O*-methylellagic acid (**1G.3**) (Bai et al. 2008), heptaphylline (**1G.4**), 7-methoxymukonal (**1G.5**), dentatin (**1G.6**) (Songsiang et al. 2012), sinapyl aldehyde (**1G.7**) (Hiltunen et al. 2006), gallic acid (**1G.8**) (Gottlieb et al. 1991), 2,6-dimethoxy-4H-pyran-4-one (**1G.9**) (Zhu et al. 2012) and β-sitosterol (**1G.10**) (Figure 1G.1). Their structures were determined using spectroscopic data and compared with those data reported in the literature.

   Compound **1G.1** was obtained as colorless needles, and its molecular formula, $C_{19}H_{16}O_{10}$, was determined from the HRESITOFMS (observed m/z 427.0645 [M + H]$^+$), indicating 12 degrees of unsaturation. The IR spectrum of **1G.1** showed absorption bands of hydroxyl (3295 cm^{-1}) and two carbonyl (1733 and 1688 cm^{-1}) groups. The UV spectrum showed absorption maxima at 247, 368, and 384 nm. The ^{13}C NMR and DEPT spectra of **1G .1** displayed 19 carbon signals, contributable to five methoxyl, 14 sp^2 quaternary (including two carbonyl) carbons. The ^{1}H NMR spectroscopic data showed a downfield signal at δ 10.47 characteristic of a chelated hydroxyl proton at C-5 located *ortho* to the carbonyl ester. Five methoxyl groups appeared at δ_H 4.27 (s, 3-OCH$_3$), 4.25 (s, 4'-OCH$_3$), 4.04 (s, 5' -OCH$_3$),

4.02 (s, 4-OCH$_3$), 4.02 (s, 3'-OCH$_3$). The phenolic hydroxyl group at C-5 was confirmed by the HMBC correlations of it proton to C-5 (δ_C 152.8). Whereas the five methoxyl groups are located at C-3, C-4, C-3', C-4' and C-5' resulted from the correlations of methoxyl protons to those carbons. The structure of **1G.1** was similar to 3,3',4,4'-tetra-*O*-methylflavellagic acid reported from stems of *Rhodomyrtus tomentosa*, except for the H-5' of **1G.1** was replaced by a methoxy group. Thus, the structure of **1G.1** was determined as a new flavellagic acid derivative, which has been named 3, 3',4,4',5'-penta-*O*-methylflavellagic acid.

Compounds **1G.1**-**1G.6** were evaluated for their biological activity, antimalarial, anti-TB, and cytotoxicity to NCI-H187, KB and MFC-7 cell lines. However, **1G.1**-**1G.3** showed no active for the tested. Compounds **1G.4**-**1G.6** have been reported to be a potent lipid peroxidation inhibitory (IC$_{50}$ 14.1, 1.45, 78.4 μM, respectively), cytotoxicity against two cholangiocarcinoma cell line (KKU-OCA17 and KKU-214) (IC$_{50}$ value in range 43.5-178.6 μM) and compounds **1G.4** and **1G.6** exhibited cytotoxicity against two cancer cell line (NCI-H187 and KB) (rang of IC$_{50}$ value 1.32-113.98 μM).
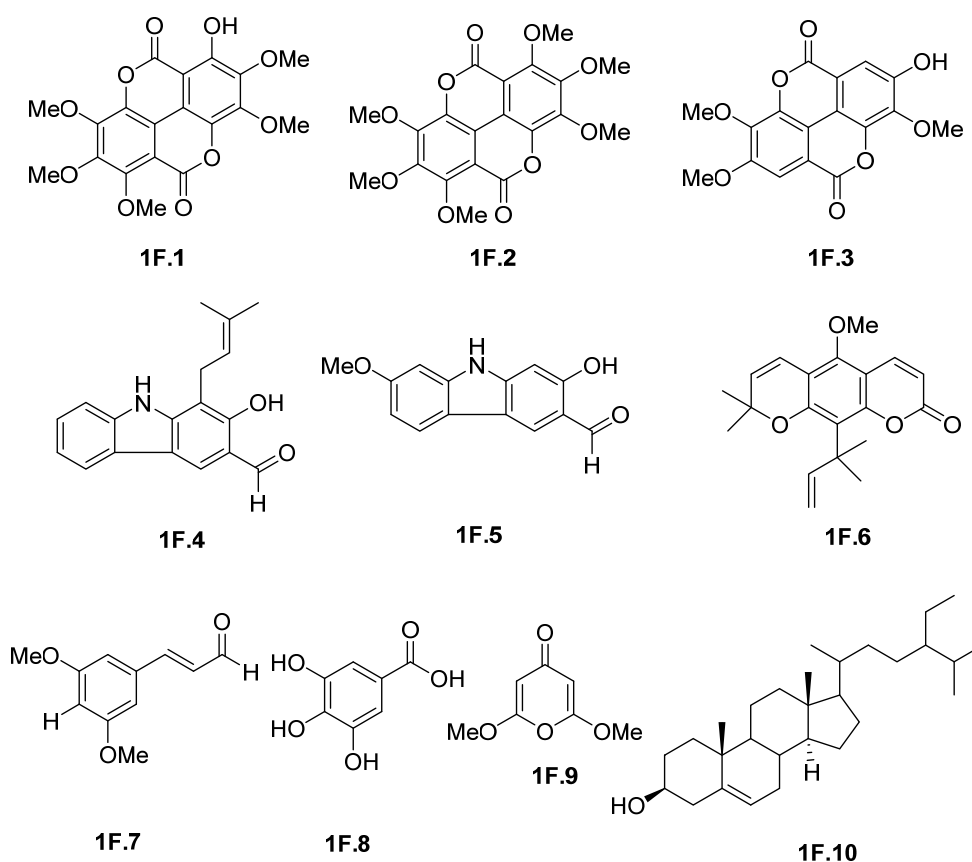

Figure 1G.1 Isolated compounds from the stems of *Rhodamnia dumetorum.*

References

Bai N, He K, Roller M, Zheng B, Chen X, Shao Z, Peng T, Zheng Q. 2008. Active compounds from *Lagerstroemia speciosa*, insulin-like glucose uptake-stimulatory/inhibitory and adipocyte differentiation-inhibitory activities in 3T3-L1 cells. J Agric Food Chem. 56:11668–11674.

Brophy JJ, Goldsack RJ, Forster PI. 1997. The leaf essential oils of the Australian species of *Rhodamnia* (Myrtaceae). Flavour Fragr J. 12:345–354.

Chansuwanit N, Chanprasert C. 2011. Medicinal plants and local-used plants in Paknampran, Pranburi District, Prachup-khiri-khan Province. Reg 7 Med J. 13:145–164.

Choi SJ, Kim YS, Kim JH, Bach TT, Kim JS. 2015. Screening of herbal medicines from Vietnam with inhibitory activity on advanced glycation end products formation (XIV). Korean J Pharmacogn. 46:268–278.

Gottlieb HE, Kumar S, Sahai M, Ray AB. 1991. Ethyl brevifolin carboxylate from *Flueggea microcarpa*. Phytochemistry. 30:2435–2438.

Geevananda YA, Gunawardana P, Kumar NS, Sultanbawa MUS. 1979. Three hydroxy ellagic acid methyl ethers, chrysophanol and scopoletin from *Shorea worthingtonii* and *Vatica obscura*. Phytochemistry. 18:1017–1019.

Hiltunen E, Pakkanen TT, Alvila L. 2006. Phenolic compounds in silver birch (*Betula pendula* Roth) wood. Holzforschung. 60:519–527.

Ratanadomrongpinyo C. 2008. The study of diversity and utilization of herbs in the area of the project of conservation and development of natural resorces in H.M. private development project Chumphon Province. Chumphon: Protected Areas Regional Office, Department of National Parks, Wildlife and Plant Conservation.

Songsiang U, Thongthoom T, Zeekpudsa P, Kukongviriyapan V, Boonyarat C, Wangboonskul J, Yenjai C. 2012. Antioxidant activity and cytotoxicity against cholangiocarcinoma of carbazoles and coumarins from *Clausena harmandiana*. Science Asia. 38:75-81.

Zhu M, Xiong L, Wang Y, Chen M, Jiang B, Lin S, Zhu C, Yang Y, Shi J. 2012. Lignans from *Sinocalamus affinis*. China J Chin Mater Medica. 37:1968–1972.

5) Research Outcome

Publication

Lakornwong, W., Kanokmedhakul, K., Kanokmedhakul, S. "A new coruleoellagic acid derivative from stems of *Rhodamnia dumetorum*" Natural Product Research, 2018, 32(14) 1653–1659.

Project 1H: Investigate on Roots of *Uvaria cherrevensis*

1) **Keyword**

    Uvaria cherrevensis, polyoxygenated, antimalarial, cytotoxicity

2) **Objective**

    To investigate secondary metabolizes and their cytotoxicity from the roots of *Uvaria cherrevensis*

3) **Introduction**

    Uvaria cherrevensis (Pierre ex Finet & Gagnep.) L. L. Zhou, Y. C. F. S (Annonaceae) is a shrub that reaches up to 1.5 m in height and is found in deciduous forests throughout Thailand. Its synonym is *Ellipeiopsis cherrevensis* (Pierre ex Finet & Gagnep.) R. E. Fr and is known as "Nom maeo pa", "Phi phuan noi", and "Phi khao" in Thai [1]. A water decoction of its roots is used as traditional medicine to treat urinary disorders [2]. The genus *Uvaria* is known to be a rich source of polyoxygenated cyclohexene derivatives [3-8]. Previous investigations of the aerial parts of *E. Cherrevensis* (*U. cherrevensis*) led to the isolation of several polyoxygenated cyclohexene derivatives [9-10], as well as a cytotoxic C-benzoylated chalcone, flavonoids and alkaloids [10]. Recently, Auranwiwat et al. reported 2-phenylnaphthalenes and a cyclohexene from the stems and roots extracts of this plant [11]. In our continuing search for bioactive constituents from Thai plants, we noted that the roots extracts (EtOAc and MeOH) of *U. cherrevensis* showed cytotoxicity against KB cell lines with an IC_{50} 12.6 μg/mL.

4) Result and Discussion

    Structures of isolated compounds were identified by physical and spectroscopic data measurements (IR, ^{1}H and ^{13}C NMR, 2D NMR) as well as mass spectrometry. Obtained data of known compounds were also compared with published values. Fifteen compounds were identified as (-)-uvaribonol F (**1H.4**) [11], benzoylbenzoate (**1H.5**) [12], 2-methoxybenzyl benzoate (**1H.6**) [12], endo-5-methoxy-3-patchoulene (**1H.7**) [13], (6S)-patchoulan-4-ene-6-ol (**1H.8**) [14], (-)-1,6-desoxytingtanoxide (**1H.9**) [3], (-)-1,6-desoxysenepoxide (**1H.10**) [3], tingtanoxide (**1H.11**) [3], α-senepoxide (**1H.12**) [3], uvarigranol B (**1H.13**) [15], curcuminol F (**1H.14**) [16], ellipeiopsol D (**1H.15**) [10], 2′,4′-dihydroxy-3′-(2-hydroxybenzyl-6′)-methoxychalcone (**1H.16**) [10], chamanetin 5-methyl ether (**1H.17**) [17] and (±)-dichamanetin 5-methylether (**1H.18**) [18] (Figure 1H.1).
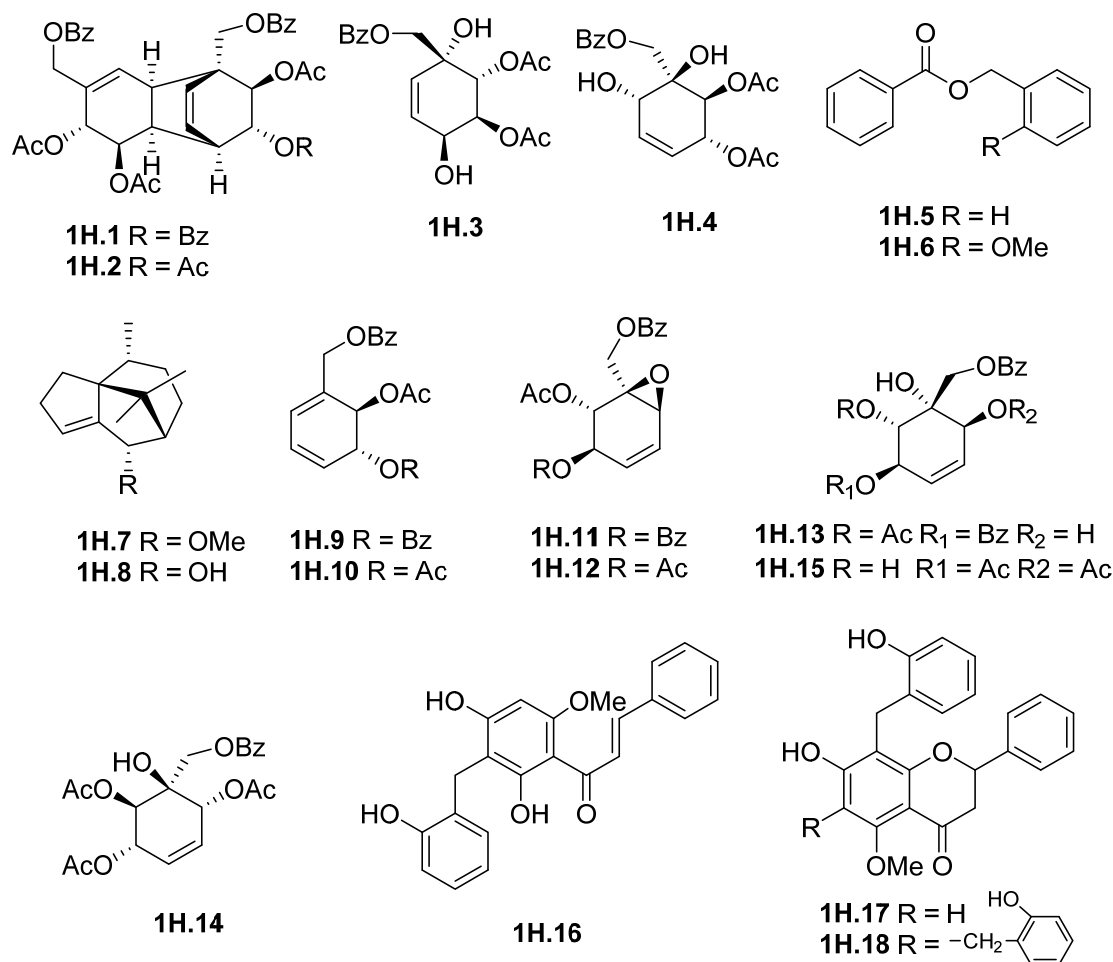
Figure 1H.1. Isolated compounds from the roots of *Uvaria cherrevensis*

Compound **1H.1** was obtained as a white amorphous solid. The molecular formula, $C_{41}H_{38}O_{12}$, was deduced from the HRESIMS (m/z 745.2269 [M+Na]$^+$), implying 23 degrees of unsaturation. The IR spectrum indicated bands for a mono-substituted benzene (1601, 1491 and 707 cm^{-1}) and an ester carbonyl group (1717 cm^{-1}). The ^{1}H and ^{13}C NMR spectroscopic data of **1H.1** showed resonances corresponding to 15 protons of three mono-substituted aromatic benzene rings, together with resonances for two sets of oxymethylene protons at δ_H 4.79 (2H, ABq, J=12.8 Hz, H-7), and δ 4.56 and 4.69 (both d, J=11.6 Hz, H-7′) revealing two sets of benzoyl methylene (-CH$_2$OCOPh) groups and a benzoyl (-OCOPh) group in the molecule. The resonances at $\delta_{H/C}$ 5.86 (d, J=8.0Hz, H-6′)/132.6 and 6.47 (dd, J=8.0, 6.8 Hz, H-5′)/129.8, and $\delta_{H/C}$ 6.11 (brs, H-6)/128.0 were attributed to a di-substituted and a tri-substituted double bond, respectively. Analysis of the ^{1}H and ^{13}C NMR spectroscopic data and 2D NMR spectra (COSY, HSQC, HMBC and NOESY), combined with MS, led us to

conclude that **1H.1** contained two cyclohexene moieties of (-)-1,6-desoxysenepoxide (**1H.9**) and (-)-1,6-desoxytingtanoxide (10), which was the endo-addition product from their Diels-Alder reaction. The COSY correlations of H-2/H-3/H-5/H-6/H-7 (allylic coupling) and H-2′/H-3′/H-4′/H-5′/H-6′, revealing the partial cyclohexene units in the molecule. Key HMBC correlations showed two linked cyclohexene moieties from H-4 to C-3′ and C-4′; as well as oxymethylene protons of 1′-CH$_2$OBz to C-5, C-1′, C-2′; and H-2′ to C-5. The relative stereochemistry of **1H.1** was determined by analysis of coupling constants and from NOESY experiment. A trans-diaxial relationship between H-2 and H-3 was indicated by the vicinal coupling constant J2,3 of 9.2 Hz. In contrast, the coupling constant, J2′,3′ of H-2′ and H-3′ is 3.2 Hz corresponding to axial and equatorial orientations. The NOESY correlation between H-2 and H-5′, H-3′ and H-5′ and the structural constraints of the bridged ring structure indicated that H-2′ and H-3′ were in axial and equatorial orientations, respectively. On the basis of the above data, the relative stereochemistry of **1H.1** was assigned as 2*R*,3*R*. Since compound **1H.1** was deduced from Diels-Alder reaction of compounds **1H.9** and **1H.10**, which both have been clearly reported for their absolute configurations as 2*R*,3*R* [3]. Therefore, **1H.1** would retain the same absolute configuration as 2*R*,3*R* and 2′*R*,3′*R*. Thus **1H.1** was assigned to a new dimer polyoxygenated cyclohexene, which was named cherrevenisyl A.

Compound **1H.2** was obtained as a white amorphous solid. It has a molecular formula of C$_{36}$H$_{36}$O$_{12}$ based on the HRESIMS (m/z 683.2109 [M + Na]+), implying 19 degrees of unsaturation. The IR spectrum showed similar absorption bands to those of 1. Analysis of the ^{1}H and ^{13}C NMR spectroscopic data with 2D NMR techniques (COSY, HSQC, HMBC, and NOESY) indicated that **1H.2** has a similar core structure to **1H.1**, except for the benzoyl group at C-3′ which was replaced by an acetyl group (δ_H 2.06, δ_C 20.4, 170.9). Compound **1H.2** contained two cyclohexene moieties of (-)-1,6-desoxytingtanoxide (**1H.10**), which was also the endo-addition adduct from their Diels-Alder reaction. The relative configuration of **1H.2** was deduced from the coupling constants and NOESY spectrum as well as the comparison with those of **1H.1,** indicating that compound **1H.2** possesses the same relative configuration as **1H.1.** The absolute configuration of **1H.2** would be 2*R*,3*R* and 2′*R*,3′*R* as described for compound **1H.1** above. Thus, the structure of **1H.2** was deduced as a new dimer polyoxygenated cyclohexene, which was named cherrevenisyl B.

Compound **1H.3** was obtained as a pale yellow amorphous solid, and its molecular formula C$_{18}$H$_{20}$O$_8$ was deduced from HRESIMS (m/z 387.1062 [M +Na]+), implying nine degrees of unsaturation. The IR spectrum showed absorption bands for a hydroxy group (3372 cm^{-1}), monosubstituted aromatic rings (1601, 1583 and 714 cm^{-1}), and ester carbonyl

groups (1719 cm^{-1}). The 1H NMR spectroscopic data of **1H.3** showed resonances for a mono-substituted benzene of benzoyl methyl group, three oxymethines (δ_H 5.28, H-2; 5.48, H-3; 4.08, H-4), an oxymethylene (δ_H 4.12, 4.32, H2-7), and two olefinic protons (δ_H 5.82, H-5; 5.58, H-6), together with two acetoxy groups. In addition, the ^{13}C NMR spectroscopic data showed 18 carbon resonances including five oxygenated sp3 carbons (δ_C 66.8, 68.9, 71.1, 72.2, and 74.3), two olefinic carbons (δ_C126.3 and 130.6), and two acetate groups. Analysis of the COSY and HMQC spectra revealed the partial connections (bold line) of H-2/H-3/H-4/H-5/H-6 which were further connected based on long-range HMBC correlations. The HMBC spectrum of 3 revealed long range correlations of the oxymethylene protons at δ_H 4.12, 4.32 (H2-7) to the oxymethine carbon at δ_C 72.2 (C-2) and the quaternary oxygenated carbon at δ 74.3 (C-1). Furthermore, significant correlations of the oxymethine protons at δ_H 5.28 (H-2) and 5.48 (H-3) to the carbonyl carbons at δ_C 170.5 proved the location of each acetate group at C-2 and C-3, respectively. The H2-7 oxymethylene protons and the aromatic protons at δ_H 8.02 (H-2′,6′) correlated to the ester carbonyl carbon at δ_C 166.1 which indicated the presence of the benzoyl group at C-7. An additional hydroxy group was placed at the C-1 position based on the molecular formula and the ^{13}C NMR chemical shift of C-1. The location of the secondary hydroxy group at the C-4 was indicated by COSY correlations and also supported by the chemical shift of H-4. The relative stereochemistry of compound 3 was further confirmed by the NOESY spectrum. H-3 showed a through-space correlation with H-4. The same type of interaction was observed between H-2 and H-7. 1D and 2D NMR spectroscopic analyses indicated that compound **1H.3** has the same structure skeleton as an unnamed synthetic intermediate of crotepoxide [20], which was later isolated as a natural product named artabotrol A from the fungus *Artabotrys madagascariensis*. However, the absolute configurations of carbons C-1 and C-4 of **1H.3** were opposite to those reported for artabotrol A. Besides the sign of optical rotation for **1H.3** (-165.0^o) was also opposite to that of artabotral A (+89.4^o). Thus, compound **1H.3** was determined as a new polyoxygenated cyclohexene, which was named ellipeiopsol E.

Compounds **1H.1**, **1H.2** and **1H.5** exhibited antimalarial activity against *Plasmodium falciparum* with IC$_{50}$ 7.34, 3.97 and 3.34 μg/mL, respectively. Only compound **1D.5** showed a weak antimycobacterial activity against *Mycobacterium tuberculosis* with MIC 50.0 μg/mL. Most of the isolated compounds, with the exception of **1H.2**, **1H.6** and **1H.13**, showed cytotoxicity against three human cancer cell lines (KB, MCF-7 and NCIH187) with IC$_{50}$ values ranging from 1.26 - 48.84 μg/mL. It should be noted that **1H.2** is the most potent antimalarial agent which is not cytotoxic against the three cancer cell lines tested. Compound **1H.1** also showed cytotoxicity against the NCI-H187 cell line, suggesting that the presence of the

benzoyl and acetyl groups on structures **1H.1** and **1H.2** plays a role in these activities. On the other hand, 2-methoxybenzylbenzoate (**1H.6**), bearing a methoxy group at C-2, was inactive when compared with benzylbenzoate (**1H.5**). Moreover, compound **1H.5** was reported to have cytotoxicities against other cancer cells.

References

1) T. Smitinand, Thai Plant Names, Revised Edition, Prachachon Co. Limited, Bangkok, 2001, p. 357.

2) Mahidol University Foundation, Kok Ya E-San, Amarin Printing, Bangkok, 2000, pp.103.

3) M. Kodpinid, C. Sadavongvivad, C. Thebtaranonth, Y. Thebtaranonth, Structures of *β*-senepoxide, tingtanoxide, and their diene precursors. Constituents of *Uvaria ferruginea,* Tetrahedron Lett. 24 (1983) 2019–2022.

4) S.D. Jolad, J.J. Hoffmann, K.H. Schram, J.R. Cole, M.S. Tempesta, R.B. Bates, Structures of zeylenol and zeylena, constituents of *Uvaria zeylanica* (Annonaceae), J. Org. Chem. 46 (1981) 4267–4272.

5) V.S. Parmar, O.D. Tyagi, A. Malhotra, S.K. Singh, K.S. Bisht, R. Jain, Novel constituents of *Uvaria* species, Nat. Prod. Rep. 11 (1994) 219–224.

6) Y.H. Liao, Z.M. Zou, J. Guo, L.Z. Xu, M. Zhu, S.L. Yang, Five polyoxygenated cyclohexenes from *Uvaria grandiflora*, J. Chin. Pharm. Sci. 9 (2000) 170–173.

7) X.P. Pan, R.-Y. Chen, D.Q. Yu, Polyoxygenated cyclohexenes from *Uvaria grandiflora*, Phytochemistry 47 (1988) 1063–1066.

8) G.X. Zhou, Y.J. Zhang, R.Y. Chen, D.Q. Yu, Three polyoxygenated cyclohexenes from *Uvaria calamistrata*, J. Asian Nat. Prod. Res. 12 (2010) 696–701.

9) A. Kijjoa, J. Bessa, M.M.M. Pinto, C. Anatachoke, A.M.S. Solva, G. Eaton, W. Herz, Polyoxygenated cyclohexene derivatives from *Ellipeiopsis cherrevensis*, Phytochemistry 59 (2002) 543–549.

10) L. Wirasathien, T. Pengsuparp, M. Moriysu, K. Kawanishi, R. Suttisri, Cytotoxic C-benzylated chalcone and other constituents of *Ellipeiopsis cherrevensis*, Arch. Pharm.Res. 29 (2006) 497–502.

11) C. Auranwiwat, P. Wongsomboon, T. Thaima, R. Rattanajak, S. Kamchonwongpaisan, A.C. Willis, W. Lie, S.G. Pyne, T. Limtharakul (nee Ritthiwigrom), 2-Phenylnaphthalenes and a polyoxygenated cyclohexene from the stem and root extracts of *Uvaria cherrevensis* (Annonaceae), Fitoterapia 120 (2017) 103–107.

12) M. Kodpinid, C. Sadavongvivad, C. Thebtaranonth, Y. Thebtaranonth, Benzyl benzoates from the roots of *Uvaria purpurea*, Phytochemistry 23 (1984) 199–200.

52

13) T.A. Yapi, J.B. Boti, B.K. Attioua, A.C. Ahibo, A. Bighelli, J. Casanova, F. Tomi, Three new natural compounds from the root bark essential oil from *Xylopia aethiopica*, Phytochem. Anal. 23 (2012) 651–656.

14) S.J. Kim, H.J. Kim, H.J. Kim, Y.P. Jang, M.S. Oh, D.S. Jang, New patchoulane-type sesquiterpenes from the rhizomes of *Cyperus rotundus*, Bull. Kor. Chem. Soc. 33 (2012) 3115–3118.

15) X.P. Pan, D.Q. Yu, Two polyoxygenated cyclohexenes from *Uvaria grandiflora*, Phytochemistry 40 (1995) 1079–1711.

16) Z.J. Ma, Z.K. Meng, P. Zhang, Chemical constituents from *Curcuma wenyujin*, Fitoterapia 80 (2009) 374–376.

17) M. Kodpinid, C. Thebtaranonth, Y. Thebtaranonth, Benzyl benzoates and O-hydroxybenzyl flavanones from *Uvaria ferruginea*, Phytochemistry 24 (1985) 3071–3072.

18) H.N. El-Sohly, W.L. Lasswell, C.D. Hufford, Two new C-benzylated flavanones from *Uvaria chamae* and ^{13}C NMR analysis of flavanone methyl ethers, J. Nat. Prod. 42 (1979) 264–270

5) Research Outcome

Publication

Lekphrom, R., Kanokmedhakul, K., Schevenels, F., Kanokmedhakul, S. Antimalarial polyoxygenated cyclohexene derivatives from the roots of *Uvaria cherrevensis*. Fitoterapia (2018) 217, 420-424.

Project 1I: Investigate on Roots of *Asparagus racemosus*

1) Keywords

Asparagus racemosus, spirosteroid saponin, spiro 20-norsteroid, α-glucosidase inhibitory

2) Objective

To investigate the chemical constituents and their α-glucosidase inhibitory from roots of *Asparagus racemosus*

3) Introduction

Asparagus racemosus, also well known as Shatarari, belongs to the family Asparagaceae and is commonly distributed in tropical and subtropical regions [1–2]. In several countries, *A. racemosus* which is an important herbal in Ayurvedic medicine, has been

used to treat various human disorders. In India, this plant is used to increase milk secretion in lactating women, to combat menopausal symptoms, and used with *Azardichta indica* to control blood sugar level [2]. Its roots have also been used as stimulant, anti-abortifacient and demulcent agents in India and Thailand [3]. Besides, the potent biological and pharmacological activities of *A. racemosus* have been reported, such as galactagogue effect, immunomodulatory activity, anticancer activity, cardiovascular effect, immunological activity, antidiabetic effect, and antioxidant activity [4]. Previous phytochemical investigation of fruits and roots of *A. racemosus* have identified the alkaloids [5–6] and steroid saponins [1,7–9]. To further biological investigation of compounds from roots of *A. racemosus* for α-glucosidase inhibitory was our focus.

4) Result and Discussion

Chromatographic separation of the extracts from the roots of *A. racemosus* obtained four new compounds, asparacosins B-E (**1I.1-4**), along with seven known compounds including asparacosin A (**1I.5**) [20], (25*R*)-12*β*-acetyl-17*α*-hydroxyspirost-4-en-3-one (**1I.6**) [20], nyasol (**1I.7**) [21], asparenydiol (**1I.8**) [20,22], 4-[5-(4-methoxyphenoxy)-3-penten-1-ynyl]phenol (**1I.9**) [22], 3"-methoxyasparenydiol (**1I.10**) [20], and stigmasterol [23]. Their sturctures are shown in Figure 1I.1.

Compound **1I.1** was obtained as colorless crystal and its molecular formula $C_{27}H_{42}O_5$ based on the ^{13}C NMR and HRESITOFMS at *m/z* 469.2923 [M + Na]$^+$ (calcd for $C_{27}H_{40}NaO_5$, 469.2930) data, implying seven degrees of unsaturation. The ^{13}C NMR and DEPT spectral data showed the presence of 27 carbons attributable to four methyls (δ_C 22.4, 17.0, 11.3, and 7.3), ten methylenes (δ_C 66.9, 42.2, 37.0, 36.9, 31.2, 30.7, 28.7, 28.0, 26.5, and 25.6), eight methines (δ_C 90.9, 71.7, 51.4, 45.2, 43.9, 39.5, 33.9, and 30.0), and five quaternary [δ_C 212.7 (C=O), 110.3, 90.6, 49.4, and 35.0] carbons. The ^{1}H NMR spectroscopic data displayed four methyl groups at δ_H 1.00 (3H, s, Me-19), 0.90 (3H, d, *J* = 7.2 Hz, Me-21), 0.78 (3H, s, Me-18), and 0.76 (3H, d, *J* = 6.4 Hz, Me-27), as well as two signals of oxymethine protons at δ_H 3.99 (1H, dd, *J* = 11.2, 4.8 Hz, H-12) and 3.96 (1H, t, *J* = 8.0 Hz, H-16). These NMR spectral data suggested that compound **1I.1** was a spirostane-type steroid [20,24] and similar to asparacosin A which isolated from *A.cochinchinensis* [20]. The main difference was the absence of alkene at C-4, and C-5 in **1I.1**. The ketone group was defined at δ_C 212.7 in ^{13}C NMR spectrum as well as the IR absorption band at V_{max} 1711 cm^{-1} (Supplementary data). The methylene signals appeared at δ_H 2.59 (1H, t, *J* = 14.0 Hz, H-4a) and δ_H 1.98 (1H, m, H-4b)/δ_C 42.2 (C-4), and a methine signal at δ_H 1.78 (1H, m)/δ_C 43.9 (C-5). These were supported by HMBC correlations of H-4 to C-3 (δ_C 212.7), C-5 (δ_C 43.9), C-6 (δ_C 26.5) and C-10 (δ_C 35.0); H-5 to C-6 (δ_C 26.5), C-9 (δ_C 39.5) and C-10 (δ_C 35.0). The hydroxyl group

at C-12 was assigned as β-oriented by coupling pattern of H-12 (dd, J = 11.2, 4.8 Hz) [20]. The absolute configurations of **1I.1** was assigned as 5*R*, 8*R*, 9*S*, 10*S*, 12*R*, 13*R*, 14*S*, 16*S*, 17*S*, 20*S*, 22*R*, 25*R* by a single crystal X-ray based on its anomalous dispersion data with the Flack parameter of - 0.02(9). Thus, compound **1I.1** defined as a new spirosteroid and was named asparacosin B.
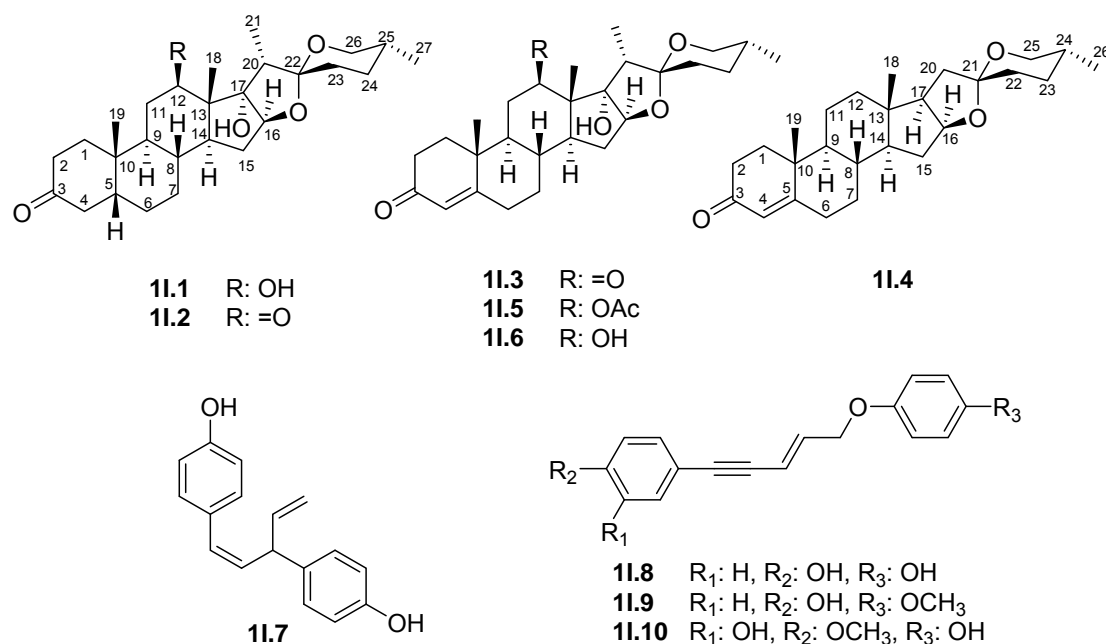

1I.1	R: OH
1I.2	R: =O

1I.3	R: =O
1I.5	R: OAc
1I.6	R: OH

1I.4

1I.8	R₁: H, R₂: OH, R₃: OH
1I.9	R₁: H, R₂: OH, R₃: OCH₃
1I.10	R₁: OH, R₂: OCH₃, R₃: OH

1I.7

Figure 1I.1. Isolated compounds from the roots of *Asparagus racemosus*

Compound **1I.2** had a molecular formula $C_{27}H_{40}O_5$ based on the ^{13}C NMR and HRESITOFMS at *m/z* 467.2779 [M + Na]$^+$ (calcd for $C_{27}H_{40}NaO_5$, 467.2773) data, revealing eight degrees of unsaturation. Comparison of its NMR spectroscopic data with those of **1I.1** suggested that a hydroxyl group at C-12 was oxidized to be a carbonyl group. The ^{13}C NMR spectral data revealed a signal of carbonyl carbon at δ_C 215.5. This was supported by HMBC correlations of H-14 (δ_H 2.38) and H-18 (δ_H 1.06) to C-12. The absolute configuration of **1I.2** was determined as 5*R*, 8*R*, 9*S*, 10*S*, 13*S*, 14*S*, 16*S*, 17*S*, 20*S*, 22*R*, and 25*R* by a single crystal X-ray analysis [Flack parameter of -0.08(18)]. Thus compound **1I.2**, an asparacosin C was elucidated as a new spirosteroid (Figure 1I.1).

Compound **1I.3** possessed a molecular formula $C_{27}H_{38}O_5$ by ^{13}C NMR and HRESITOFMS at *m/z* 465.2619 [M + Na]$^+$ (calcd for $C_{27}H_{38}NaO_5$, 465.2617) data, revealing nine degrees of unsaturation. The of ^{1}H and ^{13}C NMR spectral data of **1I.3** was similar to that of **1I.2**, except for the presence of an α,β-unsaturated ketone at δ_C 198.6 (C-3), $\delta_{H/C}$

5.47/124.7 (H/C-4), and δ_C 168.2 (C-5) in **1I.2**. The HMBC spectrum showed correlations of an olefinic proton H-4 to C-2 (δ_C 33.6), C-6 (δ_C 32.3), and C-10 (δ_C 38.6); H-1 (δ_H 2.65 and 1.86) and H-2 (δ_H 2.33) to C-3; H-6 (δ_H 2.43 and 2.33) to C-4 and C-5, and of H-10 (δ_H 1.23) to C-5 confirmed the location of those functional groups. The ECD spectrum of **1I.3** was similar to that of **1I.2** as well as its specific rotation was the same sign $[\alpha]_D^{19.8}$ –9.2° (*c* 0.1, MeOH) for **1I.3** and $[\alpha]_D^{19.6}$ –11.2° (*c* 0.1, MeOH) for **1I.2**. This indicates that **1I.2** and **1I.3** had the same absolute configuration. Thus compound **1I.3** was elucidated as a new spirosteroid and has been named asparacosins D (Figure 1I.1).

Compound **1I.4** had a molecular formula $C_{26}H_{38}O_3$ based on the ^{13}C NMR and HRESITOFMS at *m/z* 421.2716 $[M + Na]^+$ (calcd for $C_{26}H_{38}NaO_3$, 421.2719) data, indicating eight degrees of unsaturation. The ^1H and ^{13}C NMR spectral data showed resonance signals closely to that of **1I.3**, excepted for the absences of a ketone group at C-12, a hydroxyl group at C-17, and a methyl group at C-20. This supported by the IR absorption bands at V_{max} 2931 and 1677 cm^{-1} (Supplementary data), which indicates the characteristic of C-H and unsaturated C=O stretching, respectively. The NMR spectral data indicated that **1I.4** was an unusual steroid skeleton, 20-norsteroid [1]. It displayed signals of two methylene groups at $\delta_{H/C}$ 1.85 (m, H$_a$-20) and 1.70 (m, H$_b$-20)/37.0, and δ_H 1.69 (m, H$_a$-12) and 1.10 (m, H$_b$-12)/δ_C 39.0] and one methine [$\delta_{H/C}$ 2.16 (m, H-17)/54.6]. This assignment was confirmed by HMBC correlations of H-11 (δ_H 1.41), H-17 (δ_H 2.16), and H-18 (δ_H 0.78) to C-12; H-15 (δ_H 2.09) and H-18 to C-13; and H-17 (δ_H 2.16) to C-20. In addition, the COSY spectrum of **1I.4** showed the correlations of H-9↔H-11↔H-12; H-14↔H-15↔H-16↔H↔H-17↔H↔H-20 confirmed an occurring of two methylene groups at positions C-12 and C-20. The relative configuration of **1I.4** determined by the NOESY correlations between H-16 (δ_H 4.51) and H-14 (δ_H 1.16), H-14 and H-25β (δ_H 3.38). Finally, the absolute configuration of **1I.4** was determined by a single crystal X-ray analysis [Flack parameter of 0.04(7)] as 8*S*, 9*S*, 10*R*, 13*S*, 14*S*, 16*S*, 17*R*, 22*R*, and 25*R*. Thus compound **1I.4**, asparacosin D was elucidated as a new spiorosteroid 20-norsteroid.

All isolated compounds (**1I.1**–**1I.10**) were elucidated for their *α*-glucosidase inhibitory activity. Compounds **1I.7**–**1I.10** show high potential inhibition of *α*-glucosidase with IC$_{50}$ values in a range of 0.003–0.004 *µ*M which are stronger than positive control drug acarbose (171.47 µM). Unfortunately, all steroids were proved to be inactive with *α*-glucosidase inhibitory activity.

56

References

1) D. N., Quang, P., Nanthalath, V. A., Khamko, X., Soulinhong, V., Vidavone, Acemosin- a cytotoxic 20-norsteroid from *Asparagus racemosus*, Fitoterapia 131 (2018) 221–224.

2) S., Thakur, K. L., Tiwari, S. K., Jadhav, Approaches for conservation of an ethnomedicinal plant: *Asparagus racemosus* Wild, Online J. Biol. Sci. 15 (2015) 126–133.

3) F., Ikegami, Active constituents in Chinese, Ayurvedic and Thai herbal medicines: Applicable separation procedures, Thai J. Health Res. 19 (2005) 1–12.

4) P., Shaha, A., Bellankimath, Pharmacological profile of *Asparagus racemosus*: A review, Int. J. Curr. Microbiol. App. Sci. 6 (2017) 1215–1223.

5) T., Sekine, N., Fukasawa, Y., Kashiwagi, N., Ruangrungsi, I., Murakoshi, Structure of asparagamine A, a novel polycyclic alkaloid from *Asparagus racemosus*, Chem. Pharm. Bull. 42 (1994) 1360–1362.

6) T., Sekine, F., Ikegami, N., Fukasawa, Y., Kashiwagi, T., Aizawa, Y., Fujii, N., Ruangrungsi, I., Murakoshi, Structure and relative stereochemistry of a new polycyclic alkaloid, asparagamine A, showing anti-oxytocin activity, isolated from *Asparagus racemosus*, J. Chem. Soc., Perkin Trans. 1 (1995) 391–393.

7) P. Y., Hayes, A. H., Jahidin, R., Lehmann, K., Penman, W., Kitching, J. J., De Voss, Asparinins, asparosides, curillins, curillosides and shavatarins: structural clarification with the isolation of shatavarin V, a new steroidal saponin from the root of *Asparagus racemosus*, Tetrahedron Lett. 47 (2006) 8683–8687.

8) D., Mandal, S., Banerjee, N. B., Mondal, A. K., Chakravarty, N. P., Sahu, Steroidal saponins from the fruits of *Asparagus racemosus*, Phytochemistry 67 (2006) 1316–1321.

9) C., Onlom, W., Phromittayarat, W., Putalun, N., Waranuch, K., Ingkaninan, Immunoaffinity knockout of saponin glycosides from *Asparagus racemosus* to assess anti-lipid peroxidation, Phytochem. Anal. 28 (2017) 316–323.

10) T., Okimura, Z., Jiang, Y., Liang, K., Yamaguchi, T., Oda, Suppressive effect of ascophyllan HS on postprandial blood sugar level through the inhibition of α-glucosidase and stimulation of glucagon-like peptide-1 (GLP-1) secretion, Int. J. Biol. Macromol. 125 (2019) 453–458.

11) F. A., Al-Dhabaan, Kinetics of hypoglycemic α-glucosidase inhibitory protein, J. Pure Appl. Microbio. 12(2018) 119–126.

12) L., Xu, W., Li, Z., Chen, Q., Guo, C., Wang, R. K., Santhanam, H., Chen, Inhibitory effect of epigallocatechin-3-O-gallate on α-glucosidase and its hypoglycemic effect via targeting PI3K/AKT signaling pathway in L6 skeletal muscle cells, Int. J. Biol. Macromol. 125 (2019) 605–611.

13) Y. Y., Zhong, H. S., Chen, P. P., Wu, B. J., Zhang, Y., Yang, Q. Y., Zhu, C. G., Zhang, S. Q., Zhao, Synthesis and biological evaluation of novel oleanolic acid analogues as potential α-glucosidase inhibitors, Eur. J. Med. Chem. 164 (2019) 706–716.

14) G. M., Sheldrick, XT, Acta. Cryst. A71 (2015) 3–8.

15) O. V., Dolomanov, L. J., Bourhis, R. J., Gildea, J. A. K., Howard, H., Puschmann, Olex2: A complete structure solution, refinement and analysis program, J. Appl. Cryst. 42 (2009) 339–341.

16) G. M., Sheldrick, XL, Acta. Cryst. C71 (2015) 3–8.

17) Y. H., Song, D. W., Kim, M. J., Curtis-Long, C., Park, M., Son, J. Y., Kim, H. J., Yuk, K. W., Lee, K. H., Park, Cinnamic acid amides from *Tribulus terrestris* displaying uncompetitive α-glucosidase inhibition, Eur. J. Med. Chem. 114 (2016) 201–208.

18) I. G., Hwang, H. Y., Kim, K. S., Woo, J. T., Hong, B. Y., Hwang, J. K., Jung, J., Lee, H. S., Jeong, Isolation and characterisation of an α-glucosidase inhibitory substance from fructose-tyrosine Maillard reaction products, Food Chem. 127 (2011) 122–126.

19) Y. M., Kim, M. H., Wang, H. I., Rhee, A novel α-glucosidase inhibitor from pine bark, Carbohydr. Res. 339 (2004) 715–717.

20) H. J., Zhang, K., Sydara, G. T., Tan, C., Ma, B., Southavong, D. D., Soejarto, J. M., Pezzuto, H. H. S., Fong, Bioactive constituents from *Asparagus cochinchinensis*, J. Nat. Prod. 67 (2004) 194–200.

21) G. B., Marini-Bettolo, M., Nicoletti, I., Messana, C., Galeffi, J. D., Msonthi, W. A., Chapya, Research on African medicinal plants – X1: Glucosides of *Hypoxis nyasica* bak. The structure of nyasoside, a new glucoside biologically related to hypoxoside, Tetrahedron 41 (1985) 665–670.

22) K., Terada, C., Honda, K., Suwa, S., Takeyana, H., Oku, W., Kamisako, Acetylenic compounds isolated from cultured cells of *Asparagus officinalis*, Chem. Pharm. Bull. 43 (1995) 564–566.

23) P., Forgo, K. E., Kover, Gradient enhanced selective experiments in the ^{1}H NMR chemical shift assignment of the skeleton and side-chain resonances of stigmasterol, a phytosterol derivative, Steroids 69 (2004) 43–50.

5) Research Outcome

Manuscript will be submitted to Phytochemistry.

Tantapakula, C., Chaiyosanga, B., Suthiphasilp, V., Kanokmedhakul, K., Laphookhieo, S., Andersen, R.J., Patrick, B. O., Kanokmedhakul, S., Spirosteroid saponins and acetylenic derivatives with α-glucosidase inhibitory from *Asparagus racemosus* roots.

Project 1J: Investigate on Leaves and Stems of *Croton poomae* Esser

1) Keywords

anti-inflammatory, nitric oxide, *Croton poomae,* clerodane diterpenoids

3) Objective

To investigate the chemical constituents and their inhibition of nitric oxide (NO) production inhibitory from leaves and stems of *Croton poomae*

3) Introduction

Croton is a large genus in the Euphorbiaceae family. Many species have long been used as traditional medicines in Asia, Africa and South America (Salatino et al., 2007). Previous investigations of *Croton* have shown a wide range of secondary metabolites, such as alkaloids (Suárez et al., 2004), phenolics (Tala et al., 2013), terpenoids (Aguilar-Guadarrama and Rios, 2004; Kuo et al., 2013) and volatile oils (Cavalcanti et al., 2012; Silva-Alves et al., 2015). Some of these compounds display interesting biological activities, for example anti-inflammatory (Cordeiro et al., 2016; Kuo et al., 2013; Suárez et al., 2006; Yang et al., 2016), cytotoxic (Liu et al., 2014; Sommit et al., 2003; Zhang et al., 2013), antiviral (Wang et al., 2012), and antimicrobial (Liu et al., 2014). In Thailand, *Croton poomae* is locally known as "Plau Phu Wua", named after Phu Wua, the single locality where it is commonly found. *C. poomae* is a tree, 10 m in height, and widely distributed in the North-Eastern part of Thailand (Esser, 2002). Although *C. poomae* has been reported as a new species since 2002, its phytochemistry and biological activity have not been reported. Recently, there was a report of clerodane diterpenoids from the genus *Croton* that displayed nitric oxide (NO) inhibition (Zhang et al., 2017). Therefore, the investigation of *C. poomae* became a focus of our work.

4) Result and Dicussion

The *n*-hexane, EtOAc and MeOH extracts of dried leaves and stems of *C. poomae* were separated by silica gel column chromatography (CC), silica gel flash column chromatography (FCC) and Sephadex LH-20 column chromatography to yield two new clerodane diterpenoids, crotonolide K (**1J.1**) and furocrotinsulolide A acetate (**1J.2**) and eighteen known compounds (**1J.3**-**1J.20**). Structures of known compounds were identified by spectroscopic data measurements, as well as by comparing the data obtained with published values, as furocrotinsulolide A (**1J.3**) (Graikou et al., 2005), 3,4,15,16-diepoxy-cleroda-13(16),14-diene-12,17-olide (**1J.4**) (Pudhom and Sommit, 2011), 15,16-epoxy-3 β-hydroxy-5(10),13(16),14-ent-halimatriene-17,(12*S*)-olide (**1J.5**) (Aldhaher et al., 2017), crotonolide E (**1J.6**) (Liu et al., 2014), crotonolide F (**1J.7**) (Liu et al., 2014), 3β,4β:15,16-diepoxy-

13(16),14-clerodadiene (**1J.8**) (Harinantenaina et al., 2006), 1-hydroxy-guai-3,10(14)-diene (**1J.9**) (Ezzat and Motaal, 2012), spathulenol (**1J.10**) (Ragasa et al., 2003), 1β-hydroxy-4(15),5E,10(14)-germacratriene (**1J.11**) (Brown et al., 2003), scopoletin (**1J.12**) (Vasconcelos et al., 1998), fraxidin (**1J.13**) (Garcez et al., 1999), 4-hydroxy-3-methoxybenzaldehyde (**1J.14**) (Ito et al., 2001), *trans*-coniferyl aldehyde (**1J.15**) (Miyazawa and Hisama, 2003), sinapyl aldehyde (**1J.16**) (Hiltunen et. al., 2006), β-sitosterol (**1J.17**) stigmasterol (**1J.18**), stigmast-5-en-7-one (**1J.19**), and 7-oxo-β-sitosterol (**1J.20**) (Pettit et al., 2000) as shown in Figure 1J.1.

Compound **1J.1** had the molecular formula $C_{20}H_{26}O_4$ deduced from the ^{13}C NMR and HRESIMS, *m/z* 3.53.1729 [M + Na]$^+$ (calcd. for $C_{20}H_{26}O_4$ + Na, 353.1727), indicating eight degrees of unsaturation. The IR spectrum showed the presence of a hydroxyl group at 3488 cm^{-1}, the carbonyl of an ester group at 1720 cm^{-1} and alkenes at 1459 and 1373 cm^{-1}. The UV spectrum indicated an ester group at 210 nm. The ^1H and ^{13}C NMR spectroscopic data of **1J.1** were similar to those of a known isolated clerodane diterpenoid, 15,16-epoxy-3β-hydroxy-5(10),13(16),14-*ent*-halimatriene-17,(12S)-olide (**1J.5**) (Aldhaher et al., 2017). The main difference was the presence of the double bond at C-5/C-6 (in **1J.1**) instead of C-5/C-10 (in **1J.5**). This was confirmed by the appearance of two methine protons at δ_H 5.63, d, *J* = 6.1 Hz, H-6/δ_C 119.5 and δ_H 2.13, m, H-10/δ_C 44.2 in **1J.1**, as well as the HMBC correlations of H-10 to C-6 and C-20, and H-6 to C-4, C-7, C-8 and C-10. The resonance of H-3 as a broad singlet at δ_H 3.51 indicated a β-equatorial orientation (Graikou et. al., 2005) which was confirmed by the NOESY correlations between H-3 and H$_3$-18, and H$_3$-18 and H-10. The correlations between H-12 and H$_3$-20 revealed that these protons were in α-orientation. From the above evidence, the relative configuration of **1J.1** was assigned as the same as that of **1J.5** except H-3 (Aldhaher et al., 2017). Moreover, the absolute configuration of **1J.1** was determined by comparison of the experimental ECD with its calculated ECD spectra. The ECD calculations were generated for two selected possible stereoisomers, 3*R*, 8*R*, 9*R*, 10*R*, 12*S* and 3*S*, 8*S*, 9*S*, 10*S*, 12*R* using Gaussian09 with DFT B3LYP/6-311++G (d,p). The ECD experimental spectrum of **1J.1** corresponded to its calculated spectrum, therefore the absolute configuration of **1J.1** was assigned as 3*R*, 8*R*, 9*R*, 10*R*, 12*S*. Thus, **1J.1** was deduced as a new celodane diterpene, 15,16-epoxy-3α-hydroxy-5(6)13(16),14-*ent*-halimatriene-17,(12S)-olide and was named crotonolide K.

Compound **1J.2** had the molecular formula $C_{22}H_{30}O_6$, deduced from the ^{13}C NMR and HRESIMS, *m/z* 413.1941 [M + Na]$^+$ (calcd. for $C_{22}H_{30}O_6$ + Na, 413.1940), indicating eight degrees of unsaturation. The IR spectrum showed the absorption bands of hydroxyl (3433 cm^{-1}), ester carbonyl (1715 cm^{-1}), and alkene (1504 cm^{-1}) groups. The UV spectrum indicated
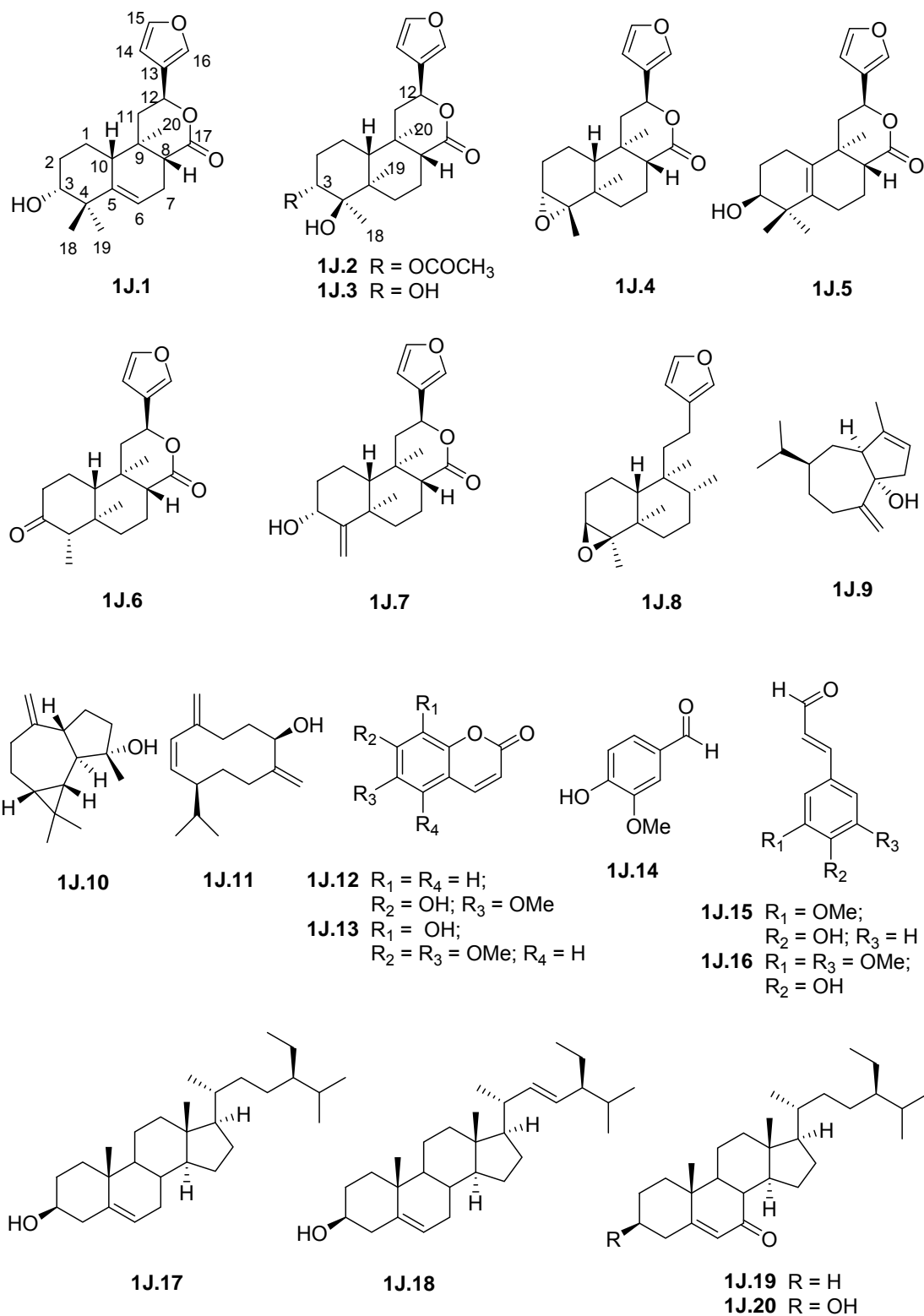
Figure 1J.1 Compounds isolated from leaves and stems of *Croton poomae* Esser

an ester group at 211 nm. The ^{1}H and ^{13}C NMR spectral data of **1J.2** were similar to those of the known isolated furocrotinsulolide A (**3**) (Graikou et al., 2005). However, the hydroxy group at C-3 in **1J.3** was replaced by an acetoxy group, which was confirmed by NMR resonances at δ_H 2.01, s/δ_C 22.8 and δ_C 170.2, and the high-field carbon signal of C-3 at δ_C 68.6. The resonance of H-3 at δ_H 4.73 appeared as a broad singlet, indicating a β-equatorial orientation of H-3 in **2J.2** was the same as those of **1J.1** and **1J.3** (Graikou et. al., 2005). The NOESY correlations between H-12 and H_3-20, H_3-18 and H_3-19, and H_3-19 and H_3-20 revealed that these protons were α-orientation, while the correlation between H-2β and H-3, H-2β and H-10, and H-8 and H-10 suggested the β-orientation of H-3, H-8 and H-10. Consequently, the relative configuration of **1J.2** was assigned to be the same as that of furocrotinsulolide A (**1J.3**) (Graikou et al., 2005). Furthermore, the absolute configuration of **1J.2** was assigned by comparison of the experimental ECD with its calculated ECD spectra of two selected possible stereoisomers (3*R*, 4*R*, 5*R*, 8*R*, 9*R*, 10*R*, 12*S* and 3*S*, 4*S*, 5*S*, 8*S*, 9*S*, 10*S*, 12*R*). The experimental ECD spectrum of **1J.2** was matched with its calculated ECD spectrum of 3*R*, 4*R*, 5*R*, 8*R*, 9*R*, 10*R*, 12*S* (Figure S5). Therefore, **1J.2** was identified as a new clerodane diterpenoid and was named furocrotinsulolide A acetate.

Compounds **1J.1-1J.8** were evaluated for their inhibition of NO production by LPS-induced RAW 264.7 macrophages. The results show that **1J.1**, **1J.2**, **1J.5**, **1J.7** and **1J.8** inhibited NO production with IC_{50} values of 46.43, 31.99, 48.85, 42.04, and 32.19 μM, respectively, which makes them more potent than the standard drugs, indomethacin (IC_{50} = 154.5 μM) and dexamethasone (IC_{50} = 56.28 μM). Compounds **1J.3**, **1J.4**, and **1J.6** showed weak inhibitory activity with IC_{50} values of 81.97, 86.98, and 74.78 μM, respectively.

References

Aguilar-Guadarrama AB, Rois MY. 2004. Three new sesquiterpenes from *Croton arboreous*. J Nat Prod. 67:914-917.

Aldhaher A, Langat M, Ndunda B, Chirchir D, Midiwo JO, Njue A, Schwikkard S, Carew M, Mulholland D. 2017. Diterpenoids from roots of *Croton dichogamus* Pax. Phytochemistry. 144:1-8.

Brown GD, Liang GY, Sy L-K. 2003. Terpenoids from the seeds of *Artemisia annua*. Phytochemistry. 64:303-323.

Cavalcanti JM, Leal-Cardoso JH, Diniz LRL, Portella VG, Costa CO, Linard FBM, Cecatto VM, Coelho-de-Souza AN. 2012. The essential oil of *Croton zehntneri* and *trans*-anethole improves cutaneous wound healing. J Ethanopharmacol. 144: 240-247.

Cordeiro KW, Felipe JL, Malange KF, Prado PR, Figueirdo PO, Garcez FR, Freitas KC, Garcez WS, Toffoli-Kadri MC. 2016. Anti-inflammatory and antinociceptive activities of *Croton urucurana* Baillon bark. J Ethanopharmacol. 183:128-135.

Esser HJ. 2002. *Croton poomae* (Euphorbiaceae), a new species from Thailand. Thai For Bull. 30:1-6.

Ezzat SM, Motaal AA. 2012. Isolation of new cytotoxic metabolites from *Cleome droserifolia* growing in Egypt. Z Naturforch. 67:266-274.

Garcez FR, Garcez WS, Martins M, Cruz AC. 1999. A bioactive lactone from *Nectandra gardneri*. Planta Med. 65:775.

Graikou K, Aligiannis N, Chinou I, Skaltsounis AL, Tillequin F, Litaudon M. 2005. Chemical constituents from *Croton insularis*. Helv Chim Acta. 88:2654-2660.

Harinantenaina L, Takahara Y, Nishizawa T, Kohchi C, Soma GI, Asakawa Y. 2006. Chemical constituents of Malagasy liverworts, Part V: prenyl bibenzyls and clerodane diterpenoids with nitric oxide inhibitiory activity from *Radula appressa* and *Thysananthus spathulistipus*. Chem Phar Bull. 54:1046-1049.

Hiltunen E, Pakkanen TT, Alvila L. 2006. Phenolic compounds in silver birch (*Berula pendula* Roth) wood. Holzforschung. 60:519-527.

Ito J, Chang FR, Wang HK, Park YK, Ikegaki M, Kilgore N, Lee KH. 2001. Anti-AIDS agents. 48. Anti-HIV activity of moronic acid derivatives and the new melliferone-related triterpenoid isolated from Brazilian propolis. J Nat Prod. 64:1278-1281.

Kuo PC, Yang ML, Hwang TL, Lai YY, Li YC, Thang TD, Wu TS. 2013. Anti-inflammatory diterpenoids from *Croton tonkinensis*. J Nat Prod. 76:230-236.

Liu CP, Xu JB, Zhao JX, Xu CH, Dong L, Ding J, Yue JM. 2014. Diterpenoids from *Croton laui* and their cytotoxic and antimicrocial activities. J Nat Prod. 77:1013-1020.

Miyazawa M, Hisama M. 2003. Antimutagenic activity of phenylpropanoids from Clove *Syzygium aromaticum*). J Agric Food Chem. 51:6413-6422.

Pettit GR, Numata A, Cragg GM, Herald DL, Takada T, Iwamoto C, Riesen R, Schmidt JM, Doudek DL, Goswami A. 2000. Isolation and structures of schleichrastatins 1-7 and schleicheols 1 and 2 from the teak forest medicinal tree *Schleichera oleosa*. J Nat Prod. 63:72-78.

Pudhom K, Sommit D. 2011. Clerodane diterpenoids and a trisubstituted furan from *Croton oblongifolius*. Phytochem Lett. 4:147-150.

Ragasa CY, Ganzon J, Hofileña J, Tamboong B, Rideout JA. 2003. A new furanoid diterpene from *Caesalpinia pulcherrima*. Chem Pharm Bull. 51:1208-1210.

Salatino A, Salatino MLF, Negri G. 2007. Traditional uses, Chemistry and Pharmacology of *Croton* species (Euphorbiaceae). J Braz Chem Soc. 18:11-33.

Silva-Alves KS, Ferreira-da-Silva FW, Coelho-de-Souza AN, Albuquerque AAC, Vale OC, Leal-Cardoso JH. 2015. Essential oil of *Croton zehntneri* and its main constituent anethole block excitability of rat peripheral nerve. Planta Med. 81:292-297.

Suárez AI, Blanco Z, Monache FD, Compagnone RS, Arvelo F. 2004. Three new glutarimide alkaloids from *Croton cuneatus*. Nat Prod Res. 18:421-426.

Suárez AI, Blanco A, Compagnone RS, Salazar-Bookaman MM, Zapata V, Alvarado C. 2006. Anti-inflammatory activity of *Croton cuneatus* aqueous extract. J Ethanopharmacol. 150:99-101.

Tala MF, Tan NH, Ndontsa BL, Tane P. 2013. Triterpenoids and phenolic compounds from *Croton macrostachyus*. Biochem Syst Ecolo. 51:138-141.

Vasconcelos JMJ, Silva AMS, Cavaleiro JAS. 1998. Chromones and flavanones from *Artemisia camoestris* subsp. *Maritima*. Phytochemistry. 49:1421-1424.

Wang GC, Li JG, Li GQ, Xu JJ, Wu X, Ye WC, Li YL. 2012. Clerodane diterpenoids from *Croton crassifolius*. J Nat Prod. 75:2188-2192.

Yang L, Zhang YB, Chen LF, Chen NH, Wu ZN, Jiang SQ, Jiang L, Li GQ, Li YL, Wang GC. 2016. New labdane diterpenoids from *Croton laui* and their anti-inflammatory activities. Bioorg Med Chem Lett. 26:4687-4691.

Zhang JS, Tang YQ, Huang JL, Li W, Zou YH, Tang GH. 2017. Bioactive diterpenoids from *Croton laevigatus*. Phytochemistry. 144:151-158.

Zhang XL, Wang L, Li F, Yu K, Wang MK. 2013. Cytotoxic phorbol esters of *Croton tiglium*. J Nat Prod. 76 ;858-864.

5) Research Outcome:

Publication

Project 2: Investigate on Two Fungi : *Apiospora montagnei* **and** *Botryotrichum*

piluliferum **and Two Plants:** *Miliusa velutina* **and** *Cissus rheifolia*

Researcher: Kwanjai Kanokmedhakul (Project Leader)

Project 2A: Investigate on the Fungus *Apiospora montagnei*

1) Keywords

Apiospora montagnei; xanthone; cytotoxicity.

2) Objective

To investigate the chemical constituents and their bioactivity from the fungus *Apiospora montagnei*

3) Introduction

The fungus *Apiospora montagnei* Sacc. belongs to the Apiosporaceae family (Klemke et al. 2004). It is the only species in the genus *Apiospora* that has been studied. Previous reports have shown that *A. montagnei* produces several secondary metabolites such as amide, coumarin (Alfatafta et al. 1994), isocoumarins (Ramos et al. 2013), cyclic peptides (Koguchi et al. 2000; Kohno et al. 2000), diterpene, monomethyl esters, polyketide and xanthone derivative (Klemke et al. 2004). Some of these compounds show antibacterial activity (Alfatafta et al. 1994), cytotoxicity (Klemke et al. 2004) and proteasome inhibitory activity (Kohno et al. 2000). Therefore, the chemical constituents and the biological activities of this fungus were our interests in this study.

4) Result and Discussion

Chromatographic separation of *n*-hexane, EtOAc and MeOH extracts yielded eight compounds. The new compound (**2A.1**) was determined by spectroscopic techniques (IR, UV, ^{1}H and ^{13}C NMR, 2D NMR, and MS), whereas the seven known compounds were identified by their physical properties and spectroscopic data measurements, as well as by comparing the data obtained with published values, as being methyl 8-hydroxy-3-methylxanthone-1-carboxylate (**2A.2**) (Li et al. 2011), methyl 8-hydroxy-6-methylxanthone-1-carboxylate (**2A.3**) (Kachi & Sassa 1986), ergosterol (**2A.4**) (Smith & Korn 1968), cyathisterone (**2A.5**) (Kawahara et al. 1994), ergosta-4,6,8(14),22-tetraen-3-one (**2A.6**) (Kawahara et al. 1994), calvasterone (**2A.7**) (Kawahara et al. 1994) and 2-hexyl-3-methylmaleic anhydride (**2A.8**) (Buttery et al. 1980) as shown in Figure 2A.1.

Compound **2A.1** was obtained as yellow needles, and its molecular formula, $C_{16}H_{12}O_6$, was deduced from HR-ESI-TOF-MS (*m/z* 301.0719 [M + H]$^+$). The IR spectrum
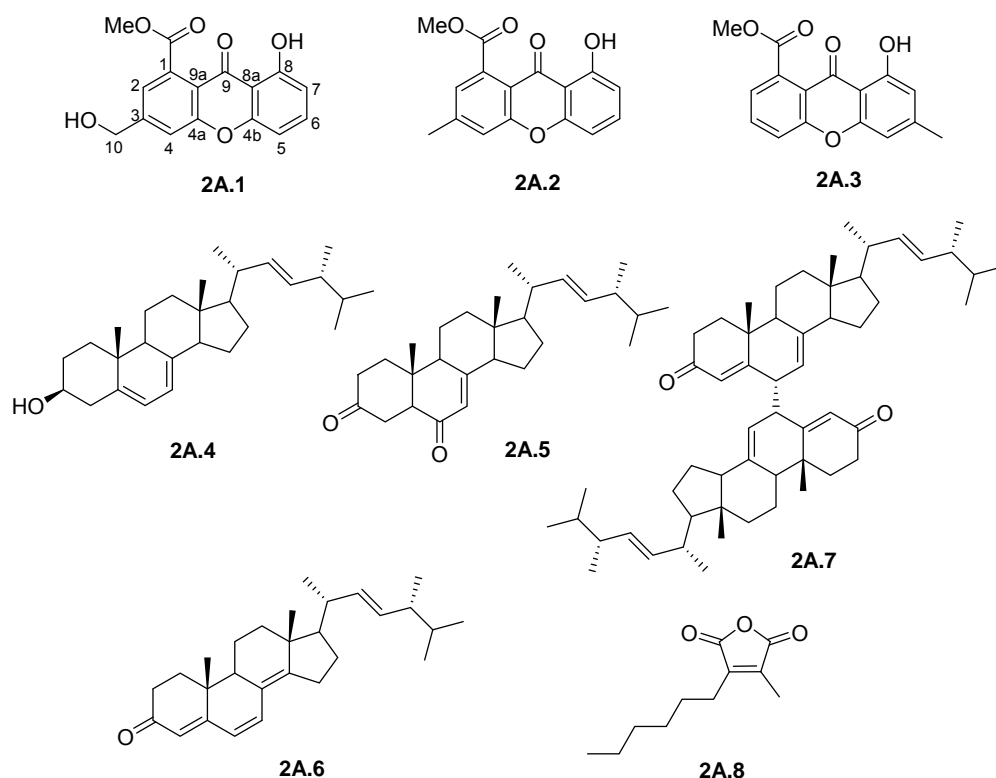
Figure 2A.1 Isolated compounds from the fungus *Apiospora montagnei.*

showed broad absorption bands at 3430 (hydroxyl), 1731 (carbonyl of ester), and 1650 (aromatic ketone) cm^{-1}. The UV spectrum exhibited adsorptions at 234, 259, 287, and 366 nm, which correspond to xanthone chromophores (Kachi & Sassa 1986; Tian et al. 2015; Daengrot et al. 2016). The ^{1}H NMR spectral data consisted of a chelated hydroxyl proton (δ_H 12.23, 1H, s, 8-OH), a set of *meta*-coupled aromatic protons [δ_H 7.53 (1H, brs, H-4) and 7.26 (1H, brs, H-2)], and a set of 1,2,3-trisubstituent aromatic protons [δ_H 7.57 (1H, t, J = 8.4 Hz, H-6), 6.88 (1H, d, J = 8.4 Hz, H-5), and 6.80 (1H, d, J = 8.4 Hz, H-7)]. The latter was confirmed by COSY correlations between H-5↔H-6↔H-7. Moreover, the 1H NMR spectrum of **1** also exhibited the characteristic signals of methyl ester [δ_H 4.01 (3H, s, CO2Me)] and oxymethylene protons [δ_H 4.85 (2H, s, H-10)]. The HMBC spectrum showed correlations of the H-2 (δ_H 7.26) and OMe (δ_H 4.01) to the carbonyl of ester (δ_C 169.6), and H-10 to C-2 (δ_C 120.5) and C-4 (δ_C 116.3), confirming the methylester and hydroxymethyl units were located at C-1 and C-3, respectively. The COSY and HMBC correlations data confirmed the sturture. Therefore, compound **2A.1** was assigned as a new methyl 8-hydroxy-3-hydroxy methylxanthone-1-carboxylate.

Compounds **2A.1**, **2A.2**, **2A.5**, **2A.6** and **2A.8** were evaluated for their biological activities. All compounds were inactive towards antimalarial test. The results showed that compound **2A.5** exhibited weak cytotoxicity against the NCI-H187 cell line with an IC$_{50}$ value

of 14.80 μM, whereas compound **2A.6** showed weak cytotoxicity against KB and NCI-H187 cell lines with IC$_{50}$ values of 48.10 and 58.80 μM, respectively.

References

Alfatafta AA, Gloer JB, Scott JA, Malloch D. 1994. Apiosporamide, a new antifungal agent from the coprophilous fungus *Apiospora montagnei*. J Nat Prod. 57:1696-1702.

Buttery RG, Seifert RM, Haddon WF, Lundin RE. 1980. 2-Hexyl-3-methylmaleic anhydride: an unusual volatile component of raisins and almond hulls. J Agric Food Chem. 28:1336-1338.

Daengrot C, Rukachaisirikul V, Tadpetch K, Phongpaichit S, Bowornwiriyapan K, Sakayaroj J, Shen X. 2016. Penicillanthone and penicillidic acids A-C from the soil-derived fungus *Penicillium aculeatum* PSU-RSPG105. RSC Adv. 6:39700-39709.

Kachi H, Sassa T. 1986. Isolation of moniliphenone, a key intermediate in xanthone biosynthesis from *Monilinia fructicola*. Agric Biol Chem. 50:1669-1671.

Kawahara N, Sekita S, Satake M. 1994. Steroids from *Calvatia cyathiformis*. Phytochemistry. 37:213-215.

Klemke C, Kehraus S, Wright AD, Konig GM. 2004. New secondary metabolites from the marine endophytic fungus *Apiospora montagnei*. J Nat Prod. 67:1058-1063.

Koguchi Y, Kohno J, Nishio M, Takahashi K, Okuda T, Ohnuki T, Komatsubara S. 2000. TMC-95A, B, C, and D, novel proteasome inhibitors produced by *Apiospora montagnei* Sacc. TC 1093. J Antibiot. 53:105-109.

Kohno J, Koguchi Y, Nishio M, Nakao K, Kuroda M, Shimizu R, Ohnuki T, Komatsubara S. 2000. Structures of TMC-95A-D: novel proteasome inhibitors from *Apiospora montagnei* Sacc. TC 1093. J Org Chem. 65:990-995.

Li C, Zhang J, Shao C, Ding W, She Z, Lin Y. 2011. A new xanthone derivative from the co-culture broth of two marine fungi (strain No. E33 and K38). Chem Nat Compd. 47:382-384.

Ramos HP, Simão MR, de Souza JM, Magalhães LG, Rodrigues V, Ambrósio SR, Said S. 2013. Evaluation of dihydroisocoumarins produced by the endophytic fungus Arthrinium state of *Apiospora montagnei* against *Schistosoma mansoni*. Nat Prod Res. 27:2240–2243

Smith FR, Korn ED. 1968. 7-Dehydrostigmasterol and ergosterol: the major sterols of an amoeba. J Lipid Res. 9:405-408.

Tian Y, Qin X, Lin X, Kaliyaperumal K, Zhou X, Liu J, Ju Z, Tu Z, Liu Y. 2015. Sydoxanthone C and acremolin B produced by deep-sea-derived fungus *Aspergillus* sp. SCSIO Ind09F01. J Antibiot. 68:703-706.

5) Research Outcome

Publication

Arthan, S.; Tantapakul, C.; Kanokmedhakul, K.; Soytong, K.; Kanokmedhakul, S. 2017**.** A new xanthone from the fungus *Apiospora montagnei* Natural Product Research, 31, 1766–1771.

Project 2B: Investigate on the Fungus _Botryotrichum piluliferum_

 1) Keywords

Botryotrichum piluliferum, Chaetomiaceae, sterigmatocystin, mycotoxin cytotoxicity**.**

2) Objective

To investigate the chemical constituents and their bioactivity from the fungus _Botryotrichum piluliferum_

3) Introduction

The fungus _Botryotrichum piluliferum_ belongs to the family Chaetomiaceae. Colonies grown on potato dextrose agar are white when young and turn pale brown when mature, at 30 °C in 7 days, with septate mycelia, branches, and setae. Conidia are chain-like on hyaline conidiophores, globose, 12.50-15.50 μm diameter, with irregularly thick walls of 3.0-3.5 μm. Teleomorphs were not found in this isolate. It was morphologically identified according to Domsch et al.[1] and Downing.[2] The fungus _B. piluliferum_ has been reported as one of the seedborne fungi of chili pepper.[3] Previous chemical investigation on the genus Botryotrichum has reported it to contain asterriquinone CT2 from _Botryotrichum_ spp.[4] and botryolides A-E,[5] decarestrictine D,[5] and sterigmatocystin from _Botryotrichum_ sp. (NRRL38180). However, no studies on the chemical constituents and bioactivity of _B. piluliferum_ have been found. Many fungi such as _Aspergillus_ species,[6] _Aschersonia coffeae_ Henn. BCC 28712,7 and _Penicillium chrysogenum_[8] including _Botryotrichum_ sp. (NRRL 38180) have been reported to produce mycotoxins. Mycotoxins have been reported as mutagenic and having carcinogenic effects in animals and humans.[9,10] In our continuing investigation on bioactive metabolites from fungi isolated from Thai soil, crude n-hexane and EtOAc extracts of _B. piluliferum_ displayed cytotoxicity against the KB cell line with 85.5 and 59.7% inhibition, respectively, at a concentration of 50 μg/mL. Moreover, the EtOAc extract presented cytotoxicity toward the MCF-7 cell line with 57.5% inhibition.

4) Result and Discussion

The chromatographic separation of biomass powder of _B. piluliferum_ gave two new sterigmatocystin derivatives, **2B.1** and **2B.2**, and nine known compounds, **2B.3**-**2B.11** (Figure **2B.1**). Their structures were identified by spectroscopic data and by comparing the data obtained to those of related known compounds published in the literature. They were oxisterigmatocystins E and F (**2B.1** and **2B.2**, respectively), oxisterigmatocystins G and H (**2B.3** and **2B.4**, respectively), sterigmatocystin (**2B.5**),[16] N-0532B (**2B.6**),17 O-methyl

sterigmatocystin (**2B.7**), N-0532A (**2B.8**),[17] 6-O-methylversicolorin A (**2B.9**), 6,8-O-dimethyl versicolorin A (**2B.10**),[19] and 8-O-methylaverufin (**2B.11**)[7] as shown in Fiure 2B.1.

Compounds **2B.1** and **2B.2** had the molecular formula $C_{21}H_{17}ClO_8$, derived from ^{13}C NMR and HR-ESI-TOFMS, signifying indices of hydrogen deficiency. The IR spectra of compounds **2B.1** and **2B.2** showed absorption bands for ester (1749/1752 cm^{-1}), aromatic ketone (1664/1659 cm^{-1}), and aromatic (1418/1452 cm^{-1}) groups. The ^{13}C NMR and DEPT spectra of these two compounds indicated 21 carbon signals attributable to 3-methyls (2 methoxy and an acetoxy group), a methylene, 3 sp2 methines, 3 sp3 methines, and 11 sp2
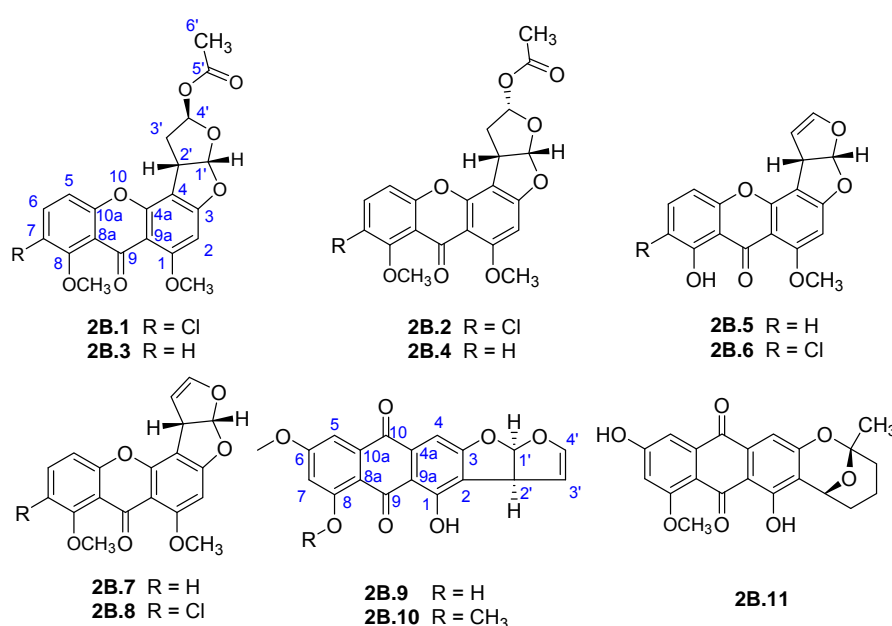
Figure 2B.1. Structures of the isolated compounds **2B.1**-**2B.11**.

quaternary (including two carbonyl) carbons. The ^{1}H and ^{13}C NMR spectroscopic data of **2B.1** agreed with those of isolated N-0532A (**2B.8**),[17] except that the double bond at C-3′ was saturated by a proton at C-3′ [$\delta_{H/C}$ 2.55 (m, H2-3′)/37.1] and an acetoxy group at C-4′ [$\delta_{H/C}$ 2.11(s)/21.2, δ_C 169.8]. The three resonances of aromatic protons appeared at δ 6.38 (s, H-2), 7.08 (d, J = 9.0 Hz, H-5), and 7.58 (d, J = 9.0 Hz, H-6). Correlations of H-1′/H-2′/H2-3′/H-4′ in the COSY spectrum confirmed the lack of a double bond at C-3′ of the bishydrofuran unit. The HMBC also indicated the connectivity of an acetoxy group through C-4′ by showing correlations of H3-6′ to C-5′ and C-4′ and H-4′ to C-5′. The ^{1}H and ^{13}C NMR spectroscopic data of **2B.2** were similar to those of 2B.1, except that the resonance of methyl protons of the acetoxy group at C-4′ of **2B.2** (δ 1.69) appeared at a higher field than that of **2B.1** (δ 2.11). The coupling constants between H-1′ and H-2′ (J = 6.0 Hz) and the NOESY correlations of

the two protons of **2B.1** and **2B.2** revealed a *cis* ring fusion, the same as in the sterigmatocystin (**2B.5**),[18] which allowed assignment of the absolute configurations at both C-1′ and C-2′ as S. The assignment of configurations at C-4′ of **2B.1** and **2B.2** as R and S were determined by comparing the ^{1}H NMR resonances of an acetoxy group to those reported for related analogues, dothistromin pentaacetate and oxisterigmatocystin D. The methyl protons of the 4′-acetoxy group of **2B.2** appeared at a higher field (δ_H 1.69) than in **2B.1** (δ_H 2.11), agreeing with that reported for endo dothistromin pentaacetate (δ_H 1.67) which was due to the strong shielding effect of xanthone. Furthermore, the optical rotation value of **2B.1** was different from that of **2B.2**, suggesting the different configurations at C-4′ of the two compounds. On the basis of the above evidence, the structure of **2B.1**, oxisterigmatocystin E, was determined as a new sterigmatocystin derivative and compound **2B.2**, oxisterigmatocystin F, was identified as the C-4′ epimer of **2B.1**.

Compounds **2B.3** and **2B.4** possessed a molecular formula of $C_{21}H_{18}O_8$ from ^{13}C NMR and HR-ESI-TOFMS, indicating 13 degrees of hydrogen deficiency. IR spectra of both **2B.3** and **2B.4** showed bands for ester (1752/1752 cm^{-1}), aromatic ketone (1659/1659 cm^{-1}), and aromatic (1462/1471 cm^{-1}) groups. The ^{1}H NMR, ^{13}C NMR, and DEPT spectroscopic data of **2B.3** were similar to those of **2B.1**, except for the presence of an additional sp2 methine proton at C-7 [δ_H 6.75 (d, J = 8.4 Hz, H-7)]. This information, together with the absence of Cl isotope in the MS data, established that the chlorine atom was displaced by an sp2 methine proton. The COSY spectrum showed correlations of H-5/H-6/H-7, indicating trisubstitution of the aromatic ring. The HMBC spectrum of **2B.3** clearly demonstrated correlations of H-7 to C-8a and C-5, H-6 to C-8 and C-10a, and H-5 to C-7, C-8a, and C-10a, confirming the structure of **2B.3**. Because the resonances of acetoxy groups of **2B.3** (δ_H 2.10) and **2 B.4** (δ_H 1.67) appeared at low and high fields in the same manner as those of **2B.1** and **2B.2**, the configurations at C-4′ of **2B.3** and **2B,4** were assigned as *R* and *S*, respectively. Moreover, the optical rotation values of them were comparable to those of **2B.1** and **2B.2**, respectively. This is the first isolation of compounds **2B.3** and **3B.4** from a natural source, and they have been named oxisterigmatocystin G (**2B.3**) and oxisterigmatocystin H (**2B.4**).

Compound **2B.9** had the molecular formula $C_{19}H_{12}O_7$, deduced from ^{13}C NMR and R-ESI-TOFMS, requiring 14 degrees of hydrogen deficiency. The IR spectrum displayed absorption bands for aromatic ketones (1629 and 1613 cm^{-1}) and aromatic (1579 cm^{-1}) groups. The ^{13}C NMR and DEPT spectra displayed 19 carbon signals for a methoxy, 5 sp2 methines, 2 sp3 methines, and 11 sp2 quaternary (including two carbonyl) carbons. Careful examination of 1D and 2D NMR data indicated that the structure of **2B.9** was similar to that of

6,8-O-dimethylversicolorin A, which has been previously reported as a methylation product of versicolorin A. The HMBC spectrum revealed correlations of hydroxyl proton at C-8 to C-7, C-8, and C-8a, onfirming the position of the hydroxyl group at C-8. Besides, the correlations of H-4 to C-2, C-3, C-10, and C-9a, H-5 to C-7, C-8a, and C-10, H-7 to C-5, C-6, C-8, and C-8a, H-1′ to C-3, C-2′, C-3′, and C-4′, H-3′ to C-1′ and C-2′ H-4′ to C-2′, methoxyl protons at C-6 to C-6, and hydroxyl proton (OH-1) to C-1, C-2, and C-9a indicated the structure of **2B.9**. The absolute configuration of **2B.9** was assigned to be the same as that of 6,8-O-dimethylversicolorin A (**2B.10**) by comparing their optical rotations, -320 (c 0.12, dioxane) for 1019 and -312.8 (c 0.1, CHCl3) for **2B.9**. Thus, this is the first report of 6-O-methylversicolorin A (**2B.9**) isolated from a natural source.

Compounds **2B.1**, **2B.3**, and **2B.4** showed antimalarial activity against *P. falciparum* with IC_{50} values of 7.9, 14.7, and 23.9 μM, respectively. Compounds 1-4 exhibited cytotoxicity against three cancer cell lines (KB, MCF-7, and NCI-H187) with IC_{50} values ranging from 3.5 to 78.6 M. Compound **2B.3** showed significant cytotoxicity against KB cells with an IC50 value of 3.5 μM, which is lower than that of the control drug ellipticine. Furthermore, **2B.3** was cytotoxic against the MCF-7 cell line with 0an IC_{50} value of 6.9 μM, which is lower than that of the control drug doxorubicin. However, **2B.3** was highly cytotoxic toward the normal cell line (*Vero* cell) with an IC_{50} value of 1.6 μM, which is lower than the that of the control drug ellipticine, 2.5 μM. Among compounds **2B.1** - **2B.4**, the influence of an exo versus an endo arrangement was noted. The exo arrangements in **2B.1** and **2B.3** showed both higher antimalarial activity and cytotoxicity against cancer cells than their endo analogues, **2B.2** and **2B.4**. It should be noted that the missing double bond at C-3′ and the presence of an acetoxy group at C-4′ of sterigmatocystin derivatives **2B.1**-**2B.4** would play important roles for cytotoxicity enhancement when compared to derivatives 2B.5−**2B.8**. Moreover, the double bond at C-3′ and C-4′ of sterigmatocystin derivatives **2B.5−2B.8** exhibited no cytotoxicity (>100 μM) toward KB and MCF-7, which corresponds to the results for related structures in a previous paper. In addition, compounds **2B.9** and **2B.10** showed strong cytotoxicity against the NCI-H187 cell line with IC_{50} values of 2.1 and 0.38 μM, respectively, which were lower than that of the control drug ellipticine. By comparison between compounds **2B.9** and **2B.10**, the presence of a methoxy group at C-8 led to a decrease in cytotoxicity toward normalcells. Interestingly, compound **2B.10** was not cytotoxic against *Vero* cells and should be further studied in detail. However, most of the isolated compounds showed cytotoxicity against Vero cells with IC_{50} values in the range from 0.65 to 12.3 μM. Sterigmatocystin (**2B.5**) has been reported to contaminate foodstuffs such as wheat, rice, coffee bean, corn, and red pepper.

Furthermore, it has been discovered in cheese contaminated with *Aspergillus versicolor*. On the basis of our results, most isolated compounds from *B. piluliferum* are mycotoxins with structures metabolically related to the aflatoxin carcinogen. These mycotoxins could be responsible for the toxicity of the fungus *B. piluliferum*. As mentioned above, the fungus *B. piluliferum* was found in the seeds of chili pepper and so the contamination of *B. piluliferum* in the food chain and agricultural soil should be monitored.

References

1) Domsch, K. H.; Gams, W.; Anderson, T.-H. Compendium of Soil Fungi, 1st ed.; IHW-Verlag: Eching, Germany, 1993; 859 pp.

2) Downing, M. H. *Botryotrichum* and *Coccospora*. Mycologia 1953, 45, 934−940.

3) Chigoziri, E.; Ekefan, E. J. Seed borne fungi of chili pepper (*Capsicum frutescens*) from pepper producing areas of Benue State, Nigeria. Agric. Biol. J. North Am. 2013, 4, 370−374.

4) Mocek, U.; Schultz, L.; Buchan, T.; Baek, C.; Fretto, L.; Nzerem, J.; Sehl, L.; Sinha, U. Isolation and structure elucidation of five new asterriquinones from *Aspergillus, Humicola* and *Botryotrichum* species. J. Antibiot. 1996, 49, 854-859.

5) Sy, A. A.; Swenson, D. C.; Gloer, J. B.; Wicklow, D. T. Botryolides A−E, decarestrictine analogues from a fungicolous *Botryotrichum* sp. (NRRL 38180). J. Nat. Prod. 2008, 71, 415−419.

6) Jurjev0ic, Ž.; Peterson, S. W.; Solfrizzo, M.; Peraica, M. Sterigmatocystin production by nine newly described *Aspergillus* species in section *Versicolores* grown on two different media. Mycotoxin Res. 2013, 29, 141-145.

7) Kornsakulkarn, J.; Saepua, S.; Srichomthong, K.; Supothina, S.; Thongpanchang, C. New mycotoxins from the scale insect fungus *Aschersonia coffeae* Henn. BCC 28712. Tetrahedron 2012, 68, 8480−8486.

8) Maskey, R. P.; Grün-Wollny, I.; Laatsch, H. Isolation, structure elucidation and biological activity of 8-O-methylaverufin and 1,8-Odimethylaverantin as new antifungal agents from *Penicillium chrysogenum*. J. Antibiot. 2003, 56, 459-463.

9) Veršilovskis, A.; De Saeger, S. Sterigmatocystin: occurrence in foodstuffs and analytical methods - an overview. Mol. Nutr. Food Res. 2010, 54, 136-147.

10) Mori, H.; Kawai, K.; Ohbayashi, F.; Kuniyasu, T.; Yamazaki, M.; Hamasaki, T.; Williams, G. M. Genotoxicity of a variety of mycotoxins in the hepatocyte primary culture/DNA repair test using rat and mouse hepatocytes. Cancer Res. 1984, 44, 2918-2923.

11) Rajachan, O.-A.; Kanokmedhakul, S.; Kanokmedhakul, K.; Soytong, K. Bioactive depsidones from the fungus *Pilobolus heterosporous*. Planta Med. 2014, 80, 1635-1640.

12) Trager, W.; Jensen, J. B. Human malaria parasites in continuous culture. Science 1976, 193, 673−675.

72

13) Desjardins, R. E.; Canfield, C. J.; Haynes, J. D.; Chulay, J. D. Quantitative assessment of antimalarial activity *in vitro* by a semiautomated microdilution technique. Antimicrob. Agents Chemother. 1979, 16, 710-718.

14) O'Brien, J.; Wilson, I.; Orton, T.; Pognan, F. Investigation of the Alamar Blue (resazurin) fluorescent dye for the assessment of mammalian cell cytotoxicity. Eur. J. Biochem. 2000, 267, 5421-5426.

15) Hunt, L.; Jordan, M.; De Jesus, M.; Wurm, F. M. GFP expressing mammalian cells for fast, sensitive, noninvasive cell growth assessment in a kinetic mode. Biotechnol. Bioeng. 1999, 65, 201-205.

16) Fremlin, L. J.; Piggott, A. M.; Lacey, E.; Capon, R. J. Cottoquinazoline A and cotteslosins A and B, metabolites from an Australian marine-derived strain of *Aspergillus versicolor*. J. Nat. Prod. 2009, 72, 666-670.

17) Nishino, Y.; Takawa, N.; Mitsumori, N.; Seki, T. Chemical compound N-0532, the manufacturing method and application. Jpn. Kokai Tokkyo Koho, JP 11080162 A, March 26, 1999.

18) Cox, R. H.; Cole, R. J. Carbon-13 nuclear magnetic resonance studies of fungal metabolites, aflatoxins, and sterigmatocystins. J. Org.Chem. 1977, 42, 112−114.

19) Hatsuda, Y.; Hamasaki, T.; Ishida, M.; Kiyama, Y. 6,8-ODimethylversicolorin A, a new metabolite from *Aspergillus versicolor*. Agric. Biol. Chem. 1971, 35, 444.

5) Research Outcome

Publication

Project 2C: Investigate on Leaves of *Miliusa velutina*

1) Keywords

Miliusa velutina, antimalarial, cytotoxicity

3) Objective

To investigate the chemical constituents and their bioactivity from leaves of *Miliusa velutina*

3) Introduction

Miliusa velutina (Dunal) Hook. f. & Thomson belongs to the family Annonaceae. This plant is found widely in Thailand with local names ''Khang hua mu" or "Kong kang". A water decoction of the wood is used traditionally as a tonic and an aphrodisiac.[1] The genus *Miliusa*

comprises ca. 50 species distributed from India, South East Asia, to Australia. At least 19 species of *Miliusa*, have been found in Thailand.[2,3] Eight of the *Miliusa* genera growing worldwide have been investigated for their phytochemistry and biological activities.[4-19] Among these species, a Thai medicinal plant, *M. velutina*, has been shown to contain the acetogenin, goniothalamusin,[17] an aporphine alkaloid, (+)-isocorydine α-*N*-oxide,[18] and four alkaloids, reticuline, liriodenine, norcorydine, and isocorydine.[19] Recently, the isolation and characterization of the linear acetogenins, cananginones A-I from the stem bark of *M. velutina* were reported.[20,21] In a continued investigation of this plant, the crude *n*-hexane and EtOAc extracts from the leaves of this plant were found to exhibit activity towards *Mycobacterium tuberculosis* with 99.6 and 98.9% inhibition at a concentration of 50 *μ*g/mL, respectively.

4) Result and Discussion

Chromatographic fractionation of n-hexane and EtOAc extracts yielded eight new bicyclic lactones, velutinones A–H (**2C.1**–**2C.8**), three cyclobutane dimers, velutinindimers A–C (**2C.9**–**2C.11**), and four known compounds (**2C.12**–**2C.15**), kawapyrone, yangonin (**2C.12**), three flavonoids, sakuranetin (**2C.13**), 7-O-methyleriodictyol (**2C.14**) and rhamnetin (**2C.15**), and an acetogenin, cananginone H (**2C.16**) (Figure 2C.1).

The IR spectra of **2C.1**–**2C.4** showed absorption bands of a glactone moiety at (1789–1771 cm^{-1}) and a conjugated carbonyl functionality (1685–1862 cm^{-1}) similar to the absorption bands of a synthetic bicyclic cyclohexenone.

Compound **2C.1** possessed the molecular formula $C_{18}H_{24}O_3$ based on the ^{13}C NMR and HRESITOFMS (m/z 311.1611 [M + Na]$^+$) data, indicating seven indices of hydrogen deficiency. The ^1H NMR data had resonances at δ 2.48 (d, *J* = 17.4 Hz, H-2a), 2.39 (d, 17.4 Hz, H-2b), 2.52 (s, 2H, H-3), 6.17 (dd, *J* = 10.3, 1.2 Hz, H-5), 6.75 (dd, *J* = 10.3, 3.3 Hz, H-6), and 4.87 (dd, *J* = 3.3, 1.2 Hz, H-6a). The ^{13}C NMR data, DEPT, and HMQC experiments indicated seven resonances which were associated with an α,β-unsaturated carbonyl (δ 196.2/C-4), a lactone carbonyl (δ 174.2/C-1), two olefinic (δ 131.2/C-5 and 141.4/C-6), two methylene (δ 38.9/C-2 and 42.6/C-3), one methine (δ 77.8/C-6a), and one quaternary (δ 44.7/C-2a) carbons. Interpretation of the COSY and HMBC correlations indicated that **2C.1** has a core structure of a five-membered lactone ring fused to an α,β-unsaturated cyclohexanone ring. This arrangement is similar to that of a compound isolated from the fruit kernels of *Otoba parvifolia* and from a total synthesis of its core structure, except for the side chain at C-2a which was replaced by a geranyl moiety in **2C.1**. This geranyl side chain ($C_{10}H_{17}$) was evident from the ^1H and ^{13}C NMR spectroscopic data. The COSY spectrum

showed the connectivity of the geranyl side chain by correlations between H-1′ and H-2′, and amongst H-4′, H-5′ and H-6′. The HMBC spectrum exhibited correlations of H-1′ to C-2, C-3, C-2a, C-6a, C-2′ and C-3′; H-2′ to C-2a, C-1′, C-3′, C-4′, and C-10′; H-4′ to C-2′, C-3′, C-5′, C-6′ and C-10′; H-6′ to C-4′, C-5′, C-8′, and C-9′ indicating that the geranyl group was linked to the stereogenic quaternary carbon C-2a. The relative configuration at C-2a and C-6a was established as syn from the NOESY correlation of H-6a and H-1′. Based on the above evidence, the new compound **2C.1** has been named velutinone A.
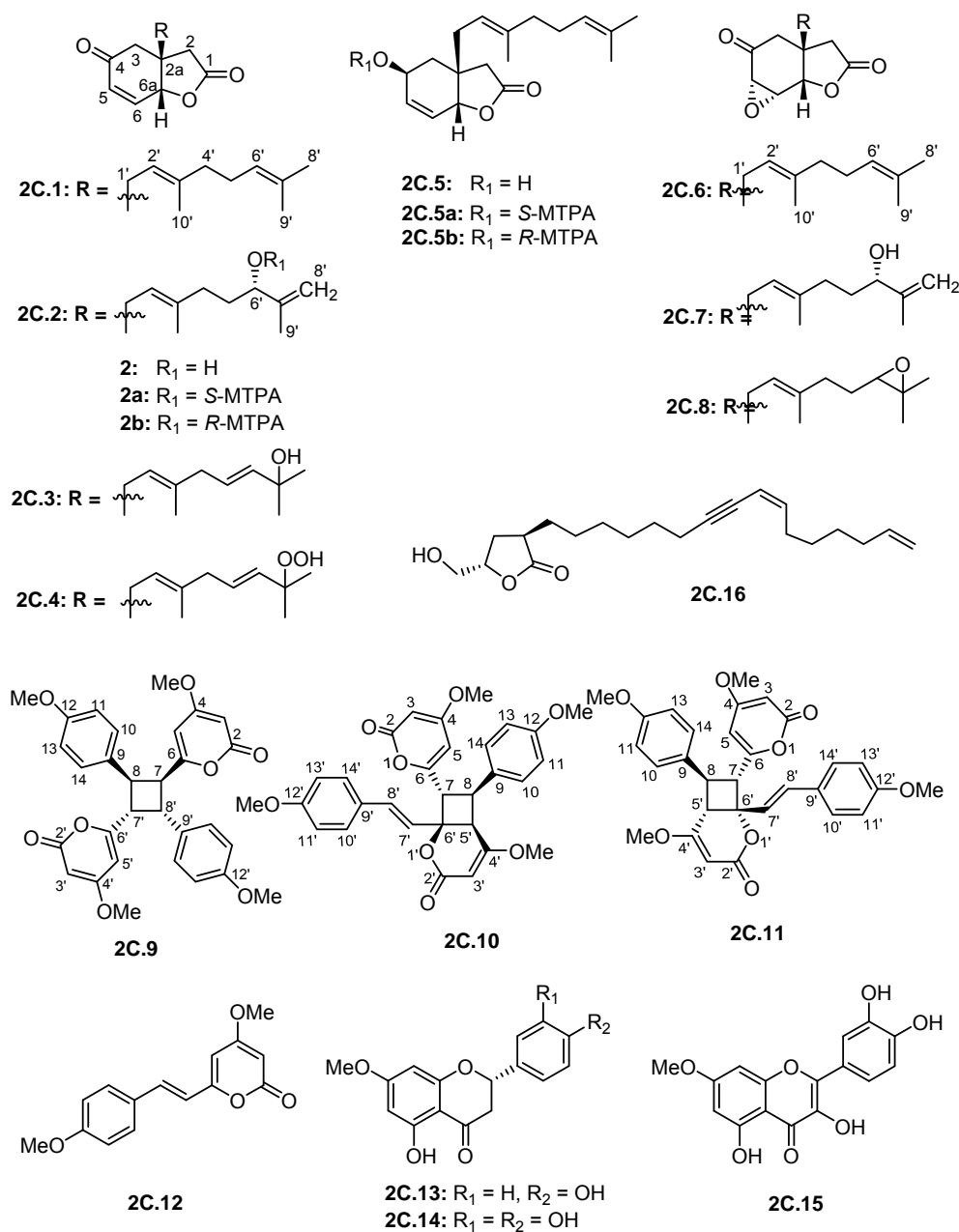
Figure 2C.1. Structures of isolated compounds **2C.1-2C.16**.

Compound **2C.2** had the molecular formula $C_{18}H_{24}O_4$ derived from the $_{13}C$ NMR and HRESITOFMS (m/z 305.1740 [M + H]$^+$) data, demonstrating the same index of hydrogen deficiency, but having one additional oxygen atom compared to **2C.1.** The ^1H and ^{13}C NMR spectroscopic data of **2C.2** were similar to those of **2C.1**, except for the geranyl side chain being oxidized at C-6′ and having a 7′, 8′ terminal double bond. The NMR spectroscopic data displayed resonances for an olefinic methylene protons at δ_H 4.82 (t, J = 1.4 Hz, 4.91 (brs), H-8′)/ δ_C 111.1 and an oxymethine at δ_H 4.00 (t, J = 6.3 Hz, H-6′)/ δ_C 75.3. The HMBC correlations of H-5′ to C-3′, C-4′, C-6′, and C-7′; H-6′ to C-4′, C-5′, C-7′, C-8′, and C-9′; and H-8′ to C-6′, C-7′, and C-9′ confirmed the position of the terminal olefinic moiety and the hydroxy group in the side chain. The assignment of the (6′S) absolute configuration was done *via* the modified Mosher's ester method. Therefore, the structure of compound **2C.2** has been named velutinone B.

Compound **2C.3** had the molecular formula $C_{18}H_{24}O_4$, deduced from ^{13}C NMR and HRESITOFMS (m/z 327.1543 [M + Na]$^+$) data, implying the same index of hydrogen deficiency, but having one additional oxygen atom compared to **2C.1**. The ^1H and ^{13}C NMR spectroscopic data of **2C.3** were similar to those of **2C.1**, except for the appearance of the olefinic protons at δ_H 5.51 (dt, J = 15.6, 6.6 Hz, H-5′) and δ_H 5.60 (d, J = 15.6 Hz, H-6′), and one additional oxygenated carbon signal at δ_C 70.4 (C-7′). The position of the hydroxy group at C-7′ on the side chain was confirmed by the HMBC correlations of H-5′ to C-3′, C-4′, C-6′, and C-7′; and H-6′ to C-4′, C-5′, C-7′ and C-8′/C-9′. Therefore, the new structure of compound **2C.3** has been named velutinone C.

Compound **2C.4** had the molecular formula $C_{18}H_{24}O_5$ derived from the ^{13}C NMR and RESITOFMS (m/z 343.1472 [M + Na]$^+$) data, demonstrating the same index of hydrogen deficiency, but having one additional oxygen atom compared to **2C.3**. The NMR spectroscopic data of **2C.4** was similar to that of **2C.3**, except for the resonance of a C-7′ hydroxy group. The ^{13}C NMR spectrum revealed the unusual down field oxygenated carbon signal at δ_C 81.8 for C-7′, suggesting the presence of a hydroperoxy group. Finally, the structure of new compound **2C.4**, has been named velutinone D,

Compound **2C.5** had the molecular formula $C_{18}H_{26}O_3$ derived from the ^{13}C NMR and HRESITOFMS (m/z 291.1935 [M + Na]$^+$) data, implying six indices of hydrogen deficiency. The IR spectrum showed hydroxy (3442 cm^{-1}) and g-lactone carbonyl (1771 cm^{-1}) functionalities. The NMR data of **2C.5** corresponded to those of **2C.1**, except that the ketone carbonyl resonance for C-4 was replaced by a resonance for an oxymethine group at δ_H 4.31 (m)/ δ_C 63.7. The assignment of (4S) absolute configuration was done via the modified Mosher's ester method. The configurations of (2aR and 6aR) were assigned by NOESY and a

molecular modeling study. NOESY correlations were observed between H-4 and H-2α, H-6a and H-1′a, H-6a and H-3β, H-1′b and H-2β, and H-3α and H-2′. Then, the structure of new compound **2C.5** has been named velutinone E.

Compound **2C.6** had the molecular formula $C_{18}H_{24}O_4$ derived from the ^{13}C NMR and HRESITOFMS (m/z 327.1562 [M + Na]$^+$) data, implying the same index of hydrogen deficiency, but having one more oxygen atom than **2C.1**. The IR spectrum showed bands for g-lactone (1789 cm^{-1} and a cyclohexanone (1719 cm^{-1}) groups. The NMR data of **2C.6** was similar to that of **2C.1**, except for the resonances of the C-5/6 double bond which were replaced by those of an epoxide moiety [δ_H 3.65 (d, J = 3.6 Hz, H-5)/ δ_C 58.6 and δ_H 3.37 (d, J = 3.6 Hz, H-6)/ δ_C 54.9)]. The relative configuration of the epoxide was assigned by the NOESY correlations between H-6 and H-6a. Hence, the structure of new compound **2C.6**, has been named velutinone F.

Compound **2C.7** had the molecular formula $C_{18}H_{24}O_5$, established from the ^{13}C NMR and HRESITOFMS (m/z 321.1690 [M + Na]$^+$) data, having the same index of hydrogen deficiency as in **2C.2**. The IR spectrum displayed an extra hydroxyl band at (3481 cm^{-1}) which differed from that of **2C.6**. The NMR data of **2C.7** corresponded to that of **2C.2**, except for the resonances of a C-5/6 double bond, which was replaced by resonances for an epoxide moiety [δ_H 3.62 (d, J = 3.6 Hz, H-5)/ δ_C 58.5 and δ_H 3.34 (d, J = 3.6 Hz, H-6)/ δ_C 54.8] as in that of **2C.6**. The 6′S configuration was assigned by comparison of the NMR data to that of **2C.2**. Thus the structure of **2C.7**, velutinone G, was defined as shown in Figure 2C.1.

Compound **2C.8** possessed the molecular formula $C_{18}H_{24}O_5$ from the ^{13}C NMR and HRESITOFMS (m/z 321.1690 [M + H]$^+$) data, having seven indices of hydrogen deficiency as in **2C.6**, but having one additional oxygen. The IR spectrum was also similar to that of **2C.6**. The NMR data of **2C.8** corresponded to that of **2C.6**, except for the resonances for a C-6′/7′ double bond which were replaced by resonances for an epoxide [dH 3.65 (t, J = 6.7 Hz, H-60/ δ_C 63.7 and δ_C 58.2, C-7′)] at this position. The configuration at C-6′ of **2C.8** was proposed to be S, based on its ring opening to give **2C.7**. Hence, structure of **2C.8**, velutinone H, was designated as shown in Figure 2C.1.

Compound **2C.9** showed an [M + Na]$^+$ ion peak at m/z 539.1651 in its HRESITOFMS, which in conjunction with the ^{13}C NMR data indicated the molecular formula $C_{30}H_{28}O_8$, requiring seventeen indices of hydrogen deficiency. The IR spectrum showed bands for unsaturated lactone (1715 cm^{-1}) and aromatic (1643 cm^{-1}) groups. The UV spectrum also indicated an aromatic moiety (286 nm). Since the NMR spectroscopic data of **2C.9** displayed half the number of resonance signals expected for 28 protons and 30 carbons, the structure

should be a symmetrical dimer. These NMR resonances corresponded to those of the cyclobutane dimer, achyrodimer A, except for hydroxy groups at C-12 and C-12′ of the aromatic rings which were replaced by methoxy groups. The ^{1}H NMR spectroscopic data showed resonances for the para-substituted benzene rings at δ_H 6.82 and 7.19 (each 4H, d, J = 8.7 Hz), four methines of the cyclobutyl ring at δ 4.16 and 4.35 (each 2H, dd, J = 7.6, 10.0 Hz), four olefinic protons for the two α-pyronemoieities at δ 5.21 and 5.71 (each 2H, d, J = 2.2 Hz), and four methoxy groups at δ 3.75 and 3.67 (each 6H, s). The ^{13}C NMR data showed resonances for the para-disubstituted benzene rings at δ 129.4 (C-9, 9′), 128.5 (C-10, 10′ and C-14, 14′), and 113.9 (C-11, 11′), the cyclobutyl methines at δ 43.0 (C-7, 7′), and 45.5(C-8, 8′) the α-pyrone methines at δ 87.7 (C-3, 30), 101.3 (C-5, 5′) and methoxy groups at δ 55.7 (4, 4′-OMe) and 55.2 (12, 12′-OMe), and a carbonyl group at 162.9 (C-6, 6′). The correlations of H-7/7′ to C-5/5′, C-6/6′, C-8/8′, and C-9/9′, and of H-8/8′ to C-6/6′, C-7/7′, C-10/10′, and C-14/14′ from the HMBC spectrum revealed the connection of a cyclobutane ring to an α-pyrone ring, and benzene rings at C-7/7′ and C-8/8′, respectively. Resonances for two sets of methoxy protons at δ_H 3.75 and 3.67 showed correlations with C-4/4′ and C-12/12′, respectively, confirming the location of methoxy groups at C-4/4′ and C-12/12′. The correlations between H-7 (7′) and H-8 (8′) in the NOESY spectrum indicated the relative configuration on the cyclobutane ring as reported for achyrodimer A.39 The specific rotation value of **2C.9** was almost zero [+0.08 (c 0.63, MeOH–CHCl$_3$; 3 : 1)] which was also the same as that reported for a symmetric achyrodimer A. Moreover, the ECD spectrum of **2C.9** showed no signal for a Cotton effect. Based on this evidence the structure of compound **2C.9** could contain a plane of symmetry. Hence, it was concluded to be a new symmetrical cyclobutane dimer of the isolated styrylpyrone, yangonin (**2C.12**), and it has been named velutinindimer A.

Compound **2C.10** possessed the molecular formula $C_{30}H_{28}O_8$ from the ^{13}C NMR and HRESITOFMS (m/z 539.1666 [M + Na]$^+$) data, having the same index of hydrogen deficiency as **2C.9**. The IR spectrum displayed bands for lactone (1699 cm^{-1}) and aromatic (1647 cm^{-1}) groups. The UV spectrum also supported an aromatic moiety (268 nm). The ^{1}H NMR data of **2C.10** showed resonances for two para-disubstituted benzene rings at δ 6.85, 7.16, and 7.34 and 6.85 (each 2H, d, J = 8.7 Hz), an E double bond at δ 6.42 and 6.86 (each 1H, d, J = 15.8 Hz), α-pyrone ring at δ 5.33 and 5.89 (each 1H, d, J = 2.2 Hz, H-3 and H-5, respectively) and 5.29 (s, H-3′), three methine protons at δ 3.55 (d, J = 9.9 Hz, H-5′), 4.26 (dd, J = 10.8, 9.9 Hz, H-8), 4.09 (d, J = 10.8 Hz, H-7), and four methoxy groups at δ 3.32, 3.69, 3.78, and 3.79. The ^{13}C NMR spectrum, DEPT and HMQC experiments of **2C.10** showed 30 resonances, including two sets of p-disubstituted benzene rings, one α-pyrone

ring, one olefinic, one cyclobutane ring, and four methoxy carbons. The HMBC spectrum displayed ³J correlations of H-3 to C-5; H-5 to C-3, and C-7; H-7 to C-5, C-9, C-5′, and C-7′; H-8 to C-6, C-1′, C-14, C-4′, and C-6′; H-1′, 14 to C-8, and C-12; H-11, 13 to C-9; H-3′ to C-5′; H-5′ to C-7, C-9, C-3′ and C-7′; H-7′ to C-7, C-5′, and C-9′; H-8′ to C-6′, C-10′, and C-14′; H-10′, 14′ to C-8′ and C-12′; H-11′, 13′ to C-9′ and C-12′; 4-OMe to C-4; 12-OMe to C-12; 4′-OMe to C-4′; and 12′-OMe to C-12′ confirming the structure of **2C.10**. The NMR data was comparable to the cyclobutane dimer achyrodimer D, reported from the aerial parts of *Achyrocline bogotensis*. It was found that **2C.10** was the methoxy derivative of achyrodimer D. The relative configuration of **2C.10** was determined from the relatively large coupling constants (9.9–10.8 Hz) between H-7 and H-8, and H-8 and H-5′, and the NOESY correlations between H-8 and H-5′, H-7 and H-14, H-8 and H-10, H-5 and H-7, H-7′ and H-10′, and H-8′ and H-14′. The magnitude of the coupling constant between H-7 and H-8 (*J trans* = 10.8 Hz), and H-8 and H-5′ (*J cis* = 9.9 Hz) could be correlated to the dihedral angle between those protons, which corresponded with the values from the Karplus equation for a four membered ring. The ECD measurement of **2C.10** in MeOH showed no signal of the Cotton effect, and also the specific rotation value was almost zero (+0.08). These could suggest that compound **2C.10** was a racemicmixture. Finally, the X-ray crystallographic analysis supported the structure of an isolated **2C.10** containing asymmetric units of a racemic mixture, and the one with the relative configuration (5′S, 6′R, 7S, and 8S) is shown in Figure 2C.1. Thus, the structure of **2C.10** was an unsymmetrical cyclobutane dimer of the isolated yangonin (**2C.12**), and it has been named velutinindimer B.

Compound **2C.11** exhibited an [M + Na]⁺ peak at m/z 539.1664 in the positive HRESITOFMS corresponding to the molecular formula $C_{30}H_{28}O_8Na$, the same as that of **2C.10**. The IR spectrum showed bands for a lactone moiety (1708 cm⁻¹) and an aromatic ring (1649 cm⁻¹). The UV spectrum indicated an aromatic moiety (273 nm). The NMR data and 2D NMR of **2C.11** demonstrated a similar structure to a dimeric **2C.10**. Nevertheless, slight differences in chemical shifts around compounds **2C.11** and **2C.10** in the ¹H and ¹³C NMR data at positions 7, 8, 9, 5′, 7′ and 8′ suggested different configurations at the cyclobutane ring between the two compounds. The large coupling constant of H-7 and H-8 (*J trans* = 10.3 Hz) and H-8 and H-5′ (*J trans* = 9.7 Hz) could be explained in the same way as for **2C.10**. The NOESY spectrum displayed correlations of H-5′ and H-7, H-7 and H-14, H-8 and H-10, H-7′ and H-10′, and H-8′ and H-14′, indicating its relative configuration. Compound **2C.11** also showed no signal of the Cotton effect and also its specific rotation value was almost zero (+0.3) suggesting that it should be a racemic mixture as compound **2C.10**. The X-ray crystallographic analysis cofirmed that it was a racemic mixture, and the one with the relative

configuration 5′R, 6′S, 7R, and 8S is shown in Figure 2C.1. From the above evidence, the structure of **2C.11** was determined to be another new dimeric styrylpyrone and it has been named velutinindimer C.

Biological activity of the isolated compounds had been evaluated. Compounds **2C.2**– **2C.4** and **2C.7**–**2C.11** showed antimalarial activity with IC_{50} values in the range of 5.4–10.0 µM. Moreover, **2C.1**–**2C.4** and **2C.6**–**2C.8** displayed cytotoxicity against the KB, MCF7, and NCI-H187 cancer cell lines and *Vero* cell lines with IC_{50} values in the range of 4.0–24.1 µM

References

1) Chuakul, W.; Sornthornchareonon, N. *Thai J. Phytopham.* 2003, *10,* 25-32.

2) Smitinand, T. Thai Plant Names Revised Edition. Prachachon Co. Limited, Bangkok, 2001; p 359.

3) Chaowasku, T.; Keßler, P. J. A.; *Nordic Journal of Botany* 2013, *3*, 680–699.

4) Harrigan, G. G.; Gunatilaka, A. A. L.; Kingston, D. G. I.; Chan, G. W.; Johnson, R. K. *J. Nat. Prod.* 1994, *57*, 68-73.

5) Wu, R.; Ye, Q.; Chen, N. Y.; Zhang, G. L.; *Chin. Chem. Lett.*, 2001, *12*, 247-248.

6) Kamperdick, C.; Van, N. H.; Sung, T. V. *Phytochemistry* 2002, *61*, 991-994.

7) Huong, D. T.; Kamperdick, C.; Sung, T. V.; *J. Nat. Prod.* 2004, *67*, 445-447.

8) Lei, Y.; Wu, L.; Shi, H.; Tu, P. *Helv. Chim. Acta.* 2008, *91*, 495-500.

9) Thao, N. P.; Luyen, B. T. T.; Tai, B. H.; Cuong, N. M.; Kim, Y. C.; Minh, C. V.; Kim, Y. H. *Bioorg. Med. Chem. Lett.* 2015, *25*, 3859-3863.

10) Sawasdee, K.; Chaowasku, T.; Likhitwitayawuid, K. *Molecules*, 2010, *15*, 639-648.

11) Sawasdee, K.; Chaowasku, T.; Lipipun, V.; Dufat, T. H.; Michel, S.; Likhitwitayawuid, K.; *Fitoterapia*, 2013, *85*, 49–56.

12) Sawasdee, K.; Chaowasku, T.; Lipipun, V.; Dufat, T. H.; Michel, S.; Likhitwitayawuid, K. *Tetrahedron. Lett.*, 2013, *54*, 4259–4263.

13) Sawasdee, K.; Chaowasku, T.; Lipipun, V.; Dufat, T. H.; Michel, S.; Jongbunprasert, V.; Likhitwitayawuid, K. *Biochem. Syst. Ecol.*, 2014, *54*, 179–181.

14) Chen, B.; Feng, C.; Li, B.; Zhang, G.; *Nat. Prod. Res.*, 2003, *17*, 397-402.

15) Zhang, H., Ma, C;. Hung, N. V.; Cuong, N. M.; Tan, G. T.; Santarsiero, B. D.; Mesecar, A. D. Soejarto, D. D.; Pezzuto, J. M.; Fong, H. H. S. *J. Med. Chem.*, 2006, *49*, 693-708.

16) Naphong, C.; Pompimon; W.; Sombutsiri, P. *Am J. App. Sci.*, 2013, *10*, 787-792.

17) Jumana, S.; Hasan, C. M.; Rashid, M. A. *Fitoterapia*, 2000, *71*, 559-561.

18) Hasan, C. M.; Jumana, S.; Rashid, M. A. *Nat. Prod. Lett.*, 2000, *14*, 393-397.

19) Jumana, S.; Hasan, C. M.; Rashid, M. A. *Biochem. Syst. Ecol.,* 2000, *28*, 483-485.

20) Wongsa, N.; Kanokmedhakul, S.; Kanokmedhakul, K. *Phytochemistry*, 2011, *72*, 1859-1864.

21) Wongsa, N.; Kanokmedhakul S.; Kanokmedhakul, K. *Phytochemistry*, 2015, *109*, 154.

5) Research Outcome

Publication

Wongsa, N.; Kanokmedhakul K.; Boonmak, J.; Youngme, S.; Kanokmedhakul, S. "Bicyclic lactones and racemic mixtures of dimeric styrylpyrones from the leaves of *Miliusa velutina*" RSC Adv 2017, 7(41), 25285–25297.

Project 2D: Investigate on Fruits and Flowers of *Miliusa velutina*

1) Keywords

Miliusa velutina, antimalarial, antibacterial, cytotoxicity

2) Objective

To investigate the chemical constituents and their bioactivity from leaves of *Miliusa velutina*

3) Introduction

The genus *Miliusa* (Annonaceae family) consists of 50 species that are found in the tropical rainforests of India, Malaysia, North Australia, and South China [1]. Previous phytochemical investigations of the genus *Miliusa* showed a number of different types of natural products, including alkaloids [2,3], acetogenins [4–6], flavonoids [3,7], geranylated homogentisic acid derivatives [8], terpenoids [9], bicyclic lactones and dimeric styrylpyrones [10]. Many of these compounds exhibit antibacterial, antimalarial, antiviral, cytotoxic and acetylcholinesterase inhibitory activities [3–6,10–12]. The Thai medicinal plant, *Miliusa velutina*, locally known as Khang Hua Mu or Kong Kang, grows widely in the northeastern part of Thailand [13]. The wood of this plant is used as a tonic and an aphrodisiac in Thai traditional medicine [14]. Our previous phytochemical studies of leaves and stem bark of *M. velutina* resulted in the isolation of linear acetogenins, bicyclic lactones and dimeric styrylpyrones [5,6,10]. Continued study of the fruits and flowers of *M. velutina* has shown that both of their EtOAc extracts showed cytotoxicity toward human oral epidermoid carcinoma (KB) with IC_{50} values of 76.3 and 17.1 μg/mL, respectively. In addition, the EtOAc extract from the fruits of this plant showed antibacterial activity against *Bacillus cereus* with MIC value of 160 μg/mL.

4) Result and Discussion

Chromatographic separation of the extracts from fruits and flowersof *M. velutina* gave twenty compounds. Their structures were determined by spectroscopic data (IR, UV, 1H and ^{13}C NMR, and 2D-NMR) and MS. The known compounds were identified by physical properties and spectroscopic data measurements, as well as by comparing the data obtained with their published values, as methyl-2-(1′*β*-geranyl-5′*β*-hydroxy-2′-oxocyclohex-3′-enyl)acetate (**2D.6**), 2-(1′*β*-geranyl-5′*β*-hydroxy-2′-oxocyclohex-3′-enyl)acetic acid (**2D.7**), yagonin (**2D.8**), velutinindimer A (**2D.9**), velutinindimers B (**2D.10**), cananginones A (**2D.11**), cananginones H (**2D.12**), 4-hydroxybenzonitrile (**2D.13**), 4-hydroxybenzaldehyde (**2D.14**), isovanillin (**2D.15**), 5-acetyloxymethylfurfural (**2D.16**), 5-methoxyfurfural (**2D.17**) and 5-hydroxymethylfurfural (**2D.18**). Two common phytosterols were identified by comparing their spectroscopic spectra with authentic samples as *β*-sitosterol (**2D.19**) and stigmasterol (**2D.20**) as shown in Figure 2D.1.

.   Compound **2D.1** was obtained as a yellow solid. Its molecular formula, $C_{17}H_{22}O_3$, deduced from HRESITTOFMS (*m/z* 297.1510 [M+Na]$^+$), indicates seven degrees of unsaturation. The UV spectrum shows absorption maxima at 267 and 370 nm. The IR spectrum exhibits absorbtion bands of hydroxyl (3261 cm^{-1}), aromatic aldehyde (2855 and 1631 cm^{-1}) and alkene (1587 cm^{-1}) groups. The ^{13}C NMR, HMQC and DEPT spectra reveal the presence of six sp2 quaternary groups, five sp2 methine (including one carbonyl), three methylene and three methyl carbons. The ^{1}H NMR spectrum shows an aldehyde proton at δ 9.80 with its carbonyl (C-7) chelated with the hydrogen of a hydroxyl group (δ 10.90, s) at the *ortho* position (C-2). Two doublet signals at δ 6.96 and 6.83 belong to aromatic protons with *meta* coupling (*J*=2.0 Hz) of H-4 and H-6, respectively. The resonance signals at δ 3.35 (d, *J*=8.0 Hz, H-1′), δ 5.30 (t, *J*=8.0 Hz, H-2′), δ 2.11–2.08 (m, H-4′ and H-5′), δ 5.10 (t, *J*=6.0 Hz, H-6′), δ 1.60 (s, H-8′), δ 1.68 (s, H-9′) and δ1.69 (s, H-10′) were assigned to a geranyl side chain. The COSY spectrum exhibits correlations of the side chain between H-1′/H-2′ and H-4′/H5′/H-6′. The HMBC spectrum shows correlations of H-1′ to C-2, C-3 and C-4; H-2′ to C-1′, C-4′ and C-10′; H-4′ to C-2′, C-3′ and C-5′ and C-6′; H-5′ to C-4′, C-6′ and C-7′; H-8′ to C-7′ and C-9′; H-9′ to C-7′ and C-8′; H-10′ to C-2′, C-3′ and C-4′, confirming the geranyl group which is linked to the aromatic at C-3. Based on the above evidence, compound **2D.1** exhibits a core structure the same as 3-farnesyl-2,5-dihydroxybenzaldehyde isolated from seeds of *Otoba paruifolia*. Thus, **2D.1** was deduced to be a new rare homogentisic acid derivative, 3-geranyl-2,5-dihydroxybenzaldehyde, which has been named miliusanal.
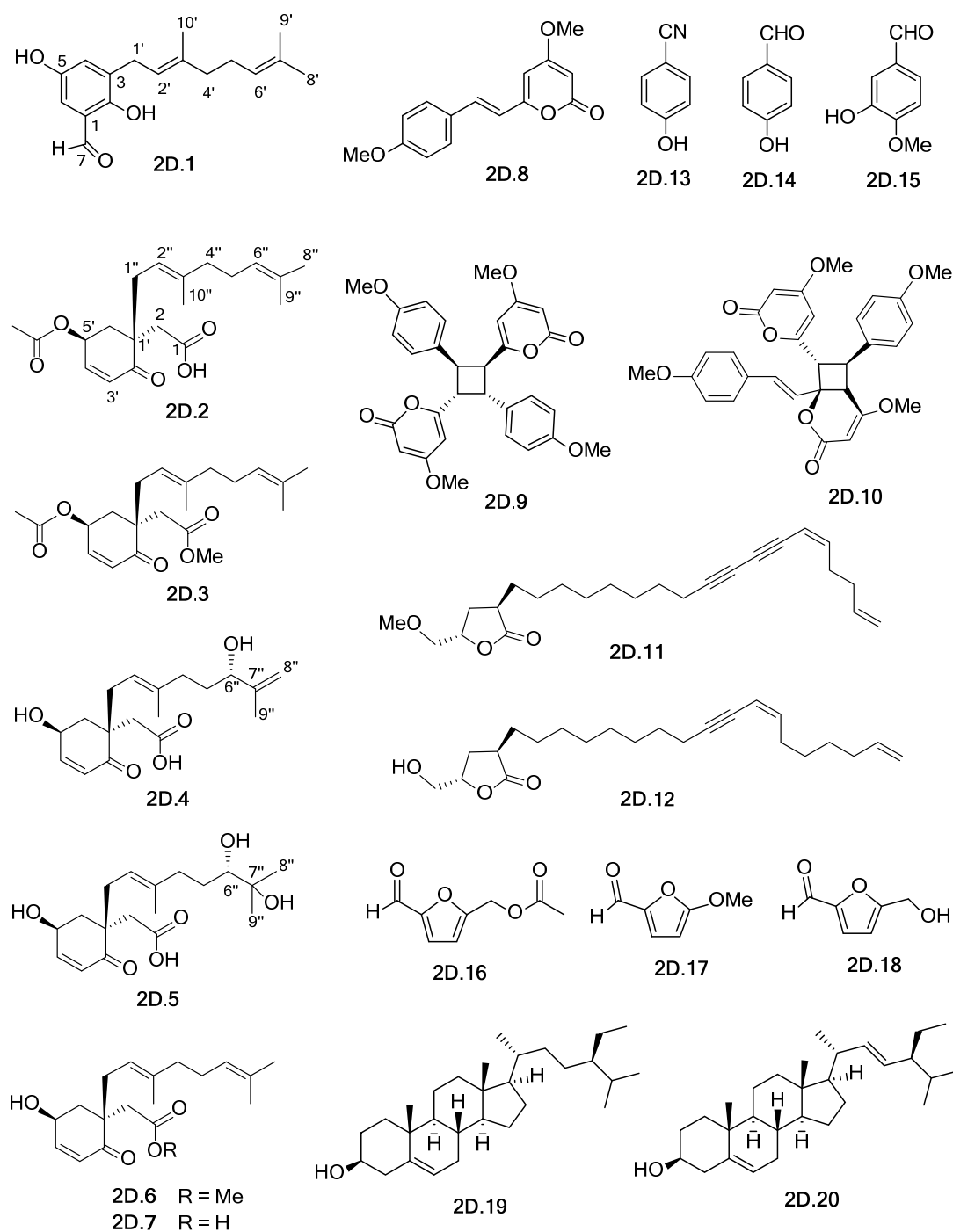
.

Figure 2D.1 Isolation compounds from fruits and flower of *Miliusa velutina*

Compound **2D.2** was obtained as a colorless viscous liquid. Its molecular formula, $C_{20}H_{28}O_5$, was deduced from HRESITTOFMS (*m/z* 371.1830 [M+Na]⁺), revealing seven degrees of unsaturation. The UV spectrum shows absorption maxima at 201 and 225 nm.

The IR spectrum exhibits characteristics of carboxylic acid (3162 and 1711 cm^{-1}), ester (1739 cm^{-1}) and conjugated ketone (1681 cm^{-1}) groupsThe ^{13}C NMR, HMQC and DEPT spectra display the presence of five sp2 quaternary (including three carbonyl groups), four sp2 methine, one sp3 quaternary, one oxymethine, five methylene and four methyl carbons. The ^{1}H NMR spectroscopic data shows sets of resonance signals for a 4,6-disubstituted-2-cyclohexenone unit at δ 6.06 (d, J=10.2 Hz, H-3′), 6.78 (dd, J=10.2, 3.6 Hz, H-4′), an oxymethine proton at δ 5.60 (m, H-5′), 2.49 (dd, J=14.8, 5.6 Hz, H-6′α), and 2.12 (dd, J=14.8, 6.0 Hz, H-6′β). The geranyl moiety shows protons ofthree methylene groups, two olefinic groups and three vinyl methyl groups as in those of **2D.1**. The α-methylene carboxylic acid (-CH$_2$-COOH) protons show two doublet signals with a germinal coupling of 16.0 Hz between δ 2.37 and 2.78. The ^{13}C NMR spectroscopic data shows a carboxylic carbon function at δ_C 176.0 (C-1), an enone carbonyl at δ_C 200.0 (C-2′), an acetate group (OAc) at δ_C 170.2 and 21.0, and a secondary oxygenated carbon at δ_C 66.0 (C-5′). The COSY spectrum shows correlations of the cyclohexenone unit, H-3′/H-4′/H-5′/H-6′. The HMBC spectrum exhibits correlations of H-1″ to C-2, C-2′, C-2″ and C-3″; H-2″ to C-1″, C-4″ and C-10″ confirming that the geranyl group is linked to the stereogenic quaternary carbon at C-1′. The relative configuration of **2D.2** was established on the basis of NOESY correlations between H-3′ and H-4′, H-5′ and H-6′α, H-1″b and H-2″, and H-6′β and H-2a to H-1″a. From the above data, **2D.2** has a core skeleton of rare homogentisic acid derivatives as in those of **2D.6** and **2D.7**. The specific rotation of **2D.2** [-48 (c, 0.1, CHCl$_3$)] and its analogues **2D.6** and **2D.7** [both -2.9 (c, 0.1, CHCl$_3$)] have the same negative sign. Since the absolute configurations of **2D.6** and **2D.7** have not been reported, the absolute configuration of **2D.2** was further determined by comparison of the experimental ECD spectrum with its ECD calculated spectra. Structures of four possible stereoisomers of **2D.2** (two chiral carbons at C-1′ and C-5′) were optimized by the B3LYP/6-31G(d) method and their ECD spectra were calculated using the time-dependent density functional theory (TD-DFT) method with CAM-B3LYP functional and 6–311++G(d,p) basis set. Polarizable continuum model (PCM) solvation model using MeOH was included in the calculations. Calculations were performed using the Gaussian09 program. The ECD calculated spectrum of (1′R,5′S)-**2D.2** shows a Cotton effect at λ_{max} 202 ($\Delta\varepsilon$+14.7), 238 nm ($\Delta\varepsilon$-38.0), and 314 ($\Delta\varepsilon$+4.0), which agrees well with that of the experimental ECD spectrum of **2D.2**. Thus, **it** was identified as a new homogentisic acid derivative with the absolute configuration (1′R,5′S)-**2D.2**, and has been named miliusanone.

Compound **2D.3** was obtained as a colorless viscous liquid. The HRESITTOFMS (*m/z* 385.1984 [M+Na]$^+$) revealed the molecular formula, C$_{21}$H$_{30}$O$_5$, which has one more carbon than **2D.2**. The UV spectrum showsabsorption similar to that of **2D.2**. The IR spectrum shows

absorption bands of ester (1735 cm^{-1}) and conjugated ketone (1681 cm^{-1}) functionalities. Analysis of the ^{1}H and ^{13}C NMR spectroscopic data and 2D NMR techniques (COSY, HSQC, HMBC and NOESY) indicates a structure similar to compound **2D.2**. However, the carboxylic acid (δ_C 176.0) of **2D.2** is replaced by an extra carbon as a methyl ester ($\delta_{H/C}$ 3.64/51.5, δ_C 171.4) in **2D.3**. The HMBC data confirms the location of the ester at C-1 by showing correlations of H-2 to C-1, C-1′, C-2′, C-6′ and C-1″, and methoxy protons to C-1. The absolute configuration of **2D.3** was assigned by comparing the ECD spectrum with calculated ECD spectra of its four possible stereoisomers (two chiral carbons at C-1′ and C-5′). The calculated spectrum of (1′R,5′S)-**2D.3** shows a Cotton effect at λ_{max} 209 nm ($\Delta\varepsilon$+6.8), 222 nm ($\Delta\varepsilon$-10.5), and 320 ($\Delta\varepsilon$+3.2), which matches the experimental ECD spectrum of **2D.3**. Thus, it was identified as a new homogentisic acid derivative with 1′R,5′S configuration, which we named miliusanone B.

Compound **2D.4** was obtained as a colorless viscous liquid. Its molecular formula, $C_{18}H_{26}O_5$, deduced from HRESITTOFMS (*m/z* 345.1679 [M+Na]$^+$), indicates six degrees of unsaturation. The UV spectrum shows absorption maxima at 204 and 236 nm. The IR spectrum exhibits the absorption bands of carboxylic acid (3395 and 1710 cm^{-1}) and conjugated ketone (1669 cm^{-1}) functionalities. The ^{1}H and ^{13}C NMR spectroscopic data of **2D.4** indicates the same core structure as that of **2D.2**. However, the acetoxy group at C-5′ of **2D.2** is replaced by a hydroxyl group ($\delta_{H/C}$ 4.61/65.0) in **2D.4**. Besides, the terminal side chain of the geranyl moiety of **2D.4** was identified as a terminal alkene [δ_C 148.0 (C-7″) and $\delta_{H/C}$ 4.77 (s), 4.85 (d, *J*=5.8 Hz)/111.4 (C-8″)] and there is an extra hydroxy group at C-6″ [δ_H/C 3.92 (q, 5.8 Hz)/75.6]. This is confirmed by the HMBC correlation of H-6″ to C-4″, C-5″, C-7″, C-8″, and C-9″. The NMR data in the side chain (C-5″- C-10″) of **2D.4**) are comparable to those of velutinone B [(CDCl$_3$) $\delta_{H/C}$ 4.00 (t, 6.3)/75.3 (C-6′), 1.58–1.65 (m)/33.0 (C-5′), δ_H 147.3 (C-7′) and 111.0 (C-8′)]. This suggests the configuration at C-6″ of **2D.4** to be 6″S, the same as 6′S in velutinone B. Finally, the absolute configuration of **2D.4** was confirmed by comparison to the calculated ECD spectra of its eight possible stereoisomers (three chiral carbons at C-1′, C-5′, and C-6″). The ECD calculated data of the generated 1′R,5′S,6″S isomer shows a Cotton effect at λ_{max} 204 ($\Delta\varepsilon$+29.1), 236 nm ($\Delta\varepsilon$-19.7), and 311 ($\Delta\varepsilon$+1.9), which is in good agreement with the experimental spectrum of **2D.4.** Thus, **2D.4** was identified as a new homogentisic acid derivative having 1′R,5′S,6″S configuration and we named it miliusanone C.

Compound **2D.5** was obtained as a colorless viscous liquid. The HRESITTOFMS (*m/z* 363.1784 [M+Na]$^+$) indicates the molecular formula, $C_{18}H_{28}O_6$, which has one more oxygen and two more hydrogen atoms than **2D.4**. It specifies five degrees of unsaturation. The UV

and IR spectral data of **2D.5** are similar to those of **2D.4**. The ^{1}H and ^{13}C NMR spectroscopic data of **2D.5** indicate the same core structure as **2D.4**. However, the appearance of an additional hydroxyl group at C-7″ (δ_C 72.4) and a missing terminal alkene at C-7″/C-8″ of the geranyl side chain is seen in **2D.5**. These are confirmed by the HMBC correlations of H-5″ to C-7″; H-6″ to C-4″, C-7″, C-8″, and C-9″; H-8″ to C-6″, C-7″, and C-9″ and H-9″ to C-6″, C-7″, and C-8″. Since **2D.5** and **2D.4** have three chiral carbons at the same positions and the comparison of their ECD spectra is in agreement, the absolute configuration of **2D.5** was designated to be 1′R,5′S,6″S, the same as that of **2D.4**. Thus, **2D.5** was elucidated as a new homogentisic acid derivative, which we named miliusanone D.

Homogentisic acid derivatives **2D.1**–**2D.7** were assayed for their bioactivity. Compounds **2D.2**, **2D.3**, **2D.6** and **2D.7** exhibited antimalarial activity against *Plasmodium falciparum* with IC$_{50}$ values of 3.8, 5.2, 3.3, and 3.9 μg/mL, respectively. This result supports a previous report of **2D.6** and **2D.7** being antiplasmodial agents against *P. falciparum* (D-6 and W-2 clones). Only **2D.6** showed weak antimycobacterial activity against *Mycobacterium tuberculosis*, with an MIC of 50 μg/mL. Compounds **2D.1**–**2D.3**, **2D.6** and **2D.7** showed cytotoxicity against KB, MCF-7 and NCI-H187 cell lines with IC$_{50}$ values in the range of 5.8–40.4 μg/mL. However, these compounds showed cytotoxicity against *Vero* cell with IC$_{50}$ values in the range of 5.8–39.1 μg/mL. Compounds **2D.1**, **2D.2**, and **2D.4**–**2D.10** were also tested for antibacterial activity using a broth microdilution method. Compounds **2D.1** and **2D.6** showed moderate antibacterial activities against three Gram-positive bacteria tested, with MICs in the range of 32–64 μg/mL. Compounds **2D.2**, **2D.7**, **2D.8** and **2D.10** showed antibacterial against *B. cereus* with MICs in the range of 64–128 μg/mL and **2D.2** also showed antibacterial against *S. aureus* with an MIC of 128 μg/mL. Moreover, compounds **2D.1**, **2D.2** and **2D.6**–**2D.10** showed antibacterial activity against Gram-negative bacteria *P. aeruginosa*, with MICs in the range of 64–128 μg/mL. Compound **2D.1** also exhibited antibacterial activity against *S.* Typhimurium with an MIC of 128 μg/mL. It should be noted that the transformations at the terminal side chain of the geranyl group in **2D.4** and **2D.5** result in the lack of activities for all tests.

References

1) T. Chaowasku, P.J.A. Keßler, Seven new species of Miliusa (Annonaceae) from Thailand, Nord. J. Bot. 31 (2013) 680–699.

2) C.M. Hasan, S. Jumana, M.A. Rashid, (+)-Isocorydine α-N-Oxide: a new aporphine alkaloid from *Miliusa velutina*, Nat. Prod. Lett. 14 (2000) 393–397.

3) T. Promchai, T. Saesong, K. Ingkaninan, S. Laphookhieo, S.G. Pyne, T. Limtharakul (née Ritthiwigrom), Acetylcholinesterase inhibitory activity of chemical constituents isolated from *Miliusa thorelii*, Phytochem. Lett. 23 (2018) 33–37.

4) S. Jumana, C.M. Hasan, M.A. Rashid, Antibacterial activity and cytotoxicity of *Miliusa velutina,* Fitoterapia. 71 (2000) 559–561.

5) N. Wongsa, S. Kanokmedhakul, K. Kanokmedhakul, Cananginones A-I, linear aceto-genins from the stem bark of *Cananga latifolia*, Phytochemistry. 72 (2011) 1859–1864.

6) N. Wongsa, S. Kanokmedhakul, K. Kanokmedhakul, Corrigendum to "Cananginones A–I, linear acetogenins from the stem bark of *Cananga latifolia*" [Phytochemistry 72 (14-15) (2011) 1859–1864], Phytochemistry. 109 (2015) 154.

7) K. Sawasdee, T. Chaowasku, V. Lipipun, T.-H. Dufat, S. Michel, V. Jongbunprasert, K. Likhitwitayawuid, Geranylated homogentisic acid derivatives and flavonols from *Miliusa umpangensis*, Biochem. Syst. Ecol. 54 (2014) 179–181.

8) H.J. Zhang, C. Ma, N.V. Hung, N.M. Cuong, G.T. Tan, B.D. Santarsiero, A.D. Mesecar, D.D. Soejarto, J.M. Pezzuto, H.H.S. Fong, Miliusanes, a class of cytotoxic agents from *Miliusa sinensis*, J. Med. Chem. 49 (2006) 693–708.

9) J.J. Brophy, R.J. Goldsack, P.I. Forster, The leaf oils of the Australian species of *Miliusa* (Annonaceae), J. Essent. Oil Res. 16 (2004) 253–255.

10) N. Wongsa, K. Kanokmedhakul, J. Boonmak, S. Youngme, S. Kanokmedhakul, Bicyclic lactones and racemic mixtures of dimeric styrylpyrones from the leaves of *Miliusa velutina*, RSC Adv. 7 (2017) 25285–25297.

11) K. Sawasdee, T. Chaowasku, K. Likhitwitayawuid, New neolignans and a phenylpropanoid glycoside from twigs of *Miliusa mollis*, Molecules. 15 (2010) 639–648.

12) C. Naphong, W. Pompimon, P. Sombutsiri, Anticancer activity of isolated chemical constituents from *Miliusa smithiae*, Am. J. Appl. Sci. 10 (2013) 787–792.

13) T. Smitinand, Thai Plant Names Revised Edition, Prachachon Co. Limited, Bangkok, 2001, pp. 359.

14) W. Chuakul, N. Sornthornchareonon, Ethnomedical uses of Thai Annonaceous plant (1). Thai J. Phytopharm. 10 (2003) 25–32.

5) Research Outcome

Publication

Promgool, T.; Kanokmedhakul, K.; Tontapha, S.; Amornkitbamrung, V.; Tongpim, S.; Jamjan, W.; Kanokmedhakul S. Bioactive homogentisic acid derivatives from fruits and flowers of *Miliusa velutina*. Fitoterapia 2019, 134, 65-72.

Project 2E: Investigate on Roots of *Cissus rheifolia*

1) Keywords

   Cissus rheifolia; flavanonol rhamnoside; berginin; antibacterial; antioxidant

2) Objective

   To isolate, characterize and evaluation of antioxidant, antibacterial and cytotoxicity of chemical constituents from roots of *Cissus rheifolia*.

3) Introduction

   Cissus is a genus of approximately 350 species of woody climbers in the grape family, Vitaceae (Wen et al. 2007). The plants of the genus *Cissus* have been widely used as a traditional folk medicine, for example *Cissus quadrangularis* for gastritis, skin infections, piles, burns and wounds (Rao and Merugu 2013), *Cissus javana* for joint pains and to heal fractured bones (Asem et al. 2014), and *Cissus aralioides* for rheumatisms, cataracts and gonorrhoea (Balogun et al. 2016). Previously phytochemical studies on this genus have led to the isolation of several types of compounds including flavonoids, iridoids, stilbenes, triterpenoids, steroids and lignan glycosides. Some of these structures showed antiulcer, antibacterial and antioxidant activities (Singh et al. 2007; Wang et al. 2007; Rao and Merugu 2013; Asem et al. 2014; Kumar et al. 2018). In addition, alkaloids, terpenoids and a flavanonol were reported from leaves and roots of *Cissus rheifolia* Planch known in Thai as "Kam Phi" or "Hun Hu Chang" (Saifah et al. 1983, 1987; Simitinand 2014). Primary screening performed by our team with the EtOAc extract from the roots of *C. rheifolia* showed antibacterial activity against Gram-negative bacteria (*Escherichia coli* DMST 4212, *Pseudomonas aeruginosa* DMST 4739, and *Salmonella enterica* serovar Typhimurium DMST 562) with MIC value of 1280 µg/mL.

4) Result and Discussion

   Chromatographic separation of the extracts from roots of *C. rheifolia* yielded two new flavanonol glycosides **2E.1** and **2E.2**, and seven known compounds **2E.3**-**2E.9**. Structures of the known compounds were identified by physical property and comparison of spectroscopic data with those of published values as 3,7-bis-α-L-rhamnopyranosyl aromadendrin (**2E.3**) (Venditti et al. 2016), (2*R*,3*R*)-engelitin (**2E.4**) (Shi et al. 2015), aromadendrin (**2E.5**) (Venditti et. al. 2013; Li et al. 2014), berginin (**2E.6**), 11-*O*-acetyl berginin (**2E.7**) (Lakornwong et al. 2014), resveratrol (**2E.8**) (Chi et al. 2014), and 4-hydroxy benzoic acid (**2E.9**) (Sukari and Said 2013). Their stuctures are shown in Figure 2E.1.
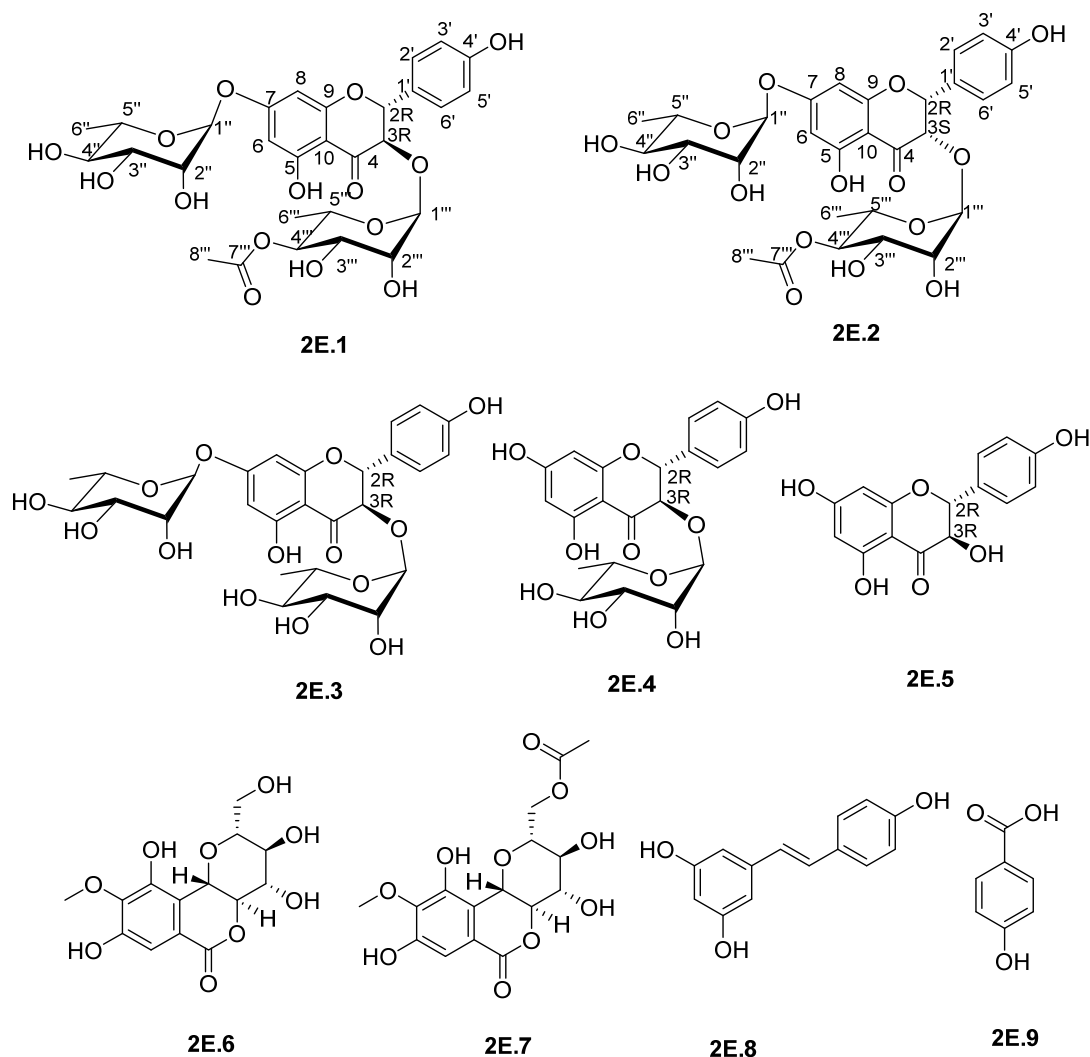
88

Figure 2E.1 Isolated compounds from roots of *Cissus rheifolia*.

Compound **2E.1** was obtained as a pale yellow solid, and its molecular formula $C_{29}H_{34}O_{15}$ was deduced from HRESITTOFMS *m/z* 645.1791 [M+Na]$^{+}$, indicating thirteen degrees of unsaturation. The IR spectrum of **2E.1** showed absorption bands of hydroxyl (3292 cm^{-1}), ester (1725 cm^{-1}), conjugated ketone (1639 cm^{-1}) and aromatic (1576 cm^{-1}) groups. The ^{13}C NMR and DEPT spectra revealed 29 signals attributable to three methyl, eighteen methine and eight quaternary (including two carbonyls) carbons. The analysis of NMR spectroscopic data indicated the glycoside skeleton. The ^{1}H NMR spectral data of **2E.1** showed resonances of an aglycone part as aromatic protons at δ_H 7.33 (2H, d, *J* = 8.9 Hz, H-2′, H-6′), 6.85 (2H, d, *J* = 8.9 Hz, H-3′,H-5′), 6.22 (1H, d, *J* = 2.0 Hz, H-8), 6.19 (1H, d, *J* = 2.0 Hz, H-6), and two *trans* oxymethine protons at 5.14 (1H, d, *J* = 11.3 Hz, H-2) and 4.58

(1H, d, J = 11.3 Hz, H-3) which consistent with a coupling pattern of an isolated flavanonol, aromadendrin (**2E.5**) with 2*R*, 3*R* configuration (Venditti et. al. 2013; Li et al., 2014). Whereas a sugar part presented as two rhamnose units via resonance signals of two anomeric protons at δ_H 5.45 (d, *J = 1.8 Hz, H*-1″) and 3.94 (brs, H-1‴) with the *α*-configuration linkages (Boutaghane et al. 2018). The resonance signals of two methyl groups of rhamnoses appeared as doublets at δ_H 1.23 (H-6″) and 1.06 (H-6‴). The linkage of carbons in the two rhamnose moieties at C-3 and C-7 were confirmed by the COSY correlations of H-1‴/H-2‴/H-3‴/H-4‴/H-5‴/H-6‴ and H-1″/H-2″/H-3″/H-4″/H-5″/H-6″ respect-tively). From data above, the structure of **2E.1** was similar to the isolated 3,7-bis-*α*-L-rhamnopyrasyl-aromadendrin (**2E.3**) (Venditti et. al. 2016), except for the appearance of an acetoxyl group at C-4‴ of a rhamnosyl unit at C-3 [$\delta_{H/C}$ 2.09 (3H, s)/21.1 (C-8‴) and 172.3 (C-7‴)] in **2E.1**. The HMBC correlations of anomeric proton H-1‴ to C-3 and reverse correlation of H-3 to C-1‴ confirmed the linkage of the acetylated rhamnose unit at C-3 position. In addition, the HMBC correlations of H-4‴ to C-7‴, H-3‴, H-6‴ to C-4‴ and reverse correlations of H-4‴ to C-3‴ and C-6‴ indicated the position of an acetyl moiety at C-4‴. Whereas, the HMBC correlation of an anomeric proton H-1″ to C-7 confirmed the location of the second rhamnose unit at C-7. Since the limitation amount of **2E.1** the absolute configurations of two rhamnose units were determined on a free rhamnose which obtained from the hydrolysis of an analogue 3,7-bis-α-L-rhamnopyranosyl aromadendrin (**2E.3**) instead. Hydrolysis of **2E.3** was carried out by a method described by Harinantenaina et al. (2002) to yield a rhamnose and an aglycone aromadendrin (**2E.5**). The ^{1}H and ^{13}C NMR spectroscopic data of a rhamnose product agree with those reported for the L-rhamnose (Bruyn and Anteunis 1976; Colson and King 1976). Furthermore, its specific rotation [+8.1, *C* = 0.29, H_2O] has the same sign as L-rhamnose reported in literature (+9.1) (Harinantenana et al. 2002) and [+7.7 (*c* 0.15, H_2O)] Zeng et al. 2012). However, the ECD spectrum of a hydrolysis product, aromadendrin (**2E.5**) showed Cotton effect the same as **2E.1** and **2E.4**. This indicated that two rhamnose units in **2E.1** and **2E.3** do not make influences on their ECD spectra. Finally, the absolute configuration of the aromadendrin moiety in **2E.1** was further confirmed to be 2*R*, 3*R* by the comparison of the ECD spectrum [λ_{max} 217 nm ($\Delta\varepsilon$ +15.1), 288 nm ($\Delta\varepsilon$ -18.5), 336 nm ($\Delta\varepsilon$ +5.0)] with that reported for (2*R*,3*R*)-engelitin (**2E.4**) [λ_{max} 220 nm ($\Delta\varepsilon$ +25), 280 nm ($\Delta\varepsilon$ -22) and 330 nm ($\Delta\varepsilon$ +9)] (Shi et al. 2015). Thus, compound **2E.1** was elucidated as a new rhamnopyranosyl aromadendrin glycoside which we named cissusfoliate A.

Compound **2E.2** was obtained as a pale yellow solid, and its HRESITTOFMS *m/z* 645.1785 [M＋Na]$^+$ revealed the molecular formula $C_{29}H_{34}O_{15}$ the same as that of **2E.1**. Analysis of IR, ^{1}H and ^{13}C NMR spectroscopic data, and 2D NMR techniques (COSY, HMQC

and HMBC) indicated that structure of **2E.2** was similar to **2E.1**. However, the ^{1}H NMR spectrum of **2E.2** showed a major difference as two doublet signals of two oxymethine protons at δ_H 5.42 (H-2) and 4.09 (H-3) with a small coupling constant value (J = 2.5 Hz). This indicated that H-2 and H-3 were *cis* isomer the same as the previously reported for (2*R*,3*S*)-engelitin isolated from *Engelhardia roxburghiana* (Shi et al. 2015). In addition, the ^{1}H NMR resonances of a methine proton H-5′′′ (δ_H 2.03-2.08, m) and methyl protons H-6′′′ (δ_H 0.75, d, J = 6.3 Hz) of a rhamnosyl unit at C-3 appeared at higher field than in those of **2E.1** suggesting the anisotropic effect of a benzene ring at C-2. The *locations* of carbons of two rhamnose units in **2E.2** were established by COSY experiments. Moreover, they were further confirmed by TOCSY correlations of H-1′′′ to H-2′′′; H-3′′′ to H-5′′′and H-6′′′; H-4′′′ to H-2′′′, H-3′′′, H-5′′′ and H-6′′′; H-5′′′ to H-6′′′ and H-1′′ to H-2′′; H-2′′ to H-3′′ and H-4′′; H-3′′ to H-4′′, H-5′′ and H-6′′; H-4′′ to H-6′′ and H-5′′ to H-6′′. In addition, the linkages of two rhamnose units to an aglycone flavononol were confirmed by the HMBC spectral data. The absolute configuration of **2E.2** was further confirmed to be 2*R*,3*S* by comparison of the ECD spectrum [λ_{max} 214 nm ($\Delta\varepsilon$ +7.9), 229 nm ($\Delta\varepsilon$ -13.0), 292 nm ($\Delta\varepsilon$ -21.0), 347 nm ($\Delta\varepsilon$ +8.4)] with that reported for (2*R*,3*S*)-engelitin [λ_{max} 213 nm ($\Delta\varepsilon$ +9.0), 227 nm ($\Delta\varepsilon$ -8.0), 298 nm ($\Delta\varepsilon$ -20.0) and 346 nm ($\Delta\varepsilon$ +9.0)] (Shi et al. 2015). The ECD spectra of **2E.1** and **2E.2** were almost similar, except for the Cotton effect at λ_{max} 229 nm ($\Delta\varepsilon$ -13.0) in **2E.2** which proposed to be a characteristic of 3*S* configuration. While, the negative Cotton effects at λ_{max} 288 for **2E.1** and λ_{max} 292 for **2E.2** were proposed for 2*R* configuration. Based on the ECD spectrum and the *cis* configuration of H-2 and H-3, the absolute configuration of **2E.2** was assigned to be 2*R*,3*S*. Thus, compound **2E.2** was determined as an *epimer* of **2E.1** and has been named 3-*epi*-cissusfoliate A.

The absolute configurations of the known aromadendrin analogues **2E.3**-**2E.5** were also assigned by the *J* coupling constant values of H-2 and H-3 and further confirmed by the comparison of their experimental ECD spectra with those reported in literature. This is the first report of experimental ECD spectrum of compound **2E.3**.

Three isolated compounds **2E.3**, **2E.6** and **2E.7** were evaluated for their antioxidant activities using ORAC, ABTS and DPPH assays. Compound **2E.6** showed strong antioxidant activity in ORAC assay, a technique recommended due to its biological relevance and extensive validation in the number of laboratories (MacDonald-Wicks et al. 2006), with a more potent IC_{50} values (8.7±1.23 µg/mL) than a standard drug, Trolox (IC_{50} value of 17.8±0.84 µg/mL). Compounds **2E.3** and **2E.7** also exhibited potent antioxidant activity using ORAC assay with IC_{50} values of 26.9±12.85 and 21.4±8.95 μg/mL, respectively. Compounds **2E.6**

and **2E.7** also showed moderate antioxidant activity using ABTS assay with IC$_{50}$ values of 80.96±1.60 and 90.18±0.36 μg/mL, respectively. However, none of them showed radical scavenging against DPPH at the concentration of 200 μg/mL. In case of antibacterial activity, compounds **2E.1**, **2E.3** and **2E.5-2E.8** showed growth-inhibitory effect against *P. aeruginosa* and *E. coli* with MIC values of 64 and 128 μg/mL, respectively. Only compound **2E.8** exhibited antibacterial activity against *Bacillus cereus* and MRSA with MIC value of 64 μg/mL. In addition, compounds **2E.3**, **2E.5** and **2E.8** showed antibacterial activity against *S. Typhimurium* with MIC value of 128 μg/mL. Compounds **2E.3**, **2E.5**, **2E.6**, and **2E.7** were evaluated for their cytotoxic activity against human cancer cell lines (Hela, KB, MCF-7, HepG2, and HT-29) and *Vero* cell and none of them showed significant activities at 100 μg/mL. Compounds **2E.2**, **2E.4** and **2E.9** were not tested due to the limitation of the samples isolated. However, compound **2E.4** has been previously reported to exhibit anti-inflammatory against the inflammatory reaction in a lipopolysaccharide (LPS)-induced endometritis mouse model (Wu et al. 2016). Moreover, compound **2E.9** has previously been reported to have oestrogenic activity in a panel of assays in breast cancer cell lines (Pugazhendhi et al. 2005).

References

Asem BD, Laitonjam WS, Oinam IS, Th J. 2014. Isolation of compounds from the aqueous methanol extract of *Cissus javana* CD leaves and determination of its trace element content through wet digestion. Asian J Chem. 26(13):3820–3822.

Balogun OS, Oladosu IA, Zhiqiang L. 2016. Chemical compositions and radical scavenging potentials of essential oils from *Tragia benthamii* (BAKER) and *Cissus aralioides* (WELW). TBAP. 6(1):59-64.

Boutaghane N, Alabdul Magid A, Abedini A, Cafolla A, Djeghim H, Gangloff SC, et al. 2018. Chemical constituents of *Genista numidica* Spach aerial parts and their antimicrobial, antioxidant and antityrosinase activities. Nat Prod Res. 6419:1–7.

Bruyn AD, Anteunis M. 1976. [1]H-N.M.R. study of L-rhamnose, methyl α-L-rhamnopyranoside, and 4-O-β-D-galactopyranosyl-L-rhamnose in deuterium oxide. Carbohydr Res. 47:158-163.

Chi X, Xing Y, Xiao Y, Dong Q, Hu F. 2014. Separation and Purification of three stilbenes from the radix of *Polygonum cillinerve* (Nakai) Ohwl by macroporous resin column chromatography combined with high-speed counter-current chromatography. Quim Nova. 37(9):1465–1468.

Colson P, King RR. 1976. The ^{13}C-N.M.R. spectra of disaccharides of D-glucose, D-

galactose, and L-rhamnose as models for immunological polysaccharides. Carbohydr Res. 47: I-13.

Harinantenaina L, Kasai R, Yamasaki K. 2002. Cussosaponins A–E, triterpene saponins from the leaves of *Cussonia racemosa*, a Malagasy endemic plant. Chem Pharm Bull. 50:1290-1293.

Kumar P, Dev K, Sharma K, Sahai M. 2018. New lignan glycosides from *Cissus quadrangularis* stems. Nat Prod Res. 6419:1–6.

Lakornwong W, Kanokmedhakul K, Kanokmedhakul S. 2014. Chemical constituents from the roots of *Leea thorelii* Gagnep. Nat Prod Res. 28(13):1015–1017.

Li W, Kim YH. 2014. Anti-inflammatory and antioxidant activities of phenolic compounds from *Desmodium caudatum* leaves and stems. Arch Pharm Res. 37(6):721–727.

Pugazhendhi D, Pope GS, Darbre PD. 2005. Oestrogenic activity of *p*-hydroxybenzoic acid (common metabolite of paraben esters) and methylparaben in human breast cancer cell lines. J Appl Toxicol. 25: 301–309.

Rao AS, Merugu R. 2013. Crystal structure of isoengelitin isolated from *Cissus quadrangularis* Linn. Int J Chem Tech Res. 5(4):1939–1941.

Saifah E, Kelley CJ, Leary JD. 1983. Constituents of the leaves of *Cissus rheifolia*. J Nat Prod. 46(3):353–358.

Saifah E, Vaisiriroj V, Kelley CJ, Higuchi Y. 1987. Constituents of the roots of *Cissus rheifolia.* J Nat Prod. 50(2):328.

Shi H, Liu M, Wang R, Gao B, Zhang Z, Niu Y. 2015. Separating four diastereomeric pairs of dihydroflavonol glycosides from *Engelhardia roxburghiana* using high performance counter-current chromatography. J Chromatogr A. 1383:79–87.

Simitinand T. 2014. Thai plant names revised edition. Bangkok: Prachachon Co. Limited; p. 137.

Singh G, Rawat P, Maurya R. 2007. Constituents of *Cissus quadrangularisy*. Nat Prod Res. 21(6):522–528.

Sukari S, Said IM. 2013. Phenolic compounds from the fruits of *Orania sylvicola*. Malaysian J Anal Sci. 17(2):276–280.

Venditti A, Serrilli AM, Rizza L, Frasca G, Cardile V, Bonina FP, Bianco A. 2013. Aromadendrine, a new component of the flavonoid pattern of *Olea europaea* L. and its anti-inflammatory activity. Nat Prod Res. 27(4-5):340–349.

Venditti A, Frezza C, Foddai S, Serafini M, Bianco A. 2016. A rare bis-rhamnopyranosyl-aromadendrin derivative and other flavonoids from the flowers of *Genista cilentina* Vals. an endemic species of Southern Italy. Arab J Chem. doi:10.1016/j.arabjc.2016.02.012.

Wang Y-H, Zhang Z-K, He H-P, Wang, J-S, Zhou H, Ding M, Hao X-J. 2007. Stilbene *C*-glucosides from *Cissus repens*. J Asian Nat Prod Res. 9(7):631-636.

Wen J, Nie Z-L, Soejima A, Meng Y. 2007. Phylogeny of Vitaceae based on the nuclear *GAI1* gene sequences. Can J Bot. 85(8):731–745.

Wu H, Zhao G, Jiang K, Li C, Qiu C, Deng G. 2016. Engeletin alleviates lipopolysaccharide-induced endometritis in mice by inhibiting TLR4-mediated NF-*K*B activation. J Agric Food Chem. 64:6171-6178.

Sukari S, Said IM. 2013. Phenolic compounds from the fruits of *Orania sylvicola*. Malaysian J Anal Sci. 17(2):276–280.

Venditti A, Frezza C, Foddai S, Serafini M, Bianco A. 2016. A rare bis-rhamnopyranosyl-aromadendrin derivative and other flavonoids from the flowers of *Genista cilentina* Vals. an endemic species of Southern Italy. Arab J Chem. doi:10.1016/j.arabjc.2016.02.012.

Zeng Y, Wang H, Zuo W, Zheng B, Yang T, Dai H, Mei W. 2012. A fatty acid glycoside from a marine-derived fungus isolated from mangrove plant S*cyphiphora hydrophyllacea*. Mar Drugs. 10:598–603.

5) Research Outcome
Publication

Promgool, T., Kanokmedhakul, K., Tantapakul, C., Suchaichit, N. P., Yahuafai, J., Siripong, P., Kelemen, C.D., Kokoska, L., Kanokmedhakul, S. Bioactive secondary metabolites from roots of *Cissus rheifolia* Planch. Natural Product Research (Under Review)

Project 3: Chemical Constituents and Their Bioactivities from roots of *Diospyros undulata*

Researcher: Panawan Moosophon (Project Leader)

2) Keywords

Diospyros undulata, Ebenaceae , naphthoquinone, plumbagin derivative

2) Objective

To isolate, characterize and evaluation of antibacterial and cytotoxicity of chemical constituents from the leaves of *D. oblonga*.

3) Introduction

Plumbagin and its derivatives are hydroxy-naphthoquinones distributed in the family Ebenceae especially Diospyros species. They exhibited highly potent bioactivities such as anticancer, antimicrobial, antimalarial, and antiinflammatory activities (Bao et al.2017). Recent investigations indicated that plumbagin derivatives have been attracted an increasing

researchers due to its promising cytotoxic activity against various cancer cell lines including breast, lung, cervical, leukemia, hepatocellular, and oral cavity cancers (Padhye et al. 2012). *Diospyros undulata* Wall. ex G. Don (Ebenaceae) is distributed in rainforest and it is a widely available medicinal plant in the north, northeast and south parts of Thailand (Smitinand 2001). Previously work, we reported the isolation of naphthoquinone derivatives and their cytotoxicity from the stem bark of *D. undulata* (Suchaichit et al. 2018).

4) Result and Discussion

Separation of the CH_2Cl_2 and MeOH extracts from *D. undulata* roots by flash column chromatography on silica gel, preparative TLC and recrystallization yielded a new plumbagin derivative **3.1** and eleven known compounds (**3.2–3.12**) (Figure 3.1). Their structures were identified by spectroscopic methods (IR, 1D and 2D NMR and MS) including comparison with data reported in the literature. The known compounds were identified as *cis*-isoshinanolone (**3.2**) (Bringmann et al. 2001), maritinone (**3.3**) (Gu et al. 2004), plumbagin (**3.4**) (Rischer et al. 2002), 3,3′-biplumbagin (**3.5**) (Higa et al. 2002), 7,7′-biplumbagin (**3.6**) (Salae et al. 2010), isodiospyrin (**3.7**) (Ruphin et al. 2014; Van der Kooy et al.2006), lupeol (**3.8**) (Abdullahi et al. 2013), friedelin (**3.9**) (Ee et al. 2004), betulin (**3.10**), betulinic acid (**3.11**) (Uddin et al. 2011), and coniferyl aldehyde (**3.12**) (Herath et al. 1998).

Compound **3.1**, obtained as an orange amorphous powder, the molecular formula based on high-resolution MS (HRESIMS) with a molecular ion peak at m/z 309.1116 [M+Na]$^+$ (calcd. For $C_{17}H_{18}O_4Na$, 309.1103), indicating nine degrees of unsaturation. The UV spectrum showed absorption maximum due to a conjugated ketone at 272 and 416 nm. The IR spectrum of **3.1** displayed the characteristic absorption bands of hydroxy (3,445 cm^{-1}) and carbonyl ketone (1,713 cm^{-1}) groups. The ^1H and ^{13}C NMR spectra of **3.1** showed characteristic of 1,4-naphthoquinone [δ_H 7.60 (1H, dd, J =1.2, 7.2 Hz, H-8), 7.55 (1H, t, J = 8.0 Hz, H-7), 7.20 (1H, dd, J = 1.2, 8.0 Hz, H-6), 2.13 (3H, s, CH_3-11) and 12.18 (1H, s, OH-5)] similar to those of plumbagin (**3.4**), except for the additional signals of methyl butyl ketone unit at C-3. The NMR data of this unit displayed the magnetic nonequivalence of four methylene protons at δ_H 2.62 (2H, t, J = 8.0 Hz, H-12), 2.49 (2H, t, J = 7.2 Hz, H-15), 1.71 (2H, quint, J = 8.0 Hz, H-14), 1.48 (2H, quint, J = 8.0 Hz, H-13), methyl protons at δ_H 2.15 (3H, s, H-17) and a carbonyl carbon at δ_C 208.0 (C-16). The COSY correlations exhibited the coupling through the sequence of H-12 to H-15 and HMBC showed correlations from H-12 to C-13/C-14, H-14 to C-12/C-15/C-16, and H-17 to C-15/C16 indicating a 5-oxohexyl unit. The HMBC data showed correlations from H-12 to C-2/C-4 confirmed that C-12 of 5-oxohexyl group connected to the 1,4-naphthoquinone at C-3. Therefore, the compound **3.1** was

identified as a new 5-hydroxy-2-methyl-3-(5-oxohexyl)naphthalene-1,4-dione and was named as 3-(5-oxohexyl)plumbagin.

The cytotoxic activity of the active constituent **3.1** was evaluated *in vitro* against human small-cell lung carcinoma (NCI-H187), human breast adenocarcinoma (MCF-7), human oral cavity carcinoma (KB) and African green monkey kidney fibroblasts (*Vero*) using MTT colorimetric method (Brien et al. 2000; Hunt et al. 1999). The results revealed potent cytotoxicity against three cancer cell lines (NCI-H187, MCF-7 and KB) with IC_{50} value 8.70, 12.90 and 28.70 μM, respectively and it was not cytotoxic to *Vero* cells. Both naphthoquinone **3.1** and **3.4** (Suchaichit et al. 2018) exhibited potent cytotoxicity to all three cancer cell lines but only **3.1** showed none cytotoxicity to normal cell, suggesting that the 5-oxohexyl group at C-3 played an important role in the decrease of cytotoxicity to normal cell and might be a lead compound for anticancer drug development in the future. Benzoquinones **3.2**-**3.7** and triterpenes **3.8**-**3.11** have previously been reported for cytotoxic against cancer cell lines (Suchaichit et al. 2018; Bishayee et al. 2011). The isolated compounds (**3.1**-**3.11**) were screened for their antibacterial activity against 1 gram-positive and 4 gram-negative bacteria using agar well diffusion method. The results showed that compounds **3.1**-**3.7** and **3.11** displayed inhibition activity against at least one pathogenic bacteriaGentamycin (GEN) and ceftazidime (CAZ) antibiotics that used as positive control showed inhibition against all tested bacteria except *B. pseudomallei* that resist to GEN. Compound **3.4** showed inspiring activity as it inhibited *E. coli*, *B. pseudomallei*, *A. baumannii* and *S. aureus* with MBC of 250, 63, 125, and 63 μg/mL that were comparable to the range of standard control drug GEN. Besides, compounds **3.4**, **3.6**, **3.7**, and **3.11** also showed respectable activity against *B. pseudomallei*, a gram-negative bacteria that caused melioidosis with the MBC of 63, 125, 125, and 125 μg/mL, respectively. Further investigation may lead to uncover the potential of these compounds as an alternative drug for the patients with melioidosis. Compound **3.4** is the most effective one in this report as it could kill *A. baumannii*, of which is an important nosocomial bacterial infection and dramatically resistance to several antibiotics. The remarkable activity against the gram-positive foodborne pathogen, S. aureus, of compounds 1, 2, 3, 4, 5, and 11 with MBC values of 250, 250, 125, 63, 250, and 250 μg/mL raised attention that these compounds could proceed further to test if any of them could be applied as antibacterial drugs in the forthcoming. Coniferyl aldehyde (**3.12**) has previously been reported for their antimicrobial activities against some oral pathogens, including *Streptococcus pyogenes*, *Streptococcus mitis*, *Streptococcus mutans* and Candida albicans (Meerungrueang and Panichayupakaranant 2014).
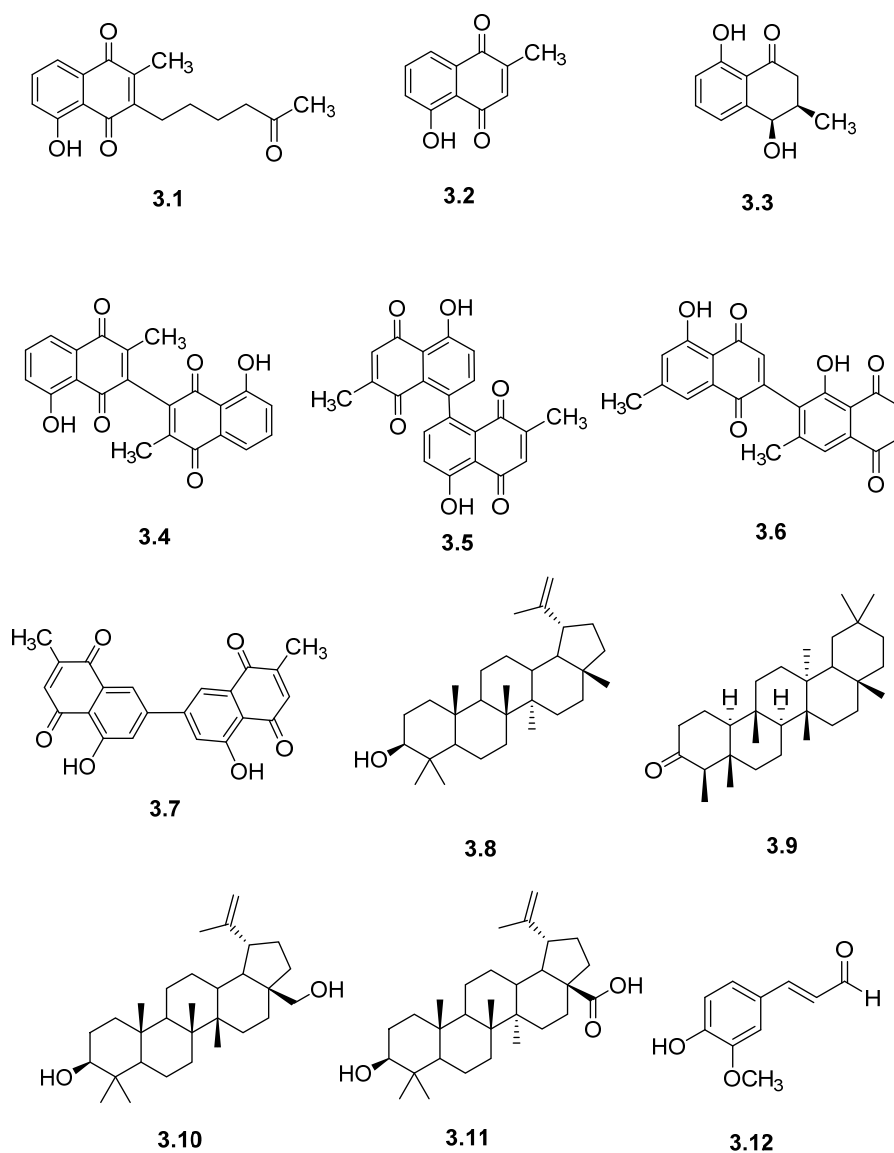
Figure 3.1 The isolated compounds from the *D.undulata* roots.

Table 3.1 Minimum bactericidal concentration (MBC) of **3.1-3.7** and **3.11**

Microorganism	MBC of Bioactive compound (µg/mL)									
	3.1	**3.2**	**3.3**	**3.4**	**3.5**	**3.6**	**3.7**	**3.11**	CAZ	GEN
Burkholderia pseudomallei	in	63	in	in	in	125	125	125	3.13	100
Acinetobacter baumannii	in	125	in	in	in	in	in	in	3.13	12.50
Pseudomonas	in	in	in	in	in	in	in	in	3.13	12.50
Staphylococcus aureus	250	63	125	250	250	in	in	in	3.13	12.50
Escherichia coli	in	250	in	in	in	in	in	250	50	50

CAZ = ceftazidime and GEN = Gentamicin (µg/mL), in = inactive

Table 3.2 Cytotoxic activity of compound **3.1** from *D. undulata* roots.

Compound	Cytotoxicity IC$_{50}$ (µM)			
	KB[a]	MCF-7[b]	NCI-H187[c]	Vero[d,e]
3.1	28.67	12.85	7.16	Non cytotoxicity
Ellipticine[f]	0.96			4.51
Doxorubicin[f]		11.18		
Tamoxifen[f]		0.15	21.05	

[a]human oral cavity carcinoma, [b]human breast adenocarcinoma, [c]human small cell lung carcinoma, [d]african green monkey kidney fibroblast, [e]the maximum test concentration at 174.63 µM (50 µg/mL), [f]positive controls.

References

Abdullahi SM, Musa AM, Abdullahi MI, Sule MI, Sani YM. 2013. Isolation of Lupeol from the Stem-bark of Lonchocarpus sericeus (Papilionaceae). Sch Acad J Biosci. 1(1):18–19.

Bao N, Ou J, Xu M, Guan F, Shi W, Sun J, Chen L. 2017. Novel NO-releasing plumbagin derivative: Design, synthesis and evaluation of antiproliferative activity. Eur J Med Chem. 13:88–95.

Bishayee A, Ahmed S, Brankov N, Perloff M. 2011. Triterpenoids as potential agents for the chemoprevention and therapy of breast cancer. Front Biosci (Landmark Ed). 16:980–996.

Brien JO, Wilson I, Orton T, Pognan F. 2000. Investigation of the alamar blue (resazurin) fluorescent dye for the assessment of mammalian cell cytotoxicity. Eur J Biochem. 267(17): 5421–5426.

Bringmann G, Messer K, Saeb W, Peters EM, Peters K. 2001. The absolute configuration of (+)-isoshinanolone and in situ LC-CD analysis of its stereoisomers from crude extracts. Phytochemistry. 56(4):387–391.

Ee GC, Ng KN, Taufiq-Yap YH, Rahmani M, Ali AM, Muse R. 2004. Mucigerin, A new coumarin from *Calophyllum mucigerum* (Guttiferae). Nat Prod Res. 18(2):123–128.

Gu JQ, Graf TN, Lee D, Chai HB, Mi Q, Kardono LB, Setyowati FM, Ismail R, Riswan S, Farnsworth NR, et al. 2004. Cytotoxic and antimicrobial constituents of the bark of *Diospyros maritima* collected in two geographical locations in Indonesia. J Nat Prod. 67(7):1156–1161.

Herath H, Dassanayake RS, Priyadarshani AMA, De Silva S, Wannigam GP, Jamie J. 1998. Isoflavonoids and a pterocarpan from *Gliricidia sepium*. Phytochemistry. 47(1):117–119.

Higa M, Noha N, Yokaryo H, Ogihara K, Yogi S. 2002. Three new naphthoquinone derivatives from *Diospyros maritima* BLUME. Chem Pharm Bull. 50(5):590–593.

98

Hunt L, Jordan M, De Jesus M, Wurm FM. 1999. GFP-expressing mammalian cells for fast, sensitive, noninvasive cell growth assessment in a kinetic mode. Biotechnol Bioeng. 65(2):201–205.

Meerungrueang W, Panichayupakaranant P. 2014. Antimicrobial activities of some Thai traditional medical longevity formulations from plants and antibacterial compounds from *Ficus foveolata*. Pharm Biol. 52(9):1104–1109.

Padhye S, Dandawate P, Yusufi M, Ahmad A, Sarkar FH. 2012. Perspectives on medicinal properties of plumbagin and itts analogs. Med Res Rev. 32(6):1131–1158.

Rischer H, Hamm A, Bringmann G. 2002. *Nepenthes insignis* uses a C2-portion of the carbon skeleton of L-alanine acquired *via* carnivorous organs, to build up the allelochemical plumbagin. Phytochemistry. 59(6):603–609.

Ruphin FP, Baholy R, Emmanuel R, Amelie R, Martin MT, Koto-Te-Nyiwa N. 2014. Isolation and structural elucidation of cytotoxic compounds from the root bark of *Diospyros quercina* (Baill.) endemic to Madagascar. Asian Pac J Trop Biomed. 4(3):16–175.

Salae AW, Karalai C, Ponglimanont C, Kanjana-Opas A, Yuenyongsawad S. 2010. Naphthalene derivatives from *Diospyros wallichii*. Can J Chem. 88(9):922–927.

Smitinand T. 2001. Thai Plant Names. Revised ed. Bangkok: Funny Publishing; p. 191.

Suchaichit NP, Suchaichit N, Kanokmedhakul K, Poopasit K, Moosophon P, Kanokmedhakul S. 2018. Two new naphthalenones from *Diospyros undulata* stem bark and their cytotoxic activity. Phytochem Lett. 24:132–135.

Uddin G, Aliullah W, Siddiqui BS, Alam M, Sadat A, Ahmad A, Uddin Khan A. 2011. Chemical constituents and phytotoxic of solvent extracted fractions of stem bark of *Grewia optiva* Drummond ex Burret. Middle-East J Sci Res. 8(1):85–91.

Van der Kooy F, Meyer JJM, Lall N. 2006. Antimycobacterial activity and possible mode of action of newly isolated neodiospyrin and other naphthoquinones from Euclea natalensis. S Afr J Bot. 72(3):349–352.

5) Research Outcome:

Publication

Suchaichit, N., Suchaichit, N.P., Kanokmedhakul, K., Boottanun, P., Sermswan, R.W., Moosophon, P., Kanokmedhakul, S. A new cytotoxic plumbagin derivative from roots of *Diospyros undulata*. Natural Product Research 2019, Published online: doi:10.1080/14786419.2019. 1630120.

Project 4: Investigate on Roots of *Buchanania lanzan*

Researcher: Nuthanat Phonkerd (Project Leader)

1) Keyword

Buchanania lanzan, steroid, antibacterial activity

2) Objective

To investigate antibacterial activity of compounds from roots of *Buachania lanzan*

3) Introduction

Buchanania lanzan is a tree species which belongs to the family Anacardiaceae. They are distributed over the tropics and subtropics. Different parts of the plant have many pharmacological actions as of traditional medicine. The gum from the tree is used against leprosy. The roots are acrid, astringent, cooling, depurative and constipating. They are useful in the treatment of diarrhoea. The leaves are used in the treatment of skin diseases. The fruits are used in treating coughs and asthma. Previous investigations on chemical constituents from leaves of *B. lanzan* has been reported, indicating the presence of flavonoid, glycoside, celidoniol, vomicine, and epinitol. However, no investigation of the phytochemical constituents and bioactivity from the roots of *B. lanzan* has yet been carried out. This drawn our attention to investigate the chemical constituents as well as searching for bioactive compounds from this plant.

4) Result and Discussion

Air-dried roots of *Buchanania lanzan* (3.5 kg) was ground into power and then extracted successively with hexane, EtOAc and MeOH three times each. Removal of solvents under reduce pressure gave crude hexane (4.52 g), crude EtOAc (22.30 g) and crude MeOH (68.80 g) extracts, respectively. Preliminary antibacterial assay of these extracts are shown in Table 4.1.

The crude hexane extract was applied on silica gel CC, gradient eluting with EtOAc-Hexane to give 24 fractions. According to TLC patterns, these fractions were combined to provide 7 Fractions, designated as HF1-HF7. Fraction HF4 was filtered out to give white solid of compound **4.1** (49.7 mg). The filtrate of HF4 (901.0 g) was subjected to silica gel CC, eluted with gradient system of EtOAc-Hexane (10-100%) to give 3 subfractions designated as HF4.1-HF4.3. Subfraction HF4.1 (277.8 mg) was filtered out to obtain white solid of compound **4.2** (16.8 mg). The filtration of subfraction HF4.2 (144.2 mg) gave an additional amount of compound **4.1** (14.7 mg).

Table 4.1 Preliminary antibacterial assay of crude extracts from roots of *B. lanzan*

Bacteria	Inhibition Zone (mm)		
	Hexane extract	EtOAc extract	MeOH extract
B. megaterium	1.23 ± 0.06	1.23± 0.12	1.10 ± 0.00
S. aureus	1.30± 0.00	1.27 ± 0.06	1.20 ± 0.00
Shigella spp	1.23± 0.06	1.40 ± 0.00	1.17 ± 0.06
S. marcescens	1.33± 0.06	1.40 ± 0.00	1.23 ± 0.06

The crude EtOAc extract (22.3 g) was separated on silica gel CC, gradient eluting with EtOAc-Hexane and MeOH-CH$_2$Cl$_2$. The 100 mL of eluent was collected for each fraction to give 34 fractions. According to TLC patterns, these fractions were combined to provide 5 fractions, designated as EF1-EF5. Fraction EF2 (1.2767 g) was separated by silica gel column chromatography (CC), eluted with a gradient solvent system of EtOAc:hexane (10-100%) to give 7 fractions, EF2.1-EF2.7. The filtration of subfraction EF2.3 obtained white solid of compound **4.3** (9.1 mg). The subfraction EF2.3 was also filtered out to obtain an additional amount of compound **4.3** (14.2 mg). The subfraction EF2.5 was filtered out to give white solid of triterpene (6.8 mg). Beside these, Fraction EF1 was filtered out to give an additional amount of compound **4.3** (6.6 mg).

The crude MeOH extract (68.80g) was chromatographed on silica gel CC, gradient eluting with EtOAc-Hexane and MeOH-CH$_2$Cl$_2$. The 100 mL of eluent was collected for each fraction to give 83 fractions. According to TLC patterns, these fractions were combined to provide 12 Fractions, designated as MF1-MF12. Fraction was filtered out to give light brown solid which was recrystallized with MeOH in CH$_2$Cl$_2$ to obtain white solid (5.7 mg). Fraction MF2 was separated by silica gel column chromatography (CC), eluted with a gradient solvent system of EtOAc:hexane (10-100%) to give 5 fractions, MF2.1-MF2.5. Fraction MF3 was subjected to silica gel CC, eluted with gradient system of EtOAc-Hexane (10-100%) to give 8 subfractions designated as MF3.1-MF3.8. Fraction MF4 was chromatographed on silica gel CC, gradient eluting with EtOAc-Hexane to give 8 subfractions designated as MF4.1-MF4.8. Fraction MF5 was separated by silica gel column chromatography (CC), eluted with a gradient solvent system of EtOAc-Hexane and MeOH-CH$_2$Cl$_2$ to give 8 fractions, MF5.1-MF5.5.

The structure of isolated compounds were elucidated by analysis of spectroscopic data and comparison of the ^{1}H and ^{13}C NMR data with those previously reported in the literature. They were determined to be betulinic acid (**4.1**), stigmastane-3,6-dione (**4.2)** and stighmasterol (**4.3**) as shown in Figure 4.1.
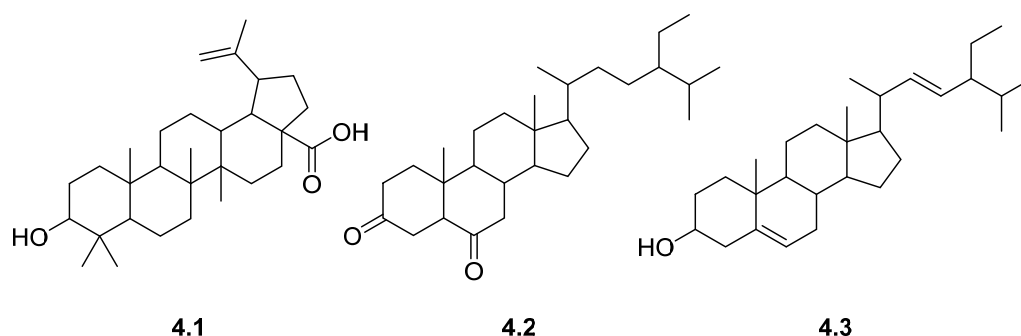
Figure 4.1. Isolated compounds from roots of *Buachania lanzan*.

5) Research Outcome

The isolation and identification of the other rest compounds are in progress.

Project 5: Investigate on Roots of *Solori thorelii*

Researcher: Nikhom Wongsa (Project Leader)

1) Keywords

*Solori thorelii***,** Fabaceae**,** bioactivity, cytotoxicity

2) Objective

2.1) To isolate and determine the chemical constituents from roots of *S. thorelii***.**

2.2) To evaluate bioactive principles of isolated compounds against human diseases such as antibacterial, TB, antimalarial and anticancer activities.

3) Introduction

The genus *Solori* (Fabaceae) in Thailand was reported 4 species, *S. microphylla, S.robusta, S. scandens* and *S. thorelii*. *Solori thorelii* (Gagnep.) Sirich. & Adema belonging to the family Fabaceae, It has common names depending on area found in Thailand such as "khruea tap pla, khruea ta pla". *Solori thorelii* has a symnonym name is *Derris thorelii.* Its root has been used for soaking in rice whisky, apply to cure a herpes zoster and poison fish and insects by the villagers in North of Thailand. *S. thorelii* has been only one reported for its phytochemicals and bioactivities.[1] It was found long chain alcohol, flemichapparin and rotenone. Rotenone showed cycotoxicity against KB cell lines with IC_{50} 0.125 µg/mL and HuCCA-1 cell lines with IC_{50} 0.125 µg/mL. Thus, it is interested to reinvestigate the chemical constituents and their biological activities from *S. thorelii*.

4) Result and Discussion

Dried and ground roots (2.25 kg) of S. thorelii were extracted with Acetone at room temperature (6 L × 3) for 3 day each time. The Acetone solution was concentrated under reduced pressure to dryness, and the residue (83.42 g) was chromatographed on a silica gel column, eluted with mixtures of *n*-hexane/EtOAc (0 to 100% EtOAc in n-hexane) and EtOAc/MeOH (0 to 100% MeOH in MeOH), to give 82 fractions. According to TLC patterns, these fractions were combined to 5 fractions designated as AF1-AF5. Compounds **5.1** and **5.2** were obtained by crystallization from the fraction AF3 and AF4, respectively. Fraction AF3 (4.47 g) was purified by CC, eluted with 30% EtOAc : Hexane gave 5 subfractions, AF3.1-AF3.5. The solid from fraction AF3.2 was crytalized to give **5.1**. Subfraction AF3.3 was subjected to silica gel CC, eluted with 30% EtOAc : Hexane to give a light yellow gum of **5.1** (0.32 g). Subfraction AF3.4 was subjected to silica gel CC, eluted with 30% EtOAc : Hexane to give a light yellow gum of **5.3** (0.04 g). Subfraction AF3.5 were subjected to silica gel CC, eluted with 30% acetone : Hexane gave 2 subfractions, AF3.5.1-AF3.5.2. The solid from subfraction AF3.5.2 was crytalized to give a colourless solid of **5.4** (0.07 g). Fraction AF4 (14.26 g) was purified by CC, eluted with 30% acetone : Hexane gave 5 subfractions, AF4.1-AF4.4. The solid from fraction AF4.2 was crytalized to give **5.1** (7.24 g). Subfraction AF4.4 was subjected to silica gel CC, eluted with 30% acetone : Hexane Hexane gave 2 subfractions, AF4.4.1-AF4.4..2. The solid from subfraction AF4.4.1 was crytalized to give a colourless solid of **5.1** (0.07 g). Subfraction AF4.4.2 was subjected to silica gel CC, eluted with 40% EtOAc : Hexane Hexane gave 2 subfractions, AF4.4.2.1-AF4.4.2.2. The solid from subfraction AF4.4.2.1 and AF4.4.2.2 were crytalized to give a colourless solid of **5.2** (0.31 g) and **5.5** (0.12 g), respectively.

Compound **5.1** is a colorless solid, mp 167.5-168.9 $^{\circ}$C. The UV spectrum showed absorption maximum at 262 nm. The IR spectrum showed 3306.5, 3237.31 cm^{-1} (C=O overtone) 2957, 2916, 2850 cm^{-1} (sp3 C-H stretching) 1730 cm^{-1} (C=O stretching) 1637 cm^{-1} (C=C stretching) 1470 cm^{-1} (CH$_2$ bending) 1392 cm^{-1} (CH$_3$ bending) and 1178 cm^{-1} (C-O stretching).

Compound **5.2** is a colorless solid, mp 170.3-171.6 $^{\circ}$C. The UV spectrum showed absorption maximum at 264 nm. The IR spectrum showed 3064 cm^{-1} (sp2 C-H stretching) 2976, 2941, 2841 cm^{-1} (sp3 C-H stretching) 1643 cm^{-1} (C=O stretching) 1634 cm^{-1} (C=C stretching) 1445 cm^{-1} (CH$_2$ bending) 1360 cm^{-1} (CH$_3$ bending) and 1138 cm^{-1} (C-O stretching). Structural elucidation of compounds **5.1** and **5.2** by using 1D and 2D NMR spectra showed

that these compounds are known flavonoids. Compounds **5.3**, **5.4** and **5.5** were assigned as three new flavonoids (Figure 5.1) based on their IR and 2D NMR spectral data.
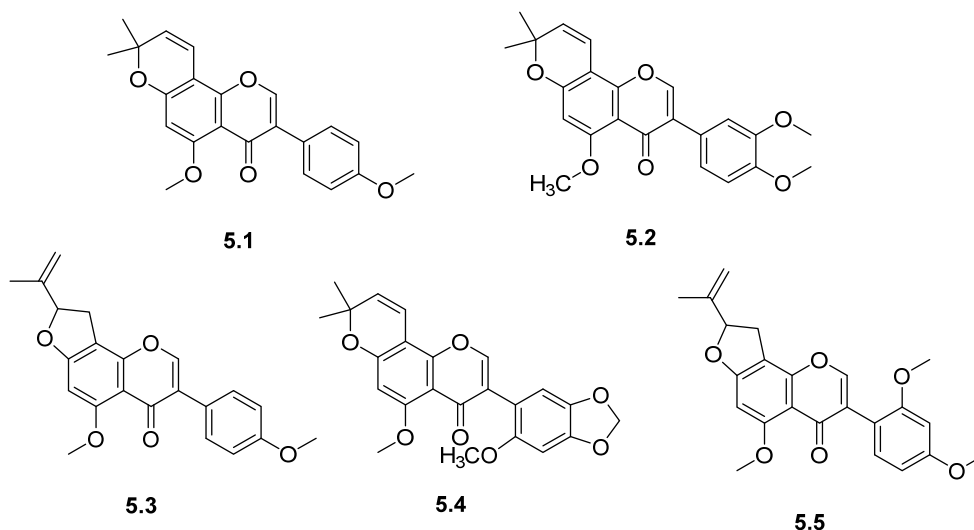

Figure 5.1. Isolated compounds from the roots of *Solori thorelii*

5) Research Outcome

Isolation and structural identification of isolated compounds have been completed. All compounds will be sent for bioactivities evaluation.

Project 6: : Investigate on Roots of *Baliospermum calycinum*

Researcher: Mongkol Nontakitticharoen (Project Leader)

1) **Keywords:** *Baliospermum calycinum*, phorbol ester, bioactive compound

2) **Objective**

2.1) To isolate and characterize phytochemicals from root of *B. calycinum.*

2.2) To evaluate the biological activity of the isolated compounds towards human disease such as Alzheimer's Disease (AD) and type 2 diabetes mellitus (T2DM), malaria, TB, and cytotoxic to cancer cell lines.

3) **Introduction**

Drugs derived from secondary metabolites in nature sources such as plants, marine creatures and microorganism still play an important role compared with synthetic drugs. Among these natural sources, compounds found in plants continue being a high potential to

be become drugs and has the potential to develop plant is being a potential source for finding new drugs. It is well known that local Thai people used medicinal plants to treat various illnesses which provide effective relief of symptoms abate until healed.   Phytochemical investigation of Thai medicinal plants creates a chance to build the knowledge and open opportunity to discover bioactive compounds that are effective in treating various diseases. There are two species of medicinal plant genus Baliospermum in the family Euphorbiaceae found in Thailand, *B. montanum* and *B. calycinum*.   Various parts of both plants including roots, leaves, and seeds are used traditionally for treatment of different ailments. Phytochemicals from roots of *B. montanum* were reported to possess anticancer, antimicrobial, immunomodulatory, and abtihelmintic activities. Thus, it is interested to study the chemical constituents and their biological activities from *B. calycinum*.

4) Result and Discussion

Air-dried powdered of *B. calycinum* roots (2.2 kg) were ground and extracted successively with organic solvents including hexane, ethyl acetate (EtOAc) and methanol (MeOH). Each 15 L of solvent extraction was carried out at room temperature for 3 days in triplicate.   The solvents were evaporated under reduced pressure to afford crude hexane (11.00 g), EtOAc (82.08 g) and MeOH (204.30 g) extracts, respectively.

Crude hexane extract (10.00 g) was subjected to silica gel flash column chromatography (FCC) eluted with gradient solvent system of hexane:EtOAc:MeOH to obtain seven fractions ($BCHF_1$ – $BCHF_7$), based on TLC analyses. The white precipitates in fraction $BCHF_4$ were filtered out and recrystallized from acetone to give compound **6.1** (18.3 mg). Fraction $BCHF_5$ was separated over silica gel column chromatography (CC) eluted with gradient solvent system of hexane:EtOAc:MeOH. The obtained fractions were combined based on TLC patterns to yield 14 fractions ($BCHF_{5.1}$ – $BCHF_{5.14}$).   The white precipitates in fraction $BCHF_{5.4}$ were filtered out to give compound **6.2** (18.7 mg).   Fraction $BCHF_{5.8}$ (0.0787 g) was further separated over silica gel CC eluted with gradient solvent system of hexane:EtOAc:MeOH to afford four sub-fractions ($BCFH_{5.8.1}$ – $BCHF_{5.8.4}$), based on TLC characteristics.   Sub-fractions $BCHF_{5.8.1}$ and $BCHF_{5.8.3}$ were separated by silica gel preparative thin layer chromatography (prep. TLC) using 20%EtOAc:hexane as eluent to afford compounds **6.3** (6.3 mg), **6.4**, and **6.5** (2.6 mg), respectively.   Fraction $BCHF_{5.12}$ (0.1228 g) was separated over silica gel CC eluted with gradient solvent system of hexane:EtOAc:MeOH to obtain three sub-fractions ($BCFH_{5.12.1}$ – $BCHF_{5.12.3}$), based on TLC patterns.   The white precipitate in sub-fraction $BCHF_{5.12.2}$ was then recrystallized from acetone to give compound **6.6** (25.9 mg).   The remaining fractions obtained from the crude hexane extract have also been purified.   Unfortunately, additional compounds have not been isolated.

Crude EtOAc extract (60.00 g) was subjected to silica gel flash column chromatography eluted by gradient solvent systems of hexane:EtOAc:MeOH to obtain eleven fractions (BCEF$_1$ – BCEF$_{11}$), based on TLC analyses. The white precipitate of BCEF$_5$ was filtered out and recrystallized from methanol to afford compound **6.7** (3.2 g). Fraction BCEF$_4$ (2.0 g) was separated by reverse phase (C-18) column chromatography eluted by 10%H$_2$O:MeOH to give ten sub-fractions (BCEF$_{4.1}$ – BCEF$_{4.10}$), based on TLC analyses. Sub-fraction BCEF$_{4.2.9}$ (150.0 mg) was separated by silica gel column chromatography eluted with gradient solvent systems of hexane:EtOAc:MeOH to give compounds **6.8** (3.8 mg) and **6.9** (9.3 mg). Fraction BCEF$_7$ (23.6 g) was recrhromatographed instead to afford 20 subfractions (BCEF$_{7.1}$ – BCEF$_{7.20}$), based on TLC analysis patterns. The subfraction BCEF$_{7.16.6}$ (117.1 mg) was purified by silica gel flash column chromatography eluted with a gradient systems of ethyl acetate and methanol to afford eight subfractions (BCEF$_{7.16.6.1}$ – BCEF$_{7.16.6.8}$). The precipitates of subfraction BCEF$_{7.16.7}$ (17.3 mg) was recrystallized from the mixture of ethyl acetate, acetone, and methanol to give compound **6.10** (7.2 mg). The subfraction BCEF$_{7.16.8}$ (1.1 g) was further separated by reverse phase RP-18 column chromatography eluted with 20%H$_2$O:MeOH to get nine subfractions, BCEF$_{7.16.8.1.1}$ - BCEF$_{7.16.8.1.9}$. Purification of these subfractions as well as all remaining subfractions from siliga gel column chromatography are in progress.

Crude methanol extract (50.00 g) was separated by silica gel flash column chromatography eluted by gradient solvent systems of hexane:EtOAc:MeOH to obtain ten fractions (BCMF$_1$ – BCMF$_{10}$), based on TLC analyses. Fraction BCMF$_2$ (0.95 g) was further separated by silica gel column chromatography eluted with gradient solvent systems of hexane:EtOAc:MeOH to give 14 sub-fractions (BCMF$_{2.1}$ – BCMF$_{2.14}$). Fraction BCMF$_7$ was subjected to Sephadex LH-20 column chromatography eluted by MeOH to afford 14 sub-fractions (BCMF$_{7.1}$ – BCMF$_{7.14}$), based on TLC analyses.

The structures of the isolated compounds were identified based on spectroscopic methods including IR, 1D and 2D NMR experiments. The results revealed that compounds **6.1** and **6.5** were known steroids as stigmasterol and stigmast-4-en-6β-ol-3-one, respectively, compound **6.2** was unsaturated fatty acid, compound **6.3** was a new phorbol ester. While compounds **6.4** and **6.6** were phenylpropanones as shown in Figure 6.1.

Structure elucidation of compounds **6.7** – **6.9** are in progress. Based on their NMR spectral data suggested that compound **6.7** is a triterpene glycoside, whereas compounds **6.8** and **6.9** are polyaromatics.
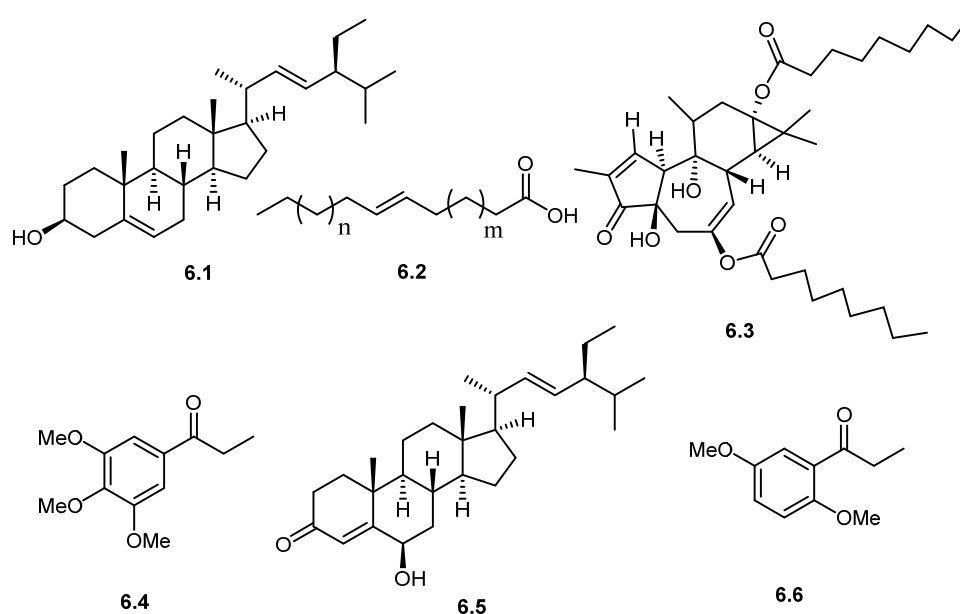
106

Figure 6.1 Some isolated compounds from the root of *B. calycinum*

5) Research Outcome

The isolation and structural determination of compounds **6.1**-**6.6** are completed. Whereas, structural identification of compounds **6.7**–**6.10** and biological evaluation of all isolated compounds are in progress.

Project 7: Investigate on Roots of *Walsura trichostemon*

Researcher: Natcha Panthama (Project Leader)

1) Keywords

Walsura trichostemon, Meliaceae,

2) Objective

2.1) To isolate and determine the chemical constituents from the roots of *W. trichostemon.*

2.2) To evaluate the antibacterial activity of isolated compounds.

3) Introduction

Walsura trichostemon Miq. is a Thai medicinal plant in the family Meliaceae. It is known as "Lamyai Pa" in Thailand, which comprises about 40 species widely distributed in

Southeast Asia. Among them, *Walsura trichostemon* or 'Lamyai Pa' in Thai and it has been used as a traditional in Thai medicine for the treatment of tendon disabilities, haemorrhoids, staunch and to clean wounds (Wongprasert et al. 2011; Sichaem, Khumkratok et al. 2014). Several *Walsura* species were reported for their antileukemic, antibacterial, antioxidant, antifeeding, and antimalarial activities. (Han et al. 2012; Sarkar et al. 2019). Phytochemical and pharmacological studies on this genus revealed a variety of bioactive constituents: limonoids showing antimalarial, cytotoxic, cell-protecting, anti-inflammatory and 11b-HSD1 inhibitory activities (Yin et al. 2007; Han et al. 2013; Nugroho et al. 2013; Ji et al. 2016; An et al. 2017); tirucallane presenting cytotoxic, anti-malarial, antifeedant, antifungal, antiplatelet aggregation, and antitubercular activities (Huang et al. 2007; Sichaem, Khumkratok et al. 2014); phenolic glycosides exhibiting antioxidant activity (Luo et al. 2006; Voravuthikunchai et al. 2010) and apotirucallane displaying cytotoxic and insecticidal activities (Sichaem et al. 2012; Sichaem, Khumkratok et al. 2014; Suri Appa Rao et al. 2015). Previous investigation of the chemical constituents of this plant provided tirucallane, apotirucallane and limonoids (Sichaem et al. 2012, Sichaem, Khumkratok et al. 2014; Phontree et al. 2014; Sichaem, Siripong et al. 2014). In order to search for further biologically active tirucallane, the EtOAc and MeOH extracts from *W. trichostemon* roots were investigated.

4) Result and Discussion

Air-dried roots of *Walsura trichostemon* (2 Kg) were ground and then extracted successively with hexane, EtOAc and MeOH, three times. The solvents were evaporated under reduced pressure to give crude hexane (8.26 g, 0.41%), EtOAc (46.08 g, 2.30%) and MeOH (93.57 g, 4.68%) extracts, respectively.

Compound **7.1** was obtained as a white solid with the molecular mormula of $C_{32}H_{50}O_5$ as determined by HRESIMS, showing an ion peak at m/z 537.3557 7 [M+ Na]$^+$. The IR spectrum of **7.1** presented the absorption bands of hydroxyl (3452 cm^{-1}), ester carbonyl (1712 cm^{-1}) and α,β-conjugated ketone (1378 cm^{-1}) groups. The ^{13}C NMR and DEPT spectra showed 32 carbons resonances corres- ponding to nine methyl, two sp2 methines, four sp2 quaternary (including two carbonyl carbons), four sp3 quaternary, seven sp3 methines, and six sp3 methylenes carbons. The ^{1}H NMR data indicated that **7.1** showed characteristic pattern of tirucallane triterpene skeleton [eight methyl (δ_H 2.17 (s), 1.96 (s), 1.10 (s), 0.90 (s), 0.89 (s), 0.88 (s), 0.74 (s) and 0.47 (d, J = 7.2 Hz)), two olefinic methine (δ_H 6.12 (s) and 5.32 (br d, J = 8.8 Hz)), three oxymethine (δ_H 4.79 (t, J = 6.4 Hz), 4.17 (s) and 3.40 (br s)), four methine and six methylene (δ_H 2.34-0.85) protons] the same as reported for 3-epimesendanin S (Han et al. 2013). However, the difference is the presence of an acetoxyl group [δ_H 2.03 (s); δ_C 171.0] at C-12 in **7.1** instead of a hydroxyl group in 3-epimesendanin

S. This acetate group was supported by HMBC correlations of downfield triplet signals of H-12 at δ_H 4.79 (J = 6.4 Hz) to acetyl carbonyl carbon at δ_H 171.0, together with the COSY correlations of H-9/H-11/H-12. The COSY correlations of H-15/H-16/H-17/H-20/H-22 and the HMBC correlation of H-22 to C-17 indicated the side chain $CH(CH_3)CH(OH)COCH=C(CH_3)_2$ connecting to a tetracyclic ring at C-17. H-3 was β-oriented and H-12 was α-oriented, based on the NOESY correlation between H-3 and CH_3-28 as well as H-12 and CH_3-18, respectively. The β-orientation of methyl group at C-20 and a-orientation of OH group at C-22 on the side chain were identified based on the similarity of the NMR spectroscopic data of **7.1** and those of 3-epimesendanin S (Han et al. 2013). From the above evidences, compound **7.1** was concluded to be a new tirucallane derivative, and was named 3-epimesendanin S 12-acetate.

By comparison of spectroscopic data with the previously reported values, the structures of known compounds **7.2**–**7.5** (Figure 7.1) were established as 3-epimesendanin S (**7.2**) [Han et al. 2013), meliasenin G (**7.3**) (Zhang et al. 2010), β-sitosterol (**7.4**) and β -sitosterol glucoside (**7.5**) (Khatun et al. 2012). The antibacterial activity of isolated compounds **7.1**–**7.3** was evaluated against three Gram-positive and three Gram-negative bacteria). Compounds **7.1** and **7.2** displayed antibacterial activity against *B. cereus* and *B. subtilis* with MIC values in the range of 16-128 µg/mL and compound **7.3** showed activity against *B. cereus* with MIC values of 64 µg/mL. Compound **7.2** exhibited activity against *B. cereus* and *B. subtilis* with MIC values of 16 and 64 µg/mL, respectively, better than **7.1**. This indicated that a hydroxyl group at C-12 might play an important role to enhance the activity. Only compound **7.3** showed activity against Gram-negative bacteria, *P. aeruginosa* and *E. coli,* with MIC values of 64 and 128 µg/mL, respectively. In addition, compounds **7.1**–**7.3** were evaluated for AChE inhibitory activity but showed no activity.

7.1 R = OAc
7.2 R = OH

7.3

7.4 R=H
7.5 R=glc
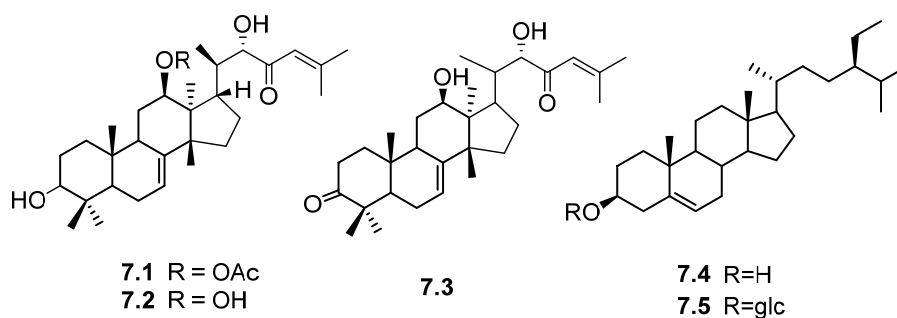
Figure 7.1. Isolated compounds from the root of *W. trichostemon*.

References

An FL, Sun DM, Li RJ, Zhou MM, Yang MH, Yin Y, Kong LY, Luo J. 2017. Walrobsins A and B, two anti-inflammatory limonoids from root barks *of Walsura robusta*. Org Lett. 19(17):4568–4571.

Han ML, Shen Y, Wang GC, Leng Y, Zhang H, Yue JM. 2013. 11b-HSD1 inhibitors from *Walsura cochinchinensis*. J Nat Prod. 76(7):1319–1327.

Han ML, Zhang H, Yang SP, Yue JM. 2012. Walsucochinoids A and B: new rearranged limonoids from *Walsura cochinchinensis*. Org Lett. 14(2):486–489.

Huang HC, Tsai WJ, Liaw CC, Wu SH, Wu YC, Kuo YH. 2007. Anti-platelet aggregation triterpene saponins from the galls of *Sapindus mukorossi*. Chem Pharm Bull. 55(9):1412–1415.

Ji KL, Li XN, Liao SG, Hu HB, Li R, Xu YK. 2016. Cytotoxic limonoids from the leaves of *Walsura robusta*. Phytochem Lett. 15:53–56.

Luo XD, Wu DG, Cai XH, Kennelly EJ. 2006. New antioxidant phenolic glycosides from *Walsura yunnanensis*. Chem Biodivers. 3(2):224–230.

Mouffok S, Haba H, Lavaud C, Long C, Benkhaled M. 2012. Chemical constituents of *Centaurea omphalotricha* Coss. & Durieu ex Batt. & Trab. Rec Nat Prod. 6(3):292–295.

Nugroho AE, Okuda M, Yamamoto Y, Hirasawa Y, Wong C-P, Kaneda T, Shirota O, Hadi AHA, Morita H. 2013. Walsogynes B–G, limonoids from *Walsura chrysogyne.* Tetrahedron. 69(20): 4139–4145.

Phontree K, Sichaem J, Khumkratok S, Siripong P, Tip-Pyang S. 2014. Trichostemonoate, a new anticancer tirucallane from the stem bark of *Walsura trichostemon.* Nat Prod Commun. 9(9): 1253–1254.

Sarkar MK, Vadivel V, Raja MRC, Kar Mahapatra S. 2019. Investigation of phytochemical constituents of anti-leukemic herbal drugs used by the traditional healers of Purulia, Birbhum and Bankura districts of West Bengal. Nat Prod Res.1–6. [2019 Feb 15]:[7 p.]. https://doi.org/10. 1080/14786419.2019.1566818.

Sichaem J, Khumkratok S, Siripong P, Tip-Pyang S. 2014. New cytotoxic apotirucallanes from the leaves of *Walsura trichostemon*. J Nat Med. 68(2):436–441.

Sichaem J, Siripong P, Tip-Pyang S, Phaopongthai J. 2014. A new cytotoxic tirucallane from the twigs of *Walsura trichostemon*. Nat Prod Commun. 9(3):367–368.

Sichaem J, Aree T, Khumkratok S, Jong-Aramruang J, Tip-Pyang S. 2012. A new cytotoxic apotirucallane from the roots of *Walsura trichostemon*. Phytochem Lett. 5(3):665–667.

110

Suri Appa Rao M, Suresh G, Ashok Yadav P, Rajendra Prasad K, Usha Rani P, Venkata Rao C, Suresh Babu K. 2015. Piscidinols H–L, apotirucallane triterpenes from the leaves of *Walsura trifoliate* and their insecticidal activity. Tetrahedron. 71(9):1431–1437.

Voravuthikunchai SP, Kanchanapoom T, Sawangjaroen N, Hutadilok-Towatana N. 2010.Antioxidant, antibacterial and antigiardial activities of *Walsura robusta* Roxb. Nat Prod Res. 24(9):813–824.

Wongprasert T, Phengklai C, Boonthavikoon T. 2011. A synoptic account of the Meliaceae of Thailand. Thai for Bull (BOT. 39:210–266.).

Yin S, Wang XN, Fan CQ, Liao SG, Yue JM. 2007. The first limonoid peroxide in the Meliaceae family: walsuronoid A from *Walsura robusta*. Org Lett. 9(12):2353–2356.

Zhang Y, Tang CP, Ke CQ, Yao S, Ye Y. 2010. Limonoids and triterpenoids from the stem bark of *Melia toosendan*. J Nat Prod. 73(4):664–668

5) Research Outcome:

Publication

Project 8: Investigation of the Luminescent Mushroom *Neonothopanus nambi* PW2

Researcher: Ratsami Lekphrom (Project Leader)

1) Keywords

Neonothopanus nambi, luminescent mushroom, antimalarial, cytotoxicity, antimycobacterial

2) Objective

2.1) To isolate and determine the chemical constituents from the luminescent mushroom *Neonothopanus nambi*

2.2) To evaluate cytotoxicity toward cancer cell lines of newly isolated compounds.

3) Introduction

　　　　Neonothopanus nambi, also called 'Hed Ruang Sang Sirin-ratsami' or Sirin-ratsami mushroom", is a bioluminescent mushroom belonging to the family Omphalotaceae. It can be found on dead wood in broad-leaved forests in the Northeastern part of Thailand. The mushroom glows with yellow greenish light under dark conditions (Buaart et al. 2011;

Kanokmedhakul et al. 2012). Bioluminescent mechanisms are often oxygen-dependent and involve a molecule called luciferin (Tsarkova et al. 2016; Bondar et al. 2011). Fungal bioluminescence is less understood, although several bioluminescent molecules have recently been reported, including 3-hydroxyhispidin found in *N. nambi* and *Panellus stipticus* as well as riboflavin contained in *Mycena chlorophos* (Purtov et al. 2015; Hayashi et al. 2012; Zernov et al. 2017; Intaraudom et al. 2013). Moreover, Tsarkova's group unveiled that many different luminophores coexist in the extract of N. nambi and could be observed under blue and green visible light (Tsarkova et al. 2016). They also reported the isolation of a novel ambiscalarane and six known secondary metabolites. We previously reported sesquiterpenes and dimeric sesquiterpenes from N. nambi. One of them, aurisin A, was reported as a biological control against a root-knot nematode (Meloidogyne incognita Chitwood) of tomatoes, chili's and potatoes (Namanusart et al. 2013). In our efforts to obtain a larger quantity of this compound, we re-investigated the phytochemical constituents of *N. nambi*.

4) Result and Discussion

The crude EtOAc extracts of two isolates of cultured mycelium of *N. nambi* PW1 and PW2 provided three new *p*-terphenyls: *p*-terphynylambi A (**8.1**), *p*-terphynylambi B (**8.2**) and *p*-terphynylambi C (**8.3**) ; along with six known sesquiterpenes: aurisin A (**8.4**) (Kanokmedhakul et al. 2012), aurisin G (**8.5**) (Intaraudom et al. 2013), aurisin Z (**8.6**) (Tsarkova et al. 2016), axinysone B (**8.7**) (Zubia et al. 2008), nambinone C (**8.8**) (Kanokmedhakul et al. 2012) and 4,8,14-trihydroxyilludala-2,6,8-triene (**8.9**) (Clericuzio et al. 1997). Besides compounds **8.1**-**8.3**, **8.5** and **8.7** are reported for the first time in the genus *Neonothopanus*. In addition, compound **8.9** is reported for the first time in the family Omphalotaceae. The structures are shown in Figure 8.1.
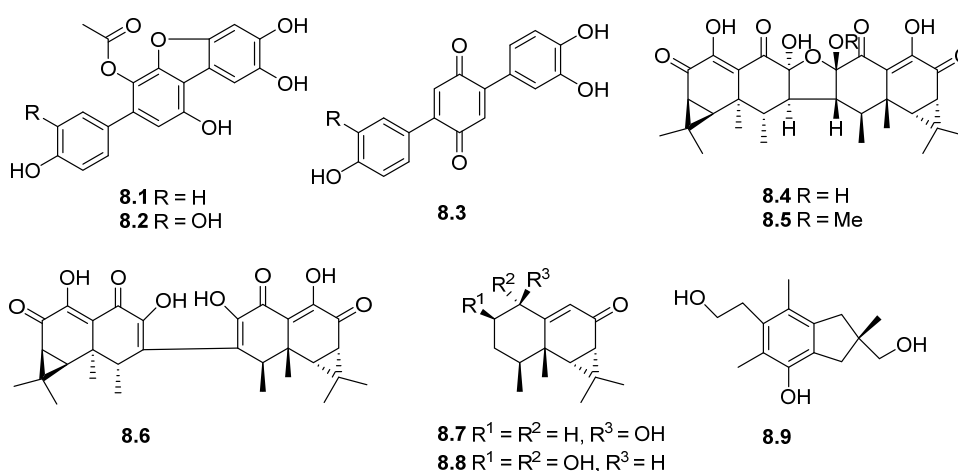
Figure 8.1 Structures of isolated compounds from *N. numbi*.

The molecular formula of **8.1** was determined as $C_{20}H_{14}O_7$ on the basis of HRESITOFMS (m/z 389.0632 $[M+Na]^+$). The IR spectrum of **8.1** showed the presence of hydroxyl (3388 cm^{-1}), ester (1749, 1732 cm^{-1}1) and aromatic (1470, 1425 cm^{-1}) groups. The ^1H NMR spectral data exhibited seven aromatic protons at δ 7.42 (H-6, 1H, s), 6.99 (H-3, 1H, s), 6.57 (H-50, 1H, s), 7.23 (H-2″ and H-6′, 2H, d, 8.4) and 6.79 (H-3″ and H-5″, 2H, d, 8.4); and acetyl protons at δ 2.19 (3H, s). The ^{13}C NMR spectral data showed the presence of three aromatic patterns including eighteen carbons δ 156.0, 150.5, 148.9,148.8, 144.6, 141.1, 132.1, 130.1x2, 129.0, 125.6, 115.2x2, 115.1, 114.0, 109.7, 107.2 and 98.2; and acetyl groups at δ 170.0 and 20.5. The COSY correlations of **8.1** showed ortho relationships of H-2″(6″) H-3″(5″). The HMBC spectrum revealed the correlations of a methine proton at δ 6.57 (H-5′) coupled to C-1′, C-3′ and C-6′; two pairs of symmetric aromatic protons, H-2″ (6″) coupled to C-4′ and H-3″(5″) correlated to C-1″and C-4″; a methine proton at δ 6.99 (H-3) correlated to C-1, C-2, C-4 and C-5; and another methine aromatic proton at 7.42 (H-6) coupled to C-1′, C-4 and C-5. Therefore, compound **8.1** was identified as a new p-terphenyl derivative, named neonambiterphenyl A. Our assignment was confirmed as the NMR spectra of **8.1** were similar to those reported for the known compound boletopsin A, a KDR kinase inhibitor isolated from the mushroom *Boletopsis leucomeles* (Kaneko et al. 2010).

The molecular formula of **8.2** was determined as $C_{20}H_{14}O_8$ on the basis of HRESITOFMS (m/z 405.0580 $[M+Na]^+$). The IR spectrum showed the presence of hydroxyl (3354 cm^{-1}), ester (1730 cm^{-1}) and aromatic (1469, 1426 cm^{-1}1) groups. The ^1H and ^{13}C NMR spectral data were similar to those of **8.1**, except for position C-3″ at δ 144.2, where H-3″ in 1 is replaced by a hydroxyl group. The key HMBC correlations between C-4′ and C-6″ with H-2″ and H-6″ supported this assignment. Therefore, **8.2** was assigned as a new p-terphenyl derivative, named neonambiterphenyl B.

The molecular formula of **8.3**, $C_{20}H_{14}O_6$, was determined on the basis of HRESITOFMS (m/z 349.0727 $[M-H]^+$). The IR spectrum showed the presence of hydroxyl (3353 cm^{-1}), ketone (1750 cm^{-1}) and aromatic (1440, 1370 cm^{-1}) groups. The ^1H NMR spectral data showed the presence of nine methine protons, including four pairs of symmetric doublets at δ 7.15 (H-2 and H-6, 2H, d, 8.4), 6.83 (H-3, H-5, H-3″ and H-5″, 4H, d, 7.6) and 7.39 (H-2″ and H-6″, 2H, d, 8.4), revealing two p-hydroxy-substituted benzene rings, and a methine at δ 6.82 (H-20, 1H, s). Moreover, the ^1H NMR data showed acetyl protons at δ 2.19 (3H, s). The ^{13}C NMR and HSQC spectral data showed three carbonyls: two of them belonging to a quinone system at δ 186.8 and 180.5 (C-3′ and C-6′), and an ester carbonyl at δ 168.7, with a methyl at δ 20.2. Furthermore, the ^{13}C NMR signals of two phydroxy-substituted benzene rings were found at δ 159.3 (C-4″), 158.3 (C-4), 131.6x2 (C-2, C-6), 131.0x2 (C-2″ and C-6″),

123.3 (C-1″), 119.3 (C-1), 115.6x2 (C-3″ and C-5″), 115.2x2 (C-3 and C-5) and four more carbons in a quinone ring were found at δ 147.2 (C-5′), 144.2 (C-1′), 134.3 (C-4′), 130.4 (C-2′). The COSY spectrum of **8.3** showed ortho correlations from two p-hydroxyphenyls: H-2(6)<->H-3(5) and H-2″ (6″)<->H-3″(5″). The HMBC spectrum of 3 showed two correlations of H-2(6) with C-1′ and C-4; H-3(5) with C-1, C-4

and C-5(3); H-3″ (5″) with C-1″, C-4″ and C-5″ (3″); H-2″ (6″) with C-4′ and C-4″. These NMR spectra were similar to those of betulinan C (El-Elimat et al. 2013). Compound **8.3** was therefore identified as a benzoquinone derivative, disubstituted by hydroxyphenyls at C-1′ and C-4′. The differences between the reported betulinan C and 3 arise from the substitution of two phenyl rings with para-hydroxyl groups and the replacement of a methoxy group at C-5′ on the quinone ring by an acetate group. Therefore, compound **8.3** was assigned as a new benzoquinone, named neonambiquinone A.

Since compounds **8.4** and **8.8** have already been reported in our previous studies [2], the newly isolated compounds (**8.1**-**8.3**, **8.5**-**8.7** and **8.9**) were tested against several targets. Compounds **8.1**-**8.3** and **8.5**-**8.7** showed cytotoxicity against NCI-H187 cell line with IC_{50} values of 16.82, 5.60, 44.69, 5.03, 9.40 and 49.31 μg/mL, respectively. While, compounds **8.1**, **8.2** and **8.5** showed cytotoxicity against KB cell line with IC_{50} values of 9.12, 40.90 and 1.45 μg/mL, respectively. Moreover, compounds **8.1** and **8.5** exhibited cytotoxicity against the MCF-7 cell line with IC_{50} values of 11.82 and 18.64 µg/mL, respectively. Compound **8.1** and **8.5** also showed cytotoxicity to *Vero* cells with IC_{50} values 38. 72 and 32. 90 µg/ mL, respectively. None of these compounds showed antimycobacterial activity against *M. tuberculosis*. Meanwhile, compound **8.3**, **8.6** and **8.7** showed specific cytotoxicity against NCI-H187 cell lines. In addition, Compounds **8.1**–**8.6** were evaluated for antibacterial activity against three Gramnegative and two Gram-positive bacteria. These bacteria are human opportunistic pathogen involved in infections acquired in a hospital setting and resistant to disinfectants as well as antibiotics. All tested compounds exhibited moderate antibacterial against *Bacillus coahuilensis* with MIC values in the range of 64–128 μg/mL. Compounds **8.1**, **8.2** and **8.3** exhibited moderate antibacterial against *Staphylococcus aureus* with MIC values of 4, 8 and 64 μg/mL, respectively. Moreover, Compounds **8.1**, **8.4** and **8.5** also exhibited moderate antibacterial against *Pseudomonas aeruginosa* with MIC values of 128 μg/mL for all. Only compound **8.1** showed antibacterial activities against *Shigella sonnei* with MIC values of 128 µg/mL.

Reference

Bondar VS, Puzyr AP, Purtov KV, Medvedeva SE, Rodicheva EK, Gitelson JI. 2011. The luminescent system of the luminous fungus *Neonothopanus nambi*. Dokl Biochem Biophys. 438:138–140.

Bua-Art S, Saksirirat W, Kanokmedhakul S, Hiransalee A, Lekphrom R. 2011. Effect of bioloactive compound from luminescent mushroom (*Neonothopanus nambi* Speg.) on root-knot nematode (Meloidogyne incognita Chitwood) and non-target organisms. KKU Res J. 16(4):726–737.

Clericuzio M, Pan F, Han F, Pang Z, Sterner O. 1997. Stearoyldelicone, an unstable protoilludane sesquiterpenoid from intact fruit bodies of *Russula delica*. Tetrahedron Lett. 38(47):8237–8240.

El-Elimat T, Figueroa M, Raja HA, Graf TN, Adcock AF, Kroll DJ, Day CS, Wani MC, Pearce CJ, Oberlies NH. 2013. Benzoquinones and terphenyl compounds as phosphodiesterase-4B inhibitors from a fungus of the order *Chaetothyriales* (MSX 47445)). J Nat Prod. 76(3):382–387.

Hayashi S, Fukushima R, Wada N. 2012. Extraction and purification of a luminiferous substance from the luminous mushroom *Mycena chlorophos*. Biophysics (Nagoya-Shi). 8:111–114.

Intaraudom C, Boonyuen N, Supothina S, Tobwor P, Prabpai S, Kongsaeree P, Pittayakhajonwut P. 2013. Novel spiro-sesquiterpene from the mushroom *Anthracophyllum* sp. BCC18695. Phytochem Lett. 6(3):345–349.

Kanokmedhakul S, Lekphrom R, Kanokmedhakul K, Hahnvajanawong C, Bua-Art S, Saksirirat W, Prabpai S, Kongsaeree P. 2012. Cytotoxic sesquiterpenes from luminescent mushroom *Neonothopanus nambi.* Tetrahedron. 68(39):8261–8266.

Namanusart W, Saksirirat W, Hirunsalee A, Lekphrom R. 2013. Efficiency of luminescent mushroom, *Neonothopanus nambi* Speg.for controlling root-knot nematodes (Meloidogyne incognita Chitwood) in tomatoes. KKU Res J. 18:824–831.

Purtov KV, Petushkov VN, Baranov MS, Mineev KS, Rodionova NS, Kaskova ZM, Tsarkova AS, Petunin AI, Bondar VS, Rodicheva EK, et al. 2015. The Chemical basis of fungal bioluminescence.Angew Chem Int Ed Engl. 54(28):8124–8128.

Tsarkova AS, Dubinnyi MA, Baranov MS, Oguienko AD, Yampolsky IV. 2016. Nambiscalarane, a novel sesterterpenoid comprising a furan ring, and other secondary metabolites from bioluminescent fungus Neonothopanus nambi. Mendeleev Commun. 26(3):191–192.

Zernov YP, Kobzeva TV, Dranova TY, Stass DV, Alekseev AA, Nefedov AA. 2017.
Luminophores of the luminous fungus Neonothopanus nambi. Biophysics. 62(2):265–270.

Zubia E, Ortega MJ, Carball Carballo JL. 2008. Sesquiterpenes from the sponge *Axinyssa Isabela*. J Nat Prod. 71(12):2004–2010.

5. Research Outcome:

Publication

Project 9: Investigate on Vines of *Salacia chinensis* Linn.

Researcher: Chulida Hemtasin (Project Leader)

1) Keywords

Salacia chinensis, freidelanes, triterpenes, Celastraceae

2) Objective

To investigate the chemical constituents and their bioactivities on
vines of *Salacia chinensis*

3) Introduction

Salacia chinensis Linn. is growing widely in Myanmar, Thailand*,* India and Malaysia.[1] This plant has gained importance as a rich repository of chemical constituents and is known to contribute to various medicinal properties. Phytochemical profiling reveals the presence of constituents such as salacinol, friedelanetype triterpene, norfriedelanetype triterpene, salaquinone, and eudesmane-type sesquiterpenes.[2,3,4] However, there have not been previously reports of the extracts from vines of *S. chinensis* Linn. We were therefore motivated to investigate its constituents and search of potentially bioactive compounds from the *S. chinensis* Linn.

4) Result and Discussion

Air-dried vines of *Salacia chinensis* (5.0 Kg) was successively immersed at room temperature in hexane, EtOAc and MeOH for 6 days. After evaporation of solvents, the brown solid of hexane extract (35.7 g), red brown solid of EtOAc extract (99.4 g) and brown viscous liquid of MeOH extract (437.5 g) were obtained. Chromatographic separation of all crude extracts gave seven compounds 9.1-9.7 as belows.

Compound **9.1** was obtaines as a yellow viscous solid. The ^{1}H NMR spectrum showed resonances of methine proton at δ 5.11 (triplet, J = 8.0 Hz, H-2), two methelene protons at δ 2.06 (dd, J = 14.8, 8.0 Hz, H$_2$.3), 1.97 (t, J = 8.0, 6.8 Hz, H$_2$-4) and methyl proton at δ 1.59 (s, H$_3$-5). The ^{13}C NMR appeared of methine carbon at δ 134.9 (C-2), quaternary carbon at δ 124.2 (C-1), two methelene carbons at δ 39.7 (C-3) and 26.7 (C-4) and meyhyl carbon at δ 16.0 (C-5). On the basis of the above evidence and SciFinder scholars 2019 data base, **9.1** was deduced to be a synthetic commercial product 1-methylcyclobut-1-ene. It should be noted that this is the first reported of **9.1** as a natural product.

Compound **9.2** was obtained as white needle solid. The IR spectrum showed the absorption bands for nonconjugate carbonyl groups (1729, 1703 cm^{-1}). The ^{1}H and ^{13}C NMR data were characteristic of 1,3-diketofriedelane triterpenoid, showing seven methyl singlets at δ 0.67 (H$_3$-24), 1.17 (H$_3$-25), 1.00 (H$_3$-26), 0.99 (H$_3$-27), 1.15 (H$_3$-28), 0.97 (H$_3$-29) and 0.92 (H$_3$-30), a methyl doublet at δ 1.03 (J = 6.5 Hz, H$_3$-23), two methylene doublets of 1,3-diketone at δ 3.22 and 3.43 (each 1H, J = 15.8 Hz, H$_2$-2) and two keto-carbonyl signals at δ 202.8 (C-1) and 204.1 (C-3). In addition to eight methyls and two carbonyls, DEPT and HSQC experiments helped categorizing the rest of its carbonyl signals as those of ten methylene (C-2, 6, 7, 11, 12, 15, 16, 19, 21, and 22), four methine (C-4, 8, 10 and 18) and six quaternary carbons (C-5, 9, 13, 14, 17 and 20). The HMBC correlations of H-2 to C-1, C-3, C-4, C-10 and C-23 confirmed the location of diketo-carbonyl at C-1 and C-2. The HMBC spectrum demonstrated correlations of H-4 to C-3, C-5, C-10, and C-24; H-10 to C-1, C-5, C-4, and C-24; H$_3$-24 to C-5, C-4, and C-10; H-8 to C-9, C-14, and C-25; H$_3$-26 to C-13, C-14, and C-15; H-18 to C-17, C-13, C-14, and C-19; H$_3$-27 to C-13, C-14, C-12, and C-18; and H$_3$-28 to C-17, C-16, C-22; establishing the friedelane triterpenoid skeleton of **9.2**. Comparison of physical properties and spectroscopic data of **9.2** with data values reported for known triterpenoid derivatives in the literature, **9.2** was defined as a known friedelane-1,3-dione which has previously been isolated from the roots of *S. campestris*.

Compound **9.3** had the molecular formula, C$_{30}$H$_{46}$O$_3$ deduced from the HRESITOFMS (m/z 455.3481 [M+H]$^+$), indicating three degrees of unsaturation. The IR spectrum displayed absorption band of ketone carbonyl (1695 cm^{-1}). The ^{1}H and ^{13}C NMR data were characteristic of 1,3-diketofriedelane triterpenoid, showing seven methyl singlets, a methyl doublet, two methylene doublets of 1,3-diketone and two keto-carbonyl signals (C-1) and (C-3). In addition to eight methyls and two carbonyls, DEPT and HSQC experiments helped categorizing the rest of its carbonyl signals as those of nine methylene (C-2, 6, 7, 11, 12, 16, 19, 21, and 22), four methine (C-4, 8, 10 and 18) and six quaternary carbons (C-5, 9,

13, 14, 17 and 20). The HMBC correlations of H-2 to C-1, C-3, C-4, C-10 and C-23 confirmed the location of diketo-carbonyl at C-1 and C-3. The HMBC spectrum demonstrated correlations of H-4 to C-3, C-5, C-10, and C-24; H-10 to C-1, C-5, C-4, and C-24; H_3-24 to C-5, C-4, and C-10; H-8 to C-9, C-14, and C-25; H_3-26 to C-13, C-14, and C-15; H-18 to C-17, C-13, C-14, and C-19; H_3-27 to C-13, C-14, C-12, and C-18; and H_3-28 to C-17, C-16, C-22; establishing the friedelane triterpenoid skeleton. These spectral data are similar to those of friedelane-1,3-dione (**9.2**) except for the absence of methylene proton (H_2-15), which was replaced by carbonyl group (δ 214.0). On the basis of the above evidence and SciFinder Scholars 2018 data base, **9.3** was deduced as a new friedelane triterpenoid (Figure 9.1).

Compound **9.4** was isolated as white solid, the molecular formula, $C_{29}H_{46}O$ deduced from the HRESITOFMS (m/z 411.3606 [M+H]$^+$), indicating two degrees of unsaturation. The IR spectrum showed the presence of hydroxyl group (3411 cm^{-1}). The ^{1}H NMR spectrum showed resonances of oxymethine proton at δ_H 3.51 (quin, *J* = 5.2 Hz, H-3) and two olefinic protons at δ_H 5.35 (d, *J* = 4.4 Hz, H-6) and 5.10 (d, *J* = 6.0 Hz, H-11). The ^{13}C and DEPT spectra confirmed the presence of 35 carbons, concisting of two olefinic (δ_C 124.2), one oxygenated methine (δ_C 71.7), seven methine, thirteen methylene, seven methyl and five quarternary carbons. The olefinic protons at C-6 and C-11 were evident from ^{1}H-^{1}H COSY correlation of H-6/H-7; H-11/H_2-12 and the key HMBC correlation between H_2-4 to C-6 and H_2-7 to C-6; H-12 to C-11. The down-field chemical shift of H-3 and the HMBC correlation of H_2-1 to C-3 and H_2-4 to C-3 in the HMBC spectrum suggested an hydroxyl group attached to the C-3.The HMBC data confirmed the location of the hydroxyl at C-3 by showing correlations of H-4 to C-3, H-1 to C-3 and H_3-23 to C-3. The methylene carbons at C-6 and C-11 were displaced with olefinic carbons at δ_C 124.2 and 121.6. The HMBC correlation of H_2-4 to C-2, C-5, C-10 and C-6; H_2-6 to C-3, C-10 and C-7; H_3-25 to C-10, C-5, C-9; H_2-7 to C-5, C-6 and C-9; H-18 to C-13, C-12, C-19, C-26 confirmed the friedelane-1,3-dione skeleton. On the basis of the above evidence and SciFinder Scholars 2019 data base, **9.4** was deduced as a new pentacyclic triterpenoid

Compound **9.5** had the molecular formula, $C_{33}H_{54}O_2$ deduced from the HRESITOFMS (m/z 483.3818 [M+H]$^+$), indicating three degrees of unsaturation. The IR spectrum showed the presence of ester group at 1729 cm^{-1}. The ^{1}H NMR spectrum gave an impression of pentacyclic triterpene because the resonances for seven methyl groups at δ_H 2.01 (H_3-2'), 1.00 x 2 (H_3-25 and H_3-27), 0.92 (H_3-28), 0.82 (H_3-29), 0.80 (H_3-30), and 0.66 (H_3-26), oxymethine proton at δ_H 4.58 (mult, *J* = 4.8 Hz, H-3) and olefinic protone at δ_H 5.35 (d, *J* = 4.4 Hz, H-6). The ^{13}C and DEPT spectra confirmed the presence of 32 carbons, concisting of one ester carbonyl (δ_C 170.4), one olefinic (δ_C 122.6), one oxygenated methine (δ_C 73.9), eleven

methylene, seven methyl and four quarternary carbons. The oxygenated proton at C-3 was evident from ^{1}H-^{1}H COSY correlation of H-7/H-9 and the key HMBC correlation between H-4 to C-6 and H-7 to C-6. The down-field chemical shift of H-3 and the HMBC correlation of H-3 with δ_C 170.4 (s) in the HMBC spectrum suggested an acetyl attached to the C-3. The HMBC correlation of H$_2$-4 to C-2, C-5, C-10 and C-6; H$_2$-6 to C-3, C-10 and C-7; H$_3$-25 to C-10, C-5, C-9; H$_2$-7 to C-5, C-6 and C-9; H-18 to C-13, C-12, C-19, C-26 confirmed the pentacyclic triterpene skeleton. On the basis of the above evidence and SciFinder Scholars 2019 data base, **9.5** was deduced as a new pentacyclic triterpenoid.

Compound **9.6** had the molecular formula, $C_{37}H_{60}O_7$ deduced from the HRESITOFMS (m/z 455.3481 [M+H]$^+$), indicating one degree of unsaturation. The IR spectrum displayed the absorption band of hydroxyl at 3384 cm^{-1}. The ^{13}C NMR and DEPT experiment revealed the presences of thirtynine carbons, attributable to fourteen methine, thirteen methylene, seven methyl and five (including a carbonyl group) quaternary carbons. The ^{1}H NMR spectrum showed the typical pattern of pentacyclic triterpenoid, connected in a pyranose acetate with five oxy-methine protons at δ_H at 3.26 (*t*, H-1'), 3.33 (*t*, H-2'), 3.40 (*q*, H-3'), 3.42 (*q*, H-4') and 4.27 (*brd*, H-5'), together with doublet signal of methylene proton at δ_H 4.33 and singlet signal of acetyl group at δ_H 2.05 (H$_3$-2''). The HMBC correlation of H-1' to C-5' and C-4': H-2' to C-1', C-3' and C-4'; H-3' to C-1'; H-4' to C-1' and C-2'; H-5' to C-1'', C-1', and C-3' confirmed the structure of pyranose acetate. The COSY spectrum of H$_2$-3''/H-1', together with the HMBC correlation of H$_2$-3'' to C-3 and C-1', confirming the connection of this unit at C-3. The ^{1}H NMR spectrum showed resonances of an olefinic protons at δ_H at 5.32 (br*d*, H-6), together with three singlet signals of methyl proton at δ_H 0.96 (H$_3$-23), 0.96 (H$_3$-24) and 0.63 (H$_3$-25). On the basis of the above evidence and SciFinder Scholars 2019 data base, **9.6** was deduced as a newpentacyclic triterpenoid glycoside (Figure 9.1).
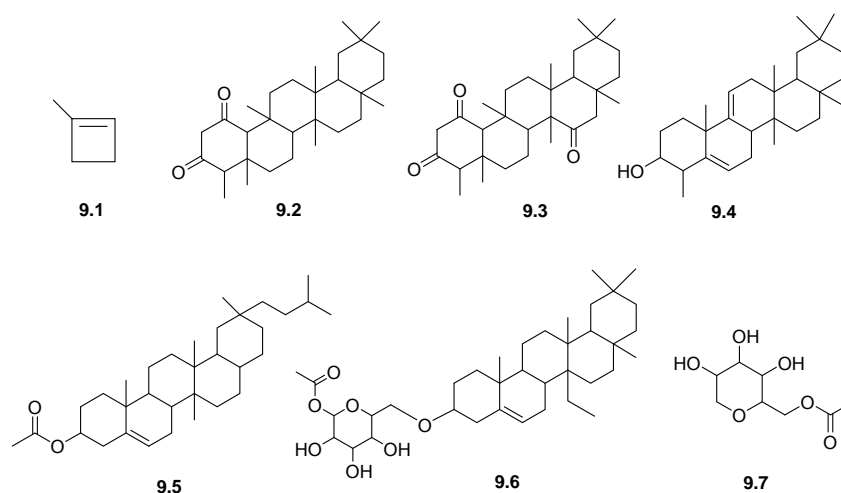
Figure 9.1 Isolated compounds from vines of *S. chinensis*

Investigation of the chemical constituents from vines of *Salacia chinensis* led to the isolation of seven compounds.They were four new compounds (**9.3-9.5** and **9.6**) and two known compounds (**9.2** and **9.7**) and a new natural product (**9.1**). Compounds **9.1-9.4** and **9.7** were inactive for antibacterial activities. Compounds **9.3** and **9.5** showed the evidence of anti α-glucosidase inhibitors for type 2 diabetes mellitus at IC_{50} 43.89 and 139.16 μM, respectively.

4) Research Outcome

All laboratory experiment have been completed. The preparation of manuscript is in progress.

Project 10: Investigate on Two Plants: *Helixanthera parasitica* Lour. and

***Croton krabas*.**

Researcher: Oue-artorn Rajachan (Project Leader)

Project 10A: Investigate on stems of *Helixanthera parasitica* Lour.

1) Keywords

Helixanthera parasitica, Loranthaceae, flavan, antimalarial activity, cytotoxic

2) Objective

2.1) To isolate and determine the chemical constituents from the stems of

H. parasitica.

2.2) To evaluate the bioactive principles from isolated compounds against some

human disease such as TB, antimalarial and cancer.

3) Introduction

Helixanthera parasitica Lour. (Loranthaceae) is parasitic plant, 1-2 m in height, found throughout Thailand. It is known in Thai as "Ka fag koh" (กาฝากก่อ). A water decoction of its stem mixing with other parasitic plants has been used in Thai traditional medicine for liver and kidney disease.[1,2] However, previous report on phytochemical investigations of *H. parasitica* has resulted in the isolation of gallic acid, ethyl gallate, quercitrin, and 4,7,3',4' - tetrahydroxyflavan.[3] Furthermore, an aqueous extract from the whole part of this plant has been reported to possess both anti-metastatic and antioxidant activity by an *in vitro* invasion test.[4] As part of our search for bioactive compounds from Thai plants, the crude EtOAc extract from the stem of *H. parasitica* exhibited anti-malarial activity against *Plasmodium*

falciparum with IC$_{50}$ value of 3.25 μg/mL. Therefore, we are interested to investigate the chemical compositions and their biological activities from this plant.

4) Result of research activity during this period

The stems of *H. parasitica* were collected from Phu ruea district, Loei province, Thailand and identified by Prof. Dr. Pranom Chantaranothai, Department of Biology, Khon Kaen University, Thailand. Air-dried stems of *H. parasitica* (2.7 kg) were ground into the powder and extracted successively with EtOAc (7L x 2) and MeOH (7L x 2) to give the corresponding crude EtOAc (109 g) and MeOH (211 g) extracts, respectively. All crude extracts were tested for their bioactivity and the result showed that the crude EtOAc exhibited anti-malarial activity against *P. falciparum* with IC$_{50}$ value of 3.25 μg/mL.

The structures of isolated compounds were identified by physical and spectroscopic data measurements (IR, 1D and 2D NMR, and MS) and by comparing the data obtained with published values, to yield four known compounds including 5,7,3',4'-tetrahydroxyflavan (**10A.1**),[5] (-)-syringaresinol (**10A.2**),[6] methyl 3,4,5-trihydroxybenzoate (**10A.4**) and (-)-epicatechin (**10A.5**). Whereas, compounds **10A.3**, **10A.6**, and **10A.7** were identified as new flavans (Figure 10A.1).

Compound **10A.3** was obtained as brown solid and its molecular formula, C$_{22}$H$_{18}$O$_9$, was deduced from the HRESITOFMS (observed m/z 449.0846 [M+Na]$^+$), indicating 14 degrees of unsaturation. The IR spectrum displayed the presence of hydroxyl (3309 cm^{-1}), and conjugated carbonyl ester (1704 cm^{-1}). The ^{13}C NMR and DEPT spectra indicated the presence of two methylene, eight methine (seven aromatic), eleven quaternary aromatic, and one carbonyl carbon moieties. The ^{1}H NMR data of **10A.3** was similar to those of the isolated 5,7,3',4'-tetrahydroxyflavan (**10A.1**),[5] except for the presence of aromatic methine proton at δ 7.17 (2H, s, H-2" and H-6", gallate ester skeleton). The HMBC also confirmed the presence of this gallate by showing the correlations of H-2" to C-1", C-3", C-4", C-6", and C-7"; and H-6" to C-1", C-2", C-4", C-5", and C-7". The HMBC correlations of H-6 to C-5, C-7, C-4a, and C-8; and H-8 to C-8a, C-7, C-4a, and C-6 demonstrated that the gallate ester connected to C-7 flavan position. Compound **10A.3** demonstrated the negative specific rotation ([α]$^{23}_D$ -45.3 *c* 0.1, MeOH), which was assigned the stereochemistry at C-2 as *S*. Based on the spectroscopic evidence, compound **10A.3** was determined as a new flavan, named (2*S*)-7-*O*-galloyl-5,3',4'-trihydroxyflavan.

The mixture of compounds **10A.6** and **10A.7** was light brown amorphous powder. Their molecular formula were determined based on the HREIMS data as C$_{29}$H$_{22}$O$_{13}$ (observed m/z 601.0960 [M+Na]$^+$), corresponding to 19 degrees of unsaturation and the presence of an

additional galloyl unit. The IR spectrum demonstrated the absorption bands of hydroxyl (3280 cm^{-1}), and conjugated carbonyl ester (1695 cm^{-1}) groups. The ^{1}H NMR spectrum of **10A.6** and **10.A7** clearly showed the mixture of two flavans, especially the signal at δ_H 4.87 (1H, d, J = 10.4 Hz, H-2) and δ_H 4.92 (1H, d, J = 10.4 Hz, H-2) of compounds **10A.6** and **10A.7**, respectively. The ratio of 2:3 (1.0:1.1) was deduced from ^{1}H NMR integrals at δ_H 6.95 (H-5', **10A.6**) and 6.88 (H-6', **10A.7**). The ^{1}H NMR spectrum of **10A.6** was similar to that of **10A.3** except for the presence of an additional proton signal at δ_H 7.22 (2H, d, 94, J = 0.8 Hz, H-2''' and H-6''') and the chemical shift of ring B, proposing the connection of galloyl group to C-3' of ring B. The HMBC exhibited correlations of this proton signal at δ_H 7.22 to C-1''', C-3''', C-4''', C-5''', and C-7''' which also confirmed an extra galloyl unit. The connection of this galloyl unit to C-3' of ring B was also supported by the HMBC correlations of H-2 (4.87, 1H, d, J = 10.4 Hz) to C-3, C-4, C-8a, C-1', C-2', and C-6'; H-5' (6.95, 1H, d, J = 8 Hz) to C-1', C-3', C-4', and C-6'; and H-6' (7.15-7.12, 1H, m, overlap with H-2') to C-2', C-4', and C-5'. Besides, the ^{1}H and ^{13}C NMR spectral data of **10A.7** were similar to those of **10A.6** except for the ^{1}H NMR chemical shift of ring B, suggesting that the galloyl ester was located at C-4'. The HMBC also revealed the correlations of H-2 (4.92, 1H, d, J = 10.4 Hz) to C-3, C-4, C-8a, C-1', C-2', and C-6'; H-5' (7.04, 1H, brd, J = 5.6 Hz) to C-1', C-3', C-4', and C-6'; and H-6' (6.88, 1H, dd, J = 8.4, 2.0 Hz) to C-2', C-4', and C-5' which corresponded to the connection of this galloyl group to C-4' of ring B. The ^{13}C NMR of **10A.7** exhibited the signal at δ_C 141.6 (C-1') which appeared at lower field than **10A.6** (δ_C 134.5, C-1') due to the lack of resonance effect of hydroxyl group at C-4'. The configuration at C-2 of **10A.6** and **10A.7** was determined as S from its specific rotation ($[\alpha]^{25}_D$ -23.5 c 0.1, MeOH). Therefore, compound **10A.6** was defined as (2S)-7,3'-O-digalloyl-5,4'-dihydroxyflavan. Whereas, compound **10A.7** was identified as a positional isomer of **10A.6**, named (2S)-7,4'-O-digalloyl-5,3'-dihydroxyflavan.

All isolated compounds were evaluated for their bioactivities (Table 10A.1). Compounds **10A.3** and the mixture of **10A.6** and **10A.7** showed significant antimalarial activity against *P. falciparum* with IC$_{50}$ values of 0.59 and 1.38 μM, respectively. In addition, compounds **10A.3** and the mixture of **10A.6** and **10A.7** exhibited moderate cytotoxicity toward NCI-H187 cancer cell with IC$_{50}$ values of 16.7 and 11.1 μM, respectively. Moreover, the mixture of **10A.6** and **10A.7** displayed cytotoxicity against KB and MCF-7 cancer cell lines with IC$_{50}$ values of 30.0 and 19.7 μM, respectively. However, the mixture of **10A.6** and **10A.7** was cytotoxic toward normal cell line (IC$_{50}$ 73.9 μM). While, the latter compounds were inactive for all bioactivity tests (IC$_{50}$ > 100 μM). The comparison of flavans **10A.1**, **10A.3**, and **10A.6** and **10A.7**, it

should be noted that the addition of galloyl groups increased the cytotoxicity toward three cancer cell lines (KB, MCF-7, and NCI-H187).
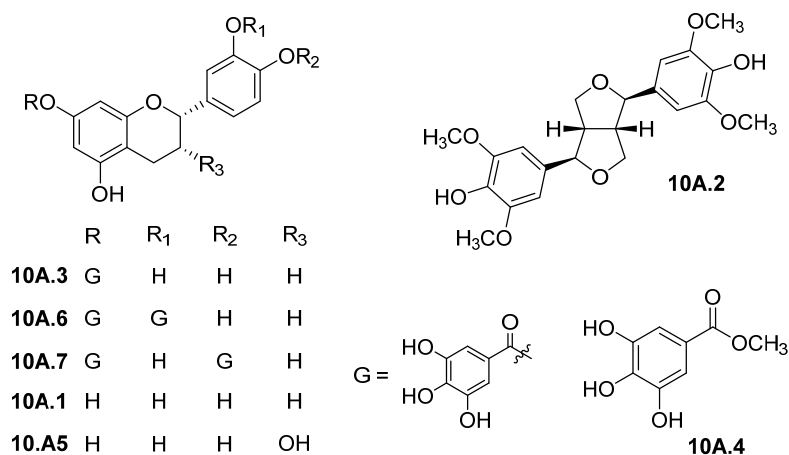

	R	R_1	R_2	R_3
10A.3	G	H	H	H
10A.6	G	G	H	H
10A.7	G	H	G	H
10A.1	H	H	H	H
10.A5	H	H	H	OH

Figure 10A.1. Structure of isolated compounds from *H. parasitica*.

Table 10A.1 Biological activity of compounds **10A.3**, **10A.6**, and **10A.7**

compound	antimalarial IC$_{50}$ (μM)	cytotoxicity IC$_{50}$ (μM)			
		KB^a	MCF-7^b	NCI-H187^c	Vero cells^d
10A.3	0.59	Inactive^e	Inactive	16.7	Inactive
10A.6 + **10A.7**	1.38	30.0	19.7	11.1	73.9
Dihydroartemisinin	0.008				
Doxorubicin			12.1		
Ellipticine		8.2		6.7	3.4

^{a}Human epidermoid carcinoma in the mouth. ^{b}Human breast adenocarcinoma. ^{c}Human small cell lung cancer. ^{d}African green monkey kidney. ^{e} > 100 μM.

References

1) Kwanda, N.; Noikotr, K.; Sudmoon, R.; Tanee, T.; Chaveerach, A. Medicinal parasitic plants on diverse hosts with their usages and barcodes. *J. Nat. Med.* 2013, *67*, 438–445.

2) Thai medicinal data base, Faculty of Pharmaceutical Sciences, Ubon Ratchathani University. Retrieved: May 2016, http://www.phargarden.com/main.php?action=viewpage&pid=203.

3) Liangqiong, L. ; Meirong, L. ; Wentao, F. Chemical constituents of Libanjisheng (*Helixanthera parasitica*). Zhongcaoyao 1994, *25*(6), 283–284.

4) Lirdprapamongkol, K.; Mahidol, C.; Thongnest, S.; Prawat, H.; Ruchirawat, S.; Srisomsap, C.; Surarit, R.; Punyarit, P.; Svasti, J. Anti-metastatic effects of aqueous extract of *Helixanthera parasitica*. *J. Ethnopharmacol.* 2003, *86*, 253–256.

5) Roemmelt, S.; Zimmermann, N.; Rademacher, W.; Treutter, D. Formation of novel flavonoids in apple (*Malusxdomestica*) treated with the 2-oxoglutarate-dependent dioxygenase inhibitor prohexadione-Ca. *Phytochemistry* 2003, *64*, 709–716.

6) Monthong, W.; Pitchuanchom, S.; Nuntasaen, N.; and Pompimon, W. (+) - Syringaresinol Lignan from New Species *Magnolia Thailandica*. *Am. J. Applied Sci.* 2011, *8*, 1268–1271.

5) Research Outcome:

Publication

Rajachan, O.; Hongtanee, L.; Chalermsaen, K.; Kanokmedhakul, K.; Kanokmedhakul, S. Bioactive galloyl flavans from the stems of *Helixanthera parasitica*. Journal Asian Natural Product, Published online: 2019 https://doi.org/10.1080/10286020.2019.1592165

Poster Presentation

Rajachan, O.; Kanokmedhakul, S.; Kanokmedhakul, K. Chemical constituents from the stem barks of *Helixanthera parasitica*. Pure and Applied Chemistry International Conference 2018 (PACCON 2018) at The 60th Anniversary of His Majesty the King's Accession to the Throne International Convention Center (ICC Hat Yai), Hat Yai, Songkhla, Thailand, 7-9 February 2018.

.

Project 10B: Investigate on Stems of *Croton krabas*.

1) Keywords

Croton krabas, Euphorbiaceae, Clerodane diterpene, antibaterial

2) Objective

2.1) To isolate and determine the chemical constituents from the stems of *Croton krabas*.

2.2) To evaluate the bioactive principles from isolated compounds against some human disease such as antibacterial and cancer.

3) Introduction

Croton krabas Gagnep. belongs to the family Euphorbiaceae which is known as "Fai nam" in Thai. It is a shrubby tree, 1–3 m in height, widely found in Lao, Cambodia and Thailand. The water decoctions of its bark and flowers are traditionally used as carminatives. The phytochemical investigations from the plant genus *Croton* have been explored. Many

compounds from this genus also exhibited many biological activities. However, the phytochemical investigation and bioactivity of the *C. krabas* has not been previously reported. Interestingly, the crude hexane and EtOAc extracts of this plant exhibited antibacterial as shown in Table 10B.1. Therefore, it is interested to study the chemical constituents and their biological activities from the stems of *C. krabas*.

Table 10B.1 Antibacterial screening of the crude extracts from the stems of

C. krabas.

Test bacterium	Zone of inhibition (mm)	
	Hexane extract	EtOAc extract
Bacillus cereus ATCC 11778	12x12	13x13

4) Result and Discussion

Air-dried powdered of the stems of *C. krabas* (3.6 kg) were extracted successively with organic solvents including hexane, EtOAc and MeOH. Each 12 L of solvent extraction was carried out at room temperature for 3 days in triplicate. The solvents were evaporated under reduced pressure to give crude hexane (43 g), EtOAc (43 g) and MeOH (118 g) extracts, respectively.

The crude hexane extract (43 g) was applied over silica gel FCC, eluted with a gradient system of *n*-hexane-EtOAc-MeOH to give nine fractions CKH1–CKH9. Recrystallization of fraction CKH2 from CH_2Cl_2-MeOH gave compound **10B.1**. Fraction CKH3 was recrystallized from CH_2Cl_2-MeOH to obtain compound **10B.2**. Fraction CKH4 was separated by silica gel CC, eluted with 10% acetone-hexane yielding three subfractions, CKH4.1–CKH4.3. Subfraction 4.3 was purified by silica gel CC, eluted with an isocratic system of 10% acetone-hexane to give four subfractions, CKH4.3.1–CKH4.3.3. Subfraction CKH4.3.1 was further separated by silica gel CC, using 2% EtOAC-CH_2Cl_2 as an eluent, to give two subfractions, CKH4.3.1.1 and CKH4.3.1.2. Subfraction CKH4.3.1.2 was subjected to Sephadex LH-20 CC, eluted with MeOH yielding compound **10B.3**. Subfraction CKH4.3.2 gave a white solid of compound **10B.4**. Fraction CKH6 was isolated by silica gel CC, eluted with an isocratic system of 2% EtOAC-CH_2Cl_2 to give four subfractions, CKH6.1–CKH6.4. Subfraction CKH6.3 was applied on reverse phase RP-18 CC, eluted with 20 H_2O-MeOH to give compound **10B.5**. Subfraction CKH7 was purified by reverse phase RP-18 CC, eluted with 20 H_2O-MeOH to obtain four sunfrations, CKH7.1–CKH7.4. Subfraction 7.3 was furture separated by silica gel CC, using 2% EtOAC-CH_2Cl_2 as an eluent, to give compound **10B.6**.

The crude EtOAc extract (43 g) was applied over silica gel FCC, eluted with a gradient system of n-hexane-EtOAc-MeOH to give seven fractions CKE1–CKE7. Fraction CKE2 was separated by silica gel CC, eluted with 10% acetone-hexane yielding compound **10B.5**. Fraction CKE6 was further separated by silica gel CC, using 15% acetone-hexane as an eluent, to give four subfractions, CKE6.1- CKE6.4. Recrystallization of subfraction CK6.2 from CH_2Cl_2-MeOH gave compound **10B.7**.

The structures of isolated compounds were identified by physical and spectroscopic data measurements (IR, ^{1}H and ^{13}C NMR) and by comparing with published values, to obtain three known compounds including lupeol (**10B.1**)[1], crotonpyrone A (**10B.3**)[2], and 12-oxo-hardwickiic acid (**10B.5**)[3] (Figure 10B.1). While, structural identificaiton of compounds **10B.2**, **10B.4**, **10B.6**, and **10B.7** are in progress.
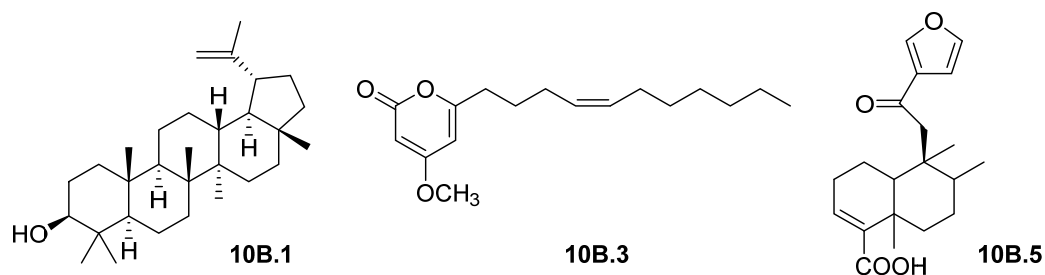
Figure 10B.1. Structure of isolated compounds from the stems of *C. krabas*.

References

1) Maciel S.; Cassia M.; Lucienir D.; Wagner M.; Ana Lucia R.; Larissa S.; Joao C.; Izabel T.; and Sidney F. Lupeol and its esters: NMR, powder XRD data in vitro evaluation of cancer cell growth.
    J. Pharm. Sci, 2017, *53*, 251–262.

2) Hui L.; Feng M.; Le-Le D.; Gai-Xia F.; Jing-Min C.; Ding-Ding G.; Zhan-Xin Z.; and Ding- Qing F. Cytotoxic and antibacterial pyran-2-one derivatives from *Croton crassifolius. Phytochemistry Lett*. 2014, *10*, 304–308.

3)   Santos, H.S.; Barros,F.W.A.; Albuquerque, M.R.J.R.; Bandeira,P.N.; Pessoa, C.; Braz-Filho, R.; Monte, F.J.Q.; Leal-Cardoso, J.H.; and Lemos, T.L.G. Cytotoxic diterpenoids from *Croton argyrophylloides*. *J. Nat. Prod*. 2009, *72*, 1884–1887.

5) Research Outcome:

The remaining of EtOAc extract of the stems of *C. krabas* will be continuously purified by chromatographic techniques. All isolated compounds will be identified and will be sent to biologically evaluation. The manuscript will be prepared.

Part II: Development of Chaetoglobosin C as a Microbial Elicitor to be Nanoproduct for Plant Immunity

Project 11: Preparation and Evaluation of Biocontrol Agent

Researcher: Kasem Soytong (Project Leader)

1) Keywords

Chaetomium chaetoglobosin C, elicitor, plant immunity**,** biocontrol

2) Objective

To develop biocontrol agents against plant diseases.

3) Introduction

Plant disease is one of the serious problems for farmers in Thailand and worldwide. The use of chemical fungicides, insecticides and herbicides for protecting their crops causes hazards in food production and environmental problems. For example, Fusarium wilt, one of the most serious diseases caused by *Fusarium oxysporum* f. sp. *lycopersici* (Sacc.) in tomatoes (*Lycopersicon esculentum* Mill.) results in yield loss and causes economic problems. Generally, chemical application has been used to control the disease. However, the pathogens have become resistant to these chemicals. This method then does not control the disease while causing health and environmental problems. In this regard, the alternative method with emphasis on biological control of plant diseases should be used to reduce chemicals used. Our collaboration research, with plant pathologist Assoc. Prof. Kasem Soytong, working on biological active compounds from antagonistic fungi both in laboratory and field trials found that some natural compounds, such as cheatoglobosin C from antagonistic fungus *Chaetomium globosm*, shows potential for biological control activity. In addition, study of *Chaetomium Chaetomium cupreum* and *Chaetomium globosum* is to develop natural products for plant disease control, induce plant immunity, and for environmental friendly agriculture.

4) Result and Discussion

4.1) Study on pathogen and antagonists

Phytophthora palmivora was isolated to pomelo and confirmed patholognecity test. It was cultured in V8 medium for morphological characterization. The isolate is confirmed identification by morphological and molecular phylogeny. Pathogenicity test was done to confirm pathogenic isolate. Morphology of *Phytophthora palmivora* was studied to confirm species (Figure **11.1**).
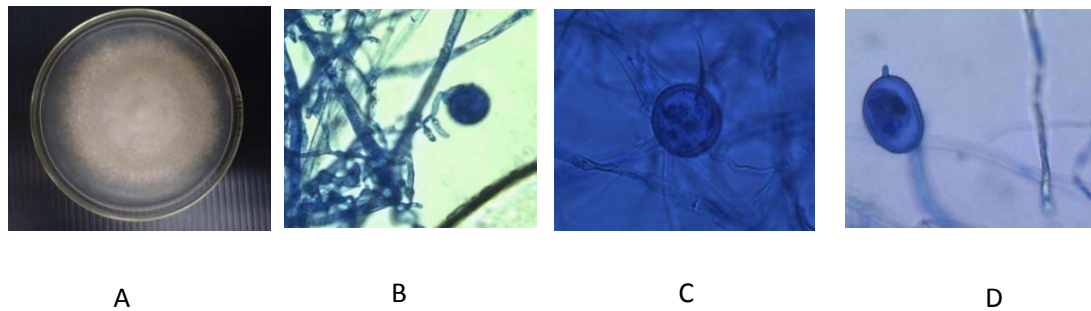
Figure 11.1 Characteristics of *Phytophthora palmivora*, A: colony on V8 medium,

B: Sporangia (400 X)   C and D: Oogonium (400 X)

Morphology: *Chaetomium cupreum* and *Chaetomium globosum* were cultured and confirm species by culturing on PAD and observation (Figures 11.2 and 11.3).
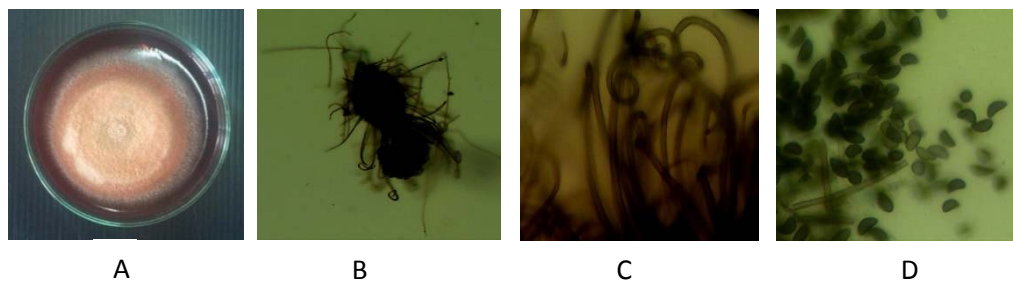
Figure 11.2. *Chaetomium cupreum*, A: colony on PDA, B: Perithecium (100 X)
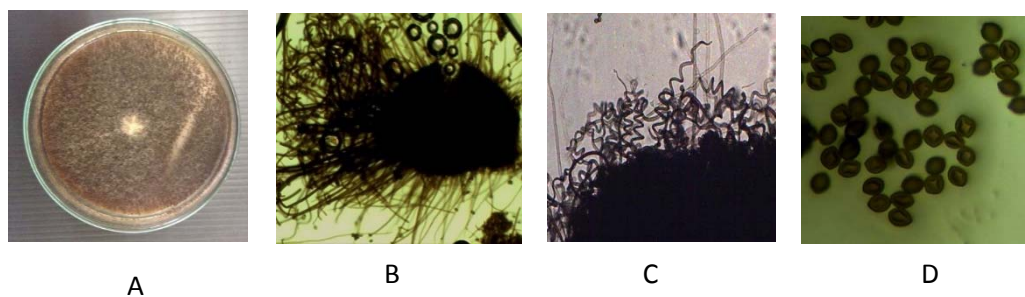
C: Terminal hairs (400X) and D: ascospores (400X).

Figure 11.3. *Chaetomium globosum*, A: colony on PDA, B: Perithecium (400X)

C: terminal hairs (400X) and D: ascospores (400X).

4.2) Pathogenicity test

Phytophthora palmivora was inoculated by detached leaf method which resulted brown lesion and invaded clearly symptom in 5 days incubation (average of four replications). The non inoculated control was no lesion (Table 11.1 and Figure 11.4).

Table 11.1 Pathogenecity test of *Phytophthora palmivora*

Isolate	Colony diameter (cm)
Control	0.50[*]
Phytophthora palmivora	4.33

*
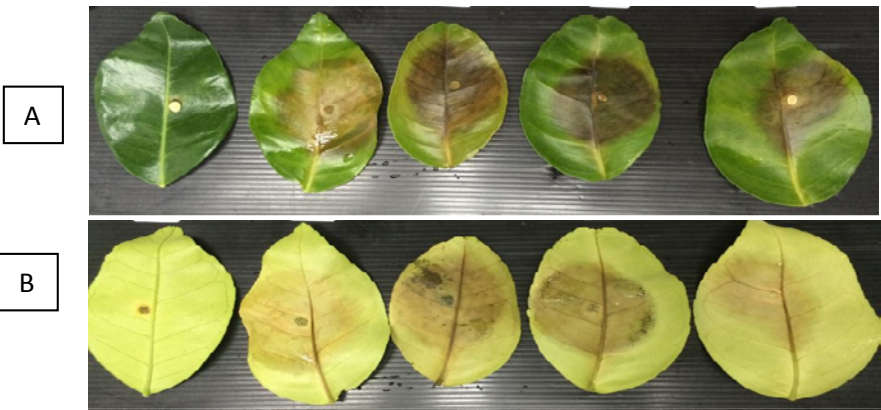
Figure 11.4. Pathogenicity test, A: Front side, B back side; First of leaf (left hand side) is non inoculated. The other four are inoculated with *Phytophthora palmivora.*

Testing nanoproducts to control *P. palmivora* causing root rot of Pamelo in laboratory

P. palmivora growing on PDA incorporated with nano-cupreum and nano-globosum at the concentrations of 3, 5 and 10 ppm were performed. The result showed that nano-globosum and nano-cupreum expressed antifungal activity against *P. palmivora* at the ED_{50} of 4.12 and 2.60 ppm, respectively (Table 11.2, Figures 11.5 and 11.6).

Table 11.2 Testing nanoproducts to control *P. palmivora* causing root rot of

pamelo in laboratory

Treatments	Conc. (ppm)	Colony dia.(cm)	%inhibition[2/]	ED$_{50}$ (ppm)
Nano-cupreum	0	5.00a[1/]		
	3	1.03b	79.4	
	5	0.5b	90	
	10	0.5b	90	4.12
Nano-globosum	0	5.00a		
	3	0.68bc	86.4	
	5	0.5b	90	
	10	0.5b	90	2.60
C.V. (%)	19.50			

1 Average of four replications. Means followed by a common letter a a column are not significantly different by DMRT at P=0.05.

2 % Inhibition = colony diameter in control plate – colony diameter in treated plate/ colony diameter in control plate X 100.
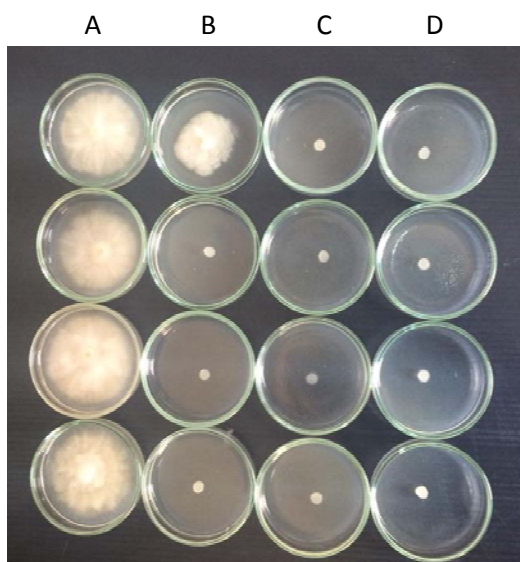
Figure 11.5 Nano-cupreum testing against *Phytophthora palmivora* at

0 ppm (A), 3 ppm (B), 5 ppm (C), 10 ppm (D)
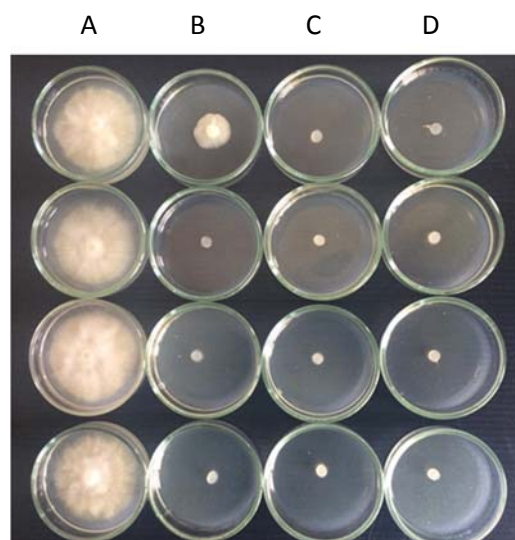
Figure 11.6 Nano-globosum testing against *Phytophthora palmivora*

at 0 ppm (A), 3 ppm (B), 5 ppm (C), 10 ppm (D)

4.3) Preparation and characterization of Nano-chaetoglobosinC

Electrospinning

The solution of chaetoglobosin C (10 mg in 0.5 ml DMSO) was drop into polylactic acid (1 grams in 5 mL tetrahydrofuran). The mixture was loaded into a syringe and placed into the electrospinning set-up. The tip of the syringe was clipped with the positive pole while the aluminum foil was clipped with the negative pole and serves as the collector. The voltage used was 25 to 30 kilovolts. The product was carefully scraped from the aluminum foil and stored in tightly capped bottles. The characteristics of the products were noted, viewed under the scanning electron microscope and the properties were analyzed using Fourier Transform Infrared spectroscopy.

5) Research Outcome

Publication

6.1 Song, J. J., Kanokmedhakul, S., Kanokmedhakul, K., Soytong, S., Application of nano-particles derived from *Chaetomium elatum* ChE01 to control *Pyricularia oryzae* causing rice Blast. International Journal of Agricultural Technology 2018,14(6), 923-932.

6.2 Song, J. J., Soytong, K., Kanokmedhakul, S. and Kanokmedhakul, K. Nano-particles from *Chaetomium lucknowense* to inhibit rice blast pathogen causded by *Pyricularia oryzae* in pot experiment. International Journal of Agricultural Technology 2018,14(7), 1961-1968.

6.3 Thongkham, D., Soytong, K., Kanokmedhakul, S., Kanokmedhakul, K. Nano-particles derived from *Chaetomium elatum* against *Phytophthora* rot of durian. International Journal of Agricultural Technology 2018, 14(7): 2115-2124.

6.4 Tongon, R., Soytong, K., Kanokmedhakul, S., Kanokmedhakul, K. Nano-particles from *Chaetomium brasiliense* to control *Phytophthora palmivora* caused root rot disease in durian var Montong. International Journal of Agricultural Technology 2018, 14(7): 2163-2170.

6.5 Udompongsuk, M.1 , Soytong, K., Kanokmedhakul, S., Kanokmedhakul, K. *In vitro* efficacy of *Chaetomium brasiliense* against *Pythium* spp. causing root rot disease of tangerine. International Journal of Agricultural Technology 2018, 14(7): 2181-2190.

6.6 Vareeket, R., Soytong, K., Kanokmedhakul, S. and Kanokmedhakul, K. Nano-particles from *Chaetomium brasiliense* against brown spot of rice. International Journal of Agricultural Technology 2018, 14(7): 2207-2214.

PROJECT OUTPUT

1. สรุปผลงานวิจัย

งานวิจัยแบ่งเป็น 2 ส่วน ในส่วนแรกเป็นการศึกษาสารองค์ประกอบและฤทธิ์ทางจากพืชและรา ส่วนที่สองเป็นการวิจัยและพัฒนาเพื่อประยุกต์ใช้ประโยชน์จากสารผลิตภัณฑ์ธรรมชาติทางด้านการเกษตรกรรม

Part 1 (Projects 1-10):

งานวิจัยในส่วนนี้เป็นการศึกษาสารออกฤทธิ์ทางชีวภาพจากพืชในภาคอีสานและราในประเทศไทย มี 10 โครงการประกอบด้วย 24 โครงการย่อย โดยแยกสารและวิเคราะห์โครงสร้างได้สารองค์ประกอบจาก ตัวอย่างพืช 14 ชนิดและรา 9 ชนิดแยกได้สารทั้งหมด 274 สาร ในจำนวนนี้พบว่าเป็นสารใหม่ 64 สาร โดยแบ่งเป็นจากพืช 14 ชนิด แยกได้ 152 สาร เป็นสารใหม่ 38 สาร และจากรา 9 ชนิด แยกได้ 122 สาร เป็นสารใหม่ 26 สาร สารเหล่านี้มีหลายกลุ่ม เช่น แอลคาลอยด์ เทอร์ปีนอยด์ สเตอรอยด์ ฟลาวานอยด์ ไตรโคทีซีน แซนโทนคิวนิดีน ออกซาฟีนาลีโนน กลัยโคไซด์ และอื่นๆ พบว่ามีสารจำนวนหนึ่งแสดงฤทธิ์ทางชีวภาพที่ดี เช่น ยับยั้งเชื้อมาลาเรีย (*Plasmodium falciparum*) ยับยั้งเชื้อวัณโรค (*Mycobacterium tuberculosis*) ยับยั้งเชื้อแบคทีเรียก่อโรคในมนุษย์ ยับยั้งแอลฟากลูโคซิเดสที่เกี่ยวกับโรคเบาหวาน ยับยั้งเอนไซม์แอซีทิลโคลีนเอสเทอเรสที่เกี่ยวกับโรคอัลไซเมอร์และยับยั้งอนุมูลอิสระ รวมถึงทดสอบความเป็นพิษต่อเซลล์มะเร็งชนิดต่างๆ เป็นต้น

Part 2 (Project 11):

สำหรับงานวิจัยส่วนที่สองนี้ได้ศึกษาฤทธิ์ของราสกุลคีโตเมียม ได้แก่ *Chaetomium brasiliense*, *Chaetomium cupreum, Chaetomium elatum, Chaetomium globosum* and *Chaetomium lucknowense* ในการยับยั้งราก่อโรคพืช เช่น โรครากเน่าในทุเรียน ส้มโอ และโรคใบไหม้ในข้าว รวมทั้งผัก เช่น มะเขือเทศ และพริก โดยพัฒนาเป็นผลิตภัณฑ์นาโนเพื่อเพิ่มประสิทธิภาพและง่ายต่อการใช้งาน โดยสาร ผลิตภัณฑ์นาโนจากสารออกฤทธิ์คือคีโตโกลโบซินซี กำลังอยู่ระหว่างการเตรียมข้อมูลสำหรับจดอนุสิทธิบัตร

2. ผลงานตีพิมพ์ในวารสารวิชาการระดับนานาชาติ

2.1 ผลงานที่ได้รับตีพิมพ์จำนวน 21 เรื่อง (ดูภาคผนวก)

2.2 ผลงานที่อยู่ระหว่างการตีพิมพ์ จำนวน 1 เรื่อง

Promgool, T., Kanokmedhakul, K., Tantapakul, C., Suchaichit, N. P., Yahuafai, J., Siripong, P., Kelemen, C.D., Kokoska, L., Kanokmedhakul, S. Bioactive secondary metabolites from roots of *Cissus rheifolia* Planch. Natural Product Research (in press 2019)

2.3 ผลงานที่อยู่ระหว่าง review จำนวน 1 เรื่อง

J. Paluka, K. Kanokmedhakul, M. Soytong, K. Soytong, J. Yahuafaid, P. Siripongd, S. Kanokmedhakul, Meroterpenoid pyrones, alkaloid and brasiliamide derivative from the fungus *Neosartorya hiratsukae*. Fitoterapia (2019 under review)

2.4 ผลงานที่อยู่ระหว่างเตรียม manuscript จำนวน 2 เรื่อง

Chaiyosang, B., Kanokmedhakul, K., Soytong, K., Soytong, M., Hadsadee, S., Jungsuttiwon, S., Yahuafai, J., Siripong, S., Kanokmedhakul, S. New pyrrolobenzoxazines terpenoid analogues from the fungus *Talaromyces trachyspermus* EU23. will be submitted to Phytochemistry.

Tantapakula, C., Chaiyosanga, B., Suthiphasilp, V., Kanokmedhakul, K., Laphookhieo, S., Andersen, R.J., Patrick, B. O., Kanokmedhakul, S., Spirosteroid saponins and acetylenic derivatives with α-glucosidase inhibitory from *Asparagus racemosus* roots. will be submitted to Phytochemistry.

3. การนำเสนอผลงานวิจัย จำนวน 17 เรื่อง

1.1 Kanokmedhakul, S.,"Thai-plant and fungal resources based anti-AD/T2 DM drug lead compound discovery and pharmacological mechanism investigation" The 6th China-Thailand Joint Workshop on Natural Products and Drug Discovery, Aonang Cliff Beach Resort, Krabi, Thailand, 16-20 October, 2016.

1.2 Lekphrom, R.," Chemical Constituents and Biological Activities from the Aerial Parts of *Sphaeranthus indicus*" The 6th China-Thailand Joint Workshop on Natural Products and Drug Discovery, Aonang Cliff Beach Resort, Krabi, Thailand, 16-20 October, 2016.

1.3 Kanokmedhakul, S. "Success Cases toward the Promotion of Neglected and Underutilized Indigenous Crop Species (NUS) in Thailand" Regional Workshop on Promotion of Neglected and underutilized indigenous crop species (NUS) for food security and nutrition in southeast Asia and EU" University of Battambang, Battambang, Cambodia, 20-22 July 2016.

1.4 Kanokmedhakul, K. "Integration Research between Agriculture and Chemistry" Regional Workshop on Promotion of Neglected and underutilized indigenous crop species (NUS) for food security and nutrition in southeast Asia and EU, University of Battambang, Battambang, Cambodia, 20-22 July 2016.

1.5 Kanokmedhakul, S. 'Neglected and underutilized plant species in northeastern part of Thailand" 2nd Regional Workshop on Promotion of Neglected and Underutilized Indigenous Crop Species (NUS) for Food Security and Nutrition in Southeast Asia and the EU, Interfaculty Centre of Environmental Sciences II (5th floor, room D551) Czech University of Life Sciences Prague, Czech Republic, 14-15 November 2016.

1.6 Paluka, J., Kanokmedhakul, S., Kanokmedhakul, K., Soytong, K. "Bioactive mero terpenoids and alkaloids from the fungus *Neosartorya pseudofischeri*" 5th International Conference on Integrating Science and Technology for Sustainable Development, Cherry Queen Hotel, Southern Shan State, Myanmar, 26-27 November 2016.

1.7 Lakornwong W, Kanokmedhakul S, Kanokmedhakul K, Soytong K. "Phytochemistry from the fungus *Myrothecium roridum*" 5th International Conference on Integrating Science and Technology for Sustainable Development, Cherry Queen Hotel, Southern Shan State, Myanmar, 26-27 November 2016.

1.8 Lakornwong W, Kanokmedhakul S, Kanokmedhakul K, Soytong K. "Chemical constituents from *Myrothecium roridum* and their bioactivities", at 116th RGJ Seminar Series, at College of Local Administration, Khon Kaen University, Khonkaen, Thailand, 9-10 August 2016.

1.9 Kanokmedhakul, S. "Bioactive Compounds from Thai (Isan) NUS" Regional Workshop on Promotion of neglected and underutilized indigenous crop species (NUS) for food security and nutrition in southeast Asia and EU, Natural Products Research Unit, Department of Chemistry, Faculty of Science, Khon Kaen University, Khon Kaen, Thailand, 20-22 April 2017.

1.10 สมเดช กนกเมธากุล นำผลงานการวิจัยไปเผยแพร่ในงานนิทรรศการ "25 ปี สกว สร้างคน สร้างความรู้ สร้างอนาคต" สยามพารากอน กรุงเทพฯ วันที่ 25-26 สิงหาคม 2560

1.11 Kanokmedhakul, S. "Secondary metabolites and their biological activities from soil-derived fungi" The 6th International Conference on Integration of Science and Technology for Sustainable Development 2017 (6th ICIST 2017) Hotel Supreme and Convention Plaza, Baguio City, Philippines, November 24-26, 2017.

1.12 Kanokmedhakul, S. "Bioactive secondary metabolites from saprophytic fungi and mushroom" Pure and Applied Chemistry International Conference 2018 (PACCON 2018), HatYai, Songkha, Thailand, 7-9 February 2018.

1.13 Rajachan, O.; Kanokmedhakul, S.; Kanokmedhakul, K. "Chemical constituents from the stem barks of *Helixanthera parasitica*" Pure and Applied Chemistry International Conference 2018 (PACCON 2018), Hat Yai, Songkhla, Thailand, 7-9 February 2018.

1.14 Moosophon, P. "Cytotoxic Naphthalenones from *Diospyros undulata*" TRF Senior Research Scholar 2018 "Research on Bioactive Compounds from ISAN Plants and Thai Fungi, Natural Products Research Unit, Department of Chemistry, Faculty of Science, Khon Kaen University, 30 June – 1 July 2018.

1.15 Kanokmedhakul, S. "Thai-plant and fungal resources based anti-T2DM/AD drug lead compound discovery and pharmacological mechanism investigation" The 7th China-Thailand Workshop on Natural Products and Drug Discovery, Nanjing, P. R. China School of Chemistry and Chemical Engineering, Nanjing University, Nanjing, Jiangsu 4-8 November 2018.

1.16 Kanokmedhakul, S.; Soytong, K.; Kanokmedhakul, K., "Microbial Elicitors for Plant Immunity" invited speaker in the 7[th]International Conference on Integration of Science and Technology for Sustainable Development 2018 (7th ICIST 2018) November 26-29, 2018 the Patra Bali Resort and Villas, Bali, Indonesia.

1.17 Kanokmedhakul, K.; Soytong, K.; Kanokmedhakul, S., "Mycotoxins in Plants Pathogenic Fungi" invited speaker in the 7[th]International Conference on Integration of Science and Technology for Sustainable Development 2018 (7th ICIST 2018) November 26-29, 2018.at the Patra Bali Resort and Villas, Bali, Indonesia.

4. การสร้างนักวิจัย

นักวิจัยหลัก 11 คน จาก 6 มหาวิทยาลัย ได้แก่ มหาวิทยาลัยขอนแก่น มหาวิทยาลัยกาฬสินธุ์ มหาวิทยาลัยมหาสารคาม มหาวิทยาลัยราชภัฏอุดรธานี มหาวิทยาลัยเทคโนโลยีราชมงคลอีสาน และ สถาบันเทคโนโลยีพระจอมเกล้าเจ้าคุณทหารลาดกระบัง โดยมีนักวิจัยอาวุโส 3 คน หลังจากโครงการ เสร็จสิ้น มีนักวิจัยได้ดำรงตำแหน่งทางวิชาการสูงขึ้น 5 คน คือ ตำแหน่งศาสตราจารย์ 1 คน และ ผู้ช่วยศาสตราจารย์ 4 คน ทั้งนี้สามารถสร้างนักวิจัยระดับต่างๆดังนี้

4.1 นักวิจัยหน้าใหม่ 8 คน โดยมีนักวิจัย 3 คน สามารถขอทุนนักวิจัยรุ่นใหม่ สกว.ได้

และอีก 5 คน สามารถขอทุนวิจัยจากแหล่งอื่นๆได้

4.2 ผู้ช่วยวิจัย 2 คน

4.3 นักศึกษา ระดับปริญญาเอก 10 คน และ ปริญญาโท 4 คน ปริญญาตรี 15 คน

5. การเชื่อมโยงทางวิชาการกับนักวิชาการอื่น ๆทั้งในและต่างประเทศ

นักวิจัยในโครงการมีงานวิจัย และมีการติดต่อเชื่อมโยงกับนักวิจัยทั้งในและต่างประเทศ ได้แก่ ประเทศเยอรมันนี แคนาดา สาธารณรัฐเช็ก ออสเตรเลีย ญี่ปุ่น และสาธารณรัฐประชาชนจีน รวมทั้ง นักวิจัยไทยในมหาวิทยาลัยต่างๆ ผ่านรูปแบบกิจกรรมต่างๆ เช่น การบรรยายในการประชุมสัมมนา การแลกเปลี่ยนประสบการณ์การวิจัย การให้คำปรึกษา และการให้ความร่วมมือในการแลกเปลี่ยน ข้อมูล ซึ่งเป็นการเพิ่มพูนและเรียนรู้ความรู้ใหม่ๆทางวิชาการอย่างต่อเนื่อง

6.การจัดการอบรม/ประชุมวิชาการ

จัดอบรมและประชุมวิชาการทั้งระดับชาติและนานาชาติ จำนวน 3 ครั้ง

6.1 จัดการประชุมโครงการความร่วมมือระหว่าง Asian and EU ที่ภาควิชาเคมี คณะวิทยาศาสตร์ มหาวิทยาลัยขอนแก่น ในหัวข้อ "Promotion of Neglected and underutilized indigenous crop species (NUS) for food security and nutrition in southeast Asia and EU" 20-22 April 2017

6.2 จัดงานประชุมสัมมนา TRF Senior Research Scholar Seminar 2018 เรื่อง Research on Bioactive Compounds from ISAN Plants and Thai Fungi ระหว่างวันที่ 30 มิถุนายน – 1 กรกฎาคม 2561 ที่ ห้องประชุมภาควิชาเคมี คณะวิทยาศาสตร์ มหาวิทยาลัยขอนแก่น

6.3 จัดงานประชุมสัมมนา TRF Senior Research Scholar Seminar 2019 เรื่อง งานวิจัยเคมีของ ผลิตภัณฑ์ธรรมชาติในประเทศไทย: อดีต ปัจจุบันและอนาคตในวันที่ 4-6 กรกฎาคม 2562 ห้อง ประชุมสาขาวิชาเคมี คณะวิทยาศาสตร มหาวิทยาลัยขอนแก่น

ภาคผนวก

ผลงานตีพิมพ์ในวารสารวิชาการนานาชาติ 21 เรื่อง

1. Lakornwong, W.; Kanokmedhakul, K.; Soytong, K.; Unartngam, A.; Tontapha, S.; Amornkitbamrung, V.; Kanokmedhakul, S. Types A and D trichothecene mycotoxins from the fungus *Myrothecium roridum*. Planta Medica **2019**, 85, 774-780.

2. J. Paluka, K. Kanokmedhakul, M. Soytong, K. Soytong, S. Kanokmedhakul, Meroditerpene pyrone, tryptoquivaline and brasiliamide derivatives from the fungus *Neosartorya pseudofischeri*. Fitoterapia **2019**, 137, 104257 (Online 03 July 2019).

3. Tantapakul, C., Promgool, T., Kanokmedhakul, K., Soytong, K., Song, J., Hadsadee, S., Jungsuttiwong, S., Kanokmedhakul, S. Bioactive xanthoquinodins and epipolythiodioxopiperazines from *Chaetomium globosum* 7s-1, an endophytic fungus isolated from *Rhapis cochinchinensis* (Lour.) Mart. Natural Product Research, Published online **2018** doi.org/10.1080/14786419.2018.1489392

4. Chaiyosaeng, B.; Kanokmedhakul, K.; Sanmanoch, W.; Boonlue, S.; Hadsadee, S.; Jungsuttiwong, S.; Kanokmedhakul, S. Bioactive oxaphenalenone dimers from the fungus *Talaromyces macrosporus* KKU-1NK8. Fitoterapia **2019**, 134, 429-434.

5. Lakornwong, W., Kanokmedhakul, K., Kanokmedhakul, S. A new coruleoellagic acid derivative from stems of *Rhodamnia dumetorum*. Natural Product Research, **2018**, 32(14) 1653–1659.

6. Lekphrom, R., Kanokmedhakul, K., Schevenels, F., Kanokmedhakul, S. Antimalarial polyoxygenated cyclohexene derivatives from the roots of *Uvaria cherrevensis*. Fitoterapia **2018**, 217, 420-424.

7. Somteds, A., Tantapakul, C., Kanokmedhakul, K., Laphookhieo, S., Phukhatmuen, P., Kanokmedhakul, S. Inhibition of nitric oxide production by clerodane diterpenoids from leaves and stems of Croton poomae Esser, Natural Product Research, Published online: 23 Sep **2019**, doi.org/10.1080/14786419.2019.1667350

8. Arthan, S.; Tantapakul, C.; Kanokmedhakul, K.; Soytong, K.; Kanokmedhakul, S. A new xanthone from the fungus *Apiospora montagnei*. Natural Product Research, **2017**. 31, 1766–1771.

9. Rajachan, O.; Kanokmedhakul, K.; Soytong, K.; Kanokmedhakul, S. Mycotoxins from the fungus *Botryotrichum piluliferu* Journal of Agricultural and Food Chemistry **2017**, 65(7), 1337-1341.

10. Wongsa, N.; Kanokmedhakul K.; Boonmak, J.; Youngme, S.; Kanokmedhakul, S. Bicyclic lactones and racemic mixtures of dimeric styrylpyrones from the leaves of *Miliusa velutina*. RSC Advances **2017**, 7(41), 25285–25297.

11. Promgool, T.; Kanokmedhakul, K.; Tontapha, S.; Amornkitbamrung, V.; Tongpim, S.; Jamjan, W.; Kanokmedhakul S. Bioactive homogentisic acid derivatives from fruits and flowers of *Miliusa velutina*. Fitoterapia **2019**, 134, 65-72.

ผลงานตีพิมพ์ในวารสารวิชาการนานาชาติ 21 เรื่อง (ต่อ)

12. Suchaichit, N., Suchaichit, N.P., Kanokmedhakul, K., Boottanun, P., Sermswan, R.W., Moosophon, P., Kanokmedhakul, S. A new cytotoxic plumbagin derivative from roots of *Diospyros undulata*. Natural Product Research, Published online: **2019**, doi:10.1080/14786419.2019.1630120.

13. Suchaichit, N.; Kanokmedhakul, K.; Promgool, T.; Moosophon, P.; Chompoosor, A.; Suchaichit, N.P., Kanokmedhakul, K. A new antibacterial tirucallane from *Walsura trichostemon* roots. Natural Product Research, Published online: **2019** doi.org/10.1080/14786419.2019.1669025

14. Sangsopha W, Lekphrom R, Schevenels FT, Saksirirat W, Bua-Art S, Kanokmedhakul K, Kanokmedhakul S. 2018.New p-terphenyl and benzoquinone metabolites from the bioluminescent mushroom *Neonothopanus nambi*. Natural Product Research, Published online: **2019**. Doi: 10.1080/14786419.2019.1578763

15. Rajachan, O.; Hongtanee, L.; Chalermsaen, K.; Kanokmedhakul, K.; Kanokmedhakul, S. Bioactive galloyl flavans from the stems of *Helixanthera parasitica*. Journal Asian Natural Product, Published online: **2019** https://doi.org/10.1080/10286020.2019.1592165

16. Song, J. J., Kanokmedhakul, S., Kanokmedhakul, K., Soytong, S., Application of nano-particles derived from *Chaetomium elatum* ChE01 to control *Pyricularia oryzae* causing rice Blast. International Journal of Agricultural Technology **2018**,14(6), 923-932.

17. Song, J. J., Soytong, K., Kanokmedhakul, S. and Kanokmedhakul, K. Nano-particles from *Chaetomium lucknowense* to inhibit rice blast pathogen causded by *Pyricularia oryzae* in pot experiment. International Journal of Agricultural Technology **2018**,14(7), 1961-1968.

18. Thongkham, D., Soytong, K, Kanokmedhakul, S., Kanokmedhakul, K. Nano- particles derived from *Chaetomium elatum* against *Phytophthora* rot of durian. International Journal of Agricultural Technology **2018**, 14(7): 2115-2124.

19. Tongon, R., Soytong, K., Kanokmedhakul, S., Kanokmedhakul, K. Nano-particles from *Chaetomium brasiliense* to control *Phytophthora palmivora* caused root rot disease in durian var Montong. International Journal of Agricultural Technology **2018**, 14(7): 2163-2170.

20. Udompongsuk, M.1 , Soytong, K., Kanokmedhakul, S., Kanokmedhakul, K. *In vitro* efficacy of *Chaetomium brasiliense* against *Pythium* spp. causing root rot disease of tangerine. International Journal of Agricultural Technology, **2018**, 14(7): 2181-2190.

21. Vareeket, R., Soytong, K., Kanokmedhakul, S. and Kanokmedhakul, K. Nano-particles from *Chaetomium brasiliense* against brown spot of rice. International Journal of Agricultural Technology **2018**, 14(7): 2207-2214.
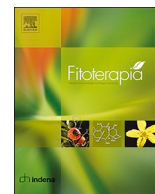
Meroditerpene pyrone, tryptoquivaline and brasiliamide derivatives from the fungus *Neosartorya pseudofischeri*

Jakkapat Paluka[a], Kwanjai Kanokmedhakul[a], Mayamor Soytong[b], Kasem Soytong[c], Somdej Kanokmedhakul[a],*

[a] *Natural Products Research Unit, Department of Chemistry and Center of Excellence for Innovation in Chemistry, Faculty of Science, Khon Kaen University, Khon Kaen 40002, Thailand*
[b] *Department of Biology, Faculty of Science, King Mongkut's Institute of Technology Ladkrabang, Bangkok 10520, Thailand*
[c] *Department of Plant Pest Management, Faculty of Agricultural Technology, King Mongkut's Institute of Technology Ladkrabang, Bangkok 10520, Thailand*

ARTICLE INFO

ABSTRACT

Two new meroditerpene pyrones, chevalone F (**1**) and 11-hydroxychevalone E (**2**), a new tryptoquivaline analog, tryptoquivaline V (**3**) and a new brasiliamide analog, brasiliamide G (**4**), together with thirteen known compounds, chevalones A-C (**5–7**), chevalone E (**8**), 11-hydroxychevalone C (**9**), pyripyropene A (**10**), iso-chaetominine C (**11**), pyrrolobenzoxazine terpenoids CJ-12662 (**12**) and CJ-12663 (**13**), fischerindoline (**14**), eurochevalierine (**15**), 1,4-diacetyl-2,5-dibenzylpiperazine-3,7″-oxide (**16**) and lecanorin (**17**) were isolated from the fungus *Neosartorya pseudofischeri*. Their structures were established on the basis of spectroscopic evidence. Compound **2** showed weak antibacterial activity against *Escherichia coli* and *Salmonella enterica* serovar Typhimurium, whereas compounds **7**, **12**, **13** and **15** showed antibacterial activity against *Bacillus cereus* and *Staphylococcus aureus*. In addition, compounds **13** and **14** showed cytotoxicity against KB and MCF-7 cancer cell lines, as well as the *Vero* cell line.

1. Introduction

The genus *Neosartorya* (Trichomaceae) is a source of bioactive secondary metabolites such as sesquiterpene alkaloids, sartorymensin analogs and meroterpenoids. These compounds show cytotoxicity against human U373 glioblastoma, MCF-7 breast cancer, and A549 non-small-cell-lung cancer cell lines [1–3]. The fungus *Neosartorya pseudofischeri* has been found in both marine and terrestrial sources, for example sea star (*Acanthaster planci*) [4,5] and soil [1,6]. Various bioactive compounds have been reported from *N. pseudofischeri* such as pyripyropenes A, 1,4-diacetyl-2,5-dibenzylpiperazine-3,7″-oxide, pseudofischerine [1] neosartin analogs, bis-*N*-norgliovictin [4], trichodermamide A and indolyl-3-acetic acid methyl ester [5]. In our search for bioactive compounds from soil fungi isolated in Thailand, we have found that the *n*-hexane extract from biomass of the fungus *N. pseudofischeri* shows anti-mycobacterial activity against *Mycobacterium tuberculosis*, with 50% inhibition at a concentration of 50 µg/mL. Herein, we report the isolation of four new compounds (**1–4**), together with thirteen known compounds (**5–17**), as well as the biological activities of the fungus *N. pseudofischeri*.

2. Experimental

2.1. General experimental procedures

Melting points were obtained using a Gallenkamp melting point apparatus (Leicestershire, U.K.) and were uncorrected. A JASCO DIP-1000 digital polarimeter was used to identify the optical rotation. The ECD and UV spectra were measured using a JASCO J-810 apparatus. IR spectra were obtained using a Bruker Tenser 27 spectrophotometer (Agilent Technologies, U.S.A.). NMR spectra were recorded on a Varian Mercury Plus 400 spectrometer (Varian, Inc., U.S.A.) using $CDCl_3$ and CD_3OD as solvents (Merck, Darmstadt, Germany). Mass spectra were determined on a Micromass Q-TOF 2 hybrid quadrupole time-of-flight (Q-TOF) mass spectrometer (Bruker, Germany) with a *Z*-spray ES source. TLC was performed on silica gel 60 PF_{254} TLC aluminum sheet (Merck, Darmstadt, Germany). The column chromatography was carried out on silica gel 0.063–0.200 mm or < 0.063 mm (Merck, Darmstadt, Germany) and sephadex LH-20 (Amersham Pharmacia, Biotech AB, Sweden). Preparative thin-layer chromatography (PLC) was carried out on glass supported silica gel 60 PF_{254} plates (Merck, Darmstadt, Germany).

* Corresponding author.
 E-mail address: somdej@kku.ac.th (S. Kanokmedhakul).

2.2. Fungal material

The fungus *N. pseudofischeri* was isolated from soil collected in a Chiang Mai forest, Thailand in 2012, and was identified by M. Soytong [6]. A voucher specimen EU13 was deposited at the Department of Plant Production Technology, Faculty of Agricultural Technology, King Mongkut's Institute of Technology Ladkrabang, Bangkok 10520, Thailand. The fungus was cultured in conical flasks (500 mL, 80 flasks) with potato dextrose (50 mL/flask) and incubated in a standing condition at 30 °C for 30 days. Dried fungal biomass was harvested and was air dried for 3 days.

2.3. Extraction and isolation

The dried biomass of *N. pseudofischeri* (135 g) was ground and extracted successively at room temperature with *n*-hexane (3 × 1 L), EtOAc (3 × 1 L), and MeOH (3 × 1 L). Removal of solvents under reduced pressure gave crude *n*-hexane (3.38 g), EtOAc (4.05 g), and MeOH (6.47 g) extracts. The *n*-hexane extract was subjected to silica gel column chromatography (CC), eluting with a gradient system of *n*-hexane-EtOAc and EtOAc-MeOH to give fifty-six fractions. On the basis of their TLC characteristics, they were combined to 9 fractions, NpH$_1$-NpH$_9$. Fractions NpH$_4$ and NpH$_6$ were recrystallized from *n*-hexane-EtOAc to afford colorless crystals of **6** (356 mg) and a white solid of **5** (60 mg), respectively. Fraction NpH$_7$ was purified by preparative thin-layer chromatography (PLC) using CH$_2$Cl$_2$-MeOH (98:2, x2) as eluent, affording a yellow solid of **13** (8 mg, R_f 0.39) and a white solid of **12** (23 mg, R_f 0.29). Fraction NpH$_8$ was purified by silica gel flash column chromatography (FCC), eluted with a gradient system of *n*-hexane-EtOAc, followed by PLC purification (3% MeOH-CH$_2$Cl$_2$, x2) to yield a yellow solid of **15** (8 mg, R_f 0.64) and a white solid of **14** (8 mg, R_f 0.53). A solid from fraction NpH$_9$ was filtered out and recrystallized from CH$_2$Cl$_2$-MeOH to afford **7** (91 mg), and the filtrate was further separated by FCC, eluted with a gradient system of *n*-hexane-EtOAc to give four subfractions, NpH$_{9.1}$-NpH$_{9.4}$. Subfraction NpH$_{9.1}$ was isolated by PLC (5% MeOH-CH$_2$Cl$_2$, x3) to yield a white solid of **1** (6 mg, R_f 0.53), a white solid of **8** (4 mg, R_f 0.37) and a yellow solid of **4** (7 mg, R_f 0.25). Purification of subfraction NpH$_{9.3}$ by PLC (30% EtOAc-*n*-hexane, x4) afforded a yellowish solid of **10** (4 mg, R_f 0.21). Subfraction NpH$_{9.4}$ was refined by Sephadex LH-20 CC, eluting with MeOH, to give a pale yellow solid of **16** (9 mg).

The EtOAc extract was separated into sixty fractions by silica gel CC, eluting with a gradient system of *n*-hexane-EtOAc and EtOAc-MeOH to yield seven fractions, NpE$_1$-NpE$_7$. Then, compounds **6** (19 mg) and **5** (60 mg) were isolated from fraction NpE$_2$ by FCC using a gradient system of *n*-hexane-EtOAc. Fraction NpE$_3$ was purified by PLC (4% MeOH-CH$_2$Cl$_2$, x4) to yield a pale yellow solid of **11** (6 mg, R_f 0.47) and **13** (16 mg, R_f 0.53). Fraction NpE$_5$ was separated by FCC, eluting with a gradient system of *n*-hexane-EtOAc to give three subfractions, NpE$_{5.1}$-NpE$_{5.3}$. Subfraction NpE$_{5.1}$ was purified by PLC (3% MeOH-CH$_2$Cl$_2$, x2) to afford **7** (5 mg, R_f 0.53). Subfraction NpE$_{5.3}$ was isolated by silica gel FCC, eluted with a gradient system of CH$_2$Cl$_2$-MeOH, to give colorless needles of **3** (6 mg), a white solid of **9** (7 mg) and an additional amount of **10** (13 mg). Fraction NpE$_6$ was separated on silica gel FCC, eluting with a gradient system of *n*-hexane-EtOAc, to give four subfractions, NpE$_{6.1}$-NpE$_{6.4}$. Subfraction NpE$_{6.1}$ was further purified by PLC (30% *n*-hexane-EtOAc) to yield **4** (49 mg, R_f 0.53). Subfraction NpE$_{6.2}$ was purified by PLC (20% *n*-hexane-EtOAc, x4) to afford **8** (27 mg, R_f 0.47). Subfraction NpE$_{6.4}$ was purified by PLC (5% MeOH-CH$_2$Cl$_2$, x4) to give white solids **2** (5 mg, R_f 0.89) and **16** (14 mg, R_f 0.61).

The MeOH extract was separated using a similar method to those of *n*-hexane and EtOAc extract, to give six fractions, NpM$_1$-NpM$_6$. Fraction NpM$_2$ yielded an additional amount of **5** (15 mg). Fraction NpM$_3$ was separated by PLC (40% *n*-hexane-EtOAc, x3) to give **11** (22 mg, R_f 0.50) and **7** (6 mg, R_f 0.37). Fraction NpM$_5$ was further purified by PLC (40% *n*-hexane-EtOAc, x7) to give **14** (7 mg, R_f 0.63). Fraction NpM$_6$ was

Table 1
^{1}H and ^{13}C NMR spectral data of compounds **1** (CDCl$_3$) and **2** (CDCl$_3$ + CD$_3$OD).

Position	1		2	
	δ_H (mult. *J* in Hz)	δ_C, type	δ_H (mult. *J* in Hz)	δ_C, type
1	1.97 (m), 1.48 (m)	39.1, CH$_2$	1.79 (m), 0.98 (m)	38.2, CH$_2$
2	2.48 (m)	33.8, CH$_2$	1.57 (m)	26.7, CH$_2$
3		217.3, C	3.06 (dd, 11.0, 5.3)	78.5, CH
4		47.2, C		37.9, C
5	1.43 (m)	54.7, CH	0.62 (m)	56.1, CH
6	1.57 (m), 1.39 (m)	19.0, CH$_2$	1.49 (m)	18.2, CH$_2$
7	1.95 (dd, 12.7, 3.8), 1.09 (m)	40.0, CH$_2$	1.76 (tt, 12.2, 2.9), 0.91 (m)	43.0, CH$_2$
8		37.2, C		37.5, C
9	1.04 (m)	59.6, CH	0.75 (m)	60.7, CH
10		36.7, C		38.8, C
11	1.73 (m), 1.42 (m)	19.1, CH$_2$	4.48 (m)	66.6, CH
12	2.12 (dd, 13.2, 3.1), 1.71 (m)	40.1, CH$_2$	2.19 (dd, 13.2, 3.6), 1.73 (m)	47.9, CH$_2$
13		84.0, C		85.3, C
14	1.51 (m)	52.2, CH	1.46 (m)	52.8, CH
15	2.55 (dd, 16.4, 4.6), 2.15 (m)	15.4, CH$_2$	2.47 (dd, 16.5, 4.7), 2.16 (m)	15.1, CH$_2$
16	1.31 (s)	20.5, CH$_3$	1.43 (s)	21.6, CH$_3$
17	0.92 (s)	15.6, CH$_3$	1.15 (s)	17.0, CH$_3$
18	0.93 (s)	16.2, CH$_3$	1.16 (s)	17.3, CH$_3$
19	1.09 (s)	26.6, CH$_3$	0.84 (s)	27.9, CH$_3$
20	1.05 (s)	20.8, CH$_3$	0.69 (s)	15.1, CH$_3$
1′				–
2′		180.5, C		163.2, C
3′		98.4, C		98.8, C
4′		162.6, C		181.0, C
5′	5.98 (s)	111.9, CH	5.69 (s)	111.0, CH
6′		160.5, C	–	161.5, C
7′	2.20 (s)	19.2, CH$_3$	2.14 (s)	18.9, CH$_3$

separated by FCC, eluted with a gradient system of CH$_2$Cl$_2$-MeOH, to afford **16** (22 mg, R_f 0.58) and the pale yellow solid **17** (22 mg).

Chevalone F (**1**): White solid; R_f = 0.61 (MeOH-CH$_2$Cl$_2$; 1:19); mp 177–178 °C; [α]$_D^{28}$ -115.3 (*c* 0.1, CHCl$_3$); ECD (*c* 240 μM, MeOH) nm 220 (+8.8), 243 (−55.9), 257 (−56.2), 301 (+4.7); UV (MeOH) λ$_{max}$ (log ε) 226 (3.87), 245 (4.08), 259 (4.11) nm; IR (Neat) ν$_{max}$ 2918, 2851, 1697, 1665, 1613, 1585, 1427, 1386 cm^{-1}; ^{1}H and ^{13}C NMR data (CDCl$_3$, 400 MHz), see Table 1; HRESITOFMS *m/z* 435.2557 [M + Na]$^+$ (calcd. for C$_{26}$H$_{36}$O$_4$ + Na, 435.2511). 11-Hydroxychevalone E (**2**): White solid; R_f = 0.39 (MeOH-CH$_2$Cl$_2$; 1:19); mp 196–198 °C; [α]$_D^{28}$ +14.1 (*c* 0.1, CHCl$_3$); ECD (*c* 230 μM, MeOH) nm 203 (−43.0), 211 (+5.8), 241 (−8.6), 262 (−8.4); UV (MeOH) λ$_{max}$ (log ε) 203 (4.05), 232 (3.61), 260 (3.53) nm; IR (Neat) ν$_{max}$ 3408, 2933, 2867, 1665, 1577, 1431 cm^{-1}; ^{1}H and ^{13}C NMR data (CDCl$_3$ + CD$_3$OD, 400 MHz), see Table 1; HRESITOFMS *m/z* 453.2622 [M + Na]$^+$ (calcd. for C$_{26}$H$_{38}$O$_5$ + Na, 453.2617). Tryptoquivaline V (**3**): Colorless needles; R_f = 0.41 (MeOH-CH$_2$Cl$_2$; 1:19); mp 250–252 °C (decomp.); [α]$_D^{28}$ +184.6 (*c* 0.1, CHCl$_3$); ECD (*c* 190 μM, MeOH) nm 203 (16.7) 208 (−3.8), 214 (+16.9), 234 (−3.6) 248 (−8.5), 266 (+1.6), 274 (+8.4); UV (MeOH) λ$_{max}$ (log ε) 209 (4.30), 225 (4.13), 255 (3.75), 301 (3.19) nm; IR (Neat) ν$_{max}$ 2962, 2926, 1725, 1671, 1606, 1473, 1262 cm^{-1}; ^{1}H NMR (CDCl$_3$, 400 MHz) δ 8.31 (1H, d, *J* = 8.0 Hz, H-20), 8.11 (1H, s, H-26), 7.81 (1H, t, *J* = 8.0 Hz, H-22), 7.75 (1H, d, *J* = 8.0 Hz, H-23), 7.78 (1H, d, *J* = 7.8 Hz, H-5), 7.55 (1H, t, *J* = 8.0 Hz, H-21), 7.52 (1H, d, *J* = 7.8 Hz, H-8), 7.41 (1H, t, *J* = 7.8 Hz, H-7), 7.28 (1H, t, *J* = 7.8 Hz, H-6), 5.76 (1H, s, H-2), 5.04 (1H, dd, *J* = 9.8, 11.4 Hz, H-12), 3.85 (1H, d, *J* = 3.9 Hz, H-15), 3.21 (1H, dd, *J* = 9.8, 10.8 Hz, H-13a), 2.68 (1H, dd, *J* = 10.8, 11.4 Hz, H-13b), 2.23 (1H, m, H-27), 1.12 (3H, d, *J* = 7.4 Hz, H-28), 1.10 (3H, d, *J* = 7.4 Hz, H-29); ^{13}C NMR (100 MHz) δ 171.5 (C-14), 171.4 (C-11), 160.2 (C-18), 147.4 (C-24), 145.7 (C-26), 137.5 (C-9), 135.0 (C-22), 133.7 (C-4),

Table 2
^{1}H and ^{13}C NMR spectral data of compounds **4a** and **4b** (CDCl$_3$).

Position	4a				4b	
	δ_H (mult. J in Hz)	δ_C	HMBC	COSY	δ_H (mult. J in Hz)	δ_C
2		128.2				125.8
3α	3.68 (d, 15.1)	38.4	1′, 7′, 9	3β	4.01 (overlap)	42.5
3β	5.50 (brd, 15.1)		1′, 5, 9	3α	4.59 (brd, 7.8)	
5	4.04 (m)	55.9	6, 7″	6, 7″	4.95 (broad)	49.7
6α	3.41 (dd, 13.0, 4.4)	46.6	7″, 7	5, 6α	3.41 (overlap)	46.7
6β	4.30 (d, 13.0)			5, 6β	4.30 (overlap)	
7		169.8				169.8
8	2.28 (s)	21.8	7		2.28 (overlap)	21.9
9		169.6				169.1
10	1.66 (s)	20.9	5, 9		1.88 (s)	21.7
1′		134.0				134.0
2′	6.48 (s)	108.9	4′, 6′, 7′		6.47 (s)	108.8
3′		143.7				143.8
4′		135.3				135.2
5′		149.2				149.3
6′	6.48 (s)	102.9	2′, 4′, 5′, 7′		6.47 (s)	102.8
7′	6.35 (brd, 6.7 Hz)	126.5	3, 1′, 2		6.38 (s)	126.7
8′	3.93 (s)	56.8	3′, 4′		3.92 (s)	56.9
9′	6.00 (brs)	101.7	4′, 5′		6.01 (s)	101.8
1″		137.1				137.2
2″, 6″	7.12 (d, 7.4)	129.2	6″, 2″	3″, 5″	7.12 (overlap)	129.2
3″, 5″	7.30 (t, 7.0)	128.9	1″, 5″, 3″	2″,4″, 6″	7.30 (overlap)	129.1
4″	7.26 (t, 7.3)	127.1	3″, 5″	3″, 5″	7.26 (overlap)	128.6
7″a	2.86 (dd, 13.4, 5.9)	37.3	1″, 2″, 6″, 5, 6	5, 7″b	3.11 (broad)	36.1
7″b	2.93 (d, 8.7)			5, 7″a	3.08 (brd, 11.9)	

130.9 (C-7), 127.9 (C-21), 127.5 (C-23), 126.8 (C-20), 126.7 (C-6), 125.4 (C-5), 121.8 (C-19), 116.3 (C-8), 91.7 (C-3), 84.9 (C-2), 70.2 (C-15), 57.8 (C-12), 33.6 (C-13), 32.1 (C-27), 18.9 (C-28), 17.4 (C-29); HRESITOFMS m/z 453.1572 [M + Na]$^+$, 431.1735 [M + H]$^+$ (calcd. for C$_{24}$H$_{22}$N$_4$O$_4$ + Na, 453.1539 and C$_{24}$H$_{22}$N$_4$O$_4$ + H, 431.1719).

Brasiliamide G (**4**): Yellow solid; R$_f$ = 0.59 (MeOH-CH$_2$Cl$_2$; 1:19); mp 87–89 ˚C; [α]$_D^{28}$ + 25.9(c 0.1, CHCl$_3$); ECD (c 59 μM, MeOH) nm 237 (+ 18.9), 280 (+ 16.2); UV (MeOH) λ$_{max}$ (log ε) 205 (4.65), 230 (4.38), 285 (4.18) nm; IR (Neat) ν_{max} 3279, 2926, 1627, 1391, 1136, 1088, 1037 cm^{-1}; ^{1}H NMR and ^{13}C NMR (CDCl$_3$, 400 MHz), see Table 2; HRESITOFMS m/z 445.1749 [M + Na]$^+$ (calcd. for C$_{24}$H$_{26}$N$_2$O$_5$ + Na, 445.1739).

2.4. Biological activity procedures

2.4.1. Antimalarial assay

Antimalarial activity was evaluated against the parasite *Plasmodium falciparum* (K1, multidrug-resistant strain), using the culture method of Trager and Jensen [7]. Quantitative assessment of activity *in vitro* was determined by means of the microculture radioisotope technique based on the method described by Desjardins [8]. The standard drug was dihydroartemisinin.

2.4.2. Antimycobacterial assay

Antimycobacterial activity was assessed against *Mycobacterium tuberculosis* H37Ra using the Microplate Alamar Blue Assay (MABA) [9]. The standard drug was isoniazid.

2.4.3. Cytotoxicity assays

Cytotoxicity assays against epidermal carcinoma of the mouth with HeLa cell contamination (KB, ATCC CCL-17), and human breast adenocarcinoma (MCF-7) were performed employing the Resazurin microplate assay (REMA) described by O'Brien and co-workers [10]. The reference substance was doxorubicin. Cytotoxicity against the primate

cell line (*Vero*) was tested using the green fluorescent protein (GFP) detection method by Hunt and co-workers [11].

2.4.4. Antibacterial assay

The minimum inhibitory concentrations (MICs) were determined by the dilution method as described in the M07-A9 [12]. Resazurin solution was used as an indicator of microbial growth. MICs were recorded by reading the lowest concentration capable of inhibiting visible growth. The tests were performed as an independent experiment and each carried out in triplicate. Five microorganism cultures, *Bacillus cereus* ATCC 11778, *Staphylococcus aureus* ATCC 25923, *Escherichia coli* ATCC 25922, *Pseudomonas aeruginosa* ATCC 27853, and *Salmonella enterica* serovar Typhimurium ATCC 13311 were used. The reference substances were vancomycin and gentamycin.

3. Results and discussion

Chromatographic separation of *n*-hexane, EtOAc and MeOH extracts from the fungal biomass of *N. pseudofischeri* gave seventeen compounds. Their structures were identified by spectroscopic data (UV, IR, ^{1}H and ^{13}C NMR), as well as by comparison to published data, as two new meroditerpene pyrones (**1** and **2**), a new tryptoquivaline analog (**3**) and a new brasiliamide analog (**4**), as well as thirteen known compounds, chevalones A-C (**5–7**) [13], chevalone E (**8**) [14], 11-hydroxychevalone C (**9**) [15], pyripyropene A (**10**) [4], isochaetominine C (**11**) [16], pyrrolobenzoxazine terpenoids CJ-12662 (**12**) and CJ-12663 (**13**) [17], fischerindoline (**14**) [18], eurochevalierine (**15**) [13], 1,4-diacetyl-2,5-dibenzylpiperazine-3,7″-oxide (**16**), and lecanorin (**17**) [1] as shown in Fig. 1.

Compound **1** had the molecular formula C$_{26}$H$_{36}$O$_4$, deduced from the HRESITOFMS (m/z 435.2557 [M + Na]$^+$), indicating nine degrees of unsaturation. The UV spectrum showed absorption maxima at 226, 245, and 259 nm. The IR spectrum showed the presence of ketone (1697 cm), α,β-unsaturated ketone (1665 cm), and alkene (1613 and 1585 cm) functionalities. Analysis of ^{1}H and ^{13}C NMR (Table 1) as well as 2D-NMR (COSY, HMBC and NOESY) spectroscopic data indicated that the main skeleton of **1** was the same as the isolated meroditerpene pyrone, chevalone C (**8**), which was reported from *Eurotium chevalieri* [13]. However, the hydroxyl group at C-3 of **8** was replaced by a carbonyl group (δ_{C-3} 217.3) in **1**. The HMBC spectrum showed the correlations of methylene protons, H-1 to C-3 and C-5; and H-5 to C-3 confirmed the position of a carbonyl group at C-3 in **1**. Based on the above analysis, compound **1** was determined as a new meroditerpene pyrone and has been named chevalone F.

Compound **2** had the molecular formula C$_{26}$H$_{38}$O$_5$, deduced from the HRESITOFMS (m/z 453.2622 [M + Na]$^+$), indicating eight degrees of unsaturation. The UV spectrum showed absorption maxima at 203, 232, and 260 nm. The IR spectrum showed the presence of hydroxyl (3408 cm), α,β-unsaturated ketone (1665 cm), and alkene (1577 cm^{-1}) groups. The ^{1}H and ^{13}C NMR spectroscopic data (Table 1) are similar to those of a known isolate 11-hydroxychevalone C (**9**), which has previously been reported from *Neosartorya spinosa* [15], except for the appearance of an acetyl group at C-3 in **9** which was replaced by a hydroxyl group ($\delta_{H/C}$ 3.06, dd/ 78.5) in **2**. The COSY spectrum exhibited a cross coupling network between H-1/H-2/H-3 and H-9/H-11/H-12, as well as the HMBC spectrum displaying correlations of H-19, H-20 to C-3 and H-12 to C-11, supporting the positions of these two hydroxy groups at C-3 and C-11. On the basis of the same characteristic of NOESY correlations and the coupling constants of these protons, the relative configuration of **2** was defined to be the same as that of **9**. Thus, **2** was assigned as a new meroditerpene pyrone and it has been named 11-hydroxychevalone E.

Compound **3** had the molecular formula C$_{24}$H$_{22}$N$_4$O$_4$, deduced from the HRESITOFMS (m/z 453.1572 [M + Na]$^+$), indicating sixteen degrees of unsaturation. The UV spectrum showed absorption maxima at 209, 225, 255, and 301 nm. The IR spectrum showed the absorption
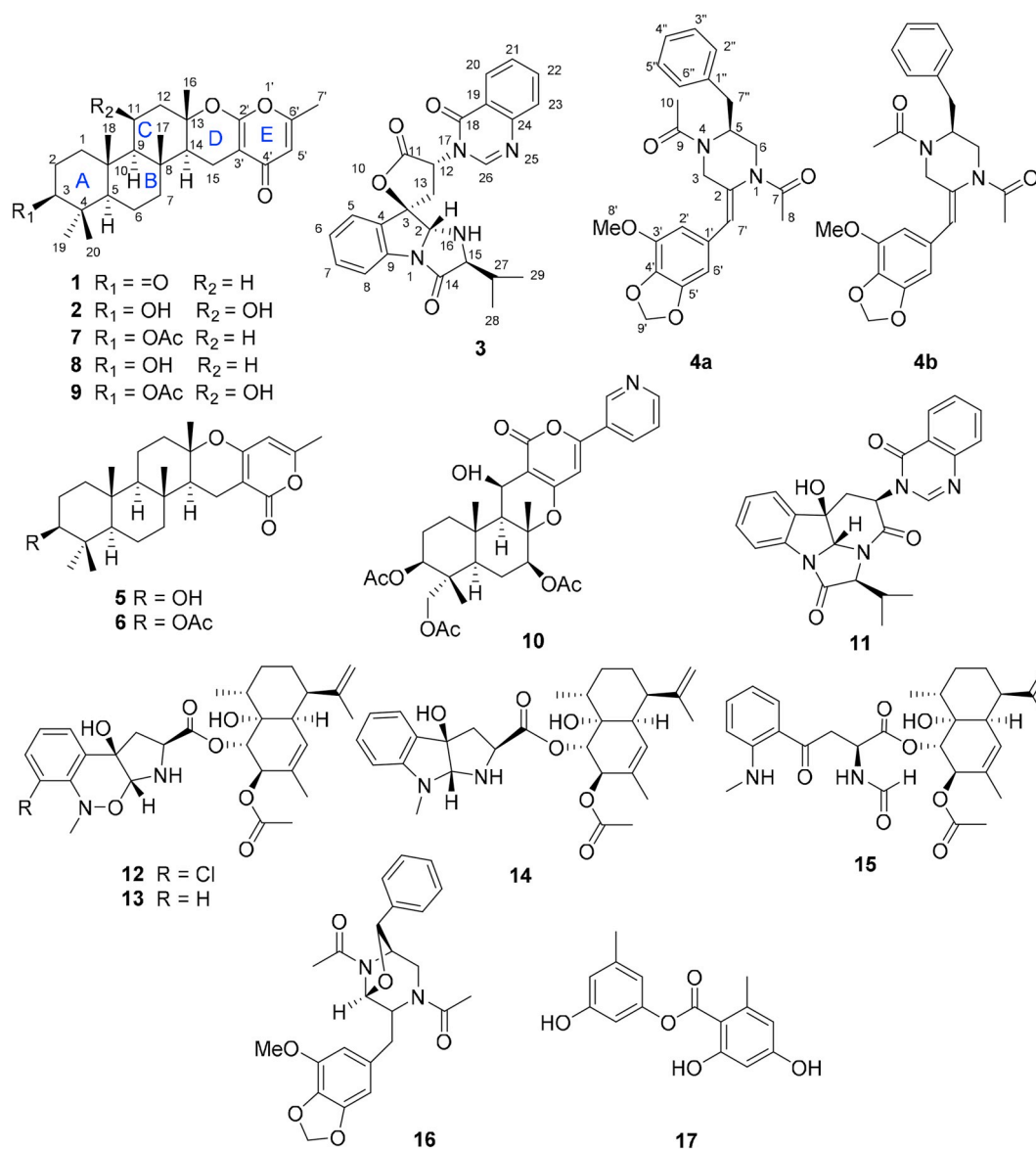
3

Fig. 1. The structures of compounds **1–17**.

bands of ester (1725 cm^{-1}), amide (1671 cm^{-1}), and alkene (1606 cm^{-1}) groups. The ^{13}C NMR and DEPT spectra showed 24 carbon signals, attributable to two methyl, one methylene, thirteen methine (including eight aromatic carbons), four aliphatic and one olefinic, together with eight quaternary (four aromatic, three carbonyl and one aliphatic) carbons. The ^{1}H NMR spectrum showed resonances of two doublets of methyl groups at δ 1.12 (d, $J = 7.4$ Hz, H$_3$–28) and 1.10 (d, $J = 7.4$ Hz, H$_3$–29), methylene protons at δ 2.68 (dd, $J = 10.8, 11.4$ Hz, H-13b) and 3.21, (dd, $J = 9.8, 10.8$ Hz, H-13a), four methine protons at δ 5.76 (s, H-2), 5.04 (dd, $J = 9.8, 11.4$ Hz, H-12), 3.85 (d, $J = 3.9$ Hz, H-15), and 2.23 (m, H-27), eight aromatic protons at δ 7.78 (d, $J = 7.8$ Hz, H-5), 7.28 (t, $J = 7.8$ Hz, H-6), 7.41 (t, $J = 7.8$ Hz, H-7), 7.52 (d, $J = 7.8$ Hz, H-8), 8.31 (d, $J = 8.0$ Hz, H-20), 7.55 (t, $J = 8.0$ Hz, H-21), 7.81 (t, $J = 8.0$ Hz, H-22), and 7.75 (d, $J = 8.0$ Hz, H-23) and an olefinic proton at δ 8.11 (s, H-26). Analysis of COSY and HMBC spectroscopic data suggested that **3** has the same core structure as the tryptoquivaline U, which has previously been isolated from *Neosartorya takakii* [19]. However, there was a difference at the C-15 position, where a *gem* dimethyl group of tryptoquivaline U is replaced by an isopropyl group in **3**. The COSY correlations between H-2/H-15/ H-27/H-28/H-29, and the HMBC correlations of H-15 to C-14, C-28,

and C-29; and H-28 and H-29 to C-15 confirmed the substituent of an isopropyl unit in the molecule.

The relative configuration of **3** was determined by NOESY correlations between H-28 and H-2, H-27 and H-15, H-13b and H-5, H-13a and H-12, and H-12 and H-26, suggesting each proton pairs were on the same phase (Fig. 2). The NOE-difference data also supported the same direction of H-12 and H-13a. Moreover, there was no correlation between H-2 and H-13 in NOESY, which was different from the corresponding position in tryptoquivaline U. In addition, the optical rotation of **3** ([α]$_D^{28}$ +184.6 (*c* 0.1, CHCl$_3$)) showed significant difference from tryptoquivaline U ([α]$_D^{28}$ -196 (*c* 0.1, CHCl$_3$)) [19], indicating a different configuration between them. Since the absolute configuration at C-3 of tryptoquivaline U was assigned as 3*S*, the configuration at C-3 in **3** should be 3*R*. Therefore, the relative configuration of **3** was assigned as 2*R*, 3*R*, 12*R* and 15*S*. From the above evidence, **3** is a new tryptoquivaline analog, and it has been named tryptoquivaline V.

Compound **4** had the molecular formula C$_{24}$H$_{26}$N$_2$O$_5$, deduced from the HRESITOFMS (*m/z* 445.1749 [M + Na]$^+$), indicating thirteen degrees of unsaturation. The UV spectrum showed absorption maxima at 205, 230, and 285 nm. The IR spectrum indicated the presence of amide (1627 cm^{-1}), and ether (1136 and 1037 cm^{-1}) functionalities. The ^{1}H
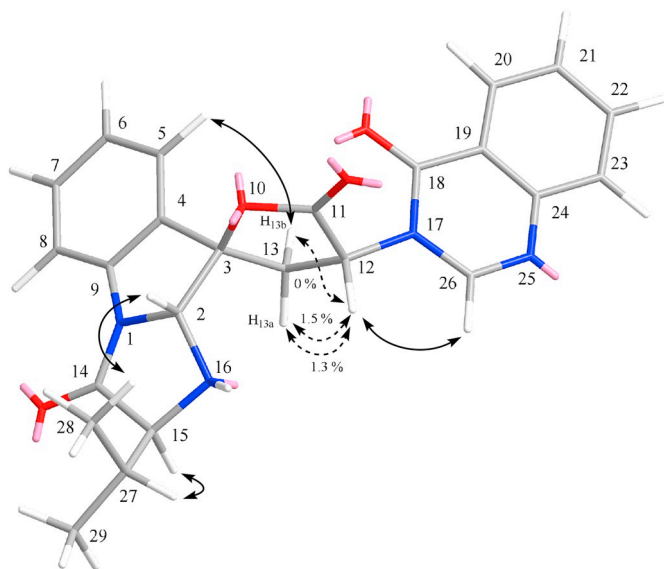
Fig. 2. The key NOESY correlations (↔) and NOE-difference (← →) data of **3** energy minimized using MM2.

NMR, ^{13}C NMR, COSY and HMBC spectroscopic data (Table 2) indicated the presence of three partial structures, including a benzyl moiety, a 3-methoxy-4,5-methylenedioxyphenyl unit, and a piperazine ring. The COSY and HMBC spectroscopic data indicated that a benzyl unit and a 3-methoxy-4,5-methylenedioxyphenyl unit were linked through the piperazine ring at C-5 and C-2, respectively. As a result, the core structure of **4** was the same as a brasiliamide B, which has previously been isolated from *Penicillium brasilianum* [20]. However, the double bond in the piperazine ring C-2/C-3 (δ_C 121.4, $\delta_{H/C}$ 6.16/112.8) of brasiliamide B was isomerized to C-2/C-7′ (δ_C 128.2, $\delta_{H/C}$ 6.35/126.5) in **4**. Moreover, the HMBC spectrum confirmed the structure of **4** by showing the correlations of olefinic proton H-7′ to C-1′ of the methylenedioxyphenyl unit, aromatic protons H-2′ and H-6′ to C-7′, and methylene proton H-3 to carbonyl carbon C-9.

According to the literature, the NMR spectra of brasiliamide analogs show a mixture of resonances of their conformers for the piperazine unit and the protons nearby due to the rotational arrangement of carbonyl groups of both acetamides [1,20,21]. A similar observation was found for the brasiliamide derivative **4**, by showing a mixture of resonances for a major **4a** and a minor **4b** conformers (Fig. 3) in the ratio of 3:1. The different NMR signals between **4a** and **4b** conformers was caused by the rotation of the acetyl group of the N-4 amide, which affects H-3, H-5, H-10 and H-7″ as shown in Table 2. In addition, the NOESY spectrum showed correlations between H-5 and H-10, H-3α, H-

6α; H-3α,β and H-2′; and H-8 and H-7′, which supports that the carbonyl acetamides at N-1 and N-4 of **4a** are arranged to C-6 and C-3 directions, respectively (Fig. 3). From the above evidence, the structure of **4** was determined to be a new (2*E*)-1,4-diacetyl-5-benzyl-2-(3-methoxy-4,5-methylenedioxybenzylidene) piperazine and has been named brasiliamide G.

Apart from four new compounds **1–4**, this is the first isolation of meroditerpene pyrones **5–9**, and pyrrolobenzoxazine terpenoids **12** and **13** from the fungus *N. pseudofischeri*. It is noticed that pyripyropene A (**10**) has been commonly found in the fungus *N. pseudofischeri* [1,4,5,18].

The new compounds **1–4** did not display anti-malarial and anti-TB activities, and were non-cytotoxic toward KB, MCF-7, and *Vero* cell lines. Since compounds **7**, **12**, and **15** have previously been reported to have anti-mycobacterial activity against *M. tuberculosis* [13], these compounds should be responsible for the anti-TB activity of the *n*-hexane extract in our screening test. Compound **13** showed weak cytotoxicity against KB and MCF-7 cell lines with IC$_{50}$ values of 36.11 and 28.31 μg/mL, respectively, while compound **14** exhibited weak cytotoxicity against the KB cell line, with an IC$_{50}$ value of 35.23 μg/mL. Moreover, compounds **13** and **14** displayed weak cytotoxicity toward *Vero* cells, with IC$_{50}$ values of 30.89 and 21.24 μg/mL, respectively. Compound **2** showed weak antibacterial activity against *E. coli* and *S. typhimurium*, both with MIC 128 μg/mL. Compounds **7**, **12**, **13** and **15** showed anti-bacterial activity against *B. cereus* with MIC values of 8, 64, 16, and 16 μg/mL, respectively, and they also exhibited activity against *S. aureus* with MIC values of 16, 128, 64, and 64 μg/mL, respectively (Table 3).

Declaration of Competing Interest

All the authors declare that there is no conflict of interest concerning this work.

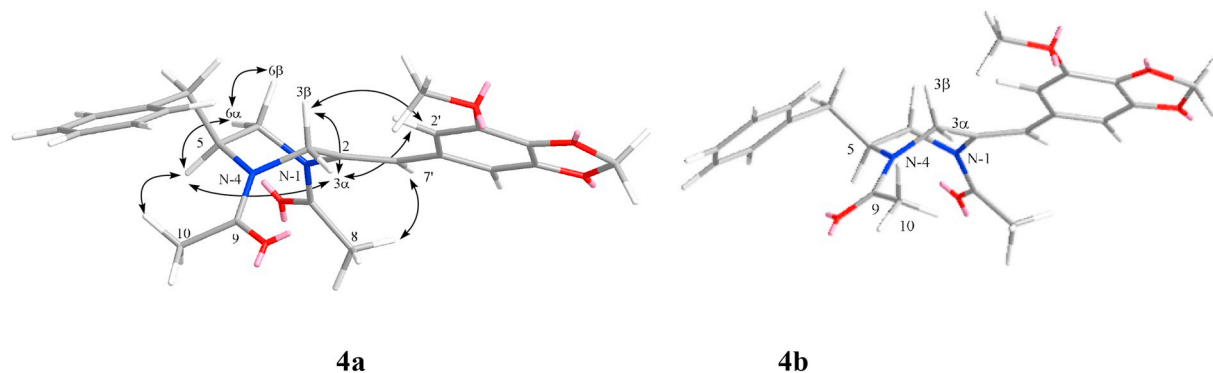**4a**   **4b**

Fig. 3. The major (**4a**), minor (**4b**) rotamers and the key NOESY correlations of **4a** energy minimized using MM2.

Table 3
Antibacterial activity of compounds **1–17**.

Compound	Antibacterial activity (MIC, μg/mL)				
	Gram-positive		Gram-negative		
	B. cereus[a]	*S. aureus*[b]	*E. coli*[c]	*P. aeruginosa*[d]	*S. typhimurium*[e]
1	>128	>128	>128	>128	>128
2	>128	>128	128	>128	128
3	>128	>128	>128	>128	>128
4	>128	>128	>128	>128	>128
5	>128	>128	>128	>128	>128
6	128	>128	>128	>128	>128
7	8	16	>128	>128	>128
8	>128	>128	>128	>128	>128
9	>128	>128	>128	>128	>128
10	>128	>128	128	>128	>128
11	>128	>128	128	>128	>128
12	64	128	>128	>128	>128
13	16	64	>128	>128	>128
14	128	>128	>128	>128	>128
15	16	64	>128	>128	>128
16	>128	>128	128	>128	>128
17	128	>128	128	>128	>128
Vancomycin	1.0	1.0	–	–	–
Gentamycin	–	–	2.0	0.5	0.5

[a] *Bacillus cereus* ATCC 11778 ATCC 11778.
[b] *Staphylococcus aureus* ATCC 25923 ATCC 25923.
[c] *Escherichia coli* ATCC 25922 ATCC 25922.
[d] *Pseudomonas aeruginosa* ATCC 27853 ATCC 27853.
[e] *Salmonella enterica* serovar Typhimurium ATCC 13311 serovar Typhimurium ATCC 13311.

Appendix A. Supplementary data

Supplementary data to this article can be found online at https://doi.org/10.1016/j.fitote.2019.104257.

References

[1] A. Eamvijarn, A. Kijjoa, C. Bruyère, V. Mathieu, L. Manoch, F. Lefranc, A. Silva, R. Kiss, W. Herz, Secondary metabolites from a culture of the fungus *Neosartorya pseusofischeri* and their in vitro cytostatic activity in human cancer cells, Planta Med. 78 (2012) 1767–1776.
[2] S. Buttachon, A. Chandrapatya, L. Manoch, A. Silva, L. Gales, C. Bruyère, R. Kiss, A. Kijjoa, Sartorymensin, a new indole alkaloid, and new analogues of tryptoquivaline and fiscalins produced by *Neosartorya siamensis* (KUFC 6349), Tetrahedron. 68 (2012) 3253–3262.
[3] A. Eamvijarn, N.M. Gomes, T. Dethoup, J. Buaruang, L. Manoch, A. Silva, M. Pedro, I. Marini, V. Roussis, A. Kijjoa, Bioactive meroditerpenes and indole alkaloids from the soil fungus *Neosartorya fischeri* (KUFC 6344), and the marine-derived fungi *Neosartorya laciniosa* (KUFC 7896) and *Neosartorya tsunodae* (KUFC 9213), Tetrahedron 69 (2013) 8583–8591.
[4] W.L. Liang, X. Le, H.J. Li, X.L. Yang, J.X. Chen, J. Xu, H.L. Liu, L.Y. Wang, K.T. Wang, K.C. Hu, D.P. Yang, W.J. Lan, Exploring the chemodiversity and biological activities of the secondary metabolites from the marine fungus *Neosartorya pseudofischeri*, Mar. Drugs 12 (2014) 5657–5676.
[5] W.J. Lan, S.J. Fu, M.Y. Xu, W.L. Liang, C.K. Lam, G.H. Zhong, J. Xu, D.P. Yang, H.J. Li, Five new cytotoxic metabolites from the marine fungus *Neosartorya pseudofischeri*, Mar. Drugs 14 (2016) 1–13.
[6] M. Soytong, S. Poeaim, Isolation and identification of Trichocomaceae from soil by morphology and three regions DNA sequencing, J. Agric. Technol. 11 (2015) 315–326.
[7] W. Trager, J.B. Jensen, Human malaria parasites in continuous culture, J. Parasitol. 91 (2005) 484–486.
[8] R.E. Desjardins, C.J. Canfield, J.D. Haynes, J.D. Chulay, Quantitative assessment of antimalarial activity in vitro by a semiautomated microdilution technique, Antimicrob. Agents Chemother. 16 (1979) 710–718.
[9] L. Collins, S.G. Franzblau, Microplate alamar blue assay versus BACTEC 460 system for high-throughput screening of compounds against *Mycobacterium tuberculosis* and *Mycobacterium avium*, Antimicrob. Agents Chemother. 41 (1997) 1004–1009.
[10] J. O'Brien, I. Wilson, T. Orton, F. Pognan, Investigation of the alamar blue (resazurin) fluorescent dye for the assessment of mammalian cell cytotoxicity: Resazurin as a cytotoxicity assay, Eur. J. Biochem. 267 (2000) 5421–5426.
[11] L. Hunt, M. Jordan, M. De Jesus, F.M. Wurm, GFP-expressing mammalian cells for fast, sensitive, noninvasive cell growth assessment in a kinetic mode, Biotechnol. Bioeng. 65 (1999) 201–205.
[12] F.R. Cockerill, M.A. Wikler, J. Alder, M.N. Dudley, G.M. Eliopoulos, M.J. Ferraro, D.J. Hardy, D.W. Hecht, J.A. Hindler, J.B. Patel, M. Powell, J.M. Swenson, R.B. Thomson, M.M. Traczewski, J.D. Turnidge, M.P. Weinstein, B.L. Zimmer, Methods for Dilution Antimicrobial Susceptibility Tests for Bacteria that Grow Aerobically, approved standard, Ninth edition, (2012).
[13] K. Kanokmedhakul, S. Kanokmedhakul, R. Suwannatrai, K. Soytong, S. Prabpai, P. Kongsaeree, Bioactive meroterpenoids and alkaloids from the fungus *Eurotium chevalieri*, Tetrahedron. 67 (2011) 5461–5468.
[14] C. Prompanya, T. Dethoup, L.J. Bessa, M.M.M. Pinto, L. Gales, P.M. Costa, A.M.S. Silva, A. Kijjoa, New isocoumarin derivatives and meroterpenoids from the marine sponge-associated fungus *Aspergillus similanensis* sp. nov. KUFA 0013, Mar. Drugs 12 (2014) 5160–5173.
[15] O. Rajachan, K. Kanokmedhakul, W. Sanmanoch, S. Boonlue, S. Hannongbua, P. Saparpakorn, S. Kanokmedhakul, Chevalone C analogues and globoscinic acid derivatives from the fungus *Neosartorya spinosa* KKU-1NK1, Phytochemistry 132 (2016) 68–75.
[16] L. Liao, M. You, B.K. Chung, D.C. Oh, K.B. Oh, J. Shin, Alkaloidal metabolites from a marine-derived *Aspergillus* sp. fungus, J. Nat. Prod. 78 (2015) 349–354.
[17] Y. Kojima, Y. Yamauchi, N. Kojima, B.F. Bishop, Antiparasitic Pyrrolobenzoxazine Compounds, Pfizer Pharm. Inc. Pat. Coop., 1995 (Treaty WO 95/19363).
[18] M. Masi, A. Andolfi, V. Mathieu, A. Boari, A. Cimmino, L. Moreno Y Banuls, M. Vurro, A. Kornienko, R. Kiss, A. Evidente, Fischerindoline, a pyrroloindole sesquiterpenoid isolated from *Neosartorya pseudofischeri*, with in vitro growth inhibitory activity in human cancer cell lines, Tetrahedron 69 (2013) 7466–7470.
[19] W.W.M. Zin, S. Buttachon, J. Buaruang, L. Gales, J.A. Pereira, M.M.M. Pinto, A.M.S. Silva, A. Kijjoa, A new meroditerpene and a new tryptoquivaline analog from the algicolous fungus *Neosartorya takakii* KUFC 7898, Mar. Drugs 13 (2015) 3776–3790.
[20] T. Fujita, D. Makishima, K. Akiyama, H. Hayashi, New convulsive compounds, brasiliamides A and B, from *Penicillium brasilianum* Batista JV-379, Biosci. Biotechnol. Biochem. 66 (2002) 1697–1705.
[21] T. Fujita, H. Hayashi, New brasiliamide congeners, brasiliamides C, D and E, from *Penicillium brasilianum* Batista JV-379, Biosci. Biotechnol. Biochem. 68 (2004) 820–826.

Bioactive xanthoquinodins and epipolythiodioxopiperazines from *Chaetomium globosum* 7s-1, an endophytic fungus isolated from *Rhapis cochinchinensis* (Lour.) Mart

Cholpisut Tantapakul, Trinop Promgool, Kwanjai Kanokmedhakul, Kasem Soytong, Jiaojiao Song, Sarinya Hadsadee, Siriporn Jungsuttiwong & Somdej Kanokmedhakul

View supplementary material

Published online: 19 Nov 2018.

Submit your article to this journal

View Crossmark data

Taylor & Francis
Taylor & Francis Group

Check for updates

Bioactive xanthoquinodins and epipolythiodioxopiperazines from *Chaetomium globosum* 7s-1, an endophytic fungus isolated from *Rhapis cochinchinensis* (Lour.) Mart

Cholpisut Tantapakul[a], Trinop Promgool[a], Kwanjai Kanokmedhakul[a], Kasem Soytong[b], Jiaojiao Song[b], Sarinya Hadsadee[c], Siriporn Jungsuttiwong[c] and Somdej Kanokmedhakul[a]

[a]Natural Products Research Unit, Department of Chemistry and Center of Excellence for Innovation in Chemistry, Faculty of Science, Khon Kaen University, Khon Kaen, Thailand; [b]Department of Plant Production Technology, Faculty of Agricultural Technology, King Mongkut's Institute of Technology Ladkrabang, Bangkok, Thailand; [c]Center for Organic Electronic and Alternative Energy, Department of Chemistry and Center of Excellence for Innovation in Chemistry, Faculty of Science, Ubon Ratchathani University, Ubon Ratchathani, Thailand

ABSTRACT

A new xanthoquinodin B9 (**1**), together with two known xanthoquinodins, xanthoquinodin A1 (**2**) and xanthoquinodin A3 (**3**), three epipolythiodioxopiperazines, chetomin (**4**), chaetocochin C (**5**) and dethio-tetra(methylthio)chetomin (**6**), and four other compounds, chrysophanol (**7**), emodin (**8**), alatinone (**9**), and ergosterol (**10**) were isolated from the endophytic fungus *Chaetomium globosum* 7s-1, isolated from *Rhapis cochinchinensis* (Lour.) Mart. All isolated structures were established based on their spectroscopic data analyses. Compounds **1–6** showed antibacterial activity against Gram positive bacteria with MICs ranging from 0.02 pM to 10.81 μM. Compounds **1–6** also exhibited cytotoxicity against KB, MCF-7 and NCI-H187 cancer cell lines (IC$_{50}$ 0.04–18.40 μM). However, they were cytotoxic towards a normal cell line (*Vero* cell) with IC$_{50}$ values ranging from 0.04 to 3.86 μM.

Xanthoquinodin B9 (1)

Chaetomium globosum 7s-1

CONTACT Somdej Kanokmedhakul ✉ somdej@kku.ac.th

Supplemental data for this article can be accessed https://doi.org/10.1080/14786419.2018.1489392.
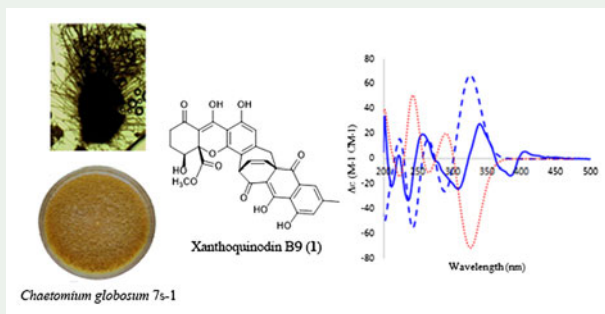
1. Introduction

Chaetomium globosum belongs to the Chaetomiaceae family (Youn et al. 2015). It has been isolated from water-damaged building materials (Green et al. 2014), animals (Chen et al. 2016), soil (Kanokmedhakul et al. 2002) and plants (Christensen et al. 1966). *C. globosum* is well-known to produce a variety of structural secondary metabolites, including anthraquinones (Kanokmedhakul et al. 2002; Wijeratne et al. 2006), azaphilones (Chen et al. 2016; McMullin et al. 2013; Wang, Zhang, et al. 2017), azaphilone alkaloids (Chen et al. 2016), cytochalasan alkaloids (Chen, Zhu, et al. 2015; Guo et al. 2017; Wang, Yan, et al 2017), depsidones (Li et al. 2008), epipolythiodioxopiperazines (Li et al. 2011; Xu et al. 2015), indole alkaloids (Xu et al. 2015), steroids (Li et al. 2011), xanthones (Li et al. 2008; Wijeratne et al. 2006), and xanthoquinodins (Kanokmedhakul et al. 2002). Most of these have exhibited a wide range of biological activities such as acetylcholinesterase inhibitory (Li et al. 2016; Ruan et al. 2018), antibacterial (Chen et al. 2016), antifungal (Li et al. 2011), anti-HIV (Chen, Zhu, et al. 2015), antioxidant (Li et al. 2016), and cytotoxic (Chen, Wang, et al. 2015; Li et al. 2008) activities. There have also been reports of its ability to degrade the cell walls of a fungal pathogen, an oomycete (*Pythium ultimum*) (Inglis and Kawchuk 2002), and to inhibit the growth and reproduction of *Myzus persicae* (Qi et al. 2011). Interestingly, derivatives of epipolythiodioxopiperazine toxins have therapeutic potential and roles in diseases (Brewer et al. 1972; Jordan and Cordiner 1987). As part of our search for bioactive compounds from endophytic fungi, EtOAc and MeOH extracts of *C. globosum* 7s-1 exhibited antibacterial activity against Gram positive and Gram negative bacteria at a concentration of 1 mg/mL. Moreover, they also showed cytotoxicity towards the KB cell line with IC_{50} values of 0.69 and 10.75 μg/mL respectively. We report herein the chemical investigation and bioactivity of xanthoquinodins and epipolythiodioxopiperazines (**1–6**) from an endophytic fungus *C. globosum* 7s-1, isolated from *Rhapis cochinchinensis* (Lour.) Mart. In addition, their antibacterial, anti-mycobacterial, and anti-malarial activities, as well as cytotoxicity towards three cell lines and *Vero* cells, are reported.

2. Results and discussion

Chromatographic separation of EtOAc and MeOH extracts of *C. globosum* 7s-1 gave a new xanthoquinodin B9 (**1**), along with nine known compounds, xanthoquinodin A1 (**2**) (Tabata, Tomoda, et al. 1993), xanthoquinodin A3 (**3**) (Tabata, Tomoda, et al. 1993), chetomin (**4**) (Fujimoto et al. 2004), chaetocochin C (**5**) (Li et al. 2006), dethio-tetra (methylthio)chetomin (**6**) (Kikuchi et al. 1982), chrysophanol (**7**) (Ghisalberti et al. 1990), emodin (**8**) (Zhou et al. 2006), alatinone (**9**) (Hemlata 1993), and ergosterol (**10**) (Ghisalberti et al. 1990) as shown in Figure 1.

Compound **1** had the molecular formula $C_{31}H_{24}O_{11}$, deduced from the ^{13}C NMR and HRESITOFMS (*m/z* 573.1390 [M + H]$^+$) data, implying 20 indices of hydrogen deficiency. The UV spectrum exhibited absorption maxima at 236, 273 and 360 nm, which is similar to that of xanthoquinodin type B (Tabata, Suzumura, et al. 1993; Tabata, Tomoda, et al. 1993). The IR absorption indicated the presence of hydroxyl (3366 cm^{-1}), carbonyl (1718 cm^{-1}) and aromatic (1594 and 1619 cm^{-1}) groups.
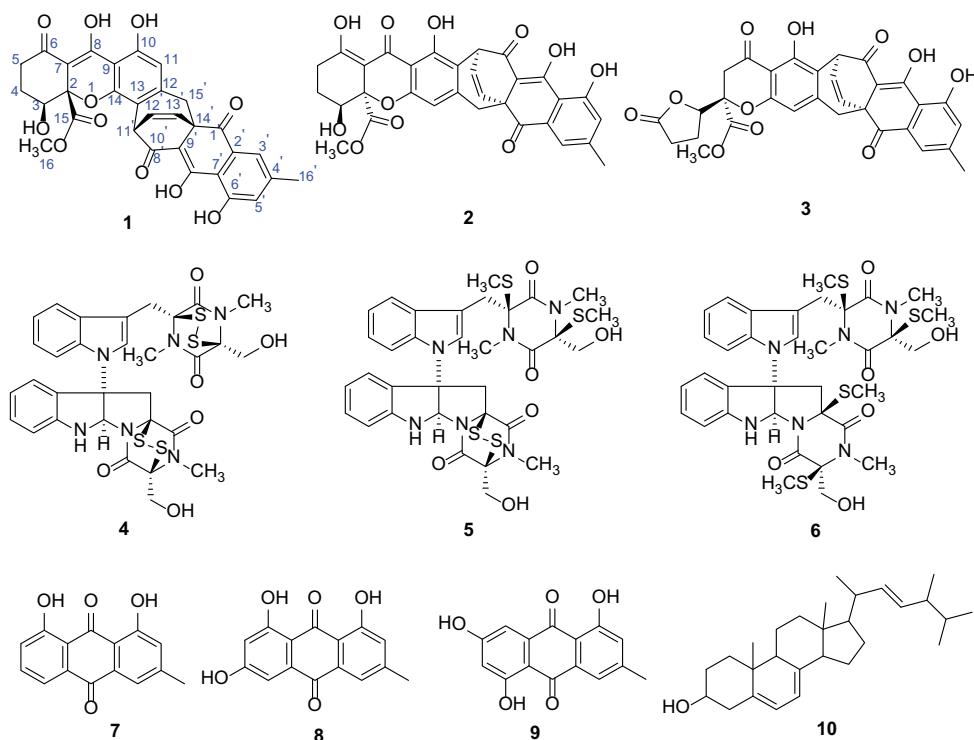
Figure 1. Chemical constituents isolated from *C. globosum* 7s-1.

The ¹³C NMR and DEPT spectral data of **1** (Table S1 in supplementary material) showed 31 carbon signals which are attributed to a methoxyl (δ_C 52.9) and a methyl (δ_C 21.7) carbons, three sp³ methylenes (δ_C 41.8, 36.0 and 26.0), two sp³ methines (δ_C 74.3 and 46.0), two sp³ quaternary carbons) δ_C 87.6 and 53.3, (five sp² methines (δ_C 133.4, 133.1, 124.6, 119.9 and 113.5) and 15 sp² quaternary carbons, three α,β-conjugated keto carbonyls (δ_C 200.2, 199.2, and 191.4) and an ester carbonyl (δ_C 174.9). The ¹H and ¹³C NMR spectroscopic data of **1** (Table S1 in supplementary material) agrees well with that of xanthoquinodin B1 (Tabata, Tomoda, et al. 1993). The ¹H NMR spectrum displayed resonances of *cis* vinyl protons showing at δ_H 6.55 (1H, d, J = 8.3 Hz, H-13′) and 6.34 (1H, dd, J = 8.3, 7.0 Hz, H-12′), which coupled to H-11′ at δ_H 4.63 (1H, d, J = 7.0 Hz). The three signals of aromatic protons appeared at δ_H 5.57 (1H, s), corresponding to a penta-substituted aromatic H-11, while δ_H 7.39 (1H, s) and 6.98 (1H, s) corresponded to *meta*-coupling of H-3′ and H-5′ respectively. An oxymethine group at C-3 appeared at δ_H 4.22 (1H, dd, J = 12.5, 4.5 Hz). Resonance signals of three methylene groups displayed at δ_H 2.99 (1H, d, J = 17.0 Hz, H$_a$-15′) and 2.70 (1H, d, J = 17.0 Hz, H$_b$-15′), 2.69 (1H, m, H-5), 2.49 (1H, dd, J = 18.0, 7.0 Hz, H-5), and two multiplet resonances at 2.20 and 1.98 of methylene protons H-4. Two singlet signals at δ_H 3.59 (3H, s) and 2.38 (3H, s) were resonances due to a methoxy carbonyl group of H-16 and a methyl group of H-16′, respectively. The significant difference between compound **1** and xanthoquinodin B1 was an arrangement of the keto-enolic system at C-6 (δ_C 191.4) and C-8 (δ_C 178.8). This was indicated by a difference in chemical shift of protons and carbons at positions 2–5 (Table S1 in supplementary material). The HMBC

spectrum of **1** clearly showed correlations of H-4 to C-6 (δ_C 191.4), H-5 to C-7 (δ_C 100.2), and ^4J correlation of the aromatic proton H-11 to C-8 (δ_C 178.8) (Figure S6 in supplementary material), confirming the location of the keto-enolic system at C-6 and C-8. The NOESY and NOE spectra (measured in DMSO-d_6, Figures S11 and S12 in supplementary material), showed a correlation of 3-OH with H-16, indicating that they are in the same orientation. The cross peak between H-11′ and H-12′ also implies that they are in the same orientation. The assignment of ^1H and ^{13}C NMR spectral data as well as HMBC correlations of **1** are summarized in Table S1 and Figure S6 in supplementary material. The absolute configuration of **1** was assigned by the predicted ECD curves of 16 possible configurations which were optimized by the B3LYP/6-31G(d,p). The predicted ECD curve of **1** corresponds to the experimental one (Figure S15 in supplementary material), therefore the absolute configuration of **1** was assigned as 2S, 3S, 11′S and 14′R. Thus, compound **1** was defined as a new xanthoquinodin type B and was named xanthoquinodin B9.

Compounds **1–6** were evaluated for their antibacterial activity against three Gram positive bacteria and three Gram negative bacteria (Table S4 in supplementary material). Xanthoquinodins **1–3** showed significant activity against *Bacillus cereus* with MIC values of 0.87, 0.44 and 0.22 μM, respectively, which were more active than standard drugs, vancomycin (1.35 μM) and kanamycin (3.43 μM). They also exhibited activity against *Staphylococcus aureus* and MRSA with MIC values ranging from 0.87 to 1.75 μM whereas vancomycin showed activity against *S. aureus* and MRSA with a MIC value of 0.67 μM, and kanamycin showed activity against *S. aureus* with a MIC value of 1.72 μM. The antibacterial activity against *S. aureus* of **2** and **3** confirmed the previous study by Tabata using the paper disc method (Tabata, Suzumura, et al. 1993). Epipolythiodioxopiperazines **4–6** exhibited a potent activity against Gram positive bacteria with the MIC values ranging from 0.02 pM to 10.81 μM. Compound **4** showed the highest activity towards *B. cereus*, *S. aureus* and MRSA with MIC values of 0.35 μM, 10.74 and 0.02 pM, respectively, which are remarkably more active than vancomycin (1.35, 0.67 and 0.67 μM) (Figure S21–S24 in supplementary material). Among these three compounds (**4–6**), the activities against all Gram positive bacteria were decreased when the sulfide bridges opened as in compounds **5** and **6**. However **6**, with both open sulfide bridges, demonstrated activity close to vancomycin against MRSA. These results support that two sulfide bridges play an important role in activity against Gram positive bacteria, as in previous reports (Brewer et al. 1972; Jordan and Cordiner 1987). In contrast, all compounds showed weak activity against the Gram negative bacteria tested (MICs of 45.06 to >223.72 μM).

In addition, compounds **1–6** were also tested for their anti-malarial, anti-TB and cytotoxic activities (Table S5 in supplementary material). They showed anti-malarial activity against *Plasmodium falciparum* with IC$_{50}$ values in the range of 0.40–6.29 μM. Epipolythiodioxopiperazines **4–6** were also active against *Mycobacterium tuberculosis* with MICs of 0.55, 4.06 and 8.11 μM, respectively, while xanthoquinodins **1–3** showed weak activity or were inactive. Furthermore, they showed strong cytotoxicity against three human cancer cell lines, KB, MCF-7 and NCI-H187, with IC$_{50}$ ranging from 0.04 to 18.40 μM. Compounds **2–6** showed cytotoxicity against MCF-7 cell line (IC$_{50}$ values of 1.09 to 13.12 μM) which were more active than the standard drug doxoburicin (17.24

μM). Among them, **4** exhibited strong cytotoxicity against NCI-H187, with an IC_{50} value of 0.04 μM, which was more active than standard drugs doxoburicin (0.40 μM) and ellipticine (9.54 μM). It should be noted that compounds **4** and **5** containing sulfide bridges in the structures are more cytotoxic against the cancer cell lines tested than the non-sulfide bridged structure, **6**. However, all compounds **1**–**6** exhibited very strong cytotoxicity towards the normal cell line (*Vero* cell) with IC_{50} values ranging from 0.04 to 3.86 μM, respectively, compared to the control drug, ellipticine (4.22 μM).

3. Experimental

3.1. Fungal material

The endophytic fungus *C. globosum* was isolated from the leaves of *R. cochinchinensis* (Lour.) Mart. collected at Ladkrabang Bangkok, Thailand and was identified by Assoc. Prof. Soytong, K. Department of Plant Production Technology, Faculty of Agricultural Technology, King Mongkut's Institute of Technology Ladkrabang, Bangkok Thailand, where the specimen (Voucher no. Cg.RL0) was deposited. Its colonies of fungus were slowly growing with little superficial mycelium and a dense olivaceous layer of ascomata. Ascomata are dark brown or black in age, globose to subglobose; lateral hairs straight, dark brown with paler tips, minutely roughened; terminal hairs, dark olive brown with paler tips, wavy or loosely coiled or undulate. There are produced asci in ascomatus, one ascus has eight ascospores. Ascospores are pale greenish to dark olive-brown, flattened lemon-shaped, hardly apiculate (von Arx et al. 1986). The fungus was cultured in 200 ml conical flasks (200 flasks) with potato dextrose broth (PDB) (50 ml/flask) and incubated in a standing condition at 25–28 °C for 30 days. The culture broth was filtered to give a wet fungal biomass, which was then air-dried at room temperature.

3.2. Extraction and isolation

Air dried fungal biomass of *C. globosum* (113 g) was ground and extracted exhaustively at room temperature with EtOAc (1L × 3) and MeOH (1L × 3) to obtain EtOAc (6.5 g) and MeOH (17.3 g) extracts, respectively. The EtOAc extract was subjected to flash column chromatography (FCC) over silica gel, eluting with a gradient system of *n*-hexane-EtOAc and EtOAc-MeOH to give eight fractions (EA − EH). Solid in fraction EA was recrystallized with MeOH to give **7** (7.5 mg) as orange solid. Fraction EC (7.2 mg) was subjected to CC on Sephadex LH-20, eluting with MeOH to obtain **8** (2.9 mg) as orange solid. Fraction EE (899.3 mg) was further separated by silica gel FCC, eluted with an isocratic system of MeOH-CH_2Cl_2 (2:98) to give **2** (39.8 mg) as yellow solid and **3** (16.4 mg) as yellow solid. Fraction EF (732.1 mg) was subjected to silica gel FCC, eluted with a gradient system of CH_2Cl_2-acetone, to give seven subfractions (EF1 − EF7). Subfraction EF2 (51.4 mg) was separated by silica gel CC using MeOH-CH_2Cl_2 (2:98) as an eluent to afford **4** (6.5 mg) as white solid. Subfraction EF4 (33.1 mg) was subjected to CC on Sephadex LH-20, eluted with MeOH, and followed by silica gel CC, eluted with acetone-CH_2Cl_2 (10:90), to give **5** (11.2 gm) as white solid. Subfraction EF6 (42.5 mg) was purified using silica gel CC, eluted with acetone-CH_2Cl_2 (15:85), to give

6 (6.0 mg) as white solid. Fraction EG (842.3 g) was subjected to silica gel FCC, eluted with a gradient system of CH_2Cl_2-MeOH to obtain four subfractions (EG1 − EG4). Subfraction EG2 (109.5 mg) was further separated by silica gel CC, eluted with MeOH-CH_2Cl_2 (10:90) to give **9** (2.6 mg) as yellow solid. Fraction EH (155 mg) was purified by silica gel CC eluted with MeOH-CH_2Cl_2 (10:90) and followed by Sephadex LH-20 CC, eluted with MeOH to obtain **1** (45.3 mg) as yellow solid. The MeOH extract (17.3 g) was subjected to FCC, eluted with a gradient system of CH_2Cl_2-MeOH to give six fractions (MA − MF). Solid in fraction MB (162.3 mg) was recrystallized with *n*-hexane to give **10** (14.8 mg) as white solid. Fraction MC (1.4 g) was chromatographed on silica gel FCC, eluting with a gradient system of CH_2Cl_2-MeOH to give seven subfractions (MC1 − MC7). Subfraction MC2 (251.9 mg) was applied on a silica gel CC, eluted with EtOAc-*n*-hexane (25:75) to give an additional amount of **8** (5.4 mg). Subfraction MC4 (197.0 mg) was purified by silica gel CC using acetone-*n*-hexane (40:60) as an eluent to yield an additional amount of **4** (25.5 mg). Subfraction MC6 (71.7 mg) was further subjected to Sephadex LH-20 CC, eluting with MeOH to give an additional amount of **3** (6.5 mg). Fraction MD (489.2 mg) was separated by CC on Sephadex LH-20 eluting with MeOH to obtain four subfractions (MD1 − MD4). Subfraction MD3 (271.7 mg) was then purified by silica gel CC, eluted with MeOH-CH_2Cl_2 (10:90) to yield an additional amount of **1** (152.6 mg). Fraction ME (318.7 mg) was subjected to CC on Sephadex LH-20, eluted with MeOH to obtain four subfractions (ME1 − ME4). Purification of subfraction ME2 (153.7 mg) by silica gel CC, using MeOH-CH_2Cl_2 (10:90) as an eluent, gave an additional amount of **1** (10.2 mg). Subfraction ME4 was further purified by CC on Sephadex LH-20, eluted with MeOH to give an additional amount of **9** (13.5 mg).

3.2.1. Xanthoquinodin B9 (1)

Yellow solid; mp 198 °C (decomp.); $[\alpha]_D^{25}$ +218 (*c* 0.1, MeOH); UV (MeOH) λ_{max} (log ε): 203 (4.47), 236 (4.36), 273 (4.11), 339 (4.25), 343 (4.26), 360 (4.28) nm; CD (*c* 0.045 mM, MeOH) λ_{max} ($\Delta\varepsilon$) 212 (−22.39), 222 (+2.47), 236 (−33.48), 259 (+18.98), 278 (−2.73), 325 (+3.66), 355 (+11.46); IR (KBr) ν_{max}: 3366, 1718, 1619, 1594, 1445, 1268, 750 cm^{-1}; ^{1}H NMR (500 MHz, CD$_3$OD): δ 13.79 (1H, s, 6′-OH), 12.12 (1H, s, 10-OH), 7.39 (1H, s, H-3′), 6.98 (1H, s, H-5′), 6.55 (1H, d, *J* = 8.3 Hz, H-13′), 6.34 (1H, dd, *J* = 8.3, 7.0 Hz, H-12′), 5.57 (1H, s, H-11), 4.63 (1H, d, *J* = 7.0 Hz, H-11′), 4.22 (1H, dd, *J* = 12.5, 4.5 Hz, H-3), 3.59 (3H, s, H-16), 2.99 (1H, d, *J* = 17.0 Hz, H-15′), 2.70 (1H, d, *J* = 7.0 Hz, H-15′), 2.69 (1H, m, H-5), 2.49 (1H, m, H-5), 2.38 (3H, s, H-16′), 2.20 (1H, m, H-4), 1.98 (1H, m, H-4); ^{13}C NMR (125 MHz, CD$_3$OD): δ 200.2 (C-1′), 199.2 (C-10′), 191.4 (C-6), 178.8 (C-8), 176.4 (C-8′), 174.9 (C-15), 162.8 (C-6′), 160.4 (C-10), 155.4 (C-14), 145.7 (C-4′), 144.8 (C-12), 133.4 (C-2′), 133.4 (C-13′), 133.1 (C-12′), 124.6 (C-5′), 119.9 (C-3′), 118.9 (C-7′), 114.2 (C-13), 113.5 (C-11), 106.3 (C-9′), 105.5 (C-9), 100.2 (C-7), 87.6 (C-2), 74.3 (C-3), 53.3 (C-14′), 52.9 (C-16), 46.0 (C-11′), 41.8 (C-15′), 36.0 (C-5), 26.0 (C-4), 21.7 (C-16′); HRESITOFMS *m/z* 573.1390 [M + H]$^+$ (calcd for C$_{31}$H$_{25}$O$_{11}$, 573.1397).

General experimental procedures, biological assay, computational method of ECD and 2D spectra for compound **1** are provided in supplementary material.

4. Conclusion

A new arrangement of keto-enolic xanthoquinodin B9 (**1**), together with nine known compounds (**2**–**10**), were isolated from the endophytic fungus *C. globosum* 7s-1. The structures were elucidated using spectroscopic methods. Xanthoquinodins (**1**–**3**) and epipolythiodioxopiperazines (**4**–**6**) showed significant activity against Gram positive bacteria, anti-malarial and anti-TB activity, and also cytotoxicity against three cancer cell lines (KB, MCF-7 and NCI-H187) as well as normal cells (*Vero* cell). Among these, the two sulfide bridge chetomin (**4**) is the most active compound against all tests. This suggests that all potently bioactive compounds need further study in detail to make use of this finding. The antibacterial activity against methicillin resistance *S. aureus* (MRSA) and *Sa. typhimurium*, as well as cytotoxicity against human epidermoid carcinoma (KB), human small cell lung cancer (NCI-H187), and normal cell (*Vero* cell), anti-mycobacterial, and anti-malarial activities of these isolated compounds were reported for the first time.

References

Brewer D, Duncan JM, Jerram WA, Leach CK, Safe S, Taylor A, Vining LC, Archibald RMcG, Stevenson RG, Mirocha CJ, et al. 1972. Ovine ill-thrift in Nova Scotia. 5. The production and toxicology of chetomin, a metabolite of *Chaetomium* spp. Can J Microbiol. 18:1129–1137.

Chen C, Wang J, Liu J, Zhu H, Sun B, Wang J, Zhang J, Luo Z, Yao G, Xue Y, Zhang Y. 2015. Armochaetoglobosins A–J: cytochalasan alkaloids from *Chaetomium globosum* TW1-1, a fungus derived from the terrestrial arthropod *Armadillidium vulgare*. J Nat Prod. 78:1193–1201.

Chen C, Wang J, Zhu H, Wang J, Xue Y, Wei G, Guo Y, Tan D, Zhang J, Yin C, et al. 2016. Chaephilones A and B, two new azaphilone derivatives isolated from *Chaetomium globosum*. Chem Biodivers. 13:422–426.

Chen C, Zhu H, Wang J, Yang J, Li XN, Wang J, Chen K, Wang Y, Luo Z, Yao G, et al. 2015. Armochaetoglobins K–R, anti-HIV pyrrole-based cytochalasans from *Chaetomium globosum* TW1-1. Eur J Org Chem. 2015:3086–3094.

Christensen CM, Nelson GH, Mirocha CJ, Bates F, Dorworth CE. 1966. Toxicity to rats of corn invaded by *Chaetomium globosum*. Appl Microbiol. 14(5):774–777.

Fujimoto H, Sumino M, Okuyama E, Ishibashi M. 2004. Immunomodulatory constituents from an ascomycete, *Chaetomium seminudum*. J Nat Prod. 67:98–102.

Ghisalberti EL, Narbey MJ, Dewan MM, Sivasithamparam K. 1990. Variability among strains of *Trichoderma harzianum* in their ability to reduce take-all and to produce pyrones. Plant Soil. 121:287–291.

Green BJ, Nayak AP, Lemons AR, Rittenour WR, Hettick JM, Beezhold DH. 2014. Production of a *Chaetomium globosum* enolase monoclonal actibody. Antib Immunodiagn Immunother. 33(6):428–437.

Guo ZL, Zheng JJ, Cao F, Wang C, Wang CY. 2017. Chemical constituents of the gorgonian-derived fungus *Chaetomium globosum*. Chem Nat Compd. 53(1):199–202.

Hemlata, SBK. 1993. Alatinone, an anthraquinone from *Cassia alata*. Phytochemistry. 32(6): 1616–1617.

Inglis GD, Kawchuk LM. 2002. Comparative degradation of oomycete, ascomycete, and basidiomycete cell walls by mycoparasitic and biocontrol fungi. Can J Microbiol. 48:60–70.

Jordan TW, Cordiner SJ. 1987. Fungal epipolythiodioxopiperazine toxins have therapeutic potential and roles in disease. Trends Pharmacol Sci. 8:144–149.

Kanokmedhakul S, Kanokmedhakul K, Phonkerd N, Soytong K, Kongsaeree P, Suksamrarn A. 2002. Antimycobacterial anthraquinone-chromone compound and diketopiperazine alkaloid from the fungus *Chaetomium globosum* KMITL-N0820. Planta Med. 68:834–836.

Kikuchi T, Kadota S, Nakamura K, Nishi A, Taga T, Kaji T, Osaki K, Tubaki K. 1982. Dethio-tetra(-methylthio)chetomin, a new antimicrobial metabolite of *Chaetomium globosum* Kinze ex Fr. Structure and partial synthesis from chetomin. Chem Pharm Bull. 30:3846–3848.

Li GY, Li BG, Yang T, Liu GY, Guo LZ. 2008. Secondary metabolites from the fungus *Chaetomium brasiliense*. Helv Chim Acta. 91:124–129.

Li GY, Li BG, Yang T, Yan JF, Liu GY, Zhang LG. 2006. Chaetocochins A-C, epipolythiodioxopiperazines from *Chaetomium cochliodes*. J Nat Prod. 69:1374–1376.

Li HQ, Li XJ, Wang YL, Zhang Q, Zhang AL, Gao JM, Zhang XC. 2011. Antifungal metabolites from *Chaetomium globosum*, an endophytic fungus in *Gingko biloba*. Biochem Syst Ecol. 39:876–879.

Li W, Yang X, Yang Y, Duang R, Chen G, Li X, Li Q, Qin S, Li S, Zhao L, et al. 2016. Anti-phytopathogen, multi-target acetylcholinesterase inhibitory and antioxidant activities of metabolites from endophytic *Chaetomium globosum*. Nat Prod Res. 30:2616–2619.

McMullin DR, Sumarah MW, Blackwell BA, Miller JD. 2013. New azaphilones from *Chaetomium globosum* isolated from the built environment. Tetrahedron Lett. 54:568–572.

Qi G, Lan N, Ma X, Yu Z, Zhao X. 2011. Controlling *Myzus persicae* with recombinant endophytic fungi *Chaetomium globosum* expressing *Pinellia ternate* agglutinin using recombinant endophytic fungi to control aphids. J Appl Microbiol. 110:1314–1322.

Ruan BH, Yu ZF, Yang XQ, Yang YB, Hu M, Zhang ZX, Zhou QY, Zhou H, Ding ZT. 2018. New bio-active compounds from aquatic endophyte *Chaetomium globosum*. Nat Prod Res. 32:1050–1055.

Tabata N, Suzumura Y, Tomoda H, Masuma R, Haneda K, Kisni M, Iwai Y, Omura S. 1993. Xanthoquinodins, new anticoccidial agents produced by *Humicola* sp. Production, isolation and physico-chemical and biological properties. J Antibiot. 46(5):749–755.

Tabata N, Tomoda H, Matsuzaki K, Omura S. 1993. Structure and biosynthesis of xanthoquinodins, anticoccidial antibiotics. J Am Chem Soc 115:8558–8564.

von Arx JA, Guarro J, Figueras MJ. 1986. The ascomycete genus *Chaetomium*. Beih Nova Hedwigia. 84:1–162.

Wang D, Zhang Y, Li X, Pan H, Chang M, Zheng T, Sun J, Qiu D, Zhang M, Wei D, et al. 2017. Potential allelopathic azaphilones produced by the endophytic *Chaetomium globosum* TY1 inhabited in *Ginkgo biloba* using the one strain-many compounds method. Nat Prod Res. 31:724–728.

Wang XY, Yan X, Fang MJ, Wu Z, Wang D, Qiu YK. 2017. Two new cytochalasan derivatives from *Chaetomium globosum* SNSHI-5, a fungus derived from extreme environment. Nat Prod Res. 31:1669–1675.

Wijeratne EMK, Turbyville TJ, Fritz A, Whitesell L, Gunatilaka AAL. 2006. A new dihydroxanthenone from a plant-associated strain of the fungus *Chaetomium globosum* demonstrates anticancer activity. Bioorg Med Chem. 14:7917–7923.

Xu GB, He G, Bai HH, Yang T, Zhang GL, Wu LW, Li GY. 2015. Indole alkaloids from *Chaetomium globosum*. J Nat Prod. 78:1479–1485.

Youn UJ, Sripisut, T, Park EJ, Kondratyuk TP, Fatima N, Simmons CJ, Wall MM, Sun D, Pezzuto JM, Chang LC. 2015. Determination of the absolute configuration of chaetoviridins and other bioactive azaphilones from the endophytic fungus *Chaetomium globosum*. Bioorg Med Chem Lett. 25:4719–4723.

Zhou X, Song B, Jin L, Hu D, Diao C, Xu G, Zou Z, Yang S. 2006. Isolation and inhibitory activity against ERK Phosphorylation of hydroxyanthraquinones from rhubarb. Bioorg Med Chem Lett. 16:563–568.

A new coruleoellagic acid derivative from stems of Rhodamnia dumetorum

Waranya Lakornwong, Kwanjai Kanokmedhakul & Somdej Kanokmedhakul

    View supplementary material ⬀

    Published online: 26 Oct 2017.

    Submit your article to this journal ⬀

    Article views: 29

    View related articles ⬀

    View Crossmark data ⬀

Taylor & Francis
Taylor & Francis Group

Check for updates

A new coruleoellagic acid derivative from stems of *Rhodamnia dumetorum*

Waranya Lakornwong, Kwanjai Kanokmedhakul and Somdej Kanokmedhakul

Natural Products Research Unit, Department of Chemistry and Center for Innovation in Chemistry, Faculty of Science, Khon Kaen University, Khon Kaen, Thailand

ABSTRACT

A new coruleoellagic acid derivative, 3,3′,4,4′,5′-pentamethyl-coruleoellagic acid (**1**) together with nine known compounds, hexamethylcoruleoellagic acid (**2**), 3,4,3′-tri-*O*-methylellagic acid (**3**), heptaphylline (**4**), 7-methoxymukonal (**5**), dentatin (**6**), sinapaldehyde (**7**), gallic acid (**8**), 2,6-dimethoxy-4H-pyran-4-one (**9**) and *β*-sitosterol (**10**) were isolated from the stems of *Rhodamnia dumetorum*. Their structures were identified by physical and spectroscopic data (IR, 1D and 2D NMR, and MS). Compounds **1**, **2** and **7**-**10** were tested for antibacterial activity against six pathogenic bacterial strains (*Bacillus cereus*, *Escherichia coli*, *Pseudomonas aeruginosa*, *Salmonella enterica* serovar Typhimurium, *Staphylococcus aureus*, and Methicillin resistant *S. aureus* (MRSA)).

Rhodamnia dumetorum
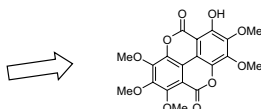
antibacterial activity against six pathogenic bacterial strains

1. Introduction

Rhodamnia dumetorum (DC.) Merr. & L.M. Perry (Myrtaceae) is a shrub or tree up to 15 m in height, growing in Cambodia, Laos, Malaysia, Thailand and Vietnam. It is known as 'Plong Kam Aon' in Thai (Smitinand 2001). The bark and leaves of *R. dumetorum* have been used as an astringent (Chansuwanit and Chanprasert 2011) and the roots has been used as an anti-pyretic in Thai traditional medicine (Ratanadomrongpinyo 2008). Moreover, the ethanol extract of the twigs of *R. dumetorum* from Vietnam has been reported to have inhibitory activity on AGEs formation (Choi et al. 2015). In a previous investigation of secondary metabolites from

---

CONTACT Somdej Kanokmedhakul ✉ somdej@kku.ac.th

Supplemental data for this article can be accessed at https://doi.org/10.1080/14786419.2017.1395430.

Rhodamnia species, only essential oil has been reported (Brophy et al. 1997). We report herein the isolation of a new coruleoellagic acid derivative (**1**) together with nine known compounds (**2**–**10**) from stems of *R. dumetorum*. This is the first phytochemical study on the stems of this plant.

2. Results and discussion

Hexane and EtOAc extracts from the stems of *R. dumetorum* were separated by chromatographic methods to give a new coruleoellagic acid derivative, 3,3′,4,4′,5′-pentamethylcoruleoellagic acid (**1**) and nine known compounds, including hexamethylcoruleoellagic acid (**2**) (Geevananda et al. 1979), 3,4,3′-tri-*O*-methylellagic acid (**3**) (Bai et al. 2008), heptaphylline (**4**), 7-methoxymukonal (**5**), dentatin (**6**) (Songsiang et al. 2012), sinapyl aldehyde (**7**) (Hiltunen et al. 2006), gallic acid (**8**) (Gottlieb et al. 1991), 2,6-dimethoxy-4H-pyran-4-one (**9**) (Zhu et al. 2012) and *β*-sitosterol (**10**) (Figure 1). Their structures were determined using spectroscopic data and compared with those data reported in the literature.

Compound **1** was obtained as yellow needles, and its molecular formula, $C_{19}H_{16}O_{10}$, was determined from the HRESITOFMS (observed *m/z* 427.0645 [M + Na]$^+$), indicating 12 degrees of unsaturation. The IR spectrum of **1** showed absorption bands of hydroxyl (3295 cm^{-1}) and two carbonyl (1733 and 1688 cm^{-1}) groups. The UV spectrum showed absorption maxima at 247, 368 and 384 nm. The ^{13}C NMR and DEPT spectra of **1** displayed 19 carbon signals attributable to five methoxy (δ_C 62.5 (5′-OCH$_3$), 62.2 (3′-OCH$_3$), 62.1 (3-OCH$_3$), 62.1 (4′-OCH$_3$)
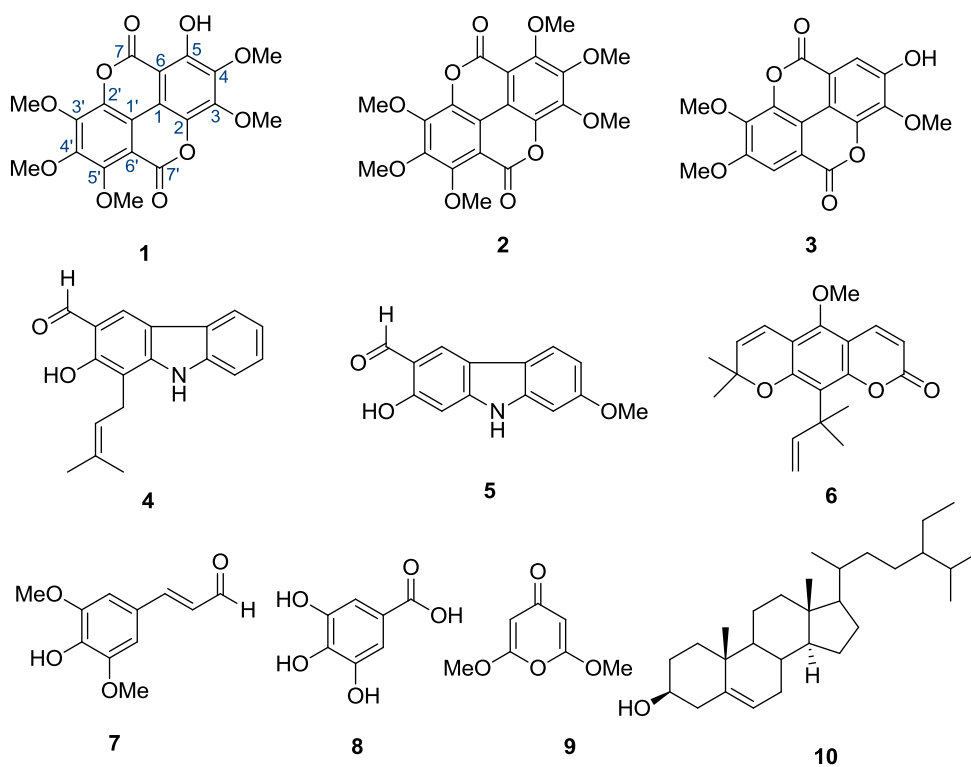

Figure 1. The structures of compounds **1**–**10**.

and 61.6 (4-OCH$_3$)), twelve hexasubstituted aromatic carbons (δ_C 111.9 (C-1), 134.7 (C-2), 148.0 (C-3), 141.8 (C-4), 152.8 (C-5), 97.2 (C-6), 114.9 (C-1'), 137.1 (C-2'), 148.7 (C-3'), 147.3 (C-4'), 154.1 (C-5') and 106.8 (C-6')) and two carbonyl lactones (δ_C 155.5 (C-7') and 163.0 (C-7)). The ^{1}H NMR spectrum showed a chelated proton at δ_H 10.45 and five methoxyl protons as five singlet signals at δ_H 4.26 (3-OCH$_3$), 4.25 (4'-OCH$_3$), 4.03 (5'-OCH$_3$), 4.02 (4-OCH$_3$) and 4.02 (3'-OCH$_3$). The phenolic hydroxyl group at C-5 was confirmed by the HMBC correlations of its proton to C-5 (δ_C 152.8), C-4 (δ_C 141.8) and C-6 (δ_C 97.2). The positions of five methoxyl groups were confirmed by HMBC correlations of methoxyl protons at 3-OCH$_3$ to C-3, 4-OCH$_3$ to C-4, 5'-OCH$_3$ to C-5', 3'-OCH$_3$ to C-3' and 4'-OCH$_3$ to C-4'. The structure of **1** was similar to that of 5'-methoxy-3,4,5,3'-tetra-O-methylflavellagic acid (Wolter-Filho et al. 1989), except for the interchange between a phenolic hydroxyl group at C-4 and a methoxyl group at C-5. Thus, the structure of **1** was determined as a new coruleoellagic acid derivative, which has been named 3,3',4,4',5'-pentamethylcoruleoellagic acid.

Compounds **1**, **2** and **7**–**10** were evaluated for antibacterial activity against three Gram-negative and three Gram-positive bacteria (Table 1). These bacteria are human opportunistic pathogen involved in infections acquired in a hospital setting and resistant to disinfectants as well as antibiotics. All tested compounds exhibited moderate antibacterial against *Pseudomonas aeruginosa* with MIC values in the range of 32–64 μg/mL. Compounds **7**-**10** exhibited moderate antibacterial against two Gram-negative bacteria (*Escherichia coli* and *Salmonella enterica* serovar Typhimurium) with MIC values in the range of 32-128 μg/mL and two Gram-positive bacteria (*Bacillus cereus* and *Staphylococcus aureus*) with MIC values in the range of 4–128 μg/mL. Moreover, compounds **7**–**9** also exhibited moderate antibacterial against MRSA with MIC values in the range of 8–128 μg/mL. The result of **7** agreed with the report for antibacterial activity against *E. coli* (Barber et al. 2000) and *B. cereus* (Chitsazian-Yazdi et al. 2015). Furthermore, the result of **8** agreed with the report for antibacterial activity against Gram-negative *P. aeruginosa*, *E. coli* and *S. enterica* serovar Typhimurium and Gram-positive *B. cereus*, *S. aureus* and MRSA (Al-Zahrani 2012; Gehrke et al. 2013; Fu et al. 2016). As to previously observed biological activities of other isolated compounds, compound **3** has been reported to possess a wide range of bioactivities, such as inhibition of on rat lens aldose reductase (RLAR), formation of AGEs, antioxidant, oxidative burst and effect on T-cell proliferation (Kim et al. 2008; Elhassan et al. 2015; Zhou et al. 2015). Compounds **4**, **5** and **6** have

Table 1. Antibacterial activity of isolated compounds **1**, **2** and **7**–**10**.

	MIC (μg/mL)					
	Gram-negative			Gram-positive		
Compounds	*Pseudomonas aeruginosa*	*Escherichia coli*	*Salmonella enterica* serovar Typhimurium	*Bacillus cereus*	*Staphylococcus aureus*	MRSA
1	64	>128	>128	>128	>128	>128
2	64	>128	>128	>128	>128	>128
7	64	128	128	128	64	128
8	64	128	128	4	64	16
9	32	64	32	32	16	8
10	64	128	128	128	128	>128
Kanamycin	–	2	–	2	1	–
Cefepime	1	0.0625	0.031	–	–	–
Vancomycin	–	–	–	2	1	1

been previously reported to be potent lipid peroxidation inhibitors and cytotoxicity towards several cancer cell lines, such as two cholangiocarcinoma (KKU-OCA17 and KKU-214), NCI-H187, KB, MCF-7, HepG2, HL-60, HeLa and HT-29 as well as *Vero* cells (Thongthoom et al. 2010; Sharif et al. 2011; Songsiang et al. 2011, 2012; Chakthong et al. 2016; Kiem et al. 2016). In addition, compounds **5** and **6** have been previously reported to exhibit antimycobacterial activity against *Mycobacterium tuberculosis*. Compound **5** also exhibited antifungal activity against *Candida albicans* (Sunthitikawinsakul et al. 2003). Moreover, compounds **4** and **6** showed antiplasmodial activity against *Plasmodium falciparum* (Yenjai et al. 2000).

3. Experimental

3.1. General experimental procedures

Melting points were determined on a SANYO Gallenkamp melting point apparatus (Leicestershire, U.K.) and are uncorrected. IR spectra were recorded as thin films using a Bruker Tensor 27 FT-IR spectrometer (Agilent Technologies, U.S.A.). UV spectra were obtained on an Agilent 8453 UV–vis spectrophotometer (Agilent Technologies, Germany). ^{1}H and ^{13}C NMR spectra were recorded in $CDCl_3$ and/or CD_3OD on a Varian Mercury Plus 400 spectrometer (Varian, Inc., U.S.A.), using residue of those solvents as internal standards. HR-ESI-TOF-MS were recorded on a Micromass Q-TOF-2 spectrometer (Bruker, Germany). Column chromatography was carried out on Merck silica gel 60 (230–400 mesh), lichroprep RP-18 (particle size 40–63 μm) (Merck, Darmstadt, Germany) and sephadex LH-20 (Amersham Pharmacia Biotech AB, Sweden). TLC was performed with precoated Merck silica gel 60 PF$_{254}$ aluminium sheets; compounds were visualised under UV light (254 and 366 nm).

3.2. Plant material

The stems of *R. dumetorum* were collected from Yasothon Province, Thailand, in May 2015. The plant was identified by Prof. Pranom Chantaranothai, Department of Biology, Faculty of Science, Khon Kaen University, where a voucher specimen (S. Kanokmedhakul-29) is deposited.

3.3. Extraction and isolation

Air-dried stems of *R. dumetorum* (6.0 Kg) were ground and extracted successively at room temperature with hexane (3 × 15 L) and EtOAc (3 × 15 L) to give crude hexane (6 g) and EtOAc (43 g) extracts, respectively. Hexane extract was separated over silica gel column chromatography (CC), eluted with a gradient system of hexane, hexane-EtOAc and EtOAc-MeOH. An aliquot of 200 mL was collected for each fraction to give 59 fractions. According to the TLC patterns, these fractions were combined to 13 subfractions, designated as H$_1$-H$_{13}$. Fraction H$_3$ was purified by silica gel flash column chromatography (FCC), eluted with an isocratic system of hexane-acetone (99:1) to give 8 subfractions H$_{3.1}$–H$_{3.8}$. Subfraction H$_{3.5}$ was purified by silica gel CC, eluted with an isocratic system of hexane-CH$_2$Cl$_2$ (80:20) to give 2 subfractions, H$_{3.5.1}$–H$_{3.5.2}$. Subraction H$_{3.5.1}$ was purified by preparative TLC using hexane-CH$_2$Cl$_2$ (30:70) as an eluent, to give a yellow solid of **4** (2.3 mg). Fraction H$_6$ was filtered out to give colourless needles of **10** (79.7 mg). Fraction H$_7$ was purified by silica gel CC, eluted

with a gradient system of hexane-CH_2Cl_2 to give 8 subfractions, $H_{7.1}$-$H_{7.8}$. Subfraction $H_{7.3}$ was purified by silica gel CC, eluted with an isocratic system of CH_2Cl_2-EtOAc (99:1) to give 3 subfractions, $H_{7.3.1}$-$H_{7.3.3}$. Subfraction $H_{7.3.2}$ was purified by preparative TLC using CH_2Cl_2–EtOAc (95:5) as an eluent, to give a yellow solid of **6** (2.0 mg) and an additional amount of **10** (242.1 mg). Subfraction $H_{7.4}$ was filtrated out to give an additional amount of **10** (27.7 mg). EtOAc extract was separated over silica gel CC, eluted with a gradient system of hexane, hexane-EtOAc and EtOAc–MeOH. An aliquot of 200 mL was collected for each fraction to give 57 fractions which were combined according to the TLC patterns into 13 subfractions, designated as E_1–E_{13}. Fraction E_5 was applied on RP-18 CC, eluted with an isocratic system of MeOH–H_2O (80:20) to give 8 subfractions, $E_{5.1}$–$E_{5.8}$. Subfraction $E_{5.3}$ was separated on Sephadex LH 20 CC, eluted with MeOH to give 7 subfractions, $E_{5.3.1}$–$E_{5.3.7}$. Subfraction $E_{5.3.2}$ was purified by preparative TLC using CH_2Cl_2–EtOAc (99:1) as an eluent, to give **5** (2.1 mg). Fraction E_6 was separated on RP-18 CC, eluted with MeOH–H_2O (80:20) to give 8 subfractions, $E_{6.1}$–$E_{6.8}$. Solid in subfraction $E_{6.5}$ was filtered to give a yellow solid of **1** (57.8 mg). Fraction E_7 was purified by CC, eluted with a gradient system of hexane-CH_2Cl_2 to give 10 subfractions, $E_{7.1}$–$E_{7.10}$. Subfraction $E_{7.2}$ was separated on RP-18 CC, eluted with MeOH–H_2O (80:20) to give 4 subfractions, $E_{7.2.1}$–$E_{7.2.4}$. Subfraction $E_{7.2.1}$ was separated on Sephadex LH 20 CC, eluted with MeOH to give 3 subfractions, $E_{7.2.1.1}$–$E_{7.2.1.3}$. Subfraction $E_{7.2.1.3}$ was separated on Sephadex LH-20 CC, eluted with MeOH to give a yellow amorphous solid of **7** (21.2 mg). Yellow needles of **9** (14.9 mg) were obtained from $E_{7.3}$ by crystallisation from CH_2Cl_2, and the filtrate was purified by preparative TLC using CH_2Cl_2-EtOAc (99:1) as eluent, to give an additional amount of **1** (12.2 mg), and pale yellow needles of **2** (15.3 mg). Solid in subfraction $E_{7.5}$ was filtered to give a pale yellow solid of **3** (1.4 mg). Subfraction $E_{7.10}$ was separated on RP-18 CC, eluted with MeOH-H_2O (80:20) to give 10 subfractions, $E_{7.10.1}$–$E_{7.10.10}$. Solid in subfraction $E_{7.10.2}$ was filtered to give colourless needles of **8** (275.8 mg).

3.3.1. 3,3′,4,4′,5′-pentamethylcoruleoellagic acid (1)

Yellow needles (CH_2Cl_2); m.p. 214–216 °C; UV (CH_2Cl_2) λ_{max} (log ε) 247 (3.71), 368 (3.14), 384 (3.16) nm; IR (film, CH_2Cl_2) v_{max} 3295 (OH), 2942, 1733 (C=O), 1688 (C=O), 1596, 1277, 1061, 931 cm^{-1}; ^{1}H NMR (CDCl$_3$, 400 MHz) δ 10.45 (1H, s, 5-OH), 4.26 (1H, s, 3-OCH$_3$), 4.25 (1H, s, 4′-OCH$_3$), 4.03 (1H, s, 5′-OCH$_3$), 4.02 (1H, s, 4-OCH$_3$), 4.02 (1H, s, 3′-OCH$_3$); ^{13}C NMR (100 MHz) δ 163.0 (C-7), 155.5 (C-7′), 154.1 (C-5′), 152.8 (C-5), 148.7 (C-3′), 148.0 (C-3), 147.3 (C-4′), 141.8 (C-4), 137.1 (C-2′), 134.7 (C-2), 114.9 (C-1′), 111.9 (C-1), 106.8 (C-6′), 97.2 (C-6), 62.5 (5′-OCH$_3$), 62.2 (3′-OCH$_3$), 62.1 (3-OCH$_3$), 62.1 (4′-OCH$_3$), 61.6 (4-OCH$_3$); HRESIMS *m/z* 427.0645 [M + Na]+ (Calcd for $C_{19}H_{16}O_{10}Na$, 427.0641).

3.4. Antibacterial assay

The minimum inhibitory concentrations (MICs) were determined by the dilution method as described in the M07-A9 (CLSI 2012). Resazurin solution was used as an indicator of microbial growth. MICs were recorded by reading the lowest concentration capable of inhibiting visible growth. The tests were performed in triplicate. Vancomycin, kanamycin and cefepime were used as positive control drugs. Six microorganism cultures (*B. cereus* ATCC 11778, *E. coli* ATCC 25922, *P. aeruginosa* ATCC 27853, *S. enterica* serovar Typhimurium ATCC 13311, *S. aureus* ATCC

6538 and Methicillin resistant *S. aureus* (MRSA)) were used. The experiment was performed at the Department of Microbiology, Faculty of Science, Khon Kaen University.

4. Conclusion

Phytochemical investigation of the hexane and EtOAc extracts from the stems of *R. dumetorum* led to the isolation of a new coruleoellagic acid derivative, 3,3′,4,4′,5′-pentamethylcoruleoellagic acid (**1**) and nine known compounds. They are a coruleoellagic acid derivative, hexamethylcoruleoellagic acid (**2**); an ellagic acid derivative, 3,4,3′-tri-*O*-methylellagic acid (**3**); two carbazoles, heptaphylline (**4**) and 7-methoxymukonal (**5**); a coumarin, dentatin (**6**); two phenolic derivatives**,** sinapaldehyde (**7**) and gallic acid (**8**); a pyrone derivative, 2,6-dimethoxy-4H-pyran-4-one (**9**); and a sterol, *β*-sitosterol (**10**). Compounds **1**–**2** showed antibacterial activity against only Gram-negative bacteria, *P. aeruginosa*. While, compounds **7**–**10** showed antibacterial activity against both Gram-negative and Gram-positive bacteria. Several of these isolated compounds have previously been reported for a wide range of biological activities. All of these compounds are isolated from stems of *R. dumetorum* for the first time. This is also the first report on the isolation of compounds **1**–**2**, **4**–**6** and **9** from the Myrtaceae family.

Disclosure statement

No potential conflict of interest was reported by the authors.

References

Al-Zahrani SHM. 2012. Antibacterial activities of gallic acid and gallic acid methyl ester on methicillin-resistant *Staphylococcus aureus*. J Am Sci. 8:7–13.

Bai N, He K, Roller M, Zheng B, Chen X, Shao Z, Peng T, Zheng Q. 2008. Active compounds from *Lagerstroemia speciosa*, insulin-like glucose uptake-stimulatory/inhibitory and adipocyte differentiation-inhibitory activities in 3T3-L1 cells. J Agric Food Chem. 56:11668–11674.

Barber MS, McConnell VS, DeCaux BS. 2000. Antimicrobial intermediates of the general phenylpropanoid and lignin specific pathways. Phytochemistry. 54:53–56.

Brophy JJ, Goldsack RJ, Forster PI. 1997. The leaf essential oils of the Australian species of *Rhodamnia* (Myrtaceae). Flavour Fragr J. 12:345–354.

Chakthong S, Bindulem N, Raknai S, Yodwaree S, Kaewsanee S, Kanjana-Opas A. 2016. Carbazolepyranocoumarin conjugate and two carbazole alkaloids from the stems of *Clausena excavata*. Nat Prod Res. 30:1690–1697.

Chansuwanit N, Chanprasert C. 2011. Medicinal plants and local-used plants in Paknampran, Pranburi District, Prachup-khiri-khan Province. Reg 7 Med J. 13:145–164.

Chitsazian-Yazdi M, Agnolet S, Lorenz S, Schneider B, Es'haghi Z, Kasaian J, Khameneh B, Iranshahi M. 2015. Foetithiophenes C-F, thiophene derivatives from the roots of *Ferula foetida*. Pharm Biol. 53:710–714.

Choi SJ, Kim YS, Kim JH, Bach TT, Kim JS. 2015. Screening of herbal medicines from Vietnam with inhibitory activity on advanced glycation end products formation (XIV). Korean J Pharmacogn. 46:268–278.

CLSI Clinical and Laboratory Standards Institute (US). 2012. Methods for dilution antimicrobial susceptibility tests for bacteria that grow aerobically; approved standard. 9th ed. M07–A9. Wayne, PA: Clinical and Laboratory Standards Institute.

Elhassan GOM, Adhikari A, Abdalla OM, Shukrulla A, Khalid A, Iqbal Choudhary M, Mesaik MA, Yagi S. 2015. Chemical constituents of *Euphorbia polyacantha* Boiss. and their immunomodulatory properties. Rec Nat Prod. 9:146–152.

Fu L, Lu W, Zhou X. 2016. Phenolic compounds and *in vitro* antibacterial and antioxidant activities of three tropic fruits: Persimmon, Guava, and Sweetsop. Biomed Res Int. [accessed 2017 Sep 20]. https://www.hindawi.com/journals/bmri/2016/4287461/; p. 9. doi:10.1155/2016/4287461.

Geevananda YA, Gunawardana P, Kumar NS, Sultanbawa MUS. 1979. Three hydroxy ellagic acid methyl ethers, chrysophanol and scopoletin from *Shorea worthingtonii* and *Vatica obscura*. Phytochemistry. 18:1017–1019.

Gehrke IT, Neto AT, Pedroso M, Mostardeiro CP, Da Cruz IB, Silva UF, Ilha V, Dalcol II, Morel AF. 2013. Antimicrobial activity of *Schinus lentiscifolius* (Anacardiaceae). J Ethnopharmacol. 148:486–491.

Gottlieb HE, Kumar S, Sahai M, Ray AB. 1991. Ethyl brevifolin carboxylate from *Flueggea microcarpa*. Phytochemistry. 30:2435–2438.

Hiltunen E, Pakkanen TT, Alvila L. 2006. Phenolic compounds in silver birch (*Betula pendula* Roth) wood. Holzforschung. 60:519–527.

Kim JM, Jang DS, Lee YM, Yoo JL, Kim YS, Kim JH, Kim JS. 2008. Aldose-reductase- and protein-glycation-inhibitory principles from the whole plant of *Duchesnea chrysantha*. Chem Biodivers. 5:352–356.

Ratanadomrongpinyo C. 2008. The study of diversity and utilization of herbs in the area of the project of conservation and development of natural resorces in HM private development project Chumphon Province. Chumphon: Protected Areas Regional Office, Department of National Parks, Wildlife and Plant Conservation.

Sharif NWM, Mustahil NA, Noor NM, Sukari MA, Rahmani M, Taufiq-Yap YH, Ee GCL. 2011. Cytotoxic constituents of *Clausena excavata*. Afr J Biotechnol. 10:16337–16341.

Smitinand T. 2001. Thai plant names revised edition. Bangkok: Prachachon Limited; p. 451.

Songsiang U, Thongthoom T, Boonyarat C, Yenjai C. 2011. Claurailas A–D, cytotoxic carbazole alkaloids from the roots of *Clausena harmandiana*. J Nat Prod. 74:208–212.

Songsiang U, Thongthoom T, Zeekpudsa P, Kukongviriyapan V, Boonyarat C, Wangboonskul J, Yenjai C. 2012. Antioxidant activity and cytotoxicity against cholangiocarcinoma of carbazoles and coumarins from *Clausena harmandiana*. Science Asia. 38:75–81.

Sunthitikawinsakul A, Kongkathip N, Kongkathip B, Phonnakhu S, Daly JW, Spande TF, Nimit Y, Rochanaruangrai S. 2003. Coumarins and carbazoles from *Clausena excavata* exhibited antimycobacterial and antifungal activities. Planta Med. 69:155–157.

Thongthoom T, Songsiang U, Phaosiri C, Yenjai C. 2010. Biological activity of the chemical constituents from *Clausena harmandiana*. Arch Pharm Res. 33:675–680.

Kiem PV, Cuong LCV, Cuc NT, Nhiem NX, Anh HLT, Tai BH, Quang TH, Minh CV, Huong LM, Kim EJ, et al. 2016. Alkaloids from the leaves of *Antidesma acidum* and their cytotoxic activity. Lett Org Chem. 13:297–301.

Wolter-Filho W, Da Rocha AI, Yoshida M, Cottlieb OR. 1989. Chemosystematics of *Rhabdodendron*. Phytochemistry. 28:2355–2357.

Yenjai C, Sripontan S, Sriprajun P, Kittakoop P, Jintasirikul A, Tanticharoen M, Thebtaranonth Y. 2000. Coumarins and carbazoles with antiplasmodial activity from *Clausena harmandiana*. Planta Med. 66:277–279.

Zhou ZH, Liu MZ, Wang MH, Qu W, Sun JB, Liang JY, Wu FH. 2015. A new ellagic acid derivative from *Polygonum runcinatum*. Nat Prod Res. 29:795–799.

Zhu M, Xiong L, Wang Y, Chen M, Jiang B, Lin S, Zhu C, Yang Y, Shi J. 2012. Lignans from *Sinocalamus affinis*. China J Chin Mater Medica. 37:1968–1972.
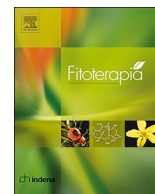
Bioactive oxaphenalenone dimers from the fungus *Talaromyces macrosporus* KKU-1NK8

Boonyanoot Chaiyosang[a], Kwanjai Kanokmedhakul[a], Wareerat Sanmanoch[b], Sophon Boonlue[b], Sarinya Hadsadee[c], Siriporn Jungsuttiwong[c], Somdej Kanokmedhakul[a],*

[a] Natural Products Research Unit, Department of Chemistry and Center of Excellence for Innovation in Chemistry, Faculty of Science, Khon Kaen University, Khon Kaen 40002, Thailand
[b] Department of Microbiology, Faculty of Science, Khon Kaen University, Khon Kaen 40002, Thailand
[c] Center for Organic Electronic and Alternative Energy, Department of Chemistry and Center of Excellence for Innovation in Chemistry, Faculty of Science, Ubon Ratchathani University, Ubon Ratchathani 34190, Thailand

ARTICLE INFO

ABSTRACT

Six new polyketide-derived oxaphenalenone dimers, talaromycesone C (**1**) and macrosporusones A-E (**2–6**), together with eight known analogs, were isolated from the mycelium of the fungus *Talaromyces macrosporus* KKU-1NK8. Their structures were established based on their spectroscopic data and MS. The absolute configurations of new compounds **1–6** were determined by ECD analyses. Compounds **3** and **8** exhibited antimalarial activity against *Plasmodium falciparum*. Compound **3** showed activity against NCI-H187 cells, while compound **8** displayed activity against KB, MCF-7 and NCI-H187 cell lines. In addition, compound **11** showed antibacterial activity against *Bacillus cereus*, *Staphylococcus aureus* and MRSA.

1. Introduction

The genus *Talaromyces*, a sexual state of the *Penicillium* species, was introduced by Benjamin in 1995. It belongs to the family Trichocomaceae [1]. Some species were isolated from soil, plants, sponges, and foods. Many species are used in food and agricultural production [2]. Previous reports on secondary metabolites from *Talaromyces* species have resulted in the isolation of many different types of compounds such as alkaloids [3], indole alkaloids [4], adenine [5], tetramic acid derivatives [6], polyesters [7], diphenyl ether lactone derivatives [8], meroterpenoids [9], oxaphenalenone dimers [8,10–13], quinones [14–16], steroids and terpenoids [17]. One interesting type is the oxaphenalenone dimer which is a polyketide-derived. Until now, only 20 natural isolated members in this type have been reported [8,10–13,18–20]. They showed various bioactive activities such as cytotoxicity against cancer cell lines [11] and antibacterial activity against Gram positive bacteria [8,12,13], as well as acetylcholinesterase inhibition [11]. Therefore, searching for bioactive compounds from the fungus *Talaromyces* is still of interest. Since no phytochemical investigation of *T. macrosporus* has been reported, our investigation found that the crude EtOAc extracts of *T. macrosporus* KKU-1NK8 exhibited cytotoxicity towards the KB cell line with 40%

inhibition at 50 μg/mL. We report herein the isolation of fourteen oxaphenalenone dimers from the fungus *T. macrosporus* (Fig. 1); six of these (**1–6**) are reported as new oxaphenalenone dimers.

2. Experimental section

2.1. General experimental procedures

Melting points were obtained using a SANYO Gallenkamp melting point apparatus and were uncorrected. Optical rotations were determined using a JASCO DIP-1000 digital polarimeter. The CD and UV spectra were measured using a JASCO J-810 apparatus. IR spectra were obtained using a Bruker Tenser 27 spectrophotometer. NMR spectra were recorded on a Varian Mercury Plus 400 spectrometer in CDCl$_3$ and CD$_3$OD, and the internal standards were referenced from the residues of these solvents. Mass spectra were determined on a Micromass Q-TOF 2 hybrid quadrupole time-of-flight (Q-TOF) mass spectrometer. TLC was performed with MERCK silica gel 60 PF$_{254}$ TLC aluminum sheets. The column chromatography was carried out on MERCK silica gel 0.063–0.200 mm or < 0.063 mm and Sephadex LH-20. Preparative layer chromatography (PLC) was carried out on silica gel 60 PF$_{254}$ (MERCK).

---

* Corresponding author at: Natural Products Research Unit, Department of Chemistry and Center of Excellence for Innovation in Chemistry, Faculty of Science, Khon Kaen University, Khon Kaen 40002, Thailand.
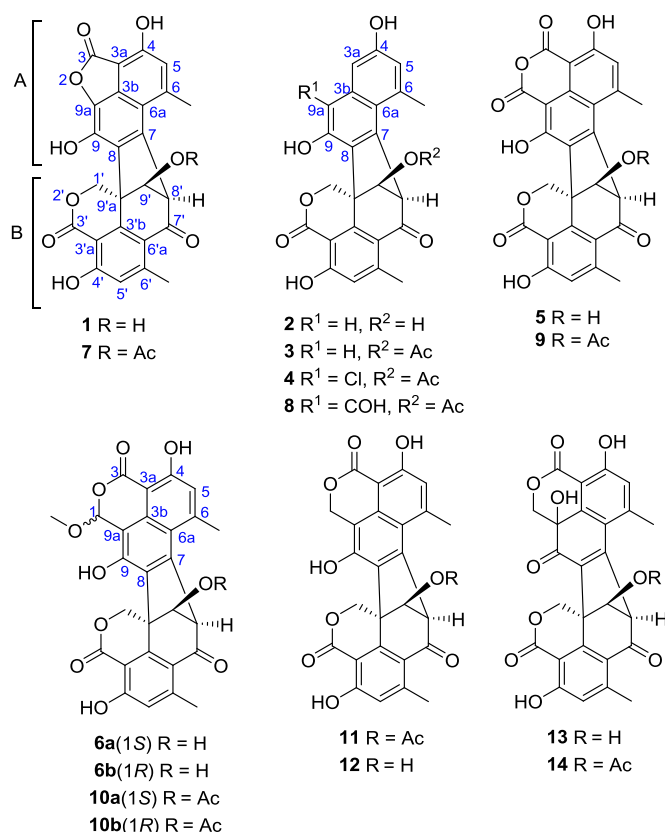*E-mail address:* somdej@kku.ac.th (S. Kanokmedhakul).

Fig. 1. Structures of compounds **1–14**.

2.2. Fungal material

The fungus *Talaromyces macrosporus* KKU-1NK8 was collected from the forest soil around the Pha Nok Kao Silvicultural Station, Khon Kaen Province, Thailand, on July 2012. The internal transcribed spacer region sequences of *T. macrosporus* KKU-1NK8 were deposited in GenBank as accession numbers MH620706. The production of bioactive metabolites condition of *T. macrosporus* KKU-1NK8 was produced on 500 mL malt extract peptone broth by incubating at 30 °C under static conditions for 28 days.

2.3. Extraction and isolation

Air-dried biomass of the fungus *T. macrosporus* (89.4 g) was extracted exhaustively three times with *n*-hexane (3 × 400 mL), EtOAc (3 × 400 mL), and MeOH (3 × 400 mL) at room temperature to yield crude *n*-hexane (10.0 g, 11.2%), EtOAc (11.8 g, 13.2%) and MeOH (26.9 g, 30.1%) extracts. The *n*-hexane extract was separated on silica gel flash column chromatography (FCC), eluted with a gradient system of *n*-hexane-EtOAc and EtOAc-MeOH to give 5 fractions, H$_1$-H$_5$. Fraction H$_2$ was further separated by FCC, eluted with an isocratic system of *n*-hexane-EtOAc (80:20) to give a pale yellow solid of **4** (8.9 mg). Fraction H$_3$ afforded a white solid of **11** (8.5 mg). Fraction H$_5$ was separated by FCC, eluting with an isocratic system of CH$_2$Cl$_2$-MeOH (99:1) and afforded a yellow powder of **7** (10.5 mg).

The EtOAc extract was separated on silica gel FCC, eluting with a gradient system of *n*-hexane-EtOAc and EtOAc-MeOH to give 6 fractions, E$_1$-E$_6$. Fraction E$_3$ was separated over silica gel FCC, eluting with an isocratic system of CH$_2$Cl$_2$-MeOH (99:1) to give 6 subfractions, E$_{3.1}$-E$_{3.6}$. Subfraction E$_{3.1}$ was carried out by PLC (CH$_2$Cl$_2$-MeOH; 97:3, ×2) to afford yellow solids of **9** (5.6 mg, R_f 0.60) and **10** (6.7 mg, R_f 0.54). Subfraction E$_{3.2}$ was separated on silica gel FCC, eluting with an isocratic system of CH$_2$Cl$_2$-MeOH (99:1) to give 3 subfractions, E$_{3.2.1}$-

E$_{3.2.3}$. Subfraction E$_{3.2.1}$ provided an additional amount of **10** (76.5 mg). Subfraction E$_{3.2.2}$ provided an additional amount of **11** (18.2 mg). Subfraction E$_{3.4}$ provided a pale yellow solid of **8** (10.3 mg). Subfraction E$_{3.6}$ afforded a pale yellow solid of **14** (2.3 mg). Fraction E$_4$ was separated by FCC, eluting with an isocratic system of *n*-hexane-CH$_2$Cl$_2$-MeOH (19.5:79.5:1) to give 4 subfractions, E$_{4.1}$-E$_{4.4}$. Separation of subfraction E$_{4.2}$ gave an additional amount of **14** (2.5 mg). Subfraction E$_{4.3}$ provided a pale yellow solid of **6** (8.0 mg). Subfraction E$_{4.4}$ gave a yellow solid of **13** (3.0 mg). Fraction E$_5$ was further separated on silica gel by FCC, eluting with an isocratic system of CH$_2$Cl$_2$ to give 4 subfractions, E$_{5.1}$-E$_{5.4}$. Subfraction E$_{5.2}$ provided a pale yellow solid of **5** (13.9 mg). Subfraction E$_{5.3}$ gave an additional amount of **7** (42.9 mg). Subfraction E$_{5.4}$ provided a pale yellow solid of **1** (3.9 mg). Separation of fraction E$_6$ by PLC (CH$_2$Cl$_2$-MeOH; 1:99, ×2) yielded a pale yellow solid of **3** (4.2 mg, R_f 0.44).

The MeOH extract was separated on silica gel FCC, eluting with a gradient system of *n*-hexane-EtOAc and EtOAc-MeOH to give 4 fractions, M$_1$-M$_4$. Separation of fraction M$_2$ by PLC (CH$_2$Cl$_2$-MeOH; 97:3, ×2) gave a pale yellow solid of **12** (3.5 mg, R_f 0.60). Fraction M$_3$ was separated by PLC (CH$_2$Cl$_2$-MeOH; 95:3, ×3) to afford a pale yellow solid of **2** (9.4 mg, R_f 0.62) and an additional amount of **7** (3.5 mg, R_f 0.58).

2.3.1. Talaromycesone C (1)

Pale yellow solid; mp 264–266 °C (dec); [α]$_D^{25.3}$ +164 (*c* 0.1, MeOH); UV (MeOH) λ$_{max}$ (log ε) 219 (4.29), 234 (4.29), 261 (4.36), 323 (3.67), 326 (3.67); ECD (*c* 50 μM, MeOH) nm 216 (−37.9), 243 (66.3), 272 (14.5), 298 (−20.2), 339 (9.4); IR (neat) ν$_{max}$ 3356, 2926, 1705, 1670, 1633, 1567, 1461, 1273, 1227 cm^{-1}; ^{1}H and ^{13}C NMR, see Tables 1 and 2; HRESITOFMS *m/z* 483.0684 [M + Na]$^+$ (calcd for C$_{25}$H$_{16}$O$_9$Na, 483.0692).

2.3.2. Macrosporusone A (2)

Pale yellow solid; mp 257–258 °C (dec); [α]$_D^{25.3}$ +160 (*c* 0.1, MeOH); UV (MeOH) λ$_{max}$ (log ε) 240 (4.30), 273 (3.80), 324 (3.35); ECD (*c* 120 μM, MeOH) nm 213 (−37.0), 247 (47.8), 302 (−7.2); IR (Neat) ν$_{max}$ 3347, 2959, 2927, 2853, 1663, 1612, 1570,1460, 1270, 1231, 1127 cm^{-1}; ^{1}H and ^{13}C NMR, see Tables 1 and 2; HRESITOFMS *m/z* 441.0940 [M + Na]$^+$ (calcd for C$_{24}$H$_{18}$O$_7$Na, 441.0950).

2.3.3. Macrosporusone B (3)

Pale yellow solid; mp 262–265 °C (dec); [α]$_D^{25.4}$ +122 (*c* 0.1, MeOH); UV (MeOH) λ$_{max}$ (log ε) 207 (3.88), 239 (4.02), 277 (3.60), 323 (3.24); ECD (*c* 110 μM, MeOH) nm 216 (−29.9), 246 (51.5), 297

Table 1
^{1}H NMR Spectroscopic Data of Compounds **1–6** (CDCl$_3$:CD$_3$OD, δ in ppm).

Position	1	2	3	4	5	6a	6b
1						6.37, s	6.44, s
3a		6.57, s	6.72, s	7.21, s			
5	6.61, s	6.62, s	6.71, s	6.84, s	6.92, s	6.77, s	6.84, s
9a		6.65, s	6.79, s				
1′	4.95, d	4.90, d	4.83, d	4.89, d	4.89, d	4.98, d	5.00, d
	(12.4)	(12.0)	(12.4)	(12.4)	(12.8)	(12.8)	(12.8)
	5.31, d	5.16, d	5.08, d	5.16, d	5.16, d	5.18,d	5.19, d
	(12.4)	(12.0)	(12.4)	(12.4)	(12.8)	(12.8)	(12.8)
5′	6.62, s	6.62, s	6.68, s	6.72, s	6.71, s	6.71, brs	6.71, brs
8′	4.61, s	4.88, s	4.99, s	5.06, s	5.00, s	4.93, s	4.95, s
9′	4.73, s	4.59, s	5.74, s	5.79, s	4.76, s	4.67, s	4.69, s
Me-6	2.46, s	2.86, s	2.86, s	2.94, s	3.06, s	2.97, s	2.99, s
Me-6′	2.83, s	2.48, s	2.50, s	2.54, s	2.50, s	2.52, brs	2.52, brs
Ac-9′			1.99, s	2.03, s			
4′-OH	11.86, s	11.77, s		11.83 s	11.91 s		
9-OH							
1-OMe						3.56, s	3.68, s

Table 2
^{13}C NMR spectroscopic data of compounds **1–6** (CDCl$_3$:CD$_3$OD, δ in ppm).

Position	1	2	3	4	5	6a	6b
1					161.8	99.1	99.4
3	166.9				165.8	168.6	168.6
3a	98.7	106.8	106.8	104.4	97.2	96.8	96.8
3b	131.6	138.4	138.6	134.5	134.4	131.0	131.3
4	158.4	154.1	154.4	155.7	164.6	163.4	163.4
5	120.3	119.2	119.4	120.4	120.1	119.8	119.8
6	131.8	136.4	136.4	137.7	149.8	146.9	147.0
6a	117.0	121.0	121.0	121.7	118.8	119.7	119.7
7	132.2	136.5	136.5	135.5	149.8	139.9	139.9
8	134.4	130.9	131.0	130.2	132.1	132.2	132.3
9	153.4	152.0	151.0	164.2	164.4	151.0	151.1
9a	136.6	110.6	110.5	113.8	99.5	109.2	109.2
1′	70.1	70.7	69.5	69.2	69.6	70.3	70.5
3′	168.4	168.7	168.2	167.9	167.9	168.3	168.3
3′a	103.5	103.8	103.1	103.2	103.6	103.2	103.3
3′b	147.7	147.9	146.7	146.0	146.7	147.3	147.6
4′	164.0	163.8	163.9	164.4	164.6	164.2	164.2
5′	120.3	120.1	120.5	121.0	120.9	120.5	120.5
6′	147.4	153.5	153.7	153.9	153.7	153.9	153.9
6′a	116.7	117.3	117.1	116.9	116.8	117.1	117.3
7′	192.6	193.2	191.6	190.9	190.8	192.3	192.3
8′	63.9	60.1	61.9	61.8	66.2	65.1	65.2
9′	86.7	86.4	86.3	86.1	86.0	86.0	86.0
9′a	50.5	49.9	48.3	48.7	49.7	50.1	50.2
Me-6	22.2	24.3	24.4	24.7	25.3	25.0	25.1
Me-6′	23.7	23.7	23.7	23.8	23.7	23.7	23.7
Ac-9			20.8	20.7			
			170.6	170.4			
1-OMe						55.8	55.9

(-13.9); IR (neat) ν_{max} 3400, 2971, 2846, 1746, 1668, 1605, 1571, 1465, 1371, 1270, 1227 cm^{-1}; ^{1}H and ^{13}C NMR, see Tables 1 and 2; HRESITOFMS m/z 459.1088 [M−H]$^-$ (calcd for C$_{26}$H$_{20}$O$_8$, 459.1080).

2.3.4. Macrosporusone C (4)

Pale yellow solid; mp 248–249 °C (dec); $[\alpha]_D^{24.7}$ +196 (c 0.1, MeOH); UV (MeOH) λ_{max} (log ε) 241 (4.41), 272 (3.96), 323 (3.43); ECD (c 100 μM, MeOH) nm 216 (-58.9), 246 (105.0), 294 (-36.9); IR (neat) ν_{max} 3425, 2972, 2931, 1740, 1670, 1632, 1569, 1463, 1268, 1228, 1045 cm^{-1}; ^{1}H and ^{13}C NMR, see Tables 1 and 2; HRESITOFMS m/z 495.0850 [M + H]$^-$ and 497.0812 [M + H + 2]$^+$ (calcd for C$_{26}$H$_{19}$ClO$_8$H, 495.0847 and C$_{26}$H$_{19}$ClO$_8$H + 2, 497.0817).

2.3.5. Macrosporusone E (5)

Pale yellow solid; mp 246–247 °C (dec); $[\alpha]_D^{24.0}$ +141 (c 0.1, MeOH); UV (MeOH) λ_{max} (log ε) 207 (3.95), 227 (3.95), 240 (3.98), 291 (3.53), 322 (3.40); ECD (c 100 μM, MeOH) nm 217 (-42.6), 243 (80.0), 272 (17.6), 301 (-20.2); IR (neat) ν_{max} 3330, 2970, 2930, 1716, 1670, 1613, 1466, 1427, 1271 cm^{-1}; ^{1}H and ^{13}C NMR, see Tables 1 and 2; HRESITOFMS m/z 487.0669 [M−H]$^-$ (calcd for C$_{26}$H$_{16}$O$_{10}$, 487.0665).

2.3.6. Macrosporusone D (6)

Pale yellow solid; mp 269–271 °C (dec); $[\alpha]_D^{25.0}$ +148 (c 0.1, MeOH); UV (MeOH) λ_{max} (log ε) 209 (3.89), 239 (4.05), 279 (3.62), 321 (3.40); ECD (c 100 μM, MeOH) nm 218 (-23.8), 245 (45.6), 298 (-15.3); IR (neat) ν_{max} 3409, 2977, 2930, 1666, 1604, 1570, 1466, 1319, 1226 cm^{-1}; ^{1}H and ^{13}C NMR, see Tables 1 and 2; HRESITOFMS m/z 503.0975 [M−H]$^-$ (calcd for C$_{27}$H$_{20}$O$_{10}$, 503.0978).

2.4. Calculation of ECD spectra

The ECD spectra of **1–5** were performed for two selected 8′R, 9′S, 9′aS and 8′S, 9′R, 9′aR stereoisomers and all calculations were performed using the Gaussian09 program [21]. The ground-state geometries of structures were optimized by B3LYP using the 6-31G (d,p) basis

set. ECD spectra were calculated using the time dependent density functional theory (TD-DFT) method with CAM-B3LYP functional and 6-311 + +G (d,p) basis set. Polarizable Continuum Model (PCM) solvation model using methanol was included in the calculations. All calculations were performed using Gaussian09 program. Gaussian bandshape with a bandwidth of 0.25 eV was used to simulate ECD spectra.

2.5. Biological activity procedures

2.5.1. Antimalarial assay

Antimalarial activity was evaluated against the parasite *Plasmodium falciparum* (K1, multidrug-resistant strain), using the culture method of Trager and Jensen [22]. Quantitative assessment of activity *in vitro* was determined by means of the microculture radioisotope technique, based upon the method described by Desjardins and co-workers [23]. The inhibitory concentration (IC$_{50}$) represents the concentration that causes a 50% reduction in parasite growth as indicated by the *in vitro* uptake of [^{3}H]-hypoxanthine by *P. falciparum*.

2.5.2. Cytotoxicity assays

Cytotoxicity assays against human epidermoid carcinoma (KB), human breast adenocarcinoma (MCF7), and human small cell lung cancer (NCI-H187) were performed employing the Resazurin microplate assay (REMA) described by O'Brien and co-workers [24]. The reference substance was doxorubicin. Cytotoxicity against the primate cell line (*Vero*) was tested using the green fluorescent protein (GFP) detection method by Hunt and co-workers [25].

2.5.3. Antibacterial assay

The minimum inhibitory concentrations (MICs) were determined by the dilution method, as described in the M07-A9 of the Clinical and Laboratory Standards Institute [26,27]. Resazurin solution (0.18%) was used as an indicator of microbial growth [24]. MICs were recorded by reading the lowest concentration capable of inhibiting visible growth. The tests were performed in triplicate. Cefepime, kanamycin and vancomycin were used as positive control drugs (Table 4). Six microorganism cultures (*Bacillus cereus* ATCC 11778, *Staphylococcus aureus* ATCC 6538, Methicillin resistant *S. aureus* (MRSA), *Escherichia coli* ATCC 25922, *Pseudomonas aeruginosa* ATCC 27853, and *Salmonella enterica* serovar Typhimurium ATCC 13311 were used. The experiment was performed at the Department of Microbiology, Faculty of Science, Khon Kaen University, Thailand.

3. Results and discussion

Chromatographic separation of extracts from the dried mycelium of the fungus *T. macrosporus* KKU-1NK8 obtained six new oxaphenalenone dimers (**1–6**) and eight known compounds (**7–14**). Their structures were elucidated by spectroscopic methods. Structures of known compounds were also compared with those reported in the literature. They were talaromycesone B (**7**) [8], bacillisporin G (**8**) [12], xenoclauxin (**9**) [10], bacillisporin F (**10a**) and 1-*epi*-bacillisporin F (**10b**) [12], bacillisporins A and B (**11** and **12**) [10,11] and bacillisporins D and E (**13** and **14**) [11].

The IR spectra of **1–6** showed mainly absorption bands of hydroxyl, lactone carbonyl, ketone, and aromatic groups (see supplementary data section).

Compound **1** possessed the molecular formula C$_{25}$H$_{16}$O$_9$, based on the ^{13}C NMR and HRESITOFMS (m/z 483.0684) [M + Na]$^+$ data, implying 18 degrees of unsaturation. Analysis of the ^{1}H and ^{13}C NMR spectroscopic data of **1** (Tables 1 and 2) with the assistance of 2D NMR techniques (COSY, HMQC, HMBC, and NOESY) concluded that the structure of **1** was similar to that of talaromycesone B (**7**) [8], except for an acetyl group at C-9′ being replaced by a hydroxyl group in **1**. The structure of **1** was confirmed by HMBC correlations of H-9′ to C-7, C-8, C-3′b, and C-7′ (Fig. 2). The absolute configuration of **1** was determined
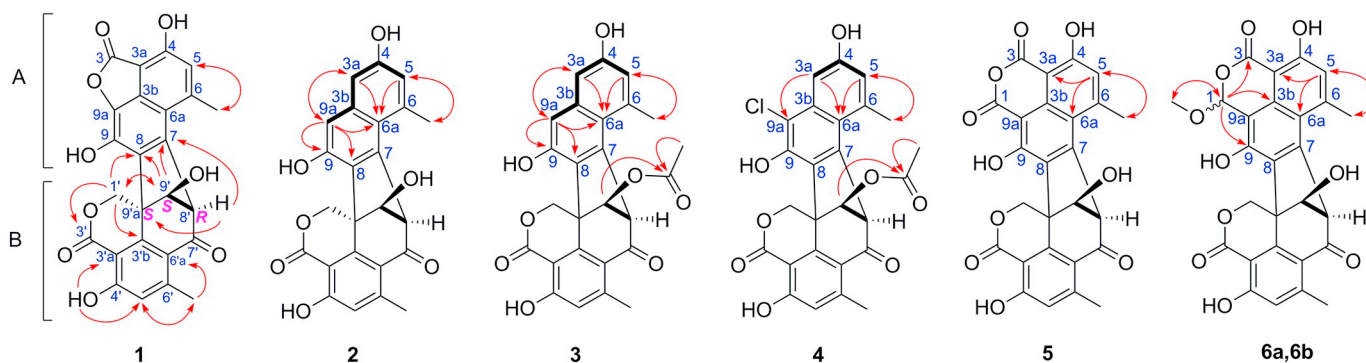
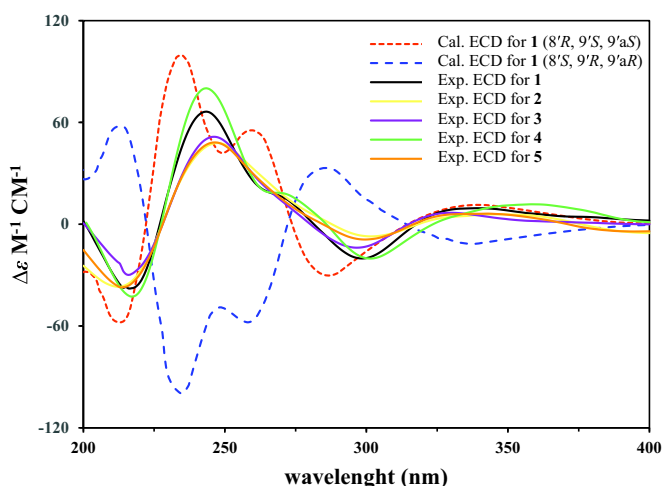Fig. 2. COSY (bold line) and selected HMBC (arrowed line) correlations of **1–6**.

Fig. 3. Comparison of calculated ECD spectrum of **1** and experimental ECD spectra of **1–5** (measured in MeOH).

by comparing its experimental and calculated ECD spectra. The ECD calculations were generated for three chiral centers of two selected possible stereoisomers, 8′*R*, 9′*S*, 9'a*S* and 8′*S*, 9′*R*, 9'a*R* using Gaussian 09 with DFT B3LYP/6-311 + +G (d,p) [21]. The ECD calculated spectrum of **1** generated for the 8′*R*, 9′*S*, 9'a*S* isomer shows a Cotton effect at 215 nm ($\Delta\varepsilon$ − 56.5), 239 ($\Delta\varepsilon$ 65.1), 258 ($\Delta\varepsilon$ 38.2) and 335 ($\Delta\varepsilon$ − 9.1), which agrees well with its experimental ECD spectrum (Fig. 3). From the above evidence, compound **1** was named talaromycesone C and was determined to be a new oxaphenalenone dimer (Fig. 1).

Compound **2** had the molecular formula $C_{24}H_{18}O_7$, based on the ^{13}C NMR and HRESITOFMS (*m/z* 441.0940) [M + Na]$^+$, indicating 16 degrees of unsaturation. The NMR spectroscopic data of **2** (Tables 1 and 2) were similar to those of bacillisporin G (**8**) [12], expect for the absence of an aldehyde group at C-9a and that an acetyl group at C-9′ was replaced by a hydroxyl group. The ^1H NMR spectral data of unit A showed resonances of three aromatic protons at δ 6.62 (s, H-5), 6.65 (s, H-9a), and 6.57 (s, H-3a). The COSY data showed meta-coupling correlations between H-5/H-3a and H-3a/H-9a (Fig. 2). The ^{13}C NMR spectral data of unit A showed three methine aromatic carbons at δ 106.8 (C-3a), 119.2 (C-5) and 110.6 (C-9a), five quaternary aromatic carbons at δ 138.4 (C-3b), 136.4 (C-6), 121.0 (C-6a), 136.5 (C-7) and 130.9 (C-8), two oxy-aromatic carbons at δ 154.1 (C-4) and 152.0 (C-9), and a methyl at δ 24.3 (Me-6). The HMBC correlations of H-3a to C-4, C-5, C-6a and C-9a; H-5 to C-3a, C-4 and C-6a; H-9a to C-3a, C-6a, C-8 and C-9; and Me-6 to C-5, C-6 and C-6a confirmed the structure of unit A (Fig. 2). The NMR spectroscopic data of unit B was similar to that of **1** (Tables 1 and 2). The absolute configuration of **2** was concluded to be

8′*R*, 9′*S*, 9'a*S*, the same as that of **1,** by comparing their ECD spectra (Fig. 3). Thus, compound **2** was determined as a new oxaphenalenone dimer and was named macrosporusone A (Fig. 1).

Compound **3** had the molecular formula $C_{26}H_{20}O_8$, based on the ^{13}C NMR and HRESITOFMS (*m/z* 459.1088) [M-H]$^-$ data, implying 17 degrees of unsaturation. The ^1H and ^{13}C NMR spectroscopic data of **3** (Tables 1 and 2) were similar to those of **2**, except that the hydroxyl group at C-9′ was replaced by an acetoxyl group (δ_C carbonyl ester group 170.6 and methyl group $\delta_{H/C}$ 1.99 (s)/20.8). The complete interpretation of the NMR data of **3** was established as a result of conclusive DEPT, COSY, HMQC, HMBC, and NOESY experiments. The ECD spectrum of **3** showed the same Cotton effect as that of **1** (Fig. 3). Therefor, the new compound **3** was named macrosporusone B (Fig. 1).

Compound **4** had the molecular formula $C_{26}H_{19}ClO_8$, based on the ^{13}C NMR and HRESITOFMS (*m/z* 495.0850) [M + H]$^+$, (*m/z* 497.0812) [M + H + 2]$^+$ data, indicating 17 degrees of unsaturation. The ^1H and ^{13}C NMR spectroscopic data of **4** (Tables 1 and 2) were similar to those of **3**. The major distinction was the presence of a chloride atom at C-9a in **4** (δ_C 113.8) which was confirmed by the HMBC correlation of H-3a to C-9a. The absolute configuration of **4** was determined by comparing its ECD spectrum with that of **1** (Fig. 3). Thus, compound **4**, macrosporusone C, was assigned as a new oxaphenalenone dimer (Fig. 1). It should be noted that this is the first oxaphenalenone dimer reported with a chlorine atom in the molecule.

Compound **5** possesses the molecular formula $C_{26}H_{16}O_{10}$, based on the ^{13}C NMR and HRESITOFMS (*m/z* 487.0669) [M-H]$^-$ data, implying 19 indices of deficiency. The NMR spectroscopic data of **5** (Tables 1 and 2) were similar to those of the isolated xenoclauxin (**9**) [10], except that an acetoxyl group at C-9′ was replaced by a hydroxyl group. The ^1H NMR spectroscopic data of unit A showed resonances of aromatic protons at δ 6.92 (s, H-5), and methyl protons at δ 3.06 (s, Me-6). The NMR spectral data of unit B were similar to those of **1**. The absolute configuration of **5** was assigned to be the same as that of **1** by comparison of its ECD spectrum with that of **1** (Fig. 3). The complete structure of **5** was confirmed by 2D NMR techniques, COSY, HMBC and NOESY. From the above evidence, compound **5,** named macrosporusone D, was determined as a new oxaphenalenone dimer (Fig. 1).

Compound **6** had the molecular formula $C_{27}H_{20}O_{10}$, based on the ^{13}C NMR and HRESITOFMS (*m/z* 503.0975) [M-H]$^-$ data, implying 18 degrees of unsaturation. The NMR spectral data of **6** (Tables 1 and 2) showed a mixture of epimers in the ratio of 1:1. Their resonance signals were similar to those of the mixture of bacillisporin F (**10a**) and 1-*epi*-bacillisporin F (**10b**) [12], except that an acetoxyl group at C-9′ was replaced by a hydroxyl group. The ^1H NMR spectral data of unit A showed a mixture of two sets of aromatic proton signals at δ 6.84/6.77 (s, H-5), methine protons at δ 6.44/6.37 (s, H-1), methoxy protons at δ 3.68/3.56 (s, MeO-1) and methyl protons at δ 2.99/2.97 (s, Me-6). The COSY spectrum showed an allylic coupling between H-5 and Me-6. The

Table 3
Biological activity of compounds **1–3**, **5**, **7–12** and **14**.

Compound	Antimalarial IC$_{50}$ (µM)	Cytotoxicity IC$_{50}$ (µM)			
		KB[a]	MCF-7[b]	NCI-H187[c]	Vero cells[d]
1	Inactive[e]	Inactive	Inactive	Inactive	Inactive
2	Inactive	74.81	104.18	58.28	69.77
3	10.28	56.66	Inactive	16.73	13.74
5	Inactive	Inactive	Inactive	Inactive	37.47
7	Inactive	48.78	64.29	32.72	Inactive
8	8.07	5.86	9.16	7.29	7.50
9	Inactive	Inactive	Inactive	Inactive	93.27
10	Inactive	33.55	Inactive	Inactive	Inactive
11	Inactive	41.50	Inactive	69.44	34.86
12	Inactive	53.47	Inactive	99.43	37.67
14	Inactive	47.02	80.34	77.35	Inactive
Dihydroartemisinin	0.003				
Doxorubicin		1.58	17.44	0.35	
Ellipticine		13.80		9.26	3.45

[a] Human epidermoid carcinoma in the mouth.
[b] Human breast adenocarcinoma.
[c] Human small cell lung cancer.
[d] African green monkey kidney.
[e] > 150 µM.

HMBC spectrum demonstrated the correlations of MeO-1 to C-1, H-1 to C-3, C-3b and C-9; H-5 to C-3, C-3a, C-4 and C-6a; and Me-6 to C-5, C-6 and C-6a (Fig. 2). The NMR spectroscopic data of unit B was similar to that of **1**. The configurations of **6a** and **6b** were determined as 1*R*, 8′*R*, 9′*S*, 9'a*S* and 1*S*, 8′*R*, 9′*S*, 9'a*S* by comparing their experimental ECD spectra with those of bacillisporin F (**10a**) and 1-*epi*-bacillisporin F (**10b**) [12]. Therefore, the compound **6** was deduced to be a mixture of two new oxaphenalenone dimers and they were named macrosporusone E (**6a**) and 1-*epi*-macrosporusone E (**6b**) (Fig. 1).

The biological activities of the isolated compounds were evaluated. Compounds **3** and **8** exhibited antimalarial activity against *P. falciparum* with IC$_{50}$ values of 10.28 and 8.07 µM, respectively. Compound **3** also showed cytotoxicity against NCI-H187 cells with an IC$_{50}$ value of 16.73 µM, while compound **8** showed cytotoxicity against KB, MCF-7 and NCI-H187 cell lines with IC$_{50}$ values of 5.86, 9.16 and 7.29 µM, respectively. Moreover, compounds **2**, **3**, **5**, **8** and **10–12** exhibited cytotoxicity against *Vero* cells with IC$_{50}$ values in the range of 7.50–93.27 µM (Table 3). In addition, compounds **1–3**, **5**, **7–12** and **14** were evaluated for their antibacterial activity against Gram positive and Gram negative bacteria and the results are shown in Table 4. Among them, compounds **11** and **14** showed the most potent antibacterial activity against *B. cereus*, *S. aureus* and MRSA with MICs in the range of 1.94–15.03 µM.

4. Conclusion

The first chemical investigation of the soil fungus *T. macrosporus* afforded six new polyketide-derived oxaphenalenone dimers, talaromycesone C (**1**) and macrosporusones A-E (**2–6**), together with eight known analogs, talaromycesone B (**7**), bacillisporin G (**8**), xenoclauxin (**9**), bacillisporin F (**10**), bacillisporins A and B (**11** and **12**) and bacillisporins D and E. Their absolute configurations were assigned based on ECD spectra analysis. The new talaromycesone C (**1**) is reported as the second analogue of oxaphenalenone dimers with 5-membered lactone ring in unit A. Compounds **3** and **8** exhibited antimalarial activity against *P. falciparum*. Compound **3** showed activity against the NCI-H187 cell line, while compound **8** showed cytotoxic activity against KB, MCF-7 and NCI-H187 cell lines. In addition, compound **11** showed antibacterial activity against MRSA, *S. aureus* and *B. cereus*; the latter had activity close to the standard drugs, vancomycin and kanamycin.

Table 4
Antibacterial activity of compounds **1–3**, **7–8**, **10–12** and **14**.

Compound	Antibacterial activity (MIC, µM)					
	Gram positive bacteria			Gram negative bacteria		
	B. cereus	*S. aureus*	MRSA[a]	*E. coli*	*P. aeruginosa*	*S.* Typhimurium
1	inactive	Inactive	Inactive	Inactive	278.21	278.21
2	153.07	Inactive	Inactive	Inactive	306.14	Inactive
3	139.10	Inactive	Inactive	Inactive	278.19	Inactive
7	254.93	Inactive	Inactive	254.93	254.93	inactive
8	32.78	131.12	Inactive	Inactive	262.24	262.24
10	Inactive	58.60	29.30	Inactive	234.38	234.38
11	1.94	7.75	3.88	248.01	124.01	248.01
12	16.87	33.75	16.87	269.99	269.99	269.99
14	3.76	15.03	7.52	240.56	240.56	Inactive
Vancomycin	1.38	0.35	0.35			
Kanamycin	4.13	2.06		8.26		
Cefepime				0.06	4.16	0.06

[a] Methicillin resistant *S. aureus*.

Conflict of interest

The authors declare no personal, financial and any other form of conflict of interest.

Acknowledgments

Appendix A. Supplementary data

Supplementary data to this article can be found online at https://doi.org/10.1016/j.fitote.2019.03.015.

References

[1] N. Yilmaz, C.M. Visagie, J. Houbraken, J.C. Frisvad, R.A. Samson, Polyphasic taxonomy of the genus *Talaromyces*, Stud. Mycol. 78 (2014) 175–341.

[2] M.M. Zhai, J. Li, C.X. Jiang, Y.P. Shi, D.L. Di, P. Crews, Q.X. Wu, The bioactive secondary metabolites from *Talaromyces* species, Nat. Products Bioprospect. 6 (2016) 1–24.

[3] H. Yang, F. Li, N. Ji, Alkaloids from an algicolous strain of *Talaromyces* sp, Chin. J. Oceanol. Limnol. 34 (2016) 367–371.

[4] J.P. Guo, J.L. Tan, Y.L. Wang, H.Y. Wu, C.P. Zhang, X.M. Niu, W.Z. Pan, X.W. Huang, K.Q. Zhang, Isolation of talathermophilins from the thermophilic fungus *Talaromyces thermophilus* YM3-4, J. Nat. Prod. 74 (2011) 2278–2281.

[5] T. Morino, M. Nishimoto, A. Masuda, T. Nishikiori, S. Saito, NK374200, a novel insecticidal agent from *Talaromyces*, found by physicochemical screening, J. Antibiot. 48 (1995) 1509–1510.

[6] S. Suzuki, T. Hosoe, K. Nozawa, K.I. Kawai, T. Yaguchi, S.I. Udagawa, Antifungal substances against pathogenic fungi, talaroconvolutins, from *Talaromyces convolutus*, J. Nat. Prod. 63 (2000) 768–772.

[7] J.W. He, Z.Q. Mu, H. Gao, G.D. Chen, Q. Zhao, D. Hu, J.Z. Sun, X.X. Li, Y. Li, X.Z. Liu, X.S. Yao, New polyesters from *Talaromyces flavus*, Tetrahedron. 70 (2014) 4425–4430.

[8] B. Wu, B. Ohlendorf, V. Oesker, J. Wiese, S. Malien, R. Schmaljohann, J.F. Imhoff, Acetylcholinesterase inhibitors from a marine fungus *Talaromyces* sp. strain LF458, Mar. Biotechnol. 17 (2015) 110–119.

[9] H. Hayashi, Y. Oka, K. Kai, K. Akiyama, A new meroterpenoid, chrodrimanin C, from YO-2 of *Talaromyces* sp, Biosci. Biotechnol. Biochem. 76 (2012) 745–748.

[10] M. Yamazaki, E. Okuyama, Isolation and structures of oxaphenalenone dimers from *Talaromyces bacillsporus*, Chem. Pharm. Bull. 28 (1980) 3649–3655.

[11] T. Dethoup, L. Manoch, A. Kijjoa, M.S.J. Nascimento, P. Puaparoj, A.M.S. Silva, G. Eaton, W. Herz, Bacillisporins D and E, new oxyphenalenone dimers from *Talaromyces bacillisporus*, Planta Med. 72 (2006) 957–960.

[12] Y. Zang, G. Genta-Jouve, A.E. Escargueil, A.K. Larsen, L. Guedon, B. Nay, S. Prado, Antimicrobial oligophenalenone dimers from the soil fungus *Talaromyces stipitatus*, J. Nat. Prod. 79 (2016) 2991–2996.

[13] Y. Zang, G. Genta-jouve, P. Retailleau, A. Escargueil, S. Mann, B. Nay, S. Prado, Talaroketals A and B, unusual bis(oxaphenalenone) spiro and fused ketals from the soil fungus Talaromyces stipitatus ATCC 10500, Org. Biomol. Chem. 14 (2016) 2691–2697.

[14] S. Natori, F. Sato, S. Udagawa, Anthraquinone metabolites of *Talaromyces avellaneus*, Chem. Pharm. Bull. 13 (1965) 385–386.

[15] R. Bara, A.H. Aly, A. Pretsch, V. Wray, B. Wang, P. Proksch, A. Debbab, Antibiotically active metabolites from *Talaromyces wortmannii*, an endophyte of Aloe vera, J. Antibiot. (Tokyo) 66 (2013) 491–493.

[16] R. Bara, I. Zerfass, A.H. Aly, H. Goldbach-Gecke, V. Raghavan, P. Sass, A. Mándi, V. Wray, P.L. Polavarapu, A. Pretsch, W. Lin, T. Kurtán, A. Debbab, H. Brötz-Oesterhelt, P. Proksch, Atropisomeric dihydroanthracenones as inhibitors of multiresistant staphylococcus aureus, J. Med. Chem. 56 (2013) 3257–3272.

[17] H. Li, H. Huang, C. Shao, H. Huang, J. Jiang, X. Zhu, Y. Liu, L. Liu, Y. Lu, M. Li, Y. Lin, Z. She, Cytotoxic norsesquiterpene peroxides from the endophytic fungus *Talaromyces flavus* isolated from the mangrove plant *Sonneratia apetala*, J. Nat. Prod. 74 (2011) 1230–1235.

[18] K.K. Chexa, C. Tamm, 186. Gilmaniellin and dechlorogilmaniellin, two novel dimeric oxaphenalenones, Helv. Chim. Acta. 62 (1979) 1785–1803.

[19] Z. Guo, C. Shao, Z. She, X. Cai, F. Liu, L.L.P. Vrijimoed, Y. Lin, H. Kong, ^{1}H and ^{13}C NMR assignments for two oxaphenalenones bacillosporin C and D from the mangrove endophytic fungus SBE-14, Magn. Reson. Chem. 45 (2007) 439–441.

[20] P. Cao, J. Yang, C. Miao, Y. Yan, X. Li, L. Zhao, S. Huang, New duclauxamide from *Penicillium manginii* YIM PH30375 and structure revision of the duclauxin family, Org. Lett. 17 (2015) 1146–1149.

[21] M.J. Frisch, G.W. Trucks, H.B. Schlegel, G.E. Scuseria, M.A. Robb, J.R. Cheeseman, G. Scalmani, Barone, V., B. Mennucci, G.A. Petersson, H. Nakatsuji, M. Caricato, X. Li, H.P. Hratchian, A.F. Izmaylov, J. Bloino, G. Zheng, J.L. Sonnenberg, M. Hada, M. Ehara, K. Toyota, R. Fukuda, J. Hasegawa, M. Ishida, T. Nakajima, Y. Honda, O. Kitao, H. Nakai, T. Vreven, J.A. Montgomery, J.E. Peralta, F. Ogliaro, M. Bearpark, J.J. Heyd, E. Brothers, K.N. Kudin, V.N. Staroverov, R. Kobayashi, J. Normand, K. Raghavachari, A. Rendell, J.C. Burant, S.S. Iyengar, J. Tomasi, M. Cossi, N. Rega, J. M. Millam, M. Klene, J.E. Knox, J.B. Cross, V. Bakken, C. Adamo, J. Jaramillo, R. Gomperts, R.E. Stratmann, O. Yazyev, A.J. Austin, R. Cammi, C. Pomelli, J.W. Ochterski, R.L. Martin, K. Morokuma, V.G. Zakrzewski, G.A Voth, P. Salvador, J.J. Dannenberg, S. Dapprich, A.D. Daniels, Ö. Farkas, J.B. Foresman, J.V. Ortiz, J. Cioslowski, D.J. Fox, Gaussian09, Inc., Wallingford CT (2010).

[22] W. Trager, J.B. Jensen, Human malaria parasites in continuous culture, J. Parasitol. 91 (2005) 484–486.

[23] R.E. Desjardins, C.J. Canfield, J.D. Haynes, J.D. Chulay, Quantitative assessment of antimalarial activity in vitro by a semiautomated microdilution technique, Antimicrob. Agents Chemother. 16 (1979) 710–718.

[24] J. O'Brien, I. Wilson, T. Orton, F. Pognan, Investigation of the Alamar Blue (resazurin) fluorescent dye for the assessment of mammalian cell cytotoxicity, Eur. J. Biochem. 267 (2000) 5421–5426.

[25] L. Hunt, M. Jordan, M. De Jesus, F.M. Wurm, GFP-expressing mammalian cells for fast, sensitive, noninvasive cell growth assessment in a kinetic mode, Biotechnol. Bioeng. 65 (1999) 201–205.

[26] Clinical and Laboratory Standards Institute, Methods for Dilution Antimicrobial Susceptibility Tests for Bacteria that Grow Aerobically. Approved Standard 9th Ed. Document M07-A9, CLSI, Wayne, PA, USA, 2012.

[27] M. Balouiri, M. Sadiki, S.K. Ibnsouda, Methods for in vitro evaluating antimicrobial activity: a review, J. Pharm. Anal. 6 (2016) 71–79.

Antimalarial polyoxygenated cyclohexene derivatives from the roots of *Uvaria cherrevensis*

Ratsami Lekphrom, Kwanjai Kanokmedhakul, Florian Schevenels, Somdej Kanokmedhakul*

Natural Products Research Unit, Department of Chemistry and Center of excellence for Innovation in Chemistry, Faculty of Science, Khon Kaen University, Khon Kaen 40002, Thailand

ARTICLE INFO

ABSTRACT

Three new polyoxygenated cyclohexene derivatives named cherrevenisyls A and B (**1** and **2**), and ellipeiopsol E (**3**), along with fifteen known compounds, were isolated from the roots of *Uvaria cherrevensis*. Their structures were determined by spectroscopic methods including 2D NMR techniques and mass spectrometry. The absolute configurations of **1** and **2** were assigned. Compounds **1**, **2** and **5** showed antimalarial activity against *Plasmodium falciparum* with IC_{50} ranging from 3.34–7.34 μg/mL. Compounds **5–18** exhibited cytotoxicity against three cancer cell lines (KB, MCF-7 and NCI-H187) with IC_{50} values in ranging from 1.26–49.03 μg/mL.

1. Introduction

Uvaria cherrevensis (Pierre ex Finet & Gagnep.) L. L. Zhou, Y. C. F. S (Annonaceae) is a shrub that reaches up to 1.5 m in height and is found in deciduous forests throughout Thailand. Its synonym is *Ellipeiopsis cherrevensis* (Pierre ex Finet & Gagnep.) R. E. Fr and is known as "Nom maeo pa", "Phi phuan noi", and "Phi khao" in Thai [1]. A water decoction of its roots is used as traditional medicine to treat urinary disorders [2]. The genus *Uvaria* is known to be a rich source of polyoxygenated cyclohexene derivatives [3–8]. Previous investigations of the aerial parts of *E. Cherrevensis* (*U. cherrevensis*) led to the isolation of several polyoxygenated cyclohexene derivatives [9,10], as well as a cytotoxic C-benzoylated chalcone, flavonoids and alkaloids [10]. Recently, Auranwiwat et al. reported 2-phenylnaphthalenes and a cyclohexene from the stems and roots extracts of this plant [11]. In our continuing search for bioactive constituents from Thai plants, we noted that the roots extracts (EtOAc and MeOH) of *U. cherrevensis* showed cytotoxicity against KB cell lines with an IC_{50} value of 12.6 μg/mL. We report herein the isolation, the structural characterization, and bioactivities of three new polyoxygenated cyclohexene derivatives (**1–3**), together with fifteen known compounds (**4–18**). Among them, compounds **7**, **8** and **14** are reported for the first time from the genus *Uvaria*.

2. Experimental

2.1. General experimental procedures

Melting points were determined using a Gallenkamp melting point

apparatus and were uncorrected. Optical rotations were obtained using a JASCO DIP-1000 digital polarimeter. IR spectra were taken on a Perkin-Elmer Spectrum One spectrophotometer. NMR spectra were recorded in $CDCl_3$ and CD_3OD on a Varian Mercury Plus 400 spectrometer, using residual $CHCl_3$ and CH_3OH as an internal standard. HRMS spectra were obtained using a Micromass LCT mass spectrometer, and the lock mass calibration was applied for the determination of accurate masses. Column chromatography and preparative TLC were carried out on silica gel 60 (230–400 mesh) and PF_{254}, respectively.

2.2. Plant materials

The roots of *U. cherrevensis* were collected from Ban Na-khum Village, Ubonratana District, Khon Kaen Province, Thailand, in July 2011 and were identified by Prof. P. Chantaranothai, Department of Biology, Khon Kaen University, Thailand, where a voucher specimen S. Kanokmedhakul 19 was deposited.

2.3. Extraction and isolation

Air-dried roots of *U. cherrevensis* (1.1 kg) were ground to powder and then extracted successively with EtOAc (3 L × 3) and MeOH (3 L × 3). Removal of solvents from each extract under reduced pressure gave the crude EtOAc (57.5 g, 5.23%) and MeOH (65.9 g, 5.99%) extracts.

The EtOAc extract (55.0 g) was separated on silica gel column chromatography (CC), eluting with a gradient system of *n*-hexane-EtOAc (90:10 to 0:100 v/v) and then EtOAc-MeOH (100:0 to 0:100 v/v) to give six fractions, EF_1-EF_6. Evaporation of EF_1 gave compound **5** as a

---

colourless oil (746.2 mg). Fraction EF$_2$ was purified by silica gel flash column chromatography (FCC), eluting with a gradient system of *n*-hexane-EtOAc (90:10 to 0:100 v/v) and then EtOAc-MeOH (100:0 to 0:100 v/v) to give ten subfractions, EF$_{2.1}$-EF$_{2.10}$. Subfraction EF$_{2.5}$ was purified on silica gel CC, eluting with a gradient system of *n*-hexane-EtOAc (80:20 to 0:100 v/v) to yield compound **6** as a colourless oil (269.8 mg). Subfraction EF$_{2.6}$ was separated by silica gel FCC, eluting with a gradient system of *n*-hexane-EtOAc to yield compound **7** as a colourless oil (190.0 mg) and an additional amount of **5** (36.3 mg). Subfraction EF$_{2.8}$ was chromatographed on silica gel FCC, eluting with a gradient system of *n*-hexane-EtOAc (80:20 to 0:100 v/v) to give compound **8** as a colourless solid (26.4 mg) and compound **9** as a colourless oil (17.3 mg). Subfraction HF$_{2.9}$ was purified on silica gel CC, gradually eluting with *n*-hexane-EtOAc (80:20 to 0:100 v/v) and EtOAc-MeOH (80:20 to 0:100 v/v) to give five subfractions, EF$_{2.9.1}$-EF$_{2.9.5}$. Subfraction MF$_{2.9.2}$ was subjected to silica gel CC, using the same solvent system as that of subfraction EF$_{2.8}$ above to give compound **10** as a colourless oil (55.6 mg). Subfraction EF$_{2.9.3}$ was purified by silica gel CC eluting with a gradient system of *n*-hexane-CH$_2$Cl$_2$ (80:30 to 0:100 v/v) to yield compounds **1** and **2** as white amorphous solids (49.0 and 25.0 mg). Subfraction EF$_{2.9.5}$ was further purified by silica gel FCC, using the same solvent system as that of subfraction EF$_{2.8}$ to give compounds **11** and **12** as two yellow oils (16.4 and 55.2 mg). Fraction EF$_3$ was chromatographed on silica gel CC and eluted with a gradient of *n*-hexane–EtOAc (90:10 to 0:100 v/v) to give nine subfractions, EF$_{3.1}$-EF$_{3.9}$. Subfraction EF$_{3.2}$ was subjected to silica gel CC, eluting with a gradient system of *n*-hexane-CH$_2$Cl$_2$ (70:30 to 0:100 v/v) to yield compound **13** as a white solid (11.5 mg). Subfraction EF$_{3.3}$ was separated by silica gel CC, using the same solvent system as that of subfraction EF$_{3.2}$ to yield compound **14** as a colourless amorphous powder (11.2 mg) and compound **15** as colourless crystals (37.1 mg). Subfraction EF$_{3.5}$ was separated by silica gel CC, eluting with a gradient system of CH$_2$Cl$_2$-EtOAc (100:0 to 0:100 v/v) to give compound **16** as orange needles (80.5 mg) and compound **17** as colourless needles (44.6 mg). Subfraction EF$_{3.9}$ was re-crystallized from *n*-hexane-EtOAc (30:70) to yield **3** as a pale yellow amorphous solid (40.2 mg). Fraction EF$_4$ was separated by silica gel CC, eluting with a gradient system of CH$_2$Cl$_2$-MeOH (100:0 to 0:100 v/v) to give compound **4** as a white amorphous solid (20.2 mg). Fraction EF$_6$ was separated by silica gel CC, eluting with a gradient system of CH$_2$Cl$_2$-MeOH (80:20 to 0:100 v/v) to give compound **18** as a yellow solid (120.5 mg).

The MeOH extract (60.0 g) was separated on silica gel CC, eluting with a gradient system of *n*-hexane-EtOAc (60:40 to 0:100 v/v) and then EtOAc-MeOH (80:20 to 0:100 v/v) to give seven fractions, MF$_1$–MF$_7$. Fraction MF$_2$ was separated by CC, eluting with a gradient system of *n*-hexane-EtOAc (60:40 to 0:100 v/v) to give four subfractions, MF$_{4.1}$-MF$_{4.4}$. Subfraction MF$_{4.1}$ afforded an additional amount of **14** (11.7 mg). Subfraction MF$_{4.2}$ was purified by preparative TLC, using *n*-hexane-CH$_2$Cl$_2$-EtOAc (20–10:70) as eluent to yield an additional amount of **11** (R_f = 0.42, 9.3 mg) and **12** (R_f = 0.40, 16.7 mg). Fraction MF$_3$ was further subjected to silica gel FCC, eluting with a gradient system of *n*-hexane-EtOAc (50:50 to 0:100 v/v) and then MeOH to give an additional amount of **14** (11.9 mg). Fraction EF$_5$ was separated by silica gel CC, eluting with a gradient system of CH$_2$Cl$_2$-MeOH (80:20 to 0:100 v/v) to give an additional amount of **17** (20.2 mg).

2.3.1. Cherrevenisyl A (1)

White amorphous solid; $[\alpha]_D^{26}$ + 94.4 (*c* 0.1, CHCl$_3$); UV (CHCl$_3$) λ_{max} (log ε) 268 (4.25) 331 (4.23); IR (KBr) ν_{max} 2927, 1717, 1601, 1491, 707 cm^{-1}; ^{1}H and ^{13}C NMR, see Table 1; HRESIMS *m/z* 745.2269 [M + Na]$^+$ (calcd for C$_{41}$H$_{38}$O$_{12}$Na 745.2261).

2.3.2. Cherrevenisyl B (2)

White amorphous solid; $[\alpha]_D^{26}$ + 9.2 (*c* 0.1, CHCl$_3$); UV (MeOH) λ_{max} (log ε) 235 (4.5); ECD (*c* 0.09 mM, MeOH) λ_{max} ($\Delta\varepsilon$): 206 (+ 80.35), 235 (− 26.49); IR (KBr) ν_{max} 2925, 1715, 1601, 1561,

712 cm^{-1}; ^{1}H and ^{13}C NMR see Table 1; HRESIMS *m/z* 683.2109 [M + Na]$^+$ (calcd for C$_{36}$H$_{36}$O$_{12}$Na 683.2104).

2.3.3. Ellipeiopsol E (3)

Pale yellow amorphous solid; $[\alpha]_D^{26}$ − 165.0 (*c* 0.1, CH$_3$OH; IR (KBr) ν_{max} 3372, 2971, 2938, 1719, 1601, 1583, 714 cm^{-1}; ^{1}H and ^{13}C NMR, see Table 2; HRESIMS *m/z* 387.1062 [M + Na]$^+$ (calcd for C$_{18}$H$_{20}$O$_8$Na 387.1056).

2.4. Antimalarial assay

Antiplasmodial activity was evaluated against the parasite *Plasmodium falciparum* (K1, multidrug resistant strain), using the method of Trager and Jensen [23]. Quantitative assessment of antimalarial activity *in vitro* was determined by means of the microculture radioisotope technique, based upon the method described by Desjardins et al. [24]. The inhibitory concentration (IC$_{50}$) represents the concentration which causes 50% reduction in parasite growth as indicated by the *in vitro* incorporation of [^{3}H]-hypoxanthine by *P. falciparum*. The standard compound was dihydroartemisinin.

Table 1
^{1}H and ^{13}C NMR spectral data (δ, ppm) for compounds **1** and **2** (CDCl$_3$).

Position	1		2	
	δ_H (*J* in Hz)	δ_C, type	δ_H (*J* in Hz)	δ_C, type
Ring A				
1		134.3, C		134.3, C
2	5.79 d (9.2)	67.6, CH	5.56 d (9.2)	67.6, CH
3	5.27 dd (9.2,7.6)	74.0, CH	5.06 dd (9.2, 7.2)	73.2, CH
4	3.34 t (7.6)	31.9, CH	3.30 br m	31.6, CH
5	3.17 brm	39.3, CH	3.10 m	39.1, CH
6	6.11 brs	128.0, C	6.07 brs	128.2, C
1-CH$_2$OBz				
1		129.8, C		129.6, C
2,6	8.05 d (7.2)	129.7, C	8.01 d (7.2)	129.5, CH
3,5	7.48 d (7.2)	128.5, CH	7.45 m	128.6, CH
4	7.5 m	133.1, CH	7.58 m	133.4, CH
CO		166.0, C		166.4, C
CH$_2$	4.79 ABq (12.8)	64.3, CH$_2$	4.73 *br s*	64.4, CH$_2$
2-OAc	1.97 s	170.2, C; 20.1, CH$_3$	2.01 s	170.7, C; 20.5, CH$_3$
3-OAc	1.92 s	170.3, C; 20.7, CH$_3$	2.01 s	170.6, C; 20.5, CH$_3$
Ring B				
1′		46.5, C		46.4, C
2′	5.17 d (3.2)	74.4, CH	5.10 d (2.8)	74.6, CH
3′	4.53 t (3.2)	78.0, CH	4.51 t (2.8)	78.2, CH
4′	3.02 dd (6.8, 3.2)	35.2, CH	3.01 dd (6.6, 2.8)	35.0, CH
5′	6.47 dd (8.0, 6.8)	129.8, CH	6.40 dd (8.0,6.6)	130.7, CH
6′	5.86 d (8.0)	132.6, CH	5.83 d (8.0)	132.6, CH
1′-CH$_2$OBz				
1		129.5, C		129.3, C
2,6	8.00 d (7.2)	129.6, CH	7.95 d (7.2)	129.5, CH
3,5	7.49 (m)	128.6, CH	7.42 m	128.5, CH
4	7.60 (m)	133.5, CH	7.58 m	133.3, CH
CO		166.1, C		166.3, C
CH$_2$	4.69 d (11.6)	61.2, CH$_2$	4.64 d (12.0)	61.2, CH$_2$
	4.56 d (11.6)		4.54 d (12.0)	
2′-OAc	2.03 s	169.7, C; 20.8, CH$_3$	2.03 s	170.4, C; 20.7, CH$_3$
3′-OBz				
1		129.3, C		
2,6	7.98 d (7.2)	129.6, CH		
3,5	7.46 m	128.4, CH		
4	7.57 m	133.4, CH		
CO		165.2, C		
3′-OAc			2.06 s	170.9, C; 20.4, CH$_3$

Table 2
^{1}H and ^{13}C NMR spectral data (δ, ppm) for compound **3** (DMSO).

Position	3	
	δ_H (J in Hz)	δ_C, type
1		74.3, C
2	5.28 d (8.0)	72.2, CH
3	5.48 m	71.1, CH
4	4.08 br s	68.9, CH
5	5.82 dd (10.0, 4.4)	130.6, CH
6	5.58 d (10.0)	126.3, CH
7	4.32 d (11.0), 4.12 d (11.0)	66.8, CH$_2$
CO		166.1, C
1′		130.3, C
2′,6′	8.02 d (8.0)	129.9, CH
3′,5′	7.50 t (7.6)	133.6, CH
4	7.62 t (7.6)	129.0, CH
2-OAc	2.0 s	170.5, C; 21.1, CH$_3$
3-OAc	1.98 s	170.5, C; 21.0, CH$_3$

2.5. Antimycobacterial assay

The antimycobacterial activity was assessed against *Mycobacterium tuberculosis* H37Ra using the Microplate Alamar Blue Assay (MABA) [25]. Standard drugs, isoniazid and kanamycin sulfate, were used as the reference compounds.

2.6. Cytotoxicity assay

The cytotoxicity assays against human epidermoid carcinoma (KB), human small cell lung cancer (NCI-H187) and human breast cancer (MCF-7) cell lines were performed employing the colorimetric method as described by Skehan et al. [26]. The reference substance was ellipticine.
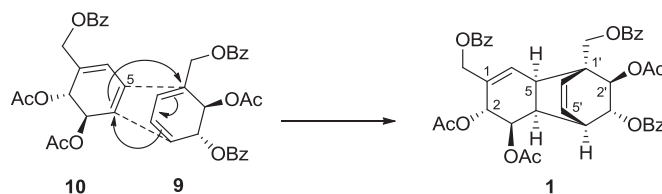
Fig. 2. Proposed mechanism of formation of **1** from **9** and **10** by Diels-Alder reaction.

3. Results and discussion

Structures of isolated compounds were identified by physical and spectroscopic data measurements (IR, ^{1}H and ^{13}C NMR, 2D NMR) as well as mass spectrometry. Obtained data of known compounds were also compared with published values. Fifteen compounds were identified as (−)-uvaribonol F (**4**) [11], benzoylbenzoate (**5**) [12], 2-methoxybenzyl benzoate (**6**) [12], *endo*-5-methoxy-3-patchoulene (**7**) [13], (6S)-patchoulan-4-ene-6-ol (**8**) [14], (−)-1,6-desoxytingtanoxide (**9**) [3], (−)-1,6-desoxysenepoxide (**10**) [3], tingtanoxide (**11**) [3], α-senepoxide (**12**) [3], uvarigranol B (**13**) [15], curcuminol F (**14**) [16], ellipeiopsol D (**15**) [10], 2′,4′-dihydroxy-3′-(2-hydroxybenzyl-6′)-methoxychalcone (**16**) [10], chamanetin 5-methyl ether (**17**) [17] and (±)-dichamanetin 5-methylether (**18**) [18] (Fig. 1).

Compound **1** was obtained as a white amorphous solid. The molecular formula, $C_{41}H_{38}O_{12}$, was deduced from the HRESIMS (*m/z* 745.2269 [M + Na]$^+$), implying 23 degrees of unsaturation. The IR spectrum indicated bands for a mono-substituted benzene (1601, 1491 and 707 cm^{-1}) and an ester carbonyl group (1717 cm^{-1}). The ^{1}H and ^{13}C NMR spectroscopic data of **1** (Table 1) showed resonances corresponding to 15 protons of three mono-substituted aromatic benzene rings, together with resonances for two sets of oxymethylene protons at δ_H 4.79 (2H, ABq, J = 12.8 Hz, H-7), and δ 4.56 and 4.69 (both d, J = 11.6 Hz, H-7′) revealing two sets of benzoyl methylene (−CH$_2$OCOPh) groups and a benzoyl (−OCOPh) group in the molecule. The resonances at $\delta_{H/C}$ 5.86 (d, J = 8.0 Hz, H-6′)/132.6 and 6.47 (dd, J = 8.0, 6.8 Hz, H-5′)/129.8, and $\delta_{H/C}$ 6.11 (brs, H-6)/128.0 were

Fig. 1. Structures of isolated compounds.
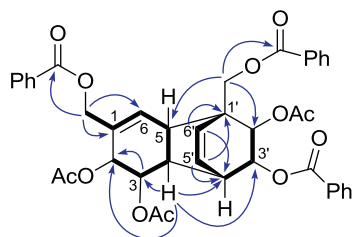
Fig. 3. COSY (bold line) and Selected HMBC (H → C) correlations for **1**.
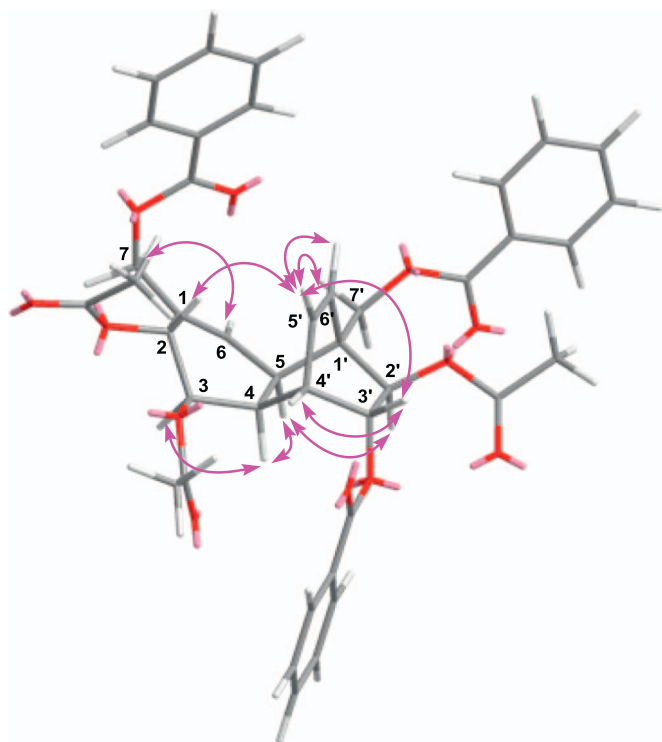
Fig. 4. NOESY correlations for **1**, energy minimized using MM2.

attributed to a di-substituted and a tri-substituted double bond, respectively. Analysis of the ^{1}H and ^{13}C NMR spectroscopic data and 2D NMR spectra (COSY, HSQC, HMBC and NOESY), combined with MS, led us to conclude that **1** contained two cyclohexene moieties of (−)-1,6-deoxyxysenepoxide (**9**) and (−)-1,6-desoxytingtanoxide (**10**), which was the *endo*-addition product from their Diels-Alder reaction [19] (Fig. 2). The COSY correlations of H-2/H-3/H-5/H-6/H-7 (allylic coupling) and H-2′/H-3′/H-4′/H-5′/H-6′, revealing the partial cyclohexene units in the molecule as highlighted in Fig. 3. Key HMBC correlations showed two linked cyclohexene moieties from H-4 to C-3′ and C-4′; as well as oxymethylene protons of 1′-CH$_2$OBz to C-5, C-1′, and C-2′; and H-2′ to C-5 (Fig. 3). The relative stereochemistry of **1** was determined by analysis of coupling constants and from NOESY experiment (Fig. 4). A *trans*-diaxial relationship between H-2 and H-3 was indicated by the vicinal coupling constant $J_{2,3}$ of 9.2 Hz. In contrast, the coupling constant, $J_{2′,3′}$ of H-2′ and H-3′ is 3.2 Hz corresponding to axial and equatorial orientations. The NOESY correlation between H-2 and H-5′, H-3′ and H-5′ and the structural constraints of the bridged ring structure indicated that H-2′ and H-3′ were in axial and equatorial orientations, respectively. On the basis of the above data, the relative stereochemistry of **1** was assigned as 2R,3R. Since compound **1** was deduced from Diels-Alder reaction of compounds **9** and **10**, which both have been clearly reported for their absolute configurations as 2R,3R [3]. Therefore, **1** would retain the same absolute configuration as 2R,3R and 2′R,3′R. Thus **1** was assigned to a new dimer polyoxygenated cyclohexene, which was named cherrevenisyl A.

Compound **2** was obtained as a white amorphous solid. It has a molecular formula of C$_{36}$H$_{36}$O$_{12}$ based on the HRESIMS (*m/z* 683.2109 [M + Na]$^+$), implying 19 degrees of unsaturation. The IR spectrum showed similar absorption bands to those of **1**. Analysis of the ^{1}H and ^{13}C NMR spectroscopic data (Table 1) with 2D NMR techniques (COSY, HSQC, HMBC, and NOESY) indicated that **2** has a similar core structure to **1**, except for the benzoyl group at C-3′ which was replaced by an acetyl group (δ_H 2.06, δ_C 20.4, 170.9). Compound **2** contained two cyclohexene moieties of (−)-1,6-desoxytingtanoxide (**10**), which was also the *endo*-addition adduct from their Diels-Alder reaction [19] (Fig. 2). The relative configuration of **2** was deduced from the coupling constants and NOESY spectrum as well as the comparison with those of **1**, indicating that compound **2** possesses the same relative configuration as **1**. The absolute configuration of **2** would be 2R,3R and 2′R,3′R as described for compound **1** above. Thus, the structure of **2** was deduced as a new dimer polyoxygenated cyclohexene, which was named cherrevenisyl B.

Compound **3** was obtained as a pale yellow amorphous solid, and its molecular formula C$_{18}$H$_{20}$O$_8$ was deduced from HRESIMS (*m/z* 387.1062 [M + Na]$^+$), implying nine degrees of unsaturation. The IR spectrum showed absorption bands for a hydroxy group (3372 cm^{-1}), monosubstituted aromatic rings (1601, 1583 and 714 cm^{-1}), and ester carbonyl groups (1719 cm^{-1}). The ^{1}H NMR spectroscopic data of **3** (Table 2) showed resonances for a mono-substituted benzene of benzoyl methyl group, three oxymethines (δ_H 5.28, H-2; 5.48, H-3; 4.08, H-4), an oxymethylene (δ_H 4.12, 4.32, H$_2$-7), and two olefinic protons (δ_H 5.82, H-5; 5.58, H-6), together with two acetoxy groups. In addition, the ^{13}C NMR spectroscopic data (Table 2) showed 18 carbon resonances including five oxygenated sp^3 carbons (δ_C 66.8, 68.9, 71.1, 72.2, and 74.3), two olefinic carbons (δ_C 126.3 and 130.6), and two acetate groups. Analysis of the COSY and HMQC spectra revealed the partial connections (bold line) of H-2/H-3/H-4/H-5/H-6 which were further connected based on long-range HMBC correlations (Fig. 5a). The HMBC spectrum of **3** revealed long range correlations of the oxymethylene protons at δ_H 4.12, 4.32 (H$_2$-7) to the oxymethine carbon at δ_C 72.2 (C-2) and the quaternary oxygenated carbon at δ 74.3 (C-1). Furthermore, significant correlations of the oxymethine protons at δ_H 5.28 (H-2) and 5.48 (H-3) to the carbonyl carbons at δ_C 170.5 proved the location of each acetate group at C-2 and C-3, respectively. The H$_2$-7 oxymethylene protons and the aromatic protons at δ_H 8.02 (H-2′,6′) correlated to the ester carbonyl carbon at δ_C 166.1 which indicated the presence of the benzoyl group at C-7. An additional hydroxy group was placed at the C-1 position based on the molecular formula and the ^{13}C NMR chemical shift of C-1. The location of the secondary hydroxy group at the C-4 was indicated by COSY correlations and also supported by the chemical shift of H-4. The relative stereochemistry of compound **3** was further confirmed by the NOESY spectrum (Fig. 5b). H-3 showed a through-space correlation with H-4. The same type of interaction was observed between H-2 and H-7. 1D and 2D NMR spectroscopic analyses indicated that compound **3** has the same structure skeleton as an unnamed synthetic intermediate of crotepoxide [20], which was later isolated as a natural product named artabotrol A from the fungus *Artabotrys madagascariensis* [21]. However, the absolute configurations of carbons C-1 and C-4 of **3** were opposite to those reported for artabotrol A. Besides,
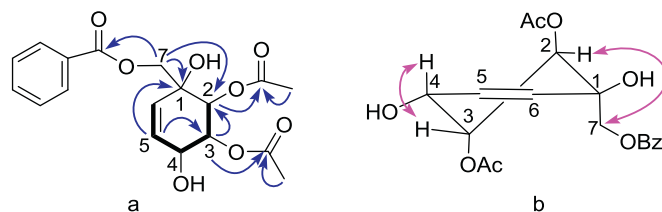

Fig. 5. a) ^{1}H,^{1}H COSY (bold line) and selected HMBC (H → C) correlations of **3**. b) Key NOESY correlation of **3**.

Table 3
Biological activities of the isolated compounds.

Compound	Antimalarial (IC$_{50}$, µg/mL)	AntiTB (MIC, µg/mL)	Cytotoxicity (IC$_{50}$, µg/mL)		
			KB[a]	MCF-7[b]	NCI-H187[c]
1	7.34	Inactive	Inactive	Inactive	13.03
2	3.97	Inactive	Inactive	Inactive	Inactive
3	Inactive	Inactive	46.63	Inactive	Inactive
4	Inactive	Inactive	Inactive	Inactive	Inactive
5	3.34	50.0	17.84	Inactive	3.46
6	Inactive	Inactive	Inactive	Inactive	Inactive
7	Inactive	Inactive	49.03	Inactive	7.01
8	Inactive	Inactive	22.93	23.99	21.34
9	Inactive	Inactive	47.75	Inactive	2.84
10	Inactive	Inactive	48.84	29.83	4.04
11	Inactive	Inactive	11.19	10.34	24.64
12	Inactive	Inactive	10.58	14.15	Inactive
13	Inactive	Inactive	Inactive	Inactive	Inactive
14	Inactive	Inactive	41.51	Inactive	10.72
15	Inactive	Inactive	11.27	21.48	Inactive
16	Inactive	Inactive	1.26	2.08	3.98
17	Inactive	Inactive	42.37	27.82	8.17
18	Inactive	Inactive	11.36	6.45	12.81
Dihydroartemisinin	0.001				
Isoniazid		0.05			
Kanamycin sulfate		2.5			
Ellipticine			0.36	0.26	0.32

[a] Human epidermoid carcinoma in the mouth.
[b] Human breast adenocarcinoma.
[c] Human small cell lung cancer.

the sign of optical rotation for **3** (-165.0°) was also opposite to that of artabotral A ($+89.4^{\circ}$). Thus, compound **3** was determined as a new polyoxygenated cyclohexene, which was named ellipeiopsol E.

The results of bioactivity tests on the isolated compounds are shown in Table 3. Compounds **1**, **2** and **5** exhibited antimalarial activity against *Plasmodium falciparum* with IC$_{50}$ 7.34, 3.97 and 3.34 µg/mL, respectively. Only compound **5** showed a weak antimycobacterial activity against *Mycobacterium tuberculosis* with MIC 50.0 µg/mL. Most of the isolated compounds, with the exception of **2**, **6** and **13**, showed cytotoxicity against three human cancer cell lines (KB, MCF-7 and NCI-H187) with IC$_{50}$ values ranging from 1.26–48.84 µg/mL. It should be noted that **2** is the most potent antimalarial agent which is not cytotoxic against the three cancer cell lines tested. Compound **1** also showed cytotoxicity against the NCI-H187 cell line, suggesting that the presence of the benzoyl and acetyl groups on structures **1** and **2** plays a role in these activities. On the other hand, 2-methoxybenzylbenzoate (**6**), bearing a methoxy group at C-2, was inactive when compared with benzylbenzoate (**5**). Moreover, compound **5** was reported to have cytotoxicities against other cancer cells. [22]. However, all compounds were not test for their cytotoxicity against a non-cancerous cell line.

Conflict of interest

All the authors declare that there is no conflict of interest concerning this work.

Acknowledgments

Appendix A. Supplementary data

Spectroscopic data of compounds 1-3 can be found online at https://doi.org/10.1016/j.fitote.2018.01.018.

References

[1] T. Smitinand, Thai Plant Names, Revised Edition, Prachachon Co. Limited, Bangkok, 2001, p. 357.
[2] Mahidol University Foundation, Kok Ya E-San, Amarin Printing, Bangkok, 2000, pp. 103.
[3] M. Kodpinid, C. Sadavongvivad, C. Thebtaranonth, Y. Thebtaranonth, Structures of β- senepoxide, tingtanoxide, and their diene precursors. Constituents of *Uvaria ferruginea*, Tetrahedron Lett. 24 (1983) 2019–2022.
[4] S.D. Jolad, J.J. Hoffmann, K.H. Schram, J.R. Cole, M.S. Tempesta, R.B. Bates, Structures of zeylenol and zeylena, constituents of *Uvaria zeylanica* (Annonaceae), J. Org. Chem. 46 (1981) 4267–4272.
[5] V.S. Parmar, O.D. Tyagi, A. Malhotra, S.K. Singh, K.S. Bisht, R. Jain, Novel constituents of *Uvaria* species, Nat. Prod. Rep. 11 (1994) 219–224.
[6] Y.H. Liao, Z.M. Zou, J. Guo, L.Z. Xu, M. Zhu, S.L. Yang, Five polyoxygenated cyclohexenes from *Uvaria grandiflora*, J. Chin. Pharm. Sci. 9 (2000) 170–173.
[7] X.P. Pan, R.-Y. Chen, D.Q. Yu, Polyoxygenated cyclohexenes from *Uvaria grandiflora*, Phytochemistry 47 (1988) 1063–1066.
[8] G.X. Zhou, Y.J. Zhang, R.Y. Chen, D.Q. Yu, Three polyoxygenated cyclohexenes from *Uvaria calamistrata*, J. Asian Nat. Prod. Res. 12 (2010) 696–701.
[9] A. Kijjoa, J. Bessa, M.M.M. Pinto, C. Anatachoke, A.M.S. Solva, G. Eaton, W. Herz, Polyoxygenated cyclohexene derivatives from *Ellipeiopsis cherrevensis*, Phytochemistry 59 (2002) 543–549.
[10] L. Wirasathien, T. Pengsuparp, M. Moriysu, K. Kawanishi, R. Suttisri, Cytotoxic C-benzylated chalcone and other constituents of *Ellipeiopsis cherrevensis*, Arch. Pharm. Res. 29 (2006) 497–502.
[11] C. Auranwiwat, P. Wongsomboon, T. Thaima, R. Rattanajak, S. Kamchonwongpaisan, A.C. Willis, W. Lie, S.G. Pyne, T. Limtharakul (nee Ritthiwigrom), 2-Phenylnaphthalenes and a polyoxygenated cyclohexene from the stem and root extracts of *Uvaria cherrevensis* (Annonaceae), Fitoterapia 120 (2017) 103–107.
[12] M. Kodpinid, C. Sadavongvivad, C. Thebtaranonth, Y. Thebtaranonth, Benzyl benzoates from the roots of *Uvaria purpurea*, Phytochemistry 23 (1984) 199–200.
[13] T.A. Yapi, J.B. Boti, B.K. Attioua, A.C. Ahibo, A. Bighelli, J. Casanova, F. Tomi, Three new natural compounds from the root bark essential oil from *Xylopia aethiopica*, Phytochem. Anal. 23 (2012) 651–656.
[14] S.J. Kim, H.J. Kim, H.J. Kim, Y.P. Jang, M.S. Oh, D.S. Jang, New patchoulane-type sesquiterpenes from the rhizomes of *Cyperus rotundus*, Bull. Kor. Chem. Soc. 33 (2012) 3115–3118.
[15] X.P. Pan, D.Q. Yu, Two polyoxygenated cyclohexenes from *Uvaria grandiflora*, Phytochemistry 40 (1995) 1079–1711.
[16] Z.J. Ma, Z.K. Meng, P. Zhang, Chemical constituents from *Curcuma wenyujin*, Fitoterapia 80 (2009) 374–376.
[17] M. Kodpinid, C. Thebtaranonth, Y. Thebtaranonth, Benzyl benzoates and *O*-hydroxybenzyl flavanones from *Uvaria ferruginea*, Phytochemistry 24 (1985) 3071–3072.
[18] H.N. El-Sohly, W.L. Lasswell, C.D. Hufford, Two new C-benzylated flavanones from *Uvaria chamae* and ^{13}C NMR analysis of flavanone methyl ethers, J. Nat. Prod. 42 (1979) 264–270.
[19] P.C. Stevenson, N.C. Veitch, M.S.J. Simmonds, Polyoxygenated cyclohexene derivatives and other compound constituents from *Kaempferia rotunda* L, Phytochemistry 68 (2007) 1579–1586.
[20] A.M. Kupchan, R.J. Hemingway, R.M. Smith, Tumor inhibitors. XLV. Crotepoxide, a novel cyclohexane diepoxide tumor inhibitor from *Croton macrostachys*, J. Org. Chem. 34 (1968) 3898–3902.
[21] B.T. Murphy, S. Cao, P.J. Brodie, J.S. Miller, F. Ratovoson, C. Birkinshaw, E. Rakotobe, V.E. Rasamison, K. Tendyke, E.M. Suh, D.G. Kingston, Antiproliferative compounds of *Artabotrys madagascariensis* from the Madagascar rainforest, Nat. Prod. Res. 22 (2008) 1169–1175.
[22] S. Lallo, S. Lee, D.F. Dibwe, Y. Tezuka, H. Morita, A new polyoxygenated cyclohexane and other constituents from *Kaempferia rotunda* and their cytotoxic activity, Nat. Prod. Res. 28 (2014) 1754–1759.
[23] W. Trager, J.B. Jensen, Human malaria parasites in continuous culture, Science 193 (1976) 673–675.
[24] R.E. Desjardins, C.J. Canfield, J.D. Haynes, J.D. Chulay, Quantitative assessment of antimalarial activity in *vitro* by a semiautomated microdilution technique, Antimicrob. Agents Chemother. 16 (1979) 710–718.
[25] L. Collins, S.G. Franzblau, Microplate Alamar Blue assay versus BACTEC 460 system for high-throughput screening of compounds against *Mycobacterium tuberculosis* and *Mycobacterium avium*, Antimicrob. Agents Chemother. 41 (1997) 1004–1009.
[26] P. Skehan, R. Storeng, D. Scudiero, A. Monks, J. McMahon, D. Vistica, J.T. Warren, H. Bokesch, S. Kenney, M.R. Boyd, New colorimetric cytotoxicity assay for anticancer-drug screening, J. Natl. Cancer Inst. 82 (1990) 1107–1112.
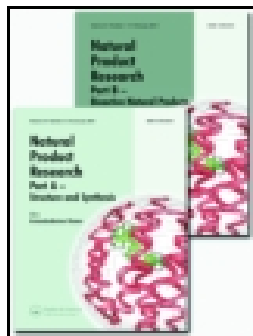
Inhibition of nitric oxide production by clerodane diterpenoids from leaves and stems of *Croton poomae* Esser

Apisara Somteds, Cholpisut Tantapakul, Kwanjai Kanokmedhakul, Surat Laphookhieo, Piyaporn Phukhatmuen & Somdej Kanokmedhakul

View supplementary material 🗗

Published online: 23 Sep 2019.

Submit your article to this journal 🗗

View related articles 🗗

View Crossmark data 🗗

Taylor & Francis
Taylor & Francis Group

Check for updates

Inhibition of nitric oxide production by clerodane diterpenoids from leaves and stems of *Croton poomae* Esser

Apisara Somteds[a], Cholpisut Tantapakul[a], Kwanjai Kanokmedhakul[a], Surat Laphookhieo[b], Piyaporn Phukhatmuen[b] and Somdej Kanokmedhakul[a]

[a]Natural Products Research Unit, Department of Chemistry and Center of Excellence for Innovation in Chemistry, Faculty of Science, Khon Kaen University, Khon Kaen, Thailand; [b]Center of Chemical Innovation for Sustainability (CIS), School of Science, Mae Fah Luang University, Chiang Rai, Thailand

ABSTRACT

Chromatographic separation of crude extracts from the leaves and stems of *Croton poomae* Esser led to the isolation of two new clerodane diterpenes crotonolide K (**1**) and furocrotinsulolide A acetate (**2**) and six known clerodane diterpenes (**3–8**), together with twelve known compounds (**9–20**). Their structures were established from spectroscopic analysis. The clerodane diterpenoids **1–8** were evaluated for inhibition of nitric oxide (NO) production in LPS-activated RAW 264.7 macrophages. Compounds **1**, **2**, **5**, **7** and **8** showed potent inhibitory effects, with IC_{50} values ranging from 32.19 to 48.85 μM, which is better than both the standard drugs indomethacin (154.5 μM) and dexamethasone (56.28 μM).

Croton poomae Esser   Inhibition of nitric oxide production
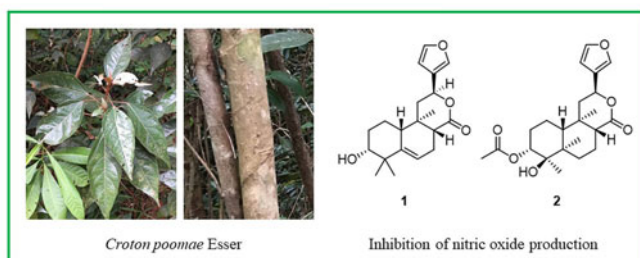
1. Introduction

Croton is a large genus in the Euphorbiaceae family consisting of approximately 1,300 species. Many species have long been used as traditional medicines in Asia, Africa and South America (Salatino et al. 2007). Previous investigations of *Croton* have shown a wide range of secondary metabolites, such as alkaloids (Suárez et al. 2004), phenolics (Tala et al. 2013), terpenoids (Aguilar-Guadarrama and Rios, 2004; Kuo et al. 2013) and

---

CONTACT Somdej Kanokmedhakul ✉ somdej@kku.ac.th

Supplemental data for this article can be accessed at https://doi.org/10.1080/14786419.2019.1667350
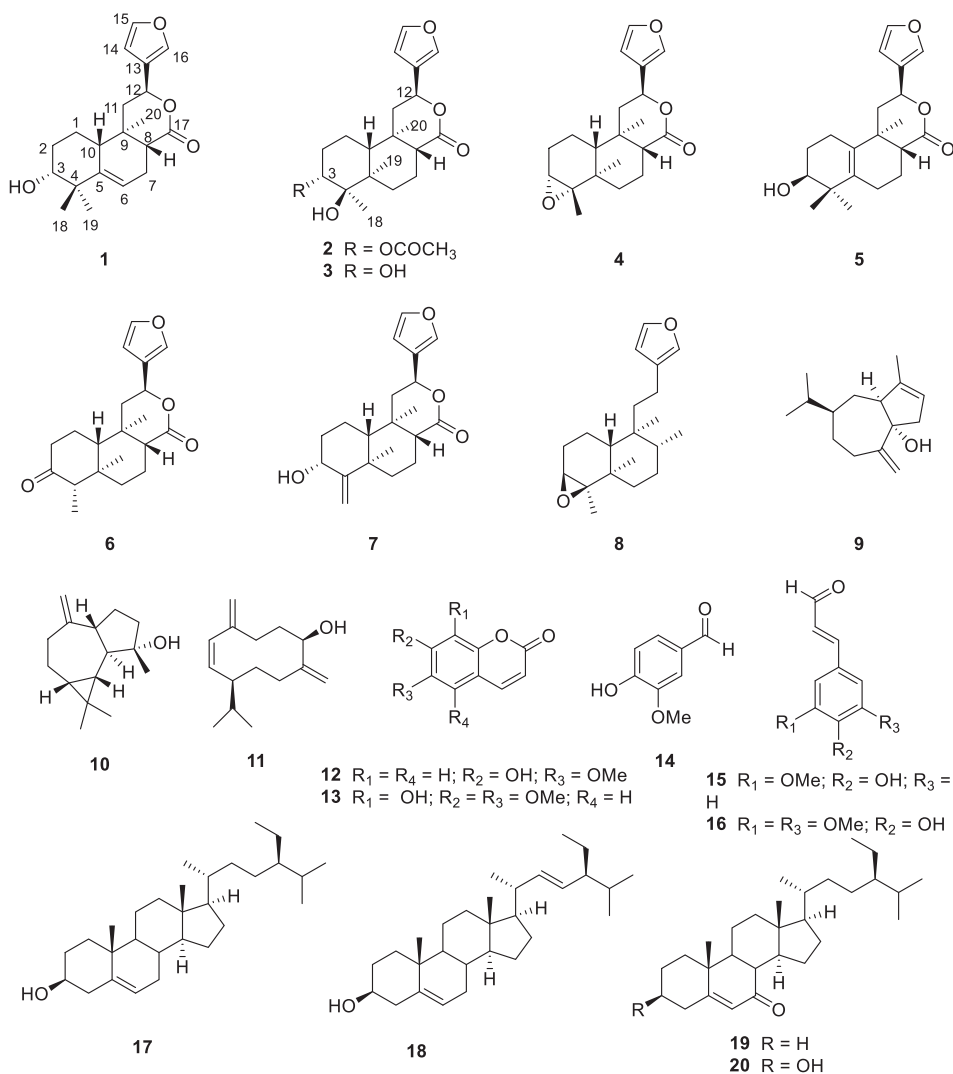
Figure 1. The structures of compounds 1–20.

volatile oils (Cavalcanti et al. 2012; Silva-Alves et al. 2015). Some of these compounds display interesting biological activities, for example anti-inflammatory (Suárez et al. 2006; Kuo et al. 2013; Cordeiro et al. 2016; Yang et al. 2016), cytotoxic (Sommit et al. 2003; Zhang et al. 2013; Liu et al. 2014), antiviral (Wang et al. 2012), and antimicrobial (Liu et al. 2014). In Thailand, *Croton poomae* is locally known as "Plau Phu Wua", named after Phu Wua, the single locality where it is commonly found. *C. poomae* is a tree, 10 m in height, and widely distributed in the North-Eastern part of Thailand (Esser, 2002). Although *C. poomae* has been reported as a new species since 2002, its phytochemistry and biological activity have not been reported. Recently, there was a report of clerodane diterpenoids from the genus *Croton* that displayed nitric oxide (NO) inhibition (Zhang et al. 2017). Therefore, the investigation of *C. poomae* became a focus of our work. Herein we report the isolation and structural determination of twenty compounds

including two new clerodane diterpenoids (**1** and **2**), as well as the inhibition of NO production activity by clerodane diterpenoids **1**–**8** from *C. poomae*.

2. Results and discussion

The *n*-hexane, EtOAc and MeOH extracts of dried leaves and stems of *C. poomae* were separated by silica gel column chromatography (CC), silica gel flash column chromatography (FCC) and Sephadex LH-20 column chromatography to yield two new clerodane diterpenoids, crotonolide K (**1**) and furocrotinsulolide A acetate (**2**) and eighteen known compounds (**3**–**20**). Structures of known compounds were identified by spectroscopic data measurements, as well as by comparing the data obtained with published values, as furocrotinsulolide A (**3**) (Graikou et al. 2005), 3,4,15,16-diepoxy-cleroda-13(16),14-diene-12,17-olide (**4**) (Pudhom and Sommit 2011), 15,16-epoxy-3*β*-hydroxy-5(10),13(16),14-*ent*-halimatriene-17,(12*S*)-olide (**5**) (Aldhaher et al. 2017), crotonolide E (**6**) (Liu et al. 2014), crotonolide F (**7**) (Liu et al. 2014), 3*β*,4*β*:15,16-diepoxy-13(16),14-clerodadiene (**8**) (Harinantenaina et al. 2006), 1-hydroxy-guai-3,10(14)-diene (**9**) (Ezzat and Motaal 2012), spathulenol (**10**) (Ragasa et al. 2003), 1*β*-hydroxy-4(15),5*E*,10(14)-germacratriene (**11**) (Brown et al. 2003), scopoletin (**12**) (Vasconcelos et al. 1998), fraxidin (**13**) (Garcez et al. 1999), 4-hydroxy-3-methoxybenzaldehyde (**14**) (Ito et al. 2001), *trans*-coniferyl aldehyde (**15**) (Miyazawa and Hisama 2003), sinapyl aldehyde (**16**) (Hiltunen et al. 2006), *β*-sitosterol (**17**) (Chang et al. 2000), stigmasterol (**18**) (Alam et al. 1996), stigmast-5-en-7-one (**19**) (Sangsopha et al. 2018), and 7-oxo-*β*-sitosterol (**20**) (Pettit et al. 2000) as shown in Figure 1.

Compound **1** had the molecular formula $C_{20}H_{26}O_4$ deduced from the ^{13}C NMR and HRESIMS, m/z 353.1729 $[M + Na]^+$ (calcd. for $C_{20}H_{26}O_4 + Na$, 353.1727) data, indicating eight degrees of unsaturation. The IR spectrum showed the presence of a hydroxyl group at 3488 cm^{-1}, the carbonyl of an ester group at 1720 cm^{-1} and alkenes at 1459 and 1373 cm^{-1}. The UV spectrum indicated an ester group at 210 nm. The ^1H and ^{13}C NMR spectroscopic data of **1** (Table S1 in supplementary material) were similar to those of a known isolated clerodane diterpenoid, 15,16-epoxy-3*β*-hydroxy-5(10),13(16),14-*ent*-halimatriene-17,(12*S*)-olide (**5**) (Aldhaher et al. 2017). The main difference was the presence of the double bond at C-5/C-6 (in **1**) instead of C-5/C-10 (in **5**). This was confirmed by the appearance of two methine protons at δ_H 5.63, d, $J = 6.1$ Hz, H-6/δ_C 119.5 and δ_H 2.13, m, H-10/δ_C 44.2 in **1**, as well as the HMBC correlations of H-10 to C-6 and C-20, and H-6 to C-4, C-7, C-8 and C-10 (Figure S1). The resonance of H-3 as a broad singlet at δ_H 3.51 indicated a *β*-equatorial orientation (Graikou et al. 2005) which was confirmed by the NOESY correlations between H-3 and H$_3$-18, and H$_3$-18 and H-10 (Figure S2). The correlations between H-12 and H$_3$-20 revealed that these protons were in α-orientation. From the above evidence, the relative configuration of **1** was assigned as the same as that of **5** except H-3 (Aldhaher et al. 2017). Moreover, the absolute configuration of **1** was determined by comparison of the experimental ECD with its calculated ECD spectra. The ECD calculations were generated for two selected possible stereoisomers, 3*R*, 8*R*, 9*R*, 10*R*, 12*S* and 3*S*, 8*S*, 9*S*, 10*S*, 12*R* using Gaussian09 with DFT B3LYP/6-311++G (d,p). The ECD experimental spectrum of **1** corresponded to its calculated spectrum (Figure S4), therefore the

absolute configuration of **1** was assigned as 3*R*, 8*R*, 9*R*, 10*R*, 12*S*. Thus, **1** was deduced as a new celodane diterpene, 15,16-epoxy-3α-hydroxy-5(6)13(16),14-*ent*-halimatriene-17,(12*S*)-olide and was named crotonolide K.

Compound **2** had the molecular formula $C_{22}H_{30}O_6$, deduced from the ^{13}C NMR and HRESIMS, *m/z* 413.1941 $[M + Na]^+$ (calcd. for $C_{22}H_{30}O_6$ + Na, 413.1940) data, indicating eight degrees of unsaturation. The IR spectrum showed the absorption bands of hydroxyl (3433 cm^{-1}), ester carbonyl (1715 cm^{-1}), and alkene (1504 cm^{-1}) groups. The UV spectrum indicated an ester group at 211 nm. The ^1H and ^{13}C NMR spectral data of **2** (Table S1 in supplementary material) were similar to those of the known isolated furo-crotinsulolide A (**3**) (Graikou et al. 2005). However, the hydroxy group at C-3 in **3** was replaced by an acetoxy group, which was confirmed by NMR resonances at δ_H 2.01, s/ δ_C 22.8 and δ_C 170.2, and the high-field carbon signal of C-3 at δ_C 68.6. The resonance of H-3 at δ_H 4.73 appeared as a broad singlet, indicating a β-equatorial orientation of H-3 in **2** was the same as those of **1** and **3** (Graikou et al. 2005). The NOESY correlations between H-12 and H$_3$-20, H$_3$-18 and H$_3$-19, and H$_3$-19 and H$_3$-20 revealed that these protons were α-orientation, while the correlations between H-2β and H-3, H-2β and H-10, and H-8 and H-10 suggested the β-orientation of H-3, H-8 and H-10 (Figure S3). Consequently, the relative configuration of **2** was assigned to be the same as that of furocrotinsulolide A (**3**) (Graikou et al. 2005). Furthermore, the absolute configuration of **2** was assigned by comparison of the experimental ECD with its calculated ECD spectra of two selected possible stereoisomers (3*R*, 4*R*, 5*R*, 8*R*, 9*R*, 10*R*, 12*S* and 3*S*, 4*S*, 5*S*, 8*S*, 9*S*, 10*S*, 12*R*). The experimental ECD spectrum of **2** was matched with its calculated ECD spectrum of 3*R*, 4*R*, 5*R*, 8*R*, 9*R*, 10*R*, 12*S* (Figure S5). Therefore, **2** was identified as a new clerodane diterpenoid and was named furocrotinsulolide A acetate.

Compounds **1–8** were evaluated for their inhibition of NO production by LPS-induced RAW 264.7 macrophages. The results show that **1**, **2**, **5**, **7** and **8** inhibited NO production with IC$_{50}$ values of 46.43, 31.99, 48.85, 42.04, and 32.19 μM, respectively, which makes them more potent than the standard drugs, indomethacin (IC$_{50}$ = 154.5 μM) and dexamethasone (IC$_{50}$ = 56.28 μM). Compounds **3**, **4**, and **6** showed weak inhibitory activity with IC$_{50}$ values of 81.97, 86.98, and 74.78 μM, respectively (Table S2 in supplementary material).

3. Experimental

3.1. Plant material

Leaves and stems of *C. poomae* Esser. were collected from Bung Kan Province, Thailand, in December 2016, and were identified by Prof. Pranom Chantaranothai, Department of Biology, Khon Kaen University, Thailand, where a voucher specimen (S. Kanokmedhakul 32) has been deposited.

3.2. Extraction and isolation

Air-dried leaves of *C. poomae* (1.6 kg) were ground and successively extracted with *n*-hexane, EtOAc, and MeOH (3 × 20 L). The solvents were evaporated to dryness under

reduced pressure to give crude *n*-hexane (39.9 g, 2.49%), EtOAc (47.9 g, 2.99%), and MeOH (225.5 g, 14.09%) extracts, respectively.

The EtOAc extract (47.9 g) was separated on silica gel CC, eluted with a gradient system of *n*-hexane-EtOAc and EtOAc-MeOH to give four fractions (EL$_1$-EL$_4$). Fraction EL$_3$ was separated by silica gel CC, eluted with CH$_2$Cl$_2$-EtOAc (99.5:0.5 to 80:20), to give five subfractions (EL$_{3.1}$-EL$_{3.5}$). Purification of subfraction EL$_{3.1}$ by silica gel CC, eluted with *n*-hexane-EtOAc (70:30) yielded a white solid of **6** (2.0 mg). Subfraction EL$_{3.2}$ was purified by silica gel CC, eluted with *n*-hexane-EtOAc (65:35) to yield a yellow oil of **5** (18.3 mg). Subfraction EL$_{3.5}$ was subjected to silica gel CC, eluted with CH$_2$Cl$_2$-EtOAc (80:20), to yield a white solid of **2** (17.1 mg). The MeOH extract (225.5 g) was subjected to silica gel CC, eluted with a gradient system of *n*-hexane-EtOAc and EtOAc-MeOH, to give five fractions (ML$_1$-ML$_5$). Fraction ML$_2$ was separated by silica gel CC, eluted with *n*-hexane-CH$_2$Cl$_2$ (40:60 to 0:100), to yield a white solid of **4** (885.4 mg), a yellow oil of **5** (23.3 mg) and colorless needles of **3** (123.5 mg).

The above extraction procedure was repeated with air-dried stems of *C. poomae* (12.4 kg) to give crude *n*-hexane (44.2 g, 0.36%), crude EtOAc (52.69 g, 0.43%), and crude MeOH (386.5 g, 3.12%) extracts, respectively. Solid in *n*-hexane extract was washed with MeOH to give a white solid of **4** (4.0 g). The *n*-hexane extract (39.3 g) was subjected to CC over silica gel, eluted with a gradient system of *n*-hexane-EtOAc and EtOAc-MeOH to give nine fractions (HS$_1$-HS$_9$). Fraction HS$_2$ was purified by silica gel CC, eluted with *n*-hexane-CH$_2$Cl$_2$ (80:20 to 50:50), to yield a white amorphous powder of **8** (168.1 mg) and colorless oil of **9** (6.7 mg). Fraction HS$_3$ was separated by silica gel CC, eluted with *n*-hexane-EtOAc (100:0 to 50:50), to afford a white amorphous powder of **10** (146.1 mg) and a white solid of **19** (76.4 mg). Fraction HS$_6$ was re-chromatographed on silica gel CC, using CH$_2$Cl$_2$-EtOAc (100:0 to 50:50) as eluent, to give a yellow oil of **5** (62.9 mg), a pale oil of **1** (39.5 mg) and a yellow oil of **7** (14.6 mg). Solid in subfraction HS$_3$ was filtered out to give a white solid of **20** (68.0 mg). Fraction HS$_7$ was separated by silica gel CC, eluted with *n*-hexane-CH$_2$Cl$_2$ (20:80), to afford a colorless oil of **11** (38.1 mg). The EtOAc extract (52.69 g) was chromatographed by silica gel flash column chromatography (FCC), eluted with a gradient system of *n*-hexane-EtOAc and EtOAc-MeOH, to afford seven fractions (ES$_1$-ES$_7$). Fractions ES$_3$ was applied to silica gel CC, eluted with *n*-hexane-EtOAc (100:0 to 70:30), to give a white amorphous powder of **10** (182.4 mg), a white solid of **17** (10.9 mg), and colorless needles of **18** (12.5 mg). Fraction ES$_4$ was purified by silica gel FCC, eluted with *n*-hexane-acetone (80:20), to give orange needles of **15** (14.3 mg), orange needles of **16** (6.8 mg), a yellow oil of **5** (16.5 mg) and colorless needles of **14** (15.5 mg). Fractions ES$_5$ was further purified by silica gel CC, eluted with a gradient system of CH$_2$Cl$_2$-MeOH (97:3 to 90:10), to afford a white solid of **12** (4.6 mg), orange needles of **13** (3.2 mg) and colorless needles of **3** (340.9 mg). The MeOH extract (386.5 g) was chromatographed on silica gel CC, eluted with a gradient system of *n*-hexane-EtOAc and EtOAc-MeOH, to give four fractions (MS$_1$-MS$_4$). Fraction MS$_2$ was subjected to silica gel CC, eluted with *n*-hexane-CH$_2$Cl$_2$ (40:60 to 0:100), to give seven subfractions (MS$_{2.1}$-MS$_{2.7}$). Subfraction MS$_{2.1}$ was chromatographed over Sephadex LH-20 CC, eluted with MeOH, to give an additional amount of **6** (6.4 mg). Subfraction MS$_{2.4}$ was further purified by silica gel CC, eluted with CH$_2$Cl$_2$-EtOAc (97:3), to yield an additional amount of **5** (8.4 mg).

3.2.1. Crotonolide K (1)

Pale oil, $[\alpha]_D^{23.4}$ -41 (c 0.1, MeOH); UV (MeOH) λ_{max} (log ε) 210 (3.92) nm; ECD (c 3.58×10^{-4} M, MeOH) λ_{max} (log ε) 202 (+4.86), 215 (-5.33) nm; IR (Neat) ν_{max} 3488, 2946, 1720, 1459, 1373, 1265, 1227, 1135, 1079, 1029, 992, 945, 910, 874, 789, 733, 702 cm^{-1}; ^{1}H NMR (400 MHz, CDCl$_3$): δ 7.45 (1H, brs, H-16), 7.39 (1H, t, $J = 1.8$ Hz, H-15), 6.42 (1H, d, $J = 1.8$ Hz, H-14), 5.63 (1H, d, $J = 6.1$ Hz, H-6), 5.42 (1H, dd, $J = 12.4$, 3.8 Hz, H-12), 3.51 (1H, brs, H-3), 2.56-2.44 (1H, m, H-7β), 2.30-2.22 (1H, m, H-11α), 2.19-2.06 (1H, m, H-7α), 2.26 (1H, m, H-8), 2.13 (1H, m, H-10), 1.94-1.82 (1H, m, H-2α), 1.78-1.68 (1H, m, H-2β), 1.78-1.68 (1H, m, H-11β), 1.65-1.58 (1H, m, H-1β), 1.57-1.48 (1H, m, H-1α), 1.15 (3H, s, H-19), 1.02 (3H, s, H-18), 0.99 (3H, s, H-20); ^{13}C NMR (100 MHz, CDCl$_3$): δ 172.9 (C-17), 143.7 (C-15), 141.5 (C-5), 139.6 (C-16), 125.4 (C-13), 119.5 (C-6), 108.6 (C-14), 76.0 (C-3), 72.3 (C-12), 46.5 (C-8), 44.2 (C-10), 42.1 (C-11), 41.1 (C-4), 34.7 (C-9), 28.5 (C-18), 27.8 (C-2), 25.3 (C-19), 23.8 (C-7), 19.4 (C-1), 15.7 (C-20); HR-ESI-MS, m/z 353.1729 [M + Na]$^+$ (calcd. for C$_{20}$H$_{26}$O$_4$ + Na, 353.1727).

3.2.2. Furocrotinsulolide a acetate (2)

White solid, $[\alpha]_D^{23.2}$ +50 (c 0.1, MeOH); UV (MeOH) λ_{max} (log ε) 211 (3.58) nm; ECD (c 5.52×10^{-4} M, MeOH) λ_{max} (log ε) 203 (+3.61), 220 (-5.02) nm; IR (Neat) ν_{max} 3433, 2950, 2929, 2855, 1715, 1504, 1456, 1394, 1369, 1243, 1137, 1071, 1034, 874, 802, 753 cm^{-1}; ^{1}H NMR (400 MHz, CDCl$_3$): δ 7.44 (1H, t, $J = 1.5$ Hz, H-16), 7.41 (1H, t, $J = 1.5$ Hz, H-15), 6.43 (1H, t, $J = 1.5$ Hz, H-14), 5.50 (1H, dd, $J = 11.5$, 5.6 Hz, H-12), 4.73 (1H, brs, H-3), 2.37 (1H, dd, $J = 13.4$, 5.6 Hz, H-11β), 2.11 (1H, m, H-8), 2.08-2.03 (1H, m, H-7β), 2.01 (3H, s, H-22), 1.80-1.65 (2H, m, H-2), 1.71-1.66 (1H, m, H-1α), 1.69 (1H, m, H-10), 1.68-1.60 (1H, m, H-11α), 1.68-1.60 (1H, m, H-7α), 1.66-1.63 (1H, m, H-6β), 1.59 (3H, s, H-18), 1.57-1.52 (1H, m, H-6α), 1.42-1.35 (1H, m, H-1β), 1.21 (3H, s, H-19), 1.10 (3H, s, H-20); ^{13}C NMR (100 MHz, CDCl$_3$): δ 172.7 (C-17), 170.2 (C-21), 143.8 (C-15), 139.4 (C-16), 126.2 (C-13), 108.6 (C-14), 88.7 (C-4), 72.2 (C-12), 68.7 (C-3), 51.3 (C-8), 47.7 (C-10), 45.0 (C-11), 42.1 (C-5), 36.9 (C-9), 31.5 (C-6), 30.3 (C-2), 22.8 (C-22), 17.8 (C-7), 17.3 (C-19), 16.2 (C-1), 15.5 (C-18), 14.9 (C-20); HR-ESI-MS, m/z 413.1941 [M + Na]$^+$ (calcd. for C$_{20}$H$_{26}$O$_4$ + Na, 413.1940).

General experimental procedures, spectroscopic data and biological assay for isolated compounds are provided in supplementary material.

4. Conclusion

This is the first report of the phytochemical and biological activity investigation of two new clerodane diterpenoids, crotonolide K (**1**) and furocrotinsulolide A acetate (**2**), and eighteen known compounds (**3**–**20**) from leaves and stems of *C. poomae*. The inhibition of NO production in LPS-activated RAW 264.7 macrophages of clerodane diterpenoids (**1**–**8**) showed that **1**, **2**, **5**, **7**, and **8** exhibited IC$_{50}$ values ranging from 31.99-48.85 μM, which is significantly more potent inhibitory activity than the standard drugs, indomethacin and dexamethasone. Compounds **3**, **4** and **6** exhibited moderate inhibition with IC$_{50}$ values ranging from 74.78-86.98 μM. This result supports the anti-inflammatory activity of clerodane diterpenoids from *Croton* species (Zhang et al.

2017). Therefore, *C. poomae* is one of the valuable sources of bioactive clerodane diterpenoids.

Disclosure statement

No potential conflict of interest was reported by the authors.

References

Aguilar-Guadarrama AB, Rios MY. 2004. Three new sesquiterpenes from *Croton arboreous*. J Nat Prod. 67(5):914–917.

Aldhaher A, Langat M, Ndunda B, Chirchir D, Midiwo JO, Njue A, Schwikkard S, Carew M, Mulholland D. 2017. Diterpenoids from roots of *Croton dichogamus* Pax. Phytochemistry. 144: 1–8.

Alam MS, Chopra N, Ali M, Niwa M. 1996. Oleanen and stigmasterol derivative from *Ambroma augusta*. Phytochemistry. 41(4):1197–1200.

Brown GD, Liang GY, Sy L-K. 2003. Terpenoids from the seeds of *Artemisia annua*. Phytochemistry. 64(1):303–323.

Cavalcanti JM, Leal-Cardoso JH, Diniz LRL, Portella VG, Costa CO, Linard CFBM, Alves K, Rocha M. V A D P, Lima CC, Cecatto VM, Coelho-de-Souza AN. 2012. The essential oil of *Croton zehntneri* and *trans*-anethole improves cutaneous wound healing. J Ethnopharmacol. 144(2):240–247.

Chang YC, Chang FR, Wu YC. 2000. The constituents of *Lindera glauca*. Jnl Chin Chem Soc. 47(2): 373–380.

Cordeiro KW, Felipe JL, Malange KF, do Prado PR, de Oliveira Figueiredo P, Garcez FR, de Cássia Freitas K, Garcez WS, Toffoli-Kadri MC. 2016. Anti-inflammatory and antinociceptive activities of *Croton urucurana* Baillon bark. J Ethanopharmacol. 183:128–135.

Esser HJ. 2002. *Croton poomae* (Euphorbiaceae), a new species from Thailand. Thai for Bull. (BOT). 30:1–6.

Ezzat SM, Motaal AA. 2012. Isolation of new cytotoxic metabolites from *Cleome droserifolia* growing in Egypt. Z Naturforch. 67(5-6):266–274.

Garcez FR, Garcez WS, Martins M, Cruz AC. 1999. A bioactive lactone from *Nectandra gardneri*. Planta Med. 65(8):775

Graikou K, Aligiannis N, Chinou I, Skaltsounis AL, Tillequin F, Litaudon M. 2005. Chemical constituents from *Croton insularis*. HCA. 88(10):2654–2660.

Harinantenaina L, Takahara Y, Nishizawa T, Kohchi C, Soma GI, Asakawa Y. 2006. Chemical constituents of Malagasy liverworts, Part V: prenyl bibenzyls and clerodane diterpenoids with

nitric oxide inhibitiory activity from *Radula appressa* and *Thysananthus spathulistipus*. Chem Pharm Bull. 54(7):1046–1049.

Hiltunen E, Pakkanen TT, Alvila L. 2006. Phenolic compounds in silver birch (*Berula pendula* Roth) wood. Holzforschung. 60(5):519–527.

Ito J, Chang FR, Wang HK, Park YK, Ikegaki M, Kilgore N, Lee KH. 2001. Anti-AIDS agents. 48.(1) Anti-HIV activity of moronic acid derivatives and the new melliferone-related triterpenoid isolated from Brazilian propolis. J Nat Prod. 64(10):1278–1281.

Kuo PC, Yang ML, Hwang TL, Lai YY, Li YC, Thang TD, Wu TS. 2013. Anti-inflammatory diterpenoids from *Croton tonkinensis*. J Nat Prod. 76(2):230–236.

Liu CP, Xu JB, Zhao JX, Xu CH, Dong L, Ding J, Yue JM. 2014. Diterpenoids from *Croton laui* and their cytotoxic and antimicrobial activities. J Nat Prod. 77(4):1013–1020.

Miyazawa M, Hisama M. 2003. Antimutagenic activity of phenylpropanoids from Clove (*Syzygium aromaticum*)). J Agric Food Chem. 51(22):6413–6422.

Pettit GR, Numata A, Cragg GM, Herald DL, Takada T, Iwamoto C, Riesen R, Schmidt JM, Doubek DL, Goswami A. 2000. Isolation and structures of schleicherastatins 1-7 and schleicheols 1 and 2 from the teak forest medicinal tree *Schleichera oleosa*. J Nat Prod. 63(1):72–78.

Pudhom K, Sommit D. 2011. Clerodane diterpenoids and a trisubstituted furan from *Croton oblongifolius*. Phytochem Lett. 4(2):147–150.

Ragasa CY, Ganzon J, Hofileña J, Tamboong B, Rideout JA. 2003. A new furanoid diterpene from *Caesalpinia pulcherrima*. Chem Pharm Bull. 51(10):1208–1210.

Salatino A, Salatino MLF, Negri G. 2007. Traditional uses, Chemistry and Pharmacology of *Croton* species (Euphorbiaceae). J Braz Chem Soc. 18(1):11–33.

Sangsopha W, Kanokmedhakul K, Lekphrom R, Kanokmedhakul S. 2018. Chemical constituents and biological activities from branches of *Colubrina asiatica*. Nat Prod Res. 32(10):1176–1179.

Silva-Alves KS, Ferreira-da-Silva FW, Coelho-de-Souza AN, Albuquerque AAC, Vale OC, Leal-Cardoso JH. 2015. Essential oil of *Croton zehntneri* and its main constituent anethole block excitability of rat peripheral nerve. Planta Med. 81:292–297.

Sommit D, Petsom A, Ishikawa T, Roengsumran S. 2003. Cytoxic activity of natural labdanes and their semi-synthetic modified derivatives from *Croton oblongifolius*. Planta Med. 69(2):167–170.

Suárez AI, Blanco Z, Monache FD, Compagnone RS, Arvelo F. 2004. Three new glutarimide alkaloids from *Croton cuneatus*. Nat Prod Res. 18(5):421–426.

Suárez AI, Blanco A, Compagnone RS, Salazar-Bookaman MM, Zapata V, Alvarado C. 2006. Anti-inflammatory activity of *Croton cuneatus* aqueous extract. J Ethanopharmacol. 150:99–101.

Tala MF, Tan NH, Ndontsa BL, Tane P. 2013. Triterpenoids and phenolic compounds from *Croton macrostachyus*. Biochem Syst Ecolo. 51:138–141.

Vasconcelos JMJ, Silva AMS, Cavaleiro J. 1998. Chromones and flavanones from *Artemisia camoestris* subsp. Maritima. Phytochemistry. 49(5):1421–1424.

Wang GC, Li JG, Li GQ, Xu JJ, Wu X, Ye WC, Li YL. 2012. Clerodane diterpenoids from *Croton crassifolius*. J Nat Prod. 75(12):2188–2192.

Yang L, Zhang YB, Chen LF, Chen NH, Wu ZN, Jiang SQ, Jiang L, Li GQ, Li YL, Wang GC. 2016. New labdane diterpenoids from *Croton laui* and their anti-inflammatory activities. Bioorg Med Chem Lett. 26(19):4687–4691.

Zhang J-S, Tang Y-Q, Huang J-L, Li W, Zou Y-H, Tang G-H, Liu B, Yin S. 2017. Bioactive diterpenoids from *Croton laevigatus*. Phytochemistry. 144:151–158.

Zhang XL, Wang L, Li F, Yu K, Wang MK. 2013. Cytotoxic phorbol esters of *Croton tiglium*. J Nat Prod. 76(5):858–864.

A new xanthone from the fungus Apiospora montagnei

Supakorn Arthan, Cholpisut Tantapakul, Kwanjai Kanokmedhakul, Kasem Soytong & Somdej Kanokmedhakul

View supplementary material ⬚

Published online: 28 Feb 2017.

Submit your article to this journal ⬚

Article views: 34

View related articles ⬚

View Crossmark data ⬚

Taylor & Francis
Taylor & Francis Group

Check for updates

A new xanthone from the fungus *Apiospora montagnei*

Supakorn Arthan[a,b], Cholpisut Tantapakul[a], Kwanjai Kanokmedhakul[a],
Kasem Soytong[c] and Somdej Kanokmedhakul[a]

[a]Natural Products Research Unit, Faculty of Science, Department of Chemistry and Center of Excellence for Innovation in Chemistry, Khon Kaen University, Thailand; [b]Chemistry program, Faculty of Science and Technology, Sakon Nakhon Rajabhat University, Sakon Nakhon, Thailand; [c]Faculty of Agricultural Technology, Department of Plant Production Technology, King Mongkut's Institute of Technology Ladkrabang, Bangkok, Thailand

ABSTRACT

A new xanthone derivative, methyl 8-hydroxy-3-hydroxymethylxanthone-1-carboxylate (**1**), and seven known compounds, 8-hydroxy-3-methylxanthone-1-carboxylate (**2**), methyl 8-hydroxy-6-methylxanthone-1-carboxylate (**3**), ergosterol (**4**), cyathisterone (**5**), ergosta-4,6,8(14),22-tetraen-3-one (**6**), calvasterone (**7**) and 2-hexyl-3-methylmaleic anhydride (**8**) were first isolated from the fungus *Apiospora montagnei*. Their structures were elucidated on the basis of spectroscopic analysis (UV, IR, MS, 1D, and 2D NMR). Compounds **5** and **6** showed weak to very weak cytotoxicity against cancer cell lines, NCI-H187 and KB.
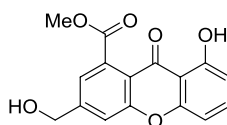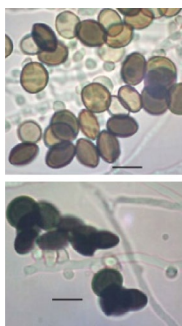
Apiospora montagnei Sacc.

1. Introduction

The fungus *Apiospora montagnei* Sacc. belongs to the Apiosporaceae family (Klemke et al. 2004). It is the only species in the genus *Apiospora* that has been studied. Previous reports have shown that *A. montagnei* produces several secondary metabolites such as amide,

coumarin (Alfatafta et al. 1994), isocoumarins (Ramos et al. 2013), cyclic peptides (Koguchi et al. 2000; Kohno et al. 2000), diterpene, monomethyl esters, polyketide and xanthone derivative (Klemke et al. 2004). Some of these compounds show antibacterial activity (Alfatafta et al. 1994), cytotoxicity (Klemke et al. 2004) and proteasome inhibitory activity (Kohno et al. 2000). Therefore, the chemical constituents and the biological activities of this fungus were our interests in this study. We report herein the isolation and elucidation of a new xanthone (**1**) and seven known compounds (**2**−**8**).

2. Results and discussion

Chromatographic separation of *n*-hexane, EtOAc and MeOH extracts yielded eight compounds (**1**−**8**). The new compound (**1**) was determined by spectroscopic techniques (IR, UV, ^{1}H and ^{13}C NMR, 2D NMR, and MS), whereas the seven known compounds were identified by their physical properties and spectroscopic data measurements, as well as by comparing the data obtained with published values, as being methyl 8-hydroxy-3-methylxanthone-1-carboxylate (**2**) (Li et al. 2011), methyl 8-hydroxy-6-methylxanthone-1-carboxylate (**3**) (Kachi & Sassa 1986), ergosterol (**4**) (Smith & Korn 1968), cyathisterone (**5**) (Kawahara et al. 1994), ergosta-4,6,8(14),22-tetraen-3-one (**6**) (Kawahara et al. 1994), calvasterone (**7**) (Kawahara et al. 1994) and 2-hexyl-3-methylmaleic anhydride (**8**) (Buttery et al. 1980).

Compound **1** was obtained as yellow needles, and its molecular formula, $C_{16}H_{12}O_6$, was deduced from HR-ESI-TOF-MS (*m/z* 301.0719 [M + H]$^+$). The IR spectrum showed broad absorption bands at 3430 (hydroxyl), 1731 (carbonyl of ester), and 1650 (aromatic ketone) cm^{-1}. The UV spectrum exhibited adsorptions at 234, 259, 287, and 366 nm, which correspond to xanthone chromophores (Kachi & Sassa 1986; Tian et al. 2015; Daengrot et al. 2016). The ^{1}H NMR spectral data consisted of a chelated hydroxyl proton (δ_H 12.23, 1H, s, 8-OH), a set of *meta*-coupled aromatic protons [δ_H 7.53 (1H, brs, H-4) and 7.26 (1H, brs, H-2)], and a set of 1,2,3-trisubstituent aromatic protons [δ_H 7.57 (1H, t, *J* = 8.4 Hz, H-6), 6.88 (1H, d, *J* = 8.4 Hz, H-5), and 6.80 (1H, d, *J* = 8.4 Hz, H-7)]. The latter was confirmed by COSY correlations between H-5↔H-6↔H-7. Moreover, the ^{1}H NMR spectrum of **1** also exhibited the characteristic signals of methyl ester [δ_H 4.01 (3H, s, CO$_2$Me)] and oxymethylene protons [δ_H 4.85 (2H, s, H-10)]. The HMBC spectrum showed correlations of the H-2 (δ_H 7.26) and OMe (δ_H 4.01) to the carbonyl of ester (δ_C 169.6), and H-10 to C-2 (δ_C 120.5) and C-4 (δ_C 116.3), confirming the methyl ester and hydroxymethyl units were located at C-1 and C-3, respectively. The COSY and HMBC correlations are shown in Figure S1 (in Supplementary material). Therefore, compound **1** was assigned as a new methyl 8-hydroxy-3-hydroxymethylxanthone-1-carboxylate.

Compounds **1**, **2**, **5**, **6** and **8** were evaluated for their biological activities (Table S1). All compounds were inactive towards antimalarial test. The results showed that compound **5** exhibited weak cytotoxicity against the NCI-H187 cell line with an IC$_{50}$ value of 14.80 μM, whereas compound **6** showed very weak cytotoxicity against KB and NCI-H187 cell lines with IC$_{50}$ values of 48.10 and 58.80 μM, respectively.

3. Experimental

3.1. General experimental procedures

Melting points were determined on a SANYO MPU350BM3.5 melting point apparatus (SANYO Gallenkamp PLC, Leicestershire, UK) and were uncorrected. IR spectra were recorded using

a Bruker Tensor 27 FT-IR spectrometer (Agilent Technologies, USA). UV spectra were measured on an Agilent 8453 UV–visible spectrophotometer (Agilent Technologies, USA). NMR spectra were obtained from a Varian Mercury Plus 400 spectrometer (Varian, Inc., USA). Chemical shifts were recorded on a δ (ppm) scale using $CDCl_3$ as the solvent, and using residual $CHCl_3$ as an internal standard. HR-ESI-TOF-MS spectra were acquired using a Micromass Q-TOF-2 spectrometer (Bruker, Germany). Column chromatography was carried out over Merck silica gel 60 (230–400 mesh) (Merck, Darmstadt, Germany). TLC was performed with precoated Merck silica gel 60 PF_{254} aluminium sheets (Merck, Darmstadt, Germany); the spots were visualised under UV light (254 and 366 nm) and further by spraying with anisaldehyde and then heating until charred.

3.2. Fungal material

3.2.1. Collection, isolation and taxonomy

The fungus *A. montagnei* was isolated from the leaf surface of *Vanilla siamensis* at Pathum Thani Province, and was identified by Assoc. Prof. Kasem Soytong. Colony is white when young and becomes brown to dark brown when mature. Mycelium is both immersed and superficial in medium. Conidiophores areseptate, single or slightly straight, smooth wall, hyaline to pale brown, sparingly septate. Conidia are lenticular, pale brown to brown, equatorial germ slit. This morphological identification is similar report of Kirk (1991). A voucher specimen (No. Am01) was deposited at the Department of Plant Production Technology, Faculty of Agricultural Technology, King Mongkut's Institute of Technology Ladkrabang, Bangkok Thailand. The fungus was cultivated on Potato Dextrose Broth (PDB) at 28–30 °C for 30 days and filtered out to yield biomass and then air-dried.

3.3. Extraction and isolation

Air-dried biomass of *A. montagnei* (140 g) was ground into powder and then extracted successively three times with *n*-hexane (1L × 3), EtOAc (1L × 3) and MeOH (1L × 3), respectively, at room temperature. The filtered extracts were evaporated to yield crude extracts of *n*-hexane (5.8 g, 4.14%), EtOAc (7.3 g, 5.21%) and MeOH (7.1 g, 5.07%). The crude *n*-hexane extract (5.8 g) was subjected to silica gel flash column chromatography (FCC), eluted with a gradient system of *n*-hexane-EtOAc, EtOAc-MeOH to give eleven fractions (HF_1–HF_{11}). Fraction HF_5 was subjected to FCC, eluted with a gradient system of *n*-hexane-EtOAc to give three subfractions ($HF_{5.1}$–$HF_{5.3}$). Subfraction $HF_{5.2}$ was separated by preparative TLC using MeOH-CH_2Cl_2 (2:98) as an eluent, to afford compound **6** (54.3 mg). Subfraction HF_6 was repeated by FCC, eluted with an isocratic system of *n*-hexane-CH_2Cl_2-EtOAc (80:10:10) to provide two fractions ($HF_{6.1}$ and $HF_{6.2}$). Subfraction $HF_{6.2}$ was further purified by preparative TLC, using CH_2Cl_2-*n*-hexane (50:50) as eluent, to yield compound **2** (12.4 mg). Fraction HF_7 was chromatographed on FCC, eluted with CH_2Cl_2 to give two subfractions ($HF_{7.1}$ and $HF_{7.2}$). Subfraction $HF_{7.2}$ was repeated on FCC, eluting with an isocratic system of *n*-hexane-CH_2Cl_2-MeOH (48:50:2) to provide three subfractions ($HF_{7.2.1}$–$HF_{7.2.3}$). Compound **5** (13.4 mg) was obtained from subfractions $HF_{7.2.2}$ and $HF_{7.2.3}$ by preparative TLC using *n*-hexane-CH_2Cl_2-MeOH (48:50:2) as evaluated solvent. Fraction HF_8 was subjected by FCC, eluted with an isocratic system of *n*-hexane-$CHCl_2$-MeOH (48:50:2) to give four subfractions ($HF_{8.1}$–$HF_{8.4}$). Subfraction $HF_{8.2}$ was then purified by preparative TLC using *n*-hexane-CH_2Cl_2 (50:50) as eluent, to yield compound

3 (6.7 mg). Compound **4** (14.2 mg) was purified from subfraction HF$_{8.4}$ by preparative TLC using MeOH–CH$_2$Cl$_2$ (2:98) as eluent. Fraction HF$_9$ was separated by FCC, eluted with an isocratic system of n-hexane-CH$_2$Cl$_2$-MeOH (48:50:2) to give two subfractions (HF$_{9.1}$ and HF$_{9.2}$). Compound **7** (5.0 mg) was then recrystallized from subfraction HF$_{9.1}$ using MeOH. The crude EtOAc extract (7.3 g) was subjected to silica gel FCC and eluted with a gradient system of n-hexane-EtOAc and EtOAc-MeOH to obtain nine fractions (EF$_1$–EF$_9$). Fraction EF$_2$ was further purified by FCC, eluting with an isocratic system of n-hexane-CH$_2$Cl$_2$ (50:50), to yield compound **8** (74.2 mg). Fraction EF$_3$ had repeated FCC using CH$_2$Cl$_2$ as eluent to provide six subfractions (EF$_{3.1}$–EF$_{3.6}$). Subfraction EF$_{3.1}$ was purified by preparative TLC with CH$_2$Cl$_2$-n-hexane (50:50) as eluent, yielding an additional amount of compounds **8** (12.6 mg) and **2** (11.4 mg). Fraction EF$_8$ was separated by FCC, eluting with an isocratic system of n-hexane-CH$_2$Cl$_2$ (50:50), to give four subfractions (EF$_{8.1}$–EF$_{8.4}$). Subfraction EF$_{8.4}$ was further purified by preparative TLC using CH$_2$Cl$_2$-n-hexane (80:20) as eluent, to obtain compound **1** (6.8 mg). The crude MeOH extract (7.1 g) was subjected to FCC, eluted with a gradient system of EtOAc-MeOH, to provide four fractions (MF$_1$–MF$_4$). Fraction MF$_1$ was further subjected to FCC, eluting with a gradient system of n-hexane-CH$_2$Cl$_2$ to give three subfractions (MF$_{1.1}$–MF$_{1.3}$). Subfraction MF$_{1.1}$ was then purified by preparative TLC using n-hexane-CH$_2$Cl$_2$ (50:50) as eluent, to yield an additional amount of compound **8** (8.2 mg). The additional amount of compound **2** (6.0 mg) was purified by preparative TLC, eluting with n-hexane-CH$_2$Cl$_2$-MeOH (50:49:1). Fraction MF$_2$ was separated by FCC using a gradient system of n-hexane-EtOAc and EtOAc-MeOH as eluent, to give three subfractions (MF$_{2.1}$–MF$_{2.3}$). Subfraction MF$_{2.2}$ was further purified by preparative TLC, eluting with n-hexane-CH$_2$Cl$_2$ (50:50), to obtain an additional amount of compound **1** (5.4 mg).

3.3.1. *Methyl 8-hydroxy-3-hydroxymethylxanthone-1-carboxylate* (1)

Yellow needles; mp 152–155 °C; UV (CH$_2$Cl$_2$) λ_{max} (log ε): 234 (4.38), 259 (4.37), 287 (3.94), 366 (3.63) nm; IR (KBr) v_{max}: 3430, 2952, 2852, 1731, 1650, 1572, 1468, 1377 cm^{-1}; ^{1}H NMR (400 MHz, CDCl$_3$): δ 12.23 (1H, s, 8-OH), 7.57 (1H, t, J = 8.4 Hz, H-6), 7.53 (1H, brs, H-4), 7.26 (1H, brs, H-2), 6.88 (1H, d, J = 8.4 Hz, H-5), 6.80 (1H, d, J = 8.4 Hz, H-7), 4.85 (2H, s, H-10), 4.01 (3H, s, CO$_2$Me); ^{13}C NMR (100 MHz, CDCl$_3$): δ 180.7 (C-9), 169.6 (1-CO$_2$Me), 161.7 (C-8), 156.3 (C-4a), 155.7 (C-4b), 149.6 (C-3), 137.0 (C-6), 133.6 (C-1), 120.5 (C-2), 116.3 (C-4), 116.2 (C-9a), 110.9 (C-7), 108.9 (C-8a), 106.8 (C-5), 63.7 (C-10), 53.1 (1-COOMe); HRESITOFMS: m/z 301.0719 [M + H]$^+$ (calcd for C$_{16}$H$_{13}$O$_6$, 301.0712).

3.4. Biological activity procedures

3.4.1. Antimalarial assay

Antimalarial activity was evaluated against the parasite *Plasmodium falciparum* (K1, multi-drug resistant strain), using the method of Targer and Jensen (Trager & Jensen 1976). Quantitative assessment of malarial activity *in vitro* was determined by means of a micro-culture radioisotope technique based upon the method of Desjardins (Desjardins et al. 1979). The inhibitory concentration (IC$_{50}$) represents the concentration which causes 50% reduction in parasite growth as indicated by the *in vitro* uptake of [^{3}H]-hypoxanthine by *P. falciparum*. The standard compound was artemisinin.
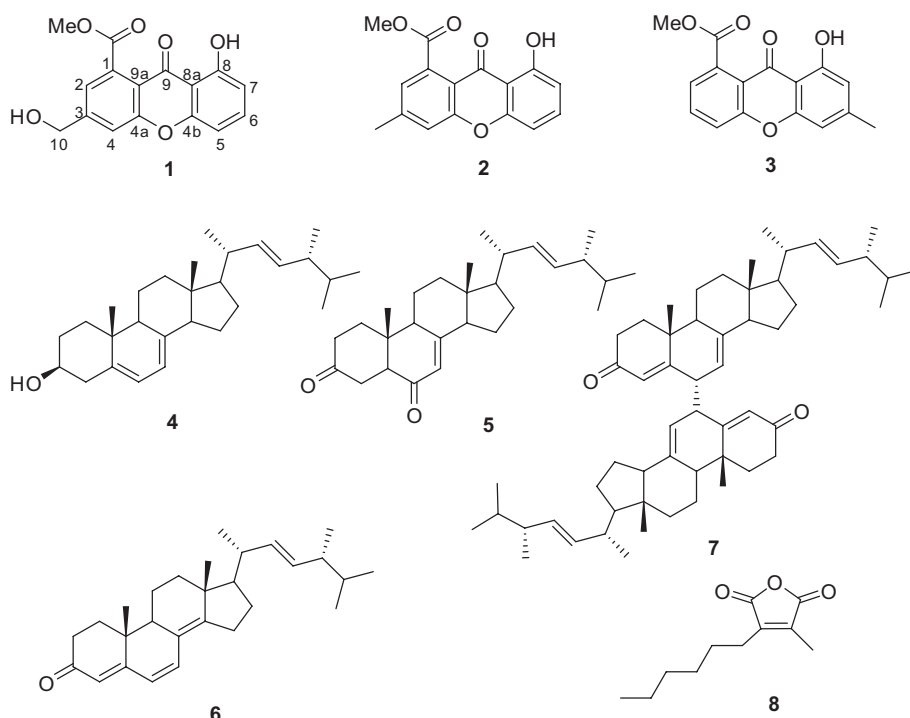
Figure 1. Structure of compounds **1**–**8**.

3.4.2. Antimycobacterial assay

Antimycobacterial activity was assessed against *Mycobacterium tuberculosis* H37Ra using the Microplate Alamar blue assay (MABA) (Collins & Franzblau 1997). The standard drug was isoniazid.

3.4.3. Cytotoxicity assay

Cytotoxicity assays against human epidermoid carcinoma (KB), human breast adenocarcinoma (MCF7) and human small cell lung cancer (NCI-H187) were performed employing the colorimetric method as described by Skehan and co-workers (Skehan et al. 1990). The reference substances were amphotericin B and ellipticine.

4. Conclusion

The investigation of constituents of the dried fungal biomass of *A. montagnei* led to the isolation of one new xanthone, methyl 8-hydroxy-3-hydroxymethylxanthone-1-carboxylate (**1**), and seven known compounds (**2**–**8**) (Figure 1). All of these compounds were reported from *A. montagnei* for the first time. The occurrence of xanthone derivatives (**1**–**3**) from this fungus is in agreement with the previous report (Klemke et al. 2004). This might be considered as one of markers for the fungus *A. montagnei*. The structures were elucidated by intensive spectroscopic analyses. Cyathisterone (**5**) exhibited weak cytotoxicity against NCI-H187 cancer cell. In addition, ergosta-4,6,8(14),22-tetraen-3-one (**6**) showed very weak cytotoxicity towards KB and NCI-H187 cancer cell lines.

References

Alfatafta AA, Gloer JB, Scott JA, Malloch D. 1994. Apiosporamide, a new antifungal agent from the coprophilous fungus *Apiospora montagnei*. J Nat Prod. 57:1696–1702.

Buttery RG, Seifert RM, Haddon WF, Lundin RE. 1980. 2-Hexyl-3-methylmaleic anhydride: an unusual volatile component of raisins and almond hulls. J Agric Food Chem. 28:1336–1338.

Collins LA, Franzblau SG. 1997. Microplate Alamar blue assay versus BATEC 460 system for high-throughput screening of compounds against *Mycobacterium tuberculosis* and *Mycobacterium avium*. Antimicrob Agents Chemother. 41:1004–1009.

Daengrot C, Rukachaisirikul V, Tadpetch K, Phongpaichit S, Bowornwiriyapan K, Sakayaroj J, Shen X. 2016. Penicillanthone and penicillidic acids A–C from the soil-derived fungus *Penicillium aculeatum* PSU-RSPG105. RSC Adv. 6:39700–39709.

Desjardins RE, Canfield CJ, Haynes JD, Chulay JD. 1979. Quantitative assessment of antimalarial activity *in vitro* by a semiautomated microdilution technique. Antimicrob Agents Chemother. 16:710–718.

Kachi H, Sassa T. 1986. Isolation of moniliphenone, a key intermediate in xanthone biosynthesis from *Monilinia fructicola*. Agric Biol Chem. 50:1669–1671.

Kawahara N, Sekita S, Satake M. 1994. Steroids from *Calvatia cyathiformis*. Phytochemistry. 37:213–215.

Kirk PM. 1991. *Apiospora montagnei*. IMI descriptions of fungi and bacteria. 1052:1–2.

Klemke C, Kehraus S, Wright AD, König GM. 2004. New secondary metabolites from the marine endophytic fungus *Apiospora montagnei*. J Nat Prod. 67:1058–1063.

Koguchi Y, Kohno J, Nishio M, Takahashi K, Okuda T, Ohnuki T, Komatsubara S. 2000. TMC-95A, B, C, and D, novel proteasome inhibitors produced by *Apiospora montagnei* Sacc. TC 1093. Taxonomy, production, isolation, and biological activities. J Antibiot. 53:105–109.

Kohno J, Koguchi Y, Nishio M, Nakao K, Kuroda M, Shimizu R, Ohnuki T, Komatsubara S. 2000. Structures of TMC-95A–D: novel proteasome inhibitors from *Apiospora montagnei* Sacc. TC 1093. J Org Chem. 65:990–995.

Li C, Zhang J, Shao C, Ding W, She Z, Lin Y. 2011. A new xanthone derivative from the co-culture broth of two marine fungi (strain No. E33 and K38). Chem Nat Compd. 47:382–384.

Ramos HP, Simão MR, de Souza JM, Magalhães LG, Rodrigues V, Ambrósio SR, Said S. 2013. Evaluation of dihydroisocoumarins produced by the endophytic fungus *Arthrinium* state of *Apiospora montagnei* against *Schistosoma mansoni*. Nat Prod Res. 27:2240–2243.

Skehan P, Storeng R, Scudiero D, Monks A, McMahon J, Vistica D, Warren JT, Bokesch H, Kenney S, Boyd MR. 1990. New colorimetric cytotoxicity assay for anticancer-drug screening. J Natl Cancer Inst. 82:1107–1112.

Smith FR, Korn ED. 1968. 7-Dehydrostigmasterol and ergosterol: the major sterols of an amoeba. J Lipid Res. 9:405–408.

Trager W, Jensen JB. 1976. Human malaria parasites in continuous culture. Science. 193:673–675.

Tian Y, Qin X, Lin X, Kaliyaperumal K, Zhou X, Liu J, Ju Z, Tu Z, Liu Y. 2015. Sydoxanthone C and acremolin B produced by deep-sea-derived fungus *Aspergillus* sp. SCSIO Ind09F01. J Antibiot. 68:703–706.

Mycotoxins from the Fungus *Botryotrichum piluliferum*

Oue-artorn Rajachan,[†] Kwanjai Kanokmedhakul,[*,†] Kasem Soytong,[§] and Somdej Kanokmedhakul[†]

[†]Natural Products Research Unit, Department of Chemistry and Center of Excellence for Innovation in Chemistry, Faculty of Science, Khon Kaen University, Khon Kaen 40002, Thailand

[§]Department of Plant Production Technology, Faculty of Agricultural Technology, King Mongkut's Institute of Technology Ladkrabang, Bangkok 10520, Thailand

Ⓢ Supporting Information

ABSTRACT: Two new sterigmatocystin derivatives, oxisterigmatocystins E and F (**1** and **2**, respectively), along with nine known compounds, oxisterigmatocystins G and H (**3** and **4**, respectively), sterigmatocystin (**5**), N-0532B (**6**), *O*-methylsterigmatocystin (**7**), N-0532A (**8**), 6-*O*-methylversicolorin A (**9**), 6,8-*O*-dimethylversicolorin A (**10**), and 8-*O*-methylaverufin (**11**), were isolated from the fungus *Botryotrichum piluliferum*. The structures of these mycotoxins were elucidated by spectroscopic evidence. Among these, compounds **3**, **4**, and **9** were discovered as natural products for the first time. Compounds **1**, **3**, and **4** displayed antimalarial activity toward *Plasmodium falciparum* (IC_{50} = 7.9−23.9 μM). In addition, compounds **1−6** and **8−11** exhibited cytotoxicity against KB, MCF-7, and NCI-H187 cell lines (IC_{50} = 0.38−78.6 μM). However, compounds **1−9** showed cytotoxic effects against the *Vero* cell line (IC_{50} = 0.65−12.3 μM). This finding should promote awareness of the contamination of *B. piluliferum* in the food chain and agricultural soil.

KEYWORDS: *Botryotrichum piluliferum*, *Chaetomiaceae*, sterigmatocystin, mycotoxin, cytotoxicity

■ INTRODUCTION

The fungus *Botryotrichum piluliferum* belongs to the family Chaetomiaceae.[1] Colonies grown on potato dextrose agar are white when young and turn pale brown when mature, at 30 °C in 7 days, with septate mycelia, branches, and setae. Conidia are chain-like on hyaline conidiophores, globose, 12.50−15.50 μm diameter, with irregularly thick walls of 3.0−3.5 μm. Teleomorphs were not found in this isolate. It was morphologically identified according to Domsch et al.[1] and Downing.[2] The fungus *B. piluliferum* has been reported as one of the seedborne fungi of chili pepper.[3] Previous chemical investigation on the genus *Botryotrichum* has reported it to contain asterriquinone CT2 from *Botryotrichum* spp.[4] and botryolides A−E,[5] decarestrictine D,[5] and sterigmatocystin[5] from *Botryotrichum* sp. (NRRL38180).[5] However, no studies on the chemical constituents and bioactivity of *B. piluliferum* have been found.

Many fungi such as *Aspergillus* species,[6] *Aschersonia coffeae* Henn. BCC 28712,[7] and *Penicillium chrysogenum*[8] including *Botryotrichum* sp. (NRRL 38180)[5] have been reported to produce mycotoxins. Mycotoxins have been reported as mutagenic and having carcinogenic effects in animals and humans.[9,10] In our continuing investigation on bioactive metabolites from fungi isolated from Thai soil, crude *n*-hexane and EtOAc extracts of *B. piluliferum* displayed cytotoxicity against the KB cell line with 85.5 and 59.7% inhibition, respectively, at a concentration of 50 μg/mL. Moreover, the EtOAc extract presented cytotoxicity toward the MCF-7 cell line with 57.5% inhibition. Herein, the isolation, structural elucidation, and bioactivities of 11 mycotoxins from *B. piluliferum* are presented.

■ MATERIALS AND METHODS

General Experimental Procedures. Optical rotations were measured on a DIP-1000 digital polarimeter (JASCO, Easton, MD, USA). IR spectra were obtained using a Bruker Tenser 27 spectrophotometer (Bruker, Ettlingen, Germany). UV spectra were recorded on an Agilent 8453 UV−visible spectrophotometer (Agilent Technologies, Santa Clara, CA, USA). NMR spectra were acquired on a Varian Mercury Plus 400 spectrometer (Varian, Palo Alto, CA, USA). HRESI-TOFMS were recorded on a Micromass Q-TOF 2 hybrid quadrupole time-of-flight (Q-TOF) mass spectrometer (Micromass, Manchester, UK). Silica gel 60 (Merck, Darmstadt, Germany) 230−400 mesh was used for CC. TLC was performed on precoated silica gel 60 PF254 (Merck).

Fungal Material. The fungus strain (no. Bp01) was isolated from forest soil collected from Three Pagoda Pass, Sangkhla Buri, Kanchanaburi province, Thailand, in 2010. It was identified as *B. piluliferum* by K. Soytong, one of the co-authors. The fungus was cultured at 25−28 °C for 9 weeks using the method described in our previous paper.[11] The biomass was collected by filtering, air-dried, and ground into a powder.

Extraction and Isolation. The biomass powder of *B. piluliferum* (240 g) was extracted successively with *n*-hexane (1 L × 3), EtOAc (1 L × 3), and MeOH (1 L × 3) by stirring at room temperature. The *n*-hexane extract (5.7 g) was separated by silica gel flash column chromatography (FCC) (45 × 5 cm), eluting with a mixture of *n*-hexane/EtOAc (95:5, 90:10, 80:20, 70:30, 60:40, 40:60, 20:80, 0:100 v/v, 300 mL each) and EtOAc/MeOH (90:10, 80:20, 70:30, 50:50, 30:70, 0:100 v/v, 300 mL each), to give 36 fractions. Analysis of TLC characteristics gave five pooled fractions, FH_1−FH_5. Recrystallization of fraction FH_1 (76 mg) from CH_2Cl_2 yielded **9** (30 mg). Fraction FH_2 (196 mg) was purified using preparative TLC, eluted with 101

Table 1. ^{1}H and ^{13}C NMR Spectroscopic Data for Compounds 1−4

	1		2		3		4	
position	δ_H	δ_C	δ_H	δ_C	δ_H	δ_C	δ_H	δ_C
1		163.7		163.6		163.4		163.3
2	6.38 s	90.9	6.38 s	90.4	6.33 s	90.6	6.33 s	90.2
3		163.7		163.9		163.1		163.3
4		105.9		106.2		105.6		106.0
4a		153.6		153.3		153.5		153.2
5	7.08 d (9.0)[a]	113.7	7.14 d (9.0)	113.8	6.89 d (8.4)	109.0	6.93 d (8.4)	109.1
6	7.58 d (9.0)	134.2	7.61 d (9.0)	134.3	7.48 t (8.4)	133.7	7.49 t (8.4)	133.7
7		124.7		124.8	6.75 d (8.4)	106.4	6.77 d (8.4)	106.5
8		156.2		156.3		160.7		160.8
8a		119.1		119.2		113.9		114.0
9		173.9		174.2		175.2		175.3
9a		108.4		108.2		109.1		108.9
10a		154.7		154.8		156.7		156.8
1′	6.51 d (6.0)	112.6	6.55 d (6.0)	113.8	6.48 d (6.0)	112.4	6.51 d (6.0)	113.6
2′	4.30 ddd (9.6, 7.2, 6.0)	42.6	4.26 ddd (7.2, 6.0, 2.4)	42.7	4.28 ddd (10.4, 6.0, 4.0)	42.7	4.25 dd (10.4, 6.0)	42.7
3′	2.55 m	37.1	2.54 dd (7.2, 4.0)	37.0	2.54 td (8.4, 4.0)	37.1	2.54 dd (6.0, 2.4)	37.0
4′	6.39 dd (9.6, 4.0)	98.6	6.46 brd (4.0)	98.7	6.38 t (4.0)	98.6	6.43 brd (2.4)	98.7
5′		169.8		169.8		169.8		169.8
6′	2.11 s	21.2	1.69 s	21.1	2.10 s	21.2	1.67 s	21.1
1-OMe	3.96 s	56.9	3.97 s	56.9	3.91 s	56.7	3.91 s	56.5
8-OMe	4.03 s	62.0	4.05 s	62.0	3.95 s	56.5	3.95 s	56.7

[a] Values in parentheses are coupling constants in hertz.

mL of *n*-hexane/CH$_2$Cl$_2$/MeOH (40:60:1, developed six times) to give **5** (44 mg, R_f = 0.47) and **6** (13 mg, R_f = 0.56). Fraction FH$_3$ (681 mg) was further subjected to a silica gel FCC (45 × 3 cm) eluting with 1.8 L of an isocratic system of *n*-hexane/CH$_2$Cl$_2$ (40:60) to give **10** (3 mg) and **8** (41 mg). Fraction FH$_4$ (154 mg) was subjected to Sephadex LH-20 (45 × 2 cm), eluting with 400 mL of MeOH to yield **11** (17 mg). Compound **7** (9 mg, R_f = 0.42) was obtained from FH$_5$ (102 mg) using preparative TLC with hexane/CH$_2$Cl$_2$/MeOH (5:95:2, developed three times). The EtOAc extract (9.3 g) was chromatographed on silica gel FCC (45 × 6 cm), eluting with a mixture of *n*-hexane/acetone (100:0, 90:10, 80:20, 70:30, 60:40, 40:60, 20:80, 0:100 v/v, 500 mL each) followed by acetone/MeOH (90:10, 80:20, 70, 60:40, 50:50, 30:70, 0:100 v/v, 300 mL each) to give 41 collected fractions. On the basis of their TLC characteristics, these gave six pooled fractions, FE$_1$−FE$_6$. Fraction FE$_4$ (325 mg) was chromatographed over silica gel FCC (45 × 3 cm), eluting with 1.5 L of *n*-hexane/CH$_2$Cl$_2$ (20:80) and pooled to two subfractions, FE$_{4.1}$ (62 mg) and FE$_{4.2}$ (115 mg). Fraction FE$_{4.1}$ was purified using preparative TLC and eluted with 100 mL of CH$_2$Cl$_2$/MeOH (98:2, developed three times) to afford **1** (7 mg, R_f = 0.49). Fraction FE$_5$ (1.25 g) was placed on silica gel FCC (45 × 4 cm), eluted with 2.4 L of an isocratic system of CH$_2$Cl$_2$/EtOAc (97:3), and pooled to two subfractions, FE$_{5.1}$ (102 mg) and FE$_{5.2}$ (720 mg). Subfraction FE$_{5.1}$ was purified using preparative TLC and eluted with 101 mL of CH$_2$Cl$_2$/EtOAc/MeOH (70:30:1, developed six times) to yield **3** (15 mg, R_f = 0.64) and **4** (11 mg, R_f = 0.57). The MeOH extract (16.1 g) was applied to silica gel FCC (45 × 6 cm), eluted with a mixture of *n*-hexane/EtOAc (100:0, 90:10, 80:20, 70:30, 60:40, 40:60, 20:80, 0:100 v/v, 300 mL each) and EtOAc/MeOH, (90:10, 80:20, 70:30, 60:40, 50:50, 30:70, 0:100 v/v, 300 mL each) to give 32 collected fractions. On the basis of their TLC characteristics, these gave four pooled fractions, FM$_1$−FM$_4$. Fraction FM$_2$ (97 mg) was chromatographed on silica gel FCC, eluting with an isocratic system of CH$_2$Cl$_2$/EtOAc (70:30, 1 L) to give **11** (6 mg). Purification of FM$_3$ (150 mg) by preparative TLC, using 101 mL of CH$_2$Cl$_2$/EtOAc/MeOH (75:25:1, developed four times), gave **1** (4 mg, R_f = 0.77) and **2** (3 mg, R_f = 0.72).

Oxisterigmatocystin E, 1: pale yellow solid; mp 223−224 °C; $[\alpha]^{25}_D$ −121.7 (*c* 0.1, CHCl$_3$); UV (MeOH) λ_{max} (log ε) 224 (3.59), 245 (3.67), 307 (3.19) nm; IR (film, CH$_2$Cl$_2$) ν_{max} 2932, 2852, 1749, 1664, 1639, 1593, 1418, 1228, 1084 cm^{-1}; ^{1}H and ^{13}C NMR data

(CDCl$_3$, 400 and 100 MHz) (Table 1); HR-ESI-TOFMS *m/z* 433.0677 [M + H]$^+$ (calcd for C$_{21}$H$_{17}$ClO$_8$ + H, 433.0690), *m/z* 435.0666 [M + 2 + H]$^+$ (calcd for C$_{21}$H$_{17}$ClO$_8$ + 2 + H, 435.0661).

Oxisterigmatocystin F, 2: pale yellow solid; mp 184−185 °C; $[\alpha]^{25}_D$ −196.5 (*c* 0.1, CHCl$_3$); UV (MeOH) λ_{max} (log ε) 220 (3.50), 243 (3.69), 309 (3.10) nm; IR (film, CH$_2$Cl$_2$) ν_{max} 2928, 2853, 1752, 1659, 1634, 1591, 1452, 1222, 1080 cm^{-1}; ^{1}H and ^{13}C NMR data (CDCl$_3$, 400 and 100 MHz) (Table 1); HR-ESI-TOFMS *m/z* 433.0689 [M + H]$^+$ (calcd for C$_{21}$H$_{17}$ClO$_8$ + H, 433.0690), *m/z* 435.0674 [M + 2 + H]$^+$ (calcd for C$_{21}$H$_{17}$ClO$_8$ + 2 + H, 435.0661).

Oxisterigmatocystin G, 3: pale yellow solid; mp 202−203 °C; $[\alpha]^{25}_D$ −99.5 (*c* 0.1, CHCl$_3$); UV (MeOH) λ_{max} (log ε) 207 (3.43), 238 (3.53), 307 (3.13) nm; IR (film, CH$_2$Cl$_2$) ν_{max} 2929, 2863, 1752, 1659, 1635, 1591, 1462, 1223, 1081 cm^{-1}; ^{1}H and ^{13}C NMR data (CDCl$_3$, 400 and 100 MHz) (Table 1); HR-ESI-TOFMS *m/z* 399.1099 [M + H]$^+$ (calcd for C$_{21}$H$_{18}$O$_8$ + H, 399.1080).

Oxisterigmatocystin H, 4: pale yellow solid; mp 180−182 °C; $[\alpha]^{25}_D$ −198.2 (*c* 0.1, CHCl$_3$); UV (MeOH) λ_{max} (log ε) 205 (3.70), 237 (3.72), 309 (3.42) nm; IR (film, CH$_2$Cl$_2$) ν_{max} 2848, 1752, 1659, 1641, 1600, 1471, 1267, 1100 cm^{-1}; ^{1}H and ^{13}C NMR data (CDCl$_3$, 400 and 100 MHz) (Table 1); HR-ESI-TOFMS *m/z* 399.1097 [M + H]$^+$ (calcd for C$_{21}$H$_{18}$O$_8$ + H, 399.1080).

6-O-Methylversicolorin A, 9: yellow needles; mp 233−235 °C; $[\alpha]^{25}_D$ −312.8 (*c* 0.1, CHCl$_3$); UV (MeOH) λ_{max} (log ε) 229 (3.34), 288 (3.54), 445 (3.06) nm; IR (film, CH$_2$Cl$_2$) ν_{max} 2927, 2852, 1629, 1613, 1579, 1383, 1305, 1212, 1155 cm^{-1}; ^{1}H NMR (CDCl$_3$, 400 MHz) δ 3.92 (3H, s, OMe-6), 4.72 (1H, dt, *J* = 7.2, 2.4 Hz, H-2′), 5.44 (1H, t, *J* = 2.4 Hz, H-3′), 6.50 (1H, t, *J* = 2.4 Hz, H-4′), 6.65 (1H, d, *J* = 2.4 Hz, H-7), 6.81 (1H, d, *J* = 7.2 Hz, H-1′), 7.32 (1H, d, *J* = 2.4 Hz, H-5), 7.33 (1H, s, H-4), 12.26 (1H, s, OH-8), and 12.38 (1H, s, OH-1); ^{13}C NMR (CDCl$_3$, 100 MHz) δ 48.3 (C-2′), 56.2 (OMe-6), 101.9 (C-3′), 103.6 (C-4), 107.0 (C-7), 108.6 (C-5), 110.0 (C-8a), 112.0 (C-9a), 113.1 (C-1′), 120.7 (C-2), 135.1 (C-4a), 136.0 (C-10a), 145.7 (C-4′), 159.6 (C-1), 164.8 (C-3), 165.2 (C-8), 166.5 (C-6), 181.5 (C-10), and 190.3 (C-9); HR-ESI-TOFMS *m/z* 375.0481 [M + Na]$^+$ (calcd for C$_{19}$H$_{12}$O$_7$ + Na, 375.0481).

Antimalarial Assay. The antimalarial assay was carried out using a method described by Trager and Jensen[12] and Desjardins et al.[13] as described in our previous paper.[11]

Cytotoxicity Assays. Cytotoxicity assays against three cancer cell lines, KB, MCF-7, and NCI-H187, were carried out by O'Brien's method.[14] The cytotoxicity assays against *Vero* cell used the method described by Hunt and co-workers,[15] as in our previous paper.[11]

■ RESULTS AND DISCUSSION

The chromatographic separation of biomass powder of *B. piluliferum* gave two new sterigmatocystin derivatives, **1** and **2**, and nine known compounds, **3−11** (Figure 1). Their
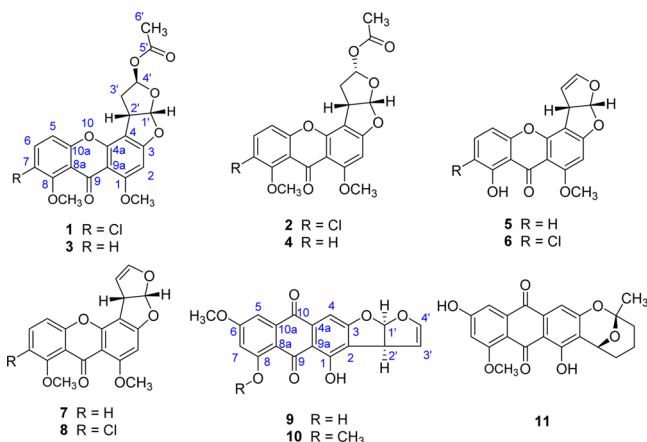

Figure 1. Structures of the isolated compounds **1−11**.

structures were identified by spectroscopic data and by comparing the data obtained to those of related known compounds published in the literature. They were oxister-igmatocystins E and F (**1** and **2**, respectively), oxisterigmato-cystins G and H (**3** and **4**, respectively), sterigmatocystin (**5**),[16] N-0532B (**6**),[17] O-methylsterigmatocystin (**7**),[18] N-0532A (**8**),[17] 6-O-methylversicolorin A (**9**), 6,8-O-dimethylversicolor-in A (**10**),[19] and 8-O-methylaverufin (**11**).[7] Compounds **3**, **4**, and **9** were isolated from the natural source for the first time.

Compounds **1** and **2** had the molecular formula $C_{21}H_{17}ClO_8$, derived from ^{13}C NMR and HR-ESI-TOFMS, signifying 13 indices of hydrogen deficiency. The IR spectra of compounds **1** and **2** showed absorption bands for ester (1749/1752 cm^{-1}), aromatic ketone (1664/1659 cm^{-1}), and aromatic (1418/1452 cm^{-1}) groups. The ^{13}C NMR and DEPT spectra of these two compounds indicated 21 carbon signals attributable to 3 methyls (2 methoxy and an acetoxy group), a methylene, 3 sp^2 methines, 3 sp^3 methines, and 11 sp^2 quaternary (including two carbonyl) carbons. The ^1H and ^{13}C NMR spectroscopic data of **1** (Table 1) agreed with those of isolated N-0532A (**8**),[17] except that the double bond at C-3′ was saturated by a proton at C-3′ [$\delta_{H/C}$ 2.55 (m, H$_2$-3′)/37.1] and an acetoxy group at C-4′ [$\delta_{H/C}$ 2.11(s)/21.2, δ_C 169.8]. The three resonances of aromatic protons appeared at δ 6.38 (s, H-2), 7.08 (d, J = 9.0 Hz, H-5), and 7.58 (d, J = 9.0 Hz, H-6). Correlations of H-1′/H-2′/H$_2$-3′/H-4′ in the COSY spectrum confirmed the lack of a double bond at C-3′ of the bishydrofuran unit. The HMBC also indicated the connectivity of an acetoxy group through C-4′ by showing correlations of H$_3$-6′ to C-5′ and C-4′ and H-4′ to C-5′ (Figure 2).

The ^1H and ^{13}C NMR spectroscopic data of **2** (Table 1) were similar to those of **1**, except that the resonance of methyl protons of the acetoxy group at C-4′ of **2** (δ 1.69) appeared at a higher field than that of **1** (δ 2.11). The coupling constants between H-1′ and H-2′ (J = 6.0 Hz) and the NOESY
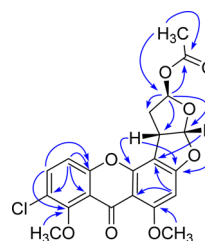

Figure 2. Selected HMBC correlations of compound **1**.

correlations of the two protons of **1** and **2** revealed a *cis* ring fusion, the same as in the sterigmatocystin (**5**),[18,20,21] which allowed assignment of the absolute configurations at both C-1′ and C-2′ as *S*. The assignment of configurations at C-4′ of **1** and **2** as *R* and *S* were determined by comparing the ^1H NMR resonances of an acetoxy group to those reported for related analogues, dothistromin pentaacetate[22] and oxisterigmatocystin D.[23] The methyl protons of the 4′-acetoxy group of **2** appeared at a higher field (δ_H 1.69) than in **1** (δ_H 2.11), agreeing with that reported for *endo* dothistromin pentaacetate (δ_H 1.67),[22] which was due to the strong shielding effect of xanthone (Figure 3). On the other hand, the 4′-acetoxy group of **1** showed a resonance at δ_H 2.11, suggesting the *exo* arrangement (Figure 3), which corresponds to that of oxisterigmatocystin D (δ_H 2.07).[23] Furthermore, the optical rotation value of **1** was different from that of **2**, suggesting the different configurations at C-4′ of the two compounds. On the basis of the above evidence, the structure of **1**, oxisterigmatocystin E, was determined as a new sterigmatocystin derivative. Compound **2**, oxisterigmatocystin F, was identified as the C-4′ epimer of **1** (Figure 1).

Compounds **3** and **4** possessed a molecular formula of $C_{21}H_{18}O_8$ from ^{13}C NMR and HR-ESI-TOFMS, indicating 13 degrees of hydrogen deficiency. IR spectra of both **3** and **4** showed bands for ester (1752/1752 cm^{-1}), aromatic ketone (1659/1659 cm^{-1}), and aromatic (1462/1471 cm^{-1}) groups. Their ^{13}C NMR and DEPT spectra displayed 21 carbon signals attributable to 3 methyls (2 methoxy groups and an acetoxy group), a methylene, 4 sp^2 methines, 3 sp^3 methines, and 10 sp^2 quaternary (including two carbonyl) carbons. The ^1H NMR, ^{13}C NMR, and DEPT spectroscopic data of **3** (Table 1) were similar to those of **1**, except for the presence of an additional sp^2 methine proton at C-7 [δ_H 6.75 (d, J = 8.4 Hz, H-7)]. This information, together with the absence of Cl isotope in the MS data, established that the chlorine atom was displaced by an sp^2 methine proton. The COSY spectrum showed correlations of H-5/H-6/-H-7, indicating trisubstitution of the aromatic ring. The HMBC spectrum of **3** clearly demonstrated correlations of H-7 to C-8a and C-5, H-6 to C-8 and C-10a, and H-5 to C-7, C-8a, and C-10a, confirming the structure of **3**. Because the resonances of acetoxy groups of **3** (δ_H 2.10) and **4** (δ_H 1.67) appeared at low and high fields in the same manner as those of **1** and **2**, the configurations at C-4′ of **3** and **4** were assigned as *R* and *S*, respectively. Moreover, the optical rotation values of **3** and **4** were comparable to those of **1** and **2**, respectively. However, compounds **3** and **4** have been previously reported as synthetic mixture products during the preparation of O-methylsterigmatocystin (**7**).[24] This is the first isolation of compounds **3** and **4** from a natural source, and they have been named oxisterigmatocystin G (**3**) and oxisterigmatocystin H (**4**). Their spectroscopic data were also reported.
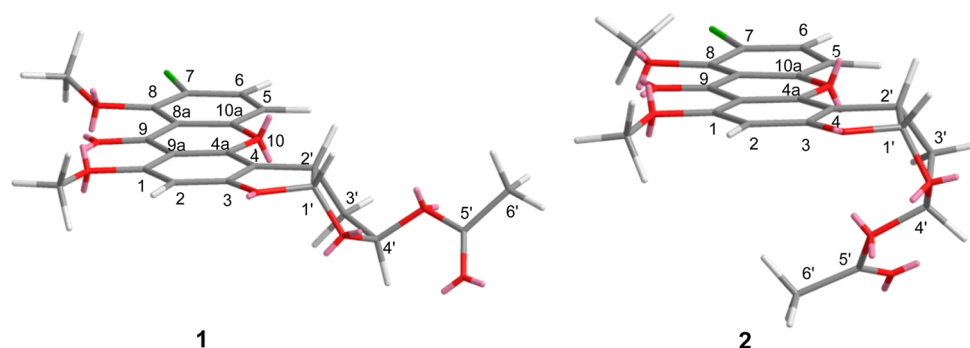
Figure 3. Structures of **1** (*exo*-form) and **2** (*endo*- form), energy minimized using MM2.

Table 2. Biological Activity of Compounds 1−11

compound	antimalarial IC$_{50}$ (μM)	cytotoxicity IC$_{50}$ (μM)			
		KB[a]	MCF-7[b]	NCI-H187[c]	Vero cell[d]
1	7.9	7.7	78.6	10.9	9.7
2	>100	25.5	38.7	25.7	4.3
3	14.7	3.5	6.9	11.6	1.6
4	23.9	25.1	33.6	22.8	6.0
5	>100	>100	>100	70.3	0.82
6	>100	>100	>100	62.2	0.65
7	>100	>100	>100	>100	12.3
8	>100	>100	>100	35.3	2.3
9	>100	>100	36.1	2.1	2.5
10	>100	>100	>100	0.38	>100
11	>100	>100	>100	44.9	>100
dihydroartemisinin	0.004				
doxorubicin		0.83	17.0	0.16	
ellipticine		4.9		4.7	2.5

[a]Human epidermoid carcinoma in the mouth. [b]Human breast adenocarcinoma. [c]Human small cell lung cancer. [d]African green monkey kidney.

Compound **9** had the molecular formula C$_{19}$H$_{12}$O$_7$, deduced from ^{13}C NMR and HR-ESI-TOFMS, requiring 14 degrees of hydrogen deficiency. The IR spectrum displayed absorption bands for aromatic ketones (1629 and 1613 cm^{-1}) and aromatic (1579 cm^{-1}) groups. The ^{13}C NMR and DEPT spectra displayed 19 carbon signals for a methoxy, 5 sp^2 methines, 2 sp^3 methines, and 11 sp^2 quaternary (including two carbonyl) carbons. Careful examination of 1D and 2D NMR data indicated that the structure of **9** was similar to that of 6,8-*O*-dimethylversicolorin A, which has been previously reported as a methylation product of versicolorin A.[25] The HMBC spectrum revealed correlations of hydroxyl proton at C-8 to C-7, C-8, and C-8a, confirming the position of the hydroxyl group at C-8. Besides, the correlations of H-4 to C-2, C-3, C-10, and C-9a, H-5 to C-7, C-8a, and C-10, H-7 to C-5, C-6, C-8, and C-8a, H-1′ to C-3, C-2′, C-3′, and C-4′, H-3′ to C-1′ and C-2′, H-4′ to C-2′, methoxyl protons at C-6 to C-6, and hydroxyl proton (OH-1) to C-1, C-2, and C-9a indicated the structure of **9**. The absolute configuration of **9** was assigned to be the same as that of 6,8-*O*-dimethylversicolorin A (**10**) by comparing their optical rotations, −320 (c 0.12, dioxane) for **10**[19] and −312.8 (c 0.1, CHCl$_3$) for **9**. Thus, this is the first report of 6-*O*-methylversicolorin A (**9**) isolated from a natural source.

Compounds **1**, **3**, and **4** showed antimalarial activity against *P. falciparum* with IC$_{50}$ values of 7.9, 14.7, and 23.9 μM, respectively. Compounds **1−4** exhibited cytotoxicity against three cancer cell lines (KB, MCF-7, and NCI-H187) with IC$_{50}$

values ranging from 3.5 to 78.6 μM. Compound **3** showed significant cytotoxicity against KB cells with an IC$_{50}$ value of 3.5 μM, which is lower than that of the control drug ellipticine. Furthermore, **3** was cytotoxic against the MCF-7 cell line with an IC$_{50}$ value of 6.9 μM, which is lower than that of the control drug doxorubicin. However, **3** was highly cytotoxic toward the normal cell line (*Vero* cell) with an IC$_{50}$ value of 1.6 μM, which is lower than the that of the control drug ellipticine, 2.5 μM. Among compounds **1−4**, the influence of an *exo* versus an *endo* arrangement was noted. The *exo* arrangements in **1** and **3** showed both higher antimalarial activity and cytotoxicity against cancer cells than their *endo* analogues, **2** and **4**. It should be noted that the missing double bond at C-3′ and the presence of an acetoxy group at C-4′ of sterigmatocystin derivatives **1−4** would play important roles for cytotoxicity enhancement when compared to derivatives **5−8**. Moreover, the double bond at C-3′ and C-4′ of sterigmatocystin derivatives **5−8** exhibited no cytotoxicity (>100 μM) toward KB and MCF-7, which corresponds to the results for related structures in a previous paper.[7] In addition, compounds **9** and **10** showed strong cytotoxicity against the NCI-H187 cell line with IC$_{50}$ values of 2.1 and 0.38 μM, respectively, which were lower than that of the control drug ellipticine. By comparison between compounds **9** and **10**, the presence of a methoxy group at C-8 led to a decrease in cytotoxicity toward normal cells. Interestingly, compound **10** was not cytotoxic against *Vero* cells and should be further studied in detail. However, most of

the isolated compounds showed cytotoxicity against *Vero* cells with IC_{50} values in the range from 0.65 to 12.3 μM (Table 2).

Sterigmatocystin (**5**) has been reported to contaminate foodstuffs such as wheat, rice, coffee bean, corn, and red pepper. Furthermore, it has been discovered in cheese contaminated with *Aspergillus versicolor*.[9] On the basis of our results, most isolated compounds from *B. piluliferum* are mycotoxins with structures metabolically related to the aflatoxin carcinogen. These mycotoxins could be responsible for the toxicity of the fungus *B. piluliferum*. As mentioned above, the fungus *B. piluliferum* was found in the seeds of chili pepper,[3] and so the contamination of *B. piluliferum* in the food chain and agricultural soil should be monitored.

ASSOCIATED CONTENT

Ⓢ Supporting Information

The Supporting Information is available free of charge on the ACS Publications website at DOI: 10.1021/acs.jafc.6b05522.

> ^{1}H and ^{13}C NMR and 2D NMR spectra for compounds **1–4** and **9** (PDF)

AUTHOR INFORMATION

Corresponding Author

*(K.K.) Phone: +66 043-009700, ext. 42174-5. Fax: +66-43-202373. E-mail: kwanjai@kku.ac.th.

ORCID Ⓘ

Kwanjai Kanokmedhakul: 0000-0002-3237-2920

Notes

The authors declare no competing financial interest.

ACKNOWLEDGMENTS

REFERENCES

(1) Domsch, K. H.; Gams, W.; Anderson, T.-H. *Compendium of Soil Fungi*, 1st ed.; IHW-Verlag: Eching, Germany, 1993; 859 pp.

(2) Downing, M. H. *Botryotrichum* and *Coccospora. Mycologia* **1953**, *45*, 934–940.

(3) Chigoziri, E.; Ekefan, E. J. Seed borne fungi of chili pepper (*Capsicum frutescens*) from pepper producing areas of Benue State, Nigeria. *Agric. Biol. J. North Am.* **2013**, *4*, 370–374.

(4) Mocek, U.; Schultz, L.; Buchan, T.; Baek, C.; Fretto, L.; Nzerem, J.; Sehl, L.; Sinha, U. Isolation and structure elucidation of five new asterriquinones from *Aspergillus, Humicola* and *Botryotrichum* species. *J. Antibiot.* **1996**, *49*, 854–859.

(5) Sy, A. A.; Swenson, D. C.; Gloer, J. B.; Wicklow, D. T. Botryolides A–E, decarestrictine analogues from a fungicolous *Botryotrichum* sp. (NRRL 38180). *J. Nat. Prod.* **2008**, *71*, 415–419.

(6) Jurjević, Ž.; Peterson, S. W.; Solfrizzo, M.; Peraica, M. Sterigmatocystin production by nine newly described *Aspergillus* species in section *Versicolores* grown on two different media. *Mycotoxin Res.* **2013**, *29*, 141–145.

(7) Kornsakulkarn, J.; Saepua, S.; Srichomthong, K.; Supothina, S.; Thongpanchang, C. New mycotoxins from the scale insect fungus *Aschersonia coffeae* Henn. BCC 28712. *Tetrahedron* **2012**, *68*, 8480–8486.

(8) Maskey, R. P.; Grün-Wollny, I.; Laatsch, H. Isolation, structure elucidation and biological activity of 8-*O*-methylaverufin and 1,8-*O*-dimethylaverantin as new antifungal agents from *Penicillium chrysogenum. J. Antibiot.* **2003**, *56*, 459–463.

(9) Veršilovskis, A.; De Saeger, S. Sterigmatocystin: occurrence in foodstuffs and analytical methods − an overview. *Mol. Nutr. Food Res.* **2010**, *54*, 136–147.

(10) Mori, H.; Kawai, K.; Ohbayashi, F.; Kuniyasu, T.; Yamazaki, M.; Hamasaki, T.; Williams, G. M. Genotoxicity of a variety of mycotoxins in the hepatocyte primary culture/DNA repair test using rat and mouse hepatocytes. *Cancer Res.* **1984**, *44*, 2918–2923.

(11) Rajachan, O.-A.; Kanokmedhakul, S.; Kanokmedhakul, K.; Soytong, K. Bioactive depsidones from the fungus *Pilobolus heterosporous. Planta Med.* **2014**, *80*, 1635–1640.

(12) Trager, W.; Jensen, J. B. Human malaria parasites in continuous culture. *Science* **1976**, *193*, 673–675.

(13) Desjardins, R. E.; Canfield, C. J.; Haynes, J. D.; Chulay, J. D. Quantitative assessment of antimalarial activity in vitro by a semiautomated microdilution technique. *Antimicrob. Agents Chemother.* **1979**, *16*, 710–718.

(14) O'Brien, J.; Wilson, I.; Orton, T.; Pognan, F. Investigation of the Alamar Blue (resazurin) fluorescent dye for the assessment of mammalian cell cytotoxicity. *Eur. J. Biochem.* **2000**, *267*, 5421–5426.

(15) Hunt, L.; Jordan, M.; De Jesus, M.; Wurm, F. M. GFP-expressing mammalian cells for fast, sensitive, noninvasive cell growth assessment in a kinetic mode. *Biotechnol. Bioeng.* **1999**, *65*, 201–205.

(16) Fremlin, L. J.; Piggott, A. M.; Lacey, E.; Capon, R. J. Cottoquinazoline A and cotteslosins A and B, metabolites from an Australian marine-derived strain of *Aspergillus versicolor. J. Nat. Prod.* **2009**, *72*, 666–670.

(17) Nishino, Y.; Takawa, N.; Mitsumori, N.; Seki, T. Chemical compound N-0532, the manufacturing method and application. Jpn. Kokai Tokkyo Koho, JP 11080162 A, March 26, 1999.

(18) Cox, R. H.; Cole, R. J. Carbon-13 nuclear magnetic resonance studies of fungal metabolites, aflatoxins, and sterigmatocystins. *J. Org. Chem.* **1977**, *42*, 112–114.

(19) Hatsuda, Y.; Hamasaki, T.; Ishida, M.; Kiyama, Y. 6,8-*O*-Dimethylversicolorin A, a new metabolite from *Aspergillus versicolor. Agric. Biol. Chem.* **1971**, *35*, 444.

(20) Zhu, F.; Lin, Y. Three xanthones from a marine-derived mangrove endophytic fungus. *Chem. Nat. Compd.* **2007**, *43*, 132–135.

(21) Cai, S.; Zhu, T.; Du, L.; Zhao, B.; Li, D.; Gu, Q. Sterigmatocystins from the deep-sea-derived fungus *Aspergillus versicolor. J. Antibiot.* **2011**, *64*, 193–196.

(22) Gallagher, R. T.; Hodges, R. The chemistry of dothistromin, a difuronanthraquinone from *Dothistroma pini. Aust. J. Chem.* **1972**, *25*, 2399–2407.

(23) Zhao, H.; Wang, G.-Q.; Tong, X.-P.; Chen, G.-D.; Huang, Y.-F.; Cui, J.-Y.; Kong, M.-Z.; Guo, L.-D.; Zheng, Y.-Z.; Yao, X.-S.; Gao, H. Diphenyl ethers from *Aspergillus* sp. and their anti-Aβ_{42} aggregation activities. *Fitoterapia* **2014**, *98*, 77–83.

(24) Rance, M. J.; Roberts, J. C. Total synthesis of (±)-*O*-methylsterigmatocystin. *Tetrahedron Lett.* **1970**, *11*, 2799–2802.

(25) Gorst-Allman, C. P.; Steyn, P. S.; Wessels, P. L.; Scott, D. B. Carbon-13 nuclear magnetic resonance assignments and biosynthesis of versicolorin A in *Aspergillus parasiticus. J. Chem. Soc., Perkin Trans. 1* **1978**, No. 9, 961.

Bicyclic lactones and racemic mixtures of dimeric styrylpyrones from the leaves of *Miliusa velutina*†

N. Wongsa,[ab] K. Kanokmedhakul, [ID]*[a] J. Boonmak, [ID][c] S. Youngme[c] and S. Kanokmedhakul[a]

A unique class of eight bicyclic lactones with a C_{18} carbon architecture, named velutinones A–H (**1–8**), three new dimeric styrylpyrones, velutinindimers A–C (**9–11**), five known compounds, the kawapyrone, yangonin (**12**), three flavonoids (**13–15**), and an acetogenin, cananginone H (**16**) were isolated from the leaves of *Miliusa velutina*. The absolute configurations of **2** and **5** were assigned by Mosher's method, whereas ECD, optical rotations, and X-ray crystallographic analysis indicated the racemic nature of compounds **10** and **11**. Compounds **2–4** and **7–11** showed antimalarial activity with IC_{50} values in the range of 5.4–10.0 μM. Moreover, **1–4** and **6–8** displayed cytotoxicity against the KB, MCF7, and NCI-H187 cancer cell lines and Vero cell lines with IC_{50} values in the range of 4.0–24.1 μM.

1. Introduction

Miliusa velutina (Dunal) Hook. f. & Thomson belongs to the family Annonaceae. This plant is found widely in Thailand with local names "Khang hua mu" or "Kong kang". A water decoction of the wood is used traditionally as a tonic and an aphrodisiac.[1] The genus *Miliusa* comprises *ca.* 50 species distributed from India, South East Asia, to Australia. At least 19 species of *Miliusa*, have been found in Thailand.[2,3] Eight of the *Miliusa* genera growing worldwide have been investigated for their phytochemistry and biological activities.[4–19] Among these species, a Thai medicinal plant, *M. velutina*, has been shown to contain the acetogenin, goniothalamusin,[17] an aporphine alkaloid, (+)-isocorydine α-*N*-oxide,[18] and four alkaloids, reticuline, liriodenine, norcorydine, and isocorydine.[19] Recently, the isolation and characterization of the linear acetogenins, cananginones A–I from the stem bark of *M. velutina* were reported.[20,21] In a continued investigation of this plant, the crude *n*-hexane and EtOAc extracts from the leaves of this plant were found to exhibit activity towards *Mycobacterium tuberculosis* with 99.6 and 98.9% inhibition at a concentration of 50 μg mL^{-1}, respectively. Herein the isolation, structural identification, and bioactivities of eight new bicyclic lactones (**1–8**),

and three new cyclobutane dimers (**9–11**), as well as five known compounds (**12–16**) from the leaves of *M. velutina* are discussed (Fig. 1).

2. Experimental section

2.1. General procedures

A Gallenkamp melting point apparatus (0–300 °C, 4 °C min^{-1}, uncorrected) was used to measure melting points. Optical rotations were recorded on a JASCO P-1020 polarimeter and ECD spectra were recorded on a JASCO J-810 apparatus. UV spectra were recorded using an Agilent 8453 UV-visible spectrophotometer. FTIR spectra were recorded on a Bruker Tensor 27 spectrophotometer. The NMR spectra were acquired on a Varian Mercury Plus 400 spectrometer. HRESITOFMS spectra were recorded on a Micromass Q-TOF-2 mass spectrometer. Flash column chromatography (FCC) was performed on MERCK silica gel 60 (230–400 mesh) and LiChroprep® RP-18 (40–63 μm). Thin layer chromatography (TLC) was performed using precoated MERCK silica gel 60 PF_{254} and RP-18 $F_{254}S$.

2.2. Plant material

The leaves of *M. velutina* were collected in Nam Som district, Udon Thani province, Thailand in November 2010. The identification of the plant was performed by Prof. Pranom Chantaranothai. A voucher specimen (S. Kanokmedhakul-17) was deposited at the herbarium of the Department of Biology, Faculty of Science, Khon Kaen University, Thailand. It should be noted that, in our previous report[20] on this plant, it was collected in different locations and was misidentified as *Cananga latifolia* because of incomplete material for species identification. It was identified based on the vegetative part (leaf and

[a] Natural Products Research Unit, Department of Chemistry and Center of Excellence for Innovation in Chemistry, Faculty of Science, Khon Kaen University, Khon Kaen 40002, Thailand. E-mail: kwanjai@kku.ac.th

[b] Division of Chemistry, Faculty of Science, Udon Thani Rajabhat University, Udon Thani 41000, Thailand

[c] Materials Chemistry Research Center, Department of Chemistry and Center of Excellence for Innovation in Chemistry, Faculty of Science, Khon Kaen University, Khon Kaen 40002, Thailand
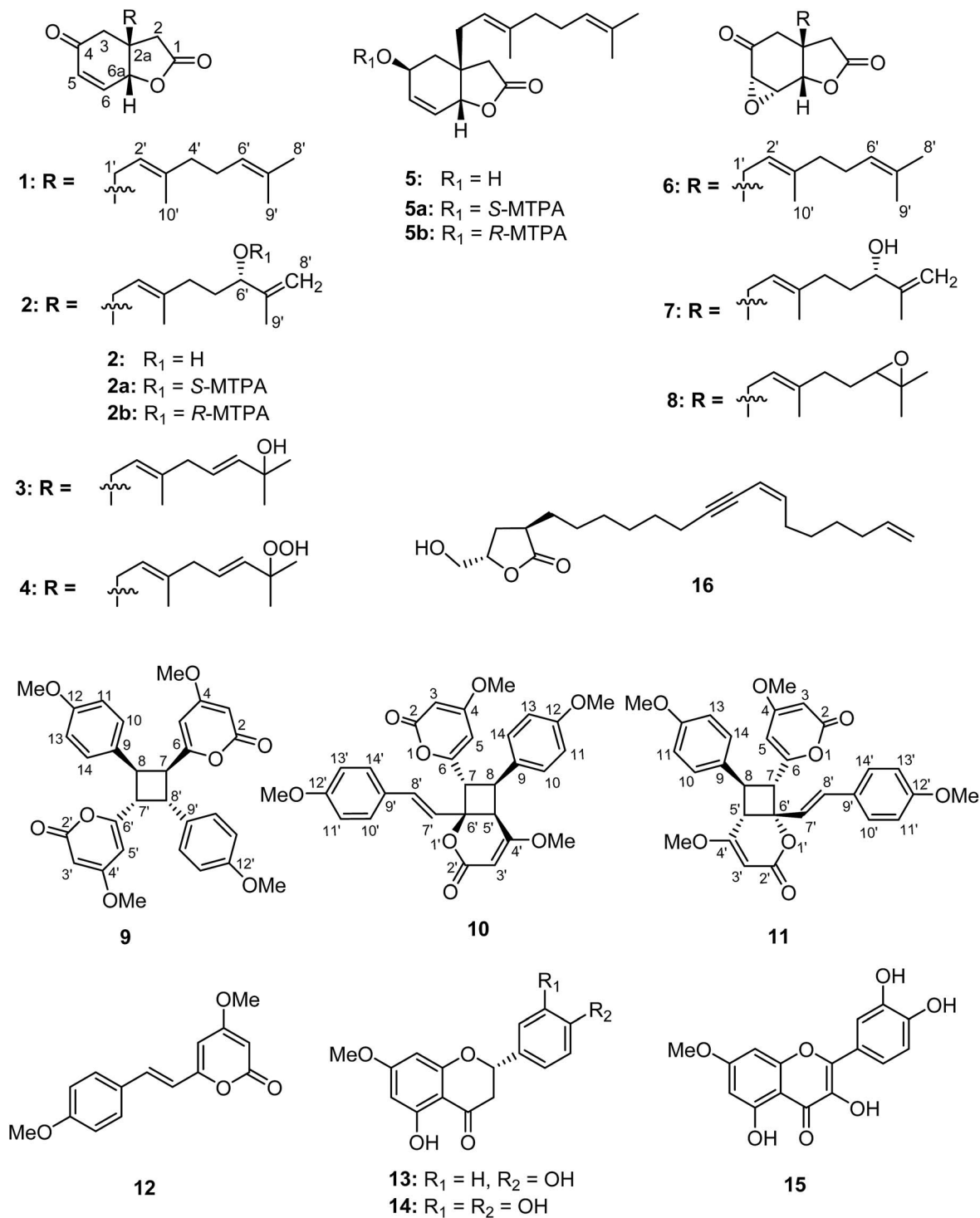
Fig. 1 Structures of isolated compounds 1–16.

stem). Later in 2015, plants with fruit from both locations were collected and the samples identified and confirmed as *Miliusa velutina*, and this has been corrected as an erratum.[21] Since the work has been published for some time, to avoid any future confusion, the names of the new compounds have not been changed.

2.3. Extraction and isolation

The dried, milled leaves of *M. velutina* (2.5 kg) were extracted with *n*-hexane (3 × 10 L) and EtOAc (3 × 10 L) to give 127 g (5.1%) and 93 g (3.7%) of *n*-hexane and EtOAc extracts, respectively. The *n*-hexane extract was separated using silica gel flash column chromatography (FCC), eluted with a gradient system of *n*-hexane–EtOAc (100 : 0, 90 : 10, 85 : 15, 70 : 30,

50 : 50, 40 : 60, 20 : 80, 0 : 100) and EtOAc–MeOH, EtOAc–MeOH (80 : 20, 50 : 50, 30 : 70, 15 : 85, 0 : 100) to afford 5 fractions, LH$_1$–LH$_5$. Fraction LH$_3$ (48.2 g) was chromatographed on silica gel FCC, eluting with n-hexane–acetone (4 : 1) to yield 3 subtractions, LH$_{3.1}$–LH$_{3.3}$. Subfraction LH$_{3.2}$ (32.8 g) was purified by LiChroprep RP-18 column chromatography, eluted with MeOH–H$_2$O (4 : 1) to give 6 fractions, LH$_{3.2.1}$–LH$_{3.2.6}$. Further purification of subfraction LH$_{3.2.1}$ (0.48 g) by silica gel FCC, eluting with n-hexane–EtOAc (4 : 1) gave compounds **4** (53.8 mg) and **2** (23 mg) as colorless viscous liquids. Subfraction LE$_{3.2.2}$ (23.6 g) was separated on silica gel FCC, eluting with n-hexane–EtOAc (85 : 15) to give **1** (20.3 g) as a colorless viscous liquid. Subfraction LH$_{3.2.3}$ (1.7 g) was chromatographed on silica gel FCC, eluting with n-hexane–EtOAc (85 : 15) to give **1** (1.59 g) and **6** (57.3 mg) as colorless viscous liquids. Subfraction LH$_{3.3}$ (9.6 g) was purified by silica gel FCC, eluting with n-hexane–acetone (7 : 1) to afford 5 subfractions, LH$_{3.3.1}$–LH$_{3.3.5}$. Further purification of subfraction LH$_{3.3.1}$ (0.28 g) by silica gel FCC, eluted with n-hexane–EtOAc (3 : 1) gave **8** (49.8 mg) as a colorless viscous liquid. Subfraction LE$_{3.3.2}$ (0.49 g) was chromatographed on silica gel FCC, eluted with n-hexane–EtOAc (1 : 1) to afford **7** (408.5 mg) as a colorless viscous liquid. Subfraction LH$_{3.4.4}$ (0.68 g) was purified by silica gel FCC, eluting with n-hexane–EtOAc (75 : 35) to give an extra amount of **2** (551.7 mg). Subfraction LH$_{3.4.5}$ (0.56 g) was purified by silica gel FCC, eluting with n-hexane–EtOAc (1 : 1) to give **3** (507.4 mg) as a colorless viscous liquid. Fraction LH$_4$ (6.7 g) was purified by silica gel FCC, eluting with acetone-CH$_2$Cl$_2$ (1 : 4) to yield 3 subfractions, LH$_{4.1}$–LH$_{4.3}$. Subfraction LH$_{4.3}$ (3.0 g) was chromatographed on silica gel FCC, eluted with n-hexane–acetone (7 : 3) to give 3 subfractions, LH$_{4.3.1}$–LH$_{4.3.3}$. Solid in subfraction LH$_{4.3.3}$ (1.6 g) was crystallized from CH$_2$Cl$_2$-n-hexane to give **12** (332 mg) as a yellow solid. Fraction LH$_5$ (1.9 g) was separated on silica gel FCC, eluted with n-hexane–acetone (7 : 3) to give 2 subfractions, LH$_{5.1}$–LH$_{5.2}$. Solid in subfraction LH$_{5.2}$ (0.62 g) was crystallized from MeOH-n-hexane to give **10** (30 mg) as colorless needles. The EtOAc extract was separated over silica gel FCC, using gradient elution with n-hexane–EtOAc (80 : 20 to 0 : 100) and EtOAc–MeOH (80 : 20 to 0 : 100) to afford 6 fractions, LE$_1$–LE$_6$. Fraction LE$_2$ (6.3 g) was then purified by silica gel FCC, eluting with n-hexane–acetone (4 : 1) to give 2 subfractions, LE$_{2.1}$–LE$_{2.2}$. Further purification of subfraction LE$_{2.2}$ (0.74 g) by silica gel FCC, eluting with n-hexane–EtOAc (4 : 1) gave **13** (552 mg) as a white solid. Fraction LE$_3$ (3.6 g) was purified by silica gel FCC, eluting with n-hexane–acetone (3 : 1) to give 2 subfractions, LE$_{3.1}$–LE$_{3.2}$. Subfraction LE$_{3.2}$ (0.31 g) was further separated by LiChroprep RP-18 column chromatography, eluting with MeOH–H$_2$O (6 : 1) to give **16** (17.6 mg) as a colorless viscous liquid. Fraction LE$_4$ (12.0 g) was separated by silica gel FCC, eluting with n-hexane–acetone (7 : 3) to give 4 subfractions, LE$_{4.1}$–LE$_{4.4}$. Subfraction LE$_{4.1}$ (2.6 g) was purified by LiChroprep RP-18 column chromatography, eluting with MeOH–H$_2$O (4 : 1) to give 2 subfractions, LE$_{4.1.1}$–LE$_{4.1.2}$. Subfraction LE$_{4.1.1}$ (1.8 g) was separated on silica gel FCC, eluting with MeOH–CH$_2$Cl$_2$ (1 : 19) to give 3 subfractions, LE$_{4.1.1.1}$–LE$_{4.1.1.3}$. Solid in subfraction LH$_{4.1.1.1}$ was crystallized from MeOH to give **12** (21 mg) as a yellow solid. Subfraction LE$_{4.1.1.2}$

(1.4 g) was purified by silica gel FCC, eluting with n-hexane–EtOAc (1 : 1) to give an additional amount of **2** (214 mg). Subfraction LE$_{4.1.2}$ (0.67 g) was purified by silica gel FCC, eluting with n-hexane–acetone (7 : 3) to give **5** (25.8 mg) as a colorless viscous liquid. Subfraction LE$_{4.2}$ (3.0 g) was purified by silica gel FCC, eluting with n-hexane–acetone (7 : 3) to give 2 subfractions, LE$_{4.2.1}$–LE$_{4.2.2}$. Solid in subfraction LH$_{4.2.1}$ was crystallized from MeOH to give an additional amount of **12** (105.3 mg). Solid in subfraction LH$_{4.2.2}$ (0.54 g) was crystallized from MeOH to give **14** (30 mg) as a white solid. Subfraction LE$_{4.3}$ (2.9 g) was purified by silica gel FCC, eluting with n-hexane–EtOAc (1 : 1), to give an additional amount of **3** (174 mg). Solid in subfraction LE$_{4.4}$ (0.12 g) was crystallized from DMF–CH$_2$Cl$_2$ to give **15** (26 mg) as a yellow solid. Fraction LE$_5$ (8.4 g) was purified by silica gel FCC, eluting with MeOH–CH$_2$Cl$_2$ (3 : 97) to give 2 subfractions, LE$_{5.1}$–LE$_{5.2}$. Solid in subfraction LE$_{5.1}$ (1.6 g) was crystallized from MeOH–CH$_2$Cl$_2$ to give **10** (1.08 g) as colorless needles and the filtrate was further purified by silica gel FCC, eluting with EtOAc–CH$_2$Cl$_2$ (15 : 85) to yield **9** (22 mg) as a white solid and **11** (75 mg) as colorless needles. Solids in subfractions LE$_{5.2}$ (6.2 g) and LE$_6$ (10.9 g) were crystallized from DMF-CH$_2$Cl$_2$ to give **15** (931 mg) as a yellow solid.

2.3.1 Velutinone A (1). Colorless viscous liquid; $R_f = 0.39$ (n-hexane–EtOAc, 7 : 3); $[\alpha]_D^{23}$ −68.0 (c 0.20, CHCl$_3$); ECD (80 μM, MeOH) λ_{max} ($\Delta\varepsilon$) 215 (−19.02) nm; IR (ATR) ν_{max} 2966, 2916, 2854, 1781, 1685, 1440, 1418, 1383, 1161, and 997 cm^{-1}; for ^{1}H and ^{13}C NMR spectroscopic data, see Table 1; HRESITOFMS m/z 311.1611 [M + Na]$^+$ (calcd for C$_{18}$H$_{24}$O$_3$ + Na, 311.1618).

2.3.2 Velutinone B (2). Colorless viscous liquid; $R_f = 0.34$ (n-hexane–EtOAc, 1 : 1); $[\alpha]_D^{24}$ −61.2 (c 0.20, CHCl$_3$); ECD (130 μM, MeOH) λ_{max} ($\Delta\varepsilon$) 215 (−28.90) nm; IR (ATR) ν_{max} 3468, 2920, 2857, 1777, 1683, 1447, 1385, 1165, 1065, 995, and 990 cm^{-1}; for ^{1}H and ^{13}C NMR spectroscopic data, see Table 1; HRESITOFMS m/z 305.1740 [M + H]$^+$ (calcd for C$_{18}$H$_{24}$O$_4$ + H$^+$, 305.1747).

2.3.3 Velutinone C (3). Colorless viscous liquid; $R_f = 0.29$ (n-hexane–EtOAc, 1 : 1); $[\alpha]_D^{23}$ −55.4 (c 0.20, CHCl$_3$); ECD (50 μM, MeOH) λ_{max} ($\Delta\varepsilon$) 213 (−7.63) nm; IR (ATR) ν_{max} 3447, 2972, 2929, 1778, 1682, 1481, 1385, 1155, and 975 cm^{-1}; for ^{1}H and ^{13}C NMR spectroscopic data, see Table 1; HRESITOFMS m/z 327.1543 [M + Na]$^+$ (calcd for C$_{18}$H$_{24}$O$_4$ + Na, 327.1572).

2.3.4 Velutinone D (4). Colorless viscous liquid; $R_f = 0.39$ (n-hexane–EtOAc, 1 : 1); $[\alpha]_D^{24}$ −58.4 (c 0.20, CHCl$_3$); ECD (56 μM, MeOH) λ_{max} ($\Delta\varepsilon$) 213 (−9.74) nm; IR (ATR) ν_{max} 3393, 2978, 2931, 1778, 1682, 1417, 1384, 1165, and 996 cm^{-1}; for ^{1}H and ^{13}C NMR spectroscopic data, see Table 1; HRESITOFMS m/z 343.1472 [M + Na]$^+$ (calcd for C$_{18}$H$_{24}$O$_5$ + Na, 343.1521).

2.3.5 Velutinone E (5). Colorless viscous liquid; $R_f = 0.37$ (n-hexane–EtOAc, 1 : 1); $[\alpha]_D^{23}$ −32.5 (c 0.20, CHCl$_3$); ECD (62 μM, MeOH) λ_{max} ($\Delta\varepsilon$) 202 (−13.84) nm; IR (ATR) ν_{max} 3442, 3030, 2967, 2921, 2856, 1771, 1668, 1446, 1419, 1377, 1328, 1167, 1069, 1030, and 990 cm^{-1}; for ^{1}H and ^{13}C NMR spectroscopic data, see Table 2; HRESITOFMS m/z 291.1935 [M + H]$^+$ (calcd for C$_{18}$H$_{26}$O$_3$ + H$^+$, 291.1955).

2.3.6 Velutinone F (6). Colorless viscous liquid; $R_f = 0.50$ (n-hexane–EtOAc, 7 : 3); $[\alpha]_D^{23}$ −29.5 (c 0.20, CHCl$_3$); ECD (72 μM, MeOH) λ_{max} ($\Delta\varepsilon$) 207 (+4.83) nm; IR (ATR) ν_{max} 2967, 2917, 2855, 1789, 1719, 1423, 1377, 1347, 1161, 1035, 857, and 802 cm^{-1}; for

Table 1 ^{1}H and ^{13}C NMR spectroscopic data of **1–4** in CDCl$_3$

No.	**1** δ_C	**1** δ_H (J in Hz)	**2** δ_C	**2** δ_H (J in Hz)	**3** δ_C	**3** δ_H (J in Hz)	**4** δ_C	**4** δ_H (J in Hz)
1	174.2		174.3		174.2		174.4	
2	38.9	2.48, d (17.4), Hα/2.39, d (17.4), Hβ	38.9	2.43, d (17.8), Hα/2.39, d (17.8), Hβ	39.0	2.40, s	39.0	2.42, s
2a	44.7		44.6		44.5		44.5	
3	42.6	2.52, s	42.7	2.55, d (16.7), Hα/2.50, d (16.7), Hβ	42.9	2.53, d (16.7), Hα/2.48, d (16.7), Hβ	43.0	2.56, d (16.7), Hα/2.50, d (16.7), Hβ
4	196.2		196.2		196.1		196.3	
5	131.2	6.17, dd (10.3, 1.2)	131.2	6.13, dd (10.3, 1.2)	131.2	6.12, dd (10.3, 1.2)	131.2	6.18, dd (10.3, 1.2)
6	141.4	6.75, dd (10.3, 3.3)	141.4[a]	6.74, dd (10.3, 3.3)	141.3	6.74, dd (10.3, 3.3)	141.4	6.76, dd (10.3, 3.3)
6a	77.8	4.87, dd (3.3, 1.2)	77.9	4.87, d (3.3)	77.9	4.86, dd, (3.3, 1.2)	78.1	4.88, dd, (3.3, 1.2)
1′	36.0	2.31, dd (14.4, 7.7), Ha/2.21, dd (14.4, 7.7), Hb	36.2	2.31, dd (14.5, 7.7), Ha/2.22, dd (14.5, 7.7), Hb	36.6	2.30, dd (14.4, 7.7), Ha/2.23, dd (14.4, 7.7), Hb	36.8	2.32, dd (14.4, 7.7), Ha/2.26, dd (14.4, 7.7), Hb
2′	116.9	5.10, td (7.7, 1.4)	116.9	5.15, td (7.7, 1.4)	117.5	5.11, td (7.7, 1.4)	117.8	5.15, td (7.7, 1.4)
3′	141.5		141.4[a]		140.3		140.0	
4′	39.9	2.10–2.02, m[a]	35.9	2.14–1.98, m	42.4	2.68, d (6.5)	42.5	2.73, d (5.5)
5′	26.2	2.10–2.02, m[a]	33.0	1.65–1.58, m	123.8	5.51, dt (15.6, 6.6)	128.0	5.62, dt (15.8, 6.0)
6′	123.7	5.01, t (5.4)	75.3	4.00, t (6.3)	140.2	5.60, d, (15.6)	135.9	5.56, d, (15.8)
7′	131.9		147.3		70.4		81.8	
8′	25.7	1.65, s	111.1	4.91, brs, Ha/4.82, t (1.4), Hb	29.7	1.28, s	24.3	1.31, s
9′	17.7	1.58, s	17.5	1.70, s	29.7	1.28, s	24.2	1.31, s
10′	16.3	1.60, s	16.4	1.61, s	16.5	1.58, s	16.6	1.60, s

[a] Overlap of the signals.

Table 2 ^{1}H and ^{13}C NMR spectroscopic data of **5–8** in CDCl$_3$

No.	**5** δ_C	**5** δ_H (J in Hz)	**6** δ_C	**6** δ_H (J in Hz)	**7** δ_C	**7** δ_H (J in Hz)	**8** δ_C	**8** δ_H (J in Hz)
1	176.2		173.8		173.9		173.7	
2	37.1[a]	2.38, d (17.4), Hα/2.19, d (17.4), Hβ	38.3	2.32, d (17.4), Hα/2.28, d (17.4), Hβ	38.4	2.30–2.24, m[a]	38.4	2.30–2.24, m[a]
2a	42.3		47.5		47.4		47.4	
3	37.2[a]	2.25–2.17, m[a], Hα/1.58–1.51, m, Hβ	39.9[a]	2.86, d (13.9), Hα/2.14, d (13.9), Hβ	39.9	2.82, d (13.9), Hα/2.11, d (13.9), Hβ	39.9	2.84, d (13.9), Hα/2.12, d (13.9), Hβ
4	63.7	4.31, m	204.6		204.5		204.5	
5	135.2	5.97, brd (10.2)	58.6	3.65, d (3.6)	58.5	3.62, d (3.6)	58.5	3.62, d (3.7)
6	125.2	6.75–5.65, m	54.9	3.37, d (3.6)	54.8	3.34, d (3.6)	54.8	3.34, d (3.7)
6a	80.1	4.62, m	76.6	4.71, d (3.6)	76.6	4.68, s	76.5	4.69, s
1′	36.5	2.25–2.09, m	36.9	2.29, dd (14.4, 7.7), Ha/2.20, dd (14.4, 7.7), Hb	36.8	2.25–2.09, m[a]	36.9[a]	2.32–2.09, m[a]
2′	117.5	5.12, td (7.7, 1.4)	116.2	5.08, td (7.7, 1.4)	116.3	5.10, td (7.8, 1.4)	116.7	5.14, td (7.7, 1.4)
3′	140.2		141.8		141.6		141.1	
4′	39.8	2.08–1.98, m[a]	39.9[a]	2.10–2.02, m[a]	35.8	2.01–1.96, m[a]	36.7[a]	2.32–2.09, m[a]
5′	26.3	2.08–1.98, m[a]	26.2	2.10–2.02, m[a]	32.8			
6′	123.8	5.01, m	123.6	5.04, t (6.6)	75.1	1.64–1.55, m	27.2	1.69–1.53, m
7′	131.6		132.0		147.3	3.98, t (6.0)	63.7	3.65, t (6.7)
8′	25.6	1.63, s	25.7	1.68, s	111.0	4.79, brs, Ha/4.89, t (0.8), Hb	58.2	
9′	17.6	1.56, s	17.7	1.59, s	17.5	1.68, s	24.7	1.27, s
10′	16.2	1.58, s	16.4	1.61, s	16.4	1.60, s	18.7	1.23, s

[a] overlapping of the signals.

^{1}H and ^{13}C NMR spectroscopic data, see Table 2; HRESITOFMS m/z 327.1562 [M + Na]$^{+}$ (calcd for $C_{18}H_{24}O_4$ + Na, 327.1567).

2.3.7 Velutinone G (7). Colorless viscous liquid; R_f = 0.42 (hexane–EtOAc, 1 : 3); $[\alpha]_D^{23}$ −25.6 (c 0.20, CHCl$_3$); ECD (94 μM, MeOH) λ_{max} ($\Delta\varepsilon$) 205 (+11.89) nm; IR (ATR) ν_{max} 3481, 2939, 2858, 1783, 1718, 1651, 1422, 1347, 1164, 1033, and 902 cm^{-1} for ^{1}H and ^{13}C NMR spectroscopic data, see Table 2; HRESITOFMS m/z 321.1690 [M + H]$^{+}$ (calcd for $C_{18}H_{24}O_5$ + H^{+}, 321.1697).

2.3.8 Velutinone H (8). Colorless viscous liquid; R_f = 0.29 (n-hexane–EtOAc, 7 : 3); $[\alpha]_D^{24}$ −23.5 (c 0.20, CHCl$_3$); ECD (75 μM, MeOH) λ_{max} ($\Delta\varepsilon$) 215 (+11.84) nm; IR (ATR) ν_{max} 2962, 2924, 2855, 1785, 1719, 1423, 1378, 1163, and 1034 cm^{-1}; for ^{1}H and ^{13}C NMR spectroscopic data, see Table 2; HRESITOFMS m/z 321.1690 [M + H]$^{+}$ (calcd for $C_{18}H_{24}O_5$ + H^{+}, 321.1697).

2.3.9 Velutindimer A (9). White solid; mp 201–203 °C; R_f = 0.13 (n-hexane–EtOAc, 1 : 1); $[\alpha]_D^{28}$ + 0.08 (c 0.63, MeOH–CHCl$_3$, 3 : 1); ECD (26 μM, MeOH) λ_{max} ($\Delta\varepsilon$) 285 (0.00) nm; UV (MeOH) λ_{max} (log ε) 226 (4.53), 285 (4.20); IR (ATR) ν_{max} 3088, 2944, 2837, 1715, 1643, 1611, 1564, 1513, 1455, 1409, 1249, 1180, 1034, and 818 cm^{-1}; for ^{1}H and ^{13}C NMR spectroscopic data, see Table 3; HRESITOFMS m/z 539.1651 [M + Na]$^{+}$ (calcd for $C_{30}H_{28}O_8$ + Na, 539.1682).

2.3.10 Velutinin dimer B (10). Colorless needles; mp 205–207 °C; R_f = 0.21 (n-hexane–EtOAc, 1 : 1); $[\alpha]_D^{28}$ +0.08 (c 0.63,

MeOH–CHCl$_3$, 5 : 3); ECD (33 μM, MeOH) λ_{max} ($\Delta\varepsilon$) 265 (0.00) nm; UV (MeOH) λ_{max} (log ε) 265 (4.45); IR (ATR) ν_{max} 2940, 2838, 1699, 1647, 1608, 1566, 1512, 1455, 1410, 1391, 1246, 1176, 1031 and 814 cm^{-1}; for ^{1}H and ^{13}C NMR spectroscopic data, see Table 3; HRESITOFMS m/z 539.1666 [M + Na]$^{+}$ (calcd for $C_{30}H_{28}O_8$ + Na, 539.1682).

2.3.11 Velutinin dimer C (11). Colorless needles; mp 207–209 °C; R_f = 0.18 (n-hexane–EtOAc, 1 : 1); $[\alpha]_D^{27}$ +0.03 (c 0.23, MeOH–CHCl$_3$, 9 : 1); ECD (22 μM, MeOH) λ_{max} ($\Delta\varepsilon$) 268 (0.00) UV (MeOH) λ_{max} (log ε) 268 (4.59); IR (ATR) ν_{max} 2924, 2837, 1708, 1649, 1625, 1608, 1567, 1513, 1455, 1406, 1248, 1176, 1031, and 821 cm^{-1}; for ^{1}H and ^{13}C NMR spectroscopic data, see Table 3; HRESITOFMS m/z 539.1664 [M + Na]$^{+}$ (calcd for $C_{30}H_{28}O_8$ + Na, 539.1682).

2.4. Preparation of the (R)-and (S)-α-methoxy-α-(trifluoromethyl) phenyl acetate of 2

The determination of configuration for the stereogenic carbinol carbons was carried out following the method reported by Ohtani et al.[22] A solution of (S)-MPTA-Cl (10 μL, 53.4 μmol) was added to a solution mixture of 2 (8 mg, 27.5 μmol) and DMAP (5 mg) in dry CH$_2$Cl$_2$ (1 mL) and stirred under N$_2$ at room temperature for 6 h. Then the solvent was removed in vacuo. The

Table 3 ^{1}H and ^{13}C NMR spectroscopic data of **9–11** in CDCl$_3$

No. position	9 δ_C	9 δ_H (J in Hz)	10 δ_C	10 δ_H (J in Hz)	11 δ_C	11 δ_H (J in Hz)
2	164.0		163.9		164.1	
3	87.7	5.21, d (2.2)	88.6	5.33, d (2.2)	88.9	5.45, d (2.2)
4	170.1		170.5		170.6	
5	101.3	5.71, d (2.2)	102.5	5.89, d (2.2)	102.0	5.99, d (2.2)
6	162.9		158.9		158.7	
7	43.0	4.35, dd (10.0, 7.6)	55.0	4.09, d (10.8)	54.5	3.64, d (10.3)
8	45.5	4.16, dd (10.0, 7.6)	38.7	4.26, dd (10.8, 9.9)	45.6	4.00, dd (10.3, 9.7)
9	129.4		127.7		131.4	
10	128.5	7.19, d (8.7)	128.6	7.16, d (8.7)	127.4	7.22, d (8.6)
11	113.9	6.82, d (8.7)	113.8	6.85, d (8.7)	114.2	6.89, d (8.6)
12	158.6		159.2		159.0	
13	113.9	6.82, d (8.7)	113.8	6.85, d (8.7)	114.2	6.89, d (8.6)
14	128.5	7.19, d (8.7)	128.6	7.16, d (8.7)	127.4	7.22, d (8.6)
2'	164.0		164.7		165.4	
3'	87.7	5.21, d (2.2)	91.7	5.29, s	89.2	5.19, s
4'	170.1		170.1		171.4	
5'	101.3	5.71, d (2.2)	45.8	3.55, d (9.9)	44.2	3.20, d (9.7)
6'	162.9		79.4		82.6	
7'	43.0	4.35, dd (10.0, 7.6)	122.2	6.42, d (15.8)	125.2	6.18, d (15.9)
8'	45.5	4.16, dd (10.0, 7.6)	130.8	6.86, d (15.8)	131.3	6.63, d (15.9)
9'	129.4		127.7		127.9	
10'	128.5	7.19, d (8.7)	128.1	7.34, d (8.7)	128.8	7.33, d (8.7)
11'	113.9	6.82, d (8.7)	114.1	6.85, d (8.7)	114.0	6.84, d (8.7)
12'	158.6		159.7		159.9	
13'	113.9	6.82, d (8.7)	114.1	6.85, d (8.7)	114.0	6.84, d (8.7)
14'	128.5	7.19, d (8.7)	128.1	7.34, d (8.7)	128.8	7.33, d (8.7)
4-OMe	55.7	3.75, s	55.8	3.69, s	55.8	3.76, s
12-OMe	55.2	3.67, s	55.3	3.79, s	55.27	3.79, s
4'-OMe	55.7	3.75, s	55.5	3.32, s	56.1	3.77, s
12'-OMe	55.2	3.67, s	55.3	3.78, s	55.30	3.80, s

residue was separated on preparative TLC (CH_2Cl_2) to give the (R)-ester (**2a**, 7 mg, 50%). The (S)-ester of **2** was prepared using the procedure described above [alcohol **2** (10 mg, 34.4 µmol), CH_2Cl_2 (1 mL), dimethylaminopyridine (5 mg), and (R)-MPTA-Cl (10 µL, 53.4 µmol)] to yield (S)-ester (**2b**, 12 mg, 71%).

2.4.1 Compound 2a. Colorless viscous liquid; ^{1}H NMR ($CDCl_3$, 400 MHz) δ 6.67 (1H, dd, J = 10.3, 3.3 Hz, H-6), 6.19 (1H, dd, J = 10.3, 1.2 Hz, H-5), 5.37 (1H, dt, J = 12.0, 6.4, 6.4 Hz, H-6′), 5.07 (1H, dt, J = 7.6, 1.1 Hz, H-2′), 5.02 (brs, H-8′a), 4.98 (1H, brs, H-8′b), 4.87 (1H, dd, J = 3.3, 1.2, H-6a), 2.56 (1H, d, J = 16.7 Hz, H-3α), 2.51 (1H, d, J = 16.6 Hz, H-3β), 2.46 (1H, d, J = 17.4 Hz, H-2α), 2.39 (1H, d, J = 17.4 Hz, H-2β), 2.32 (1H, dd, J = 14.0, 7.7 Hz, H-1′a), 2.22 (1H, dd, J = 14.6, 7.6 Hz, H-1′b), 2.05–1.65 (4H, m, H-4′ and 5′), 1.57 (3H, s, H-9′), 1.72 (3H, s, H-10′), [the α-methoxy-α-(trifluoromethyl)phenyl acetate portion exhibited δ 7.50 and 7.40 (5H, m, C_6H_5), 3.52 (3H, s, OCH_3)].

2.4.2 Compound 2b. Colorless viscous liquid; ^{1}H NMR ($CDCl_3$, 400 MHz) δ 6.76 (1H, dd, J = 10.3, 3.5 Hz, H-6), 6.19 (1H, brs, J = 10.3 Hz, H-5), 5.37 (1H, ddd, J = 17.5, 6.7, 5.5 Hz, H-6′), 5.05 (1H, dt, J = 14.3, 7.7, 7.7 Hz, H-2′), 5.02 (1H, brs, H-8′a), 4.98 (1H, brs, H-8′b), 4.87 (1H, dd, J = 3.3, 1.2 Hz, H-6a), 2.56 (1H, d, J = 16.7 Hz, H-3α), 2.51 (1H, J = 16.7 Hz, H-3β), 2.46 (1H, d, J = 17.3, Hz, H-2α), 2.39 (1H, d, J = 17.3, Hz, H-2β), 2.30 (1H, dd, J = 14.2, 7.8 Hz, H-1′a), 2.22 (1H, dd, J = 14.2, 7.6 Hz, H-1′b), 2.09–1.90 (2H, m, H-4′), 1.90–165 (2H, m, H-5′), 1.72 (3H, s, H-10′), 1.59 (3H, s, H-9′), [the α-methoxy-α-(trifluoromethyl)phenyl acetate portion exhibited δ 7.50 and 7.41 (5H, m, C_6H_5), 3.52 (3H, s, OCH_3)].

2.5. Preparation of the (R)-and (S)-α-methoxy-α-(trifluoromethyl) phenyl acetate of (5)

The esterification of **5** was carried out using the procedure described for the preparation of **2a** and **2b** to yield (S)-ester (**5a**, 7 mg, (50%)) and (R)-ester (**5b**, 12 mg, (71%)).

2.5.1 Compound 5a. Colorless viscous liquid; ^{1}H NMR ($CDCl_3$, 400 MHz) δ 6.03 (1H, d, J = 11.4 Hz, H-5), 5.97 (1H, dd, J = 11.4, 1.7 Hz, H-6), 5.65 (1H, t, J = 5.8 Hz, H-4), 5.07 (1H, t, J = 7.6 Hz, H-2′), 5.01 (1H, t, J = 6.6 Hz, H-6′), 4.64 (1H, brs, H-6a), 2.41 (1H, J = 17.4 Hz, H-2α), 2.35 (1H, J = 17.4 Hz, H-2β), 2.21 (1H, dd, J = 14.4, 8.0 Hz, H-1′a), 2.18 (1H, dd, J = 13.9, 4.8 Hz, H-3β), 2.14 (1H, dd, J = 14.4, 7.4 Hz, H-1′b), 2.08–1.98 (4H, m, H-4′ and 5′), 1.71 (1H, dd, J = 13.9, 7.9 Hz, H-3α), 1.65 (3H, s, H-8′), 1.58 (3H, s, H-10′), 1.55 (3H, s, H-9′), [the α-methoxy-α-(trifluoromethyl)phenyl acetate portion exhibited δ 7.50 and 7.41 (5H, m, C_6H_5), 3.55 (3H, s, OCH_3)].

2.5.2 Compound 5b. Colorless viscous liquid; ^{1}H NMR ($CDCl_3$, 400 MHz) δ 5.95 (1H, d, J = 11.0 Hz, H-5), 5.92 (1H, d, J = 11.0 Hz, H-6), 5.66 (1H, t, J = 6.8 Hz, H-4), 5.12 (1H, t, J = 7.7 Hz, H-2′), 5.03 (1H, t, J = 6.6 Hz, H-6′), 4.63 (1H, brs, H-6a), 2.44 (1H, J = 17.4 Hz, H-2α), 2.35 (1H, J = 17.4 Hz, H-2β), 2.24 (1H, dd, J = 14.6, 5.5 Hz, H-1′a), 2.21 (1H, dd, J = 14.0, 4.3 Hz, H-3β), 2.18 (1H, dd, J = 14.6, 7.6 Hz, H-1′b), 2.09–2.02 (4H, m, H-4′ and 5′), 1.82 (1H, dd, J = 14.0, 8.2 Hz, H-3α), 1.65 (3H, s, H-8′), 1.59 (3H, s, H-10′), 1.57 (3H, s, H-9′), [the α-methoxy-α-(trifluoromethyl)phenyl acetate portion exhibited δ 7.50 and 7.41 (5H, m, C_6H_5), 3.54 (3H, s, OCH_3)].

2.6. X-ray crystallographic analyses of 10 and 11

The reflection data were collected on a Bruker D8 Quest PHOTON100 CMOS detector with graphite-monochromated MoKα radiation using the APEX2 program.[23] Raw data frame integration was performed with SAINT,[23] which also applied correction for Lorentz and polarization effects. An empirical absorption correction using the SADABS program[23] was applied. The structure was solved by direct methods and refined by full-matrix least-squares method on F^2 with anisotropic thermal parameters for all non-hydrogen atoms using the SHELXTL software package.[24] All hydrogen atoms were placed in calculated positions and refined isotropically. Crystallographic data of **10** and **11** were deposited with the following Cambridge Crystallographic Data Centre codes: CCDC 1415288 and CCDC 1062125, respectively.

2.6.1 Crystal data of 10. $C_{30}H_{28}O_8$ (M = 516.52 g mol^{-1}): orthorhombic, space group $Pna2_1$ (no. 33), a = 23.725(4) Å, b = 5.5211(10) Å, c = 39.408(7) Å, V = 5162.0(16) Å^3, Z = 8, T = 293(2) K, μ(MoKα) = 0.096 mm^{-1}, D_{calc} = 1.329 g cm^{-3}, 135 470 reflections measured (6.204° $\leq 2\Theta \leq$ 52.798°), 10 518 unique (R_{int} = 0.0929, R_{sigma} = 0.0445) which were used in all calculations. The final R_1 was 0.0508 ($I > 2\sigma(I)$) and wR_2 was 0.1225 (all data).

2.6.2 Crystal data of 11. $C_{31}H_{29}Cl_3O_8$, MW = 635.89 g mol^{-1}, triclinic, space group $P\bar{1}$, a = 11.6555(5) Å, b = 12.1165(5) Å, c = 12.1203(5) Å, α = 113.9720(10), β = 102.4530(10), γ = 92.9570(10), V = 1508.54(11) Å^3, Z = 2, T = 293(2) K, μ(MoKα) = 0.354 mm^{-1}, D_{calc} = 1.400 g cm^{-3}, 61 914 reflections measured, 7472 unique (R_{int} = 0.0262) which were used in all calculations. The final R_1 was 0.0642 ($I > 2\sigma(I)$) and wR_2 was 0.2211 (all data).

2.7. Antimalarial assay

Antimalarial activity was performed against *P. falciparum* (K1, multidrug resistant strain, see ESI†), using the method of Trager and Jensen.[25] Quantitative assessment of malarial activity *in vitro* was determined by means of the microculture radioisotope technique based upon the method described by Desjardins *et al.*[26] The inhibitory concentration (IC_{50}) represents the concentration that causes 50% reduction in parasite growth as indicated by the *in vitro* uptake of [^{3}H]-hypoxanthine by *P. falciparum*. The standard compound was dihydroartemisinin.

2.8. Antimycobacterial assay

Antimycobacterial activity was performed against *M. tuberculosis* H37Ra (purchased from ATCC) using the MicroplateAlamar Blue Assay (MABA).[27] The standard drug streptomycin was used as reference substance.

2.9. Cytotoxicity assay

Cytotoxicity assays against human epidermoid carcinoma (KB), human breast cancer (MCF7), and human small cell lung cancer (NCI-H187) cell lines human breast adenocarcinoma Resazurin microplate assay described by O'Brien and co-workers.[28] The reference substances were ellipticine and doxorubicin. Cytotoxicity test against primate cell line (Vero) was performed using

the green fluorescent protein detection method described by Hunt and co-workers.[29] The reference substances used were ellipticine and doxorubicin. All cells were purchased from ATCC.

3. Results and discussion

Chromatographic fractionation of *n*-hexane and EtOAc extracts yielded eight new bicyclic lactones, velutinones A–H (**1–8**), three cyclobutane dimers, velutinindimers A–C (**9–11**), and four known compounds (**12–15**), kawapyrone, yangonin (**12**),[30] three flavonoids, sakuranetin (**13**),[31] 7-*O*-methyleriodictyol (**14**)[32] and rhamnetin (**15**),[33] and an acetogenin, cananginone H (**16**)[20,21] (Fig. 1).

The IR spectra of **1–4** showed absorption bands of a γ-lactone moiety at (1789–1771 cm^{-1}) and a conjugated carbonyl functionality (1685–1862 cm^{-1}) similar to the absorption bands of a synthetic bicyclic cyclohexenone.[34,35]

Compound **1** possessed the molecular formula $C_{18}H_{24}O_3$ based on the ^{13}C NMR and HRESITOFMS (m/z 311.1611 [M + Na]$^+$) data, indicating seven indices of hydrogen deficiency. The ^1H NMR data (Table 1) had resonances at δ 2.48 (d, J = 17.4 Hz, H-2α), 2.39 (d, 17.4 Hz, H-2β), 2.52 (s, 2H, H-3), 6.17 (dd, J = 10.3, 1.2 Hz, H-5), 6.75 (dd, J = 10.3, 3.3 Hz, H-6), and 4.87 (dd, J = 3.3, 1.2 Hz, H-6a). The ^{13}C NMR data (Table 1), DEPT, and HMQC experiments indicated seven resonances which were associated with an α,β-unsaturated carbonyl (δ 196.2/C-4), a lactone carbonyl (δ 174.2/C-1), two olefinic (δ 131.2/C-5 and 141.4/C-6), two methylene (δ 38.9/C-2 and 42.6/C-3), one methine (δ 77.8/C-6a), and one quaternary (δ 44.7/C-2a) carbons. Interpretation of the COSY and HMBC correlations (Fig. 2) indicated that **1** has a core structure of a five-membered lactone ring fused to an α,β-unsaturated cyclohexanone ring. This arrangement is similar to that of a compound isolated from the fruit kernels of *Otoba parvifolia*[35,36] and from a total synthesis of its core structure,[34] except for the side chain at C-2a which was replaced by a geranyl moiety in **1**. This geranyl side chain ($C_{10}H_{17}$) was evident from the ^1H and ^{13}C NMR spectroscopic data (Table 1). The COSY spectrum showed the connectivity of the geranyl side chain by correlations between H-1$'$ and H-2$'$, and amongst H-4$'$, H-5$'$ and H-6$'$. The HMBC spectrum exhibited correlations of H-1$'$ to C-2, C-3, C-2a, C-6a, C-2$'$ and C-3$'$; H-2$'$ to C-2a, C-1$'$, C-3$'$, C-4$'$, and C-10$'$; H-4$'$ to C-2$'$, C-3$'$, C-5$'$, C-6$'$ and C-10$'$; H-6$'$ to C-4$'$, C-5$'$, C-8$'$, and C-9$'$ indicating that the geranyl group was linked to the stereogenic quaternary carbon C-2a (Fig. 2). The relative configuration at C-2a and C-6a was
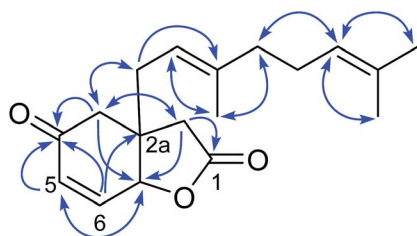
established as *syn* from the NOESY correlation of H-6a and H-1$'$. Based on the above evidence, the structure of **1**, velutinone A, was defined as shown in Fig. 1.

Compound **2** had the molecular formula $C_{18}H_{24}O_4$ derived from the ^{13}C NMR and HRESITOFMS (m/z 305.1740 [M + H]$^+$) data, demonstrating the same index of hydrogen deficiency, but having one additional oxygen atom compared to **1**. The ^1H and ^{13}C NMR spectroscopic data of **2** (Table 1) were similar to those of **1**, except for the geranyl side chain being oxidized at C-6$'$ and having a 7$'$, 8$'$ terminal double bond. The NMR spectroscopic data displayed resonances for an olefinic methylene protons at δ_H 4.82 (t, J = 1.4 Hz, 4.91 (brs), H-8$'$)/δ_C 111.1 and an oxymethine at δ_H 4.00 (t, J = 6.3 Hz, H-6$'$)/δ_C 75.3. The HMBC correlations of H-5$'$ to C-3$'$, C-4$'$, C-6$'$, and C-7$'$; H-6$'$ to C-4$'$, C-5$'$, C-7$'$, C-8$'$, and C-9$'$; and H-8$'$ to C-6$'$, C-7$'$, and C-9$'$ confirmed the position of the terminal olefinic moiety and the hydroxy group in the side chain. The assignment of the (6$'$*S*) absolute configuration was done *via* the modified Mosher's ester method[22] (Fig. 3). Therefore, the structure of compound **2**, velutinone B, was defined as shown in Fig. 1.

Compound **3** had the molecular formula $C_{18}H_{24}O_4$, deduced from ^{13}C NMR and HRESITOFMS (m/z 327.1543 [M + Na]$^+$) data, implying the same index of hydrogen deficiency, but having one additional oxygen atom compared to **1**. The ^1H and ^{13}C NMR spectroscopic data of **3** (Table 1) were similar to those of **1**, except for the appearance of the olefinic protons at δ_H 5.51 (dt, J = 15.6, 6.6 Hz, H-5$'$) and δ_H 5.60 (d, J = 15.6 Hz, H-6$'$), and one additional oxygenated carbon signal at δ_C 70.4 (C-7$'$). The position of the hydroxy group at C-7$'$ on the side chain was confirmed by the HMBC correlations of H-5$'$ to C-3$'$, C-4$'$, C-6$'$, and C-7$'$; and H-6$'$ to C-4$'$, C-5$'$, C-7$'$ and C-8$'$/C-9$'$. Therefore, the structure of compound **3**, velutinone C, was defined as shown (Fig. 1).

Compound **4** had the molecular formula $C_{18}H_{24}O_5$ derived from the ^{13}C NMR and HRESITOFMS (m/z 343.1472 [M + Na]$^+$) data, demonstrating the same index of hydrogen deficiency, but having one additional oxygen atom compared to **3**. The NMR spectroscopic data of **4** (Table 1) was similar to that of **3**, except for the resonance of a C-7$'$ hydroxy group. The ^{13}C NMR spectrum revealed the unusual downfield oxygenated carbon signal at δ_C 81.8 for C-7$'$, suggesting the presence of a hydroperoxy group.[37] Thus the structure of compound **4**, velutinone D, was determined as shown (Fig. 1).
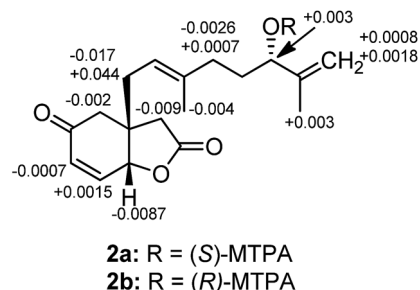

Fig. 2 Selected HMBC correlations of **1**.

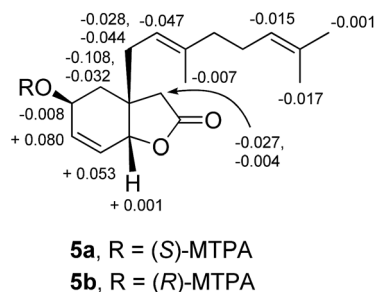**Fig. 3** $\Delta\delta$ values ($\Delta\delta = \delta_S - \delta_R$ in ppm) obtained for MTPA esters **2a** and **2b**.

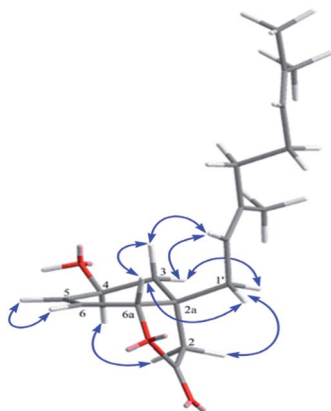Compound **5** had the molecular formula $C_{18}H_{26}O_3$ derived from the ^{13}C NMR and HRESITOFMS (m/z 291.1935 [M + Na]$^+$) data, implying six indices of hydrogen deficiency. The IR spectrum showed hydroxy (3442 cm^{-1}) and γ-lactone carbonyl (1771 cm^{-1}) functionalities. The NMR data of **5** (Table 2) corresponded to those of **1**, except that the ketone carbonyl resonance for C-4 was replaced by a resonance for an oxymethine group at δ_H 4.31 (m)/δ_C 63.7. The assignment of (4S) absolute configuration was done *via* the modified Mosher's ester method[22] (Fig. 4). The configurations of (2aR and 6aR) were assigned by NOESY and a molecular modeling study. NOESY correlations were observed between H-4 and H-2α, H-6a and H-1'a, H-6a and H-3β, H-1'b and H-2β, and H-3α and H-2' (Fig. 5). Therefore, the structure of compound **5**, velutinone E, was established as shown (Fig. 1).

Compound **6** had the molecular formula $C_{18}H_{24}O_4$ derived from the ^{13}C NMR and HRESITOFMS (m/z 327.1562 [M + Na]$^+$) data, implying the same index of hydrogen deficiency, but having one more oxygen atom than **1**. The IR spectrum showed bands for γ-lactone (1789 cm^{-1} and a cyclohexanone (1719 cm^{-1}) groups. The NMR data of **6** (Table 2) was similar to that of **1**, except for the resonances of the C-5/6 double bond which were replaced by those of an epoxide moiety [δ_H 3.65 (d, J = 3.6 Hz, H-5)/δ_C 58.6 and δ_H 3.37 (d, J = 3.6 Hz, H-6)/δ_C 54.9)]. The relative configuration of the epoxide was assigned by the NOESY correlations between H-6 and H-6a. Hence, the structure of compound **6**, velutinone F, was defined as shown (Fig. 1).

5a, R = (S)-MTPA
5b, R = (R)-MTPA

Fig. 4 $\Delta\delta$ values ($\Delta\delta = \delta_S - \delta_R$ in ppm) obtained for MTPA esters **5a** and **5b**.

Fig. 5 Key NOESY correlations of **5**, energy minimized using MM2.

Compound **7** had the molecular formula $C_{18}H_{24}O_5$, established from the ^{13}C NMR and HRESITOFMS (m/z 321.1690 [M + Na]$^+$) data, having the same index of hydrogen deficiency as in **2**. The IR spectrum displayed an extra hydroxyl band at (3481 cm^{-1}) which differed from that of **6**. The NMR data of **7** (Table 2) corresponded to that of **2**, except for the resonances of a C-5/6 double bond, which was replaced by resonances for an epoxide moiety [δ_H 3.62 (d, J = 3.6 Hz, H-5)/δ_C 58.5 and δ_H 3.34 (d, J = 3.6 Hz, H-6)/δ_C 54.8] as in that of **6**. The 6'S configuration was assigned by comparison of the NMR data to that of **2**. Thus the structure of **7**, velutinone G, was defined as shown (Fig. 1).

Compound **8** possessed the molecular formula $C_{18}H_{24}O_5$ from the ^{13}C NMR and HRESITOFMS (m/z 321.1690 [M + H]$^+$) data, having seven indices of hydrogen deficiency as in **6**, but having one additional oxygen. The IR spectrum was also similar to that of **6**. The NMR data of **8** (Table 2) corresponded to that of **6**, except for the resonances for a C-6'/7' double bond which were replaced by resonances for an epoxide [δ_H 3.65 (t, J = 6.7 Hz, H-6'/δ_C 63.7 and δ_C 58.2, C-7')] at this position. The configuration at C-6' of **8** was proposed to be S, based on its ring opening to give **7**. Hence, structure of **8**, velutinone H, was designated as shown in Fig. 1.

There are only two closely related bicyclic lactones, panamonons A and B,[38] which have NMR data similar to those of compounds **1–8**. However, the relative configuration at the ring junction (C-2a and C-6a) of **1–8** were assigned as 2aR and 6aR which different from panamonons A and B (2aR and 6aS).[38] The ECD spectra of compounds **1–4**, containing an α,β-unsaturated ketone, and compound **5**, showed negative Cotton effects in the range of 202–215 nm. While, compounds **6–8** contained a saturated ketone, exhibited positive Cotton effects in the range of 205–215 nm (Fig. 6).

To confirm the natural occurrence of **1–8**, the isolates velutinone A (**1**) with a geranyl side chain and velutinone H (**8**) with two epoxide rings were stirred with or without silica gel in EtOAc and MeOH for 4 days following the conditions of the separation process. No change on TLC was observed. We conclude that isolates **1–8** are natural occurring products not artefacts.

The putative biosynthetic pathway towards compounds **1–8** is shown in Fig. 7. The precursor, homogentisic acid,[35,36] could be prenylated by geranyl diphosphate to form intermediate **A** [38] which may be reduced and lactonized to form compound **1**. Reduction of **1** would produce **5**, while epoxidation of **1** would afford **6** or intermediate **B**. Oxidation of **5** would give **4** which could be reduced to give **3** or **B**, the latter *via* intermediate **C**. Protonation and deprotonation of **B** may give **2** and **3**. The hydroxy group of **3** could be oxidized to give **4**. Compound **8** could be derived from **6** or **B** *via* an oxidation reaction. Further protonation and deprotonation of **8** would give **7**.

Compound **9** showed an [M + Na]$^+$ ion peak at m/z 539.1651 in its HRESITOFMS, which in conjunction with the ^{13}C NMR data indicated the molecular formula $C_{30}H_{28}O_8$, requiring seventeen indices of hydrogen deficiency. The IR spectrum showed bands for unsaturated lactone (1715 cm^{-1}) and aromatic (1643 cm^{-1}) groups. The UV spectrum also indicated an aromatic moiety (286 nm). Since the NMR spectroscopic data
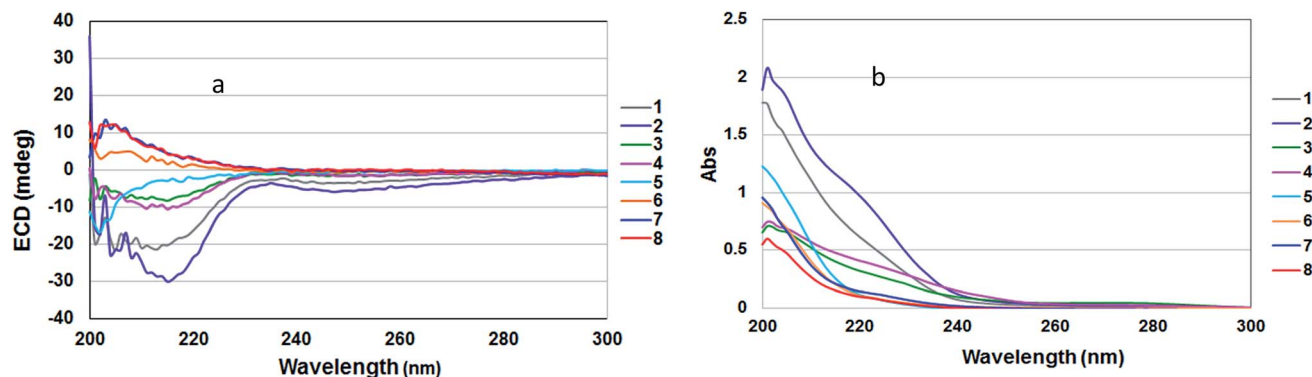
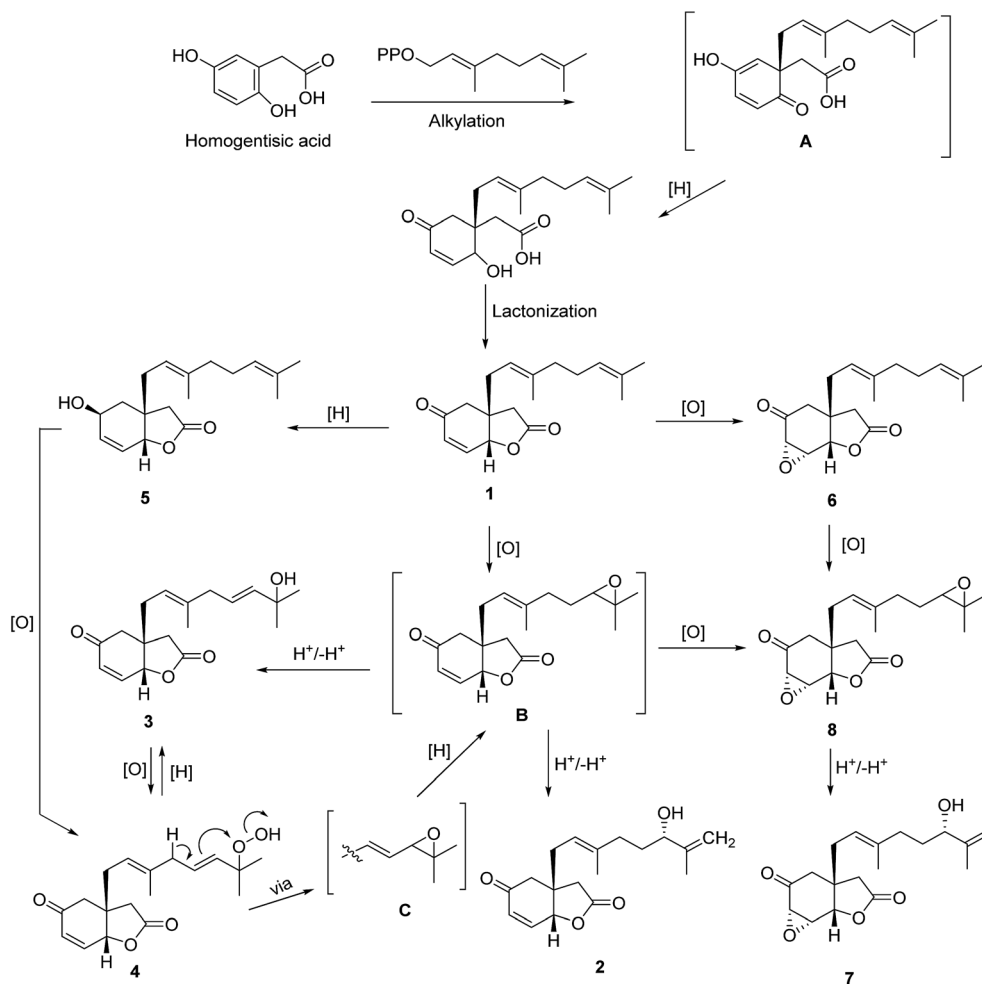Fig. 6   ECD (a) and UV (b) spectra (in MeOH) of compounds **1–8**.

Fig. 7   Plausible biogenetic pathway of **1–8**.

of **9** (Table 3) displayed half the number of resonance signals expected for 28 protons and 30 carbons, the structure should be a symmetrical dimer. These NMR resonances corresponded to those of the cyclobutane dimer, achyrodimer A,[39] except for hydroxy groups at C-12 and C-12′ of the aromatic rings which were replaced by methoxy groups. The ^{1}H NMR spectroscopic data (Table 3) showed resonances for the *para*-substituted benzene rings at δ 6.82 and 7.19 (each 4H, d, J = 8.7 Hz), four methines of the cyclobutyl ring at δ 4.16 and 4.35 (each 2H, dd, J = 7.6, 10.0 Hz), four olefinic protons for the two α-pyrone moieities at δ 5.21 and 5.71 (each 2H, d, J = 2.2 Hz), and four methoxy groups at δ 3.75 and 3.67 (each 6H, s). The ^{13}C NMR data (Table 3) showed resonances for the *para*-disubstituted benzene rings at δ 129.4 (C-9, 9′), 128.5 (C-10, 10′ and C-14, 14′),
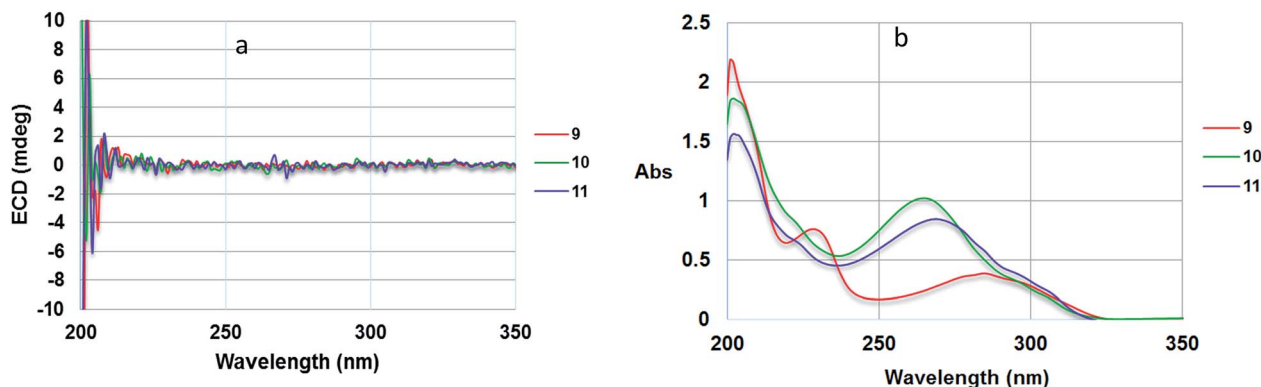
Fig. 8 ECD (a) and UV (b) spectra (in MeOH) of compounds 9, 10 and 11.

and 113.9 (C-11, 11′), the cyclobutyl methines at δ 43.0 (C-7, 7′), and 45.5(C-8, 8′) the α-pyrone methines at δ 87.7 (C-3, 3′), 101.3 (C-5, 5′) and methoxy groups at δ 55.7 (4, 4′-OMe) and 55.2 (12, 12′-OMe), and a carbonyl group at 162.9 (C-6, 6′). The correlations of H-7/7′ to C-5/5′, C-6/6′, C-8/8′, and C-9/9′, and of H-8/8′ to C-6/6′, C-7/7′, C-10/10′, and C-14/14′ from the HMBC spectrum revealed the connection of a cyclobutane ring to an α-pyrone ring, and benzene rings at C-7/7′ and C-8/8′, respectively. Resonances for two sets of methoxy protons at δ_H 3.75 and 3.67 showed correlations with C-4/4′ and C-12/12′, respectively, confirming the location of methoxy groups at C-4/4′ and C-12/12′. The correlations between H-7 (7′) and H-8 (8′) in the NOESY spectrum indicated the relative configuration on the cyclobutane ring as reported for achyrodimer A.[39] The specific rotation value of 9 was almost zero [+0.08 (c 0.63, MeOH–CHCl₃; 3 : 1)] which was also the same as that reported for a symmetric achyrodimer A.[39] Moreover, the ECD spectrum of 9 showed no signal for a Cotton effect (Fig. 8).[40] Based on this evidence the structure of compound 9 could contain a plane of symmetry. Hence, 9 was concluded to be a new symmetrical cyclobutane dimer of the isolated styrylpyrone, yangonin (12), and it was named velutinindimer A.

Compound 10 possessed the molecular formula $C_{30}H_{28}O_8$ from the ^{13}C NMR and HRESITOFMS (m/z 539.1666 [M + Na]⁺) data, having the same index of hydrogen deficiency as 9. The IR spectrum displayed bands for lactone (1699 cm⁻¹) and aromatic (1647 cm⁻¹) groups. The UV spectrum also supported an aromatic moiety (268 nm). The ^1H NMR data of 10 (Table 3) showed resonances for two *para*-disubstituted benzene rings at δ 6.85, 7.16, and 7.34 and 6.85 (each 2H, d, J = 8.7 Hz), an *E*-double bond at δ 6.42 and 6.86 (each 1H, d, J = 15.8 Hz), α-pyrone ring at δ 5.33 and 5.89 (each 1H, d, J = 2.2 Hz, H-3 and H-5, respectively) and 5.29 (s, H-3′), three methine protons at δ 3.55 (d, J = 9.9 Hz, H-5′), 4.26 (dd, J = 10.8, 9.9 Hz, H-8), 4.09 (d, J = 10.8 Hz, H-7), and four methoxy groups at δ 3.32, 3.69, 3.78, and 3.79. The ^{13}C NMR spectrum, DEPT and HMQC experiments of 10 showed 30 resonances, including two sets of *p*-disubstituted benzene rings, one α-pyrone ring, one olefinic, one cyclobutane ring, and four methoxy carbons. The HMBC spectrum displayed ^3J correlations of H-3 to C-5; H-5 to C-3, and C-7; H-7 to C-5, C-9, C-5′, and C-7′; H-8 to C-6, C-10, C-14, C-4′,

and C-6′; H-10, 14 to C-8, and C-12; H-11, 13 to C-9; H-3′ to C-5′; H-5′ to C-7, C-9, C-3′ and C-7′; H-7′ to C-7, C-5′, and C-9′; H-8′ to C-6′, C-10′, and C-14′; H-10′, 14′ to C-8′ and C-12′; H-11′, 13′ to C-9′ and C-12′; 4-OMe to C-4; 12-OMe to C-12; 4′-OMe to C-4′; and 12′-OMe to C-12′ confirming the structure of 10 (Fig. 9). The NMR data of 10 was comparable to the cyclobutane dimer achyrodimer D, reported from the aerial parts of *Achyrocline bogotensis*.[39] It was found that 10 was the methoxy derivative of achyrodimer D. The relative configuration of 10 was determined from the relatively large coupling constants (9.9–10.8 Hz) between H-7 and H-8, and H-8 and H-5′, and the NOESY correlations between H-8 and H-5′, H-7 and H-14, H-8 and H-10, H-5 and H-7, H-7′ and H-10′, and H-8′ and H-14′. The magnitude of the coupling constant between H-7 and H-8 (J_{trans} = 10.8 Hz), and

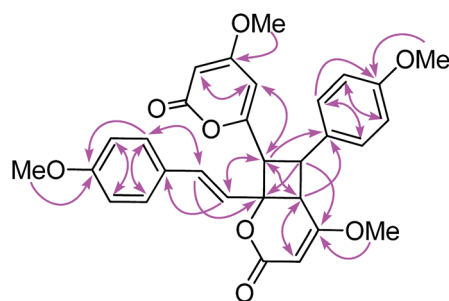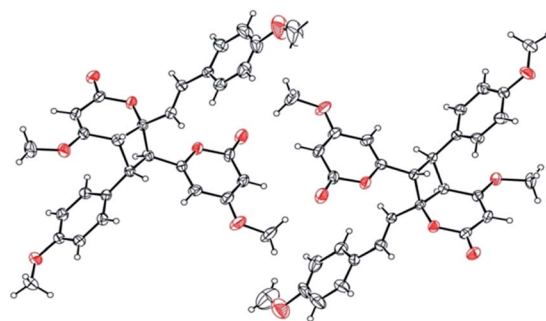

Fig. 9 Selected HMBC correlations of 10.

Fig. 10 ORTEP plot of the asymmetric units in 10. The thermal ellipsoids are shown at 40% probability.
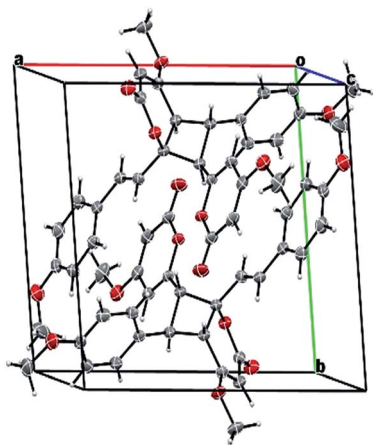
Fig. 11 Packing structure of **11** showing the inverted racemic mixture. The chloroform solvate molecule is omitted for clarity.
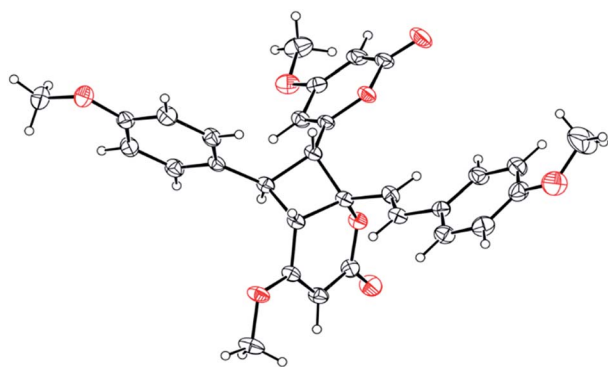

Fig. 12 ORTEP plot of the asymmetric unit in **11**. The thermal ellipsoids are shown at 30% probability level. The chloroform solvate molecule is omitted for clarity.

H-8 and H-5′ (J_{cis} = 9.9 Hz) could be correlated to the dihedral angle between those protons, which corresponded with the values from the Karplus equation for a four membered ring.[41]

The ECD measurement of **10** in MeOH showed no signal of the Cotton effect[40] (Fig. 8), and also the specific rotation value of **10** was almost zero (+0.08). These could suggest that compound **10** was a racemic mixture. Finally, the X-ray crystallographic analysis supported the structure of an isolated **10** containing asymmetric units of a racemic mixture (Fig. 10), and the one with the relative configuration (5′S, 6′R, 7S, and 8S) is shown in Fig. 1. Thus, the structure of **10** was an unsymmetrical cyclobutane dimer of the isolated yangonin (**12**), and it was named velutinindimer B.

Compound **11** exhibited an [M + Na]$^+$ peak at m/z 539.1664 in the positive HRESITOFMS corresponding to the molecular formula $C_{30}H_{28}O_8Na$, the same as that of **10**. The IR spectrum showed bands for a lactone moiety (1708 cm^{-1}) and an aromatic ring (1649 cm^{-1}). The UV spectrum indicated an aromatic moiety (273 nm). The NMR data (Table 3) and 2D NMR of **11** demonstrated a similar structure to a dimeric **10**. Nevertheless, slight differences in chemical shifts around compounds **11** and **10** in the ^{1}H and ^{13}C NMR data at positions 7, 8, 9, 5′, 7′ and 8′ (Table 3) suggested different configurations at the cyclobutane ring between the two compounds. The large coupling constant of H-7 and H-8 (J_{trans} = 10.3 Hz) and H-8 and H-5′ (J_{trans} = 9.7 Hz) could be explained in the same way as for **10**.[41] The NOESY spectrum displayed correlations of H-5′ and H-7, H-7 and H-14, H-8 and H-10, H-7′ and H-10′, and H-8′ and H-14′, indicating the relative configuration of **11**. Compound **11** also showed no signal of the Cotton effect (Fig. 7)[40] and also its specific rotation value was almost zero (+0.3) suggesting that it should be a racemic mixture as compound **10**. The X-ray crystallographic analysis confirmed that the isolated compound **11** was a racemic mixture as in **10**, and the one with the relative configuration 5′R, 6′S, 7R, and 8S is shown in Fig. 1, 11 and 12. From the above evidence, the structure of **11** was determined to be another new dimeric styrylpyrone and it was named velutinindimer C.

To confirm the natural occurrence of styrylpyrone dimers, **9**–**11**, the isolated yangonin (**12**), was stirred with silica gel in EtOAc and MeOH for a week, following the conditions for our

Table 4 Biological activities of the isolated compounds

Compound	Antimalarial (IC$_{50}$, μM)	Anti-TB (MIC, μM)	Cytotoxicity (IC$_{50}$, μM)			
			KB^a	MCF7^b	NCI-H187^c	Vero cell^d
1	Inactive	43.4	4.0	4.8	4.2	5.8
2	9.6	82.1	9.6	12.9	6.5	8.8
3	10.0	Inactive	12.9	10.9	11.4	10.3
4	9.6	Inactive	10.5	15.2	8.7	11.7
6	Inactive	Inactive	14.5	20.7	11.5	11.2
7	9.8	Inactive	24.1	21.0	14.7	17.9
8	7.3	Inactive	10.5	11.9	6.8	18.2
9	6.4	Inactive	Inactive	Inactive	Inactive	Inactive
10	5.4	Inactive	Inactive	Inactive	Inactive	Inactive
11	5.8	Inactive	Inactive	Inactive	Inactive	Inactive
Dihydroartemisinin	0.004					
Streptomycin		0.3–0.5				
Ellipticine			0.8		5.6	3.1
Doxorubicin			0.3	0.1	0.01	

^{a} Human oral epidermoid carcinoma. ^{b} Human breast cancer cells. ^{c} Human lung cancer cells. ^{d} Normal African green monkey kidney cells.

separation process. The formation of **9**, **10** and **11** was not observed. It is worth noting that isolated dimers **10** and **11** were racemic mixtures occurring from asymmetrical 2 + 2 cycloaddition of the isolated styrylpyrone, yangonin (**12**), while compound **9** has an axis of a symmetric dimer and so is not chiral.

The biological activities of the isolated compounds (purity > 95% from the NMR spectra) are shown in Table 4. Compounds **1** and **2**, with MIC values of 43.4 and 82.1 μM respectively, should be responsible for the antimycobacterial activity against *M. tuberculosis* exhibited in the primary screening. From this result, the α,β-unsaturated carbonyl in the core structure plays an important role against TB, while the hydroxy or peroxide functionalities at C-6′ or C-7′ reduce this activity. Since our previous work reported the antimalarial activity and cytotoxicity of compounds from *M. velutina*,[20,21] the compounds isolated herein have been further evaluated for their activities. Compounds **2–4** and **7–11** displayed antimalarial activity toward *P. falciparum* with IC$_{50}$ values in the range of 5.4–10.0 μM. In addition, compounds **1–4** and **6–8** exhibited cytotoxicity against three cancer cell lines tested, with IC$_{50}$ values in the range of 4.0–24.1 μM. Among these, **1**, **2** and **8** exhibited moderate cytotoxicity against NCI-H187 cell lines with IC$_{50}$ values of 4.2, 6.5 and 6.8 μM, respectively, which were close to the standard drug, ellipticine (5.6 μM). Compounds **1–4** and **6–8** exhibited cytotoxicity towards the Vero cell line with IC$_{50}$ values in the range of 5.8–18.2 μM. However, dimeric styrylpyrones **9–11** showed no cytotoxicity in the test.

4. Conclusions

Isolation of the leaves extracts of *M. velutina* yielded an unique class of eight bicyclic lactones with a C$_{18}$ carbons architecture, named velutinones A–H (**1–8**), three new dimeric styrylpyrones, velutinindimers A–C (**9–11**), five known compounds, the kawapyrone, yangonin (**12**), three flavonoids (**13–15**), and an acetogenin, cananginone H (**16**). Velutinindimers A–C (**9–11**) are dimers occurring from symmetrical and asymmetrical 2 + 2 cycloaddition of the isolated styrylpyrone, yangonin (**12**). The structures of velutinindimers B and C (**10** and **11**) were identified as mixtures which were confirmed by X-ray crystallographic, ECD and specific rotation analyses. Biological activity of the isolated compounds had been evaluated. Compounds **2–4** and **7–11** showed antimalarial activity with IC$_{50}$ values in the range of 5.4–10.0 μM. Moreover, **1–4** and **6–8** displayed cytotoxicity against the KB, MCF7, and NCI-H187 cancer cell lines and Vero cell lines with IC$_{50}$ values in the range of 4.0–24.1 μM.

Acknowledgements

Notes and references

1 W. Chuakul and N. Sornthornchareonon, *Thai J. Phytopharm.*, 2003, **10**, 25–32.

2 T. Smitinand, *Thai Plant Names Revised Edition*, Prachachon Co. Limited, Bangkok, 2001, p. 359.

3 T. Chaowasku and P. J. A. Keßler, *Nord. J. Bot.*, 2013, **3**, 680–699.

4 G. G. Harrigan, A. A. L. Gunatilaka, D. G. I. Kingston, G. W. Chan and R. K. Johnson, *J. Nat. Prod.*, 1994, **57**, 68–73.

5 R. Wu, Q. Ye, N. Y. Chen and G. L. Zhang, *Chin. Chem. Lett.*, 2001, **12**, 247–248.

6 C. Kamperdick, N. H. Van and T. V. Sung, *Phytochemistry*, 2002, **61**, 991–994.

7 D. T. Huong, C. Kamperdick and T. V. Sung, *J. Nat. Prod.*, 2004, **67**, 445–447.

8 Y. Lei, L. Wu, H. Shi and P. Tu, *Helv. Chim. Acta*, 2008, **91**, 495–500.

9 N. P. Thao, B. T. T. Luyen, B. H. Tai, N. M. Cuong, Y. C. Kim, C. V. Minh and Y. H. Kim, *Bioorg. Med. Chem. Lett.*, 2015, **25**, 3859–3863.

10 K. Sawasdee, T. Chaowasku and K. Likhitwitayawuid, *Molecules*, 2010, **15**, 639–648.

11 K. Sawasdee, T. Chaowasku, V. Lipipun, T. H. Dufat, S. Michel and K. Likhitwitayawuid, *Fitoterapia*, 2013, **85**, 49–56.

12 K. Sawasdee, T. Chaowasku, V. Lipipun, T. H. Dufat, S. Michel and K. Likhitwitayawuid, *Tetrahedron Lett.*, 2013, **54**, 4259–4263.

13 K. Sawasdee, T. Chaowasku, V. Lipipun, T. H. Dufat, S. Michel, V. Jongbunprasert and K. Likhitwitayawuid, *Biochem. Syst. Ecol.*, 2014, **54**, 179–181.

14 B. Chen, C. Feng, B. Li and G. Zhang, *Nat. Prod. Res.*, 2003, **17**, 397–402.

15 H. Zhang, C. Ma, N. V. Hung, N. M. Cuong, G. T. Tan, B. D. Santarsiero, A. D. Mesecar, D. D. Soejarto, J. M. Pezzuto and H. H. S. Fong, *J. Med. Chem.*, 2006, **49**, 693–708.

16 C. Naphong, W. Pompimon and P. Sombutsiri, *Am. J. Appl. Sci.*, 2013, **10**, 787–792.

17 S. Jumana, C. M. Hasan and M. A. Rashid, *Fitoterapia*, 2000, **71**, 559–561.

18 C. M. Hasan, S. Jumana and M. A. Rashid, *Nat. Prod. Lett.*, 2000, **14**, 393–397.

19 S. Jumana, C. M. Hasan and M. A. Rashid, *Biochem. Syst. Ecol.*, 2000, **28**, 483–485.

20 N. Wongsa, S. Kanokmedhakul and K. Kanokmedhakul, *Phytochemistry*, 2011, **72**, 1859–1864.

21 N. Wongsa, S. Kanokmedhakul and K. Kanokmedhakul, *Phytochemistry*, 2015, **109**, 154.

22 I. Ohtani, T. Kusumi, Y. Kashman and H. Kakisawa, *J. Am. Chem. Soc.*, 1991, **113**, 4092–4096.

23 Bruker, *APEX2, SAINT and SADABS*, Bruker AXS Inc., Madison, WI, USA, 2014.

24 G. M. Sheldrick, *Acta Crystallogr., Sect. A: Found. Crystallogr.*, 2008, **A64**, 112.

25 W. Trager and J. B. Jensen, *Science*, 1967, **193**, 673–675.

26 R. E. Desjardins, C. J. Canfield, J. D. Haynes and J. D. Chulay, *Antimicrob. Agents Chemother.*, 1979, **16**, 710–718.

27 D. A. Scudiere, R. H. Shoemaker, K. D. Paull, A. Monks, S. Tierney, T. H. Nofziger, M. J. Currens, D. Seniff and M. R. Boyd, *Cancer Res.*, 1988, **48**, 4827–4833.

28 J. O'Brien, I. Wilson, T. Orton and F. Pognan, *Eur. J. Biochem.*, 2000, **267**, 5421–5426.

29 L. Hunt, M. Jordan, M. D. Jesus and F. M. Wurm, *Biotechnol. Bioeng.*, 1999, **65**, 201–205.

30 T. Hashimoto, M. Suganuma, H. Fujiki, M. Yamada, T. Kohno and Y. Asakawa, *Phytomedicine*, 2003, **10**, 309–317.

31 Y. Ogawa, H. Oku, E. Iwaoka, M. Iinuma and K. Ishiguro, *Chem. Pharm. Bull.*, 2007, **54**, 675–678.

32 J. M. J. Vasconcelos, A. M. S. Silva and J. A. S. Cavaleiro, *Phytochemistry*, 1998, **49**, 1421–1424.

33 E. Lee, B. H. Moon, Y. Park, S. Hong, S. Lee, Y. Lee and Y. Lim, *Bull. Korean Chem. Soc.*, 2008, **29**, 507–510.

34 J. T. B. Ferreira, R. C. Boscaini and F. A. Marques, *Nat. Prod. Lett.*, 1993, **2**, 313–316.

35 A. G. Ferreira, J. B. Fernandes, P. C. Vieira, O. R. Gottlieb and H. E. Gottlieb, *Phytochemistry*, 1995, **40**, 1723–1728.

36 A. G. Ferreira, M. Motidome, O. R. Gottlieb, J. B. Fernandes, P. C. Vieira, M. Cojocaru and H. E. Gottlieb, *Phytochemistry*, 1989, **28**, 579–583.

37 A. G. Rücker, E. Schenkel, D. Manns, M. Falkenberg and A. Marek, *Phytochemistry*, 1996, **41**, 297–300.

38 Y.-S. Wang, R. Li, Y. Huang, W.-B. Shang, F. Chen, H.-B. Zhang and J.-H. Yang, *Phytochem. Lett.*, 2013, **6**, 26–30.

39 T. Sagawa, Y. Takaishi, Y. Fujimoto, C. Duque, C. Osorio, F. Ramos, C. Garzon, M. Sata, M. Okamoto, T. Oshikawa and S. U. Ahmed, *J. Nat. Prod.*, 2005, **68**, 502–505.

40 M. Fujiki, *Symmetry*, 2014, **6**, 677–703.

41 http://www.nmr.ch.tum.de/home/dames/J_reich_uwisc.pdf, July 2015.
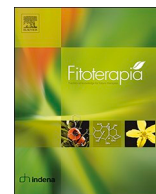
Bioactive homogentisic acid derivatives from fruits and flowers of *Miliusa velutina*

Trinop Promgool[a], Kwanjai Kanokmedhakul[a], Sarawut Tontapha[b], Vittaya Amornkitbamrung[b], Saowanit Tongpim[c], Winai Jamjan[c], Somdej Kanokmedhakul[a,*]

[a] *Natural Products Research Unit, Department of Chemistry and Center of Excellence for Innovation in Chemistry, Faculty of Science, Khon Kaen University, Khon Kaen 40002, Thailand*
[b] *Integrated Nanotechnology Research Center, Department of Physics, Faculty of Science, Khon Kaen University, Khon Kaen 40002, Thailand*
[c] *Department of Microbiology, Faculty of Science, Khon Kaen University, Khon Kaen 40002, Thailand*

ARTICLE INFO

ABSTRACT

Chromatographic separation of fruits and flowers of the Thai medicinal plant, *Miliusa velutina,* resulted in the isolation of five new rare homogentisic acid derivatives, miliusanal (**1**) and miliusanones A-D (**2–5**), together with fifteen known secondary metabolites (**6–20**). Their structures were determined through the use of extensive spectroscopic data. The absolute configurations of homogentisic acid derivatives **2–7** were identified using NOESY data and a comparison of experimental and calculated ECD spectral data. Compounds **2**, **3**, **6**, and **7** showed antimalarial activity with IC_{50} values in the range of 3.3–5.2 μg/mL. Compound **6** also showed activity against *Mycobacterium tuberculosis* with an MIC value of 50 μg/mL. Compounds **1–3**, **6** and **7** exhibited cytotoxicity againt KB, MCF-7, NCI-H187 and Vero cell lines with IC_{50} values in the range of 5.8–40.4 μg/mL. In addition, compounds **1**, **2** and **6** showed moderate antibacterial activities against three Gram-positive bacteria (*Bacillus cereus*, *Staphylococcus aureus*, and Methicillin resistant *S. aureus*) with MICs in the range of 32–64 μg/mL.

1. Introduction

The genus *Miliusa* (Annonaceae family) consists of 50 species that are found in the tropical rainforests of India, Malaysia, North Australia, and South China [1]. Previous phytochemical investigations of the genus *Miliusa* showed a number of different types of natural products, including alkaloids [2,3], acetogenins [4–6], flavonoids [3,7], geranylated homogentisic acid derivatives [8], terpenoids [9], bicyclic lactones and dimeric styrylpyrones [10]. Many of these compounds exhibit antibacterial, antimalarial, antiviral, cytotoxic and acetylcholinesterase inhibitory activities [3–6,10–12]. The Thai medicinal plant, *Miliusa velutina*, locally known as Khang Hua Mu or Kong Kang, grows widely in the northeastern part of Thailand [13]. The wood of this plant is used as a tonic and an aphrodisiac in Thai traditional medicine [14]. Our previous phytochemical studies of leaves and stem bark of *M. velutina* resulted in the isolation of linear acetogenins, bicyclic lactones and dimeric styrylpyrones [5,6,10]. Continued study of the fruits and flowers of *M. velutina* has shown that both of their EtOAc extracts showed cytotoxicity toward human oral epidermoid carcinoma (KB) with IC_{50} values of 76.3 and 17.1 μg/mL, respectively. In addition,

the EtOAc extract from the fruits of this plant showed antibacterial activity against *Bacillus cereus* with MIC value of 160 μg/mL. This work presents the isolation and structural elucidation of five new homogentisic acid derivatives (**1–5**), along with fifteen known compounds (**6–20),** from the fruits and flowers of *M. velutina*, and their biological activities.

2. Experimental

2.1. General experimental procedures

Optical rotations were determined on a JASCO P-1020 polarimeter and ECD spectra were recorded on a JASCO J-810 apparatus. UV spectra were recorded using an Agilent 8453 UV–visible spectrophotometer. IR spectra were obtained using a Bruker Tenser 27 spectrophotometer. NMR spectra were recorded using a Varian Mercury Plus 400 spectrometer; the internal standards $CDCl_3$ and CD_3OD were referenced from the residue of those solvents. HRESITOFMS spectra were recorded on a Micromass Q-TOF-2 mass spectrometer. Column chromatography was carried out on MERCK silica gel 0.063–0.200 nm

or < 0.063 mm. Preparative layer chromatography (PLC) was carried out on Merck silica gel 60 PF$_{254}$ glass plate (20 × 20 cm). TLC was performed with precoated MERCK silica gel 60 PF$_{254}$ aluminum sheets; the spots were visualized under UV light (254 and 366 nm) and further by spraying with anisaldehyde, then heating until charred.

2.2. Plant material

The fruits and flowers of *Miliusa velutina* were collected from Phu Wiang, Khon Kaen, Thailand in May 2015 and 2016, respectively. Plant specimens (KKU no. 29004 and 29,005, respectively) were identified by Prof. Pranom Chantaranothai and were deposited at the herbarium of the Department of Biology, Faculty of Science, Khon Kaen University, Thailand.

2.3. Extraction and isolation

Air-dried fruits of *M. velutina* (4.1 kg) were ground into powder and then extracted successively with *n*-hexane (3 × 10 L), EtOAc (3 × 10 L) and MeOH (3 × 10 L) at room temperature to yield crude *n*-hexane (103.4 g, 2.5%), EtOAc (110.9 g, 2.7%) and MeOH (320.6 g, 7.8%) extracts, respectively.

The *n*-hexane extract (82.5 g) was separated by silica gel flash column chromatography (FCC), with a gradient system eluting with *n*-hexane-CH$_2$Cl$_2$ and CH$_2$Cl$_2$-MeOH to give 11 fractions (FRH$_1$-FRH$_{11}$). Fraction FRH$_{10}$ (9.26 g) was subjected to silica gel FCC, eluted with a gradient system of CH$_2$Cl$_2$-EtOAc, to give nine subfractions (FRH$_{10.1}$-FRH$_{10.9}$). Subfraction FRH$_{10.5}$ (2.86 g) was recrystallized from *n*-hexane-EtOAc to afford a mixture of **19** and **20** (103.3 mg). Subfraction FRH$_{10.7}$ (0.29 g) was recrystallized from *n*-hexane-EtOAc to give **8** (5.8 mg) and subfraction FRH$_{10.7.2}$. Subfraction FRH$_{10.7.2}$ (0.22 g) was purified by preparative TLC using 5% Me$_2$CO-CH$_2$Cl$_2$ as eluent to afford **6** (10.8 mg, R$_f$ 0.38).

The EtOAc extract (90.8 g) was isolated by FCC, eluted with a gradient system of *n*-hexane-EtOAc and EtOAc-MeOH, to give 13 fractions (FRE$_1$-FRE$_{13}$). Fraction FRE$_5$ (0.34 g) was subjected to silica gel FCC, eluted with a gradient system of *n*-hexane-Me$_2$CO, to give five subfractions (FRE$_{5.1}$-FRE$_{5.5}$). Subfraction FRE$_{5.2}$ (12.6 mg) was purified by preparative TLC, using 90% CH$_2$Cl$_2$-*n*-hexane as eluent, to afford compound **3** (3.2 mg, R$_f$ 0.60). Subfraction FRE$_{5.4}$ (0.338 g) was purified by silica gel CC, eluted with CH$_2$Cl$_2$, to give **1** (38.0 mg). Fraction FRE$_6$ (1.20 g) was separated on silica gel FCC, eluted with a gradient system of *n*-hexane-CH$_2$Cl$_2$ and CH$_2$Cl$_2$-Me$_2$CO, to give seven subfractions (FRE$_{6.1}$-FRE$_{6.7}$). Subfraction FRE$_{6.3}$ (19.6 mg) was purified by preparative TLC (20% Me$_2$CO-*n*-hexane) to give **15** (3.2 mg, R$_f$ 0.56) and **16** (1.8 mg, R$_f$ 0.44). Subfraction FRE$_{6.5}$ (37.6 mg) was applied on silica gel CC, eluted with an isocratic system of 80% CH$_2$Cl$_2$-*n*-hexane, to afford **13** (2.8 mg) and **14** (1.6 mg). Fraction FRE$_8$ (3.17 g) was subjected to silica gel FCC, eluted with a gradient system of *n*-hexane-CH$_2$Cl$_2$ and CH$_2$Cl$_2$-Me$_2$CO to give eight subfractions (FRE$_{8.1}$-FRE$_{8.8}$). Subfraction FRE$_{8.4}$ (86.4 mg) was separated on silica gel CC, eluted with an isocratic system of 20% Me$_2$CO-*n*-hexane, to give **2** (19.1 mg). Fraction FRE$_9$ (6.49 g) was isolated by silica gel FCC, eluted with a gradient system of *n*-hexane-EtOAc, to give seven subfractions (FRE$_{9.1}$-FRE$_{9.7}$). Subfraction FRE$_{9.1}$ (26.0 mg) was purified by preparative TLC (20% EtOAc-*n*-hexane) to give an additional amount of **3** (3.4 mg, R$_f$ 0.64). Subfraction FRE$_{9.3}$ (1.40 g) was separated on silica gel FCC, eluted with a gradient system of *n*-hexane-EtOAc, to give eight subfractions (FRE$_{9.3.1}$-FRE$_{9.3.8}$). Subfraction FRE$_{9.3.4}$ (90.6 mg) was purified by preparative TLC (100% CH$_2$Cl$_2$) to give **6** (47.1 mg, R$_f$ 0.22). Subfraction FRE$_{9.6}$ (0.24 g) was purified by preparative TLC (60% EtOAc-*n*-hexane) to yield **7** (23.3 mg, R$_f$ 0.22). Fraction FRE$_{10}$ (1.35 g) was purified by silica gel FCC with a gradient system of *n*-hexane-Me$_2$CO, and then further purified on preparative TLC (40% Me$_2$CO-*n*-hexane), to give an additional amount of **7** (28.7 mg, R$_f$ 0.33). Fraction FRE$_{11}$ (1.11 g) was purified by silica gel FCC, eluted with a gradient

system of *n*-hexane-EtOAc, to give nine subfractions (FRE$_{11.1}$-FRE$_{11.9}$). Subfraction FRE$_{11.5}$ (0.187 g) was purified by preparative TLC (70% EtOAc-*n*-hexane, x3) to give **9** (7.4 mg, R$_f$ 0.82). Subfraction FRE$_{11.8}$ (0.18 g) was purified by preparative TLC (70% EtOAc-*n*-hexane, x 4) to give **10** (24.5 mg, R$_f$ 0.73). The MeOH extract (50.0 g) was separated on silica gel CC, eluted with a gradient of *n*-hexane-EtOAc and EtOAc-MeOH, to give eleven fractions (FRM$_1$-FRM$_{11}$). Fraction FRM$_5$ (0.29 g) was purified by silica gel FCC, eluted with a gradient system of *n*-hexane-EtOAc, to give five subfractions (FRM$_{5.1}$-FRM$_{5.5}$). Subfraction FRM$_{5.3}$ (78.0 mg) was purified by preparative TLC (5% MeOH-CH$_2$Cl$_2$) to give **17** (18.9 mg, R$_f$ 0.56). Fraction FRM$_6$ (0.34 g) was purified by Sephadex LH-20 CC, eluted with MeOH to give **18** (1.5 mg).

Air-dried flowers of *M. velutina* (500 g) were ground and extracted successively with EtOAc (3 × 1.5 L) and MeOH (3 × 1.5 L) at room temperature. Removal of solvents from the extracts under reduced pressure gave crude EtOAc (17.9 g, 3.6%) and MeOH (56.9 g, 11.4%) extracts, respectively.

The EtOAc extract (17.1 g) was separated on silica gel FCC, eluted with a gradient system of *n*-hexane-EtOAc and EtOAc-MeOH to give 9 fractions (FLE$_1$-FLE$_9$). Fraction FLE$_2$ (1.02 g) was purified on silica gel FCC, eluted with a gradient system of *n*-hexane-EtOAc, to give seven subfractions (FLE$_{2.1}$-FLE$_{2.7}$). Solid in subfraction FLE$_{2.2}$ (0.26 g) was crystallized from acetone to give **20** (12.3 mg). Subfraction FLE$_{2.3}$ (0.52 g) was purified on silica gel FCC, eluted with CH$_2$Cl$_2$, to give four subfractions (FLE$_{2.3.1}$-FLE$_{2.3.4}$). Subfraction FLE$_{2.3.3}$ (0.11 g) was subjected to Sephadex LH-20 CC, eluted with MeOH, to afford **11** (65.7 mg). Fraction FLE$_4$ (2.38 g) was separated on silica gel FCC, eluted with a gradient system of *n*-hexane-EtOAc, to give six subfractions (FLE$_{4.1}$-FLE$_{4.6}$). Solid in subfraction FLE$_{4.4}$ (0.60 g) was crystallized from *n*-hexane-EtOAc to obtain **8** (36.8 mg). Fraction FLE$_5$ (1.74 g) was separated on silica gel FCC, eluted with 40% EtOAc-*n*-hexane, to give four subfractions (FLE$_{5.1}$-FLE$_{5.4}$). Subfraction FLE$_{5.2}$ (0.040 g) was separated on silica gel FCC, eluted with a gradient system of 10–15% Me$_2$CO-CH$_2$Cl$_2$, to give **12** (9.8 mg). Subfraction FLE$_{5.3}$ (0.24 g) was purified by preparative TLC (MeOH-CH$_2$Cl$_2$) to obtain **7** (44.9 mg, R$_f$ 0.28) and **8** (7.0 mg, R$_f$ 0.89). Subfraction FLE$_{5.4}$ (1.31 g) was separated on silica gel FCC, eluted with a gradient system of 5–60% Me$_2$CO-CH$_2$Cl$_2$, to give twelve subfractions (FLE$_{5.4.1}$-FLE$_{5.4.12}$). Subfraction FLE$_{5.4.9}$ gave **4** (11.6 mg). Subfraction FLE$_{5.4.12}$ was subjected to silica gel FCC, eluted with a gradient system of 5–20% MeOH-CH$_2$Cl$_2$ to give **5** (11.4 mg). Subfraction FLE$_6$ (0.35 g) was separated on silica gel FCC, eluted with a gradient system of 2–30% MeOH-CH$_2$Cl$_2$ to give five subfractions (FLE$_{6.1}$-FLE$_{6.5}$). Subfraction FLE$_{6.1}$ (0.062 g) was purified by preparative TLC (30% Me$_2$CO-*n*-hexane, x2) to obtain **9** (18.7 mg, R$_f$ 0.21). Subfraction FLE$_7$ (0.34 g) was separated by reverse phase RP-18, eluted with a gradient system of 40% H$_2$O-MeOH, to give three subfractions (FLE$_{7.1}$-FLE$_{7.3}$). Subfraction FLE$_{7.2}$ was subjected to Sephadex LH-20 CC, eluted with MeOH, to give **10** (7.3 mg).

2.4. Physical and spectroscopic data of new compounds isolated from the fruits and flowers of Miliusa velutina

Miliusanal (**1**): Yellow solid; R$_f$ 0.41 (20% EtOAc-*n*-hexane); mp 98–99 °C; UV (MeOH) λ_{max} (log ε) 267 (4.57) and 370 (4.20) nm; IR (film)ν_{max} 3261, 2968, 2913, 2855, 1631, 1587 cm^{-1}; ^{1}H NMR (400 MHz, CDCl$_3$): δ 10.90 (s, 2-OH), 9.80 (s, CHO), 6.96 (d, $J = 2.0$ Hz, H-4), 6.83 (d, $J = 2.0$ Hz, H-6), 3.35 (d, $J = 8.0$ Hz, H-1′), 5.30 (t, $J = 8.0$ Hz, H-2′), 2.11–2.08 (m, H-4′and H-5′), 5.10 (t, $J = 6.0$, H-6′), 1.60 (s, H-8′), 1.68 (s, H-9′), 1.69 (s, H-10′); ^{13}C NMR (100 MHz, CDCl$_3$): δ 119.7 (C-1), 154.1 (C-2), 132.0 (C-3), 125.1 (C-4), 148.0 (C-5), 115.2 (C-6), 196.1 (CHO), 27.0 (C-1′), 120.7 (C-2′), 137.7 (C-3′), 39.7 (C-4′), 26.6 (C-5′), 124.2 (C-6′), 131.5 (C-7′), 17.7 (C-8′), 25.7 (C-9′), 16.1 (C-10′); HRESITTOFMS *m/z* 297.1510 [M + Na]$^+$ (calcd for C$_{17}$H$_{22}$O$_3$ + Na, 297.1467).

Miliusanone A (**2**): Colorless viscous liquid; R$_f$ 0.62 (60% Me$_2$CO-CH$_2$Cl$_2$); [α]$_D^{24.2}$ -48 (*c*, 0.1, CDCl$_3$); ECD (143.6 μM, MeOH) λ_{max} (Δε)

Table 1

^{1}H (400 MHz) and ^{13}C (100 MHz) NMR spectral data of **2**[a], **3**[a] and **4**[b], **5**[b].

No.	2 δ_C	2 δ_H (J in Hz)	3 δ_C	3 δ_H (J in Hz)	4 δ_C	4 δ_H (J in Hz)	5 δ_C	5 δ_H (J in Hz)
1	176.0		171.4		174.1		173.7	
2	39.6	2.37 d (16.0) Ha/ 2.78 d (16.0) Hb	39.9	2.35 d (16.0) Ha/ 2.73 d (16.0) Hb	44.9	2.28 d (14.4) Ha/ 2.54 d (14.4) Hb	40.7	2.30 d (16.0) Ha/ 2.59 d (16.0) Hb
1′	47.0		47.2		48.8		47.5	
2′	200.0		200.4		204.4		202.2	
3′	130.1	6.06 d (10.2)	130.1	6.06 d (10.2)	128.4	5.88 d (11.3)	127.2	5.90 d (10.2)
4′	144.0	6.78 dd (10.2, 3.6)	144.4	6.78 dd (10.2, 3.3)	153.5	6.86 d (11.3)	152.2	6.92 d (10.2)
5′	66.0	5.60 m	66.3	5.63 m	65.0	4.61 m	63.7	4.66 m
6′	34.4	2.49 dd (14.8, 5.6) Hα/ 2.12 dd (14.8, 6.0) Hβ	34.7	2.47 dd (12.0, 4.0) Hα/ 2.09 dd (12.0, 8.0) Hβ	40.0	2.39–2.30 m[c] Hα/ 2.01–1.90 m[c] Hβ	38.8	2.56–2.36 m[c] Hα/ 2.07–1.93 m[c] Hβ
1″	35.2	2.36 dd (13.6, 6.5) Ha 2.46 dd (13.6, 6.6) Hb	35.2	2.35 dd (16.0, 7.2) Ha 2.46 dd (16.0, 7.2) Hb	35.5	2.39–2.30 m[c] Ha/ 2.52–2.44 m[c] Hb	34.6	2.56–2.36 m[c]
2″	118.0	5.03 t (6.4)[c]	118.3	5.02 d (7.2)[c]	120.8	5.05 t (6.0)	119.3	5.13 t (7.4)
3″	139.5		139.2		138.4		138.4	
4″	39.9	2.09–2.01 m[c]	40.0	2.04–2.01 m[c]	36.6	2.01–1.90 m[c]	36.7	2.28–2.21 m[c] 2.07–1.93 m[c]
5″	26.4	2.09–2.01 m[c]	26.4	2.04–2.01 m[c]	33.8	1.58–1.52 m[c]	29.3	1.76–1.64 m[c] 1.39–1.23 m[c]
6″	124.0	5.03 t (6.4)[c]	124.1	5.04 d (7.2)[c]	75.6	3.92 q (5.8)	77.4	3.22 d (10.5)
7″	131.6		131.5		148.0		72.4	
8″	25.7	1.66 s	25.7	1.65 s	111.4	4.77 s Ha 4.85 d (5.8) Hb	23.6	1.12 s
9″	17.7	1.59 s	17.7	1.66 s	17.5	1.66 s	24.3	1.16 s
10″	16.4	1.59 s	16.3	1.58 s	16.5	1.58 s	15.2	1.64 s
CO_2Me	21.0	2.09 s	21.0	2.09 s				
CO_2Me	170.2		170.1					
OMe			51.5	3.64 s				

[a] Recorded in CDCl$_3$.
[b] Recorded in CDCl$_3$ + CD$_3$OD.
[c] Overlap of the signals.

Table 2

Biological activities of homogentisic acid derivatives **1**–**7**.

Compound	Antimalarial IC$_{50}$, (μg/mL)	Anti-TB MIC, (μg/mL)	Cytotoxicity (IC$_{50}$, μg/mL) KB[a]	MCF-7[b]	NCI-H187[c]	Vero[d]
1	> 10	> 50	9.3	12.6	40.4	39.1
2	3.8	> 50	11.9	23.2	6.1	16.1
3	5.2	> 50	17.9	26.4	6.2	5.8
4	> 10	> 50	> 50	> 50	> 50	> 50
5	> 10	> 50	> 50	> 50	> 50	> 50
6	3.3	50	26.5	32.7	5.8	6.3
7	3.9	> 50	11.8	> 50	6.1	17.7
Mefloquine	0.011					
Dihydroartemisinin	0.00062					
Streptomycin		0.3–0.6				
Ellipticine			2.0		2.4	1.5
Doxorubicin			0.6	8.5	0.2	

[a] Epidermal carcinoma of the mouth with HeLa cell contamination.
[b] Human breast cancer cell.
[c] Human small lung cancer cell.
[d] Normal African green monkey kidney cell.

201 (+29.9), 225 (−37.8), 340 (+5.3); IR (film)ν_{max}: 3162, 2966, 2921, 2856, 1739, 1711, 1681 cm^{-1}; for ^{1}H and ^{13}C NMR spectroscopic data, see Table 1; HRESITTOFMS m/z 371.1830 [M + Na]$^+$ (calcd for C$_{20}$H$_{28}$O$_5$ + Na, 371.8134).

Miliusanone B (**3**): Colorless viscous liquid; R$_f$ 0.44 (30% EtOAc-n-hexane); [α]$_D^{24.5}$ -40 (c, 0.1, CDCl$_3$); ECD (138.0 μM, MeOH) λ$_{max}$ (Δε) 221 (−32.9), 337 (+3.1); IR (film)ν_{max}: 2927, 2855, 1735, 1681, 1226 cm^{-1}; for ^{1}H and ^{13}C NMR spectroscopic data, see Table 1; HRESITTOFMS m/z 385.1984 [M + Na]$^+$ (calcd for C$_{21}$H$_{30}$O$_5$ + Na, 385.1985).

Miliusanone C (**4**): Colorless viscous liquid; R$_f$ 0.22 (60% Me$_2$CO-CH$_2$Cl$_2$); [α]$_D^{24.3}$ -63 (c, 0.1, MeOH); ECD (310.0 μM, MeOH) λ$_{max}$ (Δε)

206 (+17.9), 234 (−14.3), 340 (+4.3); IR (film)ν_{max}: 3395, 2920, 1710, 1669, 1450, 1379 cm^{-1}; for ^{1}H and ^{13}C NMR spectroscopic data, see Table 1; HRESITTOFMS m/z 345.1679 [M + Na]$^+$ (calcd for C$_{18}$H$_{26}$O$_5$ + Na, 345.1678).

Miliusanone D (**5**): Colorless viscous liquid; R$_f$ 0.11 (60% Me$_2$CO-CH$_2$Cl$_2$); [α]$_D^{24.8}$ -86 (c, 0.1, MeOH); ECD (290.0 μM, MeOH) λ$_{max}$ (Δε) 203 (+30.1) 234 (−20.1), 341 (+4.3); IR (film)ν_{max}: 3368, 2972, 2927, 1713, 1671, 1441, 1377 cm^{-1}; for ^{1}H and ^{13}C NMR spectroscopic data, see Table 1; HRESITTOFMS m/z 363.1784 [M + Na]$^+$ (calcd for C$_{18}$H$_{28}$O$_6$ + Na, 363.1784).

2.5. Antimalarial assay

Antimalarial activity was evaluated against *Plasmodium falciparum* (K1, multidrug resistant strain), using the method of Trager and Jensen [15]. Quantitative assessment of malarial activity *in vitro* was determined by means of the microculture radioisotope technique based upon the method described by Desjardins and co-worker [16]. The inhibitory concentration (IC_{50}) represents the concentration that causes 50% reduction in parasite growth as indicated by the *in vitro* uptake of [^{3}H]-hypoxanthine by *P. falciparum*. The standard compounds were mefloquine and dihydroartemisinin (Table 2).

2.6. Antimycobacterial assay

Antimycobacterial activity was assessed against *Mycobacterium tuberculosis* H37Ra (purchased from ATCC) using the Microplate Alamar Blue Assay (MABA), as described by Collins and co-worker [17]. The standard drug streptomycin was used as a reference substance (Table 2).

2.7. Cytotoxicity assays

Cytotoxicity assays against epidermal carcinoma of the mouth with HeLa cell contamination (KB, ATCC CCL-17), human breast adenocarcinoma (MCF7, ATCC HTB-22), and human small cell lung cancer (NCI-H187, ATCC CRL-5804) were performed employing the resazurin microplate assay (REMA) described by O'Brien and co-workers [18]. Cytotoxicity test against a primate cell line (Vero) was performed using the green fluorescent protein detection method described by Hunt and co-workers [19]. The reference substances used were ellipticine and doxorubicin (Table 2).

2.8. Antibacterial assay

The minimum inhibitory concentrations (MICs) were determined by the dilution method, as described in the document M07-A9 of the Clinical and Laboratory Standards Institute (CLSI) [20,21]. Resazurin solution (0.18%) was used as an indicator of bacterial growth. MICs were determined visually from the lowest concentrations capable of inhibiting bacterial growth. The tests were performed in triplicate. Cefepime, kanamycin and vancomycin were used as positive control

drugs (Table 3). Six bacterial cultures (*Bacillus cereus* DMST 5040, *Staphylococcus aureus* DMST 8013, methicillin resistant *S. aureus* (MRSA), *Escherichia coli* DMST 4212, *Pseudomonas aeruginosa* DMST 4739, and *Salmonella enterica* serovar Typhimurium DMST 562) were employed as the test organisms. The experiment was performed at the Department of Microbiology, Faculty of Science, Khon Kaen University, Thailand.

3. Results and discussion

Chromatographic separation of the extracts from fruits and flowers of *M. velutina* gave twenty compounds, **1–20** (Fig. 1). Their structures were determined by spectroscopic data (IR, UV, ^{1}H and ^{13}C NMR, and 2D-NMR) and MS. The known compounds were identified by physical properties and spectroscopic data measurements, as well as by comparing the data obtained with their published values, as methyl-2-(1′β-geranyl-5′β-hydroxy-2′-oxocyclohex-3′-enyl)acetate (**6**), 2-(1′β-geranyl-5′β-hydroxy-2′-oxocyclohex-3′-enyl)acetic acid (**7**) [22], yagonin (**8**), velutinindimer A (**9**), velutinindimers B (**10**) [10], cananginones A (**11**), cananginones H (**12**) [5,6], 4-hydroxybenzonitrile (**13**) [23,24], 4-hydroxybenzaldehyde (**14**) [25], isovanillin (**15**) [26], 5-acetyloxymethylfurfural (**16**), 5-methoxyfurfural (**17**) and 5-hydroxymethylfurfural (**18**) [27]. Two common phytosterols were identified by comparing their spectroscopic spectra with authentic samples as β-sitosterol (**19**) and stigmasterol (**20**). Structure elucidation of five new compounds, **1–5** and absolute configurations of new and known compounds, **2–7** are described as follows.

Compound **1** was obtained as a yellow solid. Its molecular formula, $C_{17}H_{22}O_3$, deduced from HRESITTOFMS (m/z 297.1510 [M + Na]$^+$), indicates seven degrees of unsaturation. The UV spectrum shows absorption maxima at 267 and 370 nm. The IR spectrum exhibits absorbtion bands of hydroxyl (3261 cm^{-1}), aromatic aldehyde (2855 and 1631 cm^{-1}) and alkene (1587 cm^{-1}) groups. The ^{13}C NMR, HMQC and DEPT spectra reveal the presence of six sp^2 quaternary groups, five sp^2 methine (including one carbonyl), three methylene and three methyl carbons. The ^{1}H NMR spectrum shows an aldehyde proton at δ 9.80 with its carbonyl (C-7) chelated with the hydrogen of a hydroxyl group (δ 10.90, s) at the *ortho* position (C-2). Two doublet signals at δ 6.96 and 6.83 belong to aromatic protons with *meta* coupling ($J = 2.0$ Hz) of H-4 and H-6, respectively. The resonance signals at δ 3.35 (d, $J = 8.0$ Hz, H-1′), δ 5.30 (t, $J = 8.0$ Hz, H-2′), δ 2.11–2.08 (m, H-4′ and

Table 3
Antibacterial activity of isolated compounds.

Compound	Antibacterial activity (MIC, μg/mL)					
	Gram-positive			Gram-negative		
	B. cereus[a]	*S. aureus*[b]	MRSA[c]	*E. coli*[d]	*P. aeruginosa*[e]	*S.* Typhimurium[f]
1	32	64	64	> 128	64	128
2	64	128	> 128	> 128	128	> 128
4	> 128	> 128	> 128	> 128	> 128	> 128
5	> 128	> 128	> 128	> 128	> 128	> 128
6	32	64	64	> 128	128	> 128
7	128	> 128	> 128	> 128	128	> 128
8	128	> 128	> 128	> 128	128	> 128
9	> 128	> 128	> 128	> 128	128	> 128
10	128	> 128	> 128	> 128	128	> 128
Cefepime				0.03	2	0.03
Kanamycin	2	2		2		
Vancomycin	1	1	0.5			

[a] *Bacillus cereus* DMST 5040.
[b] *Staphylococcus aureus* DMST 8013.
[c] Methicillin resistant *Staphylococcus aureus*.
[d] *Escherichia coli* DMST 4212.
[e] *Pseudomonas aeruginosa* DMST 4739.
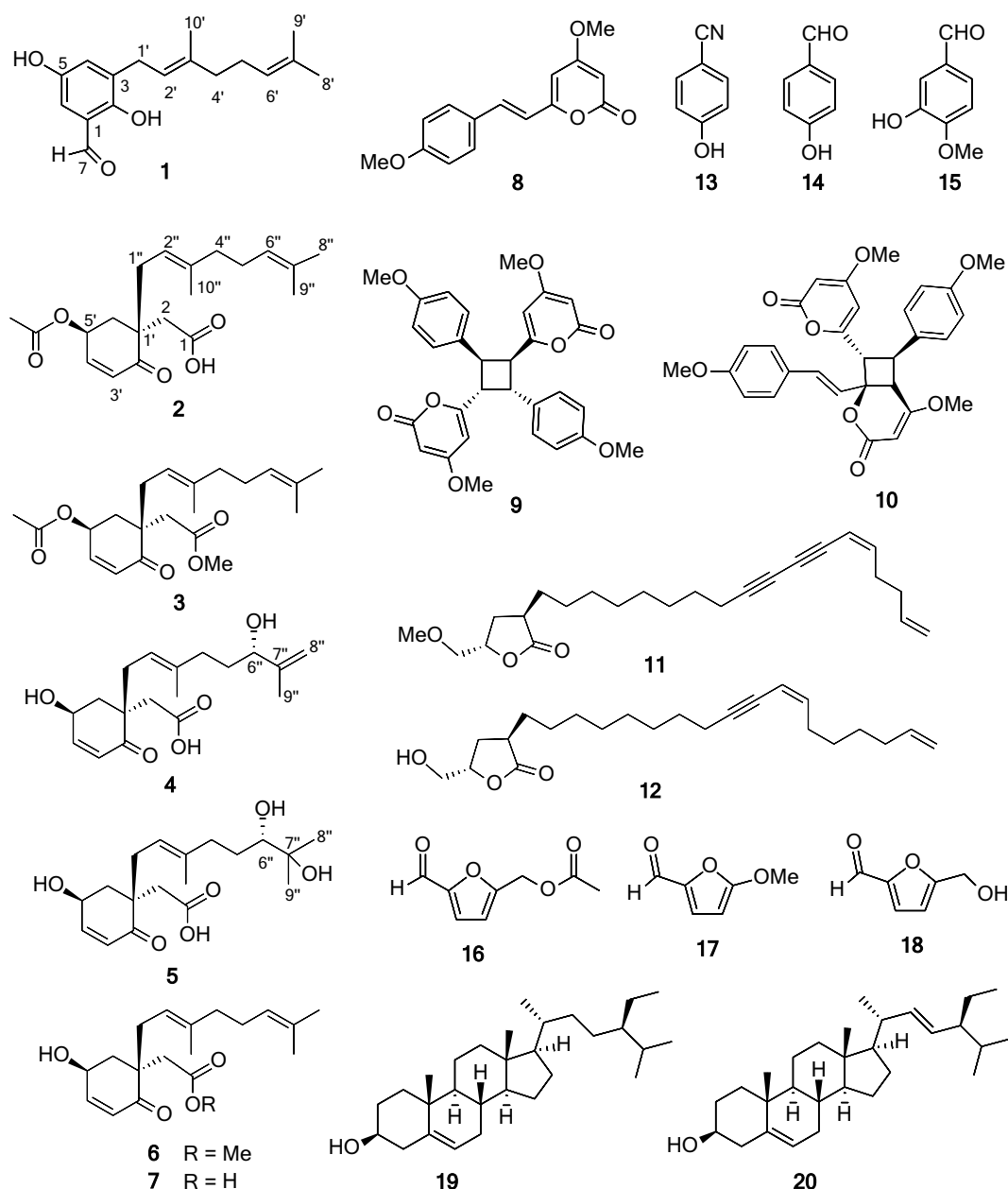[f] *Salmonella enterica* serovar Typhimurium DMST 562.
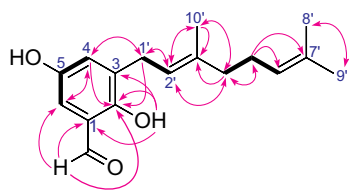
Fig. 1. Structures of compounds **1–20**.

Fig. 2. COSY (bold line) and HMBC (arrow line) correlations of **1**.

H-5′), δ 5.10 (t, $J = 6.0$ Hz, H-6′), δ 1.60 (s, H-8′), δ 1.68 (s, H-9′) and δ 1.69 (s, H-10′) were assigned to a geranyl side chain. The COSY spectrum exhibits correlations of the side chain between H-1′/H-2′ and H-4′/H5′/H-6′. The HMBC spectrum shows correlations of H-1′ to C-2, C-3 and C-4; H-2′ to C-1′, C-4′ and C-10′; H-4′ to C-2′, C-3′ and C-5′ and C-6′; H-5′ to C-4′, C-6′ and C-7′; H-8′ to C-7′ and C-9′; H-9′ to C-7′ and C-8′; H-10′ to C-2′, C-3′ and C-4′, confirming the geranyl group which is linked to the aromatic at C-3 (Fig. 2). Based on the above evidence, compound

1 exhibits a core structure the same as 3-farnesyl-2,5-dihydroxybenzaldehyde isolated from seeds of *Otoba paruifolia* [28]. Thus, **1** was deduced to be a new rare homogentisic acid derivative, 3-geranyl-2,5-dihydroxybenzaldehyde, which has been named miliusanal.

Compound **2** was obtained as a colorless viscous liquid. Its molecular formula, $C_{20}H_{28}O_5$, was deduced from HRESITTOFMS (m/z 371.1830 [M + Na]$^+$), revealing seven degrees of unsaturation. The UV spectrum shows absorption maxima at 201 and 225 nm. The IR spectrum exhibits characteristics of carboxylic acid (3162 and 1711 cm^{-1}), ester (1739 cm^{-1}) and conjugated ketone (1681 cm^{-1}) groups. The ^{13}C NMR, HMQC and DEPT spectra display the presence of five sp^2 quaternary (including three carbonyl groups), four sp^2 methine, one sp^3 quaternary, one oxymethine, five methylene and four methyl carbons. The ^{1}H NMR spectroscopic data (Table 1) shows sets of resonance signals for a 4,6-disubstituted-2-cyclohexenone unit at δ 6.06 (d, $J = 10.2$ Hz, H-3′), 6.78 (dd, $J = 10.2$, 3.6 Hz, H-4′), an oxymethine proton at δ 5.60 (m, H-5′), 2.49 (dd, $J = 14.8$, 5.6 Hz, H-6′α), and 2.12 (dd, $J = 14.8$, 6.0 Hz, H-6′β). The geranyl moiety shows protons of
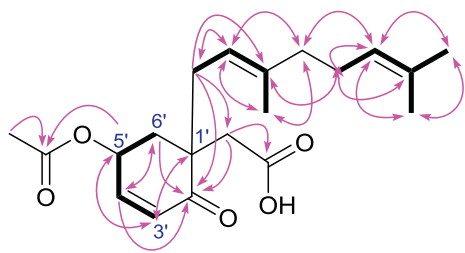
Fig. 3. COSY (bold line) and HMBC (arrow line) correlations of **2**.
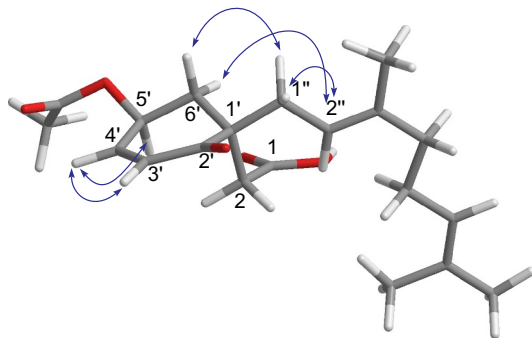
Fig. 4. Key NOESY correlations of **2**, energy minimized using MM2.

three methylene groups, two olefinic groups and three vinyl methyl groups as in those of **1**. The α-methylene carboxylic acid (-CH$_2$-COOH) protons show two doublet signals with a germinal coupling of 16.0 Hz between δ 2.37 and 2.78. The ^{13}C NMR spectroscopic data (Table 1) shows a carboxylic carbon function at δ$_C$ 176.0 (C-1), an enone carbonyl at δ$_C$ 200.0 (C-2′), an acetate group (OAc) at δ$_C$ 170.2 and 21.0, and a secondary oxygenated carbon at δ$_C$ 66.0 (C-5′). The COSY spectrum shows correlations of the cyclohexenone unit, H-3′/H-4′/H-5′/H-6′. The HMBC spectrum exhibits correlations of H-1″ to C-2, C-2′, C-2″ and C-3″; H-2″ to C-1″, C-4″ and C-10″ confirming that the geranyl group is linked to the stereogenic quaternary carbon at C-1′ (Fig. 3). The relative configuration of **2** was established on the basis of NOESY correlations between H-3′ and H-4′, H-5′ and H-6′α, H-1″b and H-2″, and H-6′β and H-2a to H-1″a (Fig. 4). From the above data, **2** has a core skeleton of rare homogentisic acid derivatives as in those of **6** and **7** [22]. The specific rotation of **2** [− 48 (c, 0.1, CHCl$_3$)] and its analogues **6** and **7** [both − 2.9 (c, 0.1, CHCl$_3$)] have the same negative sign. Since the absolute configurations of **6** and **7** have not been reported, the absolute configuration of **2** was further determined by comparison of the experimental ECD spectrum with its ECD calculated spectra. Structures of four possible stereoisomers of **2** (two chiral carbons at C-1′ and C-5′) were optimized by the B3LYP/6-31G(d) method [29] and their ECD spectra were calculated using the time-dependent density functional theory (TD-DFT) method with CAM-B3LYP functional [30] and 6–311 + +G(d,p) basis set. Polarizable continuum model (PCM) solvation model using MeOH was included in the calculations [31]. Calculations were performed using the Gaussian09 program [32]. All calculated ECD spectra are shown in the supplementary material (Fig. S31). The ECD calculated spectrum of (1′R,5′S)-**2** shows a Cotton effect at λ$_{max}$ 202 (Δε + 14.7), 238 nm (Δε − 38.0), and 314 (Δε + 4.0), which agrees well with that of the experimental ECD spectrum of **2** (Fig. 5a). Thus, **2** was identified as a new homogentisic acid derivative with the absolute configuration (1′R,5′S)-**2**, and has been named miliusanone A (Fig. 1). In addition, ECD spectra of **6** and **7** agree well with that of **2** (Fig. 5b); therefore, the absolute configurations of **6** and **7** were concluded to be 1′R,5′S, the same as that of **2**.

Compound **3** was obtained as a colorless viscous liquid. The HRE-SITTOFMS (m/z 385.1984 [M + Na]$^+$) revealed the molecular formula, C$_{21}$H$_{30}$O$_5$, which has one more carbon than **2**. The UV spectrum shows

absorption similar to that of **2**. The IR spectrum shows absorption bands of ester (1735 cm^{-1}) and conjugated ketone (1681 cm^{-1}) functionalities. Analysis of the ^{1}H and ^{13}C NMR spectroscopic data (Table 1) and 2D NMR techniques (COSY, HSQC, HMBC and NOESY) indicates a structure similar to compound **2**. However, the carboxylic acid (δ$_C$ 176.0) of **2** is replaced by an extra carbon as a methyl ester (δ$_{H/C}$ 3.64/ 51.5, δ$_C$ 171.4) in **3**. The HMBC data confirms the location of the ester at C-1 by showing correlations of H-2 to C-1, C-1′, C-2′, C-6′ and C-1″, and methoxy protons to C-1. The absolute configuration of **3** was assigned by comparing the ECD spectrum with calculated ECD spectra of its four possible stereoisomers (two chiral carbons at C-1′ and C-5′) (Fig. S32 in the supplementary material). The calculated spectrum of (1′R,5′S)-**3** shows a Cotton effect at λ$_{max}$ 209 nm (Δε + 6.8), 222 nm (Δε − 10.5), and 320 (Δε + 3.2), which matches the experimental ECD spectrum of **3** well (Fig. 5c). Thus, **3** was identified as a new homogentisic acid derivative with 1′R,5′S configuration (Fig. 1), which we named miliusanone B.

Compound **4** was obtained as a colorless viscous liquid. Its molecular formula, C$_{18}$H$_{26}$O$_5$, deduced from HRESITTOFMS (m/z 345.1679 [M + Na]$^+$), indicates six degrees of unsaturation. The UV spectrum shows absorption maxima at 204 and 236 nm. The IR spectrum exhibits the absorption bands of carboxylic acid (3395 and 1710 cm^{-1}) and conjugated ketone (1669 cm^{-1}) functionalities. The ^{1}H and ^{13}C NMR spectroscopic data of **4** (Table 1) indicates the same core structure as that of **2**. However, the acetoxy group at C-5′ of **2** is replaced by a hydroxyl group (δ$_{H/C}$ 4.61/65.0) in **4**. Besides, the terminal side chain of the geranyl moiety of **4** was identified as a terminal alkene [δ$_C$ 148.0 (C-7″) and δ$_{H/C}$ 4.77 (s), 4.85 (d, J = 5.8 Hz)/111.4 (C-8″)] and there is an extra hydroxy group at C-6″ [δ$_{H/C}$ 3.92 (q, 5.8 Hz)/75.6]. This is confirmed by the HMBC correlation of H-6″ to C-4″, C-5″, C-7″, C-8″, and C-9″. The NMR data in the side chain (C-5″- C-10″) of **4** (Table 1) are comparable to those of velutinone B [(CDCl$_3$)δ$_{H/C}$ 4.00 (t, 6.3)/75.3 (C-6′), 1.58–1.65 (m)/33.0 (C-5′), δ$_C$ 147.3 (C-7′) and 111.0 (C-8′)] [10]. This suggests the configuration at C-6″ of **4** to be 6″S, the same as 6′S in velutinone B. Finally, the absolute configuration of **4** was confirmed by comparison to the calculated ECD spectra of its eight possible stereoisomers (three chiral carbons at C-1′, C-5′, and C-6″) (Fig. S33 in the supplementary material). The ECD calculated data of the generated 1′R,5′S,6″S isomer shows a Cotton effect at λ$_{max}$ 204 (Δε + 29.1), 236 nm (Δε − 19.7), and 311 (Δε + 1.9), which is in good agreement with the experimental spectrum of **4** (Fig. 6). Thus, **4** was identified as a new homogentisic acid derivative having 1′R,5′S,6″S configuration and we named it miliusanone C (Fig. 1).

Compound **5** was obtained as a colorless viscous liquid. The HRE-SITTOFMS (m/z 363.1784 [M + Na]$^+$) indicates the molecular formula, C$_{18}$H$_{28}$O$_6$, which has one more oxygen and two more hydrogen atoms than **4**. It specifies five degrees of unsaturation. The UV and IR spectral data of **5** are similar to those of **4**. The ^{1}H and ^{13}C NMR spectroscopic data of **5** (Table 1) indicate the same core structure as **4**. However, the appearance of an additional hydroxyl group at C-7″ (δ$_C$ 72.4) and a missing terminal alkene at C-7″/C-8″ of the geranyl side chain is seen in **5**. These are confirmed by the HMBC correlations of H-5″ to C-7″; H-6″ to C-4″, C-7″, C-8″, and C-9″; H-8″ to C-6″, C-7″, and C-9″ and H-9″ to C-6″, C-7″, and C-8″. Since **5** and **4** have three chiral carbons at the same positions and the comparison of their ECD spectra is in agreement (Fig. 6), the absolute configuration of **5** was designated to be 1′R,5′S,6″S, the same as that of **4**. Thus, **5** was elucidated as a new homogentisic acid derivative, which we named miliusanone D (Fig. 1).

Geranylated homogentisic acid derivatives with a C$_{18}$ carbon are members of a rare class of plant secondary metabolites. They have been previously reported in genus *Miliusa*, including *M. balansae*, *M. sinensis*, *M. umpangensis* and *M. velutina* [7,8,10,33]. Compound **6** was obtained from *M. umpangensis* [7] and this is the first report for the isolation of **7** in the genus *Miliusa*. Therefore, the presence of geranylated homogentisic acid derivatives (**2–7**) from *M. velutina* could support the chemosystematics of *Miliusa*.
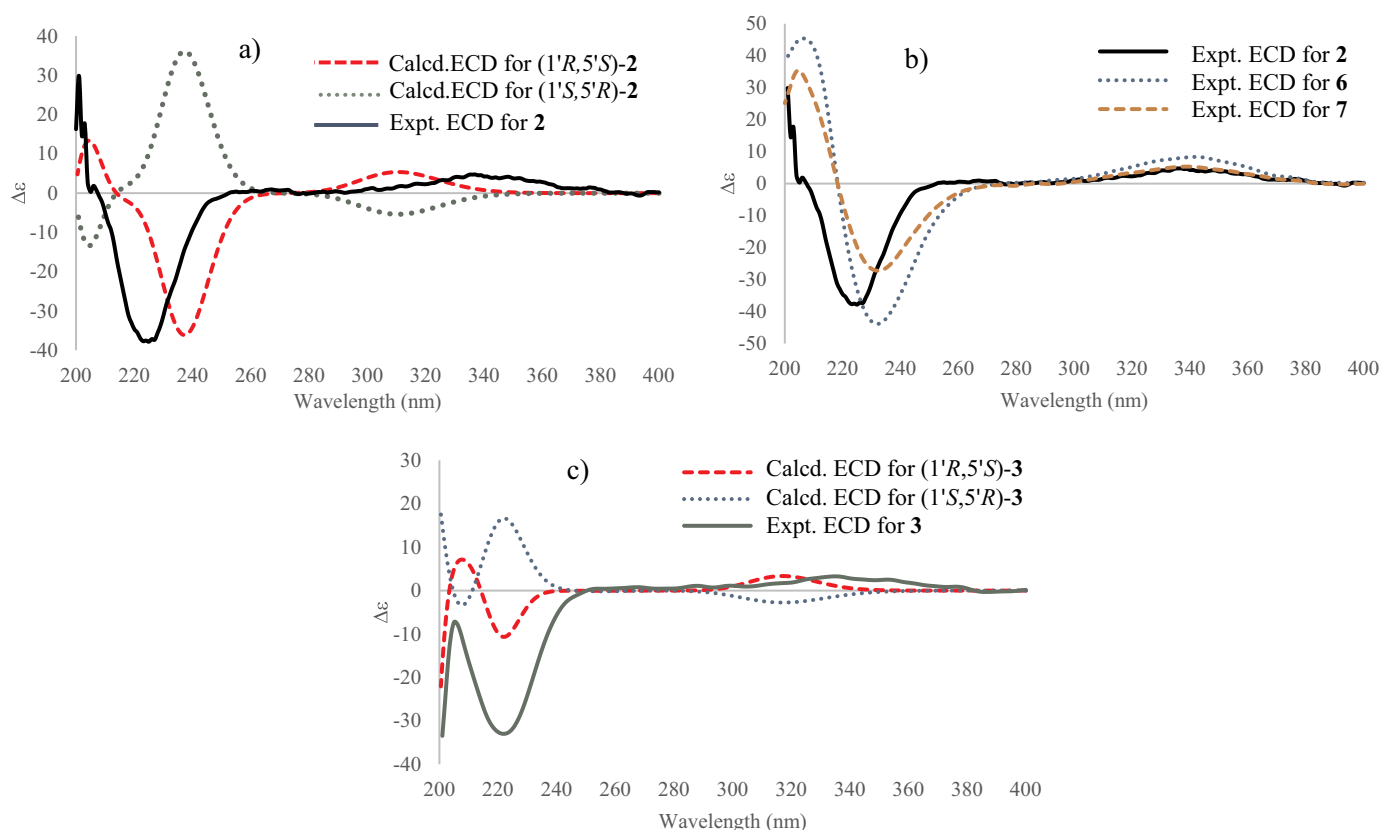
Fig. 5. a) Experimental ECD spectrum of **2** and its calculated ECD spectra of two related possible stereoisomers. b) Experimental ECD spectra of **2**, **6** and **7** in MeOH. c) Experimental ECD spectrum of **3** and its calculated ECD spectra of two related possible stereoisomers.
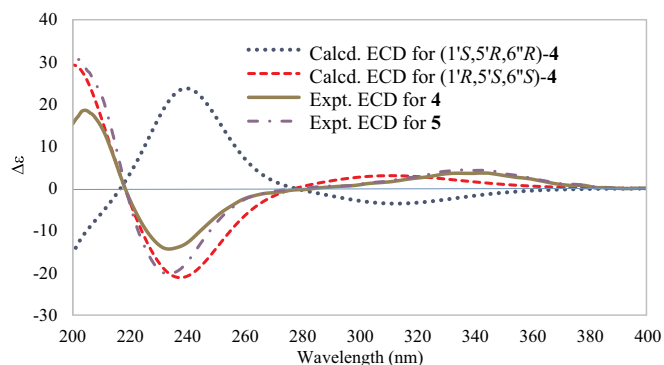

Fig. 6. Experimental ECD spectra of **4** and **5**, and calculated ECD spectra of two related possible stereoisomers of **4** in MeOH.

Homogentisic acid derivatives **1–7** were assayed for their bioactivity, and the results are shown in Tables 2 and 3. Compounds **2**, **3**, **6** and **7** exhibited antimalarial activity against *Plasmodium falciparum* with IC_{50} values of 3.8, 5.2, 3.3, and 3.9 μg/mL, respectively. This result supports a previous report of **6** and **7** being antiplasmodial agents against *P. falciparum* (D-6 and W-2 clones) [22]. Only **6** showed weak antimycobacterial activity against *Mycobacterium tuberculosis*, with an MIC of 50 μg/mL. Compounds **1–3**, **6** and **7** showed cytotoxicity against KB, MCF-7 and NCI-H187 cell lines with IC_{50} values in the range of 5.8–40.4 μg/mL. However, these compounds showed cytotoxicity against Vero cell with IC_{50} values in the range of 5.8–39.1 μg/mL (Table 2). Compounds **1**, **2**, and **4–10** were also tested for antibacterial activity using a broth microdilution method and the results are shown in Table 3. Compounds **1** and **6** showed moderate antibacterial activities against three Gram-positive bacteria tested, with MICs in the range

of 32–64 μg/mL. Compounds **2**, **7**, **8** and **10** showed antibacterial against *B. cereus* with MICs in the range of 64–128 μg/mL and **2** also showed antibacterial against *S. aureus* with an MIC of 128 μg/mL. Moreover, compounds **1**, **2** and **6–10** showed antibacterial activity against Gram-negative bacteria *P. aeruginosa*, with MICs in the range of 64–128 μg/mL. Compound **1** also exhibited antibacterial activity against *S. Typhimurium* with an MIC of 128 μg/mL. It should be noted that the transformations at the terminal side chain of the geranyl group in **4** and **5** result in the lack of activities for all tests.

4. Conclusion

Five new rare homogentisic acid derivatives, **1–5**, and fifteen known compounds **6–20** were isolated from the fruits and flowers of the Thai medicinal plant, *M. velutina*. The absolute configurations of homogentisic acid derivatives **2–7** were assigned by a combination of NOESY data and comparison of their experimental and theoretical computational ECD spectra. Most of these homogentisic acid derivatives with a geranyl side chain displayed antimalarial (*P. falciparum*), cytotoxic (KB, MCF7, NCI-H187 and Vero cell lines) and antibacterial (Gram-positive and Gram-negative bacteria) activities (Tables 2 and 3). However, compounds **4** and **5** with a hydroxyl group at the terminal side chain of the geranyl group showed no activity in all tests. Besides five new rare homogentisic acid derivatives, this investigation provides additional data supporting the utilization of the traditional medicinal plant, *M. velutina*.

Conflict of interest

All the authors declare that there is no conflict of interest concerning this work.

Appendix A. Supplementary data

Supplementary data to this article can be found online at https://doi.org/10.1016/j.fitote.2019.02.007.

References

[1] T. Chaowasku, P.J.A. Keßler, Seven new species of Miliusa (Annonaceae) from Thailand, Nord. J. Bot. 31 (2013) 680–699.

[2] C.M. Hasan, S. Jumana, M.A. Rashid, (+)-Isocorydine α-*N*−oxide: a new aporphine alkaloid from *Miliusa velutina*, Nat. Prod. Lett. 14 (2000) 393–397.

[3] T. Promchai, T. Saesong, K. Ingkaninan, S. Laphookhieo, S.G. Pyne, T. Limtharakul (née Ritthiwigrom), Acetylcholinesterase inhibitory activity of chemical constituents isolated from *Miliusa thorelii*, Phytochem. Lett. 23 (2018) 33–37.

[4] S. Jumana, C.M. Hasan, M.A. Rashid, Antibacterial activity and cytotoxicity of *Miliusa velutina*, Fitoterapia 71 (2000) 559–561.

[5] N. Wongsa, S. Kanokmedhakul, K. Kanokmedhakul, Cananginones A-I, linear acetogenins from the stem bark of *Cananga latifolia*, Phytochemistry 72 (2011) 1859–1864.

[6] N. Wongsa, S. Kanokmedhakul, K. Kanokmedhakul, Corrigendum to "Cananginones A–I, linear acetogenins from the stem bark of *Cananga latifolia*" [Phytochemistry 72 (14-15) (2011) 1859–1864], Phytochemistry 109 (2015) 154.

[7] K. Sawasdee, T. Chaowasku, V. Lipipun, T.-H. Dufat, S. Michel, V. Jongbunprasert, K. Likhitwitayawuid, Geranylated homogentisic acid derivatives and flavonols from *Miliusa umpangensis*, Biochem. Syst. Ecol. 54 (2014) 179–181.

[8] H.J. Zhang, C. Ma, N.V. Hung, N.M. Cuong, G.T. Tan, B.D. Santarsiero, A.D. Mesecar, D.D. Soejarto, J.M. Pezzuto, H.H.S. Fong, Miliusanes, a class of cytotoxic agents from *Miliusa sinensis*, J. Med. Chem. 49 (2006) 693–708.

[9] J.J. Brophy, R.J. Goldsack, P.I. Forster, The leaf oils of the Australian species of Miliusa (Annonaceae), J. Essent. Oil Res. 16 (2004) 253–255.

[10] N. Wongsa, K. Kanokmedhakul, J. Boonmak, S. Youngme, S. Kanokmedhakul, Bicyclic lactones and racemic mixtures of dimeric styrylpyrones from the leaves of *Miliusa velutina*, RSC Adv. 7 (2017) 25285–25297.

[11] K. Sawasdee, T. Chaowasku, K. Likhitwitayawuid, New neolignans and a phenylpropanoid glycoside from twigs of *Miliusa mollis*, Molecules 15 (2010) 639–648.

[12] C. Naphong, W. Pompimon, P. Sombutsiri, Anticancer activity of isolated chemical constituents from *Miliusa smithiae*, Am. J. Appl. Sci. 10 (2013) 787–792.

[13] T. Smitinand, Thai Plant Names Revised Edition, Prachachon Co. Limited, Bangkok, 2001, p. 359.

[14] W. Chuakul, N. Sornthornchareonon, Ethnomedical uses of Thai Annonaceous plant (1), Thai J. Phytopharm. 10 (2003) 25–32.

[15] J.B. Trager, W. Jensen, Human malaria parasites in continuous culture, J. Parasitol. 91 (2005) 484–486.

[16] J.D. Desjardins, R.E. Canfield, C.J. Haynes, J.D. Chulay, Quantitative assessment of antimalarial activity in vitro by a semiautomated microdilution technique, Antimicrob. Agents Chemother. 16 (1979) 710–718.

[17] S.G. Collins, L. Franzblau, Microplate alamar blue assay versus BACTEC 460 system for high-throughput screening of compounds against *Mycobacterium tuberculosis* and *Mycobacterium avium*, Antimicrob. Agents Chemother. 41 (1997) 1004–1009.

[18] J. O'Brien, I. Wilson, T. Orton, F. Pognan, Investigation of the Alamar blue (resazurin) fluorescent dye for the assessment of mammalian cell cytotoxicity, Eur. J. Biochem. 267 (2000) 5421–5426.

[19] F.M. Hunt, L. Jordan, M.D. Jesus, M. Wurm, GFP-expressing mammalian cells for fast, sensitive, noninvasive cell growth assessment in a kinetic mode, Biotechnol. Bioeng. 65 (1999) 201–205.

[20] Clinical and Laboratory Standard Institute, Methods for Dilution Antimicrobial Susceptibility Tests for Bacteria that Grow Aerobically. Approved Standard 9th Ed. Document M07-A9, CLSI, Wayne, PA, USA, 2012.

[21] M. Balouiri, M. Sadiki, S.K. Ibnsouda, Methods for in vitro evaluating antimicrobial activity: a review, J. Pharm. Anal. 6 (2016) 71–79.

[22] J.A. Mbah, P. Tane, B.T. Ngadjui, J.D. Connolly, C.C. Okunji, M.M. Iwu, B.M. Schuster, Antiplasmodial agents from the leaves of *Glossocalyx brevipes*, Planta Med. 70 (2004) 437–440.

[23] H. Yang, Y. Li, M. Jiang, J. Wang, H. Fu, General copper-catalyzed transformations of functional groups from arylboronic acids in water, Chem. Eur. J. 17 (2011) 5652–5660.

[24] L. Wu, M. Zhai, Y. Yao, C. Dong, S. Shuang, G. Ren, Changes in nutritional constituents, anthocyanins, and volatile compounds during the processing of black rice tea, Food Sci. Biotechnol. 22 (2013) 917–923.

[25] X.R. Tian, H.F. Tang, Y.S. Li, H.W. Lin, X.Y. Zhang, J.T. Feng, X. Zhang, Studies on the chemical constituents from marine bryozoan *cryptosula pallasiana*, Rec. Nat. Prod. 9 (2014) 628–632.

[26] B. Yi, L. Hu, W. Mei, K. Zhou, H. Wang, Y. Luo, X. Wei, H. Dai, Antioxidant phenolic compounds of cassava (*Manihot esculenta*) from Hainan, Molecules 16 (2011) 10157–10167.

[27] A.T. Khalil, F.R. Chang, Y.H. Lee, C.Y. Chen, C.C. Liaw, P. Ramesh, S.S.F. Yuan, Y.C. Wu, Chemical constituents from the *Hydrangea chinensis*, Arch. Pharm. Res. 26 (2003) 15–20.

[28] A.G. Ferreira, M. Motidome, O.R. Gottlieb, J.B. Fernandes, P.C. Vieira, M. Cojocaru, H.E. Gottlieb, Farnesyl-Homogentisic Acid Derivatives from *Otoba parvifolia*, vol. 28, (1989), pp. 579–583.

[29] R.G. Parr, W. Yang, Density Functional Theory of Atoms and Molecules, Oxford University Press Inc, New York, 1989.

[30] T. Yanai, D.P. Tew, N.C. Handy, A new hybrid exchange-correlation functional using the coulomb-attenuating method (CAM-B3LYP), Chem. Phys. Lett. 393 (2004) 51–57.

[31] M. Cossi, N. Rega, G. Scalmani, V. Barone, Energies, structures, and electronic properties of molecules in solution with the C–PCM solvation model, J. Comput. Chem. 24 (2003) 669–681.

[32] M.J. Frisch, G.W. Trucks, H.B. Schlegel, G.E. Scuseria, M.A. Robb, J.R. Cheeseman, G. Scalmani, V. Barone, B. Mennucci, G.A. Petersson, H. Nakatsuji, M. Caricato, X. Li, H.P. Hratchian, A.F. Izmaylov, J. Bloino, G. Zheng, J.L. Sonnenberg, M. Hada, M. Ehara, K. Toyota, R. Fukuda, J. Hasegawa, M. Ishida, T. Nakajima, Y. Honda, O. Kitao, H. Nakai, T. Vreven, J.A. Montgomery Jr., J.E. Peralta, F. Ogliaro, M. Bearpark, J.J. Heyd, E. Brothers, K.N. Kudin, V.N. Staroverov, R. Kobayashi, J. Normand, K. Raghavachari, A. Rendell, J.C. Burant, S.S. Iyengar, J. Tomasi, M. Cossi, N. Rega, J.M. Millam, M. Klene, J.E. Knox, J.B. Cross, V. Bakken, C. Adamo, J. Jaramillo, R. Gomperts, R.E. Stratmann, O. Yazyev, A.J. Austin, R. Cammi, C. Pomelli, J.W. Ochterski, R.L. Martin, K. Morokuma, V.G. Zakrzewski, G.A. Voth, P. Salvador, J.J. Dannenberg, S. Dapprich, A.D. Daniels, Ö. Farkas, J.B. Foresman, J.V. Ortiz, J. Cioslowski, D.J. Fox, Gaussian09, Revision B, 01 Gaussian Inc, Wallingford CT, 2010.

[33] D.T. Huong, C. Kamperdick, T. Van Sung, Homogentisic acid derivatives from *Miliusa balansae*, J. Nat. Prod. 67 (2004) 445–447.
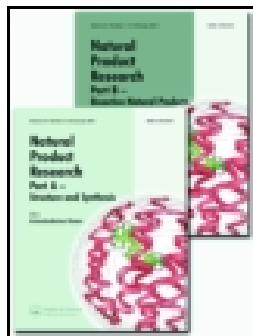
A new cytotoxic plumbagin derivative from roots of *Diospyros undulata*

Nattawut Suchaichit, Natcha P. Suchaichit, Kwanjai Kanokmedhakul, Patcharaporn Boottanun, Rasana W. Sermswan, Panawan Moosophon & Somdej Kanokmedhakul

View supplementary material

Published online: 17 Jun 2019.

Submit your article to this journal

View Crossmark data

Taylor & Francis
Taylor & Francis Group

Check for updates

A new cytotoxic plumbagin derivative from roots of *Diospyros undulata*

Nattawut Suchaichit[a], Natcha P. Suchaichit[a], Kwanjai Kanokmedhakul[b], Patcharaporn Boottanun[c,d], Rasana W. Sermswan[c,d], Panawan Moosophon[b] and Somdej Kanokmedhakul[b]

[a]Department of Applied Chemistry, Faculty of Sciences and Liberal Arts, Rajamangala University of Technology Isan, Nakhon Ratchasima, Thailand; [b]Natural Products Research Unit, Department of Chemistry and Center of Excellence for Innovation in Chemistry, Faculty of Science, Khon Kaen University, Khon Kaen, Thailand; [c]Department of Biochemistry, Faculty of Medicine, Khon Kaen University, Khon Kaen, Thailand; [d]Melioidosis Research Center, Faculty of Medicine, Khon Kaen University, Khon Kaen, Thailand

ABSTRACT

A new plumbagin derivative, 3-(5-oxohexyl)plumbagin (**1**), together with six known benzoquinone derivatives (**2–7**), four known triterpenoids (**8–11**) and coniferyl aldehyde (**12**) were isolated from *Diospyros undulata* roots. Their structures were elucidated by intensive spectroscopy including 1 D and 2 D NMR, UV, IR and MS spectrometric analysis. Compound **1** exhibited strong cytotoxicity against three cancer cell lines as lung cancer (NCI-H187), breast cancer (MCF-7), and oral cancer (KB) with IC_{50} values of 7.16, 12.85 and 28.67 μM, respectively. Moreover, it did not showed cytotoxicity to Vero cells. In addition, the antimicrobial activity of compound **1** was moderate that kill only *S. aureus* with MBC of 250 μg/mL while other compounds especially compound **4** showed a broader activity that kill all tested bacteria.
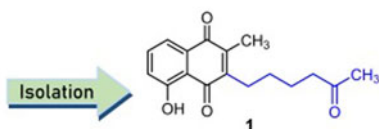
Roots of *Diospyros undulata* — Isolation — 1
- Cytotoxicity against NCI-H187, MCF-7, and KB cell lines
- Non-cytotoxicity to normal cells

CONTACT Panawan Moosophon ✉ mpanaw@kku.ac.th

Supplemental data for this article can be accessed at https://doi.org/10.1080/14786419.2019.1630120.

1. Introduction

Plumbagin and its derivatives are hydroxy-naphthoquinones distributed in the family Ebenceae especially *Diospyros* species. They exhibited highly potent bioactivities such as anticancer, antimicrobial, antimalarial, and antiinflammatory activities (Bao et al. 2017). Recent investigations indicated that plumbagin derivatives have been attracted an increasing researchers due to its promising cytotoxic activity against various cancer cell lines including breast, lung, cervical, leukemia, hepatocellular, and oral cavity cancers (Padhye et al. 2012).

Diospyros undulata Wall. ex G. Don (Ebenaceae) is distributed in rainforest and it is a widely available medicinal plant in the north, northeast and south parts of Thailand (Smitinand 2001). Previously work, we reported the isolation of naphthoquinone derivatives and their cytotoxicity from the stem bark of *D. undulata* (Suchaichit et al. 2018). In continuation of our investigation on the bioactive compounds from the roots of this plant, further isolation of the *D. undulata* roots extracts obtained a new plumbagin derivative, 3-(5-oxohexyl)plumbagin (**1**), six known benzoquinone derivatives (**2–7**), four known triterpenoids (**8–11**) and coniferyl aldehyde (**12**), as well as an evaluation for their cytotoxic and antimicrobial activities.

2. Results and discussion

Separation of the CH_2Cl_2 and MeOH extracts from *D. undulata* roots by flash column chromatography on silica gel, preparative TLC and recrystallization yielded a new plumbagin derivative (**1**) and 11 known compounds (**2–12**) (Figure 1). Their structures were identified by spectroscopic methods (IR, 1 D and 2 D NMR and MS) including
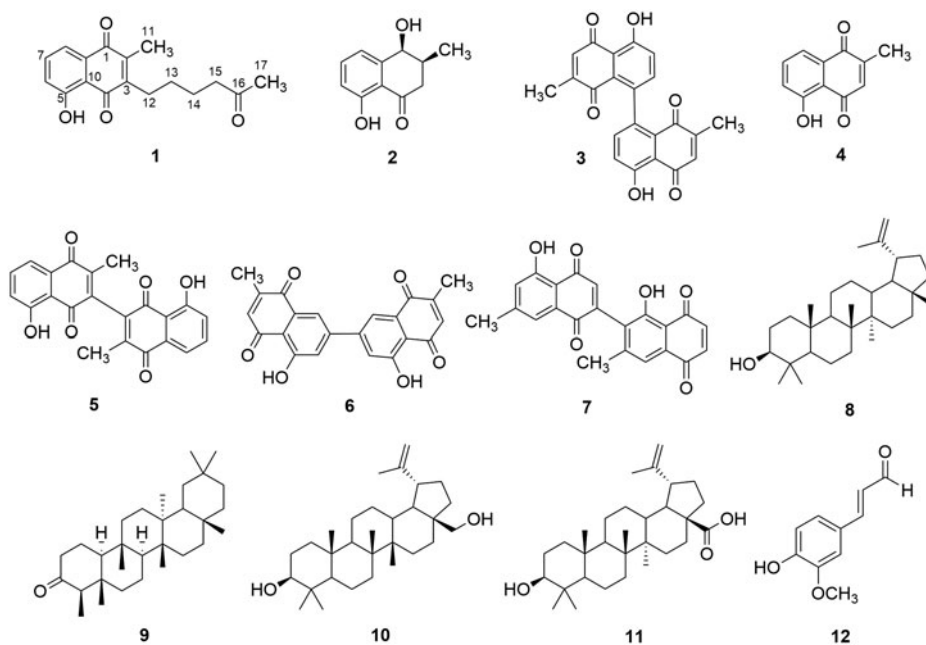

Figure 1. The structures of isolated compounds from roots of ***Diospyros undulata.***

comparison with data reported in the literature. The known compounds were identified as *cis*-isoshinanolone (**2**) (Bringmann et al. 2001), maritinone (**3**) (Gu et al. 2004), plumbagin (**4**) (Rischer et al. 2002), 3,3′-biplumbagin (**5**) (Higa et al. 2002), 7,7′-biplumbagin (**6**) (Salae et al. 2010), isodiospyrin (**7**) (Ruphin et al. 2014; Van der Kooy et al. 2006), lupeol (**8**) (Abdullahi et al. 2013), friedelin (**9**) (Ee et al. 2004), betulin (**10**), betulinic acid (**11**) (Uddin et al. 2011), and coniferyl aldehyde (**12**) (Herath et al. 1998).

Compound **1**, obtained as an orange amorphous powder, the molecular formula based on high-resolution MS (HRESIMS) with a molecular ion peak at *m/z* 309.1116 $[M + Na]^+$ (calcd. For $C_{17}H_{18}O_4Na$, 309.1103), indicating nine degrees of unsaturation. The UV spectrum showed absorption maximum due to a conjugated ketone at 272 and 416 nm. The IR spectrum of **1** displayed the characteristic absorption bands of hydroxy (3,445 cm^{-1}) and carbonyl ketone (1,713 cm^{-1}) groups. The ^{1}H and ^{13}C NMR spectra of **1** showed characteristic of 1,4-naphthoquinone [δ_H 7.60 (1H, dd, $J = 1.2$, 7.2 Hz, H-8), 7.55 (1H, t, $J = 8.0$ Hz, H-7), 7.20 (1H, dd, $J = 1.2$, 8.0 Hz, H-6), 2.13 (3H, s, CH$_3$-11) and 12.18 (1H, s, OH-5)] similar to those of plumbagin (**4**), except for the additional signals of methyl butyl ketone unit at C-3. The NMR data of this unit displayed the magnetic nonequivalence of four methylene protons at δ_H 2.62 (2H, t, $J = 8.0$ Hz, H-12), 2.49 (2H, t, $J = 7.2$ Hz, H-15), 1.71 (2H, quint, $J = 8.0$ Hz, H-14), 1.48 (2H, quint, $J = 8.0$ Hz, H-13), methyl protons at δ_H 2.15 (3H, s, H-17) and a carbonyl carbon at δ_C 208.0 (C-16). The COSY correlations exhibited the coupling through the sequence of H-12 to H-15 and HMBC showed correlations from H-12 to C-13/C-14, H-14 to C-12/C-15/C-16, and H-17 to C-15/C16 (Figure S9) indicating a 5-oxohexyl unit. The HMBC data showed correlations from H-12 to C-2/C-4 confirmed that C-12 of 5-oxohexyl group connected to the 1,4-naphthoquinone at C-3. Therefore, the compound **1** was identified as a new 5-hydroxy-2-methyl-3-(5-oxohexyl)naphthalene-1,4-dione and was named as 3-(5-oxohexyl)plumbagin.

The cytotoxic activity of the active constituent **1** was evaluated *in vitro* against human small-cell lung carcinoma (NCI-H187), human breast adenocarcinoma (MCF-7), human oral cavity carcinoma (KB) and African green monkey kidney fibroblasts (Vero) using MTT colorimetric method (Brien et al. 2000; Hunt et al. 1999). The results revealed potent cytotoxicity against three cancer cell lines (NCI-H187, MCF-7 and KB) with IC$_{50}$ value 8.70, 12.90 and 28.70 μM, respectively and it was not cytotoxic to Vero cells. Both naphthoquinone **1** and **4** (Suchaichit et al. 2018) exhibited potent cytotoxicity to all three cancer cell lines but only **1** showed none cytotoxicity to normal cell, suggesting that the 5-oxohexyl group at C-3 played an important role in the decrease of cytotoxicity to normal cell and might be a lead compound for anticancer drug development in the future. Benzoquinones **2-7** and triterpenes **8-11** have previously been reported for cytotoxic against cancer cell lines (Suchaichit et al. 2018; Bishayee et al. 2011).

The isolated compounds (**1-11**) were screened for their antibacterial activity against 1 gram-positive and 4 gram-negative bacteria using agar well diffusion method. The results showed that compounds **1-7** and **11** displayed inhibition activity against at least one pathogenic bacteria (Table S2). Gentamycin (GEN) and ceftazidime (CAZ) antibiotics that used as positive control showed inhibition against all tested bacteria except *B. pseudomallei* that resist to GEN (Table S3). Compound **4** showed inspiring

activity as it inhibited *E. coli*, *B. pseudomallei*, *A. baumannii* and *S. aureus* with MBC of 250, 63, 125, and 63 μg/mL that were comparable to the range of standard control drug GEN. Besides, compounds **4**, **6**, **7,** and **11** also showed respectable activity against *B. pseudomallei,* a gram-negative bacteria that caused melioidosis with the MBC of 63, 125, 125, and 125 μg/mL, respectively. Further investigation may lead to uncover the potential of these compounds as an alternative drug for the patients with melioidosis. Compound **4** is the most effective one in this report as it could kill *A. baumannii,* of which is an important nosocomial bacterial infection and dramatically resistance to several antibiotics. The remarkable activity against the gram-positive foodborne pathogen, *S. aureus,* of compounds **1**, **2**, **3**, **4**, **5,** and **11** with MBC values of 250, 250, 125, 63, 250, and 250 μg/mL raised attention that these compounds could proceed further to test if any of them could be applied as antibacterial drugs in the forthcoming. Coniferyl aldehyde (**12**) has previously been reported for their antimicrobial activities against some oral pathogens, including *Streptococcus pyogenes*, *Streptococcus mitis*, *Streptococcus mutans* and *Candida albicans* (Meerungrueang and Panichayupakaranant 2014).

3. Experimental

3.1. General experimental procedures

NMR spectra were measured on a Varian Mercury Plus 400 spectrometer. UV spectrum were recorded on a Shimadzu 1700 UV-visible spectrophotometer. IR were obtained using a Perkin-Elmer spectrum 100. The HRESIMS was recorded on a Bruker Micromass Q-TOF-2™ spectrometer. Column chromatography (CC) was performed with MERCK silica gel 60 (230-400 mesh) and Sephadex LH-20 (40–70 μm; GE Health care). TLC was performed with precoated MERCK silica gel 60 PF$_{254}$ aluminum sheets; the spots were detected at 254 and 366 nm and further sprayed with anisaldehyde and then heating until charred. Commercial grade solvents were distilled at their boiling point ranges prior to use for extraction and chromatographic separations (CC and TLC), whereas AR grade solvents were used for crystallization.

3.2. Plant material

Roots of *Diospyros undulata* were collected from Phu Pha Shing forest, Nong Wua So district, Udon Thani, Thailand in April 2015. The species was identified by Dr. Boonchuang Boonsuk. Voucher specimens were deposited at the herbarium of Department of Biology, Faculty of Science, Khon Kaen University, Thailand (voucher number P. Moosophon 1KKU).

3.3. Extraction and isolation

Dried and crushed roots of *D. undulata* (0.85 kg) was extracted with CH_2Cl_2 (3 × 3 L × 5 days) and MeOH (3 x 3 L × 5 days). Evaporation of all extract solvents under reduced pressure gave CH_2Cl_2 (29.2 g) and MeOH (75.3 g) extracts, respectively. The CH_2Cl_2 extract was applied to silica gel flash column chromatography (FCC) and eluted

with a gradient system of EtOAc-hexane (0:1-1:0) to yield six fractions, C1-C6. Fraction C2 was subjected to FCC eluting with EtOAc-hexane (1:9) to afford orange needles of **4** (50 mg) and colorless crystals of **8** (25 mg). Fraction C3 was subjected to FCC eluted with EtOAc-hexane (1:9-1:0) to give colorless crystals of **9** (30 mg). Purification of C4 by FCC using CH_2Cl_2-hexane (1:1-1:0) as eluent gave four subfractions (C4.1-C4.4). Further purification of subfraction C4.2 by preparative TLC developing with acetone-hexane (1:5) obtained an orange amorphous powder of **1** (18 mg) and **5** (22 mg). Subfraction C4.3 was purified by FCC using CH_2Cl_2-hexane (2:3) as a solvent to give a yellow oil of **3** (20 mg). Fraction C5 was isolated by Sephadex LH-20 CC using MeOH to yield four subfractions, C5.1-C5.4. Subfraction C5.2 was purified by preparative TLC, developed with EtOAc-hexane (1:5) to obtain a yellow oil of **7** (18 mg). Subfraction C5.4 was purified by FCC using EtOAc-hexane (3:7) as eluent to yield **6** (15 mg). Fraction C6 was separated by FCC, eluted with a gradient system of CH_2Cl_2-hexane (1:1-1:0) to give **2** (32 mg).

The MeOH extract 75.3 g was subjected to silica gel FCC, eluted with a gradient system of EtOAc-hexane (1:1-1:0) and EtOAc-MeOH (1:0-0:1) to afford five fractions, M1-M5. Fraction M1 was separated by FCC and eluted with EtOAc-hexane (1:1) to provide an additional amount of **2** (30 mg). Fraction M2 was purified by Sephadex LH-20 using MeOH as a solvent to yield four subfractions, M2.1- M2.4. Recrystallization of M2.3 with CH_2Cl_2-MeOH gave a white amorphous solid of **10** (35 mg). Fraction M3 was separated by FCC eluting with CH_2Cl_2-MeOH (1:0-1:1) to afford three subfractions, M3.1-M3.3. Purification of M3.2 by preparative TLC, developed with acetone-CH_2Cl_2 (1:5) to obtain a white solid of **12** (3 mg). Fraction M4 was separated by FCC eluting with MeOH-CH_2Cl_2 (1:9) to yield **11** (55 mg).

3-(5-oxohexyl)plumbagin or 5-hydroxy-2-methyl-3-(5-oxohexyl)naphthalene-1,4-dione **(1)**: an orange amorphous powder; UV (EtOH) λ_{max} (log ε) 272 (4.29) 416 (4.22) nm; IR (film) ν_{max} (cm^{-1}): 3445, 2923, 2853, 1713, 1631, 1607, 1456, 1360, 1263, 1156; ^{1}H NMR (400 MHz): δ = 12.18 (s, 1H, OH-5), 7.60 (dd, J = 1.2, 7.2 Hz, 1H, H-8), 7.55 (t, J = 8.0 Hz, 1H, H-7), 7.20 (dd, J = 1.2, 8.0 Hz, 1H, H-6), 2.62 (t, J = 8.0 Hz, 2H, H-12), 2.49 (t, J = 7.2 Hz, 2H, H-15), 2.15 (s, 3H, H-17), 2.13 (s, 3H, CH$_3$-11), 1.71 (quint, J = 8.0 Hz, 2H, H-14), 1.48 (quint, J = 8.0 Hz, 2H, H-13) ppm; ^{13}C NMR (100 MHz): δ = 208.0 (C-16), 190.0 (C-4), 184.4 (C-1), 161.2 (C-5), 146.6 (C-3), 144.8 (C-2), 135.9 (C-6), 132.1 (C-9), 118.9 (C-8), 114.9 (C-10), 43.2 (C-15), 30.0 (C-17), 28.1 (C-13), 26.2 (C-12), 23.8 (C-14), 12.5 (C-11) ppm; HRESIMS: m/z 309.1116 [M + Na]$^+$ (calcd for $C_{17}H_{18}O_4Na$, 309.1103).

3.4. Bioassays

3.4.1. Cytotoxicity assay

Cytotoxicity assays against human oral cavity carcinoma (KB), human breast adenocarcinoma (MCF-7), and human small cell lung carcinoma (NCI-H187) were determined by MTT colorimetric method (Brien et al. 2000). In brief, cells were diluted to 7×10^4 cell/ml for KB and 9×10^4 cell/ml for MCF-7 and NCI-H187. Successively, 5 μl of test sample diluted in 0.5% DMSO, and 45 μl of cell suspension were added to 384-well plates, incubated at 37 °C in 5% CO$_2$ incubator. After the incubator period (3 days for KB and MCF-7, and 5 days for NCI-H187), 12.5 μl of 62.5 μg/ml resazurin solution was added to

each well, and the plates were then incubated at 37 °C for 4 hours. Fluorescence signal was measured at the excitation and emission wavelengths of 530 and 590 nm.

The assay against African green monkey kidney fibroblasts (Vero) was performed by adding 45 μl of cell suspension at 3.3×10^4 cells/ml to each well of 384-well plates containing 5 μl of test compounds previously diluted in 0.5% DMSO, and then incubated for 4 days in 37 °C incubator with 5% CO_2 (Hunt et al. 1999). Fluorescence signal was measured with excitation and emission wavelengths of 485 and 535 nm.

3.4.2. Antimicrobial activity test by agar well diffusion method

Antimicrobial activities of bioactive compounds were investigated by agar well diffusion method against clinical isolates of pathogenic bacteria which are *E. coli*, *B. pseudomallei*, *A. baumannii*, *P. aeruginosa* and *S. aureus*. Approximately 10^5-10^6 CFU/mL of each bacterium were swab on Mueller-Hinton agar (MHA) plate (Umer et al. 2013). The plate was punched to obtain 6.6 mm of wells by sterile pipette tip and then 100 μl of each compound was added into each well. Methanol as the extraction solvent was used as negative control while CAZ and GEN were used as positive control. The plates were left at room temperature to let the solution diffused for 30 min. Thereafter, the plates were incubated at 37 °C for 18–24 hours. Inhibition activity was evaluated by measuring the diameter of inhibition zone against indicated bacteria.

3.4.3. Minimum bactericidal concentration (MBC) of bioactive compounds

The MBC of bioactive compounds that showed inhibition against indicated bacteria by agar well diffusion method were determined by micro-broth dilution (Hoelzer et al. 2011). The compounds at concentration of 1.0 mg/mL were diluted by two-fold serial dilution using Mueller-Hinton broth (MHB) in 96-well plate. Bacterial indicator approximately 10^5-10^6 CFU/mL were added into each well, mixed gently and then incubated at 37 °C for 18-24 hours. The last concentration that provided clear turbidity when compared to bacterial growth control was recorded as MIC. The clear turbidity wells were two-fold serially diluted with PBS, pH 7.2 and took 10 μl of each dilution to drop onto MHA plate, incubated at 37 °C for overnight and count the colony. The MBC of each compound was recorded at the concentration that caused bacterial colony decreased ≥ 3 $\log_{10}$ CFU/mL or 99.9% of bacterial cells count when compared to growth control.

4. Conclusions

A new 3-(5-oxohexyl)plumbagin (**1**) and 11 known compounds including *cis*-isoshinanolone (**2**), maritinone (**3**), plumbagin (**4**), 3,3′-biplumbagin (**5**), 7,7′-biplumbagin (**6**), isodiospyrin (**7**), lupeol (**8**), friedelin (**9**), betulin (**10**), betulinic acid (**11**) and coniferyl aldehyde (**12**) were first investigated from roots of *D. undulata*. The new compound **1** showed potent cytotoxic activity against NCI-H187, MCF-7 and KB without showing cytotoxicity towards normal cells. Moreover, compounds **1-3** and **5** exhibited antibacterial activity against only gram-positive bacteria, *S. aureus* and compounds **6** and **7** showed antibacterial activity against gram-negative, *B. pseudomallei* while compounds

4 and **11** displayed antibacterial activity against both gram-negative and gram-positive bacteria.

Acknowledgements

Disclosure statement

No potential conflict of interest was reported by the authors.

Funding

References

Abdullahi SM, Musa AM, Abdullahi MI, Sule MI, Sani YM. 2013. Isolation of Lupeol from the Stem-bark of *Lonchocarpus sericeus* (Papilionaceae). Sch Acad J Biosci. 1(1):18–19.

Bao N, Ou J, Xu M, Guan F, Shi W, Sun J, Chen L. 2017. Novel NO-releasing plumbagin derivative: Design, synthesis and evaluation of antiproliferative activity. Eur J Med Chem. 13:88–95.

Bishayee A, Ahmed S, Brankov N, Perloff M. 2011. Triterpenoids as potential agents for the chemoprevention and therapy of breast cancer. Front Biosci (Landmark Ed). 16:980–996.

Brien JO, Wilson I, Orton T, Pognan F. 2000. Investigation of the alamar blue (resazurin) fluorescent dye for the assessment of mammalian cell cytotoxicity. Eur J Biochem. 267(17): 5421–5426.

Bringmann G, Messer K, Saeb W, Peters EM, Peters K. 2001. The absolute configuration of (+)-isoshinanolone and in situ LC-CD analysis of its stereoisomers from crude extracts. Phytochemistry. 56(4):387–391.

Ee GC, Ng KN, Taufiq-Yap YH, Rahmani M, Ali AM, Muse R. 2004. Mucigerin, A new coumarin from *Calophyllum mucigerum* (Guttiferae). Nat Prod Res. 18(2):123–128.

Gu JQ, Graf TN, Lee D, Chai HB, Mi Q, Kardono LB, Setyowati FM, Ismail R, Riswan S, Farnsworth NR, et al. 2004. Cytotoxic and antimicrobial constituents of the bark of *Diospyros maritima* collected in two geographical locations in Indonesia. J Nat Prod. 67(7):1156–1161.

Herath H, Dassanayake RS, Priyadarshani AMA, De Silva S, Wannigam GP, Jamie J. 1998. Isoflavonoids and a pterocarpan from *Gliricidia sepium*. Phytochemistry. 47(1):117–119.

Higa M, Noha N, Yokaryo H, Ogihara K, Yogi S. 2002. Three new naphthoquinone derivatives from *Diospyros maritima* BLUME. Chem Pharm Bull. 50(5):590–593.

Hoelzer K, Cummings KJ, Warnick LD, Schukken YH, Siler JD, Gröhn YT, Davis MA, Besser TE, Wiedmann M. 2011. Agar disk diffusion and automated microbroth dilution produce similar antimicrobial susceptibility testing results for Salmonella serotypes newport, Typhimurium, and 4,5,12:I-, but differ in economic cost. Foodborne Pathog Dis. 8(12):1281–1288.

Hunt L, Jordan M, De Jesus M, Wurm FM. 1999. GFP-expressing mammalian cells for fast, sensitive, noninvasive cell growth assessment in a kinetic mode. Biotechnol Bioeng. 65(2):201–205.

Meerungrueang W, Panichayupakaranant P. 2014. Antimicrobial activities of some Thai traditional medical longevity formulations from plants and antibacterial compounds from *Ficus foveolata*. Pharm Biol. 52(9):1104–1109.

Padhye S, Dandawate P, Yusufi M, Ahmad A, Sarkar FH. 2012. Perspectives on Medicinal Properties of Plumbagin and Its Analogs. Med Res Rev. 32(6):1131–1158.

Rischer H, Hamm A, Bringmann G. 2002. *Nepenthes insignis* uses a C2-portion of the carbon skeleton of L-alanine acquired via carnivorous organs, to build up the allelochemical plumbagin. Phytochemistry. 59(6):603–609.

Ruphin FP, Baholy R, Emmanuel R, Amelie R, Martin MT, Koto-Te-Nyiwa N. 2014. Isolation and structural elucidation of cytotoxic compounds from the root bark of *Diospyros quercina* (Baill.) endemic to Madagascar. Asian Pac J Trop Biomed. 4(3):16–175.

Salae AW, Karalai C, Ponglimanont C, Kanjana-Opas A, Yuenyongsawad S. 2010. Naphthalene derivatives from *Diospyros wallichii*. Can J Chem. 88(9):922–927.

Smitinand T. 2001. Thai Plant Names. Revised ed. Bangkok: Funny Publishing; p. 191.

Suchaichit NP, Suchaichit N, Kanokmedhakul K, Poopasit K, Moosophon P, Kanokmedhakul S. 2018. Two new naphthalenones from *Diospyros undulata* stem bark and their cytotoxic activity. Phytochem Lett. 24:132–135.

Uddin G, Aliullah W, Siddiqui BS, Alam M, Sadat A, Ahmad A, Uddin Khan A. 2011. Chemical constituents and phytotoxic of solvent extracted fractions of stem bark of *Grewia optiva* Drummond ex Burret. Middle-East J Sci Res. 8(1):85–91.

Umer S, Tekewe A, Kebede N. 2013. Antidiarrhoeal and antimicrobial activity of *Calpurnia aurea* leaf extract. BMC Complement Altern Med. 13:21.

Van der Kooy F, Meyer JJM, Lall N. 2006. Antimycobacterial activity and possible mode of action of newly isolated neodiospyrin and other naphthoquinones from *Euclea natalensis*. S Afr J Bot. 72(3):349–352.
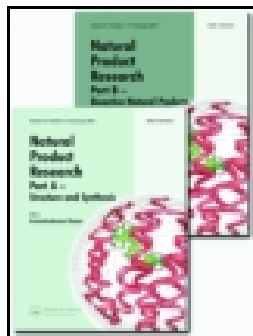
A new antibacterial tirucallane from *Walsura trichostemon* roots

Nattawut Suchaichit, Kwanjai Kanokmedhakul, Trinop Promgool, Panawan Moosophon, Apiwat Chompoosor, Natcha P Suchaichit & Somdej Kanokmedhakul

View supplementary material

Published online: 23 Sep 2019.

Submit your article to this journal

Article views: 41

View related articles

View Crossmark data

SHORT COMMUNICATION

Check for updates

A new antibacterial tirucallane from *Walsura trichostemon* roots

Nattawut Suchaichit[a], Kwanjai Kanokmedhakul[b], Trinop Promgool[b], Panawan Moosophon[b], Apiwat Chompoosor[c], Natcha P Suchaichit[a] and Somdej Kanokmedhakul[b]

[a]Department of Applied Chemistry, Faculty of Sciences and Liberal Arts, Rajamangala University of Technology Isan, Nakhon Ratchasima, Thailand; [b]Natural Products Research Unit, Department of Chemistry and Center of Excellence for Innovation in Chemistry, Faculty of Science, Khon Kaen University, Khon Kaen, Thailand; [c]Department of Chemistry, Faculty of Science, Ramkhamhaeng University, Bangkok, Thailand

ABSTRACT

Phytochemical investigation of the roots of *Walsura trichostemon*, a Thai medicinal plant, provided a new tirucallane, 3-epimesendanin S 12-acetate (**1**), together with four known compounds, 3-epimesendanin S (**2**), meliasenin G (**3**), β-sitosterol (**4**) and β-sitosterol glucoside (**5**). Their structures were characterized by intensive spectroscopy including 1 D and 2 D NMR, UV, IR and MS spectrometric analysis. The isolated compounds were evaluated for antibacterial and acetylcholinesterase inhibitory activities. Compounds **1–2** showed antibacterial activity against *Bacillus cereus* and *Bacillus subtilis* with MIC values ranging from 16–128 μg/mL. In addition, compound **3** was active against *Pseudomonas aeruginosa* and *Escherichia coli* with MIC values of 64 and 128 μg/mL, respectively.
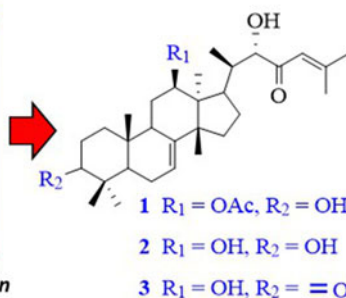
Roots of *Walsura trichostemon*

1 R$_1$ = OAc, R$_2$ = OH
2 R$_1$ = OH, R$_2$ = OH
3 R$_1$ = OH, R$_2$ = =O

Antibacterial activity

CONTACT Natcha P Suchaichit ✉ natcha.pa@rmuti.ac.th

Supplemental data for this article can be accessed at https://doi.org/10.1080/14786419.2019.1669025.

1. Introduction

There are about 40 species of the genus *Walsura* widely distributed in Southeast Asia. However, only four species are found Thailand. Among them, *Walsura trichostemon* or 'Lamyai Pa' in Thai has been used as a traditional in Thai medicine for the treatment of tendon disabilities, haemorrhoids, staunch and to clean wounds (Wongprasert et al. 2011; Sichaem, Khumkratok et al. 2014). Several *Walsura* species were reported for their antileukemic, antibacterial, antioxidant, antifeeding, and antimalarial activities. (Han et al. 2012; Sarkar et al. 2019). Phytochemical and pharmacological studies on this genus revealed a variety of bioactive constituents: limonoids showing antimalarial, cytotoxic, cell-protecting, anti-inflammatory and 11β-HSD1 inhibitory activities (Yin et al. 2007; Han et al. 2013; Nugroho et al. 2013; Ji et al. 2016; An et al. 2017); tirucallane presenting cytotoxic, anti-malarial, antifeedant, antifungal, antiplatelet aggregation, and antitubercular activities (Huang et al. 2007; Sichaem, Khumkratok et al. 2014); phenolic glycosides exhibiting antioxidant activity (Luo et al. 2006; Voravuthikunchai et al. 2010) and apotirucallane displaying cytotoxic and insecticidal activities (Sichaem et al. 2012; Sichaem, Khumkratok et al. 2014; Suri Appa Rao et al. 2015). Previous investigation of the chemical constituents of this plant provided tirucallane, apotirucallane and limonoids (Sichaem et al. 2012, Sichaem, Khumkratok et al. 2014; Phontree et al. 2014; Sichaem, Siripong et al. 2014). In order to search for further biologically active tirucallane, the EtOAc and MeOH extracts from *W. trichostemon* roots were investigated. We report herein a new tirucallane, named 3-epimesendanin S 12-acetate (**1**), two known tirucallane derivatives (**2–3**) and two known steroids (**4–5**) and their antibacterial activity from the roots of *W. trichostemon*.

2. Results and discussion

Compound **1** was obtained as a white solid with the molecular formula of $C_{32}H_{50}O_5$ as determined by HRESIMS, showing an ion peak at m/z 537.3557 $[M + Na]^+$. The IR spectrum of **1** presented the absorption bands of hydroxyl (3452 cm^{-1}), ester carbonyl (1712 cm^{-1}) and α,β-conjugated ketone (1678 cm^{-1}) groups. The ^{13}C NMR and DEPT spectra (Table S1 in supplementary material) showed 32 carbons resonances corresponding to nine methyl, two sp^2 methines, four sp^2 quaternary (including two carbonyl carbons), four sp^3 quaternary, seven sp^3 methines, and six sp^3 methylenes carbons. The ^1H NMR data (Table S1, in supplementary material) indicated that **1** showed characteristic pattern of tirucallane triterpene skeleton [eight methyl (δ_H 2.17 (s), 1.96 (s), 1.10 (s), 0.90 (s), 0.89 (s), 0.88 (s), 0.74 (s) and 0.47 (d, $J = 7.2$ Hz)), two olefinic methine (δ_H 6.12 (s) and 5.32 (br d, $J = 8.8$ Hz)), three oxymethine (δ_H 4.79 (t, $J = 6.4$ Hz), 4.17 (s) and 3.40 (br s)), four methine and six methylene (δ_H 2.34-0.85) protons] the same as reported for 3-epimesendanin S (Han et al. 2013). However, the difference is the presence of an acetoxy group [δ_H 2.03 (s); δ_C 171.0] at C-12 in **1** instead of a hydroxyl group in 3-epimesendanin S. This acetate group was supported by HMBC correlations of downfield triplet signals of H-12 at δ_H 4.79 ($J = 6.4$ Hz) to acetyl carbonyl carbon at δ_C 171.0, together with the COSY correlations of H-9/H-11/H-12. The COSY correlations of H-15/H-16/H-17/H-20/H-22 and the HMBC correlation of H-22
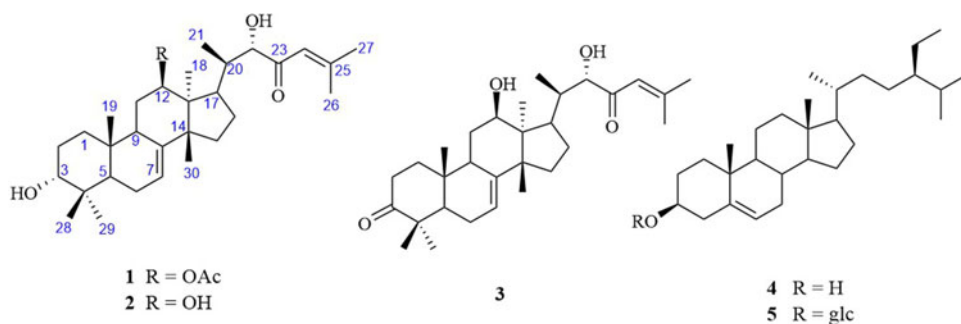
Figure 1. Chemical structures of compounds 1–5.

to C-17 indicated the side chain $CH(CH_3)CH(OH)COCH = C(CH_3)_2$ connecting to a tetracyclic ring at C-17. Selected correlations of COSY and HMBC are summarized in supplementary material (Figure S10). H-3 was β-oriented and H-12 was α-oriented, based on the NOESY correlation between H-3 and CH_3-28 as well as H-12 and CH_3-18, respectively. The β-orientation of methyl group at C-20 and α-orientation of OH group at C-22 on the side chain were identified based on the similarity of the NMR spectroscopic data of **1** and those of 3-epimesendanin S (Han et al. 2013). From the above evidences, compound **1** was concluded to be a new tirucallane derivative, and was named 3-epimesendanin S 12-acetate.

By comparison of spectroscopic data with the previously reported values, the structures of known compounds **2–5** (Figure 1) were established as 3-epimesendanin S (**2**) [Han et al. 2013], meliasenin G (**3**) (Zhang et al. 2010), β-sitosterol (**4**) (Mouffok et al. 2012) and β-sitosterol glucoside (**5**) (Khatun et al. 2012). The antibacterial activity of isolated compounds **1–3** was evaluated against three Gram-positive and three Gram-negative bacteria (Table S2 in supplementary material). Compounds **1** and **2** displayed antibacterial activity against *B. cereus* and *B. subtili*s with MIC values in the range of 16-128 μg/mL and compound **3** showed activity against *B. cereus* with MIC values of 64 μg/mL. Compound **2** exhibited activity against *B. cereus* and *B. subtilis* with MIC values of 16 and 64 μg/mL, respectively, better than **1**. This indicated that a hydroxyl group at C-12 might play an important role to enhance the activity. Only compound **3** showed activity against Gram-negative bacteria, *P. aeruginosa* and *E. coli*, with MIC values of 64 and 128 μg/mL, respectively. In addition, compounds **1–3** were evaluated for AChE inhibitory activity but showed no activity.

3. Conclusions

A new tirucallane, 3-epimesendanin S 12-acetate (**1**) and four known compounds (**2–5**) were isolated from *W. trichostemon* roots. Compounds **1–2** exhibited antibacterial activity against Gram-positive bacteria (*B. cereus* and *B. subtilis*) and compound **3** displayed activity against Gram-negative bacteria (*P. aeruginosa* and *E. coli*). Among these compounds, the isolated compound **2** showed the most potent activity against *B. cereus* with MIC value of 16 μg/mL. This is the first report of antibacterial activity of tirucallanes from this plant.

References

An FL, Sun DM, Li RJ, Zhou MM, Yang MH, Yin Y, Kong LY, Luo J. 2017. Walrobsins A and B, two anti-inflammatory limonoids from root barks of *Walsura robusta*. Org Lett. 19(17):4568–4571.

Han ML, Shen Y, Wang GC, Leng Y, Zhang H, Yue JM. 2013. 11β-HSD1 inhibitors from *Walsura cochinchinensis*. J Nat Prod. 76(7):1319–1327.

Han ML, Zhang H, Yang SP, Yue JM. 2012. Walsucochinoids A and B: new rearranged limonoids from *Walsura cochinchinensis*. Org Lett. 14(2):486–489.

Huang HC, Tsai WJ, Liaw CC, Wu SH, Wu YC, Kuo YH. 2007. Anti-platelet aggregation triterpene saponins from the galls of *Sapindus mukorossi*. Chem Pharm Bull. 55(9):1412–1415.

Ji KL, Li XN, Liao SG, Hu HB, Li R, Xu YK. 2016. Cytotoxic limonoids from the leaves of *Walsura robusta*. Phytochem Lett. 15:53–56.

Khatun M, Billah M, Quader MA. 2012. Sterols and sterol glucoside from *Phyllanthus* species. Dhaka Univ J Sci. 60(1):5–10.

Luo XD, Wu DG, Cai XH, Kennelly EJ. 2006. New antioxidant phenolic glycosides from *Walsura yunnanensis*. Chem Biodivers. 3(2):224–230.

Mouffok S, Haba H, Lavaud C, Long C, Benkhaled M. 2012. Chemical constituents of *Centaurea omphalotricha* Coss. & Durieu ex Batt. & Trab. Rec Nat Prod. 6(3):292–295.

Nugroho AE, Okuda M, Yamamoto Y, Hirasawa Y, Wong C-P, Kaneda T, Shirota O, Hadi AHA, Morita H. 2013. Walsogynes B–G, limonoids from *Walsura chrysogyne*. Tetrahedron. 69(20): 4139–4145.

Phontree K, Sichaem J, Khumkratok S, Siripong P, Tip-Pyang S. 2014. Trichostemonoate, a new anticancer tirucallane from the stem bark of *Walsura trichostemon*. Nat Prod Commun. 9(9): 1253–1254.

Sarkar MK, Vadivel V, Raja MRC, Kar Mahapatra S. 2019. Investigation of phytochemical constituents of anti-leukemic herbal drugs used by the traditional healers of Purulia, Birbhum and Bankura districts of West Bengal. Nat Prod Res.1–6.   [2019 Feb 15]:[7 p.]. https://doi.org/10.1080/14786419.2019.1566818.

Sichaem J, Khumkratok S, Siripong P, Tip-Pyang S. 2014. New cytotoxic apotirucallanes from the leaves of *Walsura trichostemon*. J Nat Med. 68(2):436–441.

Sichaem J, Siripong P, Tip-Pyang S, Phaopongthai J. 2014. A new cytotoxic tirucallane from the twigs of *Walsura trichostemon*. Nat Prod Commun. 9(3):367–368.

Sichaem J, Aree T, Khumkratok S, Jong-Aramruang J, Tip-Pyang S. 2012. A new cytotoxic apotirucallane from the roots of *Walsura trichostemon*. Phytochem Lett. 5(3):665–667.

Suri Appa Rao M, Suresh G, Ashok Yadav P, Rajendra Prasad K, Usha Rani P, Venkata Rao C, Suresh Babu K. 2015. Piscidinols H–L, apotirucallane triterpenes from the leaves of *Walsura trifoliata* and their insecticidal activity. Tetrahedron. 71(9):1431–1437.

Voravuthikunchai SP, Kanchanapoom T, Sawangjaroen N, Hutadilok-Towatana N. 2010. Antioxidant, antibacterial and antigiardial activities of *Walsura robusta* Roxb. Nat Prod Res. 24(9):813–824.

Wongprasert T, Phengklai C, Boonthavikoon T. 2011. A synoptic account of the Meliaceae of Thailand. Thai for Bull (BOT. 39:210–266.).

Yin S, Wang XN, Fan CQ, Liao SG, Yue JM. 2007. The first limonoid peroxide in the Meliaceae family: walsuronoid A from *Walsura robusta*. Org Lett. 9(12):2353–2356.

Zhang Y, Tang CP, Ke CQ, Yao S, Ye Y. 2010. Limonoids and triterpenoids from the stem bark of *Melia toosendan*. J Nat Prod. 73(4):664–668.

New *p*-terphenyl and benzoquinone metabolites from the bioluminescent mushroom *Neonothopanus nambi*

Watchara Sangsopha, Ratsami Lekphrom, Florian T. Schevenels, Weerasak Saksirirat, Sureeporn Bua-Art, Kwanjai Kanokmedhakul & Somdej Kanokmedhakul

View supplementary material

Published online: 27 Feb 2019.

Submit your article to this journal

View Crossmark data

Taylor & Francis
Taylor & Francis Group

Check for updates

New *p*-terphenyl and benzoquinone metabolites from the bioluminescent mushroom *Neonothopanus nambi*

Watchara Sangsopha[a], Ratsami Lekphrom[a], Florian T. Schevenels[a], Weerasak Saksirirat[b], Sureeporn Bua-Art[c], Kwanjai Kanokmedhakul[a] and Somdej Kanokmedhakul[a]

[a]Natural Products Research Unit, Department of Chemistry and Center for Innovation in Chemistry, Faculty of Science, Khon Kaen University, Khon Kaen, Thailand; [b]Agricultural Biotechnology Research Center for Sustainable Economy, Faculty of Agriculture, Khon Kaen University, Khon Kaen, Thailand; [c]Department of Agriculture, Plant Pathology Research Group Plant Protection Research and Development Office, Bangkok, Thailand

ABSTRACT

Two new *p*-terphenyls, neonambiterphenyls A and B (**1–2**), a new benzoquinone, neonambiquinone A (**3**), together with six known sesquiterpenes (**4–9**), were isolated from the bioluminescent mushroom *Neonothopanus nambi* PW3. The isolated compounds were identified by mass, IR and spectroscopic analyses (1D and 2D NMR). Compounds **1–3** and **5–7** showed cytotoxicity against cancer cell lines such as KB, NCI-H187 and MCF-7 with IC$_{50}$ values ranging from 1.45 to 49.31 μg/mL. In addition, compounds **1** and **5** showed cytotoxicity against *Vero* cells with IC$_{50}$ values of 38.72 and 32.90 μg/mL, respectively.

Neonothopanus nambi

1. Introduction

Neonothopanus nambi, also called 'Hed Ruang Sang Sirin-ratsami' or Sirin-ratsami mushroom", is a bioluminescent mushroom belonging to the family Omphalotaceae. It can be found on dead wood in broad-leaved forests in the Northeastern part of Thailand. The mushroom glows with yellow greenish light under dark conditions (Bua-art et al. 2011; Kanokmedhakul et al. 2012). Bioluminescent mechanisms are often oxygen-dependent and involve a molecule called luciferin (Tsarkova et al. 2016; Bondar et al. 2011). Fungal bioluminescence is less understood, although several bioluminescent molecules have recently been reported, including 3-hydroxyhispidin found in *N. nambi* and *Panellus stipticus* as well as riboflavin contained in *Mycena chlorophos* (Purtov et al. 2015; Hayashi et al. 2012; Zernov et al. 2017; Intaraudom et al. 2013). Moreover, Tsarkova's group unveiled that many different luminophores coexist in the extract of *N. nambi* and could be observed under blue and green visible light (Tsarkova et al. 2016). They also reported the isolation of a novel nambiscalarane and six known secondary metabolites. We previously reported sesquiterpenes and dimeric sesquiterpenes from *N. nambi*. One of them, aurisin A, was reported as a biological control against a root-knot nematode (*Meloidogyne incognita* Chitwood) of tomatoes, chili's and potatoes (Namanusart et al. 2013). In our efforts to obtain a larger quantity of this compound, we re-investigated the phytochemical constituents of *N. nambi*. The crude EtOAc extract of an isolate of cultured mycelium of *N. Nambi* PW3 provided two new *p*-terphenyls: neonambiterphenyl A (**1**) and neonambiterphenyl B (**2**); a new benzoquinone: neonambiquinone A (**3**); along with six known sesquiterpenes: aurisin A (**4**) (Kanokmedhakul et al. 2012), aurisin G (**5**) (Intaraudom et al. 2013), aurisin Z (**6**) (Tsarkova et al. 2016), axinysone B (**7**) (Zubia et al. 2008), nambinone C (**8**) (Kanokmedhakul et al. 2012) and 4,8,14-trihydroxyilludala-2,6,8-triene (**9**) (Clericuzio et al. 1997). The structures are shown in Figure 1.

2. Results and discussion

The molecular formula of **1** was determined as $C_{20}H_{14}O_7$ on the basis of HRESITOFMS (m/z 389.0632 $[M + Na]^+$). The IR spectrum of **1** showed the presence of hydroxyl (3388 cm^{-1}), ester (1749, 1732 cm^{-1}) and aromatic (1470, 1425 cm^{-1}) groups. The ^{1}H NMR spectral data exhibited seven aromatic protons at δ 7.42 (H-6, 1H, s), 6.99 (H-3, 1H, s), 6.57 (H-5′, 1H, s), 7.23 (H-2″ and H-6″, 2H, d, 8.4) and 6.79 (H-3″ and H-5″, 2H, d, 8.4); and acetyl protons at δ 2.19 (3H, s). The ^{13}C NMR spectral data showed the presence of three aromatic patterns including eighteen carbons δ 156.0, 150.5, 148.9, 148.8, 144.6, 141.1, 132.1, 130.1x2, 129.0, 125.6, 115.2x2, 115.1, 114.0, 109.7, 107.2 and 98.2; and acetyl groups at δ 170.0 and 20.5. The COSY correlations of **1** showed *ortho* relationships of H-2″(6″)↔H-3″(5″). The HMBC spectrum revealed the correlations of a methine proton at δ 6.57 (H-5′) coupled to C-1′, C-3′ and C-6′; two pairs of symmetric aromatic protons, H-2″(6″) coupled to C-4′ and H-3″(5″) correlated to C-1″ and C-4″; a methine proton at δ 6.99 (H-3) correlated to C-1, C-2, C-4 and C-5; and another methine aromatic proton at 7.42 (H-6) coupled to C-1′, C-4 and C-5. Therefore, compound **1** was identified as a new *p*-terphenyl derivative, named neonambiterphenyl A. Our assignment was confirmed as the NMR spectra of **1** were similar to those reported
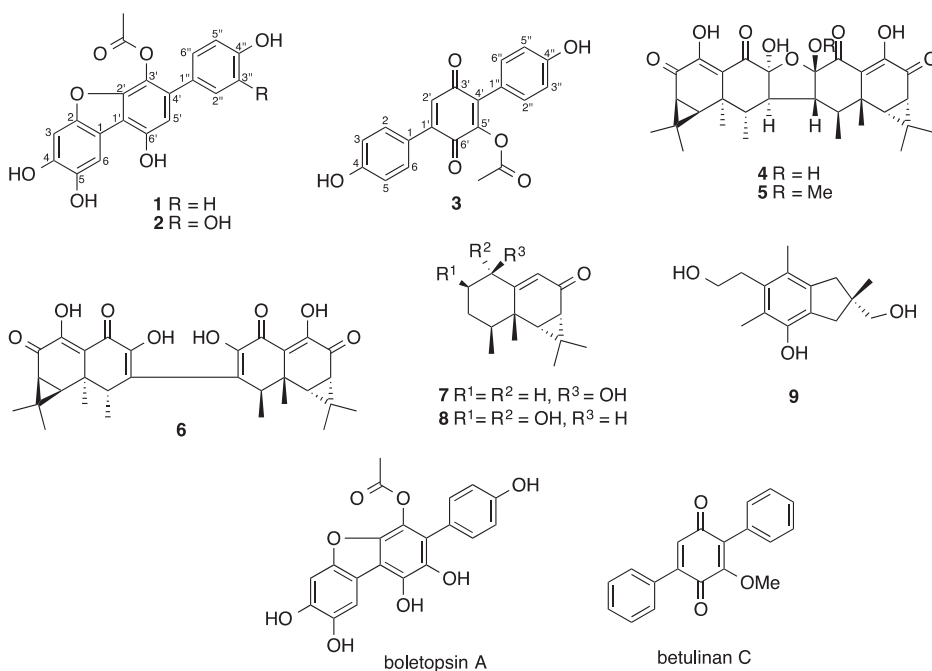
Figure 1. Structures of compounds 1–9, boletopsin A and betulinan C.

for the known compound boletopsin A, a KDR kinase inhibitor isolated from the mushroom *Boletopsis leucomeles* (Kaneko et al. 2010).

The molecular formula of **2** was determined as $C_{20}H_{14}O_8$ on the basis of HRESITOFMS (m/z 405.0580 $[M + Na]^+$). The IR spectrum showed the presence of hydroxyl (3354 cm^{-1}), ester (1730 cm^{-1}) and aromatic (1469, 1426 cm^{-1}) groups. The ^1H and ^{13}C NMR spectral data were similar to those of **1**, except for position C-3″ at δ 144.2, where H-3″ in **1** is replaced by a hydroxyl group. The key HMBC correlations between C-4′ and C-6″ with H-2″ and H-6″ supported this assignment. Therefore, **2** was assigned as a new *p*-terphenyl derivative, named neonambiterphenyl B.

The molecular formula of **3**, $C_{20}H_{14}O_6$, was determined on the basis of HRESITOFMS (m/z 349.0727 $[M-H]^+$). The IR spectrum showed the presence of hydroxyl (3353 cm^{-1}), ketone (1750 cm^{-1}) and aromatic (1440, 1370 cm^{-1}) groups. The ^1H NMR spectral data showed the presence of nine methine protons, including four pairs of symmetric doublets at δ 7.15 (H-2 and H-6, 2H, d, 8.4), 6.83 (H-3, H-5, H-3″ and H-5″, 4H, d, 7.6) and 7.39 (H-2″ and H-6″, 2H, d, 8.4), revealing two *p*-hydroxy-substituted benzene rings, and a methine at δ 6.82 (H-2′, 1H, s). Moreover, the ^1H NMR data showed acetyl protons at δ 2.19 (3H, s). The ^{13}C NMR and HSQC spectral data showed three carbonyls: two of them belonging to a quinone system at δ 186.8 and 180.5 (C-3′ and C-6′), and an ester carbonyl at δ 168.7, with a methyl at δ 20.2. Furthermore, the ^{13}C NMR signals of two *p*-hydroxy-substituted benzene rings were found at δ 159.3 (C-4″), 158.3 (C-4), 131.6x2 (C-2, C-6), 131.0x2 (C-2″ and C-6″), 123.3 (C-1″), 119.3 (C-1), 115.6x2 (C-3″ and C-5″), 115.2x2 (C-3 and C-5) and four more carbons in a quinone ring were found at δ 147.2 (C-5′), 144.2 (C-1′), 134.3 (C-4′), 130.4 (C-2′). The COSY spectrum of **3** showed *ortho* correlations from two *p*-hydroxyphenyls: H-2(6)↔H-3(5) and H-2″(6″)↔H-3″(5″). The HMBC

spectrum of **3** showed two correlations of H-2(6) with C-1′ and C-4; H-3(5) with C-1, C-4 and C-5(3); H-3″(5″) with C-1″, C-4″ and C-5″(3″); H-2″(6″) with C-4′ and C-4″. These NMR spectra were similar to those of betulinan C (El-Elimat et al. 2013). Compound **3** was therefore identified as a benzoquinone derivative, disubstituted by hydroxyphenyls at C-1′ and C-4′. The differences between the reported betulinan C and **3** arise from the substitution of two phenyl rings with *para*-hydroxyl groups and the replacement of a methoxy group at C-5′ on the quinone ring by an acetate group. Therefore, compound **3** was assigned as a new benzoquinone, named neonambiquinone A.

Since compounds **4** and **8** have already been reported in our previous study (Kanokmedhakul et al. 2012), the newly isolated compounds (**1–3**, **5–7** and **9**) were tested against several targets (Tables S1 and S2). Compounds **1–3** and **5–7** showed cytotoxicity against NCI-H187 cell lines with IC_{50} values ranging from 5.03 to 49.31 μg/mL. Among these **2**, **5** and **6** showed potent cytotoxicity with IC_{50} values of 5.60, 5.03 and 9.40 μg/mL, respectively. Compounds **1**, **2** and **5** showed cytotoxicity against KB cell lines with IC_{50} values of 9.12, 40.90 and 1.45 μg/mL, respectively. Moreover, compounds **1** and **5** exhibited cytotoxicity against MCF-7 cell lines with IC_{50} values of 11.82 and 18.64 μg/mL, respectively. However, they also showed cytotoxicity to *Vero* cells with IC_{50} values of 38.72 and 32.90 μg/mL, respectively. In addition, compounds **1–6** were evaluated for antibacterial activity against three Gram-negative and two Gram-positive bacteria (Table S2). These bacteria are human opportunistic pathogen involved in infections acquired in a hospital setting and resistant to disinfectants as well as antibiotics. All tested compounds exhibited moderate antibacterial activity against *Bacillus cereus* with MIC values in the range of 64–128 μg/mL. Compounds **1**, **2** and **3** exhibited antibacterial activity against *Staphylococcus aureus* with MIC values of 4, 8 and 64 μg/mL, respectively. Moreover, compounds **1**, **4** and **5** also exhibited moderate antibacterial activity against *Pseudomonas aeruginosa* with the equal MIC value of 128 μg/mL. Only compound **1** showed antibacterial activity against *Shigella sonnei* with MIC value of 128 μg/mL.

3. Experimental

3.1. General experimental procedures

Melting points were determined using an Electrothermal IA9200 digital melting point apparatus (Bibby Scientific Limited, Staffordshire, UK). Optical rotations were measured on a JASCO-DIP-1000 digital polarimeter (JASCO Inc., USA). IR spectra were obtained using a Bruker Tenser 27 spectrophotometer (Bruker, Germany). NMR spectra were recorded on a Varian Mercury Plus 400 spectrometer (Varian Inc., USA) using $CDCl_3$ and CD_3OD as solvents. The internal standards were referenced from the residue of those solvents. The HR-ESI-TOF-MS were recorded on a Bruker micrOTOF mass spectrometer (Bruker, Germany). Column chromatography was carried out on MERCK silica gel 60 (230–400 mesh) (Merck, Darmstadt, Germany). Thin-layer chromatography was carried out with pre-coated MERCK silica gel 60 PF254 (Merck, Darmstadt, Germany); the spots were visualized under UV light (254 and 365 nm) and further stained by spraying with anisaldehyde and then heated until charred.

3.2. Fungus material

The luminous mushroom was collected in 2015 from the Plant Genetic Conservation Project under Royal Initiation by Her Royal Highness Princess Maha Chakri Sirindhorn at Kok Phutaka area, Wiang Kao District, Khon Kaen Province, Thailand and was identified by Prof. Weerasak Saksirirat as *N. Nambi* PW3. The voucher specimen was deposited at the Department of Plant Science and Agricultural Resources, Faculty of Agriculture, Khon Kaen University, Khon Kaen, Thailand. The mushroom was cultivated on potato dextrose broth without shaking with 2 h of light per day at 25 °C for 30 days (Bua-art et al. 2011).

3.3. Extraction and isolation

The cultured mycelium of *N. nambi* PW3 (650 g) was extracted with EtOAc (3 x 4 L). Removal of solvents under reduced pressure gave 95 g of crude EtOAc extact.

The crude EtOAc extract was separated over silica gel column chromatography (CC), eluting with gradient systems of EtOAc:*n*-hexane (0:100–100:0) and MeOH:EtOAc (0:100–100:0) to give eight fractions, NnE$_1$-NnE$_8$. Fraction NnE$_1$ was separated over CC, eluting with an isocratic system of EtOAc:*n*-hexane (5:15) to give **7** (7.5 mg) as a colourless oil. Fraction NnE$_2$ was separated over CC, eluting with an isocratic system of EtOAc:*n*-hexane (7:13) to give **8** (6.6 mg) as a colourless oil. The solid in fraction NnE$_3$ was filtered and crystallized with EtOAc to give compound **4** (17.7 g) as yellow crystals. Then, fraction NnE$_3$ was further purified by CC using a gradient system of MeOH:CH$_2$Cl$_2$ (1:19) to give seven subfractions, NnE$_{3.1}$-NnE$_{3.7}$. Subfraction NnE$_{3.1}$ led to an additional amount of **4** (0.9 g). Subfraction NnE$_{3.2}$ was subjected to CC, eluting with an isocratic system of MeOH:CH$_2$Cl$_2$ (1:19) to give **6** (495.0 mg) as an orange solid. Fraction NnE$_{3.7}$ was submitted to CC using an isocratic system of MeOH:CH$_2$Cl$_2$ (7:93) to give seven subfractions, NnE$_{3.7.1}$-NnE$_{3.7.7}$. Subfraction NnE$_{3.7.4}$ led to **1** (7.0 mg) as a dark brown solid. Fraction NnE$_4$ was submitted to CC using an isocratic system of EtOAc:*n*-hexane (3:7) to give seven subfractions, NnE$_{4.1}$-NnE$_{4.7}$. Subfraction NnE$_{4.6}$ was further separated over CC, eluting with an isocratic system of EtOAc:hexane (7:13) to give **9** (3.3 mg) as a white solid and an additional amount of **1** (19.5 mg). Subfraction NnE$_{4.7}$ was subjected to CC, eluting with an isocratic system of EtOAc:hexane (9:11) to give **3** (15.5 mg) as a dark brown solid and **2** (30.5 mg) as a dark brown solid. Fraction NnE$_5$ was purified by CC, eluting with a gradient system of MeOH:CH$_2$Cl$_2$ (1:19) to give an additional amount of **2** (18.5 mg). Fraction NnE$_7$ was filtered and recrystallized with CH$_2$Cl$_2$ to give **5** (710.5 mg) as a yellow solid.

Neonambiterphenyl A (**1**): dark brown solid; m.p. 215–217 °C; R_f = 0.45 (30% EtOAc/hexane); IR (neat) ν_{max} (cm^{-1}): 3388, 1749, 1732, 1611, 1521, 1470, 1425, 1368, 1350, 1215, 1173; ^{1}H NMR (400 MHz): δ = 7.42 (s, 1H, H-6), 7.23 (d, *J* = 8.4 Hz, 2 H, H-2″ and H-6″), 6.99 (s, 1H, H-3), 6.79 (d, *J* = 8.4 Hz, 2H, H-3″ and H-5″), 2.19 (s, 3H, CH$_3$CO) ppm; ^{13}C NMR (100 MHz): δ = 170.0 (CH$_3$CO), 156.0 (C-4″), 150.5 (C-2), 148.9 (C-2′), 148.8 (C-6′), 144.6 (C-4), 141.1 (C-5), 132.1 (C-4′), 130.1 (C-2″ and C-6″), 129.0 (C-1″), 125.6 (C-3′), 115.2 (C-3″ and C-5″), 115.1 (C-1), 114.0 (C-1′), 109.7 (C-5′), 107.2 (C-6), 98.2 (C-3), 20.5 (CH$_3$CO) ppm; HRESITOFMS: *m/z* 389.0632 [M + Na]$^+$ (calcd for C$_{20}$H$_{14}$O$_7$ + Na$^+$, 389.0632).

Neonambiterphenyl B (**2**): dark brown solid; m.p. 198-200 °C; R_f =0.43 (35% EtOAc/hexane); IR (neat) ν_{max} (cm^{-1}): 3354, 1730, 1609, 1523, 1469, 1426, 1275, 1195; ^{1}H

NMR (400 MHz): δ = 7.44 (s, 1H, H-6), 6.98 (s, 1H, H-3), 6.88 (d, $J = 1.6$ Hz, 1H, H-2″), 6.79 (s, 1H, H-5″), 6.78 (d, $J = 1.6$ Hz, 1H, H-6″), 6.61 (s, 1H, H-5′), 2.19 (s, 3H, CH_3CO) ppm; ^{13}C NMR (100 MHz): δ = 170.0 ($\underline{C}H_3CO$), 150.5 (C-2), 149.1 (C-2′), 148.8 (C-6′), 144.7 (C-4), 144.2 (C-3 "and C-4″), 141.3 (C-5), 132.1 (C-4′), 129.6 (C-1″), 125.4 (C-3′), 120.9 (C-6″), 116.0 (C-2″), 115.2 (C-5″), 115.1 (C-1), 113.9 (C-1′), 109.6 (C-5′), 107.4 (C-6), 98.3 (C-3), 20.4 ($\underline{C}H_3CO$) ppm; HRESITOFMS: m/z 405.0580 [M + Na]$^+$ (calcd for $C_{20}H_{14}O_8 + Na^+$, 405.0581).

Neonambiquinone A (**3**): dark brown solid; m.p. 233-235 °C; R_f = 0.43 (25% EtOAc/hexane); IR (neat) ν_{max} (cm^{-1}): 3353, 2925, 2856, 1750, 1656, 1596, 1510, 1440, 1370, 1225, 1176, 1077, 1016, 889, 831, 707, 639; ^1H NMR (400 MHz): δ = 7.39 (d, $J = 8.4$ Hz, 2H, H-2″ and H-6″), 7.15 (d, $J = 8.4$ Hz, 2H, H-2 and H-6), 6.83 (d, $J = 7.6$ Hz, 4H, H-3, H-5, H-3″ and H-5″), 6.82 (s, 1H, H-2′), 2.19 (s, 3H, CH_3CO) ppm; ^{13}C NMR (100 MHz): δ = 186.8 (C-3′), 180.5 (C-6′), 168.7 ($\underline{C}H_3CO$), 159.3 (C-4″), 158.3 (C-4), 147.2 (C-5′), 144.2 (C-1′), 134.3 (C-4′), 131.6 (C-2 and C-6), 131.0 (C-2″ and C-6″), 130.4 (C-2′), 123.3 (C-1″), 119.3 (C-1), 115.6 (C-2″ and C-5″), 115.2 (C-3 and C-5), 20.2 ppm; HRESITOFMS: m/z m/z 349.0727 [M-H]$^+$ (calcd for $C_{20}H_{14}O_6$ -H$^+$, 349.0717).

3.4. Bioassays

3.4.1. Antiplasmodial assay

Antimalarial activity was evaluated against the parasite *Plasmodium falciparum* (K1, multidrug resistant strain), using the method of Trager and Jensen (Trager and Jensen 1976). Quantitative assessment of malarial activity *in vitro* was determined by the micro-culture radio isotope technique based on the method described by Desjardins (Desjardins et al. 1979). The inhibitory concentration (IC$_{50}$) represents the concentration which causes 50% reduction in parasite growth as indicated by the *in vitro* incorporation of [^{3}H]-hypoxanthine by *P. falciparum*. The standard compound was dihydroartemisinin.

3.4.2. Cytotoxicity assay

The cytotoxic assays against human epidermoid carcinoma (KB), human small cell lung cancer (NCI-H187) and human breast cancer (MCF-7) cell lines were performed employing the colorimetric method as described by Skehan (Skehan et al. 1990). The reference substances were ellipticine and doxorubicin.

3.4.3. Antibacterial assay

The minimum inhibitory concentrations (MICs) were determined by the dilution method as described in the M07-A9 (Clinical and Laboratory Standards Institute 2012). Resazurin in solution was used as an indicator of microbial growth. MICs were recorded by reading the lowest concentration capable of inhibiting visible growth. The tests were performed in triplicate. Kanamycin, gentamicin and vancomycin were used as positive control drugs. Five microorganism cultures (*E. coli* ATCC 25922, *P. aeruginosa* ATCC 27853, *S. sonnei* ATCC 11060, *B. cereus* ATCC 11778 and *S. aureus* ATCC 25923) were used. The experiment was performed at the Department of Microbiology, Faculty of Science, Khon Kaen University, Thailand.

4. Conclusions

The cultured mycelium of the bioluminescent mushroom *Neonothopanus nambi* PW3 was investigated and led to the isolation of nine compounds, including two new *p*-terphenyls (**1**–**2**), a new benzoquinone (**3**), and six known sesquiterpenes (**4**–**9**). Besides compounds **1**–**3**, **5** and **7** are reported for the first time in the genus *Neonothopanus* and compound **9** is reported for the first time in the family Omphalotaceae. Compounds **1**–**3** and **5**–**7** showed cytotoxicity against KB, NCI-H187 and MCF-7 cancer cell lines with IC_{50} values ranging from 1.45 to 49.31 μg/mL. Compounds **1** and **5** showed cytotoxicity against *Vero* cells with IC_{50} values of 38.72 and 32.90 μg/mL, respectively. In addition, compounds **1** and **2** showed antibacterial activity against *S. aureus* with MIC values of 4 and 8 μg/mL, respectively.

Acknowledgments

Disclosure statement

No potential conflict of interest was reported by the authors.

References

Bondar VS, Puzyr AP, Purtov KV, Medvedeva SE, Rodicheva EK, Gitelson JI. 2011. The luminescent system of the luminous fungus *Neonothopanus nambi*. Dokl Biochem Biophys. 438:138–140.

Bua-Art S, Saksirirat W, Kanokmedhakul S, Hiransalee A, Lekphrom R. 2011. Effect of bioloactive compound from luminescent mushroom (*Neonothopanus nambi* Speg.) on root-knot nematode (*Meloidogyne incognita* Chitwood) and non-target organisms. KKU Res J. 16(4):726–737.

Clericuzio M, Pan F, Han F, Pang Z, Sterner O. 1997. Stearoyldelicone, an unstable protoilludane sesquiterpenoid from intact fruit bodies of *Russula delica*. Tetrahedron Lett. 38(47):8237–8240.

Clinical and Laboratory Standards Institute. 2012. Methods for dilution antimicrobial susceptibility tests for bacteria that grow aerobically; approved standard. 9th ed. M07-A9, Wayne, PA: Clinical and Laboratory Standards Institute.

Desjardins RE, Canfield CJ, Haynes JD, Chulay JD. 1979. Quantitative assessment of antimalarial activity *in vitro* by a semiautomated microdilution technique. Antimicrob Agents Chemother. 16(6):710–718.

El-Elimat T, Figueroa M, Raja HA, Graf TN, Adcock AF, Kroll DJ, Day CS, Wani MC, Pearce CJ, Oberlies NH. 2013. Benzoquinones and terphenyl compounds as phosphodiesterase-4B inhibitors from a fungus of the order Chaetothyriales (MSX 47445)). J Nat Prod. 76(3):382–387.

Hayashi S, Fukushima R, Wada N. 2012. Extraction and purification of a luminiferous substance from the luminous mushroom *Mycena chlorophos*. Biophysics (Nagoya-Shi). 8:111–114.

Intaraudom C, Boonyuen N, Supothina S, Tobwor P, Prabpai S, Kongsaeree P, Pittayakhajonwut P. 2013. Novel spiro-sesquiterpene from the mushroom *Anthracophyllum* sp. BCC18695. Phytochem Lett. 6(3):345–349.

Kaneko A, Tsukada M, Fukai M, Suzuki T, Nishio K, Miki K, Kinoshita K, Takahashi K, Koyama K. 2010. KDR Kinase Inhibitor isolated from the mushroom *Boletopsis leucomelas*. J Nat Prod. 73(5):1002–1004.

Kanokmedhakul S, Lekphrom R, Kanokmedhakul K, Hahnvajanawong C, Bua-Art S, Saksirirat W, Prabpai S, Kongsaeree P. 2012. Cytotoxic sesquiterpenes from luminescent mushroom *Neonothopanus nambi*. Tetrahedron. 68(39):8261–8266.

Namanusart W, Saksirirat W, Hirunsalee A, Lekphrom R. 2013. Efficiency of luminescent mushroom, Neonothopanus nambi Speg.for controlling root-knot nematodes (Meloidogyne incognita Chitwood) in tomatoes. KKU Res J. 18:824–831.

Purtov KV, Petushkov VN, Baranov MS, Mineev KS, Rodionova NS, Kaskova ZM, Tsarkova AS, Petunin AI, Bondar VS, Rodicheva EK, et al. 2015. The Chemical basis of fungal bioluminescence. Angew Chem Int Ed Engl. 54(28):8124–8128.

Skehan P, Storeng R, Scudiero D, Monks A, McMahon J, Vistica D, Warren JT, Bokesch H, Kenney S, Boyd MR. 1990. New colorimetric cytotoxicity assay for anticancer-drug screening. J Natl Cancer Inst. 82(13):1107–1112.

Trager W, Jensen JB. 1976. Human malaria parasites in continuous culture. Science. 193(4254): 673–675.

Tsarkova AS, Dubinnyi MA, Baranov MS, Oguienko AD, Yampolsky IV. 2016. Nambiscalarane, a novel sesterterpenoid comprising a furan ring, and other secondary metabolites from bioluminescent fungus *Neonothopanus nambi*. Mendeleev Commun. 26(3):191–192.

Zernov YP, Kobzeva TV, Dranova TY, Stass DV, Alekseev AA, Nefedov AA. 2017. Luminophores of the luminous fungus *Neonothopanus nambi*. Biophysics. 62(2):265–270.

Zubia E, Ortega MJ, Carballo JL. 2008. Sesquiterpenes from the sponge *Axinyssa Isabela*. J Nat Prod. 71(12):2004–2010.
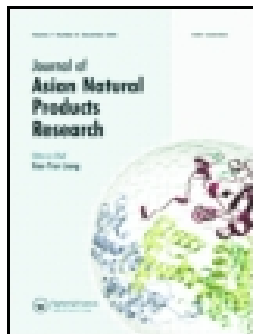
Bioactive galloyl flavans from the stems of *Helixanthera parasitica*

Oue-Artorn Rajachan, Lalitphan Hongtanee, Kasinee Chalermsaen, Kwanjai Kanokmedhakul & Somdej Kanokmedhakul

View supplementary material

Published online: 04 Apr 2019.

Submit your article to this journal

View Crossmark data

Taylor & Francis
Taylor & Francis Group

Bioactive galloyl flavans from the stems of *Helixanthera parasitica*

Oue-Artorn Rajachan[a] (iD), Lalitphan Hongtanee[b], Kasinee Chalermsaen[b], Kwanjai Kanokmedhakul[b] and Somdej Kanokmedhakul[b]

[a]Department of Chemistry and Center of Excellence for Innovation in Chemistry, Faculty of Science, Mahasarakham University, Mahasarakham 44150, Thailand; [b]Natural Products Research Unit, Department of Chemistry and Center of Excellence for Innovation in Chemistry, Faculty of Science, Khon Kaen University, Khon Kaen 40002, Thailand

ABSTRACT

Three new flavans, (2S)-7-O-galloyl-5,3′,4′-trihydroxyflavan (**1**), (2S)-7,3′-O-digalloyl-5,4′-dihydroxyflavan (**2**), and (2S)-7,4′-O-digalloyl-5,3′-dihydroxyflavan (**3**), together with four known compounds, (2S)-5,7,3′,4′-tetrahydroxyflavan (**4**), (-)-epicatechin (**5**), (-)-syringaresinol (**6**), and methyl gallate (**7**) have been isolated from the EtOAc extract of the stems of *Helixanthera parasitica*. Compounds **2** and **3** were obtained as a mixture of positional isomers. The structures of the isolated compounds were established using extensive spectroscopic data. Compound **1** and the mixture of **2** and **3** exhibited significant antimalarial activity against *Plasmodium falciparum*, with IC_{50} values of 0.59 and 1.38 μM, respectively. In addition, flavans **1**–**3** showed cytotoxicity against KB, MCF-7, and NCI-H187 cancer cell lines, with IC_{50} values in the range of 11.1–30.0 μM.

Helixanthera parasitica

	R	R_1	R_2
1	G	H	H
2	G	G	H
3	G	H	G

1. Introduction

Helixanthera parasitica belongs to the family Loranthaceae. It is a parasitic plant, 1–2 m in height [1]. In Thailand, many parasitic plants have long been used in traditional medicine. For example, a water decoction of the stems of *H. parasitica*, mixed with some other parasitic plants, has been used to treat liver and kidney diseases [2, 3]. An aqueous extract from the whole plant has been reported to exhibit anti-metastatic and antioxidant activity [3]. A phytochemical investigation of the leaves of *H. parasitica* resulted in the isolation of gallic acid, ethyl gallate, quercitrin, and 4,7,3′,4′-tetrahydroxyflavan [4]. Although, neither the chemical constituents of the stem extracts of *H. parasitica*, nor the biochemical activities of these extracts, have been reported. Our preliminary evaluation of the bioactivity of stem extracts of *H. parasitica* revealed that the crude EtOAc extract had antimalarial activity against *Plasmodium falciparum*, with an IC_{50} value of 3.25 µg/mL. Herein, we describe the isolation of three new flavans (1–3) and four known compounds (4–7) from the stems of *H. parasitica*, and report their bioactivities.

2. Results and discussion

The chemical constituents of the EtOAc extract of dried stems of *H. parasitica* were separated by chromatographic techniques, namely, column chromatography (CC), flash column chromatography (FCC), and preparative layer chromatography (PLC) resulting in seven isolated compounds (1–7). Their structures were established using their physical and spectroscopic data (IR, 1D and 2D NMR, and MS), as well as by comparison of data with those of similar compounds previously reported in the literature. The four known compounds were identified as (2*S*)-5,7,3′,4′-tetrahydroxyflavan (4) [5], (-)-epicatechin (5) [6], (-)-syringaresinol (6) [7], and methyl gallate (7) [8]. Their structures are shown in Figure 1.

Compound 1 was obtained as a light brown amorphous powder, and its molecular formula, $C_{22}H_{18}O_9$, was determined from the HRESITOFMS (observed *m/z* 449.0846 $[M + Na]^+$), indicating 14 degrees of unsaturation. The IR spectrum displayed the presence of hydroxyl (3309 cm^{-1}) and conjugated carbonyl ester (1704 cm^{-1}) groups. The ^{13}C NMR and DEPT spectra indicated that its structure contained two
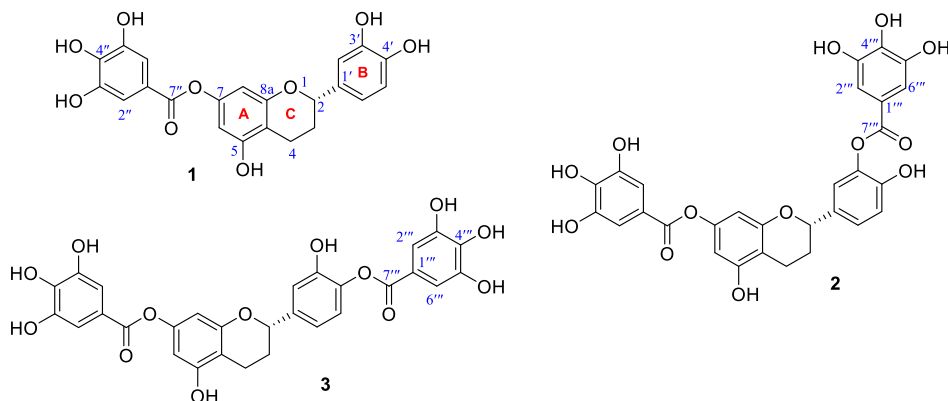

Figure 1. The structures of the isolated compounds (1–3).

Table 1. ^{1}H and ^{13}C NMR spectral data of compounds **1–3** in CD$_3$OD.

Position	1 δ_H	1 δ_C	2 δ_H	2 δ_C	3 δ_H	3 δ_C
2	4.83 brd (9.6)^a	79.0	4.87 d (10.4)	78.2	4.92 d (10.4)	78.2
3	2.18–2.08 m	30.3	2.20–2.11 m	30.0	2.20–2.11 m	29.9
	2.01–1.89 m		1.99–1.88 m		1.99–1.88 m	
4	2. 80–2.58 m	20.5	2.79–2.61 m	20.3	2.79–2.61 m	20.0
4a		108.6		108.6		108.6
5		157.2		156.9		156.9
6	6.18 d (2.4)	101.5	6.25 s	101.5	6.25 s	101.5
7		151.3		151.0		151.1
8	6.15 d (2.4)	102.4	6.24 s	102.4	6.23 s	102.4
8a		157.7		157.4		157.2
1′		134.7		134.5		141.6
2′	6.87 s	114.4	7.15 brs	121.9	7.06 brs	115.4
3′		146.1		139.9		149.8
4′		145.9		149.5		139.4
5′	6.76 d (7.2)	116.1	6.95 d (8)	117.6	7.04 brd (5.6) overlap with H-2′	123.9
6′	6.72 d (7.2)	118.8	7.13 dd (8, 2.4) overlap with H-2′	125.6	6.88 dd (8.4, 2.0)	118.4
1-galloyl unit						
1″		120.6		120.5		120.5
2″	7.17 s	110.5	7.27 s	110.7	7.27 s	110.7
3″		146.6		146.2		146.2
4″		140.5		140.2		140.2
5″		146.6		146.2		146.2
6″	7.17 s	110.5	7.27 s	110.7	7.27 s	110.7
7″		167.1		166.8		166.8
2-galloyl unit						
1‴				120.5		120.5
2‴			7.22 d (0.8)	110.5	7.21 d (0.8)	110.5
3‴				146.3		146.3
4‴				140.1		140.1
5‴				146.3		146.3
6‴			7.22 d (0.8)	110.5	7.21 d (0.8)	110.5
7‴				167.1		167.1

^{a}Values in parentheses are coupling constants in hertz.

methylene, eight methine (one oxymethine and seven aromatic), 11 quaternary aromatic, and one carbonyl carbons. The ^{1}H NMR spectroscopic data of **1** (Table 1) showed resonances of oxymethine at δ_H 4.83 (1H, brd, $J = 9.6$ Hz, H-2), δ_H 2.80–2.58 (2H, m, H-4) and of two methylene groups at δ_H 2.18–2.08 (1H, m, H-3b) and δ_H 2.01–1.89 (1H, m, H-3a). These, together with the COSY correlations of H-2/H-3/H-4 indicated the characteristic C ring of flavan moieties [9, 10]. The ^{1}H NMR resonances at δ_H 6.18 (1H, d, $J = 2.4$ Hz, H-6) and 6.15 (1H, d, $J = 2.4$. Hz, H-8) suggested a *meta*-coupling of both protons at an aromatic A ring. Three aromatic protons at δ_H 6.87 (1H, s, H-2′), 6.76 (1H, d, $J = 7.2$ Hz, H-5′), and 6.72 (1H, d, $J = 7.2$ Hz, H-6′) indicated tri-substitution of an aromatic B ring. The HMBC spectrum exhibited correlations of H-4 to C-2, C-3, C-4a, C-5, and C-8a; H-6 to C-4a, C-5, C-7, and C-8; and H-8 to C-4a, C-6, C-7, and C-8a, confirming the 4a,5,7,8a-tetra-substitution of the A ring. The HMBC correlations of H-2 to C-4, C-1′, C-2′, and C-6′ and H-2′ to C-2, C-3′, C-4′ and C-6′ revealed the connection of the C and B rings through C-2. While, the correlations of H-5′ to C-1′, C-3′, and C-4′, as well as H-6′ to C-2, C-1′, C-2′, and C-4′ represented the 1′,3′,4′-tri-substitution and also supported the position of two hydroxyl groups at C-3′ and C-4′ of the B ring. The

remaining aromatic protons at δ_H 7.17 (2H, s, H-2″ and H-6″) belong to a galloyl ester moiety, which corresponded with the HMBC correlations of H-2″ and H-6″ to C-1″, C-3″, C-4″, C-5″ and C-7″ [9, 11]. This galloyl ester group connects to the A ring at C-7 (δ_C 151.3) and appeared at high field [12]. In addition, the HMBC correlations of H-4 to C-2, C-3, C-4a, C-5, and C-8a also confirmed the position of this galloyl ester unit. Compound **1** demonstrated negative specific rotation ($[\alpha]_D^{23}$ −45.3 c 0.1, MeOH), which assigns the stereochemistry at C-2 as S [5]. Based on the spectroscopic evidence, compound **1** was determined as a new flavan, named (2S)-7-O-galloyl-5,3′,4′-trihydroxyflavan, as shown in Figure 1.

Compounds **2** and **3** were isolated as a mixture of a light brown amorphous powder. Their molecular formulas were determined, based on the HRESITOFMS data, as $C_{29}H_{22}O_{13}$ (observed m/z 601.0960 $[M + Na]^+$), corresponding to 19 degrees of unsaturation and the presence of one additional galloyl unit compared to compound **1**. The IR spectrum demonstrated the absorption bands of hydroxyl (3280 cm^{-1}) and conjugated carbonyl ester (1695 cm^{-1}) groups. The ^{1}H NMR spectrum clearly showed two sets of resonances, indicating a mixture of the two flavans **2** and **3** in the ratio of 1:1. This was especially clear for the resonance signals of the oxymethine proton H-2 (δ_H 4.87 for **2** and 4.92 for **3**, both d with $J = 10.4$ Hz) and of aromatic protons in the B ring at δ_H 7.15 and 7.06 (H-2′), 6.95 and 7.04 (H-5′), and 7.13 and 6.88 (H-6′) for **2** and **3**, respectively. The ^{1}H NMR spectrum of the mixture of **2** and **3** was similar to that of **1**, except for the presence of additional proton signals at δ_H 7.22 (2H, d, $J = 0.8$ Hz, H-2‴ and H-6‴) for **2** and δ_H 7.21 (2H, d, $J = 0.8$ Hz, H-2‴ and H-6‴) for **3**. These signals were assigned to galloyl groups [9]. The HMBC spectrum of **2** also clearly showed sets of correlations of H-2 (4.87) to C-3, C-4, C-8a, C-1′(134.5), C-2′(121.9), and C-6′(125.6); H-5′ (6.95) to C-1′(134.5), C-3′(139.9), C-4′(149.5), and C-6′; and H-6′ (7.13) to C-2′(121.9), C-4′(149.5), and C-5′(117.6), as shown in Figure 2. The HMBC spectrum of **3** exhibited correlations of H-2 (4.92) to C-3, C-4, C-8a, C-1′(141.6), C-2′(115.4), and C-6′(118.4); H-5′ (7.04) to C-1′(141.6)′, C-3′(149.8), C-4′(139.4), and C-6′(118.4); and H-6′(6.88) to C-2′(115.4), C-4′(139.4), and C-5′(123.9) as shown in Figure 2. These confirmed that the galloyl groups were located at C-3′ for **2** and C-4′ for **3**, respectively. The configurations at C-2 of **2** and **3** were determined as S from their specific rotation ($[\alpha]_D^{25}$ −23.5 c 0.1, MeOH) and their *trans* diaxial coupling ($J = 10.4$ Hz) of H-2 and H-3 [13, 14]. Therefore, compound **2** was characterized as (2S)-7,3′-O-digalloyl-5,4′-
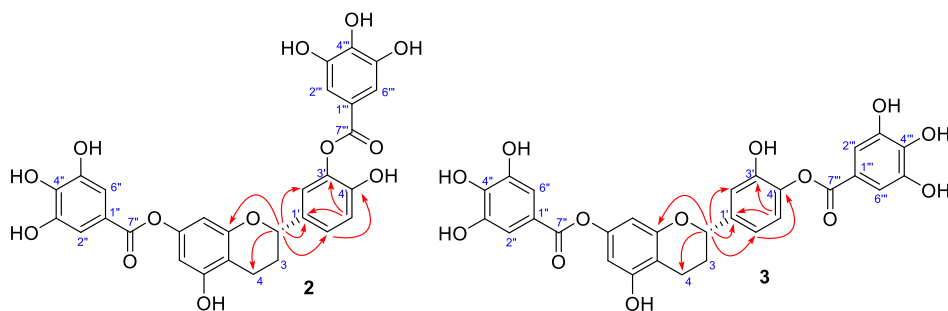

Figure 2. Selected HMBC correlations of compounds **2** and **3**.

Table 2. Biological activity of compounds **1**–**6**.

Compound	Antimalarial IC$_{50}$ (μM)	Cytotoxicity IC$_{50}$ (μM)			
		KB[a]	MCF-7[b]	NCI-H187[c]	Vero cell[d]
1	0.59	Inactive[e]	Inactive	16.7	Inactive
2 + **3**[f]	1.38	30.0	19.7	11.1	73.9
4	Inactive	Inactive	Inactive	Inactive	Inactive
5	Inactive	Inactive	Inactive	Inactive	Inactive
6	Inactive	Inactive	Inactive	Inactive	Inactive
Dihydroartemisinin	0.008				
Doxorubicin			12.1		
Ellipticine		8.2		6.7	3.4

[a]Human epidermoid carcinoma in the mouth.
[b]Human breast adenocarcinoma.
[c]Human small cell lung cancer.
[d]African green monkey kidney.
[e]>100 μM.
[f]Mixture of compounds **2** and **3**.

dihydroxyflavan, and compound **3** was elucidated as a positional isomer of **2**, named (2S)-7,4′-O-digalloyl-5,3′-dihydroxyflavan.

The bioactivities of compounds **1**–**6** were evaluated, and the result is shown in Table 2. Compound **1** and the mixture of **2** and **3** showed significant antimalarial activity against *P. falciparum* with IC$_{50}$ values of 0.59 and 1.38 μM, respectively. They also exhibited moderate cytotoxicity toward the NCI-H187 cell line, with IC$_{50}$ values of 16.7 and 11.1 μM, respectively. Only the mixture of **2** and **3** displayed cytotoxicity against KB and MCF-7 cell lines, with IC$_{50}$ values of 30.0 and 19.7 μM, respectively. However, the mixture of **2** and **3** was also cytotoxic toward the normal cell line (IC$_{50}$ 73.9 μM). Compound **7** has been previously reported for antimalarial activity against *P. falciparum*, which showed weak antimalarial activity (IC$_{50}$ 38.0 μM) [15]. In addition, compound **7** has also been reported to exhibit no cytotoxicity against MCF-7 and NCI-H187 cell lines [16, 17]. When comparing flavans **1**–**5**, it should be noted that the addition of the galloyl group in **1**–**3** increased the cytotoxicity toward the three cancer cell lines tested (KB, MCF-7, and NCI-H187).

3. Experimental

3.1. General experimental procedures

Melting points were determined on a Gallenkamp melting point apparatus (SANYO Gallenkamp PLC, Leicestershire) and are uncorrected. Optical rotations were determined using a JASCO DIP-1000 digital polarimeter (JASCO, Easton, MD). Ultraviolet (UV) spectra were measured using an Agilent 8453 UV-visible spectrophotometer (Agilent Technologies, Santa Clara, CA). IR spectra were obtained using a Bruker Tenser 27 spectrophotometer (Bruker, Ettlingen, Germany). NMR spectra were recorded with CDCl$_3$ and CD$_3$OD as solvents using a Varian Mercury Plus 400 spectrometer (Varian, Polo Alto, CA), and the residues of these solvents were used as references. Mass spectra were determined with a Micromass Q-TOF 2 hybrid quadrupole time-of-flight mass spectrometer with a Z-spray ES source (Micromass, Manchester, UK). Thin layer chromatography (TLC) was performed on silica gel 60 PF$_{254}$ (MERCK, Darmstadt, Germany) supported on an aluminum sheet; the spots

were visualized by UV light (254 and 366 nm) and also by spraying with anisaldehyde, followed by heating until charred. CC was carried out on silica gel (0.063–0.200 mm or less than 0.063 mm; MERCK), Sephadex LH-20 (40–70 μm; GE Health care, Uppsala, Sweden), and Lichroprep RP-18 (40–63 μm; MERCK). PLC was carried out on silica gel 60 PF$_{254}$ (MERCK) supported on a glass (20 × 20 cm). Commercial grade solvents were distilled at their boiling points prior to use for extraction and chromatographic separations (CC, PLC, and TLC).

3.2. Plant material

The stems of *Helixanthera parasitica* were collected on February 2013 from Ban San Tom, Phu Ruea district, Loei Province, Thailand. The plants were identified as *H. parasitica* by Prof. Pranom Chantaranothai, Department of Biology, Faculty of Science, Khon Kaen University, Thailand, where a specimen [voucher number Rajachan O-1 (MSU)] was deposited.

3.3. Extraction and isolation

Air-dried stems of *H. parasitica* (2.7 kg) were grounded and extracted successively with EtOAc (7L × 2), to give crude EtOAc extract (109 g). A portion of the crude EtOAc extract (80 g) was subjected to silica gel FCC, eluted with a gradient system of *n*-hexane-EtOAc and EtOAc-MeOH to give seven fractions, HE1–HE7. Fraction HE2 (1.43 g) was further subjected to silica gel FCC, eluted with an isocratic system of EtOAc-*n*-hexane (3:7) to give three subfractions, HE2.1–HE2.3. Recrystallization of subfraction HE2.2 (156 mg) with EtOAc yielded a white solid of **4** (92 mg). Fraction HE3 (360 mg) was subjected to Sephadex LH-20 CC, eluted with MeOH resulting in two subfractions, HE3.1 and HE3.2. Purification of subfraction HE3.1 (82 mg) by PLC using MeOH-CH$_2$Cl$_2$ (1:9) as eluent (developed 3 times) gave a light brown amorphous powder of **1** (13 mg, R$_f$ 0.63). Fraction HE4 (1.21 g) was separated by silica gel FCC, eluted with MeOH-CH$_2$Cl$_2$ (1:19) yielding three subfractions, HE4.1–4.3. Subfraction HE4.1 (150 mg) was further purified by PLC using MeOH-CH$_2$Cl$_2$ (1:9) as eluent (developed 2 times), to yield colorless needles of **6** (43 mg, R$_f$ 0.65). Recrystallization of fraction HE5 (172 mg) with EtOAc gave a white solid of **7** (78 mg). Fraction HE6 (1.58 g) was purified by silica gel FCC, eluted with an isocratic system of MeOH-EtOAc (1:19) to give two subfractions, HE6.1 and HE6.2. Subfraction HE6.1 gave a white solid of **5** (30 mg), and subfraction HE6.2 (863 mg) was further separated by Lichroprep RP-18 CC, using H$_2$O-MeOH (2:3) as an eluent, to give a light brown amorphous powder of a mixture of compounds **2** and **3** (15 mg).

3.3.1. (2S)-7-O-galloyl-5,3′,4′-trihydroxyflavan (1)

Light brown amorphous powder; mp 216 °C (dec); [α]$_D^{23}$ –45.3 (*c* 0.1, MeOH); UV (MeOH) λ_{max} (log ε) 281 (4.25) nm; IR (Neat) ν_{max} 3309, 2928, 1704, 1602, 1444, and 1206 cm^{-1}; For ^{1}H and ^{13}C NMR spectroscopic data (CD$_3$OD, 400 MHz), see Table 1; HRESITOFMS: *m/z* 449.0846 [M + Na]$^+$ (calcd for C$_{22}$H$_{18}$O$_9$Na, 449.0849).

3.3.2. The mixture of 2 and 3

Light brown amorphous powder; $[\alpha]_D^{25}$ –23.5 (c 0.1, MeOH); UV (MeOH) λ_{max} (log ε) 285 (4.43) nm; IR (Neat) ν_{max} 3280, 1695, 1603, 1514, 1444, 1334, and 1189 cm^{-1}; For ^{1}H and ^{13}C NMR spectroscopic data (CD$_3$OD, 400 MHz), see Table 1; HRESITOFMS: m/z 601.0960 [M + Na]$^+$ (calcd for C$_{29}$H$_{22}$O$_{13}$Na, 601.0958).

3.4. Antimalarial assay

Antimalarial activity against the parasite *P. falciparum* (K1, multidrug-resistant strain) was assessed using the method of Trager and Jensen [18]. Quantitative assessment of activity *in vitro* used the microculture radioisotope technique, based upon the method described by Desjardins and co-worker [19], using dihydroartemisinin as a reference drug (Table 2).

3.5. Cytotoxicity assays

Cytotoxicity assays against human epidermoid carcinoma (KB), human breast adenocarcinoma (MCF-7), and human small cell lung cancer (NCI-H187) cell lines were performed employing the Resazurin microplate assay described by O′Brien [20]. The reference substances were doxorubicin and ellipticine. Cytotoxicity against a primate cell line (Vero) was tested using the green fluorescent protein detection method described by Hunt [21]. The reference drug was ellipticine (Table 2).

Disclosure statement

No potential conflict of interest was reported by the authors.

ORCID

Oue-Artorn Rajachan 🆔 http://orcid.org/0000-0001-5681-1281

References

[1] R. Vidal-Russell and D.L. Nickrent, *Am. J. Bot.* **95**, 1015 (2008).
[2] N. Kwanda, K. Noikotr, R. Sudmoon, T. Tanee, and A. Chaveerach, *J. Nat. Med.* **67**, 438 (2013).

[3] K. Lirdprapamongkol, C. Mahidol, S. Thongnest, H. Prawat, S. Ruchirawat, C. Srisomsap, R. Surarit, P. Punyarit, and J. Svasti, *J. Ethnopharmacol.* **86**, 253 (2003).
[4] L. Li, M. Li, and W. Feng, *Chin. Tradit. Herb. Drugs* **25**, 283 (1994).
[5] X.Y. Zhang, B.G. Li, M. Zhou, X.H. Yuan, and G.L. Zhang, *J. Integr. Plant Biol.* **48**, 236 (2006).
[6] W. Lakornwong, K. Kanokmedhakul, and S. Kanokmedhakul, *Nat. Prod. Res.* **28**, 1015 (2014).
[7] E. Hiltunen, T.T. Pakkanen, and L. Alvila, *Holzforschung.* **60**, 519 (2006).
[8] G. Saxena, A.R. McCutcheon, S. Farmer, G.H.N. Towers, and R.E.W. Hancock, *J. Ethnopharmacol.* **42**, 95 (1994).
[9] Y. Li, K-T. Leung, F. Yao, L.S.M. Ooi, and V.E.C. Ooi, *J. Nat. Prod.* **69**, 833 (2006).
[10] P. Moosophon, S. Kanokmedhakul, K. Kanokmedhakul, M. Buayairaksa, J. Noichan, and K. Poopasit, *J. Nat. Prod.* **76**, 1298 (2013).
[11] L. Min-Won, S. Morimoto, G-I. Nonaka, and I. Nishioka, *Phytochemistry* **31**, 2117 (1992).
[12] T. Tanaka, G-I. Nonaka, and I. Nishioka, *Phytochemistry* **22**, (2575) 1983.
[13] J. Kang, C. Liu, H. Wang, B. Li, C. Li, R. Chen, and A. Liu, *Molecules* **19**, 4479 (2014).
[14] S. Kanokmedhakul, K. Kanokmedhakul, K. Nambuddee, and P. Kongsaeree, *J. Nat. Prod.* **67**, 968 (2004).
[15] Á.I. Calderón, L.I. Romero, E. Ortega-Barría, R. Brun, M.D. Correa A, and M.P. Gupta, *Pharm. Biol.* **44**, 487 (2006).
[16] D.S. Yang, W.B. Peng, Z.L. Li, X. Wang, J.G. Wei, Q.X. He, Y.P. Yang, K.C. Liu, and X.L. Li, *Fitoterapia* **97**, 211 (2014).
[17] Y.Y. Chan, C.Y. Wang, T.L. Hwang, S.H. Juang, H.Y. Hung, P.C. Kuo, P.J. Chen, and T.S. Wu, *Molecules* **23**, 2799 (2018).
[18] W. Trager, and J.B. Jensen, *J. Parasitol.* **91**, 484 (2005).2.0.CO;2] [16108535]
[19] R.E. Desjardins, C.J. Canfield, J.D. Haynes, and J.D. Chulay, *Antimicrob. Agents Chemother.* **16**, 710 (1979).
[20] J. O'Brien, I. Wilson, T. Orton, and F. Pognan, *Eur. J. Biochem.* **267**, 5421 (2000).
[21] L. Hunt, M. Jordan, M. De Jesus, and F.M. Wurm, *Biotechnol. Bioeng.* **65**, 201 (1999).

Application of Nano-particles Derived from *Chaetomium elatum* ChE01 to Control *Pyricularia oryzae* causing Rice Blast

Song, J. J.[1*], Kanokmedhakul, S.[2], Kanokmedhalkul, K.[2] and Soytong, K.[1]

[1]Department of Plant Production Technology, Faculty of Agricultural Technology, King Mongkut's Institute of Technology Ladkrabang (KMITL), Ladkrabang, Bangkok, Thailand; [2]Department of Chemistry, Faculty of Science, Khon Khan University, Thailand.

Abstract *Pyricularia oryzae* causing rice blast was isolated and proved for pathogenicity. *Chaetomium elatum* ChE01 was proved to be antagonized *P. oryzae* in bi-culture antagonistic test which averaged inhibition of 60.40 % within 15 days. Fungal metabolites from *C. elatum* ChE01 were extracted and tested to inhibit *P. oryzae*. Results showed that crude ethyl acetate expressed antifungal activity against *P. oryzae* which the effective dose$_{50}$ (ED$_{50}$) was 231 ppm., followed by crude methanol and crude hexane which the ED$_{50}$ were 460 and 2,122 ppm. respectively. It was shown that nano-CCE gave the highest inhibition *P. oryzae* which the ED$_{50}$ was 8.25 ppm, and followed by nano-CEM and nano-CEH which the ED$_{50}$ values were 11.21 and 65.52 ppm, respectively. Further research findings are investigated in pot and field experiments.

Keywords: Nano-particles, *Chaetomium*, Rice Blast

Introduction

The need to discover the alternative ways to safe human and environment as effective and efficient methods to control plant diseases is desired. One of the method is the application of nanotechnology. Nanotechnology is to build, re-structure, control and devise materials to be molecular level. A nanometer (nm) is one-billionth of a meter. Molecular nanotechnology applies to build the organic materials into molecule by molecule for agricultural application that is being studied (Li *et al.,* 2011). The scientists are actively studied the synthesis of organic nanoparticles are still having unusual properties like physical and biological ones (Elibol *et al.*, 2000; Salata, 2004). Application of nanotechnology in agriculture are being investigated (Soutter, 2012). Nanoparticles can be easily penetrate through plant cells (Perlatti *et al*., 2013).

---

* **Corresponding Author:** Song, J. J.; **Email:** misssongjiaojiao@gmail.com

Bioactive compounds from *Chaetomium* species has been reported by Soytong *et al*. (2001; 2013) as antifungal agent against several phytopathogens. It is safe for environmentally friendly method to control plant diseases (Dar and Soytong, 2014). Emmanuel *et al.* (2013) reported crude extracts of *Chaetomium globosum* coud inhitbit Philippine strain of *P. oryzae*. Soytong *et al.* (2013) found that pure compounds of Chaetoglobosin C, chaetomanone A derived from *Chaetomium* sp. act as microbial elicitors to elicit tomatine in tomato leading to immunity against *Fusarium oxysporum* f sp *lycopersici* causing tomato wilt. Crude extracts and pure compound derived from *Chaetomium* sp were confirmed to be effectively inhibited several plant pathogens. Research finding is further investigated to be nano-particles of those metabolites or compounds to control plant pathogen effectively. Dar and Soytong (2014) developed nano-particles from *C. globosum* and *Chaetomium cupreum* to test for inhibition of several plant pathogens. Tann and Soytong (2016) reported that nano-CGH, nano-CGE, and nano-CGM from *C. globosum* KMITL-N0805 expressed antifungal activity (ED_{50} values of 1.21, 1.19, and 1.93ppm/mL, respectively) against *Curvularia lunata*, the causal agent of leaf spot disease of rice var. Sen Pidoa.

C. *elatum* ChE01 was identified and studied its metabolites as reported by Thohinung *et al.* (2010) that it produced a new chaetoglobosin V, two new natural products, prochaetoglobosin III and prochaetoglobosin III(ed), six known chaetoglobosins B-D, F , and G and isochaetoglobosin D. All these pure compounds expressed cytotoxicity against the human breast cancer (IC_{50}) 2.54-21.29 microM and cholangiocarcinoma cell lines (IC_{50}) 3.41-86.95 microM. This isolate was proved to inhibit *P. oryzae* causing rice blast by using crude extracts and further research investigated those crude extracts to be nano-particles. Preliminary research finding found that nano-particles of *C. elatum* ChE01 actively expressed antifungal activitytest against *P. oryzae*. Nano-particles derived from *C. elatum* ChE01 as nano-CEH, nano-CEE and nano-CEM were significantly inhibited *P. oryzae* at low concentration (Song and Soytong, 2016). The objective was to prove further evaluation nano-particles derived from *C. elatum* ChE01 to inhibit rice blast caused by *P. oryzae* and control mechanism.

Materials and methods

Rice blast pathogen

The diseased samples were taken from leaves which appeared blast symptom and taken into laboratory. Tissue transplanting technique was done for isolation into pure culture. Pure cultures were morphologically identified.

Antagonistic fungus

Chaetomium elatum ChE01 is derived from Biocontrol Reserch Unit, Department of Plant Production Technology, King Mongkut's Institute of Technology Ladkrabang (KMITL), Bangkok. It was cultured on potato dextrose agar (PDA) at room temperature (27-30 C) for 3 weeks for studying morphological characters under binocular compound microscope.

Bi-culture antagonistic test

Treatments were bi-culture between pathogen and antagonist plate and pathogen alone which followed the method of Soytong and Quimio (1989). The agar culture of *C. elatum* ChE01 was cut by sterilized cock borer at peripheral colony and transferred to one side of PDA plate and the agar culture plug of pathogen was done the same and placed in opposite site at equal distance. Bi-culture plates were incubated at room temperature for 30 days.

Bioactivity test of crude extracts from Chaeomium elatum ChE01

Crude extracts from *C. elatum* ChE01 was done by followed the method of Phonkerd *et al*. (2008). Each crude extract with hexane, ethyl acetate and methanol was tested to inhibit the rice blast pathogen, *P. oryzae* at the concentrations of 0, 10, 50, 100, 500 and 1000 ppm. An agar plug of pathogen was moved the middle of potato dextrose agar (PDA) incorporated with each crude extract. The tested plates were incubated at room temperature (30 C) for 15 days.

Nano-particle testing for inhibition of rice blast pathogen

Nano –particles derived from Chaetomium sp was done by followed the method of Dar and Soytong (2014). The tested nano-CCH, nano CCE and nano-CEM) of *C. elatum* ChE01 was tested to inhibit *P. oryzae* causing rice blast with different concentrations (0, 3, 5, 7, 10 and 15 ppm.). A plug of rice blast pathogen was transferred onto the middle of each concentration plate containing PDA, then incubated at room temperature (30 C) for 15 days.

Statistical analysis

Bi-culture antagonistic test was set up using Completely Randomized Design (CRD) with four replications. The bioactivity tests were performed

using two factor factorial experiment in Completely Randomized Design with four replications. Data were collected as colony diameter (cm), number of spores and statistically computed analysis of variance. Treatment means were compared using DMRT at p = 0.05 and 0.01. The Effective dose at 50 % (ED_{50}) was computed by probit analysis program.

Results

Rice blast pathogen

Rice blast specimens were collected from rice-fields and brought into laboratory. Isolation was done by using tissue transplanting technique. Pure culture of *Pyricularia oryzae* wa cultured in rice flour agar (RFA) at room temperature (27-30 C) and morphological identified (Fig.1) and tested for pathogenicity.

Antagonistic fungus

Chaetomium elatum ChE01 offered from Biocontrol Research Laboratory, and culture on potato dextrose agar (PDA) for 3 weeks. It is an ascomycetous fungus which produces perithecia, asci and ascospores (Fig.2).

Bi-culture antagonistic test

Result showed that *C. elatum* ChE01 expressed antifungal activity against *P. oryzae* causing rice blast disease in bi-culture antagonistic test averaged 60.40 % within 15 days. The colony diameter in control plate was 9.00 while colony in bi-culture plate was averaged 3.56 cm. (Fig. 3). The colony of *C. elatum* ChE01 grew over the pathogen colony.

Bioactivity test of Crude extracts from antagonistic fungi

Crude extracts from *C. elatum* ChE01 were tested to inhibit *P. oryzae* by poisionous technique. Result showed that crude hexane, crude ethyl acetate and crude methanol at concentration 0f 1,000 ppm gave significantly highest inhibition of colony growth which averaged of 2.73, 1.48 and 2.13 cm., respectively (Table 1) while the control (o ppm) was 5.00 cm. However, crude ethyl acetate gave the most highly significant inhibited sporulation (3.93×10^{6} spores), and followed by   crude methanol and crude hexane which were 2.56×10^{6} and 3.93×10^{6} spores), respectively. Moreover, crude ethyl acetate

expressed antifungal activity against *P. oryzae* which the effective dose$_{50}$ (ED$_{50}$) was 231 ppm and followed by crude methanol and crude hexane which the ED$_{50}$ were 460 and 2,122 ppm, respectively (Table 1).
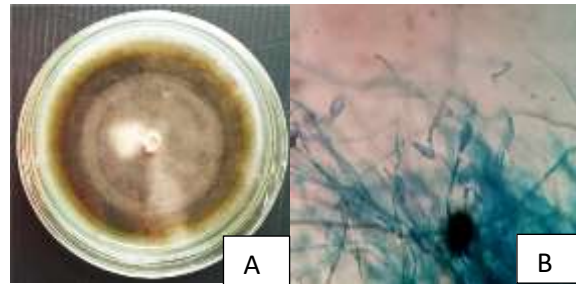

Figure 1. Rice blast pathogen *Pyriculria oryzae*, A = culture on PDA and B = Conidia
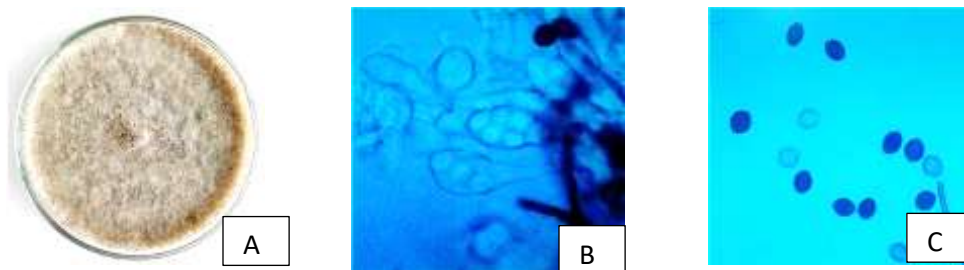

Figure 2. Antagonistic fungus *Chaetomium elatum,* A = culture on PDA, B = Asci, C = bi-culture test and D = ascospores
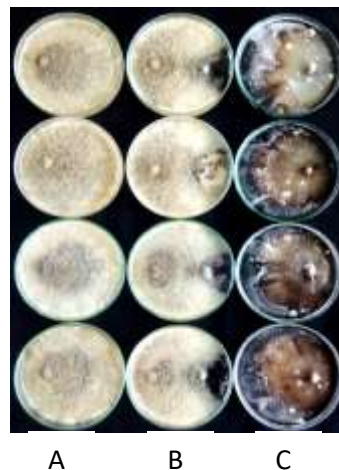

A   B   C

Figure 3. Bi-culture antagonistıc test between *Chaetomium elatum* and *Pyricularia oryzae,* A = antagonist, B = Bi-culture and C = pathogen

Table 1. Crude extracts of *Chaetomium elatum* testing for growth inhibition of *Pyricularia oryzae* at 8 days, spore production inhibition at 15 days and effective dose (ED$_{50}$) values.

Crude extracts	Concentration (ppm)	Colony diameter (cm)[1]	Growth inhibition (%)	Number of spores [1](10^6)	Spore Inhibition (%)[2,3]	ED$_{50}$(ppm)
	0	5.00^a	-	6.50^a	-	
	10	4.73^b	5.25^l	6.25^{ab}	3.61^i 2.25	
Crude	50	4.47^c	10.50^k	5.87^{abc}	8.96^{ghi}	2122
Hexane	100	4.27^d	14.50^j	5.43^{bcd}	15.54^{fgh}	
	500	3.67^f	26.50^h	5.12^{cde}	20.29^{fg}	
	1000	2.73^i	45.25^e	3.93^{fgh}	38.68^{cd}	
	0	5.00^a	-	6.50^a	-	
	10	4.36^{cd}	12.75^{jk}	5.93^{abc}	8.25^{hi}	
Crude	50	3.57^f	28.50^h	4.31^{efg}	33.70^{de}	
EtOAc	100	3.02^h	39.50^f	3.31^{hij}	49.06^{bc}	231
	500	2.00^k	60.00^c	2.62^{ij}	59.56^{ab}	
	1000	1.48^l	70.25^b	2.37^j	63.43^a	
	0	5.00^a	-	6.50^a	-	
	10	4.64^b	7.00^l	6.06^{abc}	6.53^{hi}	
Crude	50	4.12^e	17.50^i	5.31^{bcd}	27.27^{ef}	
MeOH	100	3.23^g	35.25^g	4.81^{def}	35.21^{de}	460
	500	2.13^j	57.25^d	3.75^{gh}	42.06^{cd}	
	1000	1.48^m	69.00^a	2.56^{ghi}	58.62^{ab}	
C.V.(%)		1.70	4.23	12.89	19.01	

[1]/Average of four replications. Means followed by a common letter are not significantly differed by DMRT at P=0.01.

[2]/Inhibition(%)=R1-R2/R1x100 where R1 was colony diameter of pathogen in control and R2 was colony diameter of pathogen in treated plates.

Nano-particle testing for inhibition of rice blast pathogen

Result showed that nano-CCE at 15 ppm gave highly significant inhibited colony growth of *P. oryzae* (3.00 cm) and followed by nano-CEM and

928

nano-CEH   3.40 and 3.65 ppm., respectively. Nano-CEH gave significantly better inhibited sporulation of *P. oryzae* (3.43 X 10^6 spores) than nano-CEE (1.25 X 10^6 spores) and nano CEM (1.81 X 10^6 spores). Morever, nano-CEE gave the highest inhibition *P. oryzae* which the ED_{50} was 8.25 ppm, and followed by nano-CEM and nano-CEH which the ED_{50} values were 11.21 and 65.52 ppm, respectively (Table 2). Nano-CEE at 15 ppm gave highest significantly in spore inhibition of *P. oryzae* (79.39 %) and followed by nano-CEE at concentration of 5 ppm (41.18 %) and nano-CEH at 14 ppm (42.29%).

Table 2. Nano particles of *Chaetomium elatum* ChE01 testing for growth inhibition of *Pyricularia oryzae* at 8 days, spore production inhibition at 15 days and effective dose (ED_{50}) values.

Crude extracts	Concentration (ppm)	Colony diameter $(cm)^{/1}$	Growth inhibition $(\%)^{/2}$	Number of spores $^{/1}(10^6)$	Spore Inhibition $(\%)^{/2}$	ED_{50}(ppm)
	0	5.00^a	-	6.00^a	-	
	3	4.79^b	4.00^i	5.68^{bcd}	4.85^i	
Nano-CEH	5	4.60^{de}	8.00^{fg}	4.81^{bcd}	18.80^g	65.52
	10	4.00^g	10.00^f	4.12^{de}	30.15^f	
	15	3.65^h	20.00^d	3.43^{ef}	42.29^e	
	0	5.00^a	-	6.00^a	-	
	3	4.64^{cd}	7.00^{jh}	4.56^{cd}	23.43^g	
Nano-CEE	5	4.30^f	14.00^e	3.50^{ef}	41.18^e	
	10	3.60^h	28.00^c	2.18^g	63.28^c	8.25
	15	3.00^j	40.00^c	1.25^{hi}	79.39^b	
	0	5.00^a	-	6.00^a	-	
	3	4.75^{bc}	5.00^{hi}	5.31^{abc}	11.60^h	
Nano-CEM	5	4.50^e	10.00^f	4.68^{cd}	21.32^g	
	10	3.95^g	21.00^d	3.06^f	49.20^d	11.21
	15	3.40^i	32.00^b	1.81^{gh}	70.03^c	
C.V.(%)		1.17	7.17	12.89	19.01	

[1]/Average of four replications. Means followed by a common letter are not significantly differed by DMRT at P=0.05.
[2]/Inhibition(%)=R1-R2/R1x100 where R1 was colony diameter of pathogen in control and R2 was colony diameter of pathogen in treated plates.

Discussion

P. oryzae causing rice blast was isolated and proved for pathogenicity. Te Beest (2007) stated that rice blast, caused by a fungus, *Magnaporthe oryzae* (anamorph: *Pyricularia oryzae*) and it infected rice to appear the symptom on leaves, stems, peduncles, panicles, seeds, and roots. *C. elatum* ChE01 used in this experiment as the same isolate that reported by Thohinung *et al.* (2010) which that it produced antimicrobial activity eg. chaetoglobosin V, prochaetoglobosin III and prochaetoglobosin III against the human breast cancer and cholangiocarcinoma cell lines. These compounds may possible actively prove as antibiosis in bi-culture antagonistic test that *C. elatum* ChE01 may possible release to be antagonize *P. oryzae*. Moreover, fungal metabolites from *C. elatum* ChE01 were extracted and tested to inhibit *P. oryzae*. The crude ethyl acetate gave better antifungal activity against *P. oryzae* than crude methanol and crude hexane. Similar results was reported by Sibounnavong *et al*. (2012); Soytong *et al.* (2013) which reported that crude extracts from *Chaetomium* spp. actively inhibited *Fusarium oxysporum* f sp *lycopersici* causing tomato wilt. The research finding revealed that nano-CCE gave the highest inhibition *P. oryzae* which the ED50 was 8.25 ppm, and followed by nano-CEM and nano-CEH which the ED_{50} values were 11.21 and 65.52 ppm, respectively. Tan and Soytong (2016) reported that Nano-CGH, nano-CGE, and nano-CGM derived from *Chaetomium globosum* KMITL-N0805 gave a good control *Curvularia lunata* causing leaf spot disease of rice var. Sen Pidoa. Moreover, the effect of nanoparticles showed to be broken the pathogen cell and lost pathogenicity.

Acknowledgment

References

Dar, J. and Soytong, K. (2014). Construction and characterization of copolymer nanomaterials loaded with bioactive compounds from Chaetomium species. Journal of Agricultural Technology. 10:823-831.

Elibol, O. H., Morisette, D. D., Denton, J. P. and Bashir, R. (2003). Integrated nanoscale silicon sensors using top-down fabrication. Applied Physics Letters. 83:4613-4615.

Emmanuel, E. G., Divina, C. C. and Dar, D. J. (2013). Inhibitory activity of Chaetomium globosum Kunze extract against Philippine strain of Pyricularia oryzae Cavara. International Journal of Agricultural Technology. 9:333-348.

Li, X., Xu, H., Chen, Z. S. and Chen, G. (2011). Biosynthesis of nanoparticles by microorganisms and their applications. Journal of Nanomaterials. 16:270-974.

Perlatti, B., de Souza Bergo, P. L., das Graas Fernandes da Silva, M. F., Fernandes, J. B. and Forim, M. R. (2013). Polymeric nanoparticle-based insecticides: a controlled release purpose for agrochemicals. In S. T. Technologies (Ed.), Insecticides – Development of Safer and More Effective (pp. 20). In Tech Open Access, Croatia, Ch.

Phonkerd, N., Kanokmedhakul, S., Kanokmedhakul, K., Soytong, K., Prabpai, S. and Kongsearee, P. (2008). Bis-spiro-Azaphilones and Azaphilones from the Fungi *Chaetomium cochliodes* VTh01 and *C. cochliodes* CTh05. Tetrahedron. 64:9636-9645.

Salata, O. V. (2004). Applications of nanoparticles in biology and medicine. Journal of Nanobiotechnology. 2-3.

Sibounnavong, P., Chaoenporn, C., Kanokmedhakul, S. and Soytong, K. (2012). Antifungal metabolites from antagonistic fungi used to control tomato wilt fungus, *Fusarium oxysporum f sp lycopersici*. Africa Journal of Biotechnology. 10:19714-19722.

Song, J. J. and Soytong, K. (2016). Antifungal activity of *Chaetomium elatum* against *Pyricularia oryzae* causing rice blast. International Journal of Agricultural Technology. 12:1437-1447.

Soutter, W. (2012). Nanotechnology in agriculture. AZoNano.com Publishers. Available at http://www.azonano.com/article.aspx?Article ID=3141#1%204.

Soytong, K. and Quimio, T. H. (1989). Antagonism of *Chaetomium globosum* to the rice blast pathogen, *Pyricularia oryzae*. Kasetsart Journal (Natural Science). 23:198-203.

Soytong, K., Charoenporn, C. and Kanokmedhakul, S. (2013). Evaluation of microbial elicitors to induce plant immunity for tomato wilt. African Journal of Microbiology Research. 7:1993-2000.

Soytong, K., Kanokmedhakul, S., Kukongviriyapan, V., Isobe, M. (2001). Application of Chaetomium species (Ketomium) as a new broad spectrum biological fungicide for plant disease control: a review article. Fungal Diversity. 7:1-15.

Tann, H. and Soytong, K. (2016). Effects of nanoparticles loaded with *Chaetomium globosum* kmitl-n0805 extracts against leaf spot of rice var. Sen Pidoa. Malaysia Jounal of Application Biology. 45:1-7.

Te Beest, D.O., Guerber, C. and Ditmore, M. (2007). Rice blast. The Plant Health Instructor. DOI: 10.1094/PHI-I-2007-0313-07. Reviewed 2012.

Thohinung, S., Kanokmedhakul, S., Kanokmedhakul, K., Kukongviriyapan, V., Tusskorn, O. and Soytong, K. (2010). Cytotoxic 10-(indol-3-yl)-[13]cytochalasans from the fungus Chaetomium elatum ChE01. Arch Pharm Res. 8:1135-41.

Nano-particles from *Chaetomium lucknowense* to inhibit rice blast pathogen causded by *Pyricularia oryzae* in pot experiment

Song, J. J. [1*], Soytong, K. [1], Kanokmedhakul, S. [2] and Kanokmedhakul, K. [2]

[1]Department of Plant Production Technology, Faculty of Agricultural Technology, King Mongkut's Institute of Technology Ladkrabang, Bangkok, Thailand; [2]Department of Chemistry, Faculty of Science, Khon Khan Unviersity, Khon Khan, Thailand.

Abstract Nano-particles derived from *Chaetomium lucknowense* proved to be antagonized *Pyricularia oryzae* causing rice blast disease var. RD57. Result showed that nano-ECL, nano-MCL and nano-HCL expressed antifungal activities against *P. oryzae* (rice blast disease) at the ED_{50} values were 82, 114, 181ppm, respectively. In pot experiment, the nano-CL gave significantly better to control rice blast than the chemical fungicide (Tricyclazole) in rice var. RD57. Rice blast disease showed that nano-CL gave the highest reduction of 54 %, when compared to the chemical fungicide that the disease decreased 29.26 %. Application of nano-CL gave the highest plant strands of 87.62 cm when compared to Tricyclazole (74.91 cm). Nano-particles from *C. lucknowense* is being developed to be nano-elicitors for plant immunity.

Keywords: Chaetomium, nano-particles, rice blast

Introduction

Oryza sativa L. recognized as Asian rice. The origins of rice are numerously debated. (Harris *et al.,* 1996) found that genetic variation had expressed to all forms of Asian rice that occurred 8,200–13,500 years ago in China. Rice was first domesticated in the region of Yangtze valley in China (Normile, 1997). There are many pathogens that infected to rice and caused the yield loss, the blast disease seems to be the most important one caussed by *Pyricularia oryzae* (perfect stage: *Magnaporthe oryzae*).

It is pathogenic to rice which highly destructive to 30% yield loss worldwide (Skamnioti and Gurr, 2009). Moreover, *P. oryzae* isolates from rice are also reported to be a host-specific (OU, 1985). *Chaetomium* spp. are reported to antogonized to many phythopathogens (Soytong *et al.,* 2001). The application of chemical fungicides for disease control has been used for years and gradually caused pollution to surrounding environment. It is recorded that

---

[*] **Corresponding Author:** Song, J. J.; **Email:** misssongjiaojiao@gmail.com

the over use of fungicides can be detrimental affected to human health (Soytong, 2001). *Chaetomium* species are unique isolated from fertile soil and animal dungs (von Arx, 1986). It is reported to control *P. oryzae* (Soytong and Quimio, 1989), *Phytophora palmivora* causing root rot of Pomelo (Hung *et al.* 2015). *Colletotrichum gloeosporioides*, *Fusarium oxysporum* f. sp. *lycopersici* (Soytong *et al.,* 2001). The objective was to evaluate the constructed nano-particles from *Chaetomium lucknowense* to control rice blast disease caused by *P. oryzae*.

Materials and methods

Pathogen, antagonists and nano-partcles preparation

Pyricularia oryzae was isolated from rice var. RD57, identified and tested pathogenicity from previous experiment used in this study. The original isolate of*Chaetomium lucknowense* used in this study is reported to produce bioactive substances to be effectice against human (Thahinung *et al.,* 2010) and phytopathogen (Charoenporn *et al*., 2011). Bioactive substances extracted from *C. lucknowense* were done by following the method of Phokerd *et al.* (2008). The bioactive compound was constructed to be nano-particles by followiong the method of Dar and Soytong, 2014).

Biological activity of nano-particles against Pyricularia oryzae

Testing biological activity was followed the method of Charoenporn *et al*. (2011). Two factors experiment were conducted with four replications, and the factor A was nano-particles derived from nano-particles derived from *C. lucknowense* (nano-HCL, nano-ECL, nano-MCL) and factor B was the concentrations of 0,1,3,5 and 10 ppm.

Evaluation of nano-particles to control rice blast in pot experiment

The 15 days of rice seedings var. RD57 were planted in sterilized clay soil in pot experiment for 15 days before treatment. Treaments were set up as follows:- treatment 1(T1) was inoculated with *P. oryzae*, treatment 2 (T2) was inoculated with *P. oryzae* and treated with nano-CL, and treatment 3 (T3) was inoculated with *P. oryzae* and treated with chemical fungicide,Tricyclazole. All treatments were done at the same manner of inoculated the pathogen through wounds, which made by sterilized syrinse at 0.5 mm. dia. One wound was

inoculated with inoculum suspension of 1 ml. Each treatment was done as mentioned above at every 15 days.

Experimental design and staistical analysis

The experiment for biological activity was set up as 3 x 5 factorial experiment in Completely Randomized Design (CRD). Colony diameter (cm) and spore number were collected and computed inhibition percentage. The effective dise (ED_{50}) was computed by probit analysis. The pot experiment was performed by using Randomized Completely Block Design (RCBD) with four repeated experiments. Disease index(DI) was scored and computed disease reduction (%), plant height(cm), plant fresh and dry weight (g) were statistical analyzed. Means in each experiment were compared by using Duncan's New Multiple Range Test (DMRT) at P=0.05 and 0.01.

Results

Efficacy of nano-particles derived from Chaetomium lucknowense against Pyricularia oryzae

Result showed that the nano-particles derived from *C. lucknowense* namely nano-HCL, nano-ECL and nano-MCL expressed biological activity against *P. oryzae* causing rice blast disease. It was significantly highest spore inhibition whren treated at the concentration of 10 ppm with nano-ECL and nano-MCL which inhibited the spore production at 81.93 and 81.80 %, respectively, and followed by nano-HCL which was 77.26 %. The ED_{50} values of nano-ECL, nano-MCL and nano-HCL actively inhibited the sporulation of *P. oryzae* at the concentration of 82, 114, 181 ppm., respectively as seen in Table 1 and Figure 1).

Evaluation of nano-particles to control rice blast in pot experiment

The nano-particles derived from*C. lucknowense* gave a good result to inhibit *P. oryzae* causing blast disease in pot experiment. The treated nano-CL gave significantly better to control rice blast disease than the chemical fungicide, Tricyclazole in rice var. RD57 after 20 days. It was not significantly differed in plant height of all treatments, when started the experiment which inoculated with *P. oryzae*, treated with nano-CL, and and treated with chemical fungicide,Tricyclazole. Plant height parameters at 20 days were 62, 65 and 62 cm., repectively. The application of nano-CL at 40 days gave the highest plant

growth of 87 cm when compared to inoculated with *P. oryzae* and treated with chemical fungicide,Tricyclazole which were 77 and 74 cm., respectively as seen in Table 2. It is noted that the rice blast disease showed the highest disease reduction of 54 % when compared to the chemical fubgicide that the disease reduction of 29.26 % (Table 2).

Table 1. Testing of nano-particles from *Chaetomium lucknowense* against *Pyricularia oryzae*

Bioactive metabolites	conc. (ppm)	colony dia. (cm)	growth inhibition,%	spores(10^5 spores/ml)	spore inhibition,%	ED_{50} (ppm)
nano-HCL	0	5.00^{a1}	-	47.63^a	-	
	1	4.88^b	$2^.50^c$	37.80^b	20.52^f	
	3	4.80^b	4.00^c	35.30^b	25.82^f	
	5	4.72^b	5.50^c	26.15^c	45.02^{de}	181
	7	4.80^b	4.00^c	20.20^{cd}	57.67^c	
	10	4.13^c	17.50^a	10.85^e	77.26^b	
nano-ECL	0	5.00^a	-	$47.63a$	-	
	1	4.90^b	2.00^c	$34.00b$	28.55^f	
	3	4.90^b	2.00^c	$27.75c$	41.75^{de}	
	5	4.80^b	4.00^c	$21.70c$	54.46^d	82
	7	4.80^b	4.00^c	$17.45d$	63.39^c	
	10	4.67^b	6.50^c	$8.60e$	81.93^a	
nano-MCL	0	5.00^a	-	47.63^a	-	
	1	4.85^b	3.00^c	37.40^b	21.48^f	
	3	4.85^b	3.00^c	31.45^b	33.81^f	
	5	4.80^b	4.00^c	22.35^c	53.05^d	114
	7	4.73^b	5.50^c	17.60^d	62.97^c	
	10	4.47^b	10.50^b	8.65^e	81.80^a	
	C.V. (%)	2.06		11.31		

[1] Means of four repeated experiment which followed by a common letter in each column were not significantly differed at DMRT = P 0.01.

Figure 1. Testing nano-particles derived from *Chaetomium lucknowense* against *Pyricularia oryzae*

Table 2. Disease reduction and plant height of rice var. RD 57 treated with nano-particles derived from *Chaetomium lucknowense*

Treatments	plant height(20 day) cm.)[1]	plant height(40 days) (cm)[1]	Disease reduction, %
inoculated *P. oryzae*	62[a]	77[b]	-
P. oryzae + **nano-CL**	65[a]	87[a]	54
P. oryzae + **Tricyclazole**	62[a]	74[b]	29
C.V. (%)	2.52	12.48	

[1] Means of four repeated experiment which followed by a common letter in each column were not significantly differed at DMRT = P 0.01.

Moreover, the further result showed that Tricyclazole gave significanlty highest fresh weight of stems which was 66 g and followed by nano-CL (55 g) when compared to inoculated control with *P. oryzae* which was 45 g as seen in Table 3. Nano-CL was significantly differed in fresh root weight of 79.14 g when compared to the inoculated control with *P. oryzae* and Tricyclazole 58 and 44 g, respectively.

Table 3. Fresh and dry weight of rice var. RD57 treated with nano-particles derived from *Chaetomium lucknowense*

Treatments	fresh weight (g)	
	stems[1]	roots[2]
inocullated control with *P. oryzae*	45c	58b
P. oryzae + **nano-CL**	55b	79a
P. oryzae + **Tricyclazole**	66a	44c
C.V. (%)	22.82	29.87

[1] Means of four repeated experiment which followed by a common letter in each column were not significanly differed at DMRT = P 0.01.

Table 4. Dry weight of stems and roots in rice var. RD 57 treated with nano-particles derived from *Chaetomium lucknowense*

Treatments	dry weight (g)	
	stems[1]	roots[2]
inoculated control with *P. oryzae*	14b	6b
P. oryzae + **nano-CL**	20a	12a
P. oryzae + **Tricyclazole**	11bc	11a
C.V. (%)	29.29	28.96

[1] Means of four repeated experiment which followed by a common letter in each column were not significantly differed at DMRT = P 0.01.

The tested nano-CL was significantly highest stem drty weight (20 g) and follwed by inoculated control with *P. oryzae*, nano-CE, Tricyclazole which were 14 and11 g., respectively. Nano-CL and Tricyclazole were not significantly differed which root dry weight were12 and 11 g respectively, when compared to the inoculated control with *P. oryzae* which was 6 g as seen in Table 4.

Discussion

Morphological study was done in previous experiment to prove identification of *P. oryzae* which cultured on Rice Flour Agar. The colony is geryish white, slow growing, septate mycelia, conidiaare pyriform shape, 3 septa in a cell, 17-23 × 8-11 micron that similar reports by Bussaban, *et al* (2005) and Wang (2016). Skamnioti *et al.* (2019) stated that the causing agent of blast disease that widely distributed and is destructive to rice production of 30% yield loss. It is interesting that Ou (1985) reported that isolate of *P. oryzae* from rice is mostly host-specific.

It was found that nano-particles derived from *C. lucknowense* gave actively inhibited the rice blast pathogen. As results, nano-ECL, nano-MCL and nano-HCL were actively against *P. oryzae* which the ED_{50} values were 82, 114, and 181ppm, rtespectively. As similar in the previous report found that that nano-particles of *C. elatum* was actively against *P. oryzae* causing rice blast (Song, *et al,* 2016). This result is similar reported by Tann and Soytong (2016) found that Nano-CGH, nano-CGE, and nano-CGM derived *Chaetomium globosum* gave antifungal activity against *Curvularia lunata* (leaf spot disease of rice var. Sen Pidoa), which the ED_{50} values of 1.21, 1.19, and 1.93 ppm/mL, respectively). It was also found in pot experiment that the nano-particles derived from *C. lucknowense* resulted to control the rice blast disease.

Application of nano-CL gave better disease control than chemical fungicide, Tricyclazole. Similar report was stated by Tann and Soytong (2016) tested in a pot experiment showed that nano-CGH, nano-CGE, and nano-CGM derived *Chaetomium globosum* resulted to decrease leaf spot of rice var. Sen Pidoa in pot experiment. Result showed that the nano-CL gave better plant strands than the inoculated control. Tann and Soytong (2016) also reported similar result that the nano-CGH, nano-CGE, and nano-CGM derived *C. globosum* significantly increased the height of the rice plant when compared to the non-treated control.

The research finding is confirmed that *C. elatum* produces bioactive metabolites against the teated pathogen, *P. oryzae* as a control mechanism and the crude extracts of *C. lucknowense* gave significantly inhibited the tested pathogen in

higher rate of application when compared to nano-particles derived from *C. lucknowense*. Similar discussion searched from Vilavong and Soytong (2017) stated that using nano-rotiorinol, dericed from *Chaetomium cupreum*, nano-trichotoxin derived from *Trichoderma harzianum* and ascospore suspension of *C. cupreum* resulted to reduce coffee anthracnose of 46.23, 42.71 and 18.59 %, respectively. It is needed to develop new approach of non-toxic agricultural inputs to be used instead of the chemical fungicides. As known, the chemical fungicides are ready recognized to cause human diseases, pollution, residue in the soil, water and agriculture products. It is proved that continuous chemical fungicide application will let the pathogen resistant to chemical fungicides (Soytong *et al,* 2001).

As result in pot experiment the tested nano-particles from *C. lucknowense* significantly controlled rice blast disease better than the chemical fungicide. Similar report from Vilavong and Soytong (2017) that bio-formulation of *C. cupreum* in powder form, nano- rotiorinol, from *C. cupreum* and nano-trichotoxin from *T. harzianum* gave a good control of coffee anthracnose.

It is concluded that *C. lucknowense* is proved to be effectively against rice blast disease caused by *P. oryzae*. Its metabolites could be inhibited the pathogen inoculum and reduced the disease incidence of rice blast. Research and development on nanotechnology for crop protection is done by construction of nano-particles from the crude extracts and pure compound of *C. lucknowense* would become a new strategy for rice disease protection. Further research finding is to develop these natural product to be used in crop production.

Acknowledgement

References

Bussaban, B., Lumyong, S., Lumyong, P., Seelanan, T., Park, D. C., McKenzie, E. H. C., Hyde, K. D. (2005). Molecular and morphological characterization of *Pyricularia* and allied genera. Mycologia. 97:1002-1011.

Charoenporn, C., Kanokmedhakul, S., Lin, F. C., Poeaim, S. and Soytong, K. (2011). Evaluation of bio-agent formulations to control Fusarium wilt of tomato. African Journal of Biotechnology. 9:5836-5844.

Dar, Joselito and Soytong, K. (2014). Construction and characterization of copolymer nanomaterials loaded with bioactive compounds from *Chaetomium* species. International Journal of Agricultural Technology. 10:823-831.

Hung, P. M., Pongnak, W., Soytong, K. and Poeaim, S. (2015). Efficacy of Chaetomium Species as Biological Control Agents against *Phytophthora nicotianae* Root Rot in Citrus. International Journal of Agricultural Technology. 10:833-844.

Normile, Dennis (1997). Yangtze seen as earliest rice site. Science. 275: 309-310.

Phonkerd, N., Kanokmedhakul, S., Kanokmedhakul, K. soytong, K., Prabpai, S. and Kongsearee, P. (2008). Bis-sprio-azaphilones and azaphilones from the fungi *Chaetomium cochliodes* Vth01 and *Ch. cochlioides* Cth05. Tetrahedron. 64:9636-9645.

Skamnioti, Par and Gurr, Sarah J. (2009). Against the grain: safeguarding rice from rice blast disease. Trends in Biotechnology. 27:141-150.

Soytong, K. and Quimio, T. (1992). Antagonism of *Chaetomium cupreum* to *Pyricularia oryzae*: A case study in biocontrol of rice blast disease. Journal of Plant Protection in the Tropics. 9:17-23.

Soytong, K. (2014). Bio-formulation of *Chaetomium cochliodes* for controlling brown leaf spot of rice. International Journal of Agricultural Technology. 10:321-337.

Soytong, K., Kanokmedhakul, S., Kukongviriyapan, V. and Isobe, M. (2001). Application of *Chaetomium* species (Ketomium) as a new broad spectrum biological fungicide for plant disease control: A review article. Fugal Diversity. 7:1-15.

Tann, H. and Soytong, K. (2016). Effects of nanoparticles loaded with *Chaetomium globosum* KMITL-N0805 extracts against leaf spot of rice var. Sen Pidoa. Malaysian Applied Biology Journal. 45:1-7.

Ou, S. H. (1985). Rice diseases. CAB International; Wallingford, UK.

Vilavong, S. and Soytong, K. (2017). Application of A New Bio-Formulation of *Chaetomium cupreum* For Biocontrol of *Colletotrichum gloeosporioides* Causing Coffee Anthracnose on Arabica Variety in Laos   Agrivita 39.

Von Arx, J. A., Guarro J. and Figueras, M. J. (1986). The Ascomycete Genus *Chaetomium*. Nova Hedwigia Beihefte, Lubrecht & Cramer Ltd.

Wang, X. W. (2016) Diversity and taxonomy of *Chaetomium* and chaetomium-like fungi from indoor environments. State Key Laboratory of Mycology, Institute of Microbiology, Chinese Academy of Sciences. 84:145-224.

Nano-particles derived from *Chaetomium elatum* against Phytophthora rot of durian

Thongkham, D.[1*], Soytong, K.[1], Kanokmedhakul, S.[2] and Kanokmedhakul, K.[2]

[1]Department of Plant Production Technology, Faculty of Agricultural Technology, King Mongkut's Institute of Technology Ladkrabang, Bangkok, Thailand; [2]Department of Chemistry and Center for Innovation in Chemistry, Faculty of Science, Khon Kaen University, Khon Kaen, Thailand.

Abstract Durian are the economically fruit trees in Thailand. The important problem of durian is root rot disease caused by *Phytophthora palmivora*. This study was used *Chaetomium elatum* to control the *P. palmivora* causing root rot disease of durian by dual culture method, crude extract test and nano particles test derived from *Ch. elatum*. Dual-culture test showed that *Ch. elatum* gave efficiency to inhibit of spore and colony growth of *P. palmivora* which were 46.13 and 38.89%, respectively. Testing efficacy of crude extract from *Ch. elatum* to control *P. palmivora* found that crude ethyl acetate from *Ch. elatum* gave significantly highest against pathogen of *P. palmivora* at the concentration of 1000 ppm which the ED_{50} of 175.31 ppm. Nano particles testing, nano particles of crude hexane, ethyl acetate and methanol from *Ch. elatum* showed the ED_{50} values of 3.49, 3.47 and 3.41 ppm.

Keywords: *Chaetomium elatum*, *Phytophthora palmivora*, durian

Introduction

Durian(Durio zibethinus Murr.) is king of tropical fruit refer to two facts of the fruit. Its superlative fresh, which is highly nutritional and its appearance, which resembles the thorny thrones of the Asian kings of old. Durian is one of the most famous fruit in South-East Asia. The fruit is very famous not only due to the taste richness but also the strong odour. Durian is an economically fruits in Thailand. The country is the world's largest producer and exporter of durian, followed by Malaysia and Indonesia (Somsri, 2014). In past, root rot has been reported to the serious rate of infection of durian because monoculture planting and high fertilizer applications could lead the increment of disease incidence caused by fungi such as *P. palmivora* and *Pythium* spp. Chemical compounds

---

[*] **Coressponding Author**: Thongkham, D.; **Email** : Danupatbb_2538@hotmail.com

have been used to control plant diseases, but abuse in their employment has favored the development of pathogens resistant to fungicides. The objective was to use of Chaetomium elatum that antagonize plant pathogens is risk-free when it results in enhancement of resident antagonists. Moreover, biological control agents (BCAs) could reduce levels of fungicide.

Materials and methods

Morphological Studies

Soil samples were collected plant disease. Soil samples were isolated by using soil plate method on glucose-ammonium nitrate agar media(GANA) and incubated at 28-30°C for 2 days, then the fungal growing mycelium tip of it was sub-cultured and purified in potato dextrose agar (PDA) until get the pure culture.

The macroscopic characteristics of colony appearance were determined including growth pattern and texture and growth rate onto PDA plates. For microscopic characteristics shapes of zoosporangia were observed by using a light microscope.

Pathogenicity Test

Pathogenicity test was done by agar plug method. The healthy durian detached leaves were sterilized by 10% sodium hypochlorite. The surface detached leaves were made wounds by sterilized needle. The agar plug of pathogen inoculated to wound on detached leaves. The controls were processed similarly but transferred an agar plug without the pathogen.

Bi-culture test

The experiment was conducted using a Completely Randomized Design (CRD) with 4 replications. The antagonistic fungi and pathogen were separately cultured on PDA at room temperature for 7 day. A 0.5 cm diameter sterilized cork borer was used to remove agar plugs from the actively growing edge of cultures of the pathogenic and antagonistic fungi and transferred onto 9 cm diameter PDA plates, an agar plug of the pathogen was placed on one side of the plate which opposited an agar plug of an antagonistic fungus. PDA plates were transferred with a single plug of an antagonistic fungus or of the pathogen acted as the controls. The bi-culture plates were incubated at room temperature for 30 days. Data were collected regarding colony diameter (cm) and the number of conidia reduced by the pathogen.

Crude extract test

The experiment was conducted by using factorials in Completely Randomized Design (CRD) with four replications. Each crude extract was dissolved in 2% dimethyl sulfoxide and added to PDA before autoclaving at 121 ℃ (15 psi) for 30 minutes. The agar plug of pathogen was transferred to the middle of PDA plates (amending with each crude extracts) in each concentration(0, 10, 50, 100, 500, 1000 ppm) and incubated at room temperature until the pathogen on the control plates growing full. Data were collected as colony diameter, Percentage inhibition of pathogen colony growth and conidia and The effective dose (ED_{50}). Data was statistically computed analysis of variance. Treatment means were compared with DMRT at P=0.05.

Testing nano-particles from Ch. elatum

Preparation of nano particles derived from *Ch.elatum* were used the method of Dar and Soytong (2014). Testing for inhibition of mycelial growth and sporangium formation of *P. palmivora* was done by using poison food method.The Experiment was conducted by using factorials in CRD with four replications. The concentration of nano particles; nano-CEH, nano-CEE, nano-CEM were as follows: 0, 3, 5, 10 and 15 ppm. Each concentration was dissolved in 2% dimethyl sulfoxide, then mixed into potato dextose agar(PDA) and added chitosan before autoclave at 121 ℃ for 30 minutes. The agar plug of pathogen was removed to PDA plates in each solvent and concentration. After incubated at room temperature until the pathogen on the control plates growing full collected data as colony diameter, number of sporangia, inhibition percentage and Effective dose ED_{50}. Data was statistically computed analysis of variance. Treatment means were compared with DMRT at P=0.05.

Results

Morphological Studies of P. palmivora

The fungal growth rapidly and colonized the plate within 4 days on PDA. Colony morphology on PDA is a chrysanthemum pattern with aerial mycelium. Sporangia are globose and ovoid shape, which was papillate. Zoospores were directly released from sporangia when flooded in water (Fig.1).

Pathogenicity test

Pathogenicity test on detached leaves after 3 days by the plug inoculation method. Leaves showed symptoms of brown hydrolysis expand around agar plug of pathogen. In control, Leaves remained healthy (Fig.2).
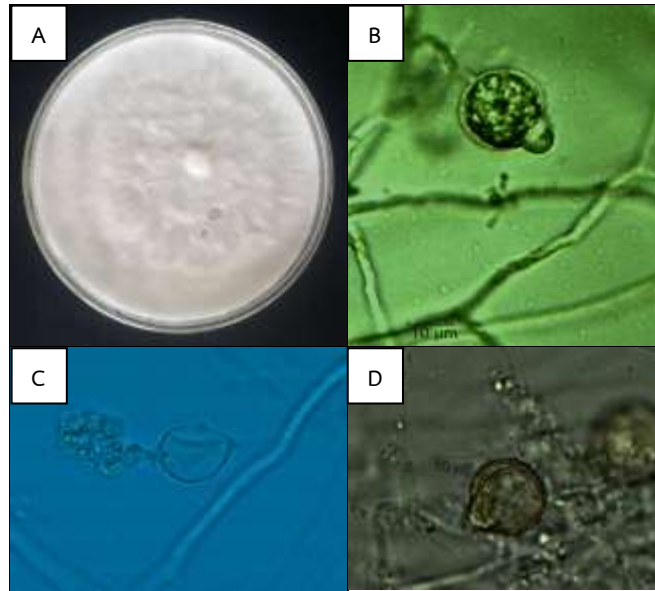
Figure 1. Morphological characteristics of *P. pamivora* (A); Colony appearance on PDA (B); Shape of sporangia (C); Zoospore release from sporangia (D); Oogonia

Figure 2. Pathogenicity test of *P. palmivora* on detached leaves. (A); The inoculated pathogen (B); The non - inoculated pathogen

Bi-culture test

    Ch.elatum was proved its abilities to inhibit the growth of *P. palmivora* by using bi-culture test (Fig.3).The result showed that *Ch. elatum* inhibited colony growth and production of spore by *P. palmivora* of 38.89 and 46.13% inhibition, respectively (Table 1).

Table 1. Colony and spore inhibition of *P. palmivora*

| Antagonist fungi | *P. palmivora* | |
	Colony inhibition (%)	spore inhibition (%)[2,3]
Ch. elatum	38.89	46.13
C.V. (%)	1.05	

Ch. elatum *P. palmivora* *P. palmivora*
+ *Ch. elatum*
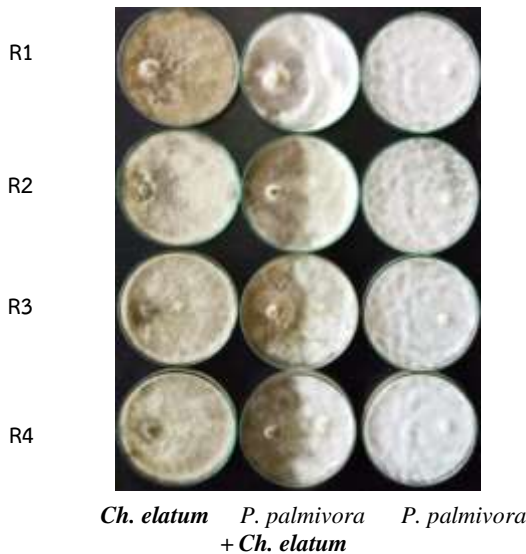
Figure 3. *Ch. elatum* inhibited colony growth of *P. palmivora* by using bi-culture test

Crude extract test

Crude-CEH at concentrations of 10, 50, 100, 500 and 1000 ppm were tested the colony growth inhibition of *P. palmivora* which were 19.25, 39.25, 46.5, 58.00 and 58.5% respectively (Fig 4). Test inhibition of sporangia information of *P. palmivora* which were 13.46, 25.88, 38.30, 53.86 and 62.73% respectively (Table 2) when compared to the control. Crude-CEE at concentrations of 10, 50, 100, 500 and 1000 ppm were tested the colony growth inhibition of *P. palmivora* which were 37.5, 39.75, 45.75, 60.5 and 76.5% respectively (Fig 4). Test inhibition of sporangia information of *P. palmivora* which were 20.04, 30.68, 39.87, 56.47 and 80.79% respectively (Table 2) when compared to the control. Crude-CEM at concentrations of 10, 50, 100, 500 and 1000 ppm were tested the colony growth inhibition of *P. palmivora* which were 12.25, 30.75, 45.25, 45.75 and 51.00% respectively (Fig 4). Test inhibition of sporangia information of *P. palmivora* which were 14.09, 20.45, 31.41, 43.73 and 54.69% respectively (Table 2) when compared to the control. Meanwhile

ED$_{50}$ values of crude-CEH, CEE, CEM were 341.97, 175.31 and 58.96 µg/ml respectively.

Nano-particles test

Nano-CEH at concentrations of 3, 5, 10, 15 ppm were tested the colony growth inhibition of *P. palmivora* which were 31.25, 38.25, 38.75 and 58.5% respectively (Fig 5). Test inhibition of sporangia information of *P. palmivora* which were 26.15, 40.94, 51.60 and 76.65% respectively (Table 3) when compared to the control. Nano-CEE at concentrations of 3, 5, 10, 15 ppm were tested the colony growth inhibition of *P. palmivora* which were 2.5, 19.75, 28.5 and 37.75% respectively (Fig 5). Test inhibition of sporangia information of *P. palmivora* which were 20.22, 28.47, 42.55 and 62.77% respectively (Table 3) when compared to the control. Nano-CEM at concentrations of 3, 5, 10, 15 ppm were tested the colony growth inhibition of *P. palmivora* which were 14.00, 23.75, 36.5 and 40.75% respectively (Fig 5). Test inhibition of sporangia information of *P. palmivora* which were 12.77, 31.48, 52.21 and 61.46% respectively (Table 3) when compared to the control. Meanwhile ED$_{50}$ values of nano-CEH, CEE, CEM were 3.49, 3.47 and 3.81 µg/ml respectively (Table 3).

Table 2. Effect of crude extracts from *Ch. elatum* to inhibit *P. palmivora*

Nano particles	Concentration (ppm)	Colony diameter (cm)	Inhibition of colony growth (%)	Number of sporangia ($\times 10^6$)	Inhibition of sporangia (%)	ED$_{50}$ (µg/ml)
Crude CEH	0	5.00[a]	0[i]	59.87[a]	0[h]	341.97
	10	4.03[c]	19.25[g]	51.81[b]	13.46[g]	
	50	3.03[e]	39.25[e]	44.37[cd]	25.88[fe]	
	100	2.67[g]	46.5[d]	36.93[e]	38.30[d]	
	500	2.1[h]	58.00[b]	27.62[f]	53.86[c]	
	1000	2.02[h]	58.5[b]	22.31[g]	62.73[b]	
Crude CEE	0	5.00[a]	0[i]	59.87[a]	0[h]	175.31
	10	3.12[e]	37.5[e]	47.87[c]	20.04[f]	
	50	3.01[e]	39.75[e]	41.5[d]	30.68[e]	
	100	2.71[f]	45.75[d]	36.00[e]	39.87[d]	
	500	1.97[h]	60.5[b]	26.06[f]	56.47[c]	
	1000	1.17[i]	76.5[a]	11.5[h]	80.79[a]	
Crude CEM	0	5.00[a]	0[i]	59.87[a]	0[h]	58.96
	10	4.38[b]	12.25[h]	51.43[b]	14.09[g]	
	50	3.46[d]	30.75[f]	47.62[c]	20.45[f]	
	100	2.73[f]	45.25[d]	41.06[d]	31.41[e]	
	500	2.71[f]	45.75[d]	33.68[f]	43.73[d]	
	1000	2.45[h]	51.00[c]	27.12[f]	54.69[c]	
C.V.(%)		4.16		5.93		

2120
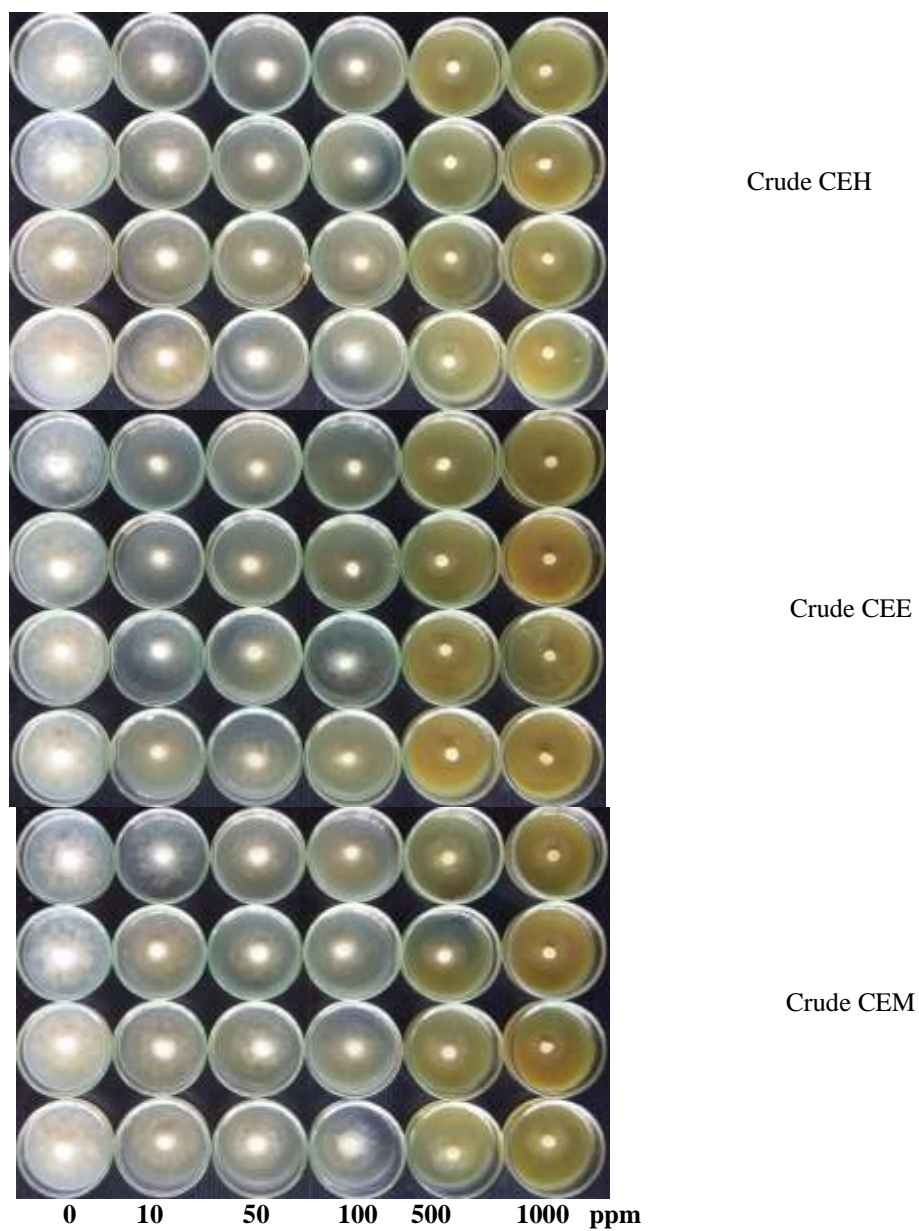
Figure 4. Testing crude extracts from *Ch. elatum* against *P. palmivora*
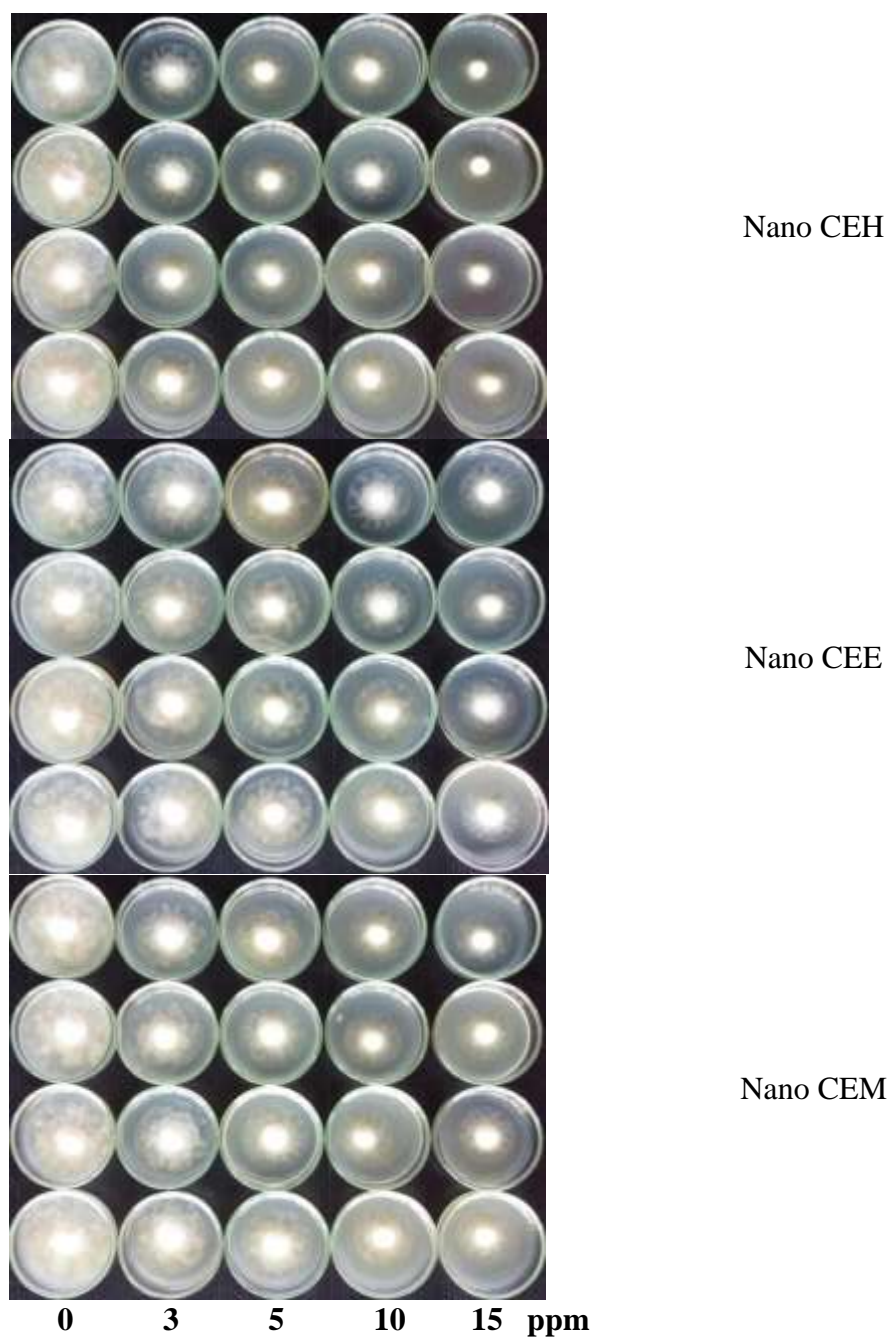
0   3   5   10   15   ppm

Figure 5. Testing nano particles from *Ch. elatum* against *P. palmivora*

Table 3. Effect of nano particles from *Ch. elatum* to inhibit *P. palmivora*

Nano particle	Concentration (ppm)	Colony diameter (cm)	Inhibition of colony growth (%)	Number of sporangia ($\times 10^6$)	Inhibition of sporangia (%)	ED_{50} ($\mu g/ml$)
Nano CEH	0	5.00^a	0^i	62.12^a	0^h	3.49
	3	3.43^f	31.25^d	45.87^d	26.15^e	
	5	3.08^g	38.25^c	36.68^e	40.94^d	
	10	3.06^{gh}	38.75^{cb}	30.06^f	51.60^c	
	15	2.07^i	58.5^a	14.5^h	76.65^a	
Nano CEE	0	5.00^a	0^i	62.12^a	0^h	3.47
	3	4.87^a	2.5^i	49.56^c	20.22^f	
	5	4.01^c	19.75^g	44.43^d	28.47^e	
	10	3.57^e	28.5^e	35.68^e	42.55^d	
	15	3.11^g	37.75^c	23.12^g	62.77^b	
Nano CEM	0	5.00^a	0^i	62.12^a	0^h	3.81
	3	4.3^b	14.00^h	54.18^b	12.77^g	
	5	3.81^d	23.75^f	42.56^d	31.48^e	
	10	3.17^g	36.5^c	29.68^f	52.21^c	
	15	2.96^h	40.75^b	23.93^g	61.46^b	
C.V.(%)		4.79		6.68		

Average of four replications. Means followed by a common letter are not significantly different by DMRT at P = 0.05

Discusion

The bi-culture tests *Ch. elatum* gave significantly inhibition colony growth of *P.palmivora* and production of spore by P. palmivora of 38.89 and 46.13%, respectively. Similar reported by Tathan (2012) *Ch. elatum* gave significantly inhibition colony growth of *P.palmivora* and production of spore by *P. palmivora* of 32.49 and 26.23%, respectively. The crude extracts of *Ch. elatum* gave significantly highest inhibited sporangia production of *P. palmivora* at concentration of 1,000 ppm. Meanwhile ED_{50} values of Crude-CEE was 175.31 μg/ml. Similar reported by Soythong (2015) that crude extract of *Ch. elatum* gave significantly highest inhibited *Fusarium oxysporum* f.sp. *lycopersici* causing wilt of tomato at concentration of 1,000 ppm with the ED_{50} value of 5.94 μg/ml. The nano particle of *Ch. elatum* gave significantly highest inhibited sporangia production of *P. palmivora* at concentration of 15 ppm. Meanwhile ED_{50} values of Crude-CEH was 3.49 μg/ml. Similar reported by Song and Soytong (2016) that nano particle of *Ch. elatum* gave significantly highest inhibited *Pyricularia oryzae* causing blast of rice at concentration of 15 ppm.

Acknowledgement

References

Joselito, D. and Soytong, K. (2014). Construction and characterization of copolymer nanomaterials loaded with bioactive compounds from *Chaetomium* species. Journal of Agricultural Technology.10:823-831.

Somsri, S. (2014). Current status of durian breeding program in Thailand. Acta Hortic. 1024: 51-60.

Song J. J. and Soytong K. (2016). Antifungal activity of *Chaetomium   elatum* against *Pyricularia oryze* causing rice blast. International Journal of Agricultural Technology. 12:1437-1447.

Soytong K., 2015. Testing bioformulation of *Chaetomium elatum* ChE01 to control Fusarium wilt of tomato. Journal of Agricultural Technology. 11:996-9752015.

Tathan, S., Sibounnavong, P., Sibounnavong, P. S., Soytong, K. and To-anun, C. (2012). Biological metabolites from Chaetomium spp to inhibit Drechslera oryzae causing leaf spot of rice. Jornal of Agricultural Technology. 8:1691-1701.

Nano-particles from *Chaetomium brasiliense* to control *Phytophthora palmivora* caused root rot disease in durian var Montong

Tongon, R.[*1]**, Soytong, K.**[1]**, Kanokmedhakul, S.**[2]** and Kanokmedhakul, K.**[2]

[1]Department of Plant Production Technology, Faculty of Agricultural Technology, King Mongkut's Institute of Technology Ladkrabang, Bangkok, Thailand; [2]Department of Chemistry and Center for Innovation in Chemistry, Faculty of Science, Khon Kaen University, Khon Kaen, Thailand.

Abstract The antagonistic fungus, *Chaetomium brasiliense* was tested to control *Phytophthora palmivora* causing rot disease of Durian (*Durio zibithenus* L.) var Montong by crude extracts and Nano-particles derived from *Ch. brasiliense*. Crude extracts of antagonistic fungus was tested for antifungal biological activities. The crude extracts from antagonistic fungus with hexane, ethyl acetate and methanol were tested against *P. palmivora*. Crude ethyl acetate from *Ch. brasiliense* gave significantly against *P. palmivora* which the ED_{50} values was 17.46 μg/ml. Testing Nano-particles were tested for antifungal activities. The results showed nano - particles from *Ch. brasiliense* gave effectively significantly inhibition of colony growth and spore production which the ED_{50} values were 1.08 μg/ml, and 8.68 μg/ml respectively. Application of Nano - particles to control the *P. palmivora* causing root rot disease of durian in pot experiment was successfully done. The results showed nano-particles from *Ch. brasiliense* reduced the root rot disease on durain of 40%. The nano–particles from *Ch. brasilense* gave significiantly high plant growth which were 79.5 cm when compared to the non-trated control.

Keywords: Nano-particles, *Chaetomium brasiliense*, *Phytophthora palmivora*, biological control

Introduction

Durian (*Durio zibithenus* L) is originated from the region of Borneo and Sumatra, growing wild in the Malay peninsula, cultivated in a wide region from India to New Guinea four hundred years ago. It was across to Myanmar, and cultivated throug Thailand and South Vietnam (Morton, 2000). The problem for durian cultivation in Thailand faced the root rot which caused by *Phytophthora* spp. It can infect all stages of growing durian trees. The symptoms are appeared as root rot, leaves and stem blight, bark and fruit rot. Chemical fungicides have

---

been used to control this disease and trened to lead the negative side effect to the environment. In addition, Phytophthora spp become resistant to those fungicide application eg. metalaxyl and related compounds (Erwin and Ribeiro, 1996). Tye eco-friendly management of *Phytophthora* diseases would be done to reduce the application cost. The application of biocontrol agents against *Phytophthora* rot has become an importance research aspect and is being carried out all over the world (Naqvi, 2004).

Biological control of plant pathogen is known as using antagonists against plant pathogens. The antagonism is the control mechanism to reduce the pathogen onocullum and disease incidence. Antagonism is expressed betweeb two organisms including antibiosis, competition and parasitism (Cook and Baker, 1983). However, thereare many reports indicated that the antagonists can express to against seversal plant pathogens eg such as *Chaetomium* spp; *and Emericella nidulans*. (Xu *et al.,* 2017; Hung, *et al.,* 2015a; Arjona-Girona *et al.,* 2018; Tran *et al.,* 2007; Song *et al.,* 2017).

The objective was to test the nano-particles derived from *Ch. brasiliense* to inhibit *Phytophthora* sp causing root rot in durian var Montong.

Materials and methods

Isolation of pathogen and testing pathogenicity

Phytophthora sp was isolated the durian diseased plant parts eg bark and root rot using tissue transplanting method. The collected diseased samples were washed with sterilized water, and and cut it into small pieces, soaked 1% clorox for 3 min. The piece samples of diseased part was moved to water agar (WA), then incubated at room temperature to observe growing colonies, them gentle moved to PDA to get pure culture. Morphology was identified and observed the characters of fungus under compound microscope. The pathogenicity was tested using detached leaves technique. The agar plugs of *Phytophthora* sp were transferred to wounded leaves. The non -inoculated leaves with steriled agar discs was done to serve as controls, and incubated at room temperature (27-30 ℃) for seven days. The experiment was replicated four times. Disease incidence was calculated as number of infected plants/ total number of tested plants x 100, and disease ratings was evaluated as 0= healthy plants, and 3= seriously infected plants (Soytong, 2010).

Morphological study of Chaetomium brasilense

Chaetomium brasilense used in this reserch study is offered from Assoc. Prof. Dr. Kasem Soytong, Department of Plant Production Technology, Faculty

of Agricultural Technlogy, King Monkut's Institute of Technology Ladkrabang (KMITL), Bangkok, Thailand. The culture was grown on patotao dextrose agar and observed morphological characters under compound microscope.

Dual culture test

The experimental design was used as Completely Randomization with four replications. Dual culture was done by followed the methods of Soytong (1992). *Ch. brasilense* and *Phytophthora* sp. were separately cultured on PDA at room temperature (27-30 ℃) for seven days. The 0.5 cm diameter of sterilized cork borer was cut at the peripheral colony in each culture and moved to PDA plates (9 cm). The agar plug of *Phytophthora* sp. was moved to PDA plate on one side of the plate that opposited the agar plug of *Ch. brasilense*. The plug of each fungus was transferred to PDA plate served as the controls. All plates were incubated at room temperature for 30 days. Colony diameter (cm) and conidia production in the dual culture plates and control plates were recorded. The number of conidia was counted by using haemacytometer.

The inhibition of colony growth or conidia production were calculated using the following formula:

$$\% \text{ inhibition} = (A\text{-}B) / A \times 100$$

Where, A was the colony diameter or number of conidia produced by the pathogen on the control plates and B was the colony diameter or number of conidia produced by the pathogen in the dual culture plate.

Testing crude extracts of Chaetomium brasilense to against Phytophthora spp in vitro

Crude extracts of *Ch. brasilense* were evaluated to inhibit *Phytophthora* sp. The experimental design was conducted using factorial experiment in Completely Randomization, and repeated four times. Factor A was crude hexane, crude ethyl acetate and crude methanol. Factor B was 0, 10, 50, 100, 500, and 1,000 μg/ml. Each crude extract was poured to 2% dimethyl sulphite and mixed to 30 ml potato dextrose agar, then autoclaved at 121 ℃,15 lbs/inch^2 for 35 minutes. *Phytophthora* sp colony was cut at peripheral colony with sterilized cock borer (0.5 mm). Agar plug of pathogen was transferred to the middle of PDA media in plate incorporated with each and incubated at room temperature (27-30 ℃) until the pathogen growing full plate. Data were recorded as colony diameter, number of conidia. The pathogen colony growth and conidia production were calculated the inhibition using the above formula. Data were statistically computed analysis of variance. Means were compared using Duncan Multiple's Range Test. The effective dose was computed using probit analysis.

In vitro testing nano-particles from Chaetomium brasilense to control root rot disease in durian var Montong

   Chaetomium brasilense was cultured in potato dextrose broth (PDB) at room temperature (27-30 C) for 30 days. The biomass was filtered through cheesecloth and air-dried. Fresh and dried biomass were weighted. The biomass was ground in electrical blender, then extracted by adding the same volume of hexane, and kept in stationary phase for 7 days at room temperature. The filtrate was get it through Whatman filter paper, evaporated in rotary vacuum evaporator to yield crude hexane. The remaining marc was consecutively extracted with ethyl acetate and methanol to get crude extracts using the same procedure as hexane to yield crude ethyl acetate (EtOAc) and crude methanol (MeOH). The nano- particles were done by followed the method of Dar and Soytong (2014), to yield Nano-CBH, Nano-CBE and Nano-CBM. Those nano-particles were evaluated to inhibit *Phytophthora* sp. The experimental design was used two factors factorial experiment in Completely Randomization. The experiment was repeated four times. Factor A was Nano-CBH, Nano-CBE and Nano- CBM. Factor B was 0, 1, 5 and 10 µg/ml. Each Nano-particle was dissolved in 2% dimethyl sulfoxide, and mixed to PDA before autoclaved at 121°C,15 lbs/inch^2 for 30 min. The culture of *Phytophthora* sp was cut at peripheral colony with sterilized cock borer (0.5 mm). Agar plug of *Phytophthora* sp was moved to the middle of PDA mixed with each nano-particles. All plates were incubated at room temperature until the pathogen in control growing full plate. The pathogen from each treatment were observed abnormal spores under compound microscope. Data were stistaically computed. The effective dose was calculated using probit analysis.

Results

Pathogenicity test

   Pathogenicity test was conducted by detached leaves method which resulted durian leave var Montong showed brown hydrolysis expand around agar plug of pathogen. In control, leaves remained healthy as seen in Fig.1.

Dual culture test

   Ch. brasiliense was proved it ability to inhibit plant pathogen *P. palmivora* causing disease of durian by using dual culture tests. The results showed that *Ch. brasiliense* gave significantly growth inhibition of *P. palmivora* which were 58.33% and showed significantly inhibited the spore production of pathogen of 88.82% (Table 1).

Figure1. Pathogenicity test of Phytophthora sp on Durian leaves

Testing crude extracts of Chaetomium brasilense to against Phytophthora spp in vitro

The crude extracts from *Ch. brasiliense* were used to test their abilities to control the growth of *P. palmivora*. The results showed that crude ethyl acetate (EtOAc) extract gave highest inhibition of *P. palmivora* colony growth which was 57.75% at the concentration of 1,000 μg/ml with the ED_{50} values of 204.28 μg/ml when compared to the control. Crude hexane and crude ethyl acetate (EtOAc) extract and showed significantly highest inhibition for the spore production of *P. palmivora* as 100% at the concentration of 1,000 μg/ml. Crude methanol extract gave the best to inhibit the trsed pathogen wghivh the ED50 was 5.94 ppm, and followed by crude ethyl acetate and crude hexane extracts which the ED50 values were 17.46 and 28.56 μg/ml., respectively (Table 2).

Table 1. Colony growth and number of spore on antagonistic dual-culture tests

Antaginistic fungi	P. palmivora			
	Colony diameter (cm)	Growth inhibition (%)	Spore number (10^4/ml)	Spore inhibition (%)
Control	9.00[a1]	-	27.43[a]	-
Ch. brasiliense	3.75[b]	58.33[b]	5.31[b]	88.82[a]
C.V. (%)	7.90		19.39	

[1] Means of four repeated experiments. Means followed by the same letters are not significantly differed by DMRT at P=0.01.

In vitro testing nano-particles from Chaetomium brasilense to control Phytohthora sp causing durian rot var Montong

Result from nano-particles showed high efficacy antifungal activity of nanoparticles from *Ch. brasilense* against *P. palmivora* The result of Nano particles from *Ch. brasilense* was showed that Nano-CBH, Nano-CBE and Nano-CBM gave highly significant inhibited the colony growth of *P. palmivora* as 90.00% which the ED_{50} values of 1.25, 1.12, 1.08 μg/ml., respectively and gave highly significant inhibition for the spore production of *P. palmivora* as 100% which the ED_{50} values of 8.68, 12.20 and 10.77ppm (Table 3).

Table 2. Crude extracts of *Ch. brasilense* testing for growth inhibition of *P. palmivora*

Crude extracts	Concentration (ppm)	Colony diameter (cm)[/1]	Growth Inhibition(%)	ED$_{50}$ (µg/ml)	Number of spores (10^7)	Inhibition (%)	ED$_{50}$ (µg/ml)
Hexane	0	5.00^a	-		1.475^a	-	
	10	5.00^a	0.00^g		0.49^{bc}	63.19^{de}	
	50	5.00^a	0.00^g	770.60	0.53^{bc}	63.87^{de}	28.56
	100	5.00^a	0.00^g		0.39^{cd}	72.13^{cde}	
	500	3.29^c	34.00^e		0.17^{efg}	87.90^{abc}	
	1000	2.02^e	57.75^c		0.00^g	100^a	
Ethyl Acetate	0	5.00^a	-		1.475^a	-	
	10	5.00^a	0.00^g		0.63^b	55.85^e	
	50	5.00^a	20.00^f	204.28	0.32^{cde}	78.17^{bcd}	17.46
	100	3.37^e	32.5^e		0.31^{cde}	78.29^{bcd}	
	500	1.25^f	75.00^b		0.00^g	100^a	
	1000	0.86^g	82.75^a		0.00^g	100^a	
Methanol	0	5.00^a	-		1.475^a	-	
	10	5.00^a	0.00^g		0.48^{bc}	65.88^{de}	
	50	5.00^a	0.00^g	-	0.39^{cd}	71.85^{bcd}	5.93
	100	5.00^a	0.00^g		0.23^{efg}	83.51^{bcd}	
	500	4.12^b	17.5^f		0.13^{efg}	91.40^{ab}	
	1000	2.65^d	47.00^d		0.02^{fg}	97.91^a	
C.V. (%)		3.96			29.34		

[1] Means of four repeated experiments. Means followed by the same letters are not significantly differed by DMRT at P=0.01.

Table 3. Nano particle extracts of *Ch. brasilense* testing for growth inhibition of *P. palmivora*

Nano particles	Concentration (ppm)	Colony diameter (cm)[/1]	Growth inhibition (%)	ED$_{50}$ (µg/ml)	Number of spores (10^7)	Inhibition (%)	ED$_{50}$ (µg/ml)
Nano-CBH	0	5.00^a	-		0.56^a	-	
	1	2.75^b	45.00^e		0.22^b	57.45^b	
	3	1.41^e	71.75^{cd}	1.25	0.00^c	100^a	8.68
	5	1.35^{ef}	73.00^{cd}		0.00^c	100^a	
	7	1.11^g	77.75^{bc}		0.00^c	100^a	
	10	0.5^h	90.00^a		0.00^c	100^a	
Nano-CBE	0	5.00^a	-		0.56^a	-	
	1	2.60^{bc}	47.50^e		0.32^b	36.67^c	
	3	1.67^d	66.50^d	1.12	0.00^c	100^a	12.20
	5	1.00^g	80.00^b		0.00^c	100^a	
	7	1.17^{fg}	76.50^{bc}		0.00^c	100^a	
	10	0.5^h	90.00^a		0.00^c	100^a	
Nano-CBM	0	5.00^a	-		0.56^a	-	
	1	2.50^c	50.00^e		0.28^b	47.95^{bc}	
	3	1.52^{de}	69.50^d	1.08	0.00^c	100^a	10.77
	5	1.12^{fg}	77.50^{bc}		0.00^c	100^a	
	7	0.5^h	90.00^a		0.00^c	100^a	
	10	0.5^h	90.00^a		0.00^c	100^a	
C.V. (%)		8.74			51.16		

[1] Means of four repeated experiments. Means followed by the same letters are not significantly differed by DMRT at P=0.01.

Discussion

Morphological study was done in previous experiment to prove identification of *P. palmivora* which cultured on potato dextrose agar. The colony is white, slow growing, non septate mycelia, sporangia produce readily and abundantly. The identity in morphological characteristics are consistent with descriptions of *Phytophthora palmivora* (Erwin and Ribiero, 1996).

The results showed that crude ethyl acetate (EtOAc) extract from *Ch. brasilense* gave highest inhibition of *P. palmivora* colony growth which was 57.75% at the concentration of 1,000 μg/ml with the ED_{50} values of 204.28 ppm when compared to the control. As similar in the previous report, found that crude extract of *Ch. globosum* CG05, *Ch. cupreum* CC3003, *Ch. lucknowense* CL01 showed ability to inhibit mycelial growth and spore production of *P. palmivora* PHY02 in laboratoty test (Hung *et al.,* 2015b). This result is also similar reported by Hung *et al.,* (2015a) found that crude extracts of these *Chaetomium* species exhibited antifungal activities against mycelial growth of *P. nicotianae*, with effective doses of 2.6~101.4 μg/ml.

It was found that nano-particles derived from *Ch. brasilense* was actively inhibited the *P. palmivora*. Nano-CBH, Nano-CBE and Nano-CBM gave highly significant inhibition of the colony growth of *P. palmivora* at 90.00% and gave highly significant inhibition for the spore production of *P. palmivora* at 100%. This result is similar reported by Thongkham (*et al.,* 2017) found that nano-particles derived from *Ch. cupreum* to inhibit mycelial growth and spore production of *Phytophthora* spp causing root rot in durian. This study was also similar to Dar *et al*. (2013) that nano particles of *Ch. globosum* and *Ch. cuperum* were proved to againt *F. oxysporum* f.sp. *lycopersici* and *Colletotrichum capsici*.

Acknowledgement

References

Arjona-Girona, I. and López-Herrera, C. J., (2018). Study of a new biocontrol fungal agent for avocado white root rot. Biological Control. 117:6-12.

Cook, R. J. and Baker, K. F. (1983). The nature and practice of biological control of plant pathogen. American Phyto pathological Society, St. Paul, MN. 539.

Dar, J. and Soytong, K. (2014) Construction and characterization of copolymer nanomaterials loaded with bioactive compounds from *Chaetomium* species. Journal of Agricultural Technology. 10:823-831.

Dar, J. and Soytong, K. (2013). In-vitro testing of nanomaterials containing globosum ethyl acetate extract against *Fusariumoxysporum* f. sp. *lycopersici* (race 2). International Conference on Integration of Science and Technology for Sustainable Development 2013, KMITL, Bangkok, Thailand November 28-29, 2013. pp. 5.

Erwin, D. C. and Ribeiro, O. K. (1996). Phytophthora diseases worldwide. St. Paul: APS Press.

Hung, P. M., Wattanachai, P., Kasem, S. and Poeaim, S. (2015a). Efficacy of Chaetomium species as biological control agents against Phytophthora nicotianae root rot in citrus. Mycobiology. 43:288-296.

Hung, P.M., Wattanachai, P., Kasem, S. and Poaim, S. (2015b). Biological control of *Phytophthora palmivora* causing root rot of pomelo using *Chaetomium* spp. Mycobiology. 43:63-70.

Morton, J. F. (200). Fruits of warm climates. Echo Point Books and Media. Brattleboro, United States. pp. 505.

Naqvi, S. A. (2004). Diagnosis and management of certain important fungal diseases of citrus. In: Naqvi SA, editor. Diseases of fruits and vegetables. Dordrecht: Kluwer Academic Publishers. pp. 247-290.

Song, J., Soytong, K. and Kanokmedhakul, S., (2017). Antifungal activity of *Emericella nidulans* against *Pyricularia oryzae* causing rice blast. Journal of Agricultural Technology. 13:1205-1209.

Soytong, K. (2010). Evaluation of Chaetomium-biological fungicide to control Phytophthora stem and root rot of durian. Research Journal. 3:117-124.

Thongkham, D., Soytong, K. and Kanokmedhakul, S. (2017). Efficacy of nano particles from *Chaetomium cupreum* to control *Phytophthora* spp. causing root rot of durian. Journal of Agricultural Technology. 13:1295-1300.

Tran, H., Ficke, A., Asiimwe, T., Höfte, M. and Raaijmakers, J. M. (2007). Role of the cyclic lipopeptide massetolide A in biological control of Phytophthora infestans and in colonization of tomato plants by Pseudomonas fluorescens. New Phytologist. 175:731-742.

Xu, T., Li, Y., Zeng, X., Yang, X., Yang, Y., Yuan, S., Hu, X., Zeng, J., Wang, Z., Liu, Q. and Liu, Y., (2017). Isolation and evaluation of endophytic *Streptomyces endus* OsiSh-2 with potential application for biocontrol of rice blast disease. Journal of the Science of Food and Agriculture. 97:1149-1157.

In vitro efficacy of *Chaetomium brasiliense* against *Pythium* spp. causing root rot disease of tangerine

Udompongsuk, M.[1] * , Soytong, K.[1], Kanokmedhakul, S.[2] and Kanokmedhakul, K.[2]

[1]Department of Plant Production Technology, Faculty of Agricultural Technology, King Mongkut's Institute of Technology Ladkrabang (KMITL), Ladkrabang, Bangkok, Thailand; [2]Department of Chemistry and Center for Innovation in Chemistry, Faculty of Science, Khon Kaen University, Khon Kaen 40002, Thailand.

Abstract Root rot is one of the most serious disease in Tangerine which caused by *Pythium* spp. This study tested efficacy of *Ch. brasiliense* to control *Pythium* sp. by bi – culture, crude extracts and nano particles testing from *Ch. brasiliense* to control *Pythium* sp., in vitro. The results from the bi – culture testing, *Ch. brasiliense* inhibited mycelium growth and sporangia production by 42.50% and 48.41%, respectively. In crude extracts from *Ch. brasiliense* gave ED_{50} values of 30.15, 58.71 and 37.25 ppm for the hexane, EtOAc and MeOH, respectively. The efficacy of nano particles against *Pythium* sp. with the ED_{50} values of 2.69, 3.00 and 3.96 ppm for the hexane, EtOAc and MeOH, respectively.

Keywords: *Chaetomium brasiliense*, Root rot, Tangerine

Introduction

Thailand office of agricultural economics reported in 2007 – 2015 tangerine production tends to decrease from 757,000 to 141,000 ton due to yield loss and decline of tangerine tree. The major problem is root rot disease (Molina *et al*., 1998). Growers used fungicide for control this disease and were faced with high cost of production, poor yield and low prices. They quit cultivation of tangerines. In 2016, they turned to reactivate their orchards because the price hiked.

The symptoms after *Pythium* spp. infected, the leaves turn yellow and some drop, twinge and branch dieback. Roots turn soft and brown, sometimes bark cracks through which gum exudation. Plant will grow poorly, decline and die in the end (Vichitrananda, 1998). For controlling this disease has been applied chemical fungicides in orchards but application chemical fungicides have resulted in accumulation of toxics in environment and resistance of

* **Coressponding Author:** Udompongsuk, M.; **Email:** zw.mink@gmail.com

fungicides. To avoide them, there are many researches for alternative control by effective of biological control agents (BCAs) e.g. *Ch. globosum Ch. cupreum* and *Ch. lucknowense* were reported to control *Phytophthora palmivora and Phytophthora nicotianae* causing root rot in pomelo and citrus (Hung *et al.,* 2014; 2015). Chaetoglobosin – C that produce from *Ch.globosum* gave significantly inhibited colony and sporangia of *Phytophthora parasitica* (Quyet *et al*., 2016). The aim of this study was to evaluation of efficiency of *Ch. brasiliense* to control *Pythium* spp. causing root rot of tangerine, in vitro.

Materials and methods

Isolation and identification

Soil samples, at a depth of 15 – 30 cm, were collected from the tangerine orchards and isolated by baiting method. The soil samples were ground and placed into sterilized petri dish, added sterilized distilled water above the soil and floated leaf pieaces of tangerines (0.5 × 0.5 cm) on the water surface and incubated petri dish for 24-72 hours at room temperature. Place baits onto water agar (WA). When mycelia grown on WA agar were transferred to Potato Dextrose Agar (PDA) until get pure culture and incubated room temperature. For morphological studies, according to their cultural appearances and observation of sporangium and other structures of *Pythium* spp. Sporangia were produced by floating some mycelial discs in distilled water and sterilized grass blades.

Pathogenicity test

Pathogenicity was tested by detached leaf method from healthy leaves leaves of *Citrus reticulata.* The leaves were washed with distilled water, then surface sterilized with 70% ethyl alcohol and placed with the upper leaf surface in sterile petri dish moisture chambers. Wounding by sterile needle on the leaves for easy access of the fungus, then leaves were inoculated with mycelium discs of *Pythium* spp. on the wound. Non-inoculated controls were inoculated with an agar plug without the fungus. 4 replications of each treatment were used in the experiment. After inoculation petri dishes were incubated at room temperature and symptoms were observed after 3 days.

Bi-culture test

Mycelial disc (0.5 m in diameter) of *Pythium* spp. was placed on PDA at one side of petri dish and *Ch. brasiliense* was placed at the opposite side of

petri dish with 4 replications and incubated at room temperature. As control an agar disc of *Pythium* spp. and *Ch. brasiliense* was placed alone on PDA. All petri dishes were incubated at room temperature until the pathogen in control growing full. The data were collected as colony diameter and the number of sporangium. The inhibition of mycelial growth and sporangium formation of pathogen was calculated as a percentage according to the formula:

Percent inhibition (I) = C – T/C $\times$ 100

Where, C = colony diameter / number of sporangium of the control

T = colony diameter / number of sporangium of the in bi-culture test

In vitro test of crude extract from Ch. brasiliense to control Pythium spp.

Ch. brasiliense was cultured in potato dextrose broth (PDB) for 30 days. The fungal biomass was collected, air-dried, ground and extracted with hexane, ethyl acetate (EtOAc) and methanol (MeOH) to produce crude hexane, crude EtOAc and crude MeOH extract, respectively. The crude exract from *Ch. brasiliense* were tested to control *Pythium* spp. by poisioned food technique with different concentrations (0, 10, 50, 100, 500 and 1000 ppm). Each crude exract was dissolved in 2% dimethyl sulfoxide (DMSO), and mixed into PDA before autoclaving at 121˚C, 15lbs/inch2 for 20 min. Mycelial disc of *Pythium* spp. was placed on the center of PDA in plate (5 cm diameter) incorporated with each crude exract. All petri dishes were incubated at room temperature until *Pythium* spp. in control growing full. Experiment was designed by using 2 factors factorial experiment in Completely Randomized Design (CRD) with 4 replications. Factor A represented solvents and factor B represented concentrations

The data were collected as colony diameter and the number of sporangium. The inhibition of mycelial growth and sporangium formation of pathogen was calculated as a percentage and the effective dose (ED_{50}) value was then calculated using probit analysis. Data was statistically computed and analysis of variance. Treatment means were compared with Duncan's multiple range test (DMRT) (p=0.05)

In vitro test of nano particles from Ch. brasiliense to control Pythium spp.

Nano particles were done using the method of Dar and Soytong (2014) to get Nano-CBH, Nano-CBE and Nano-CBM and were tested to control *Pythium* spp. by poisioned food technique. Experiment was designed by using 2 factors factorial experiment in CRD with 4 replications. Factor A represented nano particles and factor B represented concentrations at 0, 3, 5, 10 and 15 ppm.

Each nano particle was dissolved in 2% dimethyl sulfoxide (DMSO), and then mixed into PDA and added chitosan before autoclaving at 121˚C, 15lbs/inch2 for 20 min. Mycelial disc of *Pythium* spp. (7mm) was placed on the center of PDA in plate incorporated with each nano particles. All petri dishes incubated at room temperature until the pathogen in control plates growing full.

The data were collected as colony diameter and the number of sporangium. The inhibition of mycelial growth and sporangium formation of pathogen was calculated as a percentage and the effective dose (ED_{50}) value was then calculated using probit analysis. Data was statistically computed and analysis of variance. Treatment means were compare with Duncan's multiple range test (DMRT) (p=0.05).

Results

Pythium spp. was isolated from soil samples by baiting method and identified based on morphological characteristic. The cultural appearances were observed on PDA. Colony has a cottony aerial mycelium. The fungus grows fast, mycelium hyaline (Fig. 1, A). Sporangia formed on sterile grass blades in water cultures. Sporangia are of filamentous inflated (Fig. 1, B). Oogonia are smooth-walled, spherical, terminal, intercalary (Fig. 1, C-D). Oospores are aplerotic (Fig. 1, C-D).

Figure 1. Colony patterns and morphology of *Pythium* spp. A; Colony patterns on PDA, B; Filamentous inflated sporangium, C; Oogonium with monoclinous antheridium, D; Oogonium with aplerotic oospores

Inoculated leaves under moist chamber condition showed water-soaked brownish lesions expand around agar plug of pathogen size 1.5×3.2 cm. Non-inoculated leaves showed no symptoms, leaves remained healthy.

In bi – culture test, result showed that *Ch. brasiliense* grew over and degraded *Pythium* spp. after inoculation 30 days. *Pythium* spp. was inhibited 42.5% growth colony and 48.1% sporangia production when compare to control.

Figure 2. Pathogenicity test of *Pythium* spp. on detached tangerine leaves. A; Inoculated control. B; Non-inoculated control

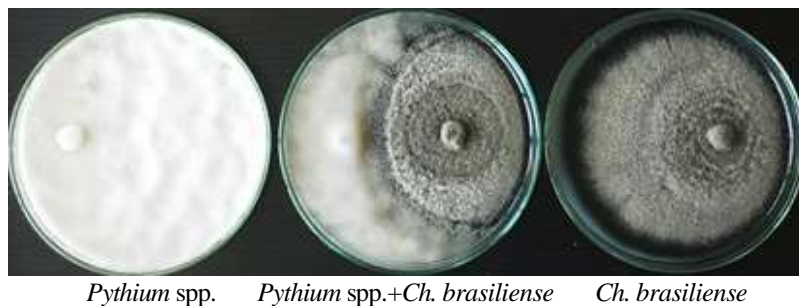*Pythium* spp.   *Pythium* spp.+*Ch. brasiliense*   *Ch. brasiliense*

Figure 3. Growth of *Pythium* spp. in bi–culture test of *Pythium* spp. (at 30 days)

Efficacy of crude extract and nano particles from *Ch. brasiliense* to control *Pythium* spp. were tested by poisioned food technique with different concentrations when *Pythium* spp. in control petri dishes grew fully (2 days).

All of concentrations gave significantly different when compare to the control (0 ppm) and at 1000 ppm gave the best growth inhibition and sporangia inhibition and follow by 500, 100, 50 and 10 ppm. All of crude extracts at the concentrations of 1000 ppm, *Pythium* spp. did not grow from mycelial discs. The hexane extract of *Ch. brasiliense* at the concentrations of 500, 100, 50 and 10 ppm inhibited the colony growth of 88, 76.5, 58.25 and 34.25%, respectively when compared to the control. The EtOAc extract of *Ch. brasiliense* at the concentrations of 500, 100, 50 and 10 ppm inhibited the colony growth of 88, 69.25, 42.75 and 27.5%, respectively when compare to the control. The MeOH extract of *Ch. brasiliense* at the concentrations of 500, 100, 50 and 10 ppm inhibited the colony growth of 86, 71, 51.5 and 44 %, respectively when compared to the control (Table 1).

There is sporangia production 46.81×10^6 spore/ml in control. When calculated the sporangia inhibition at the concentrations of 1000, 500, 100, 50 and 10 ppm, the hexane extract of *Ch. brasiliense* inhibited the sporangia production of 95.59, 88.12, 73.56, 55.14 and 32.18%, respectively when compare to the control. The EtOAc extract of *Ch. brasiliense* inhibited the sporangia production of 95.33, 87.72, 59.41, 35.38 and 25.23%, respectively when compare to the control. The MeOH extract of *Ch. brasiliense* inhibited the sporangia production of 95.46, 86.78, 63.68, 43.92 and 36.98%, respectively when compare to the control (Table 1).

The crude extracts gave ED_{50} values of 30.15, 58.71 and 37.25 ppm for the hexane, EtOAc and MeOH, respectively (Table 1).

Table 1. Effect of crude extracts from *Ch. brasiliense* to inhibit *Pythium* spp.

Crude extract	Concentration (ppm)	Colony diameter (cm)	Growth inhibition (%)	Number of sporangia ($\times 10^6$)	Sporangia inhibition (%)	ED_{50} (ppm)
hexane	0	5.00a	-	46.81a	-	30.15
	10	3.29c	34.25h	31.75c	32.18i	
	50	2.09f	58.25e	21.00f	55.14f	
	100	1.18h	76.50c	12.38i	73.56c	
	500	0.60ij	88.00ab	5.56j	88.12b	
	1000	0.50j	90.00a	2.06k	95.59a	
ethyl acetate	0	5.00a	-	46.81a	-	58.71
	10	3.63b	27.5i	35.00b	25.23j	
	50	2.86d	42.75g	30.25d	35.38h	
	100	1.54g	69.25d	19.00g	59.41e	
	500	0.60ij	88.00ab	5.75j	87.72b	
	1000	0.50j	90.00a	2.19k	95.33a	
methanol	0	5.00a	-	46.81a	-	37.25
	10	2.80d	44.00g	29.50d	36.98h	
	50	2.43e	51.50f	26.25e	43.92g	
	100	1.45g	71.00d	17.00h	63.68d	
	500	0.70i	86.00b	6.19j	86.78b	
	1000	0.50j	90.00a	2.13k	95.46a	
C.V. (%)		4.28		3.98		

[1]Average of 4 replications. Means followed by the same letters in each antagonist were not significantly different by DMRT at P=0.05.

The nano particles were done from all crude extracts of *Ch. brasiliense* according to the method of Dar and Soytong (2014). All of concentrations gave significantly different when compare to the control and at 15 ppm gave the best growth inhibition and sporangia inhibition and follow by 10, 5 and 3 ppm.

All of nano particles at the concentrations of 15 ppm, *Pythium* spp. did not grow from mycelial discs. Nano-CBH at the concentrations of 10, 5 and 3

ppm inhibited the colony growth of 77.75, 55.5 and 41.75 %, respectively when compare to the control. Nano-CBE at the concentrations of 10, 5 and 3 ppm inhibited the colony growth of 67.5, 44 and 22.4 %, respectively when compare to the control. Nano-CBM at the concentrations of 10, 5 and 3 ppm inhibited the colony growth of 78.25, 57 and 47.25 %, respectively when compare to the control (Table 2).
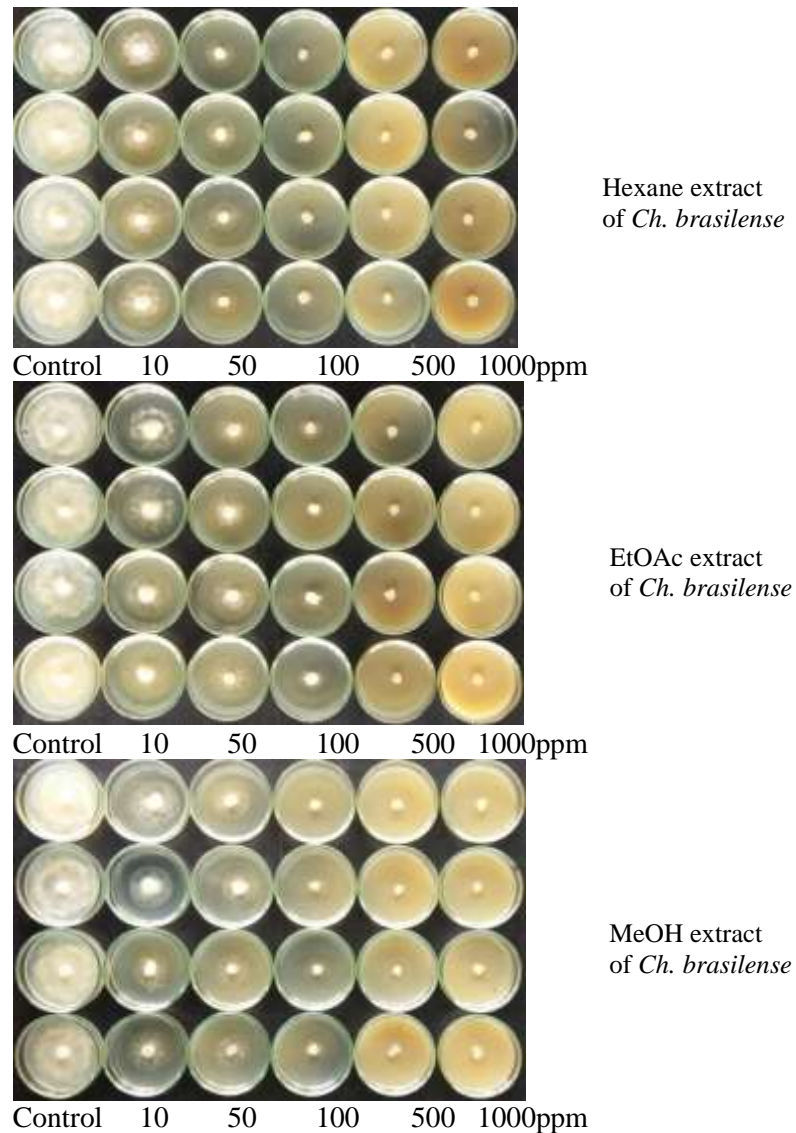

Hexane extract of *Ch. brasilense*

EtOAc extract of *Ch. brasilense*

MeOH extract of *Ch. brasilense*

Figure 4. Testing crude extracts from *Ch. brasiliense* to inhibit *Pythium* spp.
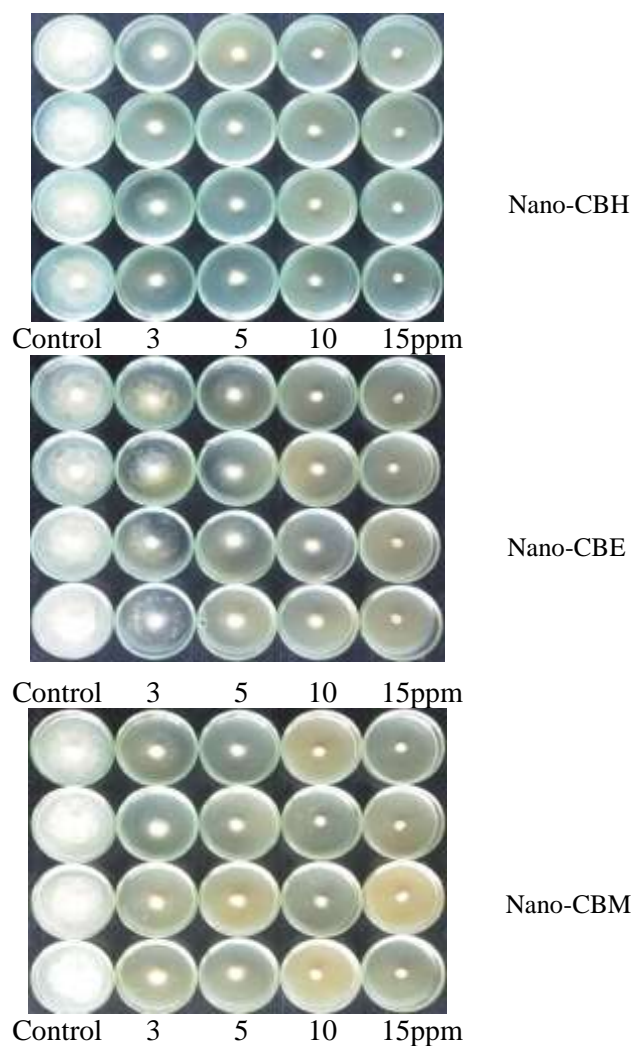
Figure 5. Testing the nano particles from *Ch. brasiliense* to inhibit *Pythium* spp.

In control, the number of sporangia was 42.38×10^6 spore/ml. When compare to the control, Nano-CBH at the concentrations of 15, 10, 5 and 3 ppm inhibited the sporangia production of 95.13, 86.43, 54.42 and 41.45 %, respectively. Nano-CBE at the concentrations of 15, 10, 5 and 3 ppm inhibited the sporangia production of 94.99, 86.43, 54.42 and 41.45 %, respectively when compare to the control. Nano-CBM at the concentrations of 15, 10, 5 and 3 ppm inhibited the sporangia production of 95.43, 89.38, 70.21 and 55.6 %, respectively when compare to the control (Table 2).

The nano particles of *Ch. brasiliense* gave ED_{50} values of 3, 3.96 and 2.69 ppm for the hexane, EtOAc and MeOH, respectively (Table 2).

2188

Table 2. Effect of the nano particles from *Ch. brasiliense* to inhibit *Pythium* spp.

Nano product	Concentration (ppm)	Colony diameter (cm)	Growth inhibition (%)	Number of sporangia ($\times 10^6$)	Sporangia inhibition (%)	ED$_{50}$ (μg/ml)
Nano-CBH	0	5.00a	-	42.38a	-	
	3	2.91c	41.75f	20.81c	50.88e	
	5	2.23e	55.50d	13.44e	68.29c	3.00
	10	1.11g	77.75b	5.00f	88.20b	
	15	0.50h	90.00a	2.06g	95.13a	
Nano-CBE	0	5.00a	-	42.38a	-	
	3	3.88b	22.40g	24.81b	41.45f	
	5	2.80cd	44.00ef	19.31cd	54.42de	3.96
	10	1.63f	67.50c	5.75f	86.43b	
	15	0.50h	90.00a	2.13g	94.99a	
Nano-CBM	0	5.00a	-	42.38a	-	
	3	2.64d	47.25e	18.81d	55.60d	
	5	2.15e	57.00d	12.63e	70.21c	2.69
	10	1.09g	78.25b	4.50f	89.38b	
	15	0.50h	90.00a	1.94g	95.43a	
C.V.(%)		5.01		6.52		

[1]Average of 4 replications. Means followed by the same letters in each antagonist were not significantly different by DMRT at P=0.05.

Discussion

The most serious root rot disease of citrus in Thailand is caused by *Phytophthora parasitica* but *Pythium* spp. is reported that caused root rot disease of citrus (Maseko and Coutinho, 2001 and Kean *et al.*, 2010).

The obvious mechanisms of action of *Ch. brasiliense* in bi – culture test is competition because at first, *Pythium* spp. grew more than 50% of petri dish and faster than *Ch. brasiliense*. After 30 days *Ch. brasiliense* can grow over *Pythium* spp. moreover, *Pythium* spp. were degraded, mycelial deflated. There is probably antibiosis mechanism, therefore studying antifungal metabolite in terms of crude extract and nano particles from *Ch. brasiliense* to control *Pythium* spp. They gave high inhibition with low ED$_{50}$ values. The ED$_{50}$ values of crude extracts were 30.15 – 58.71 ppm and nano particles were 2.69 – 3.96 ppm. It was similar to the study of Tongon and Soytong (2016) studied using crude extracts of *Ch. brasiliense* to inhibit *Fusarium solani* and got effectively inhibition of *F. solani* with ED$_{50}$ were 66.66 – 288.94 ppm. Khumkomkhet *et al.* (2009) found many depsidones from *Ch. brasiliense* and tested to control *Plasmodium falciparum*, *Mycobacterium tuberculosis* and *Candida albicans*.

Nano particles have one dimension less than 100 nm at least and ability to adsorb and carry compounds. The nano particles gave stronger inhibition than

crude extracts with lower ED_{50} values. It was similar to the report of Dar and Soytong (2014) tested nanomaterials derived *Ch. globosum* and *Ch. cupreum.* Moreover, Tongon and Soytong (2015) reported nano particles from *Ch. globosum* showed highly inhibitory effects on *Curvularia lunata* causing leaf spots of rice with low ED_{50} values.

Acknowledgement

References

Dar, J. and Soytong, K. (2014). Construction and characterization of copolymer nanomaterials loaded with bioactive compounds from *Chaetomium* species. Journal of Agricultural Technology. 10:823-831.

Hung, P. M., Wattanachai, P. and Soytong, K. (2014). Biological control of pomelo diseases using *Chaetomium* spp. Journal of Agricultural Technology. 10:833-844.

Hung P. M., Wattanachai, P., Soytong K. and Poeaim, S. (2015). Biological control of *Phytophthora palmivora* causing root rot of Pomelo using *Chaetomium* spp. Mycobiology. 43:63-70.

Kean, S., Soytong, K. and To-anun, C. (2010). Application of biological fungicides to control citrus root rot in Cambodia. Journal of Agricultural Technology. 6:219-230.

Khumkomkhet, P., Kanokmedhakul, S., Kanokmedhakul, K., Hahnvajanawong, C., and Soytong, K. (2009). Antimalarial and cytotoxic depsidones from the fungus *Chaetomium brasiliense*. Journal of natural products. 72:1487-1491.

Maseko, B. O. Z. and Coutinho, T. A. (2001). Pathogenicity of *Phytophthora* and *Pythium* species associated with citrus root rot in South Africa. South African Journal of Botany. 68:327-332.

Molina, A. B., Roa, V. N., Bay-Petersen, J., Carpio, A. T. and Joven, J. E. A. (1998). Regional Workshop on Disease Management of banana and citrus through the use of disease-free planting materials held in Davao city, Philippines. pp. 14-16.

Tongon, R. and Soytong, K. (2015). Application of nano-particles from *Chaetomium globosum* to control leaf spot of rice. Journal of Agricultural Technology. 11:1919-1926.

Tongon, R. and Soytong, K. (2016). Fungal Metabolites from chaetomium brasilense to Inhibit Fusarium solani. International Journal of Agricultural Technology. 12:1463-1472.

Quyet, N. T., Cuong, H. V., Hong, L. T. and Soytong, K. (2016). Control mechanism of *Chaetomium* spp. and its biological control of Citrus root rot in pot and field experiments in Vietnam. International Journal of Agricultural Technology. 12:329-336.

Vichitrananda, S. (1998). Disease Management of Citrus Orchards Planted with Disease-free Seedlings in Thailand. pp. 49-56. In: Proceedings of a reglonal workshop on disease management of banana and citrus throught the use of disease free planting materials helo in Davao City Philippines. October 14-16, 1998. Davao City, Philippines.

Nano-particles from *Cheatomium brasiliense* against brown spot of rice

Vareeket, R.[1*], Soytong, K.[1], Kanokmedhakul, S.[2] and Kanokmedhakul, K.[2]

[1]Department of Plant Production Technology, Faculty of agricultural Technology, King Mongkut's Institute of Technology Ladkrabang, Bangkok 10520, Thailand; [2]Department of Chemistry and Center for Innovation in Chemistry, Faculty of Science, Khon Kaen University, Khon Kaen 40002, Thailand.

Abstract *Chaetomium brasiliense* was used in this study to control rice brown spot disease pathogen, *Drechslera oryzae*. The result of bi-culture test showed that *Ch. brasiliense* gave the hightest percentage of growth inhibition at 26.38% and had the highest spore inhibition at 23.81%. In crude extracts test, it was found that crude methanol extract obtained from *Ch. brasiliense* at 1000 ppm showed the highest inhibitory effect on colony growth and spore production. *Ch. brasiliense* gave a growth inhibition and spore inhibition rates at 83.50 and 99.78% respectively. The effective dose (ED_{50}) on growth and spore inhibition of *Ch. brasiliense* was 80.54 and 0.35 μg/ml, respectively. It was also found that Nano-particles obtained from crude methanol extract of *Ch. brasiliense* (nano CBM) at 10 ppm had the best inhibitory effect in terms of growth and spore inhibition. Nano CBM can inhibit the growth at 70.00% and spore production at 79.92%. The ED_{50} values for spore inhibition of *Ch. brasiliense* was 2.86 μg/ml.

Keywords: *Chaetomium brasiliense*, biological control, rice disease

Introduction

Rice (*Oryza sativa* L) is the most widely consumed staple food for a large part of the world's human population, especially in Asia and the West Indies. It is the grain with the third-highest worldwide production (FAOSTAT, 2017). *Drechslera oryzae* is a fungus that reports to cause brown leaf spot of rice. This is one of the important plant pathogen causing a widespread disease leading to yield losses. Brown spot of rice can infect the seedlings and mature plants. The symptom appeared as blight on seedling where grown from infected seeds (Rice Department, 2018).

---

[*] **Coressponding Author:** Vareeket, R.; **Email:** rungrat.kmitl@gmail.com

This objective was to investgate the morphology of *Chaetomium brasilense* and *Drechslera oryzae*, pathogenicity test. Tesing crudec extraxts and nano-particles from *Chaetomium brasilense* to control brown leaf spot of rice var RD47 were also conducted.

Materials and methods

Isolation of pathogen and pathogenicity test

Drechslera oryzae causing brown leaf spot of rice were isolated form seed rice var. RD47. Rice seeds were soaked in sterilized water and then in 1% clorax for 3 min and then sterilized water. All seeds were moved to water agar and sub-cultured to PDA until get pure culture. Morphology was observed under compound microscope.

Morphology study of the *Drechslera oryzae*
Isolate of *Drechslera oryzae* was morphological identified. The characters of *D. oryzae* were determined under compound microscope.

Pathogenicity test
The experimental design was done by Completely Randomization with four repeated times. The pathogen isolate was proved for pathogenicity followed Koch's Postulate. The conidia suspension of 5×10^6 conidia/ml. was used for inoculation. The 15 days of rice seedlings var. RD47 were inoculated sprayed onto the wounded leaves (3 leaves/seedling). The inoculated leaves were covered with plastic sheets, then observed the infected leaves. The leaves with spraying sterilize distilled water were done to serve as controls.

Biological control of Drechslera oryzae

Strain of antagonist used for experiments
Chaetomium brasiliense was kindly provided by Assoc. Prof. Dr. Kasem Soytong.

Dual culture test
Ch. brasiliense was tested to control *D. oryzae*. Each fungus was separately cultured on PDA at room temperature for seven days. A 0.5 cm diameter sterilized cork borer was used to transfrred agar plugs from peripheral colony of each fungus to 9-cm diameter PDA plates, and put in the opposite site to each other. Control plates were transferred each fungus alone to PDA plates.

The testeds plates were incubated at room temperature for 30 days. Abnormal spores wewre observed under compound microscope and took photograph. Colony diameter, number of conidia of pathogenic fungus were collected. The growth or conidia inhibition of pathogen was calculated using formula below:

$$\text{Inhibition (\%)} = \frac{A-B}{A} \times 100 \quad\text{———————}\quad (1)$$

A = colony diameter or conidia number of pathogen in control
B = colony diameter or conidia number of pathogen in control in dual culture plate

The data were statistically computed and means were compared by using Duncan's New Multiple Range Test at P=0.01 and P=0.05.

Biological activity of antagonist against pathogen (crude extract test)

Crude extracts from *Ch. brasiliense* was tested against *D. oryzae* The fungus was cultured in potato dextrose broth at room temperature for one month. The biomass was collected, ground with the electrical blender and dissolved with solvents. The solvents were then separtately evaporated *in vacuo* to yield crude hexane, crude ethyl acetate, and crude methanol extracts, respectively.

The crude extracts were assayed to inhibit the tested pathogen, *D. oryzae.* The experimental design was conducted by using two factors factorial experiment in Compleletly Randomization withy four repatedted times. Factor A1 was crude hexane, A2 crude ethyl acetate and A3 crude methanol. Factor B1 was 0 µg/ml(control), B2 = 10 µg/ml, B3 = 50 µg/ml, B4 = 100 µg/ml, B5 = 500 µg/ml and B6 = 1,000 µg/ml. Each crude extract was dissolved in 2% dimethyl sulfoxide and added to PDA before autoclaved at $121\,^{\circ}\text{C}$ (15 psi) for 20 minutes. A sterilized 3-mm diameter cork borer was used to remove agar plugs from peripheral colony to the center of 5 cm dia Petri dishes of PDA containing crude extract at each concentration. Incubation was done until grown full plates. The number of spore was collected and calculated the inhibition. The effective dose (ED_{50}) was calculated using Probit analysis.

Testing nano-particles from Chaetomium brasiliense to control brown leaf spot

Nano-particles were performed using the method of Dar and Soytong (2014) to get Nano-CBH, Nano-CBE and Nano-CBM. Two factors factorial experiment in Complately Randomized Design was conducted with four

replications . Factor A was Nano-CBH, Nano-CBE and Nano-CBM and factor B was 0, 1, 3, 5, 7 and 10μg/ml. Each Nano-particle was dissolved in 2% dimethyl sulfoxide, mixed into PDA medium, and autoclaved at 121^0C, 15 lbs/inch2 for 30 min. The colony of *D. oryzae* was cut at the peripheral colony with sterilized cock borer (3mm), transferred to the middle of PDA incorporated with nano-particles. The plates were incubated at room temperature until the pathogen in control growing full plate. Abnormal spores were observed under compound microscope. Colony diameter and the number of spores were recorded. Inhibition was computed and the effective dose (ED_{50}) was calculated using Probit analysis.

Results

Isolation of pathogen and pathogenicity test

Rice pathogen was isolated from rice seeds of RD 47. It was found *Drechslera oryzae*. Pure culture showed brown color when mature, septate mycelia, and conidia with many septates or cells on one conidia (Figure 1).

Figure 1. *Drechslera oryzae* on PDA medium after 7 days **(A),** *Drechslera oryzae* conidiophore (B) and *Drechslera oryzae* conidium **(C)**

Figure 2. Pathogenicity test of *Drechslera oryzae* on rice. The inoculated control (left) and inoculated leaves (right) after 7 days

The pathogenicity of the isolate was confirmed; the symptoms appear in from of minute light brown or brownish red spots and these leaf spots becomes dark brown with a surrounding halo region (Figure 2).

Biological control of Drechslera oryzae

Ch. brasiliense resulted to inhibit mycelial growth of *D. oryzae* which averaged colony was 6.62 cm when compared to control plate (9.00 cm). It significantlyt inhibited the mycelia growth of 26.38%. *Ch. brasiliense* alsp espressed significantly spore inhibition of *D. oryzae* 23.81% as seen in Figure 3, and Table 2].

Figure 3. Bi-culture antagonistic test between *Drechslera oryzae* and *Chaetomium brasiliense*

Table 1. *Chaetomium brasiliense* against *Drechslera oryzae* in bi-culture tests

	Chaetomium brasiliense		Growth Inhibition percent	C.V. (%)
	Control	Bi-culture		
Colony growth(cm)	9.00[a1]	6.62[b]	26.38	0.55
Spore number (10^7/ml)	22.2[a]	16.90[b]	23.81	7.24

1/: Means four repeated experiments and followed by the same letter are not significantly differed by DMRT at P=0.01.

Biological activity of antagonist against pathogen

Crude ethyl acetate extract of *Chaetomium brasiliense* gave significantly highest inhibition of *Drechslera oryzae* which the ED_{50} of 0.24 μg/ml, and followed by crude hexane and methanol extracts which the ED_{50} of 0.32 and

0.35 μg/ml, respectively. Crude methanol extract at 1,000 ppm showed significantly highest spore inhibition of 99.78 %, and followed by crude hexane (99.77 %) and ethyl acetate extracts (99.60 %). Crude methanol extract significantly inhibited colony growth by 83.50 %, and followed by the crude ethyl acetate (82 %) and hexane extracts (74.50 %) as seen in Table 2.

Table 2. Crude extracts of *Chaetomium brasiliense* testing to inhibit *Drechslera oryzae*

Crude extracts	Concentration (ppm)	Colonydiameter (cm)	Growth inhibition (%)	ED_{50} (μg/ml)	Number of spore[1/]	Spore inhibition (%)	ED_{50} (μg/ml)
	0	5.00[al]	-		185.06[a]	-	
	10	3.50[c]	30.00[k]		22.78[bc]	87.65[e]	
Crude	50	3.30[de]	34.00[ij]	93.09	20.35[bcd]	88.99[de]	0.32
hexane	100	2.80[h]	44.00[h]		12.23[de]	93.34[c]	
	500	1.53[j]	69.50[d]		0.76[f]	99.58[a]	
	1000	1.27[k]	74.50[c]		0.40[f]	99.77[a]	
	0	5.00[a]	-		185.06[a]	-	
	10	3.22[e]	35.50[i]		20.56[bcd]	88.81[e]	
Crude	50	2.47[g]	50.50[g]	85.77	18.13[cd]	90.18[d]	0.24
ethyl	100	2.12[i]	57.50[e]		12.76[de]	93.09[c]	
acetate	500	1.05[l]	79.00[b]		1.16[f]	99.36[a]	
	1000	0.90[m]	82.00[a]		0.73[f]	99.60[a]	
	0	5.00[a]	-		185.06[a]	-	
	10	4.07[b]	18.50[l]		29.32[b]	84.13[f]	
Crude	50	3.38[cd]	32.50[jk]	80.5	21.43[bcd]	88.38[e]	0.35
methanol	100	2.32[h]	53.50[f]		8.02[ef]	95.66[b]	
	500	1.27[k]	74.50[c]		2.18[f]	98.79[a]	
	1000	0.83[m]	83.50[a]		0.38[f]	99.78[a]	
	C.V. (%)	3.25			14.92		

1/: Means four repeated experiments and followed by the same letter are not significantly differed by DMRT at P=0.01.

Testing nano-particles from Chaetomium brasiliense to control brown leaf spot

The nano-CBH, nano-CBE, and nano-CBM at the concentration of 10 ppm inhibited spore production by 85.25%, 77.86%, and 79.92%, respectively. These nanoparticles expressed antifungal activity against *Drechslera oryzae* with ED_{50}values of 5.86, 4.92, and 2.86 μg/ml, respectively (Table 3).

Table 3. Nano-particles of *Chaetomium brasiliense* testing to inhibit *Drechslera oryzae*

Crude extracts	Concentration (ppm)	Colonydiameter (cm)	Growth inhibition (%)$^{/2}$	ED$_{50}$ (µg/ml)	Number of spore	Spore inhibition (%)	ED$_{50}$ (µg/ml)
	0	5.00^{al}	-		5.45^a	-	
	1	1.91^{de}	61.75^b		2.37^{cde}	55.67^{efg}	
Nano-CBH	3	2.09^c	58.25^c	-	1.62^{efg}	69.50^{bcde}	5.86
	5	2.31^b	53.75^f		1.28^{fgh}	76.35^{abcd}	
	7	2.10^c	58.00^f		0.99^{gh}	81.73^{ab}	
	10	1.80^{ef}	64.00^h		0.77^h	85.25^a	
	0	5.00^a	-		5.45^a	-	
	1	2.07^c	58.50^b		2.89^c	46.71^g	
Nano-CBE	3	2.05^{cd}	59.00^d	168.00	2.57^{cd}	52.36^{fg}	4.92
	5	1.95^{cd}	61.00^e		2.03^{def}	62.50^{def}	
	7	1.97^{cd}	60.50^g		1.99^{def}	62.80^{def}	
	10	1.53^g	69.50^h		1.20^{gh}	77.86^{ab}	
	0	5.00^a	-		5.45^a	-	
	1	2.02^{cd}	59.50^b		3.96^b	25.60^h	
Nano-CBM	3	2.00^{cd}	60.00^{cd}	237.00	2.35^{cde}	56.84^{efg}	2.86
	5	1.68^f	66.50f		2.01^{def}	63.32^{def}	
	7	1.53^g	69.50^f		1.26^{fgh}	77.13^{def}	
	10	1.50^g	70.00^h		1.12^{gh}	79.92^{ab}	
	C.V. (%)	4.10			19.39		

1/: Means four repeated experiments and followed by the same letter are not significantly differed by DMRT at P=0.01.

Discussion

The brown spot of rice caused by *Drechslera oryzae* was isolteds and proved pathogenicityn as similar report of Tan and Soytong (2016b). *Ch brasiliense* proved to be antagonised the tested pathogen in bi-culture test was also similar result of Tan and Soytong (2016a). As a result, the crude hexane and methanol extracts from *Ch. brasiliense* actively against *D. oryzae* causing brown spot of rice var RD 47 which the ED$_{50}$ values of 0.32 and 0.35 µg/ml, respectively. Tan and Soytong (2017) reported that bioformulation including crudec extrtacts from *Chaetomium cupreum* CC3003 gave a good control leaf spot of rice var. Sen Pidao in Cambodia. Each crude crude extract of *Ch. brasiliense* was performed to be nano-particles as nano-CBH, nano-CBE, and nano-CBM and tested to inhibit *D. oryzae* causing brown leaf spot of rice var RD47. As results, it showed that nanoparticles, nano-CBH, nano-CBE, and nano-CBM gave significantly inhiubited expressed *D. oryzae* at the ED$_{50}$values of 5.86, 4.92, and 2.86 µg/ml, respectively. It concluded that nanoparticles from *Ch. brasiliense* gave successfully inhibitred the tested pathogen. Further study would be applied the the fields and also tested to control the other plantb pathogens. As reports of Vilavong and Soytong (2017) stated that the

application of bio-formulation including nano-elicitor of *Ch. cupreum* could control *Colletotrichum gloeosporioides* causing Coffee Anthracnose on Arabica Variety in Laos.

Acknowledgement

References

Joselito, D. and Soytong, K. (2014). Construction and characterization of copolymer nanomaterials loaded with bioactive compounds from *Chaetomium* species. International Journal of Agricultural Technology. 10:823-831.

Rice Department (2018). Rice Knowledge Bank. Retrieved by 5 September 2018. http://www.ricethailand.go.th/rkb/disease%20and%20insect/index.phpfile=content.php &id=113.htm.

Tann, H. and Soytong, K. (2016a). Bioformulations and nano product from *Chaetomium cupreum* CC3003 to control leaf spot of rice var. Sen Pidao in Cambodia. International Journal of Plant Biology. 7:6413.

Tann, H. and Soytong, K. (2016b). Effects of nanoparticles loaded with *Chaetomium globosum* KMITL-N0805 extracts against leaf spot of rice var. Sen Pidoa. Malaysian Applied Biology Journal. 45:1-7.

Tann, H. and Soytong, K. (2017). Biological control of brown leaf spot disease caused by *Curvularia lunata* and field application method on rice variety IR66 in Cambodia. Agrivita Journal of Agricultural Science. 39:111-117.

Vilavong, S. and Soytong, K. (2017). Application of a new bio-formulation of *Chaetomium cupreum* for biocontrol of *Colletotrichum gloeosporioides* causing coffee anthracnose on arabica variety in laos. AGRIVITA Journal of Agricultural Science. 39:303-310.

UN Food and Agriculture Organization, Corporate Statistical Database (FAOSTAT). (2017). Retrieved by 10 September 2017. http://www.fao.org/faostat/en/#data/QC.